UNITED STATES PATENT AND TRADEMARK OFFICE

BEFORE THE PATENT TRIAL AND APPEAL BOARD

SHENZHEN HUIDING TECHNOLOGY CO., LTD.

Petitioner

v.

SYNAPTICS INCORPORATED

Patent Owner

PTAB Case No. IPR2016-00465

Patent No. 8,952,916 B2

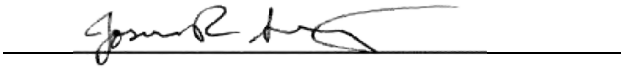
DECLARATION OF PROF. JOSHUA R. SMITH IN SUPPORT OF PETITION FOR *INTER PARTES* REVIEW OF U.S. PATENT NO. 8,952,916 B2

Ex. 1006

I hereby declare that all the statements made in this Declaration are of my own knowledge and true; that all statements made on information and belief are believed to be true; and further that these statements were made with the knowledge that willful false statements and the like so made are punishable by fine or imprisonment, or both, under 18 U.S.C. 1001 and that such willful false statements may jeopardize the validity of the application or any patent issued thereon.

I declare under the penalty of perjury that all statements made in this Declaration are true and correct.

Executed this Second day of February, 2016 in Seattle, WA.



Joshua R. Smith

TABLE OF CONTENTS

Page

LIST OF APPENDICES iv

I. INTRODUCTION 1

II. SUMMARY OF OPINIONS 3

III. QUALIFICATIONS AND EXPERIENCE 5

A. Education and Work Experience 5

B. Compensation 15

C. Documents and Other Materials Relied Upon 15

IV. STATEMENT OF LEGAL PRINCIPLES 17

A. Claim Construction 17

B. Anticipation 18

C. Obviousness 18

V. LEVEL OF ORDINARY SKILL IN THE ART 19

VI. TECHNOLOGY BACKGROUND OF THE 916 PATENT 22

A. A capacitive position sensor and a controller for a capacitive position sensor 24

B. Capacitive touch sensing circuitry that transmits and receives distinct signals based on distinct digital codes 28

C. Frequency modulation (FM), phase modulation (PM) or amplitude modulation (AM) of a carrier signal according to distinct digital codes 33

D. Specific distinct digital codes in spread spectrum modulation: Walsh-Hadamard codes, Gold codes, Kasami codes, and Barker codes 36

E. Adjustment of a frequency of a distinct signal based on observed noise in the resultant signal 37

VII. OVERVIEW OF THE 916 Patent 41

VIII. IDENTIFICATION OF THE PRIOR ART AND SUMMARY OF OPINIONS 45

IX. CLAIM CONSTRUCTION 45

Shenzhen Huiding Tech. Co., Ltd. - Exhibit 1006

TABLE OF CONTENTS
(continued)

Page

X. CLAIMS 1-20 IN THE 916 PATENT CONTAIN NOTHING NEW 47

A. GROUND 1: CLAIMS 1-20 CONTAIN NOTHING NEW OVER THE COMBINATION OF UMEDA, INOUE AND JAEGER 47

1. Overview of Umeda 48

2. Overview of Inoue 53

3. Overview of Jaeger 56

4. Motivations and reasons exist to combine Umeda, Inoue, and Jaeger 57

a. Motivations and reasons exist to combine Umeda and Inoue 57

b. Motivations and reasons exist to further combine Umeda and Inoue with Jaeger 62

5. Claim 1-20 Are Unpatentable Over Umeda, Inoue and Jaeger 69

a. Claim 1 69

b. Claim 2 104

c. Claim 3 105

d. Claim 4 111

e. Claim 5 113

f. Claim 6 114

g. Claim 7 114

h. Claim 8 120

i. Claim 9 120

j. Claim 10 122

k. Claim 11 122

l. Claim 12 123

m. Claim 13 124

Shenzhen Huiding Tech. Co., Ltd. - Exhibit 1006

TABLE OF CONTENTS
(continued)

Page

n. Claim 14.....125
o. Claim 15.....126
p. Claim 16.....126
q. Claim 17.....127
r. Claim 18.....127
s. Claim 19.....128
t. Claim 20.....128

Shenzhen Huiding Tech. Co., Ltd. - Exhibit 1006

LIST OF APPENDICES

Appendix A	Curriculum Vitae of Joshua R. Smith
Appendix B	Claim Chart Showing Teachings of Prior Art References (Exs. 1007, 1008, 1011) Pertinent to Challenged Claims of U.S. Patent No. 8,952,916 (Ex 1004)
Appendix AA.	E. A. Johnson, *Touch display—a novel input/output device for computers*, Electronics Letters, Volume 1, Issue 8, p. 219 – 220 (Oct. 1965).
Appendix BB.	David Allport, Earl Rennison, and Lisa Strausfeld, *Issues of Gestural Navigation in Abstract Information Space*, CHI'95 Mosaic of Creativity, May 1995.
Appendix CC.	Joshua Reynolds Smith, *Toward Electric Field Tomography*, MIT Master of Science Thesis in 1995.
Appendix DD.	U.S. Patent No. 5,914,701 to Neil Gersheneld, Thomas Zimmerman, and David Allport of MIT Media Lab, entitled "*Non-contact system for sensing and signalling by externally induced intra-body currents*" ("Gersheneld").
Appendix EE.	Paul Michael Yarin, *Toward the Distributed Visualization of Usage History*, MIT Master of Science Thesis in 1999 (Degree not awarded) ("Yarin")
Appendix FF.	Paul H. Dietz and Darren Leigh at Mitsubishi Electric Research Laboratories (Cambridge, MA) "*Diamond Touch: A Multi-User Touch Technology*" in UIST '01 Proceedings of the 14th annual ACM symposium on User interface software and technology, p. 219-226, ACM New York (2001).
Appendix GG.	Joshua Reynolds Smith, *Code-Division Multiplexing of a Sensor Channel: A Software Implementation*, IEEE J. on Selected Areas in Commc'ns; pp. 725-731; Vol. 17, No. 4, Apr. 1999.
Appendix HH.	Robert C. Dixon, *Spread Spectrum Systems*, (2d ed. 1984) (Excerpt).

Shenzhen Huiding Tech. Co., Ltd. - Exhibit 1006

Appendix II. Marvin K. Simon, Jim K. Omura, and Robert A. Scholtz, *Spread Spectrum Communications Handbook*, Electronic Edition, McGraw-Hill, Inc. 2002 and 1994 (Excerpt).

Appendix JJ. Thomas G. Zimmerman, Joshua R. Smith, Joseph A. Paradiso, David Allport, and Neil Gersheneld, *Applying electric field sensing to human-computer interfaces*, CHI '95 Mosaic of Creativity, 280-87, May 7-11, 1995.

Appendix KK. U.S. Patent No. 4,698,461 to Robert D. Meadows, Philip T. Krein, and Bruce Murdock, entitled "*Touch panel with automatic frequency control*" ("Meadows '461").

Appendix LL. Joshua Reynolds Smith, *Electric Field Imaging*, MIT Doctoral Dissertation in 1999.

Appendix MM. Qingxin Chen et al., *Multicarrier CDMA with Adaptive Frequency Hopping for Mobile Radio Systems*, IEEE Journal on Selected Areas in Communications, vol. 14, no. 9, Dec. 1996 ("Chen").

Appendix NN. Matthew C. Davey & David MacKay, *Low-density parity check codes over GF(q)*, IEEE Commc'ns Letters, Vol 2, No 6, pp 165-167, June 1998.

Appendix OO. U.S. Patent No. 5,565,658 to George E. Gerpheide and Michael D. Layton ("Gerpheide").

Shenzhen Huiding Tech. Co., Ltd. - Exhibit 1006

I. INTRODUCTION

1. My name is Joshua R. Smith. I am a tenured Associate Professor in the departments of Computer Science and Engineering and Electrical Engineering at the University of Washington in Seattle, Washington. I am submitting this declaration as an independent professional, not as a representative of the University of Washington.

2. I have been engaged by Shenzhen Huiding Technology Co., Ltd. (the "company") to investigate and opine on certain issues relating to U.S. Patent No. 8,952,916 B2 (the "916 Patent") entitled "Method and systems for detecting a position-based attribute of an object using digital codes" in connection with the company's second Petition for *Inter Partes* Review of the 916 Patent ("IPR Petition") over prior art references Umeda, Inoue, and Jaeger. This second IPR Petition requests the Patent Trial and Appeal Board ("PTAB") to review and cancel all claims of the 916 Patent—claims 1 through 20 ("Challenged Claims"). I have been engaged by the company to investigate and opine on certain issues relating to the 916 Patent over different prior art references in the company's earlier, first IPR petition filed under PTAB Case No. IPR2015-01740. I have also been engaged to investigate and opine on certain issues relating to three other patents that are related to the 916 Patent— U.S. Patent Nos. 7,868,874 B2,

8,338,724 B2 and 8,558,811 B2 in additional petitions for *inter partes* review, including an IPR petition on the 811 Patent under PTAB Case No. IPR2015-01739, an IPR petition on the 724 Patent under PTAB Case No. IPR2015-01741, two IPR petitions on 68 claims of the 874 Patent under PTAB Case Nos. IPR2015-01742 and IPR2015-01743. I understand that Synaptics Incorporated ("Synaptics") is asserting all four patents against Shenzhen Huiding Technology Co., Ltd. in an on-going patent infringement lawsuit, No. 5:15-cv-01742, filed in the Northern District of California on April 17, 2015, and a Section 337 Investigation, Inv. No. 337-TA-957, filed in the U.S. International Trade Commission ("ITC") on April 21, 2015 and instituted on May 19, 2015.

3. I understand that the 916 Patent was assigned from the inventor J. Kurth Reynolds to Synaptics. Synaptics is therefore referred to as the "Patent Owner" in this declaration.

4. In this declaration, I will first discuss the technology background related to the 916 Patent and then provide my analyses and opinions on claims 1-20 of the 916 Patent. The discussion of the technology background includes an overview of that technology as it was known before November 15, 2005, which I understand as the earliest invention date of the 916 Patent claimed by the inventor in his inventor declaration submitted to the USPTO during the original prosecution

of the 916 Patent. This overview provides some of the bases for my opinions with respect to the 916 Patent.

5. This declaration is based on the information currently available to me. To the extent that additional information becomes available, I reserve the right to continue my investigation and study, which may include a review of documents and information that may be produced, as well as testimony from depositions that may not yet be taken.

6. In forming my opinions, I have relied on information and evidence identified in this declaration, including the 916 Patent, the prosecution history of the 916 Patent, and prior art references listed as Exhibits to the IPR Petition and listed as appendices of this declaration.

II. SUMMARY OF OPINIONS

7. Claims 1 through 20 of the 916 Patent relate to methods and systems for detecting a position-based attribute of an object using digital codes. For reasons explained below, none of the features described in claims 1 through 20 of the 916 Patent were novel as of November 15, 2005 because each of these features was disclosed by the cited prior art; nor does the 916 Patent teach any new way of combining these known features because the claimed combinations are predictable or apparent combinations in light of the prior art teachings and in light of the

knowledge of a person of ordinary skill in the art of the technology of the 916 Patent.

8. Claims 1 through 20 of the 916 Patent relate to well-known touch screen or capacitive position sensor technology commonly used in input devices for computers, portable devices, and consumer electronics. No element of Claims 1 through 20 is novel, and Claims 1 through 20 do not provide combinations of these elements together in a way that brings any benefit beyond what a person of ordinary skill in art in touch sensing would expect from the known functions of the individual components. Claims 1 through 20 describe techniques that were well-known in the field, and combine them in ways that would have been readily apparent or trivial to a person of ordinary skill in the art with predictable results.

9. It is my opinion that each of Claims 1 through 20 contains nothing new and is a trivial or predictable combination of known features. Therefore, Claims 1 through 20 are obvious under the patentability standard of 35 U.S.C. §103(a) as I understand it and as explained to me by the counsel of Shenzhen Huiding Technology Co., Ltd. Within this declaration, I discuss specific grounds of invalidity of Claims 1 through 20; however, my opinion that Claims 1 through 20 are not new is not limited to these specific grounds, and indeed, it is my opinion that Claims 1 through 20 would have been trivial or predictable combinations of

known features in light of the general knowledge of a person of ordinary skill in the art at the time of the alleged invention in the 916 Patent.

10. The subsequent sections of this declaration first provide my qualifications and experience and then describe details of my analyses and observations.

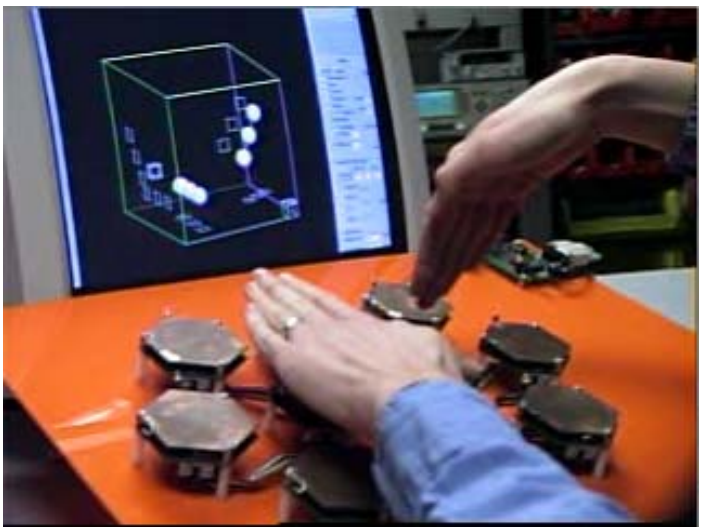
III. QUALIFICATIONS AND EXPERIENCE

A. Education and Work Experience

11. I am a tenured Associate Professor, jointly appointed in the departments of Electrical Engineering, and Computer Science and Engineering, at the University of Washington in Seattle. In 2013, the Paul G. Allen Family Foundation named me an Allen Distinguished Investigator. I am the Theme Leader for Low Power Sensing and Computing in the Intel Science and Technology Center for Pervasive Computing. I am the Thrust Leader for Communications and Interface in the National Science Foundation-funded Engineering Research Center for Sensorimotor Neural Engineering.

12. I received Ph.D. and M.S. degrees from the Massachusetts Institute of Technology in 1999 and 1995, respectively. I received an M.A. in Physics from the University of Cambridge in 1997 (originally conferred as a B.A. in 1993). I received a B.A. in Computer Science and Philosophy from Williams College in 1991. The core focus of my Ph.D. research at MIT was capacitive sensing of an

object (e.g., a human hand) relative to sensing electrodes, based on measurements of changes of the electric fields at the sensing electrodes that are caused by the object. My dissertation describes much of the research I performed at MIT. It covers techniques for sensing and interpretation of capacitance measurements, in order to infer geometrical information about human hands, for computer input applications. The dissertation includes hardware and signal processing techniques for making the measurements (the issue in the present case), techniques for inferring geometrical information from the measurements, and applications of these techniques.



Tracking two hands with the capacitive sensing device nicknamed "School of Fish," which I designed as part of my PhD research at MIT

13. My MIT dissertation covers several related projects and hardware systems. Around 1994, my MIT colleagues and I learned that several species of

fish sense their environments by making electric field measurements, and so we named the various sensing hardware systems we developed "Fish" of one sort or another. The first sensing circuit board built by my group was called the "Fish sensor." With one transmit channel and four receivers, this first sensing circuit board used a conventional analog implementation of synchronous detection, meaning that it used analog multipliers to demodulate the signal. This hardware was the basis of several of our early publications, including the CHI 1995 paper (Applying electric field sensing to human-computer interfaces, Thomas G Zimmerman, Joshua R Smith, Joseph A Paradiso, David Allport, Neil Gershenfeld, CHI '95 Proceedings of the SIGCHI conference on Human factors in computing systems, pp 280-287, ACM Press/Addison-Wesley Publishing Co. 1995), the 1996 IBM Systems Journal paper (Field mice: Extracting hand geometry from electric field measurements, Joshua R. Smith, IBM Systems Journal 35 (3-4), 587-608), and the 1998 Computer Graphics and Applications paper (Electric field sensing for graphical interfaces, J Smith, T White, C Dodge, J Paradiso, N Gershenfeld, D Allport, IEEE Computer Graphics and Applications, 18 (3), 54-60, May/June 1998). The 1995-1996 publications arose from my master's thesis research at MIT, which was completed in August 1995. The CHI 1995 paper mentions the use of

spread spectrum techniques, although the idea was not explored in detail in that paper.

14. When I became a Ph.D. student in September of 1995, I took a break from electric field sensing to work on a side project: the use of spread spectrum techniques for digital watermarking. The term digital watermarking means embedding a message (such as a copyright notice) in a picture by making many small (and thus imperceptible) modifications to a large number of the pixels. I took what was at the time a new view of digital watermarking by treating it as equivalent to the problem of communicating through a noisy channel: the pre-existing image pixels were the noise, and the small modifications were the signal. The challenge in digital watermarking was that the signal amplitude had to be much less than the noise amplitude for the modifications to be imperceptible. I had learned from our early work at MIT on capacitive sensing that modulation techniques could allow one to overcome any amount of noise, if sufficient signal energy can be collected. In all cases (ordinary radio communication, digital watermarking, and capacitive sensing) noise can be overcome by using modulation techniques, which allow large amounts of signal energy to be collected, thus improving signal to noise ratio. The large signal energy can be spread over time or

Shenzhen Huiding Tech. Co., Ltd. - Exhibit 1006

over frequency; different modulation schemes spread the signal energy in different ways.

15. I ended up presenting a paper ("Modulation and Information Hiding in Images") on my research on digital watermarking at the first workshop on Information Hiding, held at the Isaac Newton Institute for Mathematical Sciences in Cambridge, England, 1996. It also became Chapter 9 of my MIT dissertation in 1999.

16. After completing the digital watermarking paper (which became Chapter 9), I returned to electric field sensing (which is another term for capacitive sensing), and spent the next two years or so of my Ph.D. thesis research time designing and building the capacitive sensing device I named "School of Fish." This device was a network of intelligent electrodes, each of which included a microcontroller, and each of which could function as either a transmitter or receiver of electric fields. The School of Fish generates and detects electric fields in order to measure the capacitance between each pair of electrodes. In particular, it can detect changes in measured capacitance values caused by fingers or other body parts. Once I had finished the School of Fish, I started working on algorithms for interpreting the signals. At the same time, I started a new, small exploratory hardware project, to see whether the spread spectrum techniques I had

Shenzhen Huiding Tech. Co., Ltd. - Exhibit 1006

used in the digital watermarking research could be used for electric field sensing. There was a call for papers for a special issue of the IEEE Journal on Selected Areas in Communication ("JSAC") on Software Defined Radio. I thought that this idea, if it turned out to work, would fit well into this special issue.

17. My advisor allowed me to hire an undergraduate, Chris Salthouse (now a professor of electrical engineering at U. Mass Amherst) to help with this project. We implemented a system with 4 transmit electrodes, 1 receive electrode, 1 analog front end, and one analog to digital converter. We programmed a microcontroller (a PIC 16C741) to apply 4 distinct coded waveforms (each a different phase of a maximum length LFSR) to four of its General Purpose IO (GPIO) pins (configured as outputs). The technique did turn out to work well; it was published in the IEEE JSAC as intended, and became Chapter 8 of my thesis. I then designed an improved version of the prototype hardware from the paper and Chapter 8, which I called the LazyFish. The LazyFish had 4 transmit and 2 receive channels, and by default was configured for narrowband operation (with a resonant transmitter). However, as I explain in Chapter 8 of my dissertation, "By short-circuiting the inductor and removing the capacitor that comprise the tuned transmit, the LazyFish hardware can easily be used to implement CDMA sensing." The LazyFish was described in Chapter 2 of Smith, as well as Appendix A of Smith.

There is also a photo of the LazyFish hardware (with 4 transmit and 2 receive channels) in the IEEE JSAC article about CDMA sensing. The JSAC article also contains a photo of the apparatus actually used to perform the CDM experiments; which does not have resonant transmitters.

18. One application I explored in the course of my Ph.D. thesis at MIT was the use of capacitive sensing for automobile airbag safety. The technology I developed at MIT uses mutual capacitance measurements to detect out-of-position occupants and suppress airbag firing when a dangerous body pose is detected. This MIT capacitive sensing technology for automobile airbags was licensed by NEC, now Elesys/Honda, and I believe was incorporated in every Honda car for many years starting around 2000. The MIT capacitive sensing technology for automobile airbags was also incorporated into 4.5 million cars manufactured by General Motors.

19. After finishing my Ph.D. at MIT in 1999, I was hired to start a hardware research lab for a small software company called the Escher Group. When I joined, the company was privately held, with no outside investors other than the founders; while I was there a portion of the company was sold to a private equity firm, and now it is publicly traded on the London Stock Exchange. The Escher Group's primary product is postal counter automation software. This

software was used to perform a variety of counter transactions at post offices around the world, most notably the U.K. Post Office, where 40,000 workstations were deployed. In addition to mail-related transactions, in the U.K. the software is used to perform financial and other transactions, such as distribution of welfare benefits.

20. The U.K. Post Office postal counter automation system was one of the first large commercial deployments of touch screens. Because of the commercial importance of touch screens to Escher's business, I worked on developing new, improved forms of touch screen sensing technology. I developed a new type of mutual-capacitance-based touch screen that detected the user's finger before contact. This allows an interaction that present day touch screens do not support (but ordinary computer mice do): the user can hover the pointer over an icon/button/hyperlink without clicking; context sensitive help pops up, indicating what will happen if the link were to be clicked.

21. In the course of developing the new touch screen research prototypes, I designed and had fabricated several different Indium Tin Oxide (ITO, a transparent conductive material), electrodes, and the electronics to drive them.



Escher Group's prototype non-contact touch screen, which I designed and built while I was director of Escher Labs, showing raw sensor values



Escher Group's prototype non-contact touch screen, which I designed and built while I was director of Escher Labs, being used for icon selection

22. As a researcher and professor of electrical engineering, I have authored 102 technical journal and conference articles, and edited one book. My papers have won 9 best paper awards, including the Best Paper Award at the 2009

IEEE International Conference on RFID, for "A Capacitive Touch Interface for Passive RFID Tags." I won the best paper award again at the same conference in 2014. I won a Best Paper Award at the 2012 ACM Conference on Ubiquitous Computing ("Ubicomp 2012") for "An Ultra-Low- Power Human Body Motion Sensor Using Static Electric Field Sensing." In 2013, I won the Best Paper Award at the ACM SIGCOMM 2013, a very selective conference, for a paper that introduced a completely new way communicate. Another project of mine was given a 2015 "Best of What's New" award by Popular Science.

23. Additionally, I was named a Herchel Smith Scholar at the University of Cambridge, and recognized as a Motorola Fellow during my time at MIT.

24. I have 29 issued U.S. patents, many foreign patents, and numerous patents pending. These patents cover the following subject areas: capacitive sensing, electronic textile sensing, document security, Radio Frequency Identification sensing, power harvesting, wireless power transfer, and mail piece tracking.

25. My curriculum vitae, which provides a detailed summary of my education, work experience, publication, teaching history, etc. is attached to this declaration as Appendix A.

B. Compensation

26. I am compensated for the services I provide to Shenzhen Huiding Technology Co., Ltd. in connection with its IPR petitions on the 916 Patent and three other patents by Synaptics. The compensation is not contingent upon my performance, the outcome of this *inter partes* review or any other proceedings, or any issues involved in or related to this *inter partes* review or any other proceedings.

C. Documents and Other Materials Relied Upon

27. The documents on which I rely for the opinions expressed in this declaration are documents and materials identified in this declaration, including the 916 Patent, patents related to the 916 Patent, the prosecution history for the 916 Patent and other patents related to the 916 Patent, the prior art references and information discussed in this declaration, including the references attached as exhibits of the IPR Petition for the 916 Patent: Synaptics 916 Patent (Ex. 1004), Synaptics 7,868, 874 U.S. Patent Family Tree including the 916 Patent (Ex. 1005), Umeda (Ex. 1007), Inoue (Ex. 1008), Lohbihler (Ex. 1009), the Prasad 1998 Article (Ex. 1010), Jaeger (Ex. 1011), 1965 article entitled "Touch display—a novel input/output device for computers" by E. A. Johnson in Electronics Letters, Volume 1, Issue 8, p. 219 – 220 (Oct. 1965) (Appendix AA), David Allport, Earl Rennison, and Lisa Strausfeld, "Issues of Gestural Navigation in Abstract

Information Space" in CHI'95 Mosaic of Creativity, May 1995 (Appendix BB), Joshua Reynolds Smith, Toward Electric Field Tomography, MIT Master of Science Thesis in 1995 (Appendix CC), U.S. Patent No. 5,914,701 to Neil Gersheneld, Thomas Zimmerman, and David Allport of MIT Media Lab (Appendix DD), Paul Michael Yarin, Toward the Distributed Visualization of Usage History, MIT Master of Science Thesis in 1999 (Degree not awarded) (Appendix EE), Paul H. Dietz and Darren Leigh at Mitsubishi Electric Research Laboratories (Cambridge, MA) "Diamond Touch: A Multi-User Touch Technology") in UIST '01 Proceedings of the 14th annual ACM symposium on User interface software and technology, p. 219-226, ACM New York (2001) (Appendix FF), Joshua Reynolds Smith article entitled "Code-Division Multiplexing of a Sensor Channel: A Software Implementation" IEEE Journal on Selected Areas in Communications, vol. 17, No. 4, pp. 725-731, Apr. 1999 (Appendix GG), Robert C. Dixon: Spread Spectrum Systems, 2nd Edition, John Wiley & Sons 1984 (Appendix HH), Marvin K. Simon, Jim K. Omura, and Robert A. Scholtz: Spread Spectrum Communications Handbook, Electronic Edition, McGraw-Hill, Inc. 2002 and 1994 (Appendix II), co-authored by me along with Zimmerman, et al. an ACM SIGHCHI article entitled "Applying Electric Field Sensing to Human-Computer Interfaces," Thomas G Zimmerman, Joshua R Smith,

Joseph A Paradiso, David Allport, Neil Gershenfeld, CHI '95 Proceedings of the SIGCHI conference on Human factors in computing systems, pp 280-287, ACM Press/Addison-Wesley Publishing Co. (Appendix JJ), U.S. Patent No. 4,698,461 to Robert D. Meadows, Philip T. Krein, and Bruce Murdock ("Meadows") (Appendix KK), Joshua Reynolds Smith, Electric Field Imaging, MIT doctoral dissertation in 1999 ("Smith") (Appendix LL), Qingxin Chen et al., Multicarrier CDMA with Adaptive Frequency Hopping for Mobile Radio Systems, IEEE Journal on Selected Areas in Communications, vol. 14, no. 9, Dec. 1996 ("Chen") (Appendix MM), Low-density parity check codes over GF(q), MC Davey, DJC Mackay, IEEE Communications letters, Vol 2, No 6, pp 165-167, 1998 (Appendix NN), U.S. Patent No. 5,565,658 to George E. Gerpheide and Michael D. Layton ("Gerpheide") (Appendix OO), and any other references specifically identified in this declaration, in their entirety, even if only portions of these documents are discussed here in an exemplary fashion.

IV. STATEMENT OF LEGAL PRINCIPLES

A. Claim Construction

28. It is my understanding that, when construing claim terms of an unexpired patent, a claim subject to *inter partes* review receives the broadest reasonable interpretation (BRI) in light of the specification of the patent in which it appears.

B. Anticipation

29. It is my understanding that in order for a patent claim to be valid, the claimed invention must be novel. If each and every element of a claim is disclosed in a single prior art reference, then the claimed invention is not new, is anticipated, and the claimed invention is not patentable according to pre-AIA 35 U.S.C. § 102 effective before March 16, 2013. In order for an invention in a claim to be anticipated under pre-AIA 35 U.S.C. § 102, all of the elements and limitations of the claim must be disclosed in a single prior reference, arranged as in the claim. A claim is anticipated only if each and every element as set forth in the claim is found, either expressly or inherently described, in a single prior art reference. In order for a reference to inherently disclose a claim limitation, that claim limitation must necessarily be present in the reference.

C. Obviousness

30. It is my understanding that obviousness under pre-AIA 35 U.S.C. § 103 effective before March 16, 2013 is a basis for invalidity. I understand that where a prior art reference does not disclose all of the limitations of a given patent claim, that patent claim is invalid if the differences between the claimed subject matter and the prior art reference are such that the claimed subject matter as a whole would have been obvious at the time the invention was made to a person having ordinary skill in the relevant art. Obviousness can be based on a single

prior art reference or a combination of references that either expressly or inherently disclose all limitations of the claimed invention. In an obviousness analysis, it is not necessary to find precise teachings in the prior art directed to the specific subject matter claimed because inferences and creative steps that a person of ordinary skill in the art would employ can be taken into account.

V. LEVEL OF ORDINARY SKILL IN THE ART

31. I understand that the claims and specification of a patent must be read and construed through the eyes of a person of ordinary skill in the art at the time of the priority date of the claims. It has been explained to me by counsel that to determine the appropriate level of a person having ordinary skill in the art, the following factors may be considered: (a) the types of problems encountered by those working in the field and prior art solutions thereto; (b) the sophistication of the technology in question, and the rapidity with which innovations occur in the field; (c) the educational level of active workers in the field; and (d) the educational level of the inventor.

32. The "Background" section of the 916 Patent describes a "touchpad sensor" as one "common type" of sensor that responds to a stimulus on a sensing region from a finger or a stylus that creates "a capacitive, inductive or other electrical effect upon a carrier signal applied to the sensing region that can be

detected and correlated to the position or proximity of the stimulus with respect to the sensing region." Ex 1004 at 1:27-36. The 916 Patent cites U.S. Pat. No. 5,880,411 as "[o]ne example of a touchpad-type position sensor that is based on capacitive sensing technologies." *Id.* at 1:39-42. The "Background" section further describes that "[w]hile touchpad-type sensors have been in use for several years, engineers continue to seek design alternatives that reduce costs and/or improve sensor performance." *Id.* at 1:43-45. Moreover, "reducing the effects of noise generated by display screens, power sources, radio frequency interference and/or other sources outside of the sensor" is identified as a problem receiving significant attention at the time. *Id.* at 45-51. The 916 Patent recognizes the desire to have a device for "quickly, effectively and efficiently detecting a position-based attribute of an object in the presence of noise." *Id.* at 1:52-54.

33. To solve this problem and to address some perceived issues in the existing art, the 916 Patent discloses applying "spread spectrum techniques" "within a position sensor such as a touchpad to improve noise immunity and/or to provide performance enhancements." *Id.* at 2:49-52. The 916 Patent states that the disclosed technology can increase the effective power of the applied signals and maintain a uniform minimum signal-to-noise ratio (SNR) for each useful signal channel by (1) using "[c]ode division multiplexing (CDM) to create two or more

distinct modulation signals that are applied to sensing electrode(s)" and (2) "selecting digital codes to produce frequency-domain signals that avoid known sources of noise." *Id*. at 2:49-3:2.

34. In light of the disclosed technology in the 916 Patent, a person of ordinary skill in the art for the 916 Patent would need education or work experience in capacitive sensing. Because the 916 Patent is focused on applying "spread spectrum techniques" "within a position sensor", (*id.* at 2:49-3:2), a person of ordinary skill in the art would require some knowledge and experience with spread spectrum techniques used in wireless communications.

35. Based on the above considerations and factors, it is my opinion that a person having ordinary skill in the art should have a Master of Science or equivalent degree in media arts and sciences, electrical engineering, computer engineering, or computer science and engineering, or alternatively a Bachelor of Science or equivalent degree in media arts and sciences, electrical engineering, computer engineering, or computer science and engineering, with at least 5 years of experience in a technical field related to sensor technologies and communications theories. This description is approximate and additional educational experience could make up for less work experience and vice versa.

VI. TECHNOLOGY BACKGROUND OF THE 916 PATENT

36. The 916 Patent describes and claims capacitive position sensors and capacitive sensing touch screens and touch sensor in combinations of several features. Claim 1 of the 916 Patent, for example, recites method of detecting a position of an input object with respect to a touch-sensitive region, where the method comprising the steps of: (1) simultaneously applying a first one of a plurality of distinct modulation signals to a first electrode and a second one of the plurality of distinct modulation signals to a second electrode to obtain resultant signals that are electrically affected by the position of the input object, (2) wherein each of the plurality of distinct modulation signals is based on a different one of a plurality of distinct digital codes; (3) demodulating the resultant signals using the plurality of distinct digital codes to thereby discriminate electrical effects produced by the input object; and (4) determining the position of the input object from the electrical effects.. Claim 1 is representative of the three independent claims, Claims 1, 13 and 20, of the 916 Patent because Claims 13 and 20 more or less mimic the combination in Claim 1: Claim 13 recites a controller for a position sensor and Claim 20 recites an input device, both having a combination of features that are similar as recited in Claim 1.

37. As I explain below based on printed publications, all of those and other features in Claims 1, 13, 20 and their dependent claims of the 916 Patent were well known and published long before November of 2005, the earliest priority date of the 916 Patent. In addition, as I explain in my detailed analyses in this declaration, the combinations of those well-known features as claimed in Claims 1-20 were known, predictable and/or obvious combinations and were documented in printed publications.

38. In this section of my declaration, I provide an overview of some basic capacitive touch sensing techniques and features that were understood and documented in the published technical literature and in published patent documents before the filing of the 916 Patent, and that would be within the knowledge of a person of ordinary skill in the art for the technology areas related to the 916 Patent, such as a capacitive position sensor for capacitive sensing, application of spread spectrum signaling in wireless communications to capacitive touch sensing applications, circuitry that transmits and receives distinct signals based on distinct digital codes, modulating a carrier signal based on the distinct digital codes, adjustment of a frequency of a distinct signal based on observed noise in the resultant signal, and others. I use certain references, both patents and non-patent literature, as examples to illustrate the background knowledge of a person of

Shenzhen Huiding Tech. Co., Ltd. - Exhibit 1006

ordinary skill in the art, but the knowledge of a person of ordinary skill in the art at the time regarding the claimed features would not have been limited to these specific references.

A. A capacitive position sensor and a controller for a capacitive position sensor

39. It is well known in the touch screen industry that a capacitive position sensor and a controller for a capacitive position sensor were developed, published and commercialized well before 2005, which I understand to be the earliest priority date of the 916 Patent. One of the early publications describing a touchscreen with a capacitive position sensor and a controller for a capacitive sensor was the 1965 article entitled "Touch display—a novel input/output device for computers" by E. A. Johnson in *Electronics Letters*, Volume 1, Issue 8, p. 219 – 220 (Oct. 1965). Appendix AA. MicroTouch Systems, a Massachusetts touch sensing technology company founded in the early-1980s, commercialized surface capacitive technology and was acquired as part of the 3M Touch Systems formed in 2001.

40. In the 1990s, MIT Media Lab researchers, including me, published a number of innovations on capacitive position sensors using the human body to capacitively couple transmitters and receivers. In May of 1995, David Allport, Earl Rennison, and Lisa Strausfeld published an article entitled "Issues of Gestural Navigation in Abstract Information Space" in the proceedings of CHI'95

describing a user interface that uses capacitive-type electric field sensing to interpret natural hand gestures as motion controllers. Appendix BB. In August of 1995, I was an MIT student and published my Master's Thesis describing capacitive type electric field sensors for determining three dimensional location and shape information. Appendix CC. In November of 1998, I defended my Ph.D. Dissertation on using capacitive sensors as a new physical user interface for performing machine electric field perception. Appendix LL. MIT published my Ph.D. Dissertation in March of 1999. MIT obtained U.S. Patent No. 5,914,701 (Gersheneld) filed Aug. 6, 1997 and issued Jun. 22, 1999 for a capacitive type electric field sensor that uses a pseudorandom codes to produce spread spectrum signals for increasing noise immunity and allowing multiple transmitters. Appendix DD. I also collaborated with Paul Michael Yarin who integrated my LazyFish capacitive sensors into an LED display device for capacitive position sensing which was published as a part of his Master's Thesis in August 1999. Appendix EE at 20-24.

41. In 2001, Mitsubishi developed a capacitive multi-touch sensing screen to detect touches from multiple users and published an article on the technology entitled "DiamondTouch: a multi-user touch technology" by Paul Dietz and Darren Leigh at Mitsubishi Electric Research Laboratories (Cambridge, MA) in *UIST '01*

Shenzhen Huiding Tech. Co., Ltd. - Exhibit 1006

Proceedings of the 14th annual ACM symposium on User interface software and technology, p. 219-226, ACM New York (2001). Appendix FF. The capacitive multi-touch sensing screen developed by Mitsubishi is a natural extension and application of the capacitive sensors in my 1998 MIT Ph.D. dissertation and those in MIT's U.S. Patent No. 5,914,701 (Appendix DD).

42. The 916 Patent acknowledges that "[p]osition sensors are commonly used as input devices for computers, personal digital assistants (PDAs), media players, video game players, consumer electronics, wireless phones, payphones, point-of-sale terminals, automatic teller machines, kiosks and the like." Ex. 1004 at 1:23-27. "One common type of sensor used in such applications is the touchpad sensor" which detects a "stimulus" from a user's finger or a stylus "near a sensing region of the sensor" that "creates a capacitive, inductive or other electrical effect upon a carrier signal applied to the sensing region of the sensor that can be detected and correlated to the position or proximity of the stimulus with respect to the sensing region." *Id*. at 1:27-36. The 916 Patent identifies Synaptics' prior U.S. Patent No. 5,880,411 based on a filing on Jun. 8, 1992 as an example of a prior art "touchpad-type position sensor that is based on capacitive sensing technologies". *Id*. at 1:39-42. In the DETAILED DESCRIPTION section, the 916 Patent describes the sensing region 101 of FIGS. 1A-B as "any capacitive, resistive,

inductive or other type of sensor that is capable of detecting the position, proximity and/or other position-based attribute of a finger, stylus or other object 121" including "various sensors produced by Synaptics Inc. of Santa Clara, Calif., which appropriately detect a one dimensional, two dimensional or multi-dimensional position of an object 121 using capacitive or inductive coupling, although many other sensing regions 101 could be used in a wide array of alternate embodiments." *Id*. at 5:10-19. Thus, the capacitive sensing touch devices or touch screens in the 916 Patent combine preexisting capacitive touch sensing techniques and spread spectrum signal modulation. The "touch" in such capacitive sensing devices that separate the object from the underlying sensing electrodes by a dielectric material in Umeda, Inoue and Jaeger and in the 916 Patent means the object is in close proximity to the sensing electrodes without directly contacting a sensing electrode and the "touch" is between the object and the dielectric material that covers the underlying sensing electrodes. Such capacitive touch sensors mostly do not measure physical contact; rather, the capacitance induced by the proximity between the object and the electrodes behind the top dielectric material or cover is detected. Some devices are designed to sense the motion of the object at large distances from the sensing electrodes separated by air, a dielectric material, and may be referred to as "non-contact" capacitive sensing. Therefore, the term

"touchpad", "touch screen" or "touch capacitive sensing" is a misnomer in the context of the subject matter of capacitive touch sensing in the 916 Patent because there is no direct touch or direct contact between the object and a sensing electrode.

B. Capacitive touch sensing circuitry that transmits and receives distinct signals based on distinct digital codes

43. The 916 Patent discloses capacitive touch sensing circuitry that transmits and receives distinct signals based on distinct digital codes uses signal modulation and demodulation based on spread spectrum techniques, including code division multiplexing (CDM) and code division multiple access (CDMA) in radio communications. *Id*. at 4:47-5:9. The spread spectrum techniques and CDM/CDMA implementations in radio communications were long used many years before 2005. For example, the CDMAone standard used as one of the standard in 2G wireless digital communications was released in the standard IS-95A in 1995. The benefits of CDM and other spread spectrum techniques as illustrated in FIG. 3 of the 916 Patent were always known as part of the inherent benefits of spread spectrum techniques and caused creation of various spread spectrum implementations such as CDM and CDMA techniques. For example, IEEE Communications Surveys in 1998 published an article by Prasad titled "CDMA evolution: toward wideband CDMA." Ex. 1010 at Abstract. The Prasad 1998 Article provides a history of CDMA with the origin of CDMA going back to

1949 in "military field and navigation systems." *Id.* at left col. lines 41-44 at p. 3 - right col. last line. A chronological history of CDMA from its 1949 origin to narrowband CDMA in 1978 to wideband CDMA in 1995 can be seen in Table 1 at page 3 of Prasad. In addition, the Prasad 1998 Article describes the technical concepts of CDMA including the ability to reject a narrow band interference signal: "Cross-correlating the code signal with a narrowband signal will spread the power of the narrowband signal thereby reducing the interfering power in the information bandwidth." *Id*. at left col. lines 6-12 at p. 5; Fig. 3.

44. In fact, Fig. 3 of the Prasad 1998 Article and FIG. 3 of the 916 Patent are effectively the same illustration explaining the well-known concept of interference or noise rejection using CDMA. The top figure in FIG. 3 of the Prasad 1998 Article, reproduced below, shows modulated signal 's' with an interference signal 'i' on the left panel. *Id*. at left col. lines 12-14 at p. 5. On the right panel in FIG. 3 of the Prasad 1998 Article, the demodulated signal is "despread" while the interference signal is spread, making the interference signal appear as background noise. In comparison, the bottom figure in Fig. 3 of the 916 Patent, also reproduced below, shows the modulated signal 304, the wide band noise signal 308, and the narrowband noise signal 306 on the left panel. Ex. 1004 at 10:34-43. On the right panel in Fig. 3 of the 916 Patent, the demodulated signal 352 is despread and all

other signals 354 including the wideband noise signal 308 and narrow band noise signal 306 are spread across a wider band to improve the signal to noise ratio. *Id.* at 10:51-11:6. In fact, the cited prior art Jaeger (Ex. 1011) expressly describes this application of PN codes, Walsh codes or a list of other suitable codes to touch sensing in achieving wideband spectra of the resultant signals, as well known in the spread spectrum technology. Specifically, Jaeger in its FIG. 1B illustrates this aspect and explains that, "[i]n this invention, a DSSS signal is generated by encoding the system information bits with one or more wideband codes, which occupy a given bandwidth. (These codes are called Direct Sequence (DS) codes.) By generating a signal in this way, the resulting signal bandwidth is the sum of the information bandwidth plus the bandwidth of the DS code. FIGS. 1A–1B are simple illustrations of DSSS signals and how they spread in the time and frequency domain." Ex. 1011 at 4:38-45. FIG. 1B in Jaeger is reproduced below for convenience.

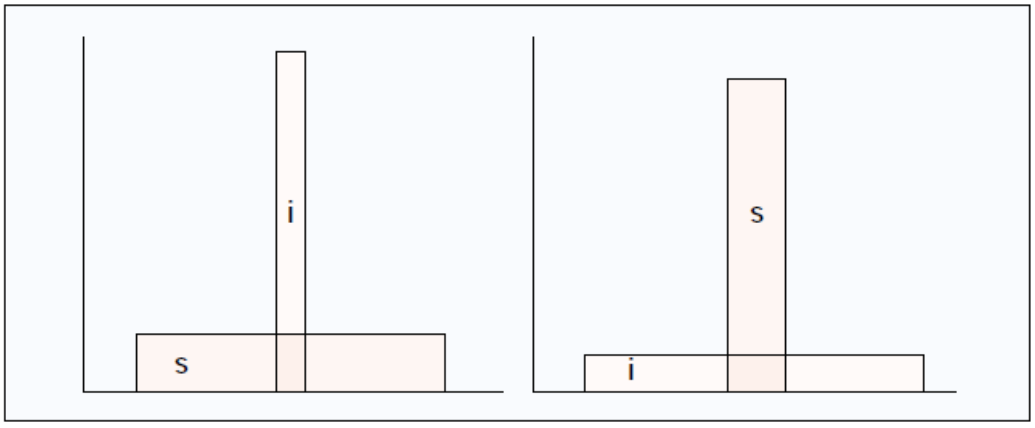


Figure 3. *Interference rejection.*

FIG. 3 in Prasad 1998 Article

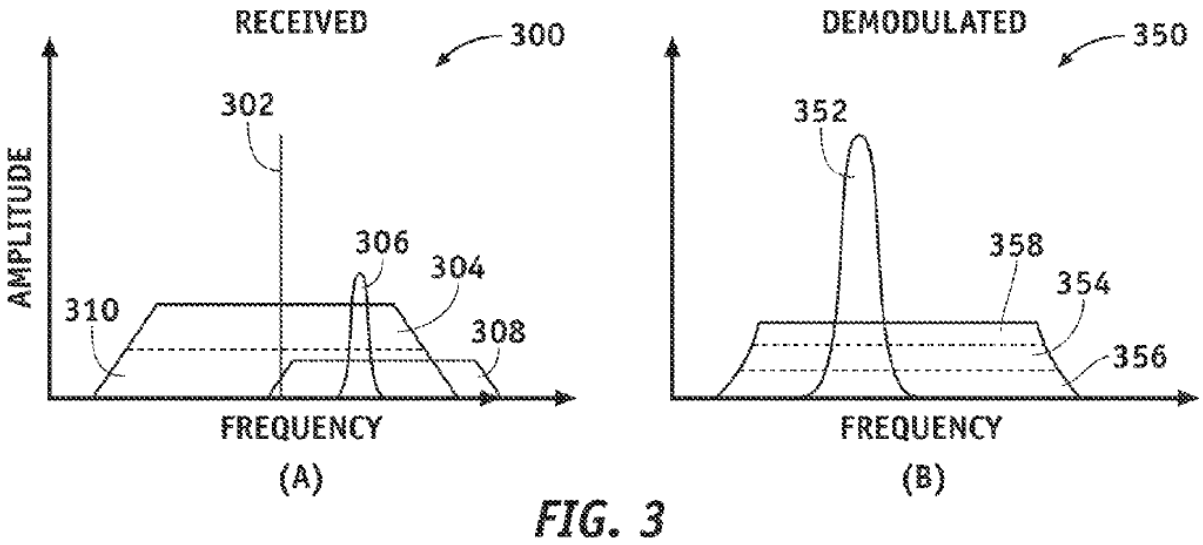


FIG. 3

FIG. 3 of the 916 Patent

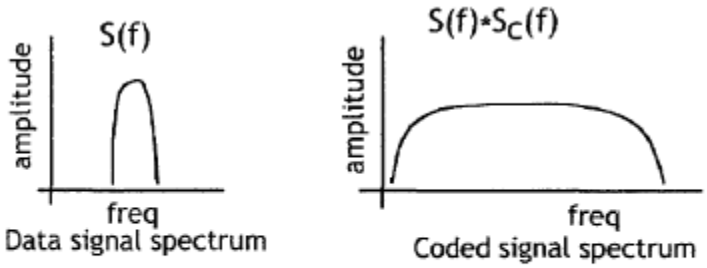


FIG. 1B

FIG. 1B in Jaeger

45. The above feature of the spread spectrum technology as described in the Prasad 1998 Article had been adopted into capacitive touch sensing around the same time where researchers published articles on the application of spread spectrum techniques, including signal modulation based on distinct digital codes for capacitive sensing of a user interaction. For example, while working on my doctoral dissertation as a Ph.D. student at MIT in the late 1990's, I used spread spectrum techniques using distinct digital codes for signal modulation for capacitive touch sensing based on impedance variations in an array of capacitor sensors and, more generally, sensing via electric fielding imaging. In 1999, I published my MIT dissertation entitled "*Electric Field Imaging*" which is cited in this Petition (Smith, Appendix LL). I also published an article entitled "Code-Division Multiplexing of a Sensor Channel: A Software Implementation" IEEE Journal; pp. 725-731; vol. 17, No. 4 in Apr. 1999 (Appendix GG).

46. Others in the touch sensing sector also recognized the need for orthogonal signals in touch sensing and developed commercial products before 2005. For example, in late 1990's and early 2000's, the above-mentioned Mitsubishi group with Paul H. Dietz and Darren Leigh built a multi-user touch screen based on code-division multiplexing of a sensor channel known as "DiamondTouch" and published their work in U.S. Patent No. 6,498,590 entitled "Multi-User Touch Surface" and issued in Dec. 2002 based on a filing in May of 2001 and published their work in "Diamond Touch: A Multi-User Touch Technology") in 2001 (Appendix FF).

47. The aforementioned publications were just some of the examples of pre-2005 publications showing that the capacitive touch sensing circuitry that transmits and receives distinct signals based on distinct digital codes of the 916 Patent was well known in the touch screen industry before 2005.

C. Frequency modulation (FM), phase modulation (PM) or amplitude modulation (AM) of a carrier signal according to distinct digital codes

48. Each of the FM, PM and AM modulations in the 916 Patent (6:16-39) were known signal modulation techniques long before 2005. In spread spectrum schemes, such as CDMA, it is well-known that the carrier signal is modulated based on distinct digital codes using one of standard modulation schemes including

frequency modulation, phase modulation, or amplitude modulation. See, for example, a book written by Robert C. Dixon entitled Spread Spectrum Systems, 2nd Edition, published by John Wiley & Sons in 1984 (Appendix HH) at 16. The type of modulation depends on the modulation scheme used, as explained by Dixon, "[d]irect sequence modulation, as mentioned in Chapter 1, is just exactly that-modulation of a carrier by a code sequence. In the general case, the format may be AM (pulse), FM, or any other amplitude- or angle-modulation form. Very common, however, is 180° biphase phase-shift keying." ***Id.*** Moreover, Dixon teaches that direct sequence spread spectrum systems (DSSS) are not only the most widely used spread spectrum system but also more exactly known as "directly carrier-modulated, code sequence modulation). ***Id.*** at 15, 109. Thus, any system that relies on DSSS expressly modulates a carrier signal.

2.1 DIRECT SEQUENCE SYSTEMS

Direct sequence (or, to be more exact, directly carrier-modulated, code sequence modulation) systems are the best known and most widely used spread spectrum systems. This is because of their relative simplicity from the standpoint that they do not require a high-speed, fast-settling frequency synthesizer. The JPL ranging technique described in Golomb et al. *Digital Communications with Space Applications*[219] and used in various space applications is a direct sequence approach. Today, direct sequence modulation is being used for communication systems and test systems, and even laboratory test equipment capable of producing a choice of a number of code sequences or operating modes is available. It is reasonable to expect that direct sequence modulation will become a familiar form of modulation in many areas in the foreseeable future. Even now, commercial applications of such systems are being contemplated.

15

Dixon (Appendix HH) at p. 15.

49. In implementing spread spectrum modulation, biphase phase-shift keying was a common technique well known before 2005. The Prasad 1998 article, for example, describes a number of standard phase shift keying based modulation techniques: "For the code modulation various modulation techniques can be used, but usually some form of phase shift keying (PSK) like binary phase shift keying (BPSK), differential binary phase shift keying (D-BPSK), quadrature phase shift keying (QPSK), or minimum shift keying (MSK) is employed." Prasad (Ex. 1010) at right col. lines 44-49 at p. 5. Similarly, a book written by Marvin K. Simon, Jim K. Omura, and Robert A. Scholtz entitled Spread Spectrum Communications Handbook, Electronic Edition, published by McGraw-Hill, Inc. in 2002 and 1994

(Appendix II) describes phase and frequency modulation techniques including BPSK and multiple frequency-shift keyed (MFSK) modulations. Appendix II at 12-13.

50. The 916 Patent specification discloses using conventional modulation designs for its modulator 107 for the disclosed modulation operations according to distinct digital codes. For example, referring to Figs. 1A and 1B, "[m]odulator 107 may be implemented using any conventional digital and/or analog circuitry, or may be partially or entirely implemented with software logic executing within controller 102 or the like." Ex. 1004 at 6:22-26. Based on my review of the 916 Patent, it is my opinion that the 916 Patent does not disclosure any new or different modulation techniques other than conventional modulation techniques that were well known before the earlier filing date of the 916 Patent.

D. Specific distinct digital codes in spread spectrum modulation: Walsh-Hadamard codes, Gold codes, Kasami codes, and Barker codes

51. It was well-known before 2005 that in spread spectrum schemes, such as CDMA, the distinct digital codes can be generated using one of standard code generation schemes including the Walsh-Hadamard codes, Gold codes, Kasami codes, and Barker codes. For example, Lohbihler describes a touch-screen device for wirelessly communicating signals for identification and accurate location

determination. Ex. 1009 at Abstract. Lohbihler uses spread spectrum techniques, such as direct sequence spread spectrum (DSSS), frequency hopping spread spectrum (FHSS), THSS, and pseudo-noise (PN) coding schemes, or combinations to perform the wireless communication. *Id.* at Abstract, ¶¶ 0014-0015, 0018-0019, 0025, 0027, 0059, 0061, 0087, 0103, 0108-0123, 0125-0128, 0134, 0136-0139. Lohbihler recognized that numerous well-known distinct codes available, including M-sequences, Walsh codes, Barker codes, Gold codes and Kasami codes. *Id.* at 0060. Similarly, Prasad specifically identifies Gold codes, Kasami codes, Reed-Solomon codes, and Walsh codes as different well-known standard spreading codes. *See* Prasad (Ex. 1010) left col. lines 12-25 at p. 22, right col. lines 28-32 at p. 22, left col. lines 10-13 at p. 14, right col. lines 37-59 at p. 14, left col. line 63 at p. 15 - left col. line 10, at p. 16, right col. lines 6-8 at p. 25, left col. lines 1-51 at p. 26, Table 2 at p. 10, Fig. 16a at p. 11, Fig. 16b at p. 12, Fig. 17 at p. 13, Fig. 18 at p. 14, Fig. 19 at p. 15, Table 4 at p. 18, Table 5 at p. 24, Fig. 38 at p. 25, Fig. 39 at p. 25, and Table 6 at p. 26.

E. Adjustment of a frequency of a distinct signal based on observed noise in the resultant signal

52. Adjustment of the carrier frequency in a communication signal to achieve better immunity to signal noise was well known for implementing spread spectrum techniques in radio communications and was extensively published

before 2005. One common way of adjusting a carrier frequency was frequency hopping, i.e., changing the carrier frequency amongst various carrier frequency channels. Adaptive frequency hopping is a form of frequency hopping in which a system measures performance at a given frequency or frequencies (e.g. measured noise or signal-to-noise ratio) and changes the frequency based on the measured performance. Adaptive frequency hopping is roughly analogous to changing channels or frequencies on a two-way radio system when there is too much static (noise) on the current channel. In 1995, more than a decade before the filing of the 916 Patent, I co-authored with Zimmerman, et al. in an CHI 1995 article entitled "Applying Electric Field Sensing to Human-Computer Interfaces", Thomas G Zimmerman, Joshua R Smith, Joseph A Paradiso, David Allport, Neil Gershenfeld, CHI '95 Proceedings of the SIGCHI conference on Human factors in computing systems, pp 280-287, ACM Press/Addison-Wesley Publishing Co. 1995 [Zimmerman-Smith article. Appendix JJ] The Zimmerman-Smith article describes "[a] non-contact sensor based on the interaction of a person with electric fields" [*Id.* at Abstract] and described "capacitance detection schemes" such as "synchronous detection" and "frequency modulation chirps (as used in radar), frequency hopping, and code modulation (e.g., spread spectrum)." *Id.* at p. 3 and Figure 3.

53. As another example, Chen's 1996 article entitled "Multicarrier CDMA with Adaptive Frequency Hopping for Mobile Radio Systems" describes adjusting the carrier frequencies of distinct signals in CDMA in form of adaptive frequency hopping scheme that enhances the signal to noise ratio, reduces channel fading and achieve multiple-access interference (MAI) reduction. Chen (Appendix MM), Abstract, 1:38-56, 11:59-12:56.

54. In fact, the interference from noise and other spurious signals was a well-known problem that had been addressed by adaptively adjusting the signal frequency in touchscreens well before 2005. For example, Gerpheide, a 1996 U.S. Patent based on a filing in 1994 (Appendix OO), refers to a 1987 U.S. Patent No. 4,698,461 issued to Meadows ("Meadows") (Appendix KK) for teaching a frequency adjustment to reduce interference: "the Meadows '461 panel also includes circuitry for automatically shifting the frequency of panel scanning signals away from spectra of spurious signals, such as those developed by cathode-ray tube transformers, which may be present in the environment. The panel seeks to avoid interference from the spurious signals, which could happen if the frequency of scanning was nearly equal to that of the spurious signals. A microcontroller determines whether the scanning frequency should be shifted by monitoring the rate at which adjustments are required in nulling of the touch

currents,." Gerpheide (Appendix OO) at 1:58-2:7. Gerpheide teaches another way of adaptively avoiding spurious signals by using a "reference frequency generator 16 [that] attempts to automatically select and generate a reference frequency which is not coherent with the most undesirable frequency of spurious signals" to "substantially eliminate[] interference even though its frequency is likely to be initially unknown and may even change during operation." *Id.* at 4:14-19. Gerpheide uses a "frequency select function [that] is activated approximately every 32 data points by the interference evaluation function 106" and "[t]he frequency having the lowest interference measure entry [in a table of frequency measurements] is selected as the new current frequency." *Id.* at 9:21-33. This adjustment of the reference frequency signal in Gerpheide is made based on the measured interference, i.e., the observed noise condition of the received signal. *Id*. 8:20-9:64 and FIG. 7.

55. In light of the above technology background, I turn to the details of the 916 Patent and my analyses and opinions of selected prior art references and its claims 1-20.

VII. OVERVIEW OF THE 916 PATENT

56. The 916 Patent describes methods, systems and devices for detecting a position-based attribute of a finger, stylus or other object with a touchpad or other sensor. Ex. 1004, Abstract.

57. The "Background" section of the 916 Patent describes a "touchpad sensor" as one "common type" of sensor that responds to a stimulus on a sensing region from a finger or a stylus that creates "a capacitive, inductive or other electrical effect upon a carrier signal applied to the sensing region that can be detected and correlated to the position or proximity of the stimulus with respect to the sensing region." Ex 1004 at 1:27-36. U.S. Pat. No. 5,880,411 is identified as "[o]ne example of a touchpad-type position sensor that is based on capacitive sensing technologies." *Id.* at 1:39-42. The "Background" section further describes that "[w]hile touchpad-type sensors have been in use for several years, engineers continue to seek design alternatives that reduce costs and/or improve sensor performance." Ex. 1004 at 1:43-45. Moreover, "reducing the effects of noise generated by display screens, power sources, radio frequency interference and/or other sources outside of the sensor" is identified as a problem receiving significant attention at the time. *Id.* at 1:45-51. Thus, it is desirable to provide systems and

methods for quickly, effectively and efficiently detecting a position-based attribute of an object in the presence of noise. *Id*., 1:43-54.

58. To solve this problem and to address some perceived issues in the existing art, the 916 Patent discloses applying "spread spectrum techniques" "within a position sensor such as a touchpad to improve noise immunity and/or to provide performance enhancements." *Id.* at 2:49-52. The 916 Patent states that the disclosed technology can increase the effective power of the applied signals and maintain a uniform minimum signal-to-noise ratio (SNR) for each useful signal channel by (1) using "[c]ode division multiplexing (CDM) to create two or more distinct modulation signals that are applied to sensing electrode(s)" and (2) "selecting digital codes to produce frequency-domain signals that avoid known sources of noise." *Id*. at 2:49-3:2.

59. Specifically, the 916 Patent describes that "principles of code gain can be readily exploited to improve the performance of sensor 100" so that the "gain of each modulation signal 110 applied to one or more transmit electrodes 112 increases with the length of the code." *Id*. at 4:60-67. To generate the modulation signal 110, the 916 Patent relies on "the use of conventional code generation techniques" because "combinatorial variations of the digital codes with well-known spectral and correlation properties are relatively easy to generate." *Id*. at

4:67-5:3. The 916 Patent describes a list of the conventional code generation techniques "suitable for use with CDM" that includes "shift register sequences such as Walsh-Hadamard codes, m-sequences, Gold codes, Kasami codes, Barker codes, delay line multiple tap sequences, and/or the like." *Id*. at 5:52-57.

According to embodiments in 916 Patent, "spread spectrum techniques can be applied within a position sensor such as a touchpad to improve noise immunity and/or to provide performance enhancements." *Id*. at 2:49-52. This appears to be the purported novelty of the 916 Patent. "By applying spread spectrum concepts commonly associated with radio communications to sensor 100, however, numerous benefits can be realized." *Id*. at 4:50-53. Thus, the 916 Patent relies on the prior art spread spectrum techniques to modulate capacitive sensor signals using prior art capacitive sensing techniques without any newly improved spread spectrum techniques or any newly improved capacitive sensing techniques.

60. The sensor in the 916 Patent includes a touch-sensitive region made up of any number of electrodes arranged in an appropriate fashion to detect user input. Modulation signals for one or more electrodes are produced as a function of any number of distinct discrete digital codes, which are substantially orthogonal to each other. The modulation signals are applied to at least one of the plurality of electrodes to obtain a resultant signal that is electrically affected by the position of

the object. The resultant signal is demodulated using the plurality of distinct digital codes to discriminate electrical effects produced by the object. The position-based attribute of the object is then determined with respect to the plurality of electrodes from the electrical effects. *Id*. at 1:60-2:11; Figs. 1A, 1B, 5 and associated text.

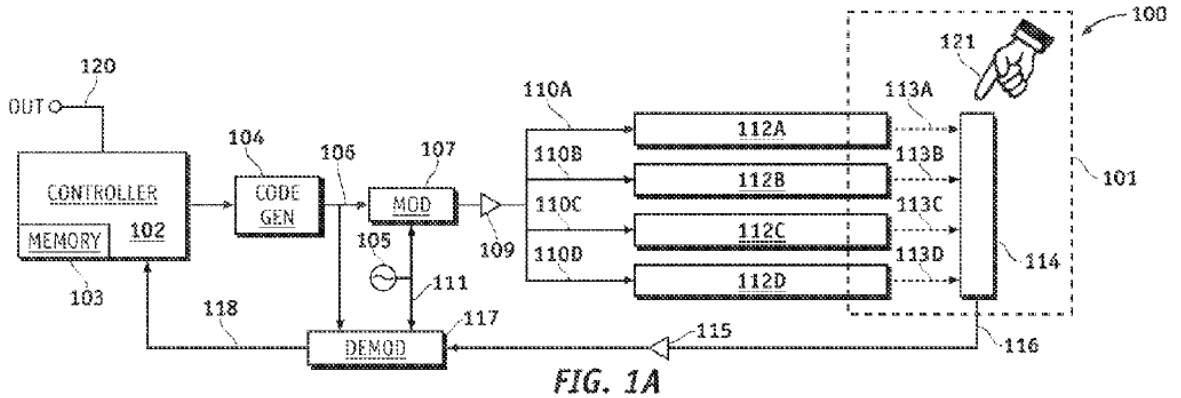


FIG. 1A

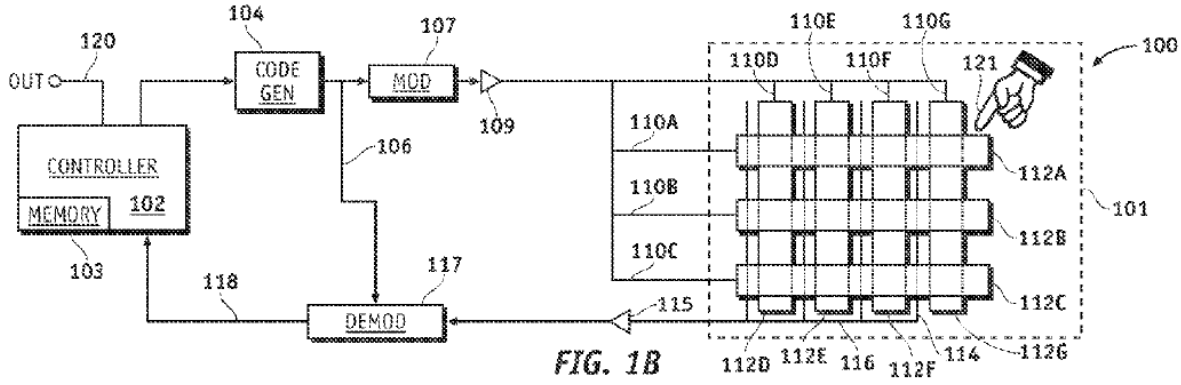


FIG. 1B

The 916 Patent: Sensing Devices in FIGS. 1A and 1B

61. Claims 1 through 20 are the only claims in the 916 Patent. As shown in this Declaration, all of the features and the combinations in Claims 1 through 20 were disclosed by prior publications and were known prior to the 916 Patent's

Shenzhen Huiding Tech. Co., Ltd. - Exhibit 1006

earliest priority date which should be no earlier than November 15, 2005. I cite and rely on references dated before November 15, 2005.

VIII. IDENTIFICATION OF THE PRIOR ART AND SUMMARY OF OPINIONS

62. As explained below, it is my opinion that the prior art references cited in this declaration disclose all technical features and the claimed combinations in Claims 1 through 20 of the 916 Patent. Therefore, neither the features in each claim nor the combination in each claim are new.

63. Based on my review of the prior art references, claims 1-20 of the 916 Patent contain nothing new over Umeda in view of Inoue and Jaeger.

IX. CLAIM CONSTRUCTION

64. In conducting my analyses of the 916 Patent, I have applied the legal understandings I set out below regarding claim constructions consistent with the "broadest reasonable interpretation" (BRI) standard described above, and offer them only for this *Inter Partes* Review. It is my understanding that the BRI claim constructions do not necessarily reflect the appropriate claim constructions to be used in a litigation proceeding in a district court or an investigation proceeding before the International Trade Commission, where a different standard applies.

65. I understand that, under the BRI claim construction, claim terms are given their ordinary and customary meaning as would be understood by one of

ordinary skill in the art in the context of the entire disclosure. An inventor may rebut that presumption by providing a definition of the term in the specification with reasonable clarity, deliberateness, and precision. In the absence of such a definition, limitations are not to be read from the specification into the claims.

66. The proposed BRI claim construction for terms in Claims 1 through 20 is plain and ordinary meaning of each term in light of the 916 Patent specification outside of few exceptions where a specific definition has been expressly or implicitly provided in the 916 Patent specification.

67. For example, the proposed claim construction for "distinct digital codes" is its plain and ordinary meaning - digital codes that are different from one another or each other - in light of the specification, e.g. Ex. 1004 at 8:2-12. *See also id.* at 5:42-6:15.

68. However, the term "mathematically independent" in Claims 9, 13, 15 and 16 is not found in the specification of the 916 Patent. The closest disclosure related to this term states that "[t]he term 'substantially orthogonal' in the context of the distinct digital codes is intended to convey that the distinct codes need not be perfectly orthogonal from each other in the *mathematical* sense, so long as the distinct codes are able to produce meaningful *independent* results" (Ex. 1004 at

5:66-6:5, emphasis added). Thus, the proposed claim construction for this term is "substantially orthogonal" under the BRI in light of the 916 Patent specification.

X. CLAIMS 1-20 IN THE 916 PATENT CONTAIN NOTHING NEW

69. In this declaration, I provide my analyses on one invalidity ground based on one prior art combination proposed by Petitioner Shenzhen Huiding Technology Co. ,Ltd.: Umeda (Ex. 1007), Inoue (Ex. 1008), and Jaeger (Ex. 1011) for Ground 1 that teaches applying the spectrum spread modulation to capacitive touch sensing.

A. GROUND 1: CLAIMS 1-20 CONTAIN NOTHING NEW OVER THE COMBINATION OF UMEDA, INOUE AND JAEGER

70. In my opinion, Claims 1 through 20 are disclosed by Umeda (Ex. 1007), Inoue (Ex. 1008), and Jaeger (Ex. 1011) as predictable or trivial combinations of known features. Umeda, Inoue and Jaeger were all published or filed in the U.S. more than one year before the earliest claimed filing date for the 916 Patent. These references collectively teach all features of, and the claimed combinations of those features of, Claims 1 through 20.

71. As I will discuss in detail below, Umeda, Inoue and Jaeger provide related teachings in the same technical field as the 916 Patent, i.e., the touch sensing field, and specifically about capacitive touching sensing. It is my opinion that the teachings in Umeda, Inoue and Jaeger provide reasons and motivations for

a person of ordinary skill in the art to combine them as claimed in claims 1-20 under pre-AIA 35 U.S.C. § 103(a).

1. Overview of Umeda

72. Umeda is a U.S. patent No. 7,084,645 issued on August 1, 2006 from an application filed on November 10, 2004, which is more than 1 year prior to the earliest priority date of the 916 Patent.

73. The capacitive position sensor in Umeda uses rows and columns of capacitive sensing electrodes to determine a position-based attribute of at least one input object, such as a finger or hand, proximate a surface of the capacitive position sensor. Umeda (Ex. 1007) at 1:19-25; 2:65-3:31; 7:44-50; Fig. 3. Umeda identifies two objectives of Umeda's sensor: (1) "provide a capacitance detection circuit and method in which the influence of external disturbance noise can be suppressed to improve the S/N [signal to noise] ratio so that very small capacitances Cs and capacitance changes ΔCs of the capacitances Cs at intersections (sensor devices) between rows lines and column lines can be detected at a sufficiently sensitivity level", and (2) "also to provide a fingerprint sensor using the above-described capacitance detecting circuit and method." *Id.* at 2:65-3:7; see also 1:8-10 and 7:29-43. Umeda identifies these two objectives to address the known issues in prior art capacitance detection circuits, and fingerprint sensors

that implement the prior art capacitance detection circuits. *Id.* at 1:11-2:61; 2:65-3:31. In fact, in the background section, Umeda identifies a number of well-known issues with prior art capacitive position sensors that must be addressed. *Id.* at 2:17-24. For example, Umeda recognizes that "a capacitance detection circuit used in, for example, a fingerprint sensor, [must] have high sensitivity since capacitance changes are very small." *Id.* at 1:56-58. Umeda also recognizes that such capacitive detection circuit "must have resistance to noise (including high-frequency noise) transmitted from a human body or noise from other circuitry" and must not be "vulnerable to crosstalk noise between adjacent row lines or column lines." *Id.* at 58-64. These well-known issues identified by Umeda are very similar to those disclosed in the 916 Patent. Thus, the technical issues that the 916 patent described were not newly identified by the 916 patent but rather were old issues previously recognized and addressed before the filing date of the 916 Patent by others such as Umeda.

74. Umeda also identifies weaknesses in a prior art capacitive position sensor that drives a single column line electrode at a time to detect capacitance changes at the intersections between that single column line and a plurality of row lines. *Id.* at 2:17-24. Umeda recognizes that driving a single column line at a time results in a very small capacitance change at each intersection of the single column

line and the row lines, and measuring the resultant small capacitance change is greatly affected by noise and interference. *Id.* at 2:17-61. Specifically, the signal-to-noise ratio ("SNR") of this prior art sensor is reduced due to external disturbance noise that cannot be removed. *Id.* at 2:17-61. To enhance the SNR of the measured capacitance change, Umeda teaches capacitive position sensing circuitry that uses a column-line driver to simultaneously drive *multiple* column lines of electrodes. *Id.* at 2:65-3:31. Umeda also teaches using a code generator to generate distinct pseudorandom (e.g., M-series PN codes) or orthogonal codes (e.g., Walsh orthogonal codes) and applying drive signals modulated using the distinct pseudorandom or orthogonal codes to the multiple column lines simultaneously. *Id.* at 2:65-3:52; 4:52-67. Driving multiple column lines simultaneously using the drive signal modulated with the distinct pseudorandom or orthogonal codes enhances the SNR properties because the effects of noise and interference on the measured capacitance change are reduced. *Id.* at 2:65-3:7; 3:32-52.

75. In my opinion, the capacitance detecting circuit in Umeda can be applied to any device for detecting a position of an input object, such as a finger because the capacitance detecting circuit in Umeda measures the capacitance change at each intersection of the column and row lines of electrodes. *Id.* at 1:19-25; 7:44-50; Figs. 2A, 2B, and 3.

FIG. 2A

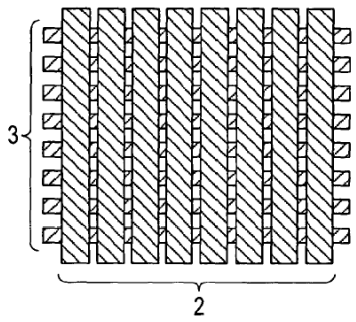


FIG. 3

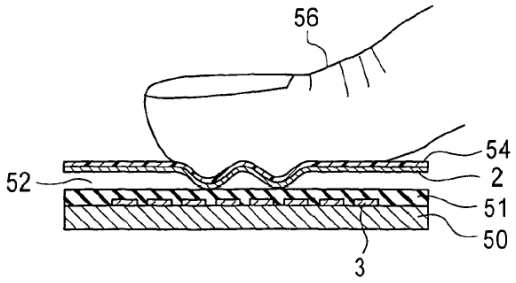
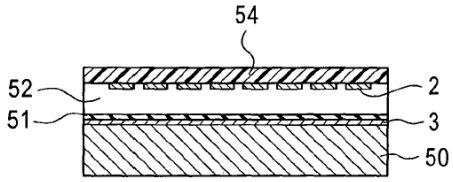


FIG. 2B



76. The location of each intersection (of column and row lines) where the corresponding capacitance change is measured can be used to detect the position of the input object, such as a finger. *Id.* For example, Umeda describes a fingerprint sensing implementation of the capacitance detecting circuit that detects the positions and spatial distributions of the "ridges" of a fingerprint by measuring the changes in the capacitances at the column-row intersections. *Id.*. The positions of the intersections associated with the measured capacitance changes caused by the ridges pressing against the top surface of the cover film 54 shown in FIGS. 2B and 3 are used to map out all the ridges and thus to identify the shape/image of the fingerprint formed by finger ridge locations. *Id.* at 1:8-25; 2:65-3:7; 3:62-4:3; 5:35-40; 27:53-59. In my opinion, the capacitance detecting circuitry in Umeda that detects the touch locations of the fingerprint's ridges with respect to the column-

row intersections (*id.*) is a high precision example of detecting the touch locations of different portions of the finger. Thus, in my opinion, a person of ordinary skill in the art would understand that the capacitance detecting circuit in Umeda is not limited to a fingerprint sensor and can be used as a general touch location sensor to detect the position of an input object, such as a finger or stylus. *Id.* at 2:65-3:7; 3:66-4:2.

77. Indeed, because a fingerprint has fine spatial features and patterns, Umeda's device must provide a sufficiently high spatial sensing resolution via its 2-D array or matrix of sensor devices 55 in FIG. 4 to perform fingerprint detection. In general, fingerprint detection is a technical superset of detecting a touch of an object because fingerprint detection demands a higher location or spatial sensing resolution and requires multi-touch detection. The 916 Patent recognizes this by defining the term "position sensor" to include biometric authentication devices (e.g. fingerprint sensors) and other devices. Ex. 1003 at 3:11-18.

Multi-touch detection is required for fingerprint sensing because in fingerprint sensing, multiple finger ridges touch the sensor simultaneously, and the touch locations of these finger ridges must be correctly determined. Since fingerprint detection is a superset of touch location detection, fingerprint sensor circuitry can be used to track the location of a touch. In particular, the circuitry for

a capacitive fingerprint sensor can be used to track finger touch locations, but the opposite is not always true: capacitive touch screen sensing circuitry cannot always be used to perform fingerprint sensing. For example, a self-capacitance-based touch screen sensor that is only capable of accurately registering a single touch location (and not capable of multi-touch) could not be used effectively as a fingerprint sensor. This is the sense in which fingerprint sensing is a technical superset of touch location sensing. Therefore, Umeda's device is a high resolution position sensor capable of sensing locations and fine features of the ridges of a fingerprint, and thus Umeda's device is within the 916 Patent's definition of the term "position sensor," which includes biometric authentication devices (e.g. fingerprint sensors) and other devices. Ex. 1004 at 3:11-18.

2. Overview of Inoue

78. Inoue is a U.S. patent No. 5,831,600 issued on November 3, 1998, more than one year before the earliest priority date of the 811 Patent. According to the front page in Inoue, Inoue is assigned to the same company in Japan, Alps Electric Co. Ltd., that owns Umeda. Because they are owned by the same company, it is not surprising that Inoue and Umeda overlap with each other with respect to various technical teachings.

79. Like Umeda, Inoue teaches a capacitive sensing coordinate input device. Inoue (Ex. 1008) at front page; Abstract. Specifically, Inoue teaches a capacitive sensing coordinate input device, such as a tablet device that can detect the contact position of at least one input object, such as an input pen or a finger, on the tablet device. *Id.* at Abstract, 1:5-2:67; 4:10-5:24; Figs. 1, 4. Like Umeda, Inoue uses a matrix of capacitive sensing electrodes arranged along the X-axis and the Y-axis. *Id*. at 1:13-2:67 and Figs. 1, 2, 4. In fact, Inoue teaches detecting circuitry similar to the circuitry disclosed in Umeda used to detect the X-Y coordinates of the touch location of an input object, such as a finger or an input pen. The similarity of the capacitive sensing electrodes in Umeda and Inoue can be seen in FIG. 2A from Umeda (left figure) and FIG. 2 from Inoue (right figure) reproduced below.

FIG. 2A of Umeda

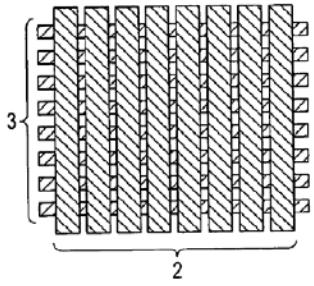
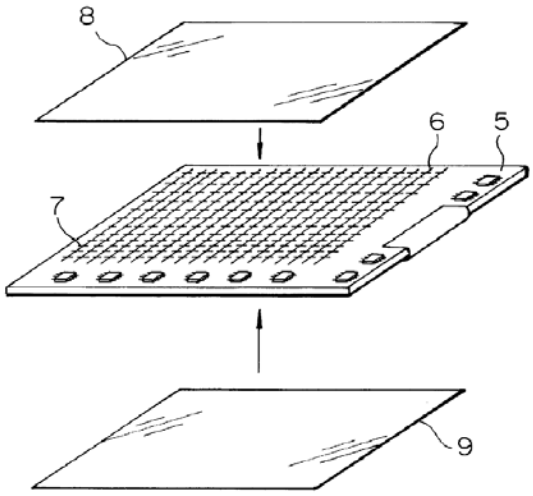


FIG. 2 of Inoue



80. Like Umeda, Inoue identifies in the Background section a known prior art touch-sensing coordinate input device, such as a tablet device that is adversely affected by external noise. *Id.* at 1:61-2:33. Specifically, Inoue teaches that the ability of the known prior art touch-sensing tablet device to detect the position of an input object, such as a finger touching the tablet device is degraded by the external noise. *Id.* For example, when the frequency of the external noise is close to the frequency of the scan signal driving the X electrodes, a frequency filter is not able to remove such noise, and thus the external noise that overlaps with the scan signal in frequency degrades the reliability of the touch position detection. *Id.* at 2:54-67. Inoue teaches a coordinate input device that minimizes the influence of the external noise by choosing the frequency of the scan signal to be at a frequency

of minimum external noise. *Id.* at 3:10-19. Specifically, Inoue teaches applying multiple scan signals of different frequencies to the X electrodes, measuring the external noise for each scan signal, and selecting the scan signal at the frequency with minimal external noise. *Id.* Thus, Inoue teaches selecting the scan signal frequency based on the measured noise level to minimize the influence of the noise and enhance the reliability of the touch position detection. *Id.* at 3:20-25.

3. Overview of Jaeger

81. Jaeger is a U.S. patent (No. 7,084,860) filed on July 25, 2002 and issued on August 1, 2006. Jaeger's filing date is more than three years before the earliest priority date of the 916 Patent.

82. In the same technical area for capacitive touch sensing as Umeda and Inoue, Jaeger teaches touch sensing input devices that can detect the contact position of an input object (such as an input pen or a finger) on a tablet based on various touch sensing techniques including capacitive touch sensing. Ex. 1011 at Abstract, 1:32-2:62, 5:10-6:27, 9:14-18:28 (the "Description of the preferred embodiment" section). Therefore, it is my opinion that the subject matter of Jaeger is closely related to the 916 Patent, because both of them relate to touch sensing technology. Specifically, Jaeger discloses that touch locations on its touch screen are determined by X-Y locator and data signal processing unit based on the

received signal strength (RSS) or amplitude of signals received by receiving sensors on the touch screen. *Id*. at 6:28-7:5, 7:39-57 and FIG. 4. Jaeger generates different signals based on distinct digital codes to distinguish different signal sources (e.g., touches by different touch devices) based on spread spectrum technology similar to Umeda.

4. Motivations and reasons exist to combine Umeda, Inoue, and Jaeger

a. Motivations and reasons exist to combine Umeda and Inoue

83. Umeda and Inoue provide related, contemporary teachings about the state of the art in sensor technology and data communication and demonstrate that the recited features and the claimed combinations in the claims of the 916 Patent cover technology that was already well-known to those of skill in the art. Umeda recognized the importance of having a capacitance detecting circuit with high sensitivity in a touch sensor to detect very small capacitance changes for fingerprint detection, for example. Umeda (Ex. 1007) at 1:56-64. Umeda also recognized that the capacitance detecting circuitry should be resistant to noise, including high frequency noise from a human body or other circuitry and crosstalk noise between columns and rows of electrodes. *Id.* In recognition of the above, Umeda teaches a capacitance detecting circuit and method for detecting very small

capacitances and capacitance changes that functions by suppressing external noise to improve the signal-to-noise ratio. *Id.* at 1:56-64 and 2:65-3:7.

84. Umeda teaches a capacitive position sensor that uses rows and columns of capacitive sensing electrodes to determine a position-based attribute of at least one input object, such as a finger or hand, near a surface of the capacitive position sensor. *Id.* at 1:19-25; 7:44-50; Fig. 3. Umeda teaches improving the signal-to-noise ratio (SNR) of the capacitive position sensor by simultaneously driving multiple column lines of the capacitive sensing electrodes using pseudorandom or orthogonal codes. *Id.* at 2:65-3:31. Like Umeda, Inoue teaches a capacitive sensing tablet device that determines the contact position of at least one input object, such as an input pen or a finger, on the tablet device and displays a cursor corresponding to the determined contact position on the display unit of the tablet device. Inoue (Ex. 1008) at Abstract, 1:5-2:67; 4:10-5:24; Figs. 1, 4. Like Umeda, Inoue uses a matrix of capacitive sensing electrodes arranged along the X-axis and the Y-axis. *Id.* at 1:29-2:15 and Figs. 1, 2, 4.

85. In my opinion, both Umeda and Inoue address similar problems as the 916 Patent, *e.g.* using channel sharing schemes to simultaneously transmit signals while enhancing the SNR properties. Thus, the combined teachings of Umeda and

Inoue show that Claims 1 through 20 of the 916 Patent do no more than articulating the use of known features in the art according to their known purposes.

86. It is my opinion that, in light of the teachings in Umeda and Inoue, a person of ordinary skill in the art would be guided by the teachings in Umeda and Inoue, and would be motivated to or have sufficient reasons, to combine teachings in Umeda and Inoue because they address the common technical issues of minimizing the influence of external noise on the ability to detect the position of the input object, such as a stylus or finger. In addition, a person of ordinary skill in the art would recognize the technical similarities between Umeda and Inoue. For example, both Umeda and Inoue teach capacitive touch sensing to determine the position of the touch location of an input object such as a finger. Umeda and Inoue share a common design for the 2-D matrix of transmit and receive electrodes arranged in X and Y axes to induce capacitances at their intersections. Both Umeda and Inoue transmit drive or scan signals to multiple transmit electrodes, and measure the resultant voltage signals at multiple receive electrodes. Both teach determining the position of the touch by the input object, such as a finger by measuring an electrical signal change at the intersections of the transmit and receive electrodes associated with a corresponding capacitance change at the intersections. As noted above, Umeda and Inoue are co-owned by the same

company Alps Electric Co. Ltd. and reflect the company's continued research and development efforts to reduce the influence of external noise to improve the reliability of detection in the company's capacitive touch sensing technology. This additional linkage between Umeda and Inoue within the capacitive touch sensing provides a further reason to a person of ordinary skill in the art to combine them.

87. Umeda and Inoue provide additional motivations or reasons to combine them. For example, Umeda recognized that an external disturbance noise source can affect the ability of the capacitance detecting circuitry to detect small capacitances with high sensitivity. Umeda at 1:56-64; 2:25-61. Specifically, Umeda observed that when the frequency of a noise source, such as the noise from the fluorescent lamp, is close to the sampling frequency of the capacitor detecting circuit, the SNR is reduced and the ability to accurately detect the position of the input object making the contact is degraded. Umeda at 2:35-61.

88. Similar to Umeda, Inoue recognized that a noise vector at a frequency close to the frequency of the scan signal will adversely affect the capacitance sensing of the location of an input finger or device over a tablet. Inoue at 2:54-67. Specifically, Inoue describes the noise problem in a conventional coordinate input device of FIG. 4 by stating that, "[i]n the known coordinate input device, when signal voltages are read from the tablet 51, external noise is superposed on the read

signal voltages. In this case, most of the external noise superposed on the signal voltages is removed by the first filter circuit 60 or a second filter circuit 66. However, when the external noise frequency is approximate to the frequency of the scan signal, the external noise cannot be removed by the first filter circuit 60 or the second filter circuit 66, and the signal voltages are input to the A/D 61 and the CPU 62 without removing the external noise from the signal voltages. For this reason, the external noise adversely affects detection of a coordinate position by the CPU 62, and the reliability of detection of the coordinate position is degraded." *Id*.

89. Because Umeda and Inoue, which are publications by the same company, recognized the same noise problem in capacitance sensing, a persons of ordinary skill in the art would have been motivated to combine them. Specifically, a person of ordinary skill in the art would have been motivated to combine the teachings of Umeda and Inoue to add the ability to adjust the frequency content of the scan signal to avoid the presence of noise and thus improve the ability to accurately detect the position of the input object touching the coordinate detecting tablet device. Inoue at 3:10-25.

b. Motivations and reasons exist to further combine Umeda and Inoue with Jaeger

90. As I discussed previously, Umeda discloses the use of distinct digital codes such as pseudorandom noise (PN) code or orthogonal code for driving electrodes of the capacitor sensors based on recognition of the use of PN codes in CDMA-based on multiplexing and demultiplexing for improving cellular communications. Ex. 1007 at 3:32-52 and 10:12-24.

91. Similar as Umeda, Jaeger also discloses using spread spectrum and CDMA techniques to transmit signals to the touch device termed "Spread Spectrum Touch Systems." Jaeger (Ex. 1011) at Abstract ("A touch sensing apparatus for receiving input from one or more touch stimulating devices [that] employs a direct sequence spread spectrum (DSSS) signal arrangement to transmit signals from the touch stimulating devices for identification and location determination."), 3:13-5:9 where CDMA is discussed in 4:46-59. Jaeger's touch sensing apparatus includes "a touch-sensing tablet (termed touch screen hereafter) [which] can be regarded as a touch screen, a digitizer, a writing panel, a modified mouse pad, or the like." *Id.* at 1:22-31. Therefore, it is my opinion that a person of ordinary skill in the art would be motivated to combine the teachings of Jaeger and Umeda, because both references are based on the common recognition of the

advantage of using distinct digital codes in capacitive touch sensing such as the codes used in CDMA.

92. Jaeger also discloses that using the spread spectrum technology for capacitive touch sensing has the benefits of (1) achieving improved SNR and (2) channelization with a plurality of different signal sources (e.g., different touch devices) to distinguish different signals in detection by using distinct digital codes for encoding signals. *Id.* at FIG. 1B; 4:30-5:9, 3:27-56, 6:22-27. This line of teaching for the benefits underlying the spread spectrum (SS) touch sensing technology in Jaeger is similar to the approach taught by Umeda of using distinctive digital codes such as PN or Walsh codes for capacitive touch sensing. Ex. 1007 at, e.g., 2:65-3:61. The techniques taught in Jaeger and Umeda are both aimed at (1) improving the S/N ratio and (2) detecting and distinguishing signals from different signal sources at intersections of column and row lines. *Id.* These common recognitions of the benefits of using distinct digital codes in touch sensing by both Jaeger and Umeda provide yet another reason, among many others, for a person of ordinary skill in the art to combine Jaeger and Umeda in designing a touch sensing device by using distinct digital codes in signal modulation for preforming the touch sensing measurements.

93. Indeed, these common techniques taught in Umeda and Jaeger were well known to a person of ordinary skill in the art at the time of the 916 patent's priority date, because of the pioneering work in applying spread spectrum and CDMA modulation to capacitive touch sensing done by the MIT Media Lab, as documented in various publications, including my IEEE publication and MIT doctoral dissertation in 1999 and further evidenced by Dietz publication from Mitsubishi Electric Research Laboratories in 2001.

94. In my view, the need in Jaeger for improved touch sensing SNR would lead a person of ordinary skill in the art to the frequency adjustment in reducing noise disclosed in Inoue. This provides one of reasons as to why a person of ordinary skill in the art would combine Umeda, Inoue and Jaeger when designing a capacitive touch sensing device based on distinct digital codes.

95. Umeda and Jaeger share additional common teachings. For example, Umeda discloses M-series PN codes and orthogonal Walsh codes as two examples of suitable distinct digital codes carried by column line voltage drive signals for the disclosed capacitive touch sensing operations. Ex. 1007 at 3:32-4:3. Jaeger, as part of its disclosure of using PN codes and other numerous suitable, well-known distinct digital codes for capacitive touch sensing, discloses more examples of suitable well-known codes in addition to the PN (M-sequence) codes and

orthogonal (Walsh) codes taught in Umeda: M-sequences, Barker codes, Walsh codes, Gold codes and Kasami codes. Ex. 1011 at 4:60-5:9. This commonality between Umeda and Jaeger provides another reason for a person of ordinary skill in the art to combine Jaeger with Umeda when selecting distinct digital codes for touch sensing purpose.

96. Umeda, Inoue and Jaeger also share the common teaching that signal modulation is used as part of the touch sensing operations of the touch sensing devices. Inoue discloses signal modulation in generating scan signals by using oscillation signals from a oscillation circuit and adjusting the frequencies of the scan signals to minimize the noise during the sensing operation. Ex. 1008 at FIG. 3 and related text. In Umeda and Jaeger, drive signals are generated based on distinct digital codes (e.g., PN codes, Walsh codes, or other proper codes). As I have previously explained in Section VI.C of this declaration, such signal modulation can be carried out by carrier modulation, either using a modulator or modulating circuit that receives and modulates a separate carrier signal, or using a circuit or chip powered by a DC voltage or current to perform directly carrier-modulated code sequence modulation to produce modulation signals or modulated carrier signals. The later approach is known as “direct sequence” systems.

97. Umeda describes this carrier modulation because it discloses amplitude and phase modulating a carrier signal according to the distinct digital code. In Umeda, when the PN code or orthogonal code value is 1, the amplitude of the column-line drive signal is set to a first voltage (high) during the first capacitance detection period; conversely, when the PN code or orthogonal code value is 0, the amplitude of the column-line drive signal is set to a second voltage (low) during the first capacitance detection period. Umeda at Abstract, 4:14-24, 7:21-28, 7:51-67, 8:53-9:3, 11:48-58, 12:4-21, 13:3-13, 13:21-27, 14:32-47, 15:1-19, 16:42-49, 16:62-17:5, 17:14-20, 21:9-23, Figs. 8 and 22. The column line drive signals are amplitude modulated by the corresponding first and second voltages.

98. Umeda also teaches phase modulating based on the bit values of the PN codes or Walsh codes. For example, the column-line drive pulse signals shown in rows (d), (e), and (f) (and zoomed out versions (h), (i), and (j)) of Figs. 8 and 22 are in-phase with each other (i.e., the same as each other) when their bit values are the same, and are out-of-phase (i.e., the opposite as each other) when their bit values are different. Umeda (Ex. 1007) at Figs. 8 and 22. Therefore, these column-line drive pulse signals are phase modulated by the distinct digital codes.

99. In addition, Umeda discloses modulating a carrier signal based on the principles of multiplexing/demultiplexing in code division multiple access

(CDMA). Ex. 1007 at 10:20-24. CDMA is one type of direct sequence spread spectrum (DSSS) technique which is more accurately known as "directly carrier-modulated, code sequence modulation." Dixon (Appendix HH) at p. 15. According to Dixon, directly carrier-modulated, code sequence modulation requires modulating a carrier signal, and Umeda indeed modulates the carrier signals using the distinct digital codes, such as pseudorandom noise (PN) codes, as I discussed in the previous paragraphs. Both alternatives resemble the disclosures of the 811 Patent, which teaches that digital codes may be modulated onto a carrier signal 111 generated by an oscillator or other signal generator 105 in some embodiments (e.g. Fig. 1(A)), while "the carrier signal 111 may therefore be eliminated and/or conceptualized as a direct current (DC) signal in various alternate embodiments," such as the embodiment of Fig. 1(B) which omits the signal generator. Ex. 1004, 6:26-27, 6:34-39.

100. Like Umeda, Jaeger discloses carrier modulation for touch screen devices using different modulation methods, including narrowband carrier modulation systems and wideband carrier modulation systems (where "a DSSS signal is generated by encoding the system information bits with one or more wideband codes"). Ex. 1011 at 2:16-62, 3:13-57, 4:30-5:9, and 16:37-59. Specifically, Jaeger discloses directly carrier-modulated, code sequence

modulation by Direct Sequence Spread Spectrum (DSSS) signals as one of the time-domain spreading methods. *Id.* at 4:30-35 ("In this invention, SS signals structures are based on time-domain spreading methods only. These methods include Direct Sequence Spread Spectrum (DSSS) signals, Time Hopping Spread Spectrum (THSS) signals, Hybrid methods of DSSS and THSS, and the like.").

101. This sharing of the same carrier modulation approach based on distinct digital codes for touch sensing in both Umeda and Jaeger provides yet another reason for a person of ordinary skill in the art to combine Umeda and Jaeger when designing a touch sensing system or device based on distinct digital codes.

102. In sum, it is my opinion that the teachings in and the relationships among Umeda, Inoue and Jaeger provide reasons or motivations for a person of ordinary skill in the art to combine these three references. In the following sections, I will discuss other specific reasons or motivations that would cause a person of ordinary skill in the art to combine Umeda, Inoue and Jaeger when analyzing these references in connection with claim limitations of Claims 1 through 20 of the 916 Patent.

5. Claim 1-20 Are Unpatentable Over Umeda, Inoue and Jaeger

103. It is my opinion that the combination of Umeda, Inoue and Jaeger teaches or suggests all the limitations of claims 1-20 and each of these claims contains nothing new over the combined teaching by Umeda, Inoue and Jaeger.

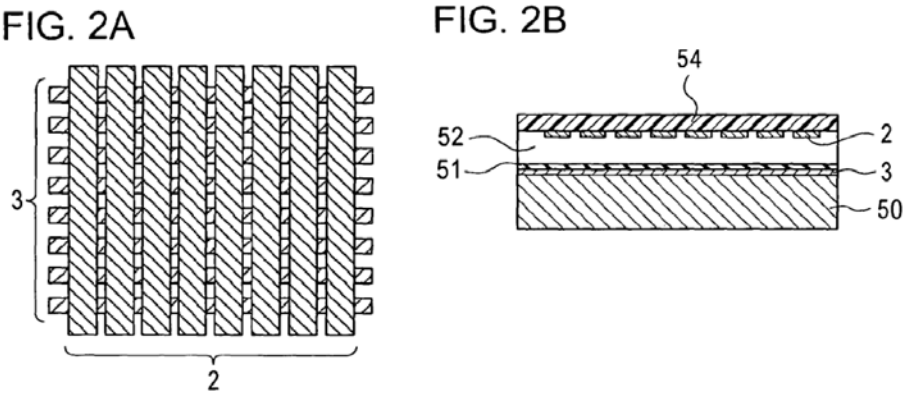
a. Claim 1

104. **Claim Element 1.Preamble:** A method of detecting a position of an input object with respect to a touch-sensitive region, comprising the steps of:

While I have been informed by counsel that the preamble of a claim is not ordinarily a limitation, to the extent that the preamble of this claim is a limitation, it is my opinion that the preamble is disclosed by the combination of Umeda, Inoue and Jaeger. As I mentioned in the TECHNOLOGY BACKGROUND section, the 916 Patent describes using preexisting capacitive sensors. For example, the 916 Patent describes in the specification that "with reference to FIGS. 1A-B, sensing region 101 is any capacitive, resistive, inductive or other type of sensor that is capable of detecting the position, proximity and/or other position-based attribute of a finger, stylus or other object 121" including "the various sensors produced by Synaptics Inc. of Santa Clara, Calif., which appropriately detect a one dimensional, two dimensional or multi-dimensional position of an object 121 using capacitive or inductive coupling, although many other sensing regions 101 could be used in a

wide array of alternate embodiments." 916 Patent at 5:10-19. In addition, the 916 Patent is not limited to just capacitive sensors and describes that "[o]ther types of sensing regions 101 capable of detecting position or proximity include sensors based upon acoustic, optical, or electromagnetic properties (e.g. radio frequency, infrared, ultraviolet or the like), and/or any other effects" can be used. *Id.* at 5:20-23.

105. The lattice arrangement of the capacitive sensing layers shown in FIGS. 2A and 2B of Umeda are similar to the overlapping electrodes shown in FIG. 5 of the 916 Patent. For comparison, I reproduce FIGS. 2A and 2B of Umeda (top left and right) and FIG. 5 of the 916 Patent (bottom) below.



FIGS. 2A and 2B of Umeda

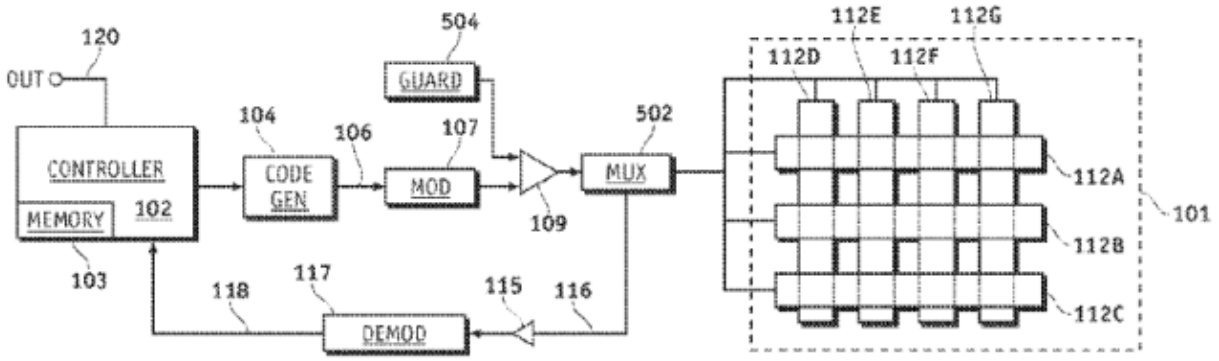


FIG. 5

FIG. 5 of 916 Patent

106. Umeda and Inoue describe a capacitive position sensor that includes transmitter and receiver electrodes arranged in a matrix of column and row lines and a controller that uses a microcontroller much the same as those described in the preamble of claim 1 and supported in the specification of the 916 Patent.

107. Specifically, Umeda discloses a capacitance detecting circuit implemented in a tablet device having a sensor area defined by a sensor unit that includes row and column lines of capacitive electrodes. Umeda at 7:25-28, Figs. 1, 2A, 2B, 4. As shown in FIGS. 1, 2A and 2B, the sensor unit 4 includes a protective film 54 over the column lines 2 and row lines 3 of capacitive electrodes for receiving a touch from the finger.

FIG. 1

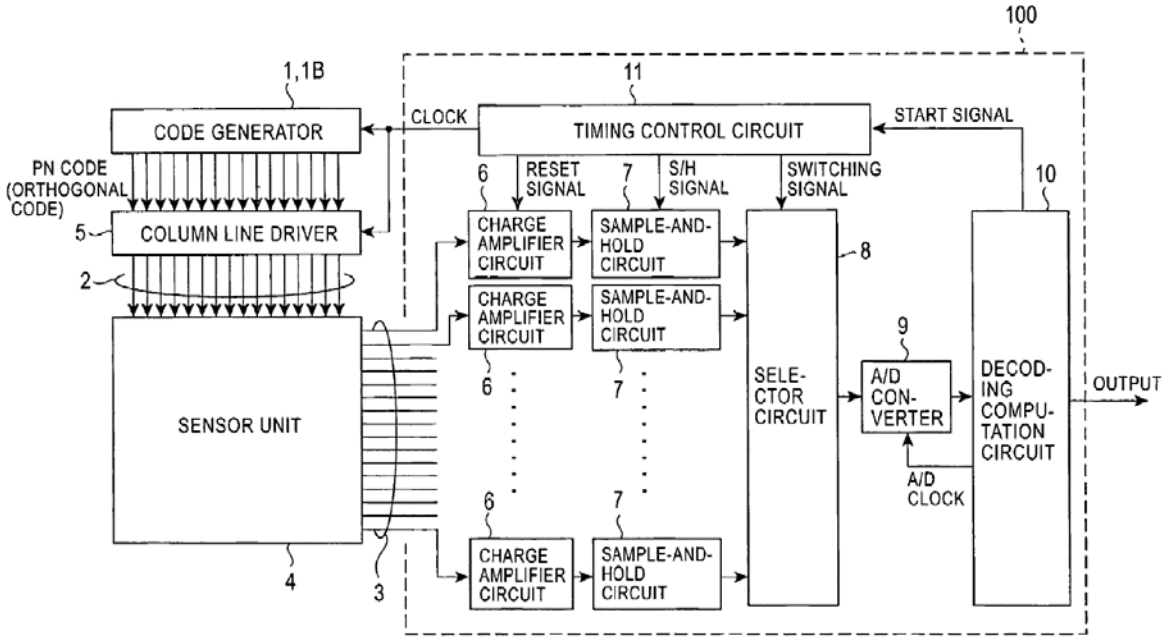


FIG. 1 of Umeda

FIG. 2A

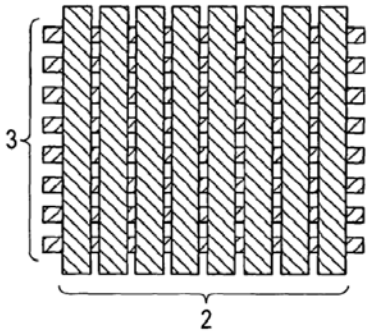
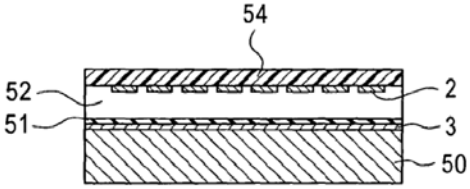


FIG. 2B



FIGS. 2A and 2B of Umeda

108. The capacitive detecting circuit in Umeda detects small capacitance changes at the intersections of the row and column lines to determine a position of an input object, such as a finger touching the sensor unit. Umeda at 1:8-9; 2:65-3:7. For example, when a user's finger touches the film 54 of the sensor unit 4, the

"ridges" of the user's fingerprint selectively cause changes to the intervals between the row lines and the column lines that correspond to the positions of the ridges, which in turn induce a capacitance change at each of the column-row intersections. *Id.* at 1:19-25; 7:44-50; Fig. 3.

FIG. 3

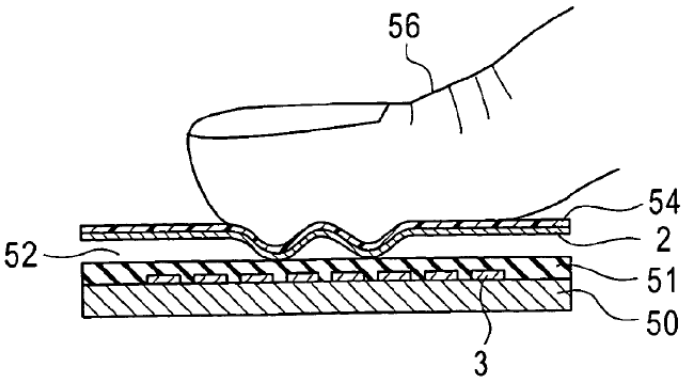


FIG. 3 of Umeda

109. Detecting the capacitance changes at the column-row intersections allows Umeda to detect the touch positions of the fingerprints' ridges to generate the shape and image of the fingerprint. *Id.* at 1:8-25; 2:65-3:7; 3:62-4:3; 5:35-40; 27:53-59.

110. As I understand the 916 Patent, the controller described in the preamble of claim 1 is any preexisting controller, such as a microcontroller. The 916 Patent specifically explains in the specification that "Controller 102 is any processor, microcontroller, neural network, analog computer, programmed

circuitry, or other module capable of processing input data 118 to extract output indicia 120 and/or the like. The particular control circuitry 102 used varies widely from embodiment to embodiment, but in exemplary embodiments controller 102 is a model T1004, T1005, T10XX or other microcontroller produced by Synaptics Inc. of Santa Clara, Calif. In many embodiments, controller 102 includes and/or communicates with a digital memory 103 that suitably stores digital instructions in any software or firmware form that are executable by controller 102 to implement the various sensing, control and other functions described herein." The 916 Patent at 5:24-36.

111. Umeda teaches using a controller for controlling operations of a capacitive position sensor and includes other circuitry such a column line driver 5, a code generator 1, and a capacitor detecting circuit 100. Umeda (Ex. 1007) at Figs. 1, 4, 17, 27. The specific details of the column line driver 5, code generator 1, and the capacitor detecting circuit 100 are discussed further for claim elements 1.A to 1.D below. In my opinion, the controller in Umeda is equivalent to the controller for a capacitive position sensor as recited in claim element 1.Preamble because detecting the position of the fingerprint's ridges is no different than detecting the position of any other input object - both require detecting the capacitance change induced by the input object. In fact, fingerprint detection in Umeda tends to be

technically more difficult than detecting a single object because fingerprint detection requires multi-touch detection when detecting the ridges of a fingerprint. Moreover, Umeda's controller can process the same capacitance changes used to determine the touch positions of the fingerprint's ridges to determine the touch position of the entire finger. Thus, a person of ordinary skill in the art would have recognized that the controller in Umeda can be used as a position sensor for detecting the touch location of input objects, such as a finger or a stylus. *Id.* at 2:65-3:7; 3:66-4:2.

112. In connection with Umeda's teachings, Inoue discloses a capacitive position sensor similar to the capacitive position sensor in Umeda that includes a matrix of capacitive sensing electrodes along X axis and Y axis. Ex. 1008 at Abstract; 1:6-20; 4:10-29; Figs. 1 and 4. Inoue discloses a controller for its capacitive position sensor to include the coordinate data generation section 3 which includes among others, X-axis side multiplexer 17, Y-axis side multiplexer 18, drive selection circuit 24 and 30, CPU 22 and scan signal switching section 28 that collectively control the operation of Inoue's position sensor (*id.* at 1:21-2:67; 4:10-7:4; Figs. 1, 3 and 4) to detect coordinates of the position of an input object, such as an input pen or finger touching an operation area formed by a matrix of X and Y electrodes. *Id.* at Abstract; 1:6-20; 4:10-29; Figs. 1 and 4. Thus, Inoue

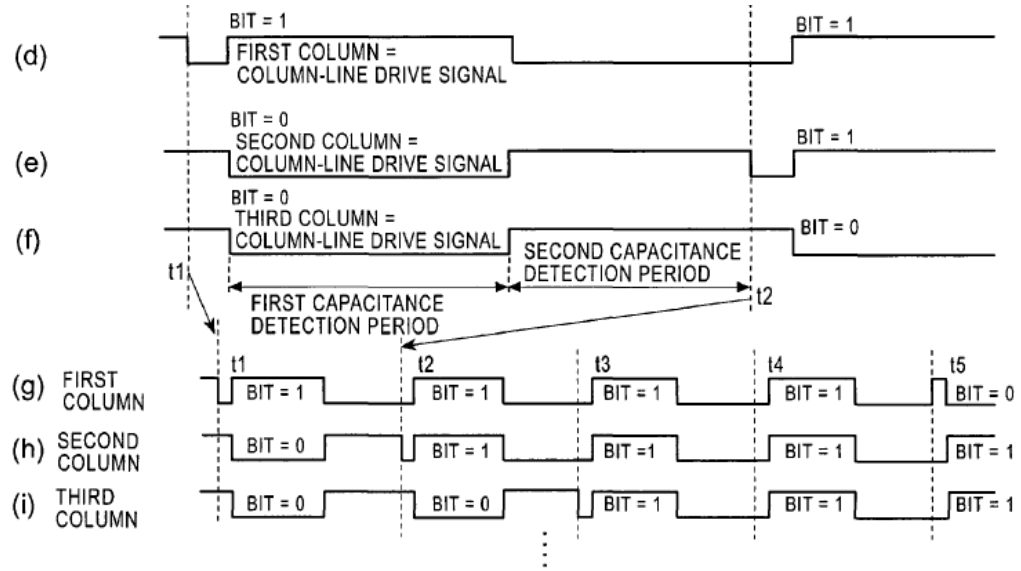
demonstrates that a capacitive position sensor similar to the one disclosed in Umeda can be used to determine the position of an input object, such as an input pen or a finger in addition to the positions of different portions of the finger, such as the fingerprint's ridges.

113. As I have previously discussed, a person of ordinary skill in the art would be motivated to combine Umeda, Inoue and Jaeger. For this claim element in particular, it is my opinion that a person of ordinary skill in the art would have been motivated to combine the teachings of Umeda and Inoue for the similar teachings shared by them. For example, both Umeda and Inoue teach a capacitive position sensor that includes a matrix of row and column lines of electrodes. Both Umeda and Inoue teach detecting capacitance changes at the intersections of the row and column lines. Both Umeda and Inoue teach measuring the magnitude and position of the measured capacitance changes at the intersection of the column-row line electrodes in response to a finger touching a surface of a touch-sensing area. In light of the similarities shared by Umeda and Inoue, a person of ordinary skill in the art would have been guided by such teachings in Umeda and Inoue and would have recognized that by combining the teachings of Umeda and Inoue, the matrix of capacitive sensing electrodes can be used to determine the position of various types of input objects including different portions of each input object.

114. **Claim Element 1.A:** simultaneously applying a first one of a plurality of distinct modulation signals to a first electrode and a second one of the plurality of distinct modulation signals to a second electrode to obtain resultant signals that are electrically affected by the position of the input object, In my opinion, the combination of Umeda, Inoue and Jaeger discloses this "simultaneously applying . . ." step.

115. Using a linear feedback shift register (LFSR) to generate pseudo random codes is a well-known technique in wireless communications as I described in the TECHNOLOGY BACKGROUND section above. Umeda discloses one exemplary implementation where a code generator is used to generate Walsh orthogonal codes or pseudorandom noise codes ("PN codes") used by a column line driver to simultaneously transmit distinct signals to different column lines. Umeda (Ex. 1007) at 3:8-52; 9:25-67; 10:47-11:9; 11:20-26; Figs. 1, 6A, 6B, 8, 9. Specifically, Figure 8 of Umeda shows the column line driver simultaneously applying distinct signals to first, second, and third column lines (see rows (g), (h), and (i)) based on distinct digital code sequences. *Id.* at 12:15-21; 13:14-20; 14:33-47; 17:6-13; Fig. 8. In this regard, a distinct signal based on a distinct digital code sequence of {1,1,1,1,0 . . .} is applied to the first column C1; a distinct signal based on a distinct digital sequence {0,1,1,1,1 . . .} is applied to the

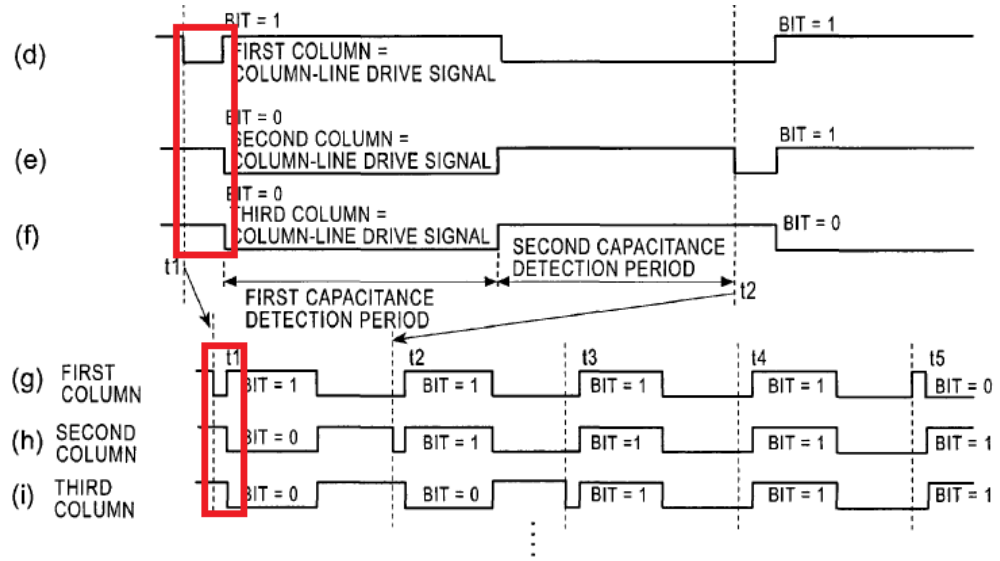
second column C2, and a distinct signal based on a distinct digital sequence {0,0,1,1,1 . . .} is applied to the third column C3. *Id.*



116. Umeda provides additional explanation of simultaneously applying the distinct signals to the different column lines as shown in Fig. 8 using a 15-bit PN code sequence. *Id.* at 7:15-20:23 (first embodiment). The 15-bit code sequence requires each capacitance measurement cycle to have 15 measurement points in time, t1 to t15. *Id.* at 10:27-35; 10:46-54. Each measurement time from t1 to t15 is further divided into a first capacitance detection period and a second capacitance detection period. *Id.* at 4:14-24; 8:54-64. The first and second detection periods are used to determine the difference of a detection signal at the rise of a column driving signal and at the fall of the column driving signal for the column lines to eliminate the offset components in a differential amplifying circuit to enhance the precision of the capacitance measurement. *Id.* at 4:14-31; 8:53-9:18; Fig. 5.

117. To initiate the capacitance measurement cycle, the code generator in Umeda generates a 15-bit pseudorandom (PN) code sequence, e.g., {1,1,1,1,0,1,0,1,1,0,0,1,0,0,0}, which is stored in a shift register having corresponding 15 registers. *Id.* at 9:25-67; 10:47-11:9; 11:20-26, Figs. 1, 6A, 6B, 9. At each time period, the code generator and the shift register in combination generate the next bit for the distinct digital codes applied to the column lines by generating a new least significant bit (LSB) and shifting the remainder (bits 1-14) of the stored PN code by one bit. *Id.* at 11:27-31, Fig. 9. For example, at the start of time t1, the shift register shifts the PN code by one bit to generate a new bit string {1,1,1,0,1,0,1,1,0,0,1,0,0,0,1}. *Id.* An inverting circuit inverts the shifted data string into {0,0,0,1,0,1,0,0,1,1,0,1,1,1,0} and outputs the inverted data string to the column line driver circuit. *Id.* at 11:41-47. The column line driver circuit then drives the corresponding column lines based on this bit string starting from the least significant bit (right to left). *Id.* at 11: 48-50. Thus, at t1, column lines C2, C3, C4, C6, C7, C10, and C12 are driven by bit "1" to a high voltage level, and the column lines C1, C5, C8, C9, C11, C13, C14, and C15 are driven by bit "0" to a low voltage level. *Id.* at 11:51-58; Fig. 8. The distinct digital codes are used to drive the column lines shown in Fig. 8 to prepare the column lines for the proper

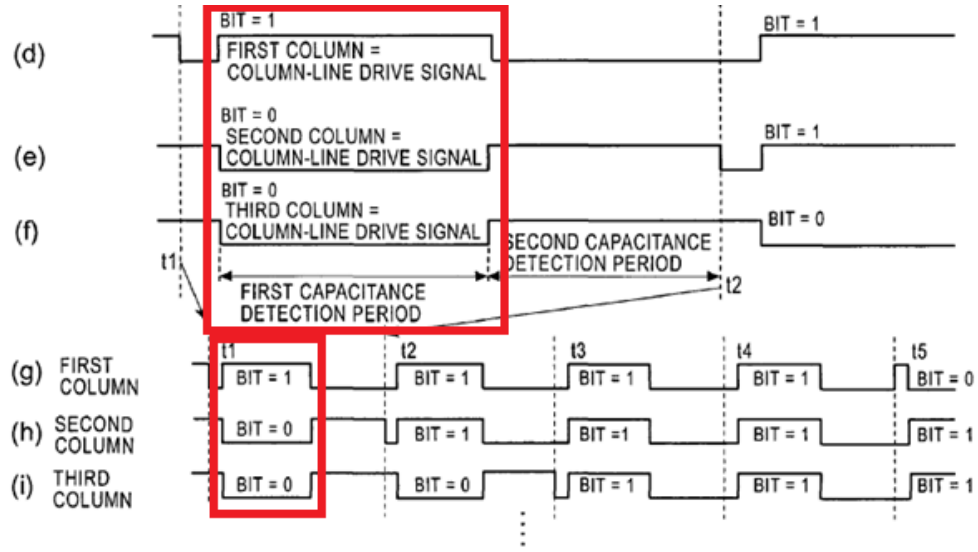
rise or fall phase of the distinct digital codes before initiating the first and second capacitance measurement period as highlighted by the red boxes. *Id.*



Umeda (Ex. 1007) at Figure 8

118. Once the "first capacitance detection period" is reached, the column line driver drives the column lines using a non-inverted version of the distinct digital code sequence. *Id.* at 11:59-64. Specifically, in the first capacitance detection period at t1, the column line driver drives the column lines using the bit string {1,1,1,0,1,0,1,1,0,0,1,0,0,0,1} to drive column line C1 to rise from low to high because the 15th bit (the least significant bit) data (counting from left) is changed from 0 to 1. *Id.* at 12:4-14. Similarly, the column line driver drives column line C2 to fall from high to low because the 14th bit data is changed from 1 to 0. *Id.* The column line driver drive other column lines in a similar fashion based on the changes in the data at the corresponding bit positions. *Id.* During the

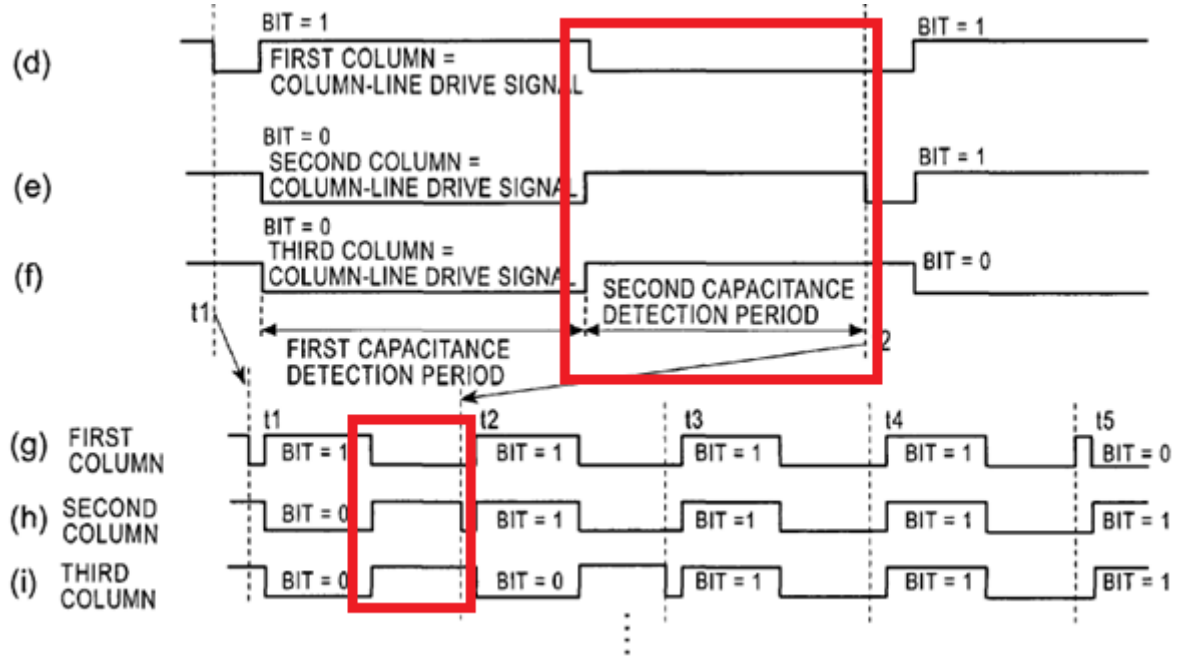
first capacitance detection period of t1, column lines C1, C5, C8, C9, C11, C13, C14, and C15 are driven as a first column line group using a high voltage, while column lines C2, C3, C4, C6, C7, C10, and C12 are driven as a second column line group using a low voltage, as highlighted in red below. *Id.* at 12:22-28; Fig. 8.



Umeda (Ex. 1007) at FIG. 8

119. During the second capacitance detection period of time period t1, the inverting circuit inverts the bit string used during the first capacitance detection period so that the column line driver can drive the column lines using the inverted bit string {0,0,0,1,0,1,0,0,1,1,0,1,1,1,0}. *Id.* at 12:57-13:13. Specifically, the column line driver drives column line C1 to fall from high to low, column line C2 to rise from low to high, column line C3 to fall from low to high, and so forth until all 15 column lines are driven simultaneously using the corresponding bit from the inverted bit string. *Id.* at 13:2-13, Fig. 8. Thus, during the second capacitance

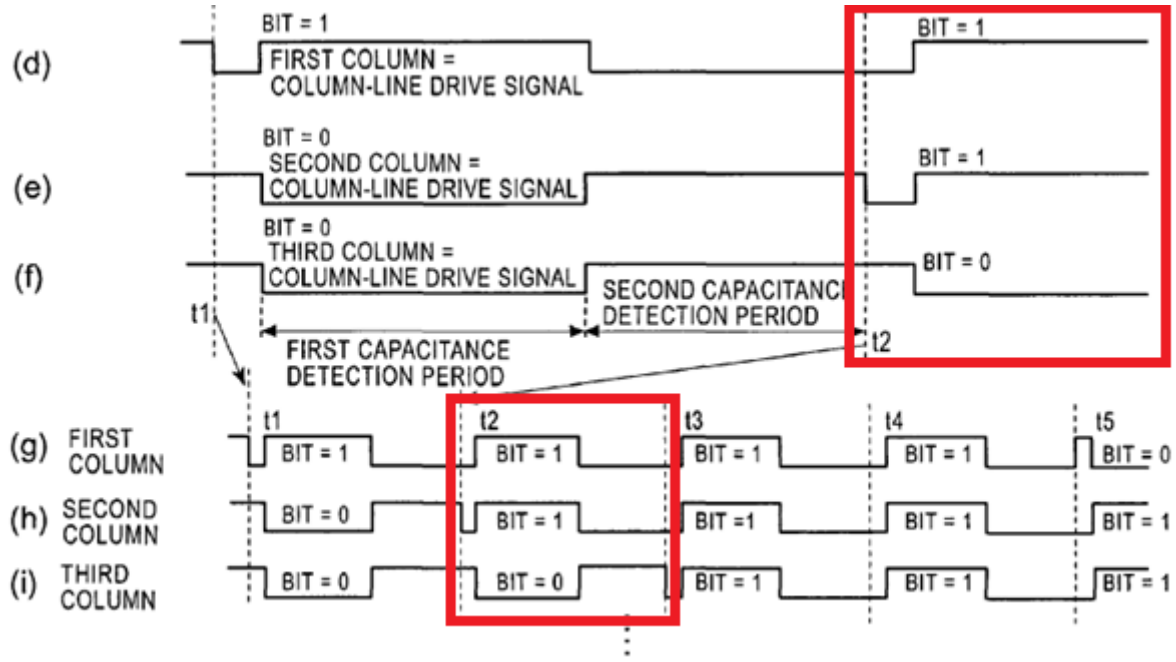
detection period, each column line is driven in the opposite direction as during the first capacitance detection period. *Id.* (the red boxes show the signals sent to the first three columns C1 - C3 during the second capacitance detection period).



Umeda (Ex. 1007) at FIG. 8

120. During each subsequent measurement period, the code generator and the storage shift register in combination generate the next bit for the distinct digital codes transmitted to the column lines by generating a new LSB and shifting bits 1-14 of the stored bit string by one bit. For example, during measurement period t2, the PN-code generating circuit of the code generator generates a new LSB (bit value "1") and the storage shift register shifts bits 1-14 of the bit string data stored in the registers to registers 2 to 15, and inputs the newly generated LSB data into register number 1. *Id.* at 16:14-22. Thus, the column line driver drives the column

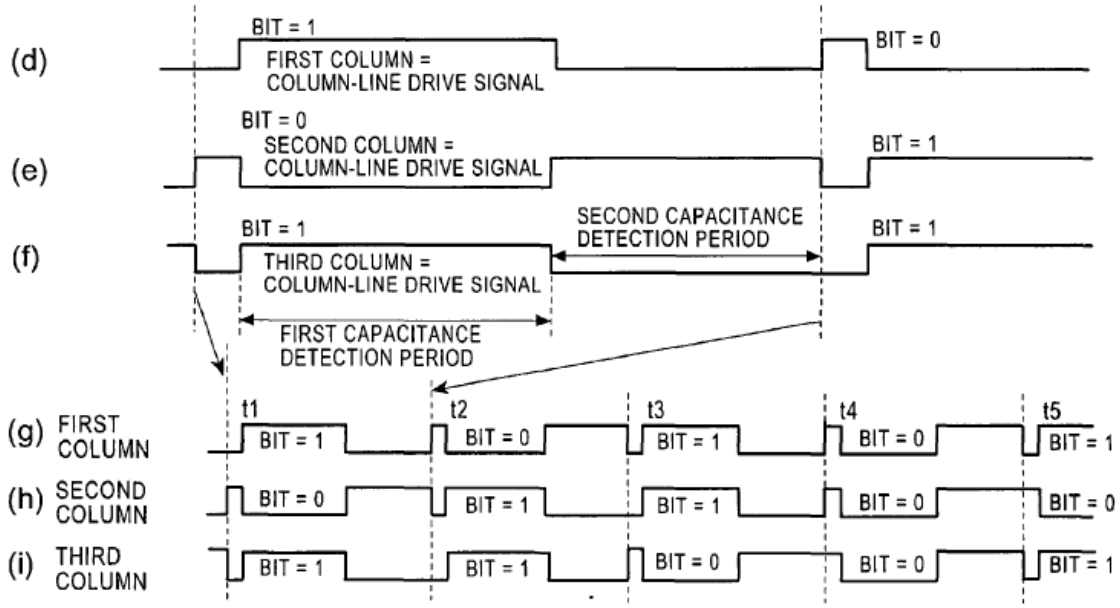
lines at time period t1 using {1,1,1,0,1,0,1,1,0,0,1,0,0,0,1} and at time period t2 using {1,1,0,1,0,1,1,0,0,1,0,0,0,1,1}. *Id.* at 16:23-18:4.



Umeda (Ex. 1007) at FIG. 8

121. Generating the next bit for the distinct digital codes continues for each of the measurement time periods t3 to t15 until the entire 15 bits are generated for each of the column lines. *Id.* at 17:46-53; Fig. 8 (showing the waveform of column line driving signals for C1, C2 and C3 during time periods t1 to t5); Fig. 14. With each subsequent bit generation, the column line driving and the first and second capacitance measuring operations are repeated as described for time periods t1 and t2 above. *Id.* Thus, Umeda teaches driving different column lines C1, C2, and C3 using different distinct 15-bit digital code sequences over the time periods t1 through t15.

122. In a second embodiment, Umeda teaches using the code generator to generate distinct digital codes such as orthogonal codes (e.g., Walsh codes) rather than PN-codes to allow the column line driver to simultaneously transmit different signals to different column lines based on the orthogonal codes. *Id.* at 20:25-26:17 (second embodiment); Figs. 1, 19-24. For example, Fig. 22 reproduced below shows the column line driver driving different column lines by distinct driving signals based on distinct orthogonal codes, such as Walsh codes. *Id.* at Fig. 22, rows (d) to (i).



Umeda (Ex. 1007) at FIG. 22.

123. Therefore, in my opinion, the code generator 1 and column line driver 5 in Umeda form a driver circuit that corresponds to the claimed driver circuitry. In addition, the timing control circuit 11 in the capacitor detecting circuit 100 may

also be considered part of this driver circuit due to the generation of the clock by circuit 11.

124. Inoue teaches driving the X electrodes of the position sensor using scan signals. Inoue (Ex. 1008) at 1:61-2:15; 2:44-53; 4:60-5:3; 5:14-16; 5:35-40; 6:1-8; 6:64-7:4. For example, Inoue discloses the claimed drive circuitry, such as circuit 3 in FIG. 1 or circuit 53 in FIG. 4. In the example in FIG. 1, Inoue's drive circuitry includes, *e.g.*, X-axis side multiplexer 17, Y-axis side multiplexer 18, drive selection circuit 24 and 30, CPU 22 and scan signal switching section 28 that collectively control the operation of Inoue's position sensor.

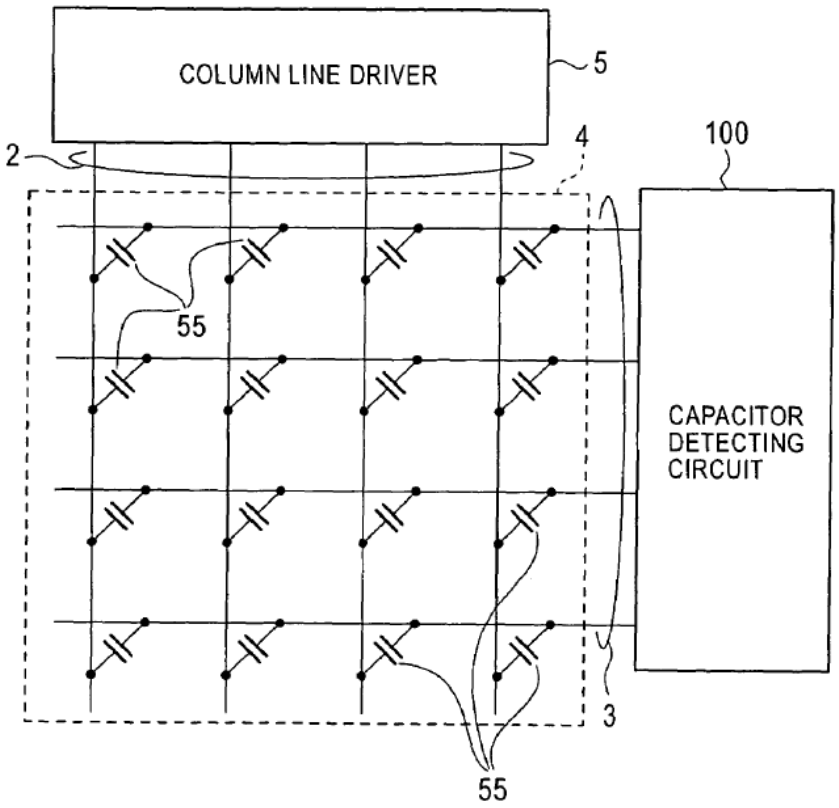
125. In the context of the combination of Umeda, Inoue and Jaeger, it is my opinion that a person of ordinary skill in the art would be motivated to apply the multi-electrodes driving method taught in Umeda in Inoue to provide the claimed drive circuitry of the claimed controller, because doing so can shorten the touch position detection time, reduce the delay in responding to a user's touch input and improve SNR properties. *Id*.

126. In addition, in my opinion, both Umeda and Inoue teach the "obtain[ing] resultant signals that are electrically affected by the position of the input object" limitation in this claim element.

127. The capacitance detecting circuit in Umeda includes a sensor unit of capacitive sensing electrodes arranged in a 2-D matrix of column lines and row lines. Ex. 1007 at 7:21-67, Figs. 1 and 4. As shown in Fig. 4, the row lines 3 of receiver electrodes are capacitively coupled to the column lines 2 of transmitter electrodes to form capacitor devices 55 at the intersections of the column lines 2 and row lines 3. *Id*. Activating the column lines using drive pulse trains generated based on the PN codes (*id.* at 7:51-67, Fig. 4) or Walsh orthogonal codes (*id.* at 20:25-21:8) induces changes in the capacitances of the capacitor devices formed by at the intersection of the row lines and the column lines. *Id.* at 7:39-43, Fig. 4. The resultant signal of the capacitance change flows through the row lines as currents based on the charge transfer in the capacitances and are converted and measured as voltages. *Id.* at 12:29-45. The capacitance detecting circuit 100 in FIGS. 1 and 4 includes circuit elements or modules that are downstream in the signal processing chain from the row lines 3. As such, in my opinion, the output terminals of the row lines 3 and part of the capacitance detecting circuit 100 can correspond to the claimed receiver circuitry. For example, the receiver circuitry may include the output terminals of the row lines 3 and the charger amplifier circuits 6 and the sample-and-hold circuits 7. The additional circuit elements, e.g., the selector circuit

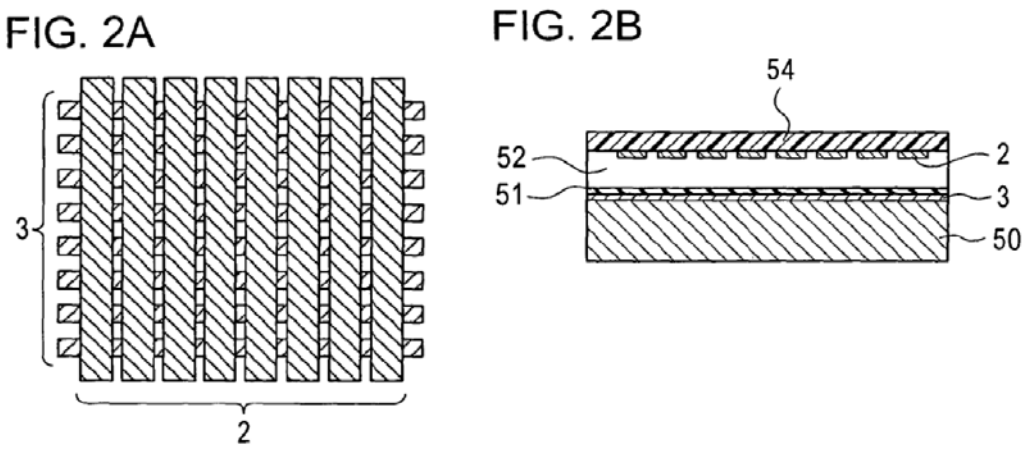
8, the A/D converter 9 and the decoding computation circuit 10 may form part of the receiver circuitry in Umeda. *Id*. at FIG. 1.

FIG. 4



Umeda (Ex. 1007) at FIG. 4

128. As shown in FIGS. 2A and 2B of Umeda, the row lines 3 of receiver electrodes are placed proximate to the column lines 2 of transmitter electrodes with only an insulating film 51 and a gap 52 separating them. *Id.* at 7:29-39, Figs. 2A, 2B.



Umeda (Ex. 1007) at FIGS. 2A and 2B

129. As discussed above in the section for overview of Inoue, Inoue teaches a capacitive sensing coordinate input device, such as a tablet device that can detect the contact position of at least one input object, such as an input pen or a finger, on the tablet device. Inoue (Ex. 1008) at Abstract, 1:5-2:67; 4:10-5:24; Figs. 1, 4. Similar to Umeda, Inoue uses a matrix of capacitive sensing X and Y electrodes arranged in corresponding X axis and Y axis forming a touch sensing area. *Id.* at 1:29-34; 4:20-29; Figs. 1, 2, 4. As shown in Fig. 2 of Inoue, the X and Y electrodes are proximate to each other with only a film substrate separating them. *Id.* at 4:20-29, Fig. 2.

FIG. 2

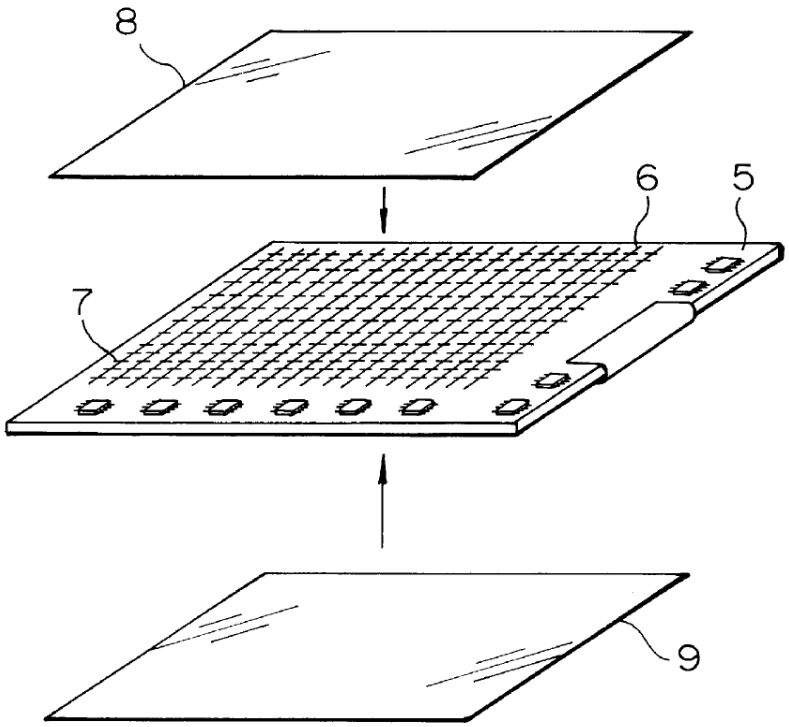


FIG. 2 of Inoue

130. Also, the X electrodes are capacitively coupled to the Y electrodes and the changes in capacitances at the intersections of the X and Y electrodes are induced in response to a scan signal applied to the X electrodes. *Id.* at 2:9-43. The resultant signal of the capacitance changes at the intersections of the capacitively coupled X and Y electrodes are measured as voltages received through the Y electrodes. *Id.* at 2:16-33; 5:25-48. Therefore, it is my opinion that the X electrodes in Inoue correspond to the claimed transmitter electrodes and Y

electrodes in Inoue correspond to the claimed receiver electrodes. The received signal voltages from Y electrodes are then used by the CPU 22 in FIG. 1 or CPU 62 in FIG. 4 to calculate the contact position of the finger on the touch sensor. ***Id.*** at 2:34-67 and 5:25-7:18. Accordingly, the claimed "receiver circuitry" may include the following receiver circuitry in Inoue: Y-axis multiplexer 18 having a plurality of (M) switches S_1 to S_M arranged in parallel in FIG. 1 and may further include other downstream circuit elements such as the first amplification circuit 19, the first filter circuit 20, the analog/digital converter (A/D) 21 and the controller (CPU) 22.

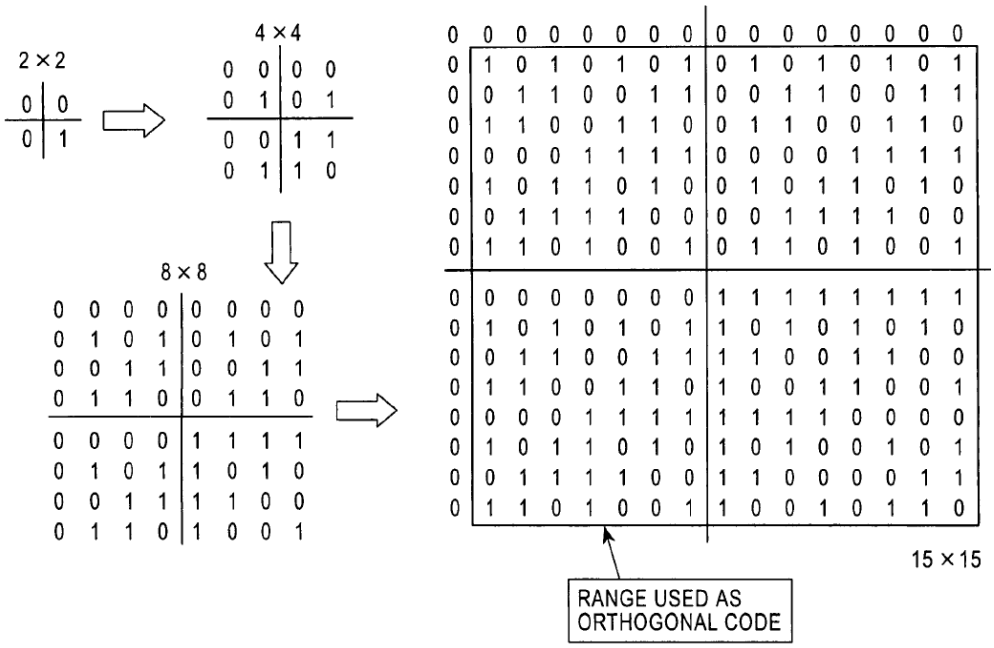
131. Because both Umeda and Inoue teach the claimed receiver circuitry, a person of ordinary skill in the art would have been motivated to combine the teachings of Umeda and Inoue due to the common teachings shared by them. For example, both of them teach detecting a position of input object, such as a finger using a matrix of columns and rows of capacitively coupled electrodes. Also, both Umeda and Inoue teach activating the transmitter electrodes and receiving the resultant signals on the receiver electrodes to determine the position of the input object. In light of the common teachings, a person of ordinary skill in the art would have recognized that combining the teachings of Umeda and Inoue will expand the applicability of the common capacitive sensing hardware to detect the

position of an input object, such as an input pen or a finger in addition to detecting the positions of different positions of the finger, such as the fingerprint's ridges.

132. **Claim Element 1.B:** wherein each of the plurality of distinct modulation signals is based on a different one of a plurality of distinct digital codes;

In my opinion, Umeda teaches generation of distinct signals based on distinct digital codes. As discussed for claim element 1.A, Umeda teaches using the code generator to generate distinct orthogonal codes, such as Walsh codes. *Id.* at 20:25-26:17 (second embodiment); Figs. 1, 19-24. The column line driver can then drive different column lines using distinct signals based on the Walsh orthogonal codes. *Id.* Figures 19 and 20 show generating an exemplary 15x15-bit matrix of Walsh orthogonal codes for driving column lines C1 to C15. *Id.* at 21:37-22:26, Figs. 19 and 20.

FIG. 19



Umeda (Ex. 1007) at FIG. 19

FIG. 20

(LSB) (MSB)

	1	2	3	4	5	6	7	8	9	10	11	12	13	14	15
t1	1	0	1	0	1	0	1	0	1	0	1	0	1	0	1
t2	0	1	1	0	0	1	1	0	0	1	1	0	0	1	1
t3	1	1	0	0	1	1	0	0	1	1	0	0	1	1	0
t4	0	0	0	1	1	1	1	0	0	0	0	1	1	1	1
t5	1	0	1	1	0	1	0	0	1	0	1	1	0	1	0
t6	0	1	1	1	1	0	0	0	0	1	1	1	1	0	0
t7	1	1	0	1	0	0	1	0	1	1	0	1	0	0	1
t8	0	0	0	0	0	0	0	1	1	1	1	1	1	1	1
t9	1	0	1	0	1	0	1	1	0	1	0	1	0	1	0
t10	0	1	1	0	0	1	1	1	1	0	0	1	1	0	0
t11	1	1	0	0	1	1	0	1	0	0	1	1	0	0	1
t12	0	0	0	1	1	1	1	1	1	1	1	0	0	0	0
t13	1	0	1	1	0	1	0	1	0	1	0	0	1	0	1
t14	0	1	1	1	1	0	0	1	1	0	0	0	0	1	1
t15	1	1	0	1	0	0	1	1	0	0	1	0	1	1	0

ORTHOGONAL CODE (15×15)

Umeda (Ex. 1007) at FIG. 20

133. Each column in Fig. 20 of Umeda represents a distinct digital code having a 15-bit sequence for applying to a corresponding column line over a time period t1 through t15. *Id.* at 21:37-22:26, Fig. 20. As discussed above, each bit of a given distinct digital code is generated at each time period from t1 to t15. As clearly shown in Fig. 20, the distinct digital codes in the 15 columns of Fig. 20 are different from one another. For example, bit sequence{1,0,1,0,1,0,1,0,1,0,1,0,1,0,1} is applied to column line C1, bit sequence {0,1,1,0,0,1,1,0,0,1,1,0,0,1,1} is applied to C2, and bit sequence {1,1,0,1,0,0,1,1,0,0,1,0,1,1,0} is applied to C15, etc., as highlighted below. To better illustrate the distinct codes applied to the columns in time scale, FIG. 20 of Umeda can be transposed to show the time period t1 through t15 in the horizontal axis and the columns of electrodes 1 thorough 15 in the vertical axis. Clearly, the transposed FIG. 20 of Umeda (see below) shows 15 distinct codes being applied to the 15 column electrodes simultaneously over the same time period t1 through t15.

	(LSB) 1	2	3	4	5	6	7	8	9	10	11	12	13	14	(MSB) 15
t1	1	0	1	0	1	0	1	0	1	0	1	0	1	0	1
t2	0	1	1	0	0	1	1	0	0	1	1	0	0	1	1
t3	1	1	0	0	1	1	0	0	1	1	0	0	1	1	0
t4	0	0	0	1	1	1	1	0	0	0	0	1	1	1	1
t5	1	0	1	1	0	1	0	0	1	0	1	1	0	1	0
t6	0	1	1	1	1	0	0	0	0	1	1	1	1	0	0
t7	1	1	0	1	0	0	1	0	1	1	0	1	0	0	1
t8	0	0	0	0	0	0	0	1	1	1	1	1	1	1	1
t9	1	0	1	0	1	0	1	1	0	1	0	1	0	1	0
t10	0	1	1	0	0	1	1	1	1	0	0	1	1	0	0
t11	1	1	0	0	1	1	0	1	0	0	1	1	0	0	1
t12	0	0	0	1	1	1	1	1	1	1	1	0	0	0	0
t13	1	0	1	1	0	1	0	1	0	1	0	0	1	0	1
t14	0	1	1	1	1	0	0	1	1	0	0	0	0	1	1
t15	1	1	0	1	0	0	1	1	0	0	1	0	1	1	0

ORTHOGONAL CODE (15×15)

Umeda (Ex. 1007) at FIG. 20

Time →

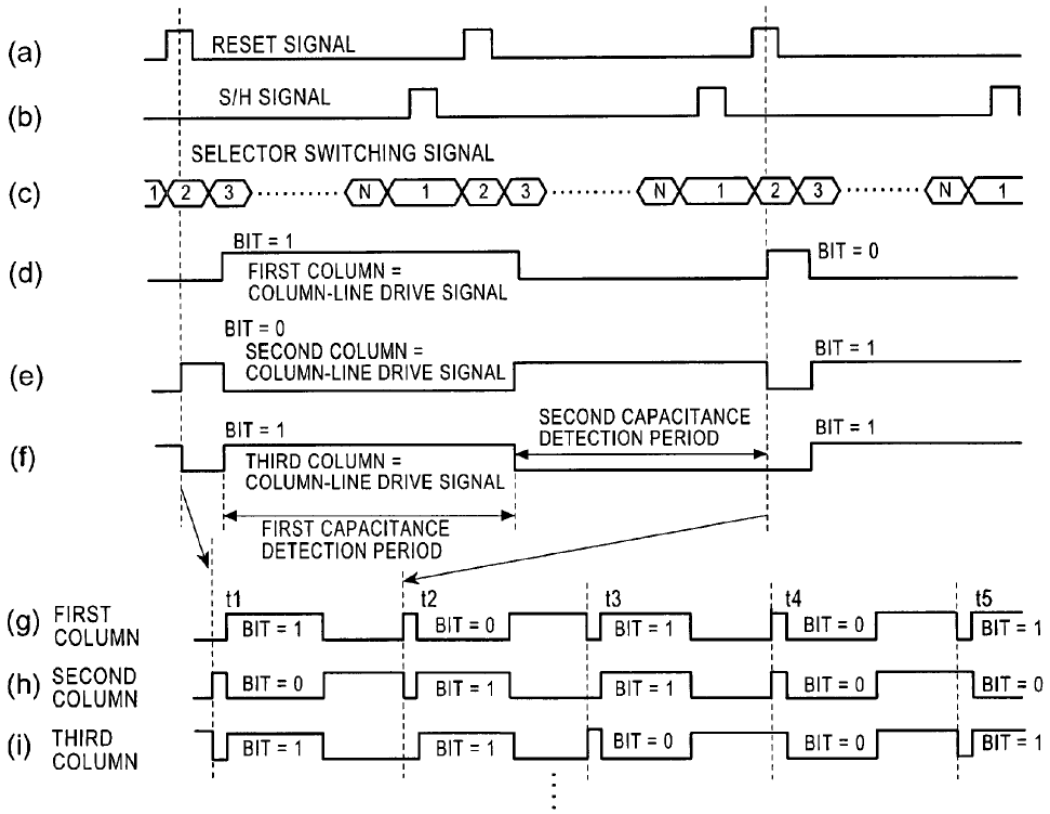
Column Electrodes	t1	t2	t3	t4	t5	t6	t7	t8	t9	t10	t11	t12	t13	t14	t15
1	1	0	1	0	1	0	1	0	1	0	1	0	1	0	1
2	0	1	1	0	0	1	1	0	0	1	1	0	0	1	1
3	1	1	0	0	1	1	0	0	1	1	0	0	1	1	0
4	0	0	0	1	1	1	1	0	0	0	0	1	1	1	1
5	1	0	1	1	0	1	0	0	1	0	1	1	0	1	0
6	0	1	1	1	1	0	0	0	0	1	1	1	1	0	0
7	1	1	0	1	0	0	1	0	1	1	0	1	0	0	1
8	0	0	0	0	0	0	0	1	1	1	1	1	1	1	1
9	1	0	1	0	1	0	1	1	0	1	0	1	0	1	0
10	0	1	1	0	0	1	1	1	1	0	0	1	1	0	0
11	1	1	0	0	1	1	0	1	0	0	1	1	0	0	1
12	0	0	0	1	1	1	1	1	1	1	1	0	0	0	0
13	1	0	1	1	0	1	0	1	0	1	0	0	1	0	1
14	0	1	1	1	1	0	0	1	1	0	0	0	0	1	1
15	1	1	0	1	0	0	1	1	0	0	1	0	1	1	0

FIG. 20 of Umeda transposed to show time on horizontal axis

134. Moreover, Umeda illustrates in Fig. 22, the time series of the distinct digital codes from Figs. 19 and 20 being applied to the different column lines. *Id.* at Fig. 22. Specifically, rows (d) to (i) in Fig. 22 represent the time series of the

distinct orthogonal codes and the distinct driving signals applied to the column lines. *Id*. For example, distinct digital code sequence {1,0,1,0,1,…} are used for driving the distinct signal transmitted to C1, distinct digital code sequence {0,1,1,0,0,…} are used for driving the distinct signal transmitted to C2, and distinct digital code sequence {1,1,0,0,1,…} are used for driving the distinct signal transmitted to C3. *Id.* at Fig. 22. These distinct digital codes are consistent with the codes shown in the columns of Fig. 20.

FIG. 22



Umeda (Ex. 1007) at FIG. 22

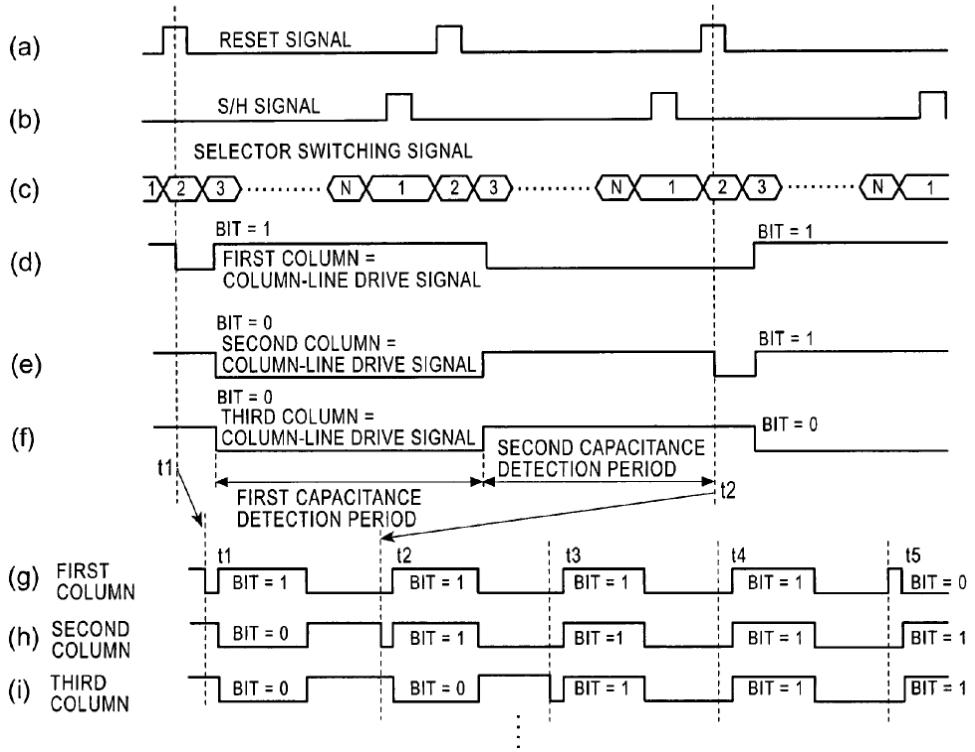
135. In addition to the Walsh orthogonal codes, Umeda teaches generating PN-codes as the distinct digital codes. Umeda at 17:46-53; Fig. 14. Similar to Fig 20 discussed for the Walsh orthogonal codes, each column of Fig. 14 in Umeda shows the 15-bit string of each PN-code stored in the storage shift register over the time periods t1 to t15. *Id*. The 15 columns of Fig. 14 contain the 15 different 15-bit PN-code sequence used to drive the column lines C1 to C15 from t1 to t15. For example, the 15-bit PN-code sequence driving C1 is shown in the first column of Fig. 14 (i.e., the LSB column): {1,1,1,1,0,1,0,1,1,0,0,1,0,0,0}, the 15-bit PN-code sequence driving C2 is contained in the second column: {0,1,1,1,1,0,1,0,1,1,0,0,1,0,0}, and the 15-bit PN-code driving C15 is shown in the last column (the MSB column) of Fig. 14: {1,1,1,0,1,0,1,1,0,0,1,0,0,1}. *Id.* at Fig. 14 (highlighted in red). In my opinion, these digital codes are "distinct digital codes" because the 916 Patent equates bit-shifted or phase-shifted codes as distinct codes: "A digital bit sequence may be simply shifted in phase, for example, to create ***multiple distinct codes***." 916 Pat. at 8:24-26; 6:11-14; 7:3-6; 8:6-12 (emphasis added).

	LSB 1	2	3	4	5	6	7	8	9	10	11	12	13	14	MSB 15	SHIFT AMOUNT
t1	1	0	0	0	1	0	0	1	1	0	1	0	1	1	1	0
t2	1	1	0	0	0	1	0	0	1	1	0	1	0	1	1	1
t3	1	1	1	0	0	0	1	0	0	1	1	0	1	0	1	2
t4	1	1	1	1	0	0	0	1	0	0	1	1	0	1	0	3
t5	0	1	1	1	1	0	0	0	1	0	0	1	1	0	1	4
t6	1	0	1	1	1	1	0	0	0	1	0	0	1	1	0	5
t7	0	1	0	1	1	1	1	0	0	0	1	0	0	1	1	6
t8	1	0	1	0	1	1	1	1	0	0	0	1	0	0	1	7
t9	1	1	0	1	0	1	1	1	1	0	0	0	1	0	0	8
t10	0	1	1	0	1	0	1	1	1	1	0	0	0	1	0	9
t11	0	0	1	1	0	1	0	1	1	1	1	0	0	0	1	10
t12	1	0	0	1	1	0	1	0	1	1	1	1	0	0	0	11
t13	0	1	0	0	1	1	0	1	0	1	1	1	1	0	0	12
t14	0	0	1	0	0	1	1	0	1	0	1	1	1	1	0	13
t15	0	0	0	1	0	0	1	1	0	1	0	1	1	1	1	14

Umeda (Ex. 1007) at FIG. 14

136. Umeda illustrates the time series of the distinct signals and the distinct digital codes shown in Fig. 14 for applying to different column lines. *Id.* at Fig. 8. Specifically, the waveforms in Fig. 8 at lines (d) through (i) represent the time series of the distinct driving signals sent to columns C1, C2 and C3 based on the distinct PN-code sequences described above. *Id.*. For example, consistent with the columns in Fig. 14, PN-code sequence{1,1,1,1,0,…} is used for driving C1, PN-code sequence {0,1,1,1,1,…} is used for driving C2, and PN-code sequence {0,0,0,1,1,…} is used for driving C3.

FIG. 8



Umeda (Ex. 1007) at FIG. 8

137. In my opinion, the driving signals transmitted to the column lines based on the Walsh orthogonal codes and the PN-codes are distinct from each other, and are based on distinct digital codes.

138. **Claim Element 1.C:** demodulating the resultant signals using the plurality of distinct digital codes to thereby discriminate electrical effects produced by the input object; It is my opinion that Umeda teaches the use of a decoding circuit which uses the distinct digital codes applied to the column lines to demodulate the signals received from the row lines to discriminate the signals applied to each column line and how the signals to each column line are affected

by the capacitance of the input object at the intersections formed by the column and row lines. Ex. 1007, Figs. 1, 4, 7:44-50.

139. For example, a charge amplifier circuit is provided in Umeda for each row line for measuring the current and voltage changes induced by capacitance changes, and the received signals for each row line are transmitted (via a series of intermediate steps) to a decoding computation circuit which demodulates the received signals to correlate the signals received from the column line drivers based on their unique digital codes, and therefore determine a two-dimensional position. *Id.*, Figs. 1, 4, 7:44-8:14, 8:34-44.

140. In addition, the distinct digital codes used in Umeda for decoding/demodulation are the same as the codes used for modulation. Umeda (Ex. 1007) at col. 3:20-24; 3:53-61; 4:56-63 ("decoding is performed by using the same PN code as that used for multiplexing, and thus, the occurrence of crosstalk between column lines can be suppressed, thereby making it possible to detect capacitance changes at the intersections with high precision"); 5:6-13; 5:49-55 ("decoding is performed by using the same PN code or orthogonal code as the code used for multiplexing so as to determine the capacitance changes as the voltages at the intersections."); 6:34-36; 6:60-62; 7:5-7; 8:34-44; 18:32-20:23; 24:22-25:67; Figs. 16, 26 and 31. Therefore, it is my opinion that Umeda teaches this claim

element. Similarly, Jaeger teaches that the signals generated using spread spectrum codes may be "de-spread" (*i.e.,* demodulated) using the same codes. Ex. 1011, 3:42-47, 4:60-63, 6:22-27, 7:59-68, 10:37-38; Figs. 4 (blocks 8, 10, 15), 5, 7B, 11A, 11B, 1.

141. **Claim Element 1.D:** determining the position of the input object from the electrical effects. In my opinion, both Umeda and Inoue teach this claim element. As discussed in Claim Element 1.Preamble, Umeda discloses a capacitance detecting circuit implemented in a tablet device having a sensor area defined by a sensor unit that includes row and column lines of capacitive electrodes. Umeda at 7:25-28, Figs. 1, 2A, 2B, 4. As shown in FIGS. 1, 2A and 2B, the sensor unit 4 includes a protective film 54 over the column lines 2 and row lines 3 of capacitive electrodes. An input object, such as a user's finger being proximate to a surface of the protective film 54 initiates the position detection as shown in FIG. 3.

Shenzhen Huiding Tech. Co., Ltd. - Exhibit 1006

FIG. 1

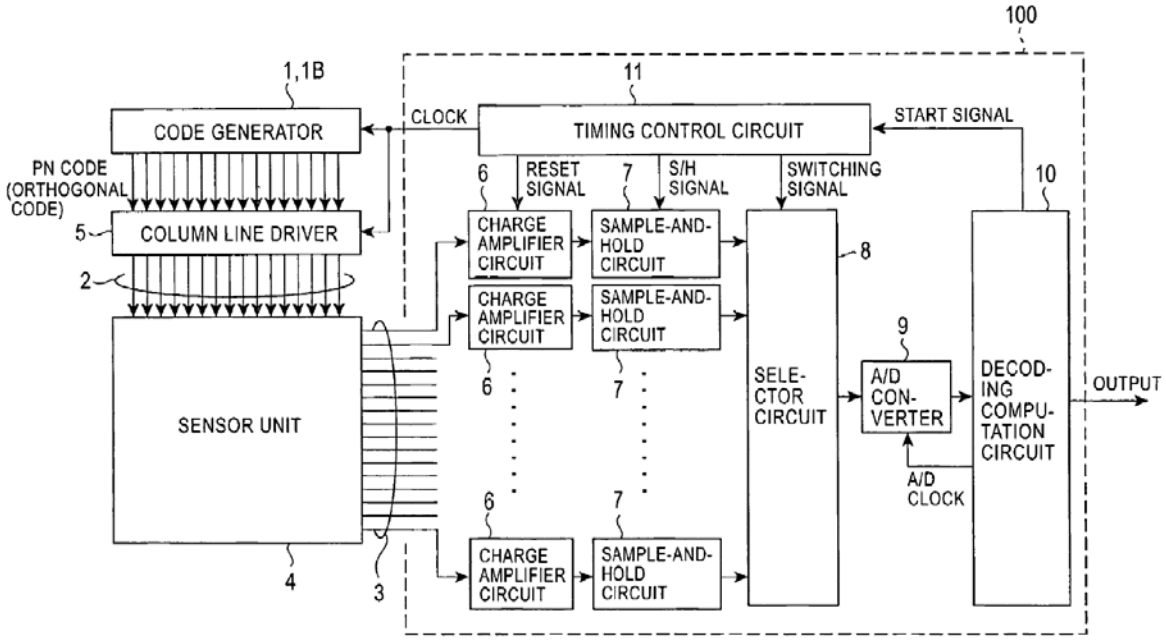


FIG. 1 of Umeda

FIG. 2A

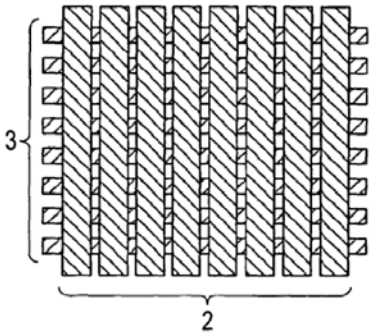
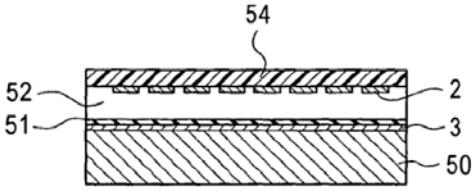


FIG. 2B



FIGS. 2A and 2B of Umeda

Shenzhen Huiding Tech. Co., Ltd. - Exhibit 1006

FIG. 3

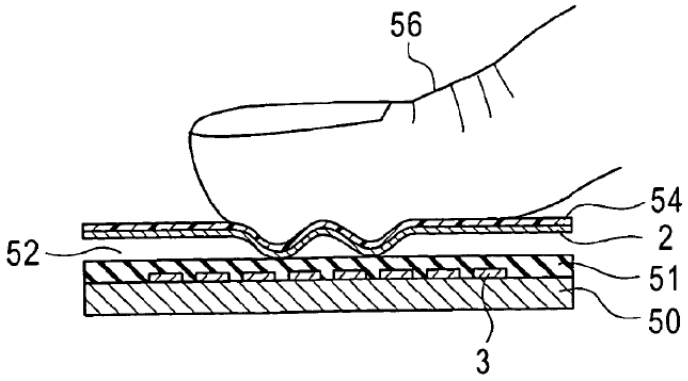


FIG. 3 of Umeda

142. Specifically, the capacitive detecting circuit in Umeda detects small capacitance changes at the intersections of the row and column lines to determine a position of an input object, such as a finger touching the surface of the film 54 on the sensor unit. Umeda at 1:8-9; 2:65-3:7; 3:8-31; 4:4-14; 24:43-50; Fig. 3, 4. For example, when a user's finger touches the film 54 of the sensor unit 4, the "ridges" of the user's fingerprint selectively cause changes to the intervals between the row lines and the column lines that correspond to the positions of the ridges, which in turn induces a capacitance change at each of the column-row intersections. *Id.* at 1:19-25; 7:44-50; Fig. 3.

143. Detecting the capacitance changes at the column-row intersections allows Umeda to detect a position-based attribute of an input object, such as the fingerprints' ridges to generate the shape and image of the fingerprint. *Id.* at 1:8-25;

2:65-3:7; 3:62-4:3; 5:35-40; 7:44-50; 27:53-59 and Fig. 3. Therefore, Umeda discloses this claim element.

144. Similar to Umeda, Inoue teaches a coordinate input device, such as a tablet device that determines a position-based attribute of an input object, such as an input pen or finger in response to the input pen or finger being proximate, i.e., touching, a surface of tablet device. Inoue at Abstract, 1:5-2:67; 4:10-5:24; Figs. 1, 4. Also similar to Umeda, the coordinate input device in Inoue uses a matrix of capacitive sensing electrodes arranged along the X-axis and the Y-axis to define a sensing area. *Id*. at 1:13-2:67 and Figs. 1, 2, 4. Specifically, Inoue teaches determining the position-based attribute of the input object as X and Y coordinates that represent the contact position of the input object on a surface of the sensing area. *Id.* at 5:54-67. In addition, the Z coordinate in Inoue represents whether the input object is close to or brought into contact with the touch sensing area. *Id.* These X, Y, and Z coordinates of the input object are determined based on the resultant signals, which is the signal voltages measured at the Y receiver electrodes. Therefore, Inoue discloses this claim element.

145. Because both Umeda and Inoue teach the features of this claim element, it would have been obvious to a person of ordinary skill in the art to combine the teachings of Umeda and Inoue in light of the common teachings

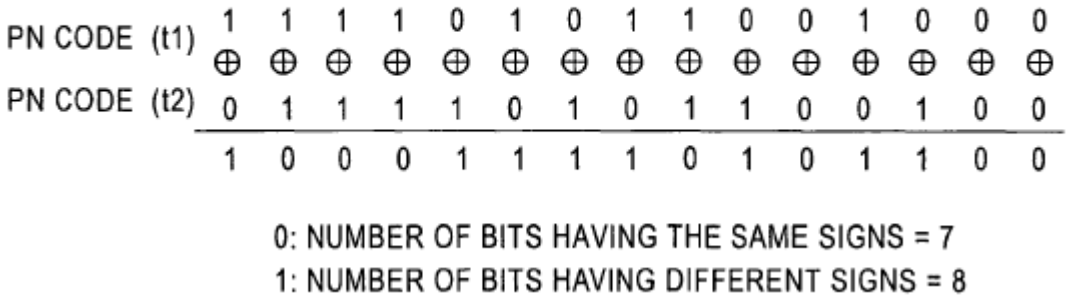
shared by both including using a matrix of X and Y electrodes to perform capacitive position sensing. In addition, a person of ordinary skill in the art would have recognized that by combining the teachings of Umeda and Inoue, additional position-based attributes can be determined including the Z coordinate of the input object, such as an input pen or finger proximate a surface of the touch sensor.

146. Therefore, it is my opinion that the combined teaching of Umeda and Inoue under the combination of Umeda, Inoue and Jaeger discloses this claim element.

b. Claim 2

147. **Claim 2.** The method of claim 1, wherein a first one of the distinct digital codes comprises a shifted digital bit sequence of a second one of the distinct digital codes. As I have previously discussed for claim element 1.B, Umeda teaches using PN codes as the claimed "distinct digital codes," and the PN codes disclosed in Umeda are bit-shifted versions of each other. For example, the PN code (t1) shown in Fig. 7B of Umeda is a "shifted digital bit sequences" of PN code (t2). Therefore, it is my opinion that claim 2 is disclosed by Umeda.

FIG. 7B



Umeda (Ex. 1007) at Fig. 7B

c. Claim 3

148. **Claim 3.** The method of claim 1, further comprising adjusting a frequency of the first and second signals based on observed noise in the resultant signals. In my opinion, the combination of Umeda, Inoue and Jaeger discloses this claim. As discussed above in the section for overview of Umeda, Umeda recognizes certain weaknesses in the prior art capacitive position sensor that results in reduced SNR. Umeda at 2:17-24. Specifically, Umeda recognizes that the changes in capacitances at the intersections of the column lines and row lines of capacitive electrodes are small when the column lines are activated one at a time and the external noise is close to the frequency of the drive signals activating the column lines. *Id*. at 2:17-61. To enhance the SNR of the measured capacitance change, Umeda teaches capacitive position sensing circuitry that use a column-line driver to simultaneously drive multiple column lines of electrodes. *Id.* at 2:65-3:31.

Umeda also teaches using a code generator to generate distinct orthogonal codes (e.g., Walsh orthogonal codes) or pseudorandom (e.g., M-series PN codes) and applying drive signals modulated using the distinct pseudorandom or orthogonal codes to the multiple column lines simultaneously. *Id*. at 2:65-3:52; 4:52-67. Driving multiple column lines simultaneously using drive signal modulated with the distinct orthogonal codes or pseudorandom codes enhances the SNR properties because effects of noise and interference on the measured capacitance change are reduced. *Id*. at 2:65-3:7; 3:32-52.

149. Similar to Umeda, Inoue recognizes certain weaknesses in the prior art capacitive sensors that apply a scan signal at a fixed frequency. The prior art capacitive sensors are adversely affected by external noise that exists at the frequency of the scan signal. Inoue at 3:10-25; 7:5-11. Inoue teaches a capacitive sensing coordinate input device, such as a tablet device that can detect the contact position of at least one input object, such as an input pen or a finger, on the tablet device and improve the SNR properties. *Id.* at Abstract, 1:5-2:67; 4:10-5:24; Figs. 1 and 4. Specifically, the controller disclosed in Inoue, as discussed in Claim Element 1.Preamble, applies multiple scan signals at different frequencies until the scan signal frequency is identified that coincides with minimal observed noise. Inoue uses a noise level measurement section to measure the current noise level of

the sensed digital signal. *Id.* at 6:57-59. When the measured noise level is at or close to the worst measurement index, the CPU 22 drives the scan signal switching section to generate another scan signal to replace the current scan signal at a different frequency. *Id.* at 6:59-7:4, *see also* 5:34-6:59, Fig. 3.

FIG. 3

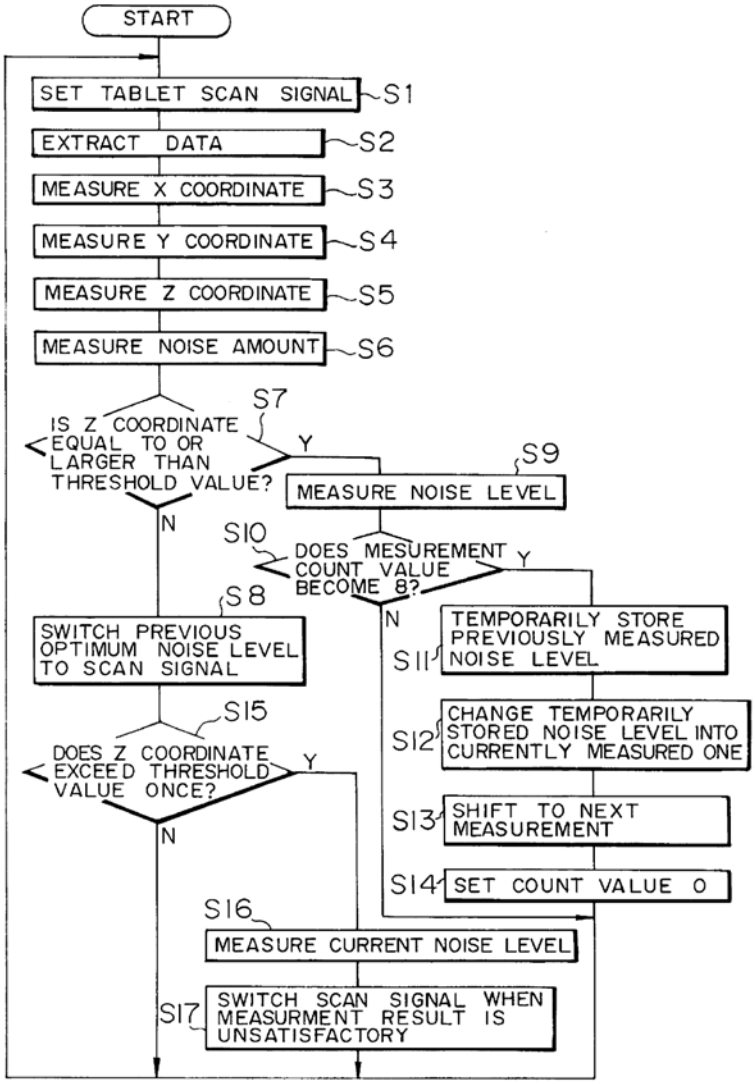


FIG. 3 of Inoue

Shenzhen Huiding Tech. Co., Ltd. - Exhibit 1006

150. By adjusting the scan signal frequency based on the observed noise level, the influence of the external noise can be minimized and the reliability of the touch position detection is improved. *Id.* at 7:26-8:10. Thus, Inoue teaches adaptively adjusting the frequency of the scan signal based on the observed external noise at the corresponding frequency of the scan signal until a frequency with the minimal external noise is selected for the scan signal. Inoue at 5:25-7:25; *see also* 3:10-25; 7:5-11. By adaptively adjusting the frequency of the scan signal, Inoue minimizes the influence of external noise and improves the reliability of the touch position detection. *Id.* at 3:10-25; 7:11-18. Therefore, this claimed element is taught by Inoue.

151. Similar to Inoue, Umeda recognizes various noise-related technical issues in capacitive touch sensing due to the small changes in the capacitances at the intersections to be measured and due to other sources that generate noise. Ex. 1007 at 2:9-61. In particular, as discussed above, Umeda recognizes the need to improve the SNR of the prior art capacitive sensors. Umeda chooses to simultaneously apply distinct orthogonal or PN codes to multiple column lines to increase the capacitance change and reduce the influence of external noise. Umeda also recognizes that an external noise source, such as a fluorescent light at a frequency close to the sampling frequency of the capacitor detecting circuit can

adversely affect the SNR. *Id.* at 2:51-61. Specifically, Umeda recognizes that the disturbance caused by the external noise source at the conflicting frequency reduces the SNR of the capacitor detecting circuit. *Id.* at 2:51-61.

152. To improve the SNR, Umeda's controller uses the capacitance detecting circuit 100, the code generator 1 and column line driver 5 to apply various driving modes to drive the column lines in the sensor unit 4 based on distinct digital codes to improve the noise performance in capacitive touch sensing. Applying different PN codes or Walsh codes in the drive signals will cause differences in the wideband spectra of the resultant signals, as well known in the spread spectrum technology explained by Jaeger's description related to FIG. 1B for touch sensing. Ex. 1011 at 4:30-5:9, 3:27-56, 6:22-27. Therefore, the teachings in Umeda and Jaeger on using PN or Walsh codes for touch sensing is based on spreading the signal spectrum over a wide band to improve the signal to noise ratio in the signal detection. Such teachings in Umeda and Jaeger are related to signal manipulation to cause a change in the signal spectral pattern in touch sensing but, do not explicitly disclose adjusting a frequency of the signals based on observed noise in the resultant signals.

153. In light of the various connections and relationships between Umeda, Jaeger and Inoue, faced with the similar noise interference problem described in

Umeda and Jaeger, a person of ordinary skill in the art would be motivated to look into closely related literature for a solution such as Inoue which teaches adjusting the operating frequency or the frequency of the drive signal to minimize the noise interference at the conflicting frequency and to enhance the SNR, in the touch sensing in Umeda and Jaeger. For example, in light of the teachings in Inoue, Umeda can be modified to select one Walsh code verses another since different Walsh codes have different frequency content. A person of ordinary skill in the art would have recognized that Inoue provides an additional tool to improve the SNR of the capacitive sensors in Umeda, which will improve the reliability and accuracy of the position sensing. For example, a person of ordinary skill in the art may apply the frequency adjustment feature taught in Inoue to Umeda's device by adjusting the carrier frequency that is being spread by the distinct digital codes. One way of performing such carrier frequency adjustment is to change the speed for clocking out the pseudo-random bits. Just as taught in Inoue, the observed noise would be used to choose the clocking (or carrier) frequency associated with the minimal noise. The rate at which the distinct digital codes of Umeda and Jaeger are clocked out to the drive electrodes would be controlled by the "adjust a frequency of the first and second signals based on observed noise in the resultant signals" as taught by Inoue. Adjusting the clocking frequency (as taught by Inoue) will affect the

Shenzhen Huiding Tech. Co., Ltd. - Exhibit 1006

rate at which the first and second (and all other) distinct digital codes are applied to the drive electrodes.

d. Claim 4

154. **Claim 4.** The method of claim 1, wherein simultaneously applying comprises: applying the first modulation signal using a first signal path coupled to the first transmitter electrode; and applying the second modulation signal using a second signal path coupled to the second transmitter electrode. In my opinion, both Umeda and Inoue teach applying modulation signals to first and second transmitter electrodes using different signal paths. For example, in Umeda, the modulation signal applied to the first transmitter electrode C1 is applied through the signal path comprising shift register 23_1, inverting circuit 24_1, and driver circuit 5_1. *See, e.g.*, Umeda (Ex. 1007) at Fig. 9. In comparison, the modulation signal applied to the second transmitter electrode C2 is applied through another signal path, comprising shift register 23_2, inverting circuit 24_2, and driver circuit 5_2. *Id.*

Shenzhen Huiding Tech. Co., Ltd. - Exhibit 1006

FIG. 9

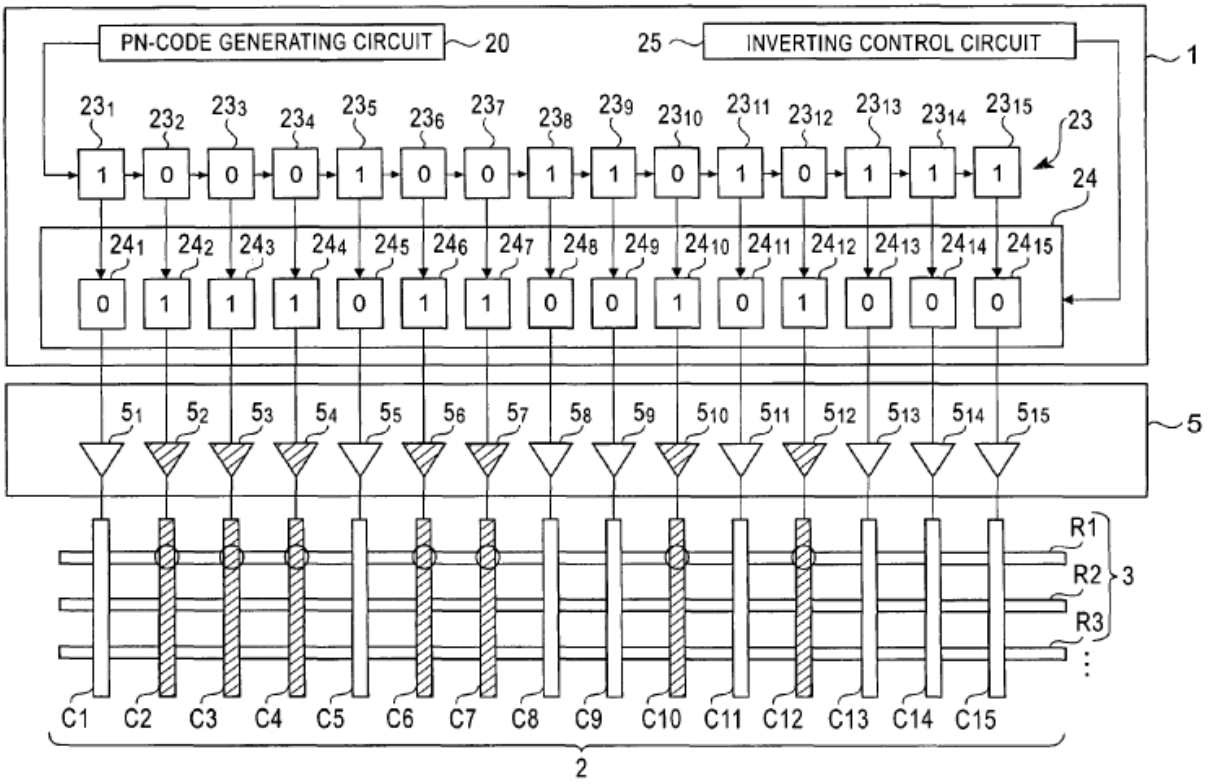


Fig. 9 of Umeda

155. Similarly, in Inoue, the modulation signal applied to the first transmitter electrode X_1 is applied through signal path comprising oscillation circuit 23, drive selection circuit 24, and switch S1, and the modulation signal applied to the second transmitter electrode X_2 is applied through signal path comprising oscillation circuit 23, drive selection circuit 24, and switch S2. *See, e.g.*, Inoue at Fig. 1. Therefore, it is my opinion that both Umeda and Inoue teaches this claim.

e. Claim 5

156. **Claim 5.** The method of claim 4, wherein the first and second signal paths each comprise at least one of an amplifier and a driver. In my opinion, both Umeda and Inoue teach the use of an amplifier, a driver, or both, in their touch sensing devices. In Umeda, the capacitance detecting circuit includes, among other components, charge amplifier circuits 6, which further contain operational amplifiers 121 in them. *See, e.g.*, Umeda at 6:5-6; 6:25-27; 8:1-14; 9:10-24; Figs. 1, 5, 13, 17 and 27. Column-line drivers are also disclosed in Umeda, which can drive the plurality of column lines based on the distinct digital codes, as discussed in claim 1. *See, e.g.*, *id.* at Abstract, 3:13-16, 3:24-31, 7:53-61; 8:45-52; Figs. 4, 9-12, 17, 21, 23, 24 and 27.

157. Similar as Umeda, Inoue's touch sensing device also contains an amplifier and a driver, as represented by the triangle symbol in the oscillation circuit 23. *See, e.g.*, Inoue at Fig. 1. In addition, Inoue's device uses amplification circuits 19 and 25 to amplify signal voltages. *See, e.g.*, Inoue at 4:30-41; 5:4-49; Fig. 1.

158. In addition to the teachings in Umeda and Inoue, it is my opinion that amplifiers and drivers are standard off-the-shelf circuit components, and a person

Shenzhen Huiding Tech. Co., Ltd. - Exhibit 1006

of ordinary skill in the art would find it obvious to use both amplifiers and drivers in signal paths that transmit modulation signals to electrodes, as recited in claim 5.

f. Claim 6

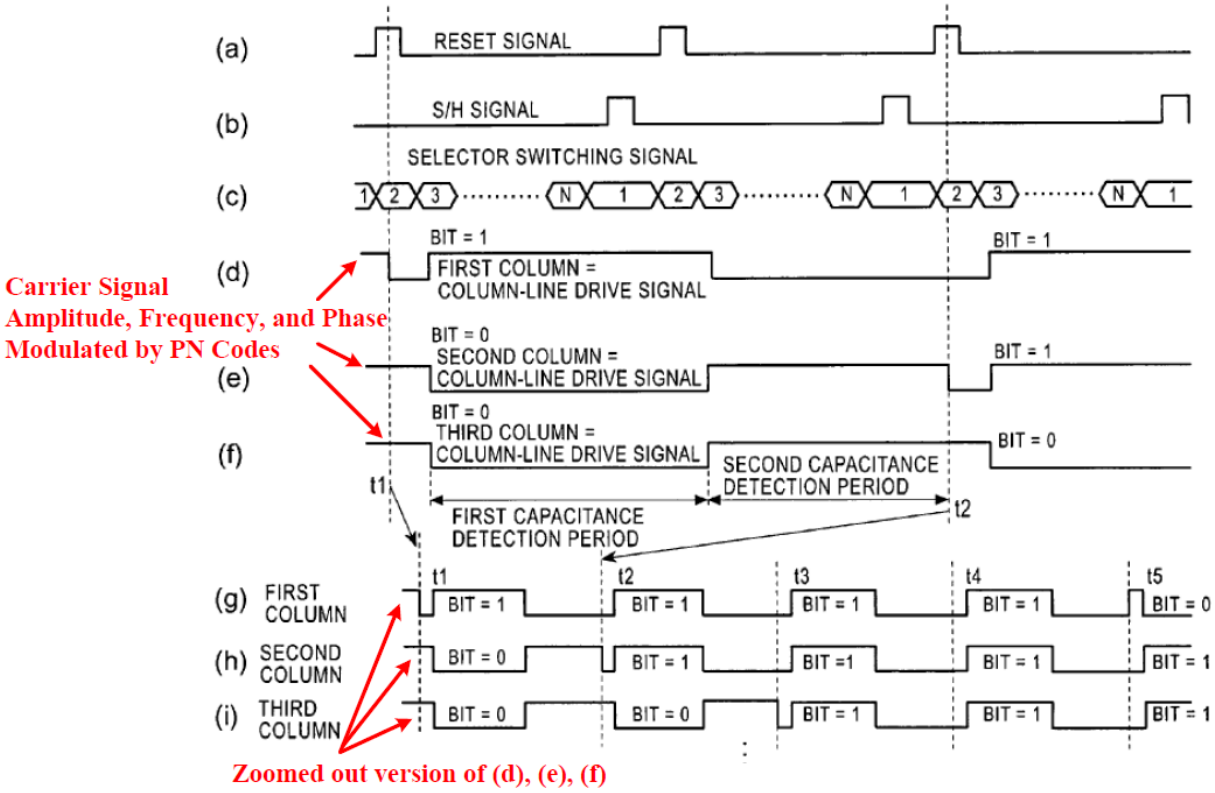
159. **Claim 6.** The method of claim 1, wherein simultaneously applying comprises frequency modulating a carrier signal according to the distinct digital codes. Frequency modulation is expressly taught in Jaeger, which discloses that "process of spectral spreading is accomplished by, e.g., coding the information bits or the carrier frequency with one or more wideband codes having continuous bandwidths." Jaeger (Ex. 1011) at 3:42-46. In addition, as I described in the TECHNOLOGY BACKGROUND section, it is well known in communications to modulate a carrier signal according to the distinct digital codes using one of several standard modulation schemes that uses frequency, amplitude, or phase modulation.

g. Claim 7

160. **Claim 7.** The method of claim 1, wherein simultaneously applying comprises phase modulating a carrier signal according to the distinct digital codes. In my opinion, Umeda teaches two such modulation schemes, specifically amplitude and phase modulating a carrier signal according to the distinct digital code. Umeda (Ex. 1007) at Abstract, 4:14-24, 7:21-28, 7:51-67, 8:53-9:3, 11:48-58, 12:4-21, 13:3-13, 13:21-27, 14:32-47, 15:1-19, 16:42-49, 16:62-17:5, 17:14-20, 21:9-23, Figs. 8 and 22. FIGS. 8 and 22 of Umeda are timing charts that illustrate

the carrier signals modulated by the distinct digital codes, such as the pseudorandom noise (PN) codes (*see* Fig 8, (d), (e), (f), (g), (h), and (i)) or orthogonal codes, e.g., Walsh codes (*see* Fig 22, (d), (e), (f), (g), (h), and (i)). In Fig. 8, when the value of the orthogonal Walsh code or PN code is 1, the amplitude of the column-line drive signal is modulated to shift from a first voltage to a second voltage during the first capacitance detection period. *Id.* at 4:14-24, 8:53-9:3, 11:48-58, 12:4-21, 13:3-13, 13:21-27, 14:32-47, 15:1-19, 16:42-49, 16:62-17:5, 17:14-20, 21:9-23, Figs. 8 and 22. When the value of the orthogonal Walsh code or PN code is 0, the amplitude of the column-line drive signal is modulated to shift from the second voltage to the first voltage during the first capacitance detection period. *Id*. Thus, Umeda amplitude modulates the carrier signal by the values of the first and second voltages based on whether the bit value of the distinct digital code is 1 or 0. Similarly Umeda phase modulates the carrier signal since the changes between first and second voltage levels result in modulated signals that are out of phase with each other.

FIG. 8



Id. at FIG. 8

FIG. 22

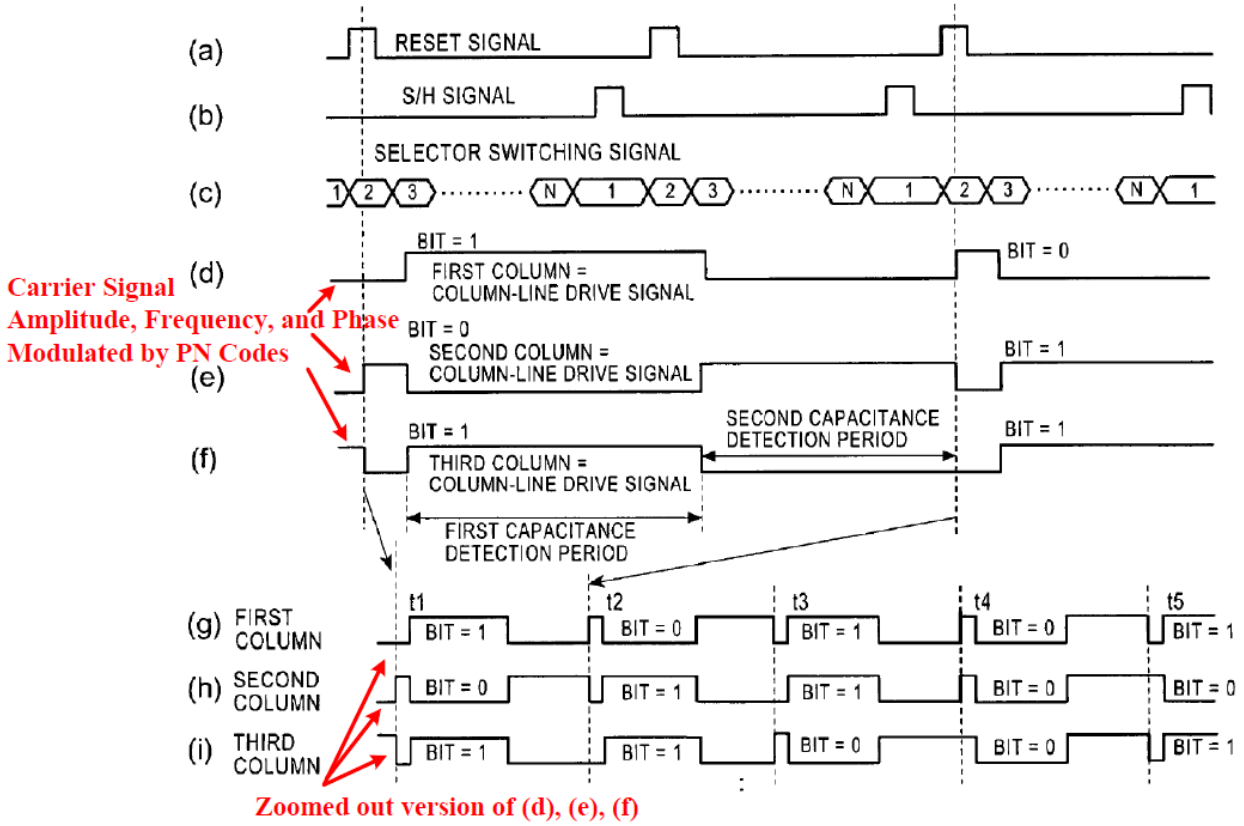


FIG. 22 of Umeda

161. In addition, Umeda teaches phase modulating the carrier signal during the second capacitance detection period when complementarily driving the column lines "using the inverted data of the bit data of the PN code that drove the column lines in the first capacitance detection period." *Id.* at Abstract, 3:32-52; 5:14-21; 10:41-54; 22:29-23:59; 24:32-25:35; 26:27-25; 27:46-67. Complementarily driving the column lines using the inverted data results in inverted modulated signals that are 180 degrees out of phase with the signal driven with the non-inverted data.

162. As shown in the timing charts of Figs. 8 and 22, the column-line drive signals modulated by the distinct digital codes (d), (e), and (f) (and zoomed out versions (g), (h), and (i)) are carrier signals because they are periodic pulse signals having a steady waveform -- constant voltage amplitude and frequency. The modulated signals (d), (e), (f), (g), (h), and (i) used to drive the column lines are -- the carrier signals modulated by the PN codes or Walsh codes to drive the column lines at a specific voltage depending on the value of the PN codes or Walsh code. For example, see 11:48-58 and 12:15-21 of Umeda describing the column line drive pulses modulated by the PN codes to modulate the amplitude to predetermined voltage levels H and L.

> Then, the driver circuit **5** drives the corresponding column lines based on the bit string {0, 0, 0, 1, 0, 1, 0, 0, 1, 1, 0, 1, 1, 1, 0} input from the inverting portions $\mathbf{24}_{15}$ through $\mathbf{24}_{1}$.
>
> Then, in the column lines C**1** through C**15**, column lines C**2**, C**3**, C**4**, C**6**, C**7**, C**10**, and C**12** are shifted as a second column line group to the second voltage (predetermined voltage at H level) in accordance with the bit data **1**, while column lines C**1**, C**5**, C**8**, C**9**, C**11**, C**13**, C**14**, and C**15** are shifted as a first column line group to the first voltage (predetermined voltage at L level) in accordance with the bit data **0**.

Id. at 11:48-58

Shenzhen Huiding Tech. Co., Ltd. - Exhibit 1006

> That is, the column line driver **5** drives the column lines C**15**, C**14**, C**13**, C**12**, C**11**, C**10**, C**9**, C**8**, C**7**, C**6**, C**5**, C**4**, C**3**, C**2**, and C**1** by the driver circuits $\mathbf{5}_{15}$, $\mathbf{5}_{14}$, $\mathbf{5}_{13}$, $\mathbf{5}_{12}$, $\mathbf{5}_{11}$, $\mathbf{5}_{10}$, $\mathbf{5}_{9}$, $\mathbf{5}_{8}$, $\mathbf{5}_{7}$, $\mathbf{5}_{6}$, $\mathbf{5}_{5}$, $\mathbf{5}_{4}$, $\mathbf{5}_{3}$, $\mathbf{5}_{2}$, $\mathbf{5}_{1}$, respectively, according to drive pulses having predetermined regular pulse widths based on the clock signal output from the timing control circuit **11** (see (d) through (i) of FIG. **8** and (b) of FIG. **13**).

Id. at 12:15-21

163. Umeda clearly teaches driving the column lines using drive pulses as illustrated in "(d) through (i)" of Figs. 8 and 22 indicating that both the column line drive pulses and the PN code or Walsh code are used to generate the modulated drive signals. *Id.* at 4:14-24, 8:53-9:3, 11:48-58, 12:4-21, 13:3-13, 13:21-27, 14:32-47, 15:1-19, 16:42-49, 16:62-17:5, 17:14-20, 21:9-23, Figs. 8 and 22.

164. In addition, because Umeda teaches using the Walsh orthogonal codes or PN codes to simultaneously drive the column lines, a person of ordinary skill in the art would have been motivated to use any of the standard amplitude, frequency, or phase modulation schemes available for modulating with the Walsh orthogonal codes or PN codes. In addition, Umeda understood the usefulness of code division multiple access (CDMA) techniques for simultaneously activating multiple column lines using drive signals based on PN-code bit strings by recognizing that "[t]he characteristics of this PN code is similar to the principle of multiplexing/demultiplexing in code division multiple access (CDMA) used in cellular telephones . . . ." *Id.* at 10:20-24. As discussed above, a number of

standard modulation schemes exist in CDMA for modulating a carrier signal using frequency, amplitude, or phase modulation. *See* Dixon (Appendix HH) at 16; Prasad (Ex. 1010) at right col., lines 44-49 at p. 5; Simon (Appendix II) at pp.12-13. In light of the recognition by Umeda of the usefulness of CDMA techniques in simultaneously activating multiple column lines using PN codes and Walsh orthogonal codes, a person of ordinary skill in the art would have been motivated to select any one of the standard modulation schemes available in CDMA, including amplitude, frequency, and phase modulation.

h. Claim 8

165. **Claim 8.** The method of claim 1, wherein simultaneously applying comprises amplitude modulating a carrier signal according to the distinct digital codes. See my discussions above for claim 7.

i. Claim 9

166. **Claim 9.** The method of claim 1, wherein the distinct digital codes are mathematically independent. In my opinion, Umeda teaches the features of this claim. In simultaneously activating multiple column lines, Umeda teachings generating two types of distinct digital codes. Umeda (Ex. 1007) at 3:48-52; 4:56-67; 6:42-44; 7:21-28; 9:43-55; 19:64-20:2; 20:33-41; 21:56-61; 22:10-13; 22:24-26. The two types of distinct digital codes in Umeda include PN-codes, such as M-series codes (also known as maximum length sequence) and orthogonal codes,

Shenzhen Huiding Tech. Co., Ltd. - Exhibit 1006

such as Walsh codes. *Id.* The Walsh codes are mathematically independent because Walsh codes by definition are orthogonal to one other. The M-series codes are mathematically independent because the M-series codes are substantially orthogonal to one another. *Id.* at Abstract; 3:48-52; 4:56-67; 6:42-44; 7:21-28; 9:43-55; 19:64-20:2; 20:33-41; 21:56-61; 22:10-13; 22:24-26; Figs. 7A, 7B, 18.

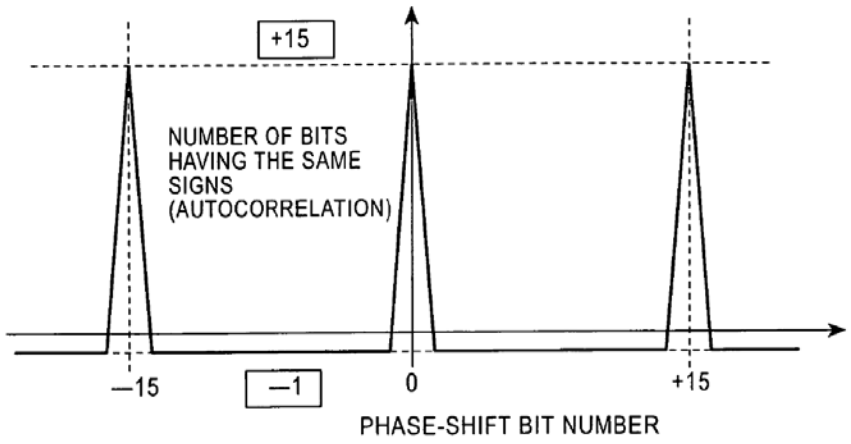


FIG. 7B

PN CODE (t1)	1	1	1	1	0	1	0	1	1	0	0	1	0	0	0
	⊕	⊕	⊕	⊕	⊕	⊕	⊕	⊕	⊕	⊕	⊕	⊕	⊕	⊕	⊕
PN CODE (t2)	0	1	1	1	1	0	1	0	1	1	0	0	1	0	0
	1	0	0	0	1	1	1	1	0	1	0	1	1	0	0

0: NUMBER OF BITS HAVING THE SAME SIGNS = 7
1: NUMBER OF BITS HAVING DIFFERENT SIGNS = 8

FIGS. 7A and 7B of Umeda

Shenzhen Huiding Tech. Co., Ltd. - Exhibit 1006

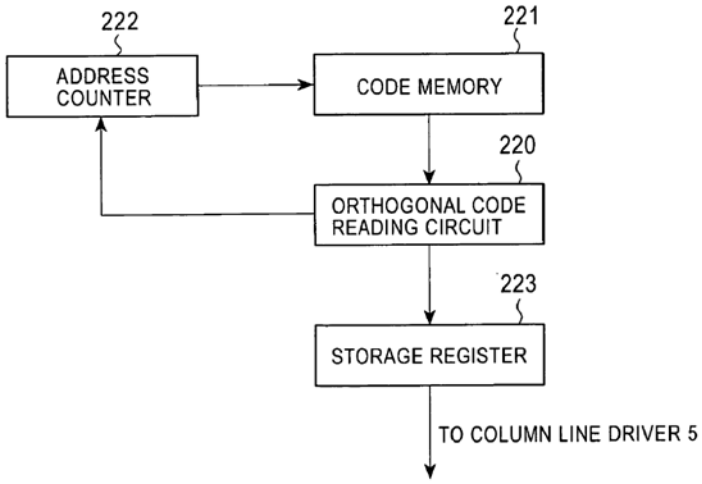


FIG. 18 of Umeda

167. In addition, it is my opinion that Jaeger further discloses using distinct digital codes that are mathematically independent for touch sensing. Ex. 1011 at 4:46-5:9. Examples of such mathematically independent distinct digital codes disclosed by Jaeger include PN code, M-sequences, Barker codes, Walsh codes, Gold codes, and Kasami codes. *Id.*

j. Claim 10

168. **Claim 10.** The method of claim 1, wherein each of a plurality of the distinct digital codes comprises a shifted digital bit sequence of another one of the plurality of distinct digital codes. *See* discussions in claim 2.

k. Claim 11

169. **Claim 11.** The method of claim 1, wherein the distinct digital codes comprise Pseudo-Random codes. *See* discussions in claim 1, claim 2 and claim 9. Specifically, in my opinion, both Umeda and Jaeger teach the claimed pseudo-

random codes. As discussed for claim element 1.B and claim 4, Umeda discloses using pseudorandom codes such as M-series codes to simultaneously activate multiple column lines in the capacitive sensing circuit. Umeda (Ex. 1007) at 3:32-52; 4:52-63; 5:48-55; 7:21-28; 7:51-67; 8:36-11:26; 12:29-34; 13:28-33; 13:48-58; 14:32-51; 15:1-19; 16:18-22; 17:21-26; 17:46-20:2; 26:35-40; 26:53-57; 26:59-27:24; 27:60-28:8; claim 9; Figs. 6A, 6B, 7B, 9-12, 14, 15, 16. In addition, Jaeger discloses PN codes as examples of suitable distinct digital codes for touch sensing. Ex. 1011 at 4:46-5:9 (disclosing a "pseudo-random (PN) code"); Fig. 1A (showing a 7-bit PN code).

l. Claim 12

170. **Claim 12.** The method of claim 1, wherein the distinct digital codes are binary. In my opinion, both Umeda and Jaeger teach the claimed binary distinct digital codes. *See* above discussions for claims 1, 2 and 9. Umeda teaches examples of using orthogonal codes such as Walsh codes or PN codes to simultaneously activate multiple column lines. Umeda at 2:65-3:52; 4:52-67; 9:25-67; 10:47-11:9; 11:20-26; Figs. 1, 6A, 6B, 8, 9. The Walsh orthogonal codes and the PN codes used in Umeda are binary codes having values of 0 and 1. *Id.* at Figs. 6A, 6B, 14-16, 20, 31.

Shenzhen Huiding Tech. Co., Ltd. - Exhibit 1006

171. In addition, Jaeger discloses PN codes which can be binary. Ex. 1011 at 4:46-5:9; Fig. 1A (showing a binary PN code). For other types of codes disclosed in Jaeger, i.e., "M-sequences, Barker codes, Walsh codes, Gold codes and Kasami codes," a person of ordinary skill in the art readily understands that they can be binary too. Ex. 1011 at 4:46-5:9.

m. Claim 13

172. **Claim Element 13.Preamble:** A controller for a position sensor, comprising: *See* discussions for Claim Element 1.Preamble.

173. **Claim Element 13.A:** drive circuitry configured to simultaneously transmit a first signal based on a first one of a plurality of mathematically independent binary codes with a first transmitter electrode, and to transmit a second signal based on a second one of the plurality of mathematically independent binary codes with a second transmitter electrode; *See* discussions for Claim Element 1.A, claim 9 and claim 12.

174. **Claim Element 13.B:** receiver circuitry coupled to at least one receiver electrode and configured to receive electrical effects associated with the first and second signals; *See* discussions for Claim Elements 1.A, 1.C.

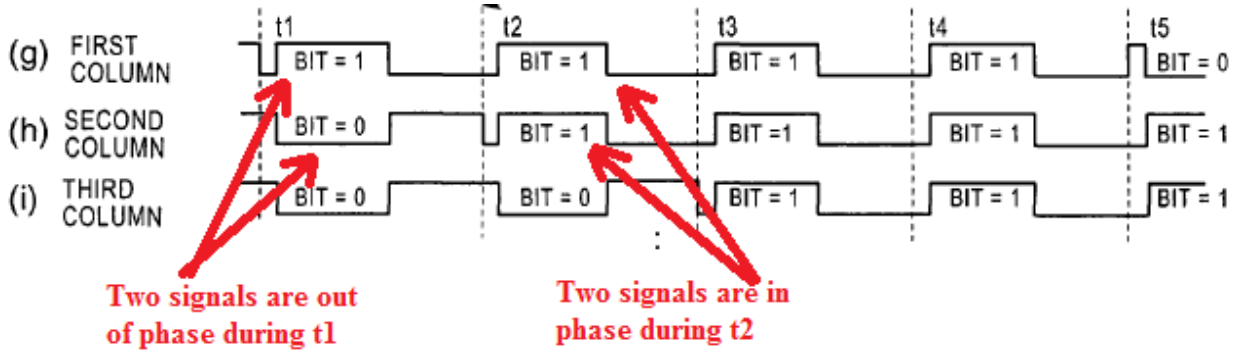
Shenzhen Huiding Tech. Co., Ltd. - Exhibit 1006

175. **Claim Element 13.C:** wherein the controller is configured to determine a position-based attribute of an input object based on the electrical effects. *See* discussions for Claim Element 1.D.

n. Claim 14

Claim 14. The controller of claim 13, wherein the first and second digital codes define the first signal to be in phase with the second signal during a first time, and the first signal to be out of phase with the second signal during a second time. In my opinion, Umeda teaches that the distinct digital codes (PN or Walsh codes) modulate the signals so that the square waveforms applied to different column line drivers are in phase at certain times and out of phase at others. For example, Umeda's Fig. 8, rows (g) and (h) show that the column-line drive signals on the first and second columns are in phase - i.e., are the same as each other - during certain time periods (e.g., during t2, t3, and t4) and 180 degrees out of phase - i.e., are the inverse of each other - during other time periods (e.g., during t1 and t5). Umeda at Fig. 8; *see also id.* at 4:52-55; 6:11-13; 10:1-35; 11:20-26; 13:56-58; 17:54-18:22; 19:52-63; claim 9; Figs. 7A, 7B, 23.

Shenzhen Huiding Tech. Co., Ltd. - Exhibit 1006



Umeda (Ex. 1007) Fig. 8

o. Claim 15

176. **Claim 15.** The controller of claim 13, wherein each of the plurality of mathematically independent binary codes comprises a shifted version of another one of the plurality of mathematically independent binary codes. *See* discussions for Claim 2.

p. Claim 16

177. **Claim 16.** The controller of claim 13, wherein the drive circuitry is further configured to simultaneously transmit a third signal based on a third one of a plurality of mathematically independent binary codes with a third transmitter electrode. *See* discussions for Claim Element 1.Preamble, claim 9 and claim 12. Specifically, Umeda's figures illustrated that 15-bit PN or orthogonal codes can be used to simultaneously transmit 15 signals based on 15 mathematically independent binary codes to 15 transmitter electrodes. *See, e.g.*, Umeda at Figs. 9-12, 21, 23 and 24. Therefore, the claimed limitation of "simultaneously

transmit[ting] a third signal based on a third one of a plurality of mathematically independent binary codes with a third transmitter electrode" is disclosed by Umeda.

q. Claim 17

178. **Claim 17.** The controller of claim 13, further comprising a code generation module configured to generate each of the distinct digital codes. *See* discussions for Claim 1. Specifically, Umeda teaches the claimed "code generation module" because it teaches "a code generator for generating code having orthogonality in chronological order." *See, e.g.*, Umeda at Abstract; 3:11-13; Figs. 1 and 17 (item 1, 1B). Figs. 9-12, 28, and 30 of Umeda further illustrate the internal structure of the code generator 1, which generates PN code using a PN-Code Generating Circuit 20. *Id.* at 4:52-63; 6:7-10; 7:21-25; 9:39-67; Figs. 6, 9-12, 28, 30. Alternatively, the code generator 1B may also generate orthogonal codes by reading out such codes pre-stored in code memory 221, as shown in Figures 21 and 23. *Id.* at 4:64-67; 6:40-49; Figs. 18-21, 23.

r. Claim 18

179. **Claim 18.** The controller of claim 13, wherein the drive circuitry comprises a first signal path between the controller and the first transmitter electrode, and a second signal path between the controller and the second transmitter electrode. *See* discussions for Claim 4.

s. Claim 19

180. **Claim 19.** The controller of claim 18, wherein the first and second signal paths each comprise at least one of an amplifier and a driver. *See* discussions for Claim 5.

t. Claim 20

181. **Claim Element 20.Preamble:** An input device comprising: *See* discussions for Claim Element 1.Preamble. Specifically, an "input device" is explicitly taught by Inoue, which discloses a "coordinate input device." *See, e.g.*, Inoue (Ex. 1008) at Abstract.

182. **Claim Element 20.A:** a first transmitter electrode, a second transmitter electrode, and a plurality of receiver electrodes proximate to and configured to be capacitively coupled with the first transmitter electrode and the second transmitter electrode; *See* discussions for Claim Elements 1.A, 1.C and 13.B.

183. **Claim Element 20.B:** a controller configured to: *See* discussions for Claim Element 13.Preamble.

184. **Claim Element 20.C:** simultaneously apply a first one of a plurality of distinct modulation signals to a first signal path connecting the controller to the first electrode, and a second one of the plurality of distinct

modulation signals to a second signal path connecting the controller to the second electrode, *See* discussions for Claim Element 1.A and claim 4.

185. **Claim Element 20.D:** wherein each of the plurality of distinct modulation signals is based on a different one of a plurality of distinct digital codes; *See* discussions for Claim Element 1.B.

186. **Claim Element 20.E:** receive resultant signals that are electrically affected by the position of the input object from the; plurality of receiver electrodes; *See* discussions for Claim Elements 1.A and 13.B.

187. **Claim Element 20.F:** demodulate the resultant signals using the plurality of distinct digital codes to thereby discriminate electrical effects produced by the input object; *See* discussions for Claim Element 1.C.

188. **Claim Element 20.G:** determine the position of the input object from the electrical effects. *See* discussions for Claim Element 1.D.

189. I have provided as Appendix B a claim chart illustrating how the Challenged Claims are disclosed by Umeda, Inoue and Jaeger on an element-by-element basis.

190. This is the END of my declaration.

Shenzhen Huiding Tech. Co., Ltd. - Exhibit 1006

JOSHUA R. SMITH

Curriculum Vitæ

Computer Science & Engineering
Office Number 556
Paul G. Allen Center for Computer Science & Engineering
Box 352350
Seattle, WA 98195

Phone: 206-685-2094
Fax: 206-543-2969
Email: jrs / cs . uw . edu

EDUCATIONAL HISTORY

Massachusetts Institute of Technology, Cambridge, MA
PhD, Media Arts and Sciences
1999
Electric Field Imaging. Citations: 73

Massachusetts Institute of Technology, Cambridge, MA
MS, Media Arts and Sciences
1995
Toward Electric Field Tomography

University of Cambridge, Cambridge, UK
MA, Natural Sciences (Physics and Theoretical Physics)
1997
Information Processing in Fraunhoffer Diffraction: A Case Study in the Physics of Information

Williams College, Williamstown, MA
BA, Magna Cum Laude, Computer Science, Philosophy
1991
Evolving Dynamical Systems with the Genetic Algorithm

EMPLOYMENT HISTORY

University of Washington
Seattle, WA
Associate Professor (with tenure)
Department of Computer Science and Engineering & Electrical Engineering, 9/14 – Present

University of Washington
Seattle, WA
Associate Professor without tenure (tenure track)
Department of Computer Science and Engineering & Electrical Engineering, 2/11 – 9/14

Intel Research Seattle
Seattle, WA
Principal Engineer, 4/08 – 1/11
Senior Research Scientist, 7/05 - 4/08
Research Scientist, 7/04 – 7/05

Tiax LLC (formerly Arthur D. Little)
Cambridge, MA
Senior Technologist, 1/04 – 7/04

Escher Group LTD.
Cambridge, MA
Chief Scientist & Director, Escher Labs, 4/01 – 12/03
Vice President & Director, Escher Labs, 4/00 – 4/01
Founding Director, Escher Labs 11/98 – 4/00

Other Research Experience

- **Santa Fe Institute**, Santa Fe, NM & **Los Alamos National Laboratory**, Los Alamos, NM. *Research student*, 6/92-9/92, 7/93-8/93. Created Lattice Gas Automata model of polymer dynamics, with application to origin of life studies.
- **Yale University**, New Haven, CT. *NECUSE Undergraduate research fellow in department of Computer Science*, 6/89 - 8/89. Implemented multigrid method for fast modeling of Hopfield Neural Networks; implemented 3d visualization code.
- **SMALL Geometry Research Group,** Williams College, Williamstown, MA. 6/88 – 8/88. *Undergraduate researcher*. Worked on Art Gallery theorems in computational geometry; wrote interactive graph editor.
- **School for Field Studies,** Marine Biology program, St. John, USVI. *Student.* 9/86 – 12/86. Devised and tested underwater method for experimental measurement of fractal dimension of coral.
- **NASA Goddard Institute for Space Studies**, New York, NY. *Graphics Programmer for Global Climate Modeling project*, 6/85-8/85. Wrote visualization software for output of global climate model.

AWARDS AND HONORS

Best Paper Awards

Best Paper, "Sifting Through the Airwaves: Efficient and Scalable Multiband RF Harvesting," IEEE RFID, April 2014

Honorable Mention award, for "Wirelessly Powered Bistable Display Tags," Ubicomp September 2013.

Best Paper, "Ambient Backscatter: Wireless Communication Out of Thin Air," SIGCOMM, August 2013.

Finalist (one of two) for best paper, for "Hybrid Analog-Digital Backscatter: A New Approach for Battery-Free Sensing," IEEE RFID, April 2013.

Best student paper award, for "Hybrid Analog-Digital Backscatter Platform for High Data Rate, Battery-Free Sensing," WiSNet 2013, January 2013.

Best Paper award, for "An Ultra-Low-Power Human Body Motion Sensor Using Static Electric Field Sensing," Ubicomp 2012, September 2012.

Nominated for best paper, for "Optical Localization of Passive UHF RFID Tags with Integrated LEDs" at IEEE RFID 2012, April 2012.

Sezai Innovation Award, for "Promise of unrestricted mobility and freedom with wireless powering
of a Ventricular Assist Device (VAD)," at the 19th congress of the International Society of Rotary Blood Pumps, Louisville, KY September 8th to 10th, 2011.

Shenzhen Huiding Tech. Co., Ltd. - Exhibit 1006

Willem Kolff/Donald B. Olsen Award, for most promising research in the development of artificial hearts, for paper "Innovative Free-Range Resonant Electrical Energy Delivery System (Free-D System) for a Ventricular Assist Device Using Wireless Power," presented at American Society for Artificial Internal Organs (ASAIO), *June 2011.*
Best Paper, "A Capacitive Touch Interface for Passive RFID Tags," *May 2009*, IEEE RFID 2009
Best Demo, "RFID Sensor Networks with the Intel WISP," *Nov. 2008,* Sensys 08

General awards

Allen Distinguished Investigator, for grant proposal "A brain-computer interface to re-animate the limbs following spinal injury: Development of a Brain-Computer-Spinal Interface (BCSI)"
Madrona Prize, for "Ambient Backscatter," awarded to research project with most commercial potential at UW CSE Industrial Affiliates Day 2013.
First Prize, UW Inventor of the Year Poster Contest, for FREE-D, 2013.
Senior Member, IEEE. January 2013.
CIF Postdoctoral Fellow Supervision award, *2010-2011,* **CRA/CCC**
Motorola Fellow, *1995 – 1997,* MIT Media Laboratory
Herchel Smith Scholar, *1991 – 1993,* Emmanuel College, University of Cambridge

Phi Beta Kappa, *1991,***Williams College**
Sigma Xi, *1991,* **Williams College**
NECUSE summer research fellowship, *1989,* **Yale University**

Intel awards

Divisional Recognition Award, *Q4 2009,* **Intel Labs,**
"For rapid resolution of key technical challenges to mobile platform intercept of WREL technology leading to JPF definition with PCCG"
Divisional Recognition Award, *Q2 2009,* **Intel Labs,**
"For a team effort on the WISP Challenge that exceeded expectations in creating a thriving WISP Community"
Special Intel Employee Retention Award, *Oct. 2008*
Divisional Recognition Award, *Q4 2008,* **Corporate Technology Group**
"For delivering first-rate results on aggressive and risky targets to provide three captivating IR technology demonstrations for Justin's stage demos at IDF"
Divisional Recognition Award, *Q3 2008,* **Corporate Technology Group**,
"For leading the formation of a new Personal Robotics community by organizing the inaugural Workshop on Personal Robotics, thereby establishing Intel as a leader in this important emerging field"
Divisional Recognition Award, *Q3 2008,* **Corporate Technology Group**
"For innovation in wireless power with a circuit-based theory that enabled the transmission of 21 watts over 2 feet at 70% efficiency"
Divisional Recognition Award, *Q4 2007,* **Corporate Technology Group**
"For role modeling customer orientation in developing the first Phase Change Memory prototype that could be read, written, and powered wirelessly with no external antenna"
Divisional Recognition Award, *Q2 2007,* **Corporate Technology Group**

Shenzhen Huiding Tech. Co., Ltd. - Exhibit 1006

"For developing a wireless read-write capability for flash memory that led to joint pathfinding with FMG and could lead to wireless capabilities for our future PCM products"

Best Poster, *June 2007,* **Intel Research Symposium**,
Award for "Electric Field Pretouch for Robotic Grasping"

Best Short Talk, *Dec. 2006,* Intel Fellows Mini-Conference on Power
Award for short talk "RF Power Harvesting for Power Efficiency"

AFFILIATIONS AND OTHER APPOINTMENTS

Affiliate Associate Professor, Computer Science & Engineering and Electrical Engineering, *University of Washington, 7/10-2/11*
Affiliate Assistant Professor, Computer Science & Engineering and Electrical Engineering, University of Washington, 6/06 – 7/10 (CSE), 7/05 – 7/10 (EE)
Graduate Faculty Member, University of Washington, 7/08 – 7/13

PUBLICATIONS

Citations: Total Citations: 5196. H-index: 37. i10-index: 76. Citations listed when 10 or more. Source: Google Scholar.

Co-Author Key
1: Graduate students under my supervision
2: Postdoctoral scholars under my supervision
3: Undergraduate students under my supervision
4: Graduate student interns under my supervision (mostly at Intel)
5: Employees under my supervision

Refereed archival journal publications

J1. Power Delivery and Leakage Field Control Using and Adaptive Phased Array Wireless Power System, Benjamin Waters, Brody Mahoney, Vaishnavi Ranganathan, Joshua R. Smith, IEEE Transactions on Power Electronics, Special Issue on Wireless Power Transfer, February 2015.

J2. Energy transmission and power sources for mechanical circulatory support devices to achieve total implantability, JX Wang, JR Smith, P Bonde The Annals of thoracic surgery, Vol 97, Issue 4, pp. 1467-1474, Feb 2014.

J3. Innovative Free-Range Resonant Electrical Energy Delivery System (FREE-D System) for a Ventricular Assist Device Using Wireless Power, Benjamin H. Waters[1], Joshua R. Smith, Pramod Bonde, ASAIO Journal Vol. 60, No. 1, pp. 31-37.

J4. The Emergence of RF-Powered Computing, S. Gollakota, M. Reynolds, J.R. Smith, D. Wetherall, IEEE Computer, Vol. 47, No. 1, pp. 32-39, Jan 2014.

J5. **Enabling Seamless Wireless Power Delivery in Dynamic Environments**, Alanson P. Sample[2], Benjamin H. Waters[1], Scott Wisdom, Joshua R. Smith, (Invited) Proceedings of the IEEE, Vol 101, Issue 6, pp. 1343-1358, June 2013. Citations: 37

J6. **Evaluation of Wireless Resonant Power Transfer Systems with Human Electromagnetic Exposure Limits**, Andreas Christ, Mark G. Douglas, John Roman, Emily B. Cooper, Alanson P. Sample[1], Benjamin H. Waters[1], Joshua R. Smith, Niels

Shenzhen Huiding Tech. Co., Ltd. - Exhibit 1006

Kuster, IEEE Transactions on Electromagnetic Compatibility, Vol. 55, Issue 2, pp. 265-275. April 2013. Citations: 40

J7. **Physical Human Interactive Guidance: Identifying Grasping Principles From Human-Planned Grasps**, Ravi Balasubramanian[2], Ling Xu[4], Peter Brook[3], Joshua R. Smith, Yoky Matsuoka, IEEE Transactions on Robotics (T-RO), Vol. 28 No. 4, pp. 899-910, Aug. 2012. Citations: 22

J8. **Powering a Ventricular Assist Device (VAD) with the Free-range Resonant Electrical Energy Delivery (FREE-D) System,** B. H. Waters[1], A. P. Sample[1], P. Bonde, J.R. Smith. (Invited) Proceedings of the IEEE, vol. 100, No. 1, pp. 138-149, January 2012. Citations: 48

J9. **Toward Total Implantability Using Free-Range Resonant Electrical Energy Delivery System: Achieving Untethered Ventricular Assist Device Operation Over Large Distances**, Benjamin Waters[1], Alanson Sample[1], Joshua Smith, and Pramod Bonde, Cardiology Clinics, Volume 29, Number 4, pp. 609-625. November 2011.

J10. **Wireless strain measurement for structural testing and health monitoring of carbon fiber composites**, Federico Gasco, Paolo Feraboli, Jeff Braun[1], Joshua Smith, Patrick Stickler, Luciano DeOto, Composites: Part A 42, pp. 1263–1274, 2011. Citations: 25

J11. **Analysis, Experimental Results, and Range Adaptation of Magnetically Coupled Resonators for Wireless Power Transfer,** Alanson P. Sample[1], David T. Meyer[3], Joshua R. Smith, IEEE Transactions on Industrial Electronics, Vol. 58, No. 2, pp 544-554, Feb 2011. Citations: 533

J12. **RFID: From Supply Chains to Sensor Nets**, S. Roy, V. Jandhyala, J.R. Smith, D.J. Wetherall, B.P. Otis, R. Chakraborty, M. Buettner[1], D.J. Yeager[1], Y.-C. Ko, A.P. Sample[1], Proceedings of the IEEE, vol.98, no.9, pp.1583-1592, Sept. 2010. Citations: 41

J13. **NeuralWISP: A Wirelessly Powered Neural Interface with 1-m Range,** Daniel J. Yeager[1], Jeremy Holleman, Richa Prasad, Joshua R. Smith, and Brian Otis, IEEE Transactions on Biomedical Circuits and Systems, Volume 3, Issue 6, pp. 379-387, Oct 2009. Citations: 41

J14. **Design of an RFID-Based Battery-Free Programmable Sensing Platform**. A.P. Sample[1], D.J. Yeager[1], P.S. Powledge, A.V. Mamishev, J.R. Smith. IEEE Transactions on Instrumentation and Measurement, Vol. 57, No. 11, Nov. 2008, pp. 2608-2615. Citations: 328

J15. **RFID MAC Performance Evaluation Based on ISO/IEC 18000-6 Type C.** You-Chang Ko, Sumit Roy, Joshua R. Smith, Hyong-Woo Lee, and Choong-Ho Cho, IEEE Communications Letters, Vol. 12, No. 6, June 2008. Citations: 25

J16. **Energy scavenging for inductively coupled passive RFID systems.** B. Jiang[4], J. R. Smith, M. Philipose, S. Roy, K. Sundara-Rajan[4], and A. Mamishev. IEEE Transactions on Instrumentation and Measurement, February 2007, Vol. 56, No. 1, pp. 118-125. Citations: 131

J17. **RFID-Based Techniques for Human Activity Detection.** Joshua R. Smith, Kenneth P. Fishkin, Bing Jiang[4], Alexander Mamishev, Matthai Philipose, Adam Rea, Sumit Roy, Kishore Sundara-Rajan[4]. Communications of the ACM, v48, no. 9, Sep 2005, pp. 39-44. Citations: 159

J18. **Battery-Free Wireless Identification and Sensing.** Matthai Philipose, Joshua R. Smith, Bing Jiang[4], Kishore Sundara-Rajan[4], Alexander Mamishev, Sumit Roy. IEEE Pervasive Computing, Vol. 4, No. 1, January-March 2005, pp. 37-45. Citations: 189

J19. **Imperceptible Sensory Channels.** Joshua R. Smith, (Invited) IEEE Computer, Vol. 37, No. 6, pp. 84-85, June 2004.

J20. **Code Division Multiplexing of a Sensor Channel: A Software Implementation**. Joshua R. Smith, Christopher Salthouse[3], and Neil Gershenfeld. IEEE Journal on

Shenzhen Huiding Tech. Co., Ltd. - Exhibit 1006

Selected Areas in Communications, Vol. 17, No. 4, April 1999, pp 725-731.

J21. **Distributing Identity**. Joshua R. Smith. IEEE Robotics and Automation Magazine, Vol. 6, No. 1, March 1999, pp 49-56. Citations: 30

J22. **Electric Field Sensing for Graphical Interfaces**. Joshua R. Smith, Tom White, Christopher Dodge, David Allport, Joseph Paradiso, and Neil Gershenfeld. Computer Graphics and Applications, Vol. 18, No. 3, 1998, pp 54-61. Citations: 107

J23. **Field Mice: Extracting Hand Geometry From Electric Field Measurements**. Joshua R. Smith. IBM Systems Journal, Vol. 35, No. 3&4, 1996, pp 587-608. Citations: 94

J24. **Lattice Polymer Automata** Steen Rasmussen and Joshua R. Smith. Berichte der BunsenGesellschaft fur Physikalische Chemie 98, No. 9., pp. 1185-1193. 1994, pp 1185-1193. Citations: 24

Conference proceedings and other non-journal articles

C1. **Co-optimization of Efficiency and Load Modulation Data Rate in a Wireless Power Transfer System**, Xingyi Shi,[1] Aaron N. Parks,[1] Benjamin Waters,[1] Joshua R. Smith, ISCAS 2015.

C2. **Active Power Summation for Efficient Multiband RF Energy Harvesting**, Aaron N. Parks,[1] Joshua R. Smith, International Microwave Symposium, Phoenix, AZ, May 2015.

C3. **SAR distribution for a Strongly Coupled Resonant Wireless Power Transfer System**, Xingyi Shi,[1] Benjamin Waters,[1] Joshua R. Smith, IEEE Wireless Power Transfer Conference, Boulder, CO, May 2015.

C4. **Sensor-Aided Teleoperated Grasping of Transparent Objects**, Kevin Huang, Liang-Ting Jiang,[1] Joshua R. Smith and Howard Jay Chizeck, IEEE International Conference on Robotics and Automation (ICRA 2015), Seattle, May 25-30, 2015

C5. **Simultaneously Tuning and Powering Multiple Wirelessly Powered Devices**, Benjamin Waters,[1] Peter Fidelman,[3] Jeffrey Raines,[3] Joshua Smith, IEEE Wireless Power Transfer Conference, Boulder, CO, May 2015.

C6. **WISPCam: A Battery-Free RFID Camera**, Saman Naderiparizi,[1] Aaron N. Parks,[1] Zerina Kapetanovic,[3] Benjamin Ransford,[2] Joshua R. Smith, IEEE RFID, April 15-17 2015. Nominated for best paper award.

C7. **NFC-WISP: A Sensing and Computationally Enhanced Near-Field RFID Platform**, Yi Zhao,[1] Joshua R. Smith, Alanson Sample, IEEE RFID 2015. Nominated for best paper award.

C8. **A Battery-free Object Localization and Motion Sensing Platform**, Yi Zhao[1], Anthony Lamarca, Joshua R. Smith, Ubicomp 2014.

C9. **Powering Wireless Sensor Nodes with Ambient Temperature Changes**, Chen Zhao, Sam Yisrael, Joshua R. Smith, Shwetak Patel, Ubicomp 2014.

C10. **Turbocharging Ambient Backscatter Communication**, AN Parks, A Liu, S Gollakota, JR Smith, Proceedings of the ACM SIGCOMM 2014 conference

C11. **Wi-Fi Backscatter: Internet Connectivity for RF-Powered Devices**, B Kellogg, A Parks, S Gollakota, JR Smith, D Wetherall, Proceedings of the ACM SIGCOMM 2014 conference

C12. **Optimal Coil Size Ratios for Wireless Power Transfer Applications,** Benjamin Waters,[1] Brody Mahoney,[1] Gunbok Lee,[1] Joshua Smith, IEEE International Symposium on Circuits and Systems (ISCAS) 2014.

C13. **Sifting Through the Airwaves: Efficient and Scalable Multiband RF Harvesting**, Aaron Parks[1], Joshua R. Smith, IEEE RFID 2014. ***Winner, Best Paper Award.***

C14. **Wirelessly Powered Bistable Display Tags**, Artem Dementyev[1], Aaron N. Parks[1], Jeremy Gummeson, Deepak Ganesan, Joshua R. Smith, Alanson P. Sample[2], Ubicomp 2013. ***Honorable Mention Award.***

Shenzhen Huiding Tech. Co., Ltd. - Exhibit 1006

C15. **Ambient Backscatter: Wireless Communication out of Thin Air,** Vincent Liu, Aaron Parks[1], Vamsi Talla[1], Shyam Gollakota, David Wetherall, Joshua R. Smith, SIGCOMM 2013. Citations: 67. ***Winner, Best Paper Award.***

C16. **Hybrid Analog-Digital Backscatter: A New Approach for Battery-Free Sensing,** Vamsi Talla[1] and Joshua R. Smith, Proceedings of IEEE RFID, Orlando, Florida, April 2013. ***Finalist (one of two) for best paper award.***

C17. **A Wearable UHF RFID-Based EEG System,** Artem Dementyev[1] and Joshua R. Smith, Proceedings of IEEE RFID, Orlando, Florida, April 2013. Citations: 10

C18. **A battery-free RFID-based indoor acoustic localization platform,** Yi Zhao[1] and Joshua R. Smith, Proceedings of IEEE RFID, Orlando, Florida, April 2013.

C19. **A Unified Framework for Grasping and Shape Acquisition Via Pretouch Sensing**, Liang-Ting Jiang[1], Joshua R. Smith, Proceedings of ICRA 2013, Karlsruhe Germany, May 6-10, 2013.

C20. **Hybrid Analog-Digital Backscatter Platform for High Data Rate, Battery-Free Sensing**, Vamsi Talla[1], Michael Buettner[1], David Wetherall and Joshua R. Smith. IEEE Topical Conference on Wireless Sensors and Sensor Networks (WiSNet 2013), January 20-23, 2013. ***Winner, best student paper award.***

C21. **Design Considerations for Asymmetric Magnetically Coupled Resonators used in Wireless Power Transfer Applications**, Gunbok Lee[1], Benjamin H. Waters[1], Chen Shi[3], Wee Sang Park, Joshua R. Smith, 2013 IEEE Topical Conference on Biomedical Wireless Technologies, Networks & Sensing Systems (BioWireleSS 2013).

C22. **A Wireless Sensing Platform Utilizing Ambient RF Energy**, Aaron Parks[1], Alanson Sample[2], Yi Zhao[1], Joshua R. Smith. IEEE Topical Conference on Wireless Sensors and Sensor Networks (WiSNet 2013), January 20-23, 2013. Citations: 30

C23. **Power consumption analysis of Bluetooth Low Energy, ZigBee, and ANT sensor nodes in cyclic sleep scenario**, Artem Dementyev[1], Stuart Taylor, Joshua R. Smith, Steven Hodges. IEEE Topical Conference on Wireless Sensors and Sensor Networks (RWW 2013). Citations: 15

C24. **Towards falls prevention: a wearable wireless and battery-less sensing and automatic identification tag for real time monitoring of human movements**, Damith Ranasinghe, Roberto Luis Shinmoto Torres, Alanson P. Sample[2], Joshua R. Smith, Keith Hill, and Renuka Visvanathan. 34th Annual International Conference of the IEEE Engineering in Medicine and Biology Society (EMBC 2012), San Diego, 2012. Citations: 10

C25. **An Ultra-Low-Power Human Body Motion Sensor Using Static Electric Field Sensing**, Gabe Cohn, Tien-Jui Lee, Sidhant Gupta, Dan Morris, Josh Smith, Matt Reynolds, Desney Tan, Shwetak Patel. Ubicomp 2012, Pittsburgh, PA. Citations: 19. ***Winner of best paper award.***

C26. **Adaptive Impedance Matching for Magnetically Coupled Resonators,** Benjamin H. Waters[1], Alanson P. Sample[2], Joshua R. Smith. Progress in Electromagnetics Research Symposium (2012), pp. 694-701. Moscow, Russia, 19-23 August 2012. Citations: 15

C27. **Biologically Inspired Grasp Planning Using Only Orthogonal Approach Angles**, Eric Rombokas, Peter Brook[3], Joshua R. Smith, Yoky Matsuoka, Proceedings of the 4th IEEE RAS/EMBS International Conference on Biomedical Robotics and Biomechatronics (BioRob2012), Rome Italy, June 24-27,2012.

C28. **Seashell Effect Pretouch Sensing for Robotic Grasping**, Liang-Ting Jiang[1], Joshua R. Smith, Proceedings of ICRA 2012, St. Paul, MN, USA, May 14-18, 2012. Citations: 12

C29. **Interactive Singulation of Objects from a Pile**, Lillian Chang[2], Joshua R. Smith, Dieter Fox, Proceedings of ICRA 2012, St. Paul, MN, USA, May 14-18, 2012. Citations: 33

C30. **Automatic Extraction of Command Hierarchies for Adaptive Brain-Robot Interfacing**, Matthew Bryan, Griffin Nicoll[3], Vibinash Thomas[3], Mike Chung, Joshua R.

Shenzhen Huiding Tech. Co., Ltd. - Exhibit 1006

Smith, Rajesh P. N. Rao, Proceedings of ICRA 2012, St. Paul, MN, USA, May 14-118, 2012.

C31. **Optical Localization of Passive UHF RFID Tags with Integrated LEDs**, Alanson Sample[1], Craig Macomber[3], Liang-Ting Jiang[1], Joshua R. Smith, Proceedings of the 2012 IEEE RFID Conference, April 3-5, 2012. Citations: 17. ***Nominated for best paper award.***

C32. **An Adaptive Brain-Computer Interface for Humanoid Robot Control**, Matthew Bryan, Joshua Green, Mike Chung, Joshua Smith, Rajesh Rao, Reinhold Scherer, Humanoids 2011, 11th IEEE-RAS International Conference on Humanoid Robots, Bled, Slovenia, October 26th - 28th, 2011. Citations: 19

C33. **Photovoltaic Enhanced UHF RFID Tag Antennas for Dual Purpose Energy Harvesting**, Alanson P. Sample[1], Jeffrey Braun[1], Aaron N. Parks[3], Joshua R. Smith, IEEE RFID 2011. Citations: 24

C34. **Wireless Power for Ventricular Assist Devices: Innovation with the Free-Range Resonant Electrical Energy Delivery System (FREE-D) for Mechanical Circulatory Assist,** Pramod Bonde, Alanson Sample[1], Benjamin Waters[1], Emily Cooper, Yoshiya Toyoda, Robert Kormos, Joshua R. Smith. Proceedings 91st Annual Scientific Meeting of American Association of Thoracic Surgeons, Philadelphia, May 7-11, 2011

C35. **Promise of unrestricted mobility and freedom with wireless powering of a Ventricular Assist Device (VAD),** B. Waters[1], A. Sample[1], J. Smith, P. Bonde, 19th congress of the International Society of Rotary Blood Pumps, Louisville, KY September 8th to 10th, 2011. ***Winner of the Sezai Innovation Award.***

C36. **Innovative Free-range Resonant Electrical Energy Delivery System (FREE-D system) for a Ventricular Assist Device (VAD) using wireless power**, Joshua R. Smith, Alanson Sample[1], Benjamin Waters[1], Yoshiya Toyoda, Robert Kormos, Pramod Bonde. Proceedings 31st Annual Scientific meeting of the American Society for Artificial Internal Organs (ASAIO), Washington, DC, June 10-12, 2011. ***Winner of ASAIO Willem J. Kolff / Don B Olsen Award.***

C37. **Gambit: An Autonomous Chess-Playing Manipulator**, Cynthia Matuszek, Brian Mayton[3], Roberto Aimi, Lifeng Bo, Marc Peter Deisenroth, Robert Chu, Michael Kung, Joshua R. Smith, Dieter Fox, Proceedings of ICRA, Shanghai, China, May 9-13, 2011. Citations: 20

C38. **Numerical Electromagnetic Analysis of Human Exposure for Wireless Power Transfer Systems**, Andreas Christ, Mark G. Douglas, John Roman, Emily B. Cooper, Alanson P. Sample[1], Joshua R. Smith, Niels Kuster. Proceedings of the Tenth International Congress of the European Bioelectromagnetics Association (EBEA 2011), Rome, Italy Feb 21-24, 2011.

C39. **Robot, Feed Thyself: Plugging In to Unmodified Electrical Outlets by Sensing Emitted AC Electric Fields.** Brian Mayton[3], Louis LeGrand[5], Joshua R. Smith. Proceedings of ICRA May 2010.

C40. **Human-Guided Grasp Measures Improve Grasp Robustness on Physical Robot.** Ravi Balasubramanian[2], Ling Xu[4], Peter Brook[3], Joshua R. Smith, Yoky Matsuoka. Proceedings of ICRA May 2010. Citations: 41

C41. **An Electric Field Pretouch System for Grasping and Co-Manipulation.** Brian Mayton[3], Louis LeGrand[5], Joshua R. Smith. Proceedings of ICRA, May 2010. Citations: 26

C42. **A Spotlight on Security and Privacy Risks with Future Household Robots: Attacks and Lessons,** Tamara Denning, Cynthia Matuszek, Karl Koscher, Joshua R. Smith, Tadayoshi Kohno. In the Proceedings of the 11th International Conference on Ubiquitous Computing (UbiComp 2009). Citations: 36

Shenzhen Huiding Tech. Co., Ltd. - Exhibit 1006

C43. **A Capacitive Touch Interface for Passive RFID Tags**, Alanson Sample[1], Daniel Yeager[1], Joshua R. Smith, 2009 IEEE International Conference on RFID (IEEE RFID 2009), April 27-28, 2009. ***Winner of Best Paper award*** Citations: 36

C44. **Experimental Results with two Wireless Power Transfer Systems**, Alanson Sample[1], Joshua R. Smith, 2009 IEEE Radio and Wireless Symposium (RawCon 2009). January 18-22, 2009. Citations: 146

C45. **NeuralWISP: An Energy-Harvesting Wireless Neural Interface with 1-m Range,** Jeremy Holleman, Dan Yeager[1], Richa Prasad, Joshua R. Smith, and Brian Otis, IEEE Biomedical Circuits and Systems Conference (BioCAS 2008), November 20-22, 2008. Citations: 19

C46. **RFID Sensor Networks with the Intel WISP.** Michael Buettner[1], Ben Greenstein, Richa Prasad, Alanson Sample[1], Joshua R. Smith, Daniel Yeager[1], David Wetherall. 6th ACM Conference on Embedded Networked Sensor Systems (Sensys 2008), November 5-7 2008. ***Winner of Best Demo award***. Citations: 31

C47. **RFIDs and Secret Handshakes: Defending Against Ghost-and-Leech Attacks and Unauthorized Reads with Context-Aware Communications,** Alexei Czeskis, Karl Koscher, Joshua R. Smith, Tadayoshi Kohno. 15th ACM Conference on Computer and Communications Security, October 27-31, 2008. Citations: 72

C48. **Revisiting Smart Dust with RFID Sensor Networks** Michael Buettner[1], Ben Greenstein, Alanson Sample[1], Joshua R. Smith, David Wetherall. Seventh ACM Workshop on Hot Topics in Networks (HotNets-VII), Alberta, Canada, Oct 6-7 2008. Citations: 93

C49. **Electric Field Servoing for Robotic Manipulation,** Ryan Wistort[3], Joshua R. Smith. Proceedings of IEEE/RSJ 2008 International Conference on Intelligent Robots and Systems (IROS 2008). Citations: 27

C50. **Wirelessly-Charged UHF Tags for Sensor Data Collection,** Daniel Yeager[1], Richa Prasad, David Wetherall, Pauline Powledge[5], Joshua Smith. IEEE International Conference on RFID 2008. Citations: 86

C51. **An Enhanced RFID Multiple Access Protocol for Fast Inventory.** You-Chang Ko, Sumit Roy, Joshua R. Smith, Hyung-Woo Lee, Choong-Ho Cho. Proc. IEEE Globecom 2007.

C52. **Electric Field Imaging Pretouch for Robotic Graspers.** Joshua R. Smith, Eric Garcia[4], Ryan Wistort[3], Ganesh Krishnamoorthy[4]. Proceedings of IEEE/RSJ 2007 International Conference on Intelligent Robots and Systems (IROS 2007). Citations: 23

C53. **Design of a Passively-Powered, Programmable Sensing Platform for UHF RFID Systems.** Alanson P. Sample[1], Daniel J. Yeager[1], Pauline S. Powledge[5], and Joshua R. Smith. Proceedings IEEE RFID 2007, March 26-28, 2007, Gaylord, Texas, USA. Citations: 111

C54. **A wirelessly powered platform for sensing and computation.** Joshua R. Smith, Alanson Sample[1], Pauline Powledge[5], Alexander Mamishev, Sumit Roy. Proceedings of Ubicomp 2006: 8th International Conference on Ubiquitous Computing. Orange Country, CA, USA, September 17-21 2006, pp. 495-506. Citations: 110

C55. **Energy Harvesting in RFID Systems** Alanson P. Sample[1], Daniel J. Yeager[1], Joshua R. Smith, Pauline S. Powledge[5], Alexander V. Mamishev. International Conference on Actual Problems of Electron Devices Engineering (APEDE), Saratov, Russia, September 2006.

C56. **Sensor Applications in RFID Technology** Daniel J. Yeager[1], Alanson P. Sample[1], Joshua R. Smith, Pauline S. Powledge[5], Alexander V. Mamishev. International Conference on Actual Problems of Electron Devices Engineering (APEDE), Saratov, Russia, September 2006.

Shenzhen Huiding Tech. Co., Ltd. - Exhibit 1006

C57. **ID Modulation: Embedding Sensor Data in an RFID Timeseries**. Joshua R. Smith, Bing Jiang[4], Sumit Roy, Matthai Philipose, Kishore Sundara-Rajan[4], Alexander Mamishev. Proceedings of the Information Hiding Workshop 2005, LNCS 3727, pp 234-246. Citations: 28

C58. **Energy Scavenging for Inductively Coupled Passive RFID Systems**. Bing Jiang[4], Sumit Roy, Kishore Sundara-Rajan[4], Matthai Philipose, Joshua R. Smith, and Alexander V. Mamishev. Proceedings of the IEEE Instrumentation and Measurement Technology Conference, Ottawa, Canada, May 17-19 2005, pp. 984-989. Citations: 37

C59. **FiberFingerprint Identification**. Eric Metois[5], Paul M. Yarin[5], Noah Salzman[5], and Joshua R. Smith. Proceedings of the Third Workshop on Automatic Identification, Tarrytown, NY, March 2002, pp. 147-154. Citations: 35

C60. **Developments in Steganography**. Joshua R. Smith and Christopher Dodge[5]. Proceedings of Information Hiding: Third International Workshop, Dresden, Germany, September/October 1999. Springer-Verlag Lecture Notes in Computer Science Vol. 1768, pp. 77-87. Citations: 30

C61. **Microstructure-Based Indicia**. Joshua R. Smith and Andrew V. Sutherland. Proceedings of the Second Workshop on Automatic Identification Advanced Technologies, Morristown, NJ, October 1999, pp 79-83. Citations: 13

C62. **Stealth Barcodes**. Joshua R. Smith and Barrett Comiskey[3]. Proceedings of the First Workshop on Automatic Identification Advanced Technologies, Stony Brook, N.Y., November 1997.

C63. **Distributed Protocols for ID Assignment**. Joshua R. Smith. Proceedings of the First Workshop on Automatic Identification Advanced Technologies, Stony Brook, N.Y., November 1997.

C64. **Modulation and Information Hiding in Images**. Joshua R. Smith and Barrett O. Comiskey[3]. Presented at the Workshop on Information Hiding, Isaac Newton Institute, University of Cambridge, UK, May 1996; Springer-Verlag Lecture Notes in Computer Science Vol. 1174, pp 207-226. Citations: 342

C65. **Applying Electric Field Sensing to Human-Computer Interfaces** Tom Zimmerman, Joshua R. Smith, Joe Paradiso, David Allport, and Neil Gershenfeld. Proceedings of the ACM Conference on Human Factors in Computing Systems (CHI-95), May 1995. Citations: 190

C66. **Evolving Models of Dynamical Systems with a Genetic Algorithm**. Joshua R. Smith and Donald House. Proceedings of IEE Colloquium on Genetic Algorithms for Control and Systems Engineering, London, April 1992. IEE Digest 1992/106.

C67. **Designing Biomorphs with an Interactive Genetic Algorithm**. Joshua R. Smith. Proceedings of the Fourth International Conference on Genetic Algorithms, San Diego, June 1991. Interactive evolution code from this paper is open source and downloadable via menu option in Ubuntu Linux. Citations: 101

Parts of books (chapters in edited books)

H1. Physical human interactive guidance: Identifying grasping principles from human-planned grasps, R. Balasubramanian, L. Xu, PD Brook, JR Smith, Y Matsuoka, in The Human Hand as an Inspiration for Robot Hand Development, Balasubramanian and Santos Eds, Springer 2014. Citations: 24

H2. **WISP: A Passively Powered UHF RFID Tag with Sensing and Computation,** D.J. Yeager[1], A.P. Sample[1], J.R. Smith, in S.A. Ahson, M. Ilyas Ed., "*RFID Handbook: Applications, Technology, Security, and Privacy*," CRC Press, March 2008. Citations: 49

H3. **Development of Sensing and Computing Enhanced Passive RFID tags Using the Wireless Identification and Sensing Platform,** A.P. Sample[1], D.J. Yeager[1], M.

Shenzhen Huiding Tech. Co., Ltd. - Exhibit 1006

Buettner[1], J.R. Smith, *Development and Implementation of RFID Technology*, Christina Turcu, Ed. , pp. 127-144, InTech, January 2009.

H4. **Range Scaling of Wirelessly Powered Sensor Systems**, Joshua R. Smith, in Wirelessly Powered Sensor Networks and Computational RFID, Joshua R. Smith, Ed., Springer SBM, New York, February 2013.

H5. **History of the WISP Program**, Joshua R. Smith, in Wirelessly Powered Sensor Networks and Computational RFID, Joshua R. Smith, Ed., Springer SBM, New York, February 2013.

H6. **The Wireless Identification and Sensing Platform,** Alanson P. Sample[1], Joshua R. Smith, in Wirelessly Powered Sensor Networks and Computational RFID, Joshua R. Smith, Ed., Springer SBM, New York, February 2013.

H7. **Maximalist Cryptography and Computation on the WISP UHF RFID Tag,** Hee-Jin Chae, Mastooreh Salajegheh, Daniel J. Yeager[1], Joshua R. Smith, and Kevin Fu, in Wirelessly Powered Sensor Networks and Computational RFID, Joshua R. Smith, Ed., Springer SBM, New York, February 2013. Citations: 77

H8. **Wireless Ambient Radio Power,** Alanson P. Sample[1], Aaron N. Parks[1], Scott Southwood[3], Joshua R. Smith, in Wirelessly Powered Sensor Networks and Computational RFID, Joshua R. Smith, Ed., Springer SBM, New York, February 2013.

H9. **A Portable Transmitter for Wirelessly Powering a Ventricular Assist Device Using the Free-Range Resonant Electrical Energy Delivery (FREE-D) System,** Benjamin H. Waters[1], Jordan T. Reed[3], Kara R. Kagi[3], Alanson P. Sample[2], Pramod Bonde, and Joshua R. Smith, in Wirelessly Powered Sensor Networks and Computational RFID, Joshua R. Smith, Ed., Springer SBM, New York, February 2013.

H10. **RFID-Vox: A Tribute to Leon Theremin,** Pavel V. Nikitin, Aaron Parks[1], and Joshua R. Smith, in Wirelessly Powered Sensor Networks and Computational RFID, Joshua R. Smith, Ed., Springer SBM, New York, February 2013.

Books edited

B1. **Wirelessly Powered Sensor Networks and Computational RFID,** Joshua R. Smith (Ed.), Springer SBM, February 2013. Citations: 14

Shenzhen Huiding Tech. Co., Ltd. - Exhibit 1006

U.S. Patents awarded (last updated 5/23/2015)

	Patent number and date * denotes issued	Title	Inventors	Assignee	Citations
P27	*US 8,937,530--- 1/20/2015	Radio frequency identification tags adapted for localization and state indication	Joshua R. Smith, Daniel Yeager Ali Rahimi	Intel Corp	
P26	*US 8,874,451--- 10/28/2014	Personal mail piece and electronic mail tracking system	Joshua R. Smith, Paul M. Yarin, Michael J. Murphy, Andrew V. Sutherland II, Eric Metois	Escher Group LTD	
P25	*US 8,827,889--- 9/9/2014	Method and system for powering implantable devices	Joshua R. Smith, Pramod Bonde, Benjamin H. Waters, Alanson P. Sample	U. Wash & Yale Univ.	
P24	*US 8,643,475--- 2/4/2014	Radio frequency identification secret handshakes	Tadayoshi Kohno, Alexei Czeskis, Karl Koscher, Joshua R Smith	U. Wash. & Intel Corp.	
P23	*US 8,527,284-- 9/3/2013	System for personal mail piece tracking and tracing from multiple sources by user identifier	Joshua R. Smith, Paul M. Yarin, Michael J. Murphy, Andrew V. Sutherland, Eric Metois	Escher Group	
P22	*US 8,502,650 – 8/6/2013	Temporary non-responsive state for RFID tags	Joshua D. Posamentier, Joshua R. Smith	Intel Corp.	
P21	*US 8,446,045 – 5/21/2013	Flat, asymmetric, and E-field confined wireless power transfer apparatus and method thereof	Joshua R. Smith, Alanson P. Sample, Emily B. Cooper	Intel Corp.	
P20	*US 8,299,652 – 10/30/2012	Wireless power transfer apparatus and method thereof	Alanson P. Sample, Joshua R. Smith	Intel Corp.	57
P19	*US 8,222,996 – 7/17/2012	Radio frequency identification tags adapted for localization and state indication	Joshua R. Smith, Daniel Yeager, Ali Rahimi	Intel Corp.	
P18	*US 8,149,120 – 4/3/2012	Temporary non-responsive state for RFID tags	Joshua D. Posamentier, Joshua R. Smith	Intel Corp.	
P17	*US7,956,725 – 6/7/2011	RFID tag with accelerometer	Joshua R. Smith	Intel Corp.	
P16	*US7,825,776 – 11/2/2010	Device configuration with RFID	Joshua R. Smith and Dirk Haehnel	Intel Corp.	14
P15	*US7,646,214 -- 1/12/10	Power harvesting signal line termination	Joshua R. Smith	Intel Corp.	
P14	*US7,633,025 --- 12/15/09	Inertial switch using fully released and enclosed conductive contact bridge	Joshua R. Smith, Kishore Sundara-Rajan	Intel Corp.	
P13	*US7,411,505 --- 8/12/08	Switch status and RFID tag	Joshua R. Smith, Anthony Lamarca,	Intel Corp.	14

Shenzhen Huiding Tech. Co., Ltd. - Exhibit 1006

			Matthai Philipose		
P12	*US7,336,184 --- 2/26/08	Inertially controlled switch and RFID tag	Joshua R. Smith, Matthai Philipose	Intel Corp.	93
P11	*US7251347 --- 7/31/07	System and method for authentication of a workpiece using three dimensional shape recovery	Joshua R. Smith	Escher Group	23
P10	*US7035428 --- 4/25/06	Workpiece authentication based upon one or more workpiece images	Joshua R. Smith	Escher Group	
P9	*US6584214 --- 6/24/03	Identification and verification using complex, three-dimensional structural features	Ravikanth Pappu, Neil Gershenfeld, Joshua R. Smith	MIT	44
P8	*USD450759 --- 11/20/01	Postal indicia for an envelope	Will Crosby, Michael J. Murphy, Joshua R. Smith, Andrew Sutherland	Escher Group	
P7	*US6210771 --- 04/03/01	Electrically active textiles and articles made therefrom	E. Rehmi Post, Margaret Orth, Emily Cooper, Joshua R. Smith	MIT	124
P6	*US6066954 --- 05/23/00	Apparatus for resolving presence and orientation within a defined space	Neil Gershenfeld, Joshua R. Smith	MIT	36
P5	*US6051981 --- 04/18/00	Method and apparatus for characterizing movement of a mass within a defined space	Neil Gershenfeld, Joshua R. Smith	MIT	40
P4	*US6025726 --- 02/15/00	Method and apparatus for determining three-dimensional position, orientation and mass distribution	Neil Gershenfeld, Joshua R. Smith	MIT	74
P3	*US5936412 --- 08/10/99	Method for resolving presence, orientation and activity in a defined space	Neil Gershenfeld, Joshua R. Smith	MIT	41
P2	*US5914610 --- 06/22/99	Apparatus and method for characterizing movement of a mass within a defined space	Neil Gershenfeld, Joshua R. Smith	MIT	58
P1	*US5844415 --- 12/01/98	Method for three-dimensional positions, orientation and mass distribution	Neil Gershenfeld, Joshua R. Smith	MIT	67

Invention disclosures

Application #	Title	Inventors	Assignee
	Generating DC Forces with AC magnetic fields	Joshua R. Smith	University of Washington
	Hemodynamic cooling for LVADs	Joshua R. Smith, Benjamin H. Waters, Pramod Bonde, Sam Asgari	University of Washington
	Impedance Modulated Acoustic Transfer	Joshua R. Smith, Aaron Parks	University of Washington
	Leadless Pacemaker	Joshua R. Smith, Benjamin H. Waters, Pramod Bonde, Sam Asgari	University of Washington
	Wireless power for Left Ventricular	Joshua R. Smith, Benjamin H.	University of

Shenzhen Huiding Tech. Co., Ltd. - Exhibit 1006

	Assist Devices	Waters, Pramod Bonde	Washington
	Improved auto-tuning algorithms for wireless power transfer	Joshua R. Smith, Benjamin H. Waters, Scott T. Wisdom	University of Washington
	Enabling seamless wireless power delivery in dynamic environments	Joshua R. Smith, Alanson P. Sample. Benjamin H. Waters, Scott Wisdom	University of Washington
	Seashell mode acoustic pre-touch sensing	Joshua R. Smith, Liang-Ting Jiang	University of Washington
	Wirelessly Powering Ventricular Assist Devices	Joshua R. Smith, Benjamin Waters, Alanson Sample	University of Washington
	Dynamic wireless power control	Jim Walsh, Gamil Cain, Issy Kipnis, Joshua R. Smith	Intel Corporation
WO-2012-061766	Extendable wireless power delivery for small devices	E. Cooper, J. Smith, A. Sample, J. Neumann	Intel Corporation
WO-2013-066327	Presence and range detection of wireless power receiving device and method thereof	Jim Walsh, Joshua R. Smith, Issy Kipnis	Intel Corporation
2012-0153739 WO-2012-087444	Range adaptation mechanism for wireless power transfer	EB Cooper, S Yang, CJ Bonsavage, JR Smith, AP Sample, AS Konanur	Intel Corporation
WO-2011-037777	HAUT-PARLEUR ALIMENTE SANS FIL	EB Cooper, JR Smith, AP Sample	Intel Corporation
2010-0187913	Wireless power transfer apparatus and method thereof	Joshua R. Smith and Alanson P. Sample	Intel Corporation
2010-0081379	Wirelessly powered speaker	Emily B. Cooper, Joshua R. Smith, Alanson P. Sample	Intel Corporation
2009-0243813	Wireless programming of non-volatile memory with near-field UHF coupling	Joshua R. Smith, Daniel Yeager, Mostafa N. Abdulla, Sean Eilert	Intel Corporation
2007-0132587	Time domain embedding of application information in an RFID response stream	Joshua R. Smith, James A. Landay	Intel Corporation

Shenzhen Huiding Tech. Co., Ltd. - Exhibit 1006

2003-0197878	Data encoding and workpiece authentication using halftone information	Eric Metois, Joshua R. Smith, Paul M. Yarin	Escher Group
2003-0063772	System and method for authentication and tracking of a workpiece that includes an optically active medium	Joshua R. Smith, Eric Metois, Michael J. Murphy	Escher Group
2003-0026448 WO/2003/012727	Data encoding and decoding using angular symbology	Eric Metois, Joshua R. Smith	Escher Group
2002-0095306 WO-2002/027618	Personal mail piece tracing and tracking mechanism	Joshua R. Smith, Paul M. Yarin, Michael J. Murphy, Andrew Victor Sutherland II, Eric Metois	Escher Group
2002-0042808 WO-2002/027617	Method and apparatus for linking data and objects	Joshua R. Smith, Paul M. Yarin, Michael J. Murphy, Andrew V. Sutherland II	Escher Group
WO-2003/032110	System for combining postage, mailing address information, and payment services	Michael J Murphy, Joshua R. Smith, Paul M. Yarin	Escher Group
WO-2000/078032	Data encoding and decoding	Joshua R. Smith	Escher Group

Abstracts, letters, non-refereed papers, technical reports

- **Printed Low Power Amperometric Gas Sensors Employing RF Energy Harvesting**, M.T. Carter, J.R. Stetter, J.R. Smith, A.N. Parks, Y. Zhao, M.W. Findlay, V. Patel. 221st Electrochemical Society Meeting, 2012, Seattle
- **Physicality: Interacting with the Physical World, From Atoms to Humans**, Joshua R. Smith, Beverly L. Harrison, Xiaofeng Ren, Siddhartha Srinivasa. Intel Technology Journal, Volume 14, Issue 1, pp. 46-61. 2010
- **Sensors, Tags, and Security.** Joshua R. Smith. In Proceedings of the State of Technology Conference on Mobile Wireless Technologies for Persons with Disabilities, Atlanta, GA, May 11-12 2004, pp. 60-66.

Other significant research dissemination (web sites, software, Wikis, etc.)

- Wisp Challenge: Wisp hardware awarded to qualifying academic applicants. Over 30 groups using Wisp. Community website: wisp.wikispaces.com.
- WISP Summit, a workshop on WISP organized in conjunction with Sensys 2009. Videos of talks are posted.
- BUGSX artificial evolution software is available free online. It is downloadable through Ubuntu Linux Software Center.

Shenzhen Huiding Tech. Co., Ltd. - Exhibit 1006

OTHER SCHOLARLY ACTIVITY

Invited lectures and seminars

1. National Academy of Engineering 2015 Regional Meeting and Symposium on Reverse Engineering the Brain. Lecture entitled "Engineering Brain Implants," one of 3 invited lecturers from UW faculty. March 19, 2015
2. Allen Distinguished Investigator Life Science Symposium, Scripps Seaside Forum at UC San Diego. "A Brain-Computer Interface to Reanimate the Limbs Following Spinal Injury: Development of a Brain-Computer-Spinal Interface," with Chet Moritz and Adrienne Fairhall, Feb 9, 2015.
3. UW College of Engineering Lecture Series, Cutting the cord: Wireless power for implanted devices. One of 3 invited lecturers from UW Engineering faculty for 2014. November 18, 2014
4. UW CSE Industrial Affiliates, **Invited Keynote**, "Powering the Internet of Things RF-Powered Sensing, Computing, and Communication**,"** October 22, 2014.
5. IEEE RFID-TA 2014 **Invited Keynote**, "RF-Powered Sensing, Computing and Communication", Tampere, Finland, Sept 8, 2014
6. Microsoft Faculty Summit, workshop on Ultra-low Power Computing, "RF-Powered Sensing, Computing, and Communication," July 16, 2014
7. Microsoft Technical Community Network Talk, "Powering the Internet of Things: RF-Powered Sensing, Computing, and Communication," April 8, 2014.
8. ASPLOS 2014, Wild and Crazy Ideas session, **Invited Keynote**, "RF-powered computing and communication," Salt Lake City Utah, Mar 1-5, 2014.
9. PowerMEMS School, "Near field wireless power transfer," London, Dec 2-3, 2013.
10. NASA Jet Propulsion Laboratory, "RF-Powered Sensor-Actuator Systems," June 18, 2013
11. Stanford University, Electrical Engineering Computer Systems Colloquium (EE380), "Wireless Power Transfer and RF Energy Harvesting: New Options for System Designers," June 5, 2013.
12. Northeastern University, First International Summer School on Green Communications and Networking, "Mapping the Space of Wirelessly Powered Systems," May 30, 2013.
13. Robotics Institute, Carnegie Mellon University, "Pretouch Sensing for Manipulation," May 28, 2013
14. University of California, Berkeley, Berkeley Institute of Design Seminar, "Mapping the Space of Wirelessly Powered Systems," May 21, 2013.
15. Georgia Institute of Technology, "Mapping the Space of Wirelessly Powered Systems," May 17, 2013.
16. IEEE RFID 2013, **Invited keynote**, "Wireless power for Left Ventricular Assist Devices," May 2, 2013, Orlando, Fl
17. University of Notre Dame, Department of Electrical Engineering Systems Seminar, "Mapping the Space of Wirelessly Powered Systems," April 10, 2013.
18. Yale University, Yale School of Medicine, Presentation , "Mapping the Space of Wirelessly Powered Systems," March 25, 2013.
19. International Symposium on Cognitive Neuroscience Robotics, UW Seattle (joint with Osaka University), "Sensor Systems for Robotics," February 1, 2013.
20. UW Robotics Colloquium, UW Seattle, "Robotics Research in The Sensor Systems Lab," Jan 25, 2013
21. Microhams (Microsoft Ham Radio club), Redmond, WA, "Connecting Physical and Digital with Sensor Systems," January 14, 2013

Shenzhen Huiding Tech. Co., Ltd. - Exhibit 1006

22. IEEE International Conference on RFID-Technology and Applications 2012, **Invited keynote** talk, "Wirelessly powered sensor systems and computational RFID," Nice, France, November 5-7, 2012.
23. 2012 CMOS Emerging Technologies Conference, **Invited plenary** talk, "Wirelessly powered sensing platforms," July 18-20, 2012, in Vancouver, BC, Canada.
24. Semiconductor Research Corporation (SRC) /Science Foundation Ireland (SFI) / National Science Foundation (NSF) Forum on Integrated Sensors for Cybersystems - FISC 2030, "Wirelessly powered sensor systems" March 22-23, Carton House, Maynooth, Co. Kildare, Ireland. Invitation only workshop.
25. Western Washington American Society of Mechanical Engineers, "Artificial Hearts," Feb 16, 2012.
26. UW EE 592, "Connecting Physical and Digital with Sensor Systems." November 4, 2011.
27. Google (Fremont) Colloquium, "Connecting Physical and Digital with Sensor Systems." April 27, 2011.
28. Northeastern University, Communications and Digital Signal Processing Center (CDSP), Annual CDSP Research Workshop, **Invited keynote** talk: "Connecting Physical and Digital with Sensor Systems", March 25, 2011. Previous (2010) keynote: Russ Tedrake. Host: Kaushik Chowdhury.
29. MIT Enterprise Forum, Seattle WA, March 16, 2011. One of 4 invited to participate in panel entitled "The internet of things." Moderated by Brier Dudley of the Seattle Times.
30. Georgia Institute of Technology, Robotics and Intelligent Machines (RIM) Seminar, "Connecting Physical and Digital with Sensor Systems", February 2011.
31. Columbia University Nanoscale Science and Engineering Center Seminar, "Connecting Physical and Digital with Sensor Systems", January 2011.
32. ICySSS conference, Cypress Semiconductor, Lynnwood, WA, **Invited keynote** talk: "Connecting Physical and Digital with Sensor Systems," September 2010
33. Google, Mountainview, CA "Connecting Physical and Digital with Sensor Systems," April 2010
34. University of Washington, Computer Science and Engineering Colloquium, "Connecting Physical and Digital with Sensor Systems," April 2010
35. Seattle Robotics Society, "Wireless Power and Personal Robotics," March 2010
36. University of Washington, Electrical Engineering Colloquium, "Mapping the space of wirelessly powered systems," January 2010
37. Microsoft Research Colloquium, "Personal Robotics and Wireless Power," February 2009.
38. Northwestern University, McCormick Lecture in Mechanical Engineering, "Electric Field Pretouch for Robotic Manipulation," Nov. 2008.
39. Seattle Robotics Society, "Personal Robotics at Intel," November 2008
40. Semiconductor Research Corporation / National Science Foundation forum on Nanomorphic Systems (invitation only workshop), "Wirelessly-powered platform for sensing and computation: Radiative and resonant-non-radiative wireless power transfer," November 2007. Stanford University, Palo Alto, CA
41. University of Washington, Computer Science and Engineering Colloquium, "New Approaches to Identification and Sensing," May 2005.
42. Stanford University, "Computational Sensing and Perception," April 2004.
43. Intel Corporation, "Computational Sensing and Perception," April 2004.
44. Georgia Institute of Technology, "Computational Sensing and Perception," March 2004.
45. Olin College, "Computational Sensing and Perception," February 2004.
46. MediaLabEurope, "Alien Sensing," January 2004.
47. Massachusetts Institute of Technology, AI Lab Colloquium, "Computational Sensing and Perception," April 2003.

Shenzhen Huiding Tech. Co., Ltd. - Exhibit 1006

48. University of Cambridge (UK), Department of Physics, Cavendish Laboratory, Inferential Sciences Colloquium, "Intelligent Documents," May 2001.
49. Microsoft Research Colloquium, "Electric Field Imaging," June 1998.
50. IBM Research Colloquium, "Electric Field Imaging," June 1998.
51. Microsoft Research Colloquium, "Modulation and Information Hiding." April 1998.
52. University of Cambridge (UK), Department of Physics, Cavendish Laboratory, Inferential Sciences Colloquium, "Toward Electric Field Imaging," 1997.

Talks, demonstrations, ads, etc. (not already listed as conference publications)

- "Wireless Resonant Energy Link," TED Global, Oxford, UK, July 2010.
- "Range adaptation of the Wireless Resonant Energy Link," student Josh Erickson co-presented demo, Research at Intel Day, Computer Museum, Mountainview, CA, July 2010.
- I am featured by name in several Intel TV ads in Intel's "Sponsors of Tomorrow" ad campaign. In one, I am identified by name: "Joshua Smith, Pretouch Robotics Inventor." The ad references my CeBIT demo (described below). Click here to view Intel television ad referencing my robotics research. (I am played by an actor). Another ad that aired in China features a Chinese actor playing me as an "Intel Rockstar" (this is a version of the popular rockstar ad that was played in the U.S., but localized to China). The text of the ad reads "J. Smith: Pulls power from atmosphere." Click here to see Intel television ad referencing my wireless power research.
- "Sponsors of Tomorrow" I appeared in a press conference with Intel CTO Justin Rattner and Intel Fellow Ajay Bhatt (inventor of USB) to discuss my role as a "rockstar" in Intel's ad campaign, Computer Museum, Mountainview, CA, July 2009.
- "A wirelessly powered speaker," student David Meyer co-presented demo, Research at Intel Day, Computer Museum, Mountainview, CA, July 2009.
- "Launching CeBIT with E-Field Pretouch," robotics demonstration with Chancellor of Germany Angela Merkel, Governor of California Arnold Schwarzenegger, and Intel Chairman Craig Barrett. Our robot "Marvin" helped the VIPs cut the ribbon to launch the CeBIT tradeshow. Click here to view video. Student Brian Mayton participated in demo. CeBIT, Hannover, Germany, March 2009.
- "Robotics: Progress and Prospects," Presentation to Intel CEO Paul Otellini, February 2009.
- "Wireless Resonant Energy Link," Intel Developer Forum, San Francisco, CA, Intel CTO Justin Rattner demos WREL in his keynote, Aug 2008. Student Alanson Sample included in demo.
  IDF Taipei, Demo repeated in research keynote, Oct 2008.
- "Electric Field Pretouch," Intel Developer Forum, San Francisco, CA, Intel CTO Justin Rattner demos E-Field Pretouch in his keynote, Aug 2008.
  IDF Taipei, Demo repeated in research keynote, Oct 2008.
- "Personal Robotics at Intel," Presentation to leading academic roboticists at Intel Personal Robotics workshop, which I organized. Santa Clara, CA, July 2008.
- "Electric Field Pretouch for Robotic Grasping," student Ryan Wistort co-presented his novel robot hand design. Research at Intel Day, Computer Museum, Mountainview, CA, July 2008.
- "E-Field Pretouch Robotic Grasper," demonstrated to Intel CEO and Management Committee as part of Technology Strategic Long Range Plan presentation on Computational Perception. October 2007.
- "Personal Robotics," Corporate Technology Group Strategic Staff , October 2007.

Shenzhen Huiding Tech. Co., Ltd. - Exhibit 1006

- "Wisp," demonstration at Intel Developer Forum (IDF) San Francisco. Student Dan Yeager co-presented, September 2007.
- "Futures for RFID in Healthcare," Federal Trade Commission's "Protecting Consumers in the Next Tech-ade," Washington, D.C. November 6-8 2006.
- "WISP," U.W. Department of Computer Science and Engineering Industrial Affiliates Day, Oct. 2006.
- "Wisp" Research at Intel Day, Santa Clara, CA June 2006.
- Intel Capital / Intel Corporate Technology Group Oregon Venture Capital Day "WISP," demo. October 2005.
- Intel Country Fair, Jones Farm, OR, "WISP v0: RFID + 1 bit accelerometer," August 2004.
- PostExpo, Hamburg Germany, "New Technologies for postage." October 2001.
- America's Millennium (U.S. National Millennium Celebration), Hirschorn Museum, Smithsonian Institution, "FiberFingerprint technology." December 2000.
- "FiberFingerprint technology," demonstration in keynote of US Postal Service CTO Norm Lorenz, National Postal Forum, Chicago, IL, September 1999.

Presentations given at conferences (not already listed as conference publications).

- **Brian Mayton**, Eric Garcia, Louis LeGrand, Joshua R. Smith, "Electric Field Pretouch: Towards Mobile Manipulation," RSS 2009 Workshop on Mobile Manipulation in Human Environments
- **Joshua R. Smith**, Ryan Wistort, "Controlling a minimal dynamically stable structure." Poster presentation, *Dynamic Walking*, Delft, Netherlands, May 2008.
- **Joshua R. Smith**, Neil Gershenfeld. "Activating Space with Electric Field Sensing," Talk, *Siggraph Technical Sketches*, Los Angeles, August 1995.
- **Joshua R. Smith** and Donald House, "Evolving Models of Dynamical Systems with a Genetic Algorithm." Poster presentation, *Artificial Life 3*, Santa Fe, New Mexico, June 1992.

Professional society memberships.

IEEE, Member, 1999-2012; Senior Member, 2013-Present
ACM, 2004-Present

Selected Recent Press Coverage

Foreign Policy, 5/20/15, Innovations: Are Potholes a Thing of the Past?
Time, 8/15/13, From the Future: Wireless Devices that Don't Require Batteries
NBC News, 8/13/13, No batteries! Wireless tech recycles airborne radio waves
The Register (UK), 8/14/13, Boffins harvest TV, mobile signals for BATTERY-FREE comms
Technology Review, 8/14/13, Devices Connect with Borrowed TV Signals and Need No Power Source
Fox News, 8/17/13, No Battery Required for This Wireless Device
The Discovery Channel, 8/17/13, No Battery Required for This Wireless Device
Wired, 8/18/13, Ambient Backscatter for battery-free object communication, by Bruce Sterling
Scientific American, 8/19/13, Will TV Stations Power the Internet of Things?
Slashdot, 8/14/13, Wireless Devices Go Battery-Free With New Communication Technique

Shenzhen Huiding Tech. Co., Ltd. - Exhibit 1006

Gizmodo, 8/13/13, Battery-Free Wireless Devices Let You Send Texts After Your Phone Dies
Total 16 National & International Stories, 73 Tech & Specialty Sites from 8/13/2013 – 9/19/2013
International stories include stories in North America, South America, Europe, Africa, Middle East, Asia, and Australia.

Earlier Press Coverage

Daily Distruption, June 2012, Disruptor of the Day: Joshua Smith – A Researcher on The Cutting Edge of Sensor Technology [Q&A].
Technology Review, April 2012, The Computing Trend that Will Change Everything.
GreenBiz, March 2012, What innovations are possible with ultra-efficient sensors?
IEEE Spectrum, March 2012, Is There a Moore's Law for Energy Efficiency?
Technology Review, July 2011, A Heart Pump Without a Cord.
Economist, Print: June 4th 2011, online: April 12, 2011. A wireless heart
New York Times, June 18, 2010. Bye-Bye Batteries: Radio Waves as a Low-Power Source
Economist, June 10, 2010. Power from thin air
New York Times, January 30, 2010. Smart Dust? Not Quite, but We're Getting There
The Times (UK), January 25, 2010. Meet Marvin, the robot that can plug itself in
Technology Review, November 25, 2009. A Battery-Free Implantable Neural Sensor
Seattle Times, June 15, 2009. Intel aims to capture wild electricity
New York Times, August 20, 2008. Intel Moves to Free Gadgets of Their Recharging Cords on WREL & EF Pretouch. Many other press & blog stories were generated along with this one.
TechnologyReview.com, September 17, 2007. Robots That Sense Before They Touch on EF Pretouch Grasping.
CNET News.Com, May 24, 2006. *Sensors: Living off scraps of energy*. Story covers WISP.
TechnologyReview.com, May 15, 2006. *Sensors without batteries*. Story on WISP.
New York Times Magazine, June 11, 2000. *The Document That Can't Be Forged*. Story on FiberFingerprint.
CBS, The Early Show TV coverage of NEC's Occupant Position Detection System.

Shenzhen Huiding Tech. Co., Ltd. - Exhibit 1006

SERVICE

Departmental service

- Director, EE Professional Programs, 2014-2015
- Member CSE Majors Admission Committee, 2014
- Member CSE 5th year Masters Admissions Committee, 2012-2013
- Leader, Communications and Interface thrust, Center for Sensorimotor Neural Engineering (CSNE), 2012 - present
- Leader, Low Power Sensing and Communication theme, Intel Science and Technology Center for Pervasive Computing (ISTC-PC)
- Member of EE Professional Masters Committee, 2011-Present.
- Member of search committee for EE Department 2010-2011 Molecular Engineering faculty search.
- EE Direct Freshman Admits Committee, 2011-2012
- Engineering Discovery Days: 2011, 2012 (April). Demonstrations of robotics and wireless power.

Professional society and other service

Program Committee, Ubicomp 2013

Technical Program Committee Chair for Power Harvesting track, IEEE RFID 2013.

Editorial Board member, International Journal of Wireless Power Transfer Transmission Technology, Cambridge University Press, January 2013 – Present.

Associate Editor, IEEE RFID Virtual Journal. 2013 – Present.

Selection panel for NSF CISE Computer Systems Research grant panel, Arlington, VA 4/11/12—4/12/12.

Selection panel for NIH NHLBI SBIR grants on Novel Technologies for Powering Ventricular Assist Devices, Bethesda, MD, 3/8/2012.

Member of CCC/CRA Study on Robotics (Professional and Service Robotics panel, 7-8 Aug. 2008, San Francisco, CA), creating 15 year U.S. National roadmap for robotics research, which has been presented to the U.S. Congress in a series of briefings; a photo of my EF Pretouch research appears on the cover of the report. Aug 2012: Member of panel updating Robotics Roadmap.

Program Committee member for IEEE RFID 2013, 2012, 2011, 2010, 2009, MedCOMM 2012 (workshop on Medical Communication in conjunction with SigCOMM), Internet of Things (IoT) 2012, RFIDSec 2011, Ubiquitous Computing Systems (UCS) 2010, 2009, RFID Data Management 2008 (RFDM 08), UCS 2007, Pervasive Computing 2006.

Reviewer for ICRA, IROS, RSS, Ubicomp, IEEE Pervasive Computing Magazine, UIST Conference, CHI conference, IEEE Transactions on Image Processing, Eurasip Journal on Applied Signal Processing, Cambridge University Press (Physics section and Engineering section). Chaired Tactile Sensing Session at IROS in 2008 and in 2007.

Shenzhen Huiding Tech. Co., Ltd. - Exhibit 1006

International, national or governmental service

- Federal Trade Commission, "Protecting consumers in the next Techade". Testified on the future of RFID and sensing. Other speakers included Vint Cerf (Google), Eric Horvitz (Microsoft) 2006.
- United States Postal Service, Mail Technology Strategy Council, Member
  2003-2008
- U.S. President's Commission on the Postal Service. My testimony led to new U.S. "Personalized Postage" with custom photographs. Examples of my prototypes are found on pp. 24 and 179 of the report, *2003*
- United States Postal Service, Intelligent Document Task Force, Member, *1999-2003*
- United States Postal Service, Intelligence on Mail for Security Task Force, Industry co-chair for Technology and Infrastructure Sub-Committee, *10/01 – 5/02*
- Smithsonian Institution, National Postal Museum. Appointed Member of the Council of Advisors (Board of directors), National Postal Museum, 2002-2004

Industrial service/Intel Service

Wireless Strategic Patent Team
2007 – *2010*
Sets patent filing targets for the two Intel Corporation IP committees covering wireless technologies. Membership normally restricted to grade P.E. and above.

Wireless Platform Technologies IP Committee
2006 – *2010*
Votes to reject or file patent applications on invention disclosures for Intel Corporation in wireless technology.

Physicality Theme, Intel Research
2006 – *2010*
Leader of one of Intel Research's 5 content themes.

Shenzhen Huiding Tech. Co., Ltd. - Exhibit 1006

Expert Witness Consulting

Wintek vs. TPK. Retained as expert witness by TPK Touch Solutions in *Inter Partes* Review case before Patent Trial and Appeal Board. Touchscreen case. I drafted expert report and gave deposition. Case Nos. IPR2013-00567 and IPR2014-00541.

Shenzhen Huiding Tech. Co., Ltd. - Exhibit 1006

Claim No.	916 Patent Claim Language	Teachings in Umeda (Ex. 1007), Inoue (Ex. 1008) and Jaeger (Ex. 1011)
1.Preamble	A method of detecting a position of an input object with respect to a touch-sensitive region, comprising the steps of:	*See, e.g.*, Umeda at 7:25-28; Figs. 1, 2A, 2B, 4. *See, e.g.*, Umeda at 1:8-9; 2:65-3:7. *See, e.g.*, Umeda at 1:19-25; 7:44-50; Fig. 3. *See, e.g.*, Umeda at 1:8-25; 2:65-3:7; 3:62-4:3; 5:35-40; 27:53-59. *See, e.g.*, Umeda at Figs. 1, 4, 17, 27. *See, e.g.*, Umeda at 2:65-3:7; 3:66-4:2. *See, e.g.*, Inoue at Abstract; 1:6-20; 4:10-29; Figs. 1 and 4. *See, e.g.*, Inoue at 1:21-2:67; 4:10-7:4; Figs. 1, 3 and 4. *See, e.g.*, Inoue at Abstract; 1:6-20; 4:10-29; Figs. 1 and 4.
1.A	simultaneously applying a first one of a plurality of distinct modulation signals to a first electrode and a second one of the plurality of distinct modulation signals to a second electrode to obtain resultant signals that are electrically affected by the position of the input object,	*See, e.g.*, Umeda at 3:8-52; 9:25-67; 10:47-11:9; 11:20-26; Figs. 1, 6A, 6B, 8, 9. *See, e.g.*, Umeda at 12:15-21; 13:14-20; 14:33-47; 17:6-13; Fig. 8. *See, e.g.*, Umeda at 7:15-20:23. *See, e.g.*, Umeda at 10:27-35; 10:46-54. *See, e.g.*, Umeda at 4:14-24; 8:54-64. *See, e.g.*, Umeda at 4:14-31; 8:53-9:18; Fig. 5. *See, e.g.*, Umeda at 9:25-67; 10:47-11:9; 11:20-26, Figs. 1, 6A, 6B, 9. *See, e.g.*, Umeda at 11:27-31, Fig. 9. *See, e.g.*, Umeda at 11: 41-47. *See, e.g.*, Umeda at 11: 48-50. *See, e.g.*, Umeda at 11:51-58; Fig. 8. *See, e.g.*, Umeda at 11:59-64. *See, e.g.*, Umeda at 12:4-14. *See, e.g.*, Umeda at 12:22-28; Fig. 8. *See, e.g.*, Umeda at 12:57-13:13. *See, e.g.*, Umeda at 13:2-13, Fig. 8. *See, e.g.*, Umeda at 16:14-22. *See, e.g.*, Umeda at 16:23-18:4.

Claim No.	916 Patent Claim Language	Teachings in Umeda (Ex. 1007), Inoue (Ex. 1008) and Jaeger (Ex. 1011)
		See, e.g., Umeda at 17:46-53; Figs. 8 and 14. *See, e.g.*, Umeda at 20:25-26:17; Figs. 1, 19-24. *See, e.g.*, Umeda at Fig. 22, rows (d) to (i). *See, e.g.*, Inoue at 1:61-2:15; 2:44-53; 4:60-5:3; 5:14-16; 5:35-40; 6:1-8; 6:64-7:4. *See, e.g.*, Umeda at 7:21-67, Figs. 1 and 4. *See, e.g.*, Umeda at 7:51-67, Fig. 4. *See, e.g.*, Umeda at 20:25-21:8. *See, e.g.*, Umeda at 7:39-43, Fig. 4. *See, e.g.*, Umeda at 12:29-45. *See, e.g.*, Umeda at Fig. 1. *See, e.g.*, Umeda at 7:29-39, Figs. 2A, 2B. *See, e.g.*, Inoue at Abstract, 1:5-2:67; 4:10-5:24; Figs. 1, 4. *See, e.g.*, Inoue at 1:29-34; 4:20-29; Figs. 1, 2, 4. *See, e.g.*, Inoue at 4:20-29, Fig. 2. *See, e.g.*, Inoue at 2:9-43. *See, e.g.*, Inoue at 2:16-33; 5:25-48. *See, e.g.*, Inoue at 2:34-67 and 5:25-7:18.
1.B	wherein each of the plurality of distinct modulation signals is based on a different one of a plurality of distinct digital codes;	*See, e.g.*, Umeda at 20:25-26:17; Figs. 1, 19-24. *See, e.g.*, Umeda at 21:37-22:26, Figs. 19 and 20. *See, e.g.*, Umeda at 21:37-22:26, Fig. 20. *See, e.g.*, Umeda at Fig. 22. *See, e.g.*, Umeda at 17:46-53; Fig. 14. *See, e.g.*, Umeda at Fig. 14. *See, e.g.*, Umeda at Fig. 8.
1.C	demodulating the	*See, e.g.*, Umeda at Figs. 1, 4, 7:44-50.

Shenzhen Huiding Tech. Co., Ltd. - Exhibit 1006

Claim No.	916 Patent Claim Language	Teachings in Umeda (Ex. 1007), Inoue (Ex. 1008) and Jaeger (Ex. 1011)
	resultant signals using the plurality of distinct digital codes to thereby discriminate electrical effects produced by the input object; and	*See, e.g.*, Umeda at Figs. 1, 4, 7:44-8:14, 8:34-44. *See, e.g.*, Umeda at 3:20-24; 3:53-61; 4:56-63; 5:6-13; 5:49-55; 6:34-36; 6:60-62; 7:5-7; 8:34-44; 18:32-20:23; 24:22-25:67; Figs. 16, 26 and 31. *See, e.g.*, Jaeger at 3:42-47, 4:60-63, 6:22-27, 7:59-68, 10:37-38; Figs. 4 (blocks 8, 10, 15), 5, 7B, 11A, 11B, 1.
1.D	determining the position of the input object from the electrical effects.	*See, e.g.*, Umeda at 7:25-28, Figs. 1, 2A, 2B, 4. *See, e.g.*, Umeda at 1:8-9; 2:65-3:7; 3:8-31; 4:4-14; 24:43-50; Fig. 3, 4. *See, e.g.*, Umeda at 1:19-25; 7:44-50; Fig. 3. *See, e.g.*, Umeda at 1:8-25; 2:65-3:7; 3:62-4:3; 5:35-40; 7:44-50; 27:53-59 and Fig. 3. *See, e.g.*, Inoue at Abstract, 1:5-2:67; 4:10-5:24; Figs. 1, 4. *See, e.g.*, Inoue at 1:13-2:67 and Figs. 1, 2, 4. *See, e.g.*, Inoue at 5:54-67.
2.	The method of claim 1, wherein a first one of the distinct digital codes comprises a shifted digital bit sequence of a second one of the distinct digital codes.	See discussion for claim element 1.B. *See, e.g.*, Umeda at Fig. 7B.
3.	The method of claim 1, further comprising adjusting a frequency of the first and second signals based on observed noise in the resultant	*See, e.g.*, Umeda at 2:17-24. *See, e.g.*, Umeda at 2:17-61. *See, e.g.*, Umeda at 2:65-3:31. *See, e.g.*, Umeda at 2:65-3:52; 4:52-67. *See, e.g.*, Umeda at 2:65-3:7; 3:32-52. *See, e.g.*, Inoue at 3:10-25; 7:5-11.

Shenzhen Huiding Tech. Co., Ltd. - Exhibit 1006

Claim No.	916 Patent Claim Language	Teachings in Umeda (Ex. 1007), Inoue (Ex. 1008) and Jaeger (Ex. 1011)
	signals.	*See, e.g.*, Inoue at Abstract, 1:5-2:67; 4:10-5:24; Figs. 1 and 4. *See, e.g.*, Inoue at 6:57-59. *See, e.g.*, Inoue at 6:59-7:4, 5:34-6:59, Fig. 3. *See, e.g.*, Inoue at 7:26-8:10. *See, e.g.*, Inoue at 5:25-7:25; 3:10-25; 7:5-11. *See, e.g.*, Inoue at 3:10-25; 7:11-18. *See, e.g.*, Umeda at 2:9-61. *See, e.g.*, Umeda at 2:51-61. *See, e.g.*, Jaeger at 4:30-5:9, 3:27-56, 6:22-27.
4.	The method of claim 1, wherein simultaneously applying comprises: applying the first modulation signal using a first signal path coupled to the first transmitter electrode; and applying the second modulation signal using a second signal path coupled to the second transmitter electrode.	*See, e.g.*, Umeda at Fig. 9. *See, e.g.*, Inoue at Fig. 1.
5.	The method of claim 4, wherein the first and second signal paths each comprise at least one of an amplifier and a driver.	*See, e.g.*, Umeda at 6:5-6; 6:25-27; 8:1-14; 9:10-24; Figs. 1, 5, 13, 17 and 27. *See, e.g.*, Umeda at Abstract, 3:13-16, 3:24-31, 7:53-61; 8:45-52; Figs. 4, 9-12, 17, 21, 23, 24 and 27. *See, e.g.*, Inoue at Fig. 1. *See, e.g.*, Inoue at 4:30-41; 5:4-49; Fig. 1.

Shenzhen Huiding Tech. Co., Ltd. - Exhibit 1006

Claim No.	916 Patent Claim Language	Teachings in Umeda (Ex. 1007), Inoue (Ex. 1008) and Jaeger (Ex. 1011)
6.	The method of claim 1, wherein simultaneously applying comprises frequency modulating a carrier signal according to the distinct digital codes.	*See, e.g.*, Jaeger at 3:42-46.
7.	The method of claim 1, wherein simultaneously applying comprises phase modulating a carrier signal according to the distinct digital codes.	*See, e.g.*, Umeda at Abstract, 4:14-24, 7:21-28, 7:51-67, 8:53-9:3, 11:48-58, 12:4-21, 13:3-13, 13:21-27, 14:32-47, 15:1-19, 16:42-49, 16:62-17:5, 17:14-20, 21:9-23, Figs. 8 and 22. *See, e.g.*, Umeda at 4:14-24, 8:53-9:3, 11:48-58, 12:4-21, 13:3-13, 13:21-27, 14:32-47, 15:1-19, 16:42-49, 16:62-17:5, 17:14-20, 21:9-23, Figs. 8 and 22. *See, e.g.*, Umeda at Abstract, 3:32-52; 5:14-21; 10:41-54; 22:29-23:59; 24:32-25:35; 26:27-25; 27:46-67. *See, e.g.*, Umeda at 11:48-58 and 12:15-21. *See, e.g.*, Umeda at 4:14-24, 8:53-9:3, 11:48-58, 12:4-21, 13:3-13, 13:21-27, 14:32-47, 15:1-19, 16:42-49, 16:62-17:5, 17:14-20, 21:9-23, Figs. 8 and 22. *See, e.g.*, Umeda at 10:20-24.
8.	The method of claim 1, wherein simultaneously applying comprises amplitude modulating a carrier signal according to the distinct digital codes.	See discussion for claim 7.
9.	The method of claim 1, wherein the distinct digital codes are	*See, e.g.*, Umeda at 3:48-52; 4:56-67; 6:42-44; 7:21-28; 9:43-55; 19:64-20:2; 20:33-41; 21:56-61; 22:10-13; 22:24-26.

Shenzhen Huiding Tech. Co., Ltd. - Exhibit 1006

Claim No.	916 Patent Claim Language	Teachings in Umeda (Ex. 1007), Inoue (Ex. 1008) and Jaeger (Ex. 1011)
	mathematically independent.	*See, e.g.*, Umeda at Abstract; 3:48-52; 4:56-67; 6:42-44; 7:21-28; 9:43-55; 19:64-20:2; 20:33-41; 21:56-61; 22:10-13; 22:24-26; Figs. 7A, 7B, 18. *See, e.g.*, Jaeger at 4:46-5:9.
10.	The method of claim 1, wherein each of a plurality of the distinct digital codes comprises a shifted digital bit sequence of another one of the plurality of distinct digital codes.	*See* discussions in claim 2.
11.	The method of claim 1, wherein the distinct digital codes comprise Pseudo-Random codes.	*See* discussions in claim 1, claim 2 and claim 9. *See, e.g.*, Umeda at 3:32-52; 4:52-63; 5:48-55; 7:21-28; 7:51-67; 8:36-11:26; 12:29-34; 13:28-33; 13:48-58; 14:32-51; 15:1-19; 16:18-22; 17:21-26; 17:46-20:2; 26:35-40; 26:53-57; 26:59-27:24; 27:60-28:8; claim 9; Figs. 6A, 6B, 7B, 9-12, 14, 15, 16. *See, e.g.*, Jaeger at 4:46-5:9; Fig. 1A.
12.	The method of claim 1, wherein the distinct digital codes are binary.	*See* discussions for claims 1, 2 and 9. *See, e.g.*, Umeda at 2:65-3:52; 4:52-67; 9:25-67; 10:47-11:9; 11:20-26; Figs. 1, 6A, 6B, 8, 9. *See, e.g.*, Umeda at Figs. 6A, 6B, 14-16, 20, 31. *See, e.g.*, Jaeger at 4:46-5:9; Fig. 1A.
13.Preamble	A controller for a position sensor, comprising:	*See* discussions for Claim Element 1.Preamble.
13.A	drive circuitry configured	*See* discussions for Claim Element

Shenzhen Huiding Tech. Co., Ltd. - Exhibit 1006

Claim No.	916 Patent Claim Language	Teachings in Umeda (Ex. 1007), Inoue (Ex. 1008) and Jaeger (Ex. 1011)
	to simultaneously transmit a first signal based on a first one of a plurality of mathematically independent binary codes with a first transmitter electrode, and to transmit a second signal based on a second one of the plurality of mathematically independent binary codes with a second transmitter electrode; and	1.Preamble, claim 9 and claim 12.
13.B	receiver circuitry coupled to at least one receiver electrode and configured to receive electrical effects associated with the first and second signals;	See discussions for Claim Elements 1.A, 1.C.
13.C	wherein the controller is configured to determine a position-based attribute of an input object based on the electrical effects.	*See* discussions for Claim Element 1.D.
14.	The controller of claim 13, wherein the first and second digital codes define the first signal to be in phase with the second signal during a first time, and the first signal to be out of phase with the second signal during a second time.	*See, e.g.*, Umeda at Fig. 8; *see also id.* at 4:52-55; 6:11-13; 10:1-35; 11:20-26; 13:56-58; 17:54-18:22; 19:52-63; claim 9; Figs. 7A, 7B, 23.

Shenzhen Huiding Tech. Co., Ltd. - Exhibit 1006

Claim No.	916 Patent Claim Language	Teachings in Umeda (Ex. 1007), Inoue (Ex. 1008) and Jaeger (Ex. 1011)
15.	The controller of claim 13, wherein each of the plurality of mathematically independent binary codes comprises a shifted version of another one of the plurality of mathematically independent binary codes.	*See* discussions for Claim 2.
16.	The controller of claim 13, wherein the drive circuitry is further configured to simultaneously transmit a third signal based on a third one of a plurality of mathematically independent binary codes with a third transmitter electrode.	*See* discussions for Claim Element 1.Preamble, claim 9 and claim 12. *See, e.g.*, Umeda at Figs. 9-12, 21, 23 and 24.
17.	The controller of claim 13, further comprising a code generation module configured to generate each of the distinct digital codes.	*See* discussions for Claim 1. *See, e.g.*, Umeda at Abstract; 3:11-13; Figs. 1 and 17 (item 1, 1B). *See, e.g.*, Umeda at 4:52-63; 6:7-10; 7:21-25; 9:39-67; Figs. 6, 9-12, 28, 30. *See, e.g.*, Umeda at 4:64-67; 6:40-49; Figs. 18-21, 23.
18.	The controller of claim 13, wherein the drive circuitry comprises a first signal path between the controller and the first transmitter electrode, and	*See* discussions for Claim 4.

Shenzhen Huiding Tech. Co., Ltd. - Exhibit 1006

Claim No.	916 Patent Claim Language	Teachings in Umeda (Ex. 1007), Inoue (Ex. 1008) and Jaeger (Ex. 1011)
	a second signal path between the controller and the second transmitter electrode.	
19.	The controller of claim 18, wherein the first and second signal paths each comprise at least one of an amplifier and a driver.	*See* discussions for Claim 5.
20.Pre	An input device comprising:	*See* discussions for Claim Element 1.Preamble. *See, e.g.*, Inoue at Abstract.
20.A	a first transmitter electrode, a second transmitter electrode, and a plurality of receiver electrodes proximate to and configured to be capacitively coupled with the first transmitter electrode and the second transmitter electrode; and	See discussions for Claim Elements 1.A, 1.C and 13.B.
20.B	a controller configured to:	*See* discussions for Claim Element 13.Preamble.
20.C	simultaneously apply a first one of a plurality of distinct modulation signals to a first signal path connecting the controller to the first electrode, and a second one of the plurality of distinct modulation signals to a second signal path connecting the	*See* discussions for Claim Element 1.A and claim 4.

Shenzhen Huiding Tech. Co., Ltd. - Exhibit 1006

Claim No.	916 Patent Claim Language	Teachings in Umeda (Ex. 1007), Inoue (Ex. 1008) and Jaeger (Ex. 1011)
	controller to the second electrode,	
20.D	wherein each of the plurality of distinct modulation signals is based on a different one of a plurality of distinct digital codes;	*See* discussions for Claim Element 1.B.
20.E	receive resultant signals that are electrically affected by the position of the input object from the; plurality of receiver electrodes;	*See* discussions for Claim Elements 1.A and 13.B.
20.F	demodulate the resultant signals using the plurality of distinct digital codes to thereby discriminate electrical effects produced by the input object; and	*See* discussions for Claim Element 1.C.
20.G	determine the position of the input object from the electrical effects.	*See* discussions for Claim Element 1.D.

Shenzhen Huiding Tech. Co., Ltd. - Exhibit 1006

shaping results in an opposite tendency. Hence, when a notch filter is used in connection with a finite or variable load, the *RC* line should be shaped as much in the form of Fig. 1*c* of Reference 1 as possible, to reduce the effect of load resistance.

K. L. SU
Georgia Institute of Technology
Atlanta, Ga., USA

6th September 1965

References

1 SU, K. L.: 'Hyperbolic *RC* transmission line', *Electronics Letters*, 1965, **1**, p. 59
2 SU, K. L.: 'Selectivity of notch filters using non-uniform *RC* lines', *ibid.*, **1**, p. 204

STABILITY OF CONTROL SYSTEMS WITH TIME DELAY

To find the approximate stability limit on the forward gain in control systems with small time delay, this note suggests approximating the exponential in the characteristic equation by the first few terms of its series and using the Routh–Hurwitz criterion. This approximation avoids all the time-consuming graphical work and gives a somewhat pessimistic maximum bound for the gain constant.

There are many control systems in which the corrective action applied at any particular time is dependent on the error T seconds earlier. The block diagram of such a system is shown in Fig. 1, where $G(s)$ is the transfer function of the plant given by

$$G(s) = \frac{s^m + a_{m-1}s^{m-1} + \ldots + a_1 s + a_0}{s^n + b_{n-1}s^{n-1} + \ldots + b_1 s + b_0}$$

with $n > m$, and K is the gain constant of the system, which is assumed to be positive. The characteristic equation of this system is given by

$$1 + K\,G(s)\,\varepsilon^{-sT} = 0 \quad \ldots . \quad (1)$$

or

$$G(s) = -K^{-1}\,\varepsilon^{sT}$$

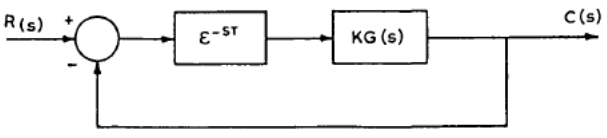


Fig. 1 *Block diagram of control system with time delay*

For a given value of the time delay T, the maximum value of K for stability can be obtained[1] by considering the intersection of the Nyquist locus of $G(j\omega)$ with the locus (circles of radius K^{-1}) of $(-K)^{-1}\exp(j\omega T)$ for different values of K and finding the value of K which gives identical frequencies on both the loci at the intersection point (Fig. 2).

The above procedure for finding the maximum value of the gain K for stability is rather time-consuming. When one is interested in finding the approximate maximum value of K for stability, this note suggests approximating the characteristic equation (eqn. 1) by

$$1 + K\,G(s)\sum_{k=0}^{n-m}\frac{(-sT)^k}{k!} = 0$$

when the time delay T is small, and using the Routh–Hurwitz criterion to find the maximum value of K for stability. This approximation avoids all the graphical work and gives a somewhat pessimistic maximum bound on K, as the following two examples show:

Example 1: Let $T = 0{\cdot}25$s, and

$$G(s) = \frac{1}{s(s+1)(s+2)(s+3)}$$

The characteristic equation is given by

$$1 + \frac{K\exp(-0{\cdot}25\,s)}{s(s+1)(s+2)(s+3)} = 0$$

Using the above approximation and considering only the first three terms of the series for the exponential, the characteristic equation may be written as

$$s^4 + 6s^3 + (11 + 0{\cdot}03125K)s^2 + (6 - 0{\cdot}25K)s + K = 0$$

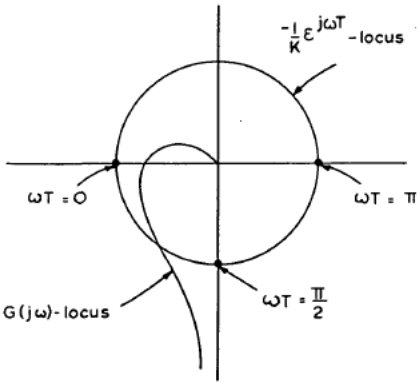


Fig. 2 *Nyquist diagram to find maximum permissible value of gain*

Application of the Routh–Hurwitz criterion to the above equation yields the maximum value of K for stability as 7·2, which compares well with the value of 7·33 obtained using the Nyquist criterion.

Example 2: Let $T = 0{\cdot}2$s, and

$$G(s) = \frac{(s+0{\cdot}5)}{s(s+1)(s+2)}$$

The characteristic equation of the system is given by

$$1 + \frac{K(s+0{\cdot}5)\exp(-0{\cdot}2s)}{s(s+1)(s+2)} = 0$$

Approximating the exponential as described earlier, the characteristic equation may be written as

$$(1 + 0{\cdot}02K)s^3 + (3 - 0{\cdot}19K)s^2 + (2 + 0{\cdot}9K)s + 0{\cdot}5K = 0$$

Applying the Routh–Hurwitz criterion to the above equation gives the maximum value of K for stability as 12·68, whereas the value obtained by using the Nyquist criterion is 13·66.

S. N. RAO
M. D. SRINATH
Department of Mechanical Engineering
Indian Institute of Science
Bangalore, India

2nd September 1965

Reference

1 KUO, B. C.: 'Automatic control systems' (Prentice-Hall, 1962)

TOUCH DISPLAY—A NOVEL INPUT/OUTPUT DEVICE FOR COMPUTERS

A novel input/output device for computer systems has wires, sensitive to the touch of a finger, on the face of a cathode-ray tube on which information can be written by the computer. This device, the 'touch display', provides a very efficient coupling between man and machine.

Touch wires

The key to the possibilities of the touch display is the provision of the 'touch wires', which are sensitive to the touch of a finger.

The touch wires themselves are completely passive, being simply pieces of tinned-copper wire (¾in long 22s.w.g.) attached to the front surface of a mask moulded to fit the front surface of a cathode-ray tube. Any convenient number, say 16, are attached to the mask and are disposed so that the computer can write an item of information against each one.

These touch wires are connected by fine insulated wires, running in grooves in the rear surface of the mask, to screened cables from the edge of the mask to the electronic equipment.

Each touch wire is made sensitive by connecting it via the screened lead to become one arm of an a.c. bridge circuit. The bridge is initially balanced but becomes unbalanced by the electrostatic capacitance of the operator.

A good clean signal is obtained (signal/noise ratio $\simeq 100:1$) on touching, but the proximity effect is negligible. Each bridge can accept two touch wires, and a number of bridges can use one amplifier and a phase-sensitive detector on a time-sharing basis.

Shenzhen Huiding Tech. Co., Ltd. - Exhibit 1006

Use of the touch display

The touch display coupled to a computer can be considered as a keyboard, the engravings of which can be varied to suit the needs of the moment; more fundamentally, it can be considered as a means by which a computer presents a list of those 'choices' which are available to a controller at any given instant and as the means by which the controller indicates his choice back to the computer.

In the way that in mathematics it is profitable to consider a complex function to be built up of simpler functions (e.g. sine waves, as in Fourier analysis), it is profitable to consider the 'control function', i.e. whatever a human controller does in a real-time computing system, as a series of 'choices', each choice being made from a limited list and the content of each list being determined by the previous choice.

It is in the light of this hypothesis, i.e. that the control function can be equated to a series of choices, that the concept of the touch display is seen to be important, because it combines the computer's ability to set up lists of choices with a facility for the controller to indicate his choice in a natural manner.

In one possible use of the touch display, at an air-traffic-control position, the computer can present to the controller the following lists on successive pictures, in each picture one item of the list being against one touch wire:

- list of call signs of the aircraft under control
- list of items in the flight plan of the aircraft selected
- list of values for the first element of the item
- list of values for the second element of the item
- list of values for the third element of the item
- list of executive actions.

A list of values for an element of an item may be the numerals 0 to 9 or symbols such as those for 'climbing', 'holding' etc., and can be displayed exactly according to the possibilities of that element; e.g. the list for the first digit of a time need not show a value greater than five (tens of minutes).

During the operation the display may show, in addition to the current list and away from the touch wire, reference data, such as the complete flight plan and the amendments so far put in.

One of the touch displays has been made up and programmed for the air-traffic-control task, and an evaluation of it in this role is being arranged.

Acknowledgment

This article is Crown copyright and is reproduced by permission of the Controller of Her Majesty's Stationery Office.

E. A. JOHNSON *8th September 1965*
Royal Radar Establishment
Malvern, Worcs., England

ONLINE DIGITAL PREDICTION AND CONTROL OF THE OUTPUT OF A LINEAR TIME-VARYING SYSTEM

The system time-varying weighting function is approximated by a grid of sample estimates. Criteria are given for specifying the sample spacing in each dimension and for predicting the sample estimates at the next sampling instant. The criteria are based on maximum sample smoothness, subject to a prescribed signal/noise ratio at the system output.

Consider the identification scheme of Fig. 1. Let us assume that the physical system has a lowpass characteristic, which for practical purposes may be represented by a weighting function bandlimited to $|\omega| < \pi/T_1$ rad/s, with a time variation of the weighting function bandlimited to $|\omega| < \pi/T_2$ rad/s. From the Nyquist sampling theorem[1] the weighting function is uniquely described by an infinite set of time-varying weights spaced at time interval T_1, where each time-varying weight is sampled over all time at instants spaced T_2 apart. The digital model of the physical system must be described by a finite number of weights; specifically, let the model output be

$$y_m = \sum_{n=0}^{N-1} w_{nm}\, x_{m+n} \qquad m = 0, \ldots M-1 \quad \ldots \quad (1)$$

where w_{nm} are time-varying weights to be determined over an output measurement interval $0 \leqslant m \leqslant M-1$ from bandlimited sampled values x_m, z_m of normal operating records $x(t)$, $z(t)$; m counts sampling instants backwards in time from the present instant $m = 0$. Let us assume that x_m, z_m are bandlimited to $|\omega| < \pi/T_3$ rad/s, and the system is able to respond to the highest significant frequency components of input; i.e. $T_3 > T_1$. The assumption that the higher-frequency components of the weighting function are not excited by the input means that a smoothed weighting function is acceptable. The choice of N in eqn. 1 and the estimation of sampling intervals T_2 and T_3 (T_3 is normalised to 1 s) are considered later. The choice of M in eqn. 1 can be shown* to be expressible in terms of N and certain statistical properties of the input signal and output noise.

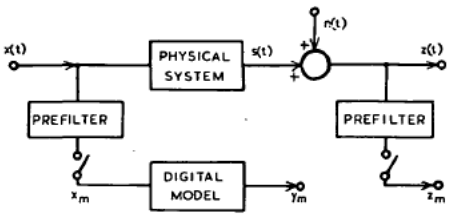


Fig. 1 *Notation used to describe the identification problem*

Smoothness of the weights

Let the sample estimates of the smoothed weighting function ($T_3 > T_1$) at any instant be called a set of weights, and let the sets of weights at instants spaced T_2 apart be called sample sets. For simplicity, let the estimate of T_2 be $(M-1)/(K-1)$, an integer, and let k $(0 \leqslant k \leqslant K-1)$ be the count of sample sets in the measurement interval $M-1$.

The kth sample set may be regarded as the strengths of a sequence of impulses spaced at 1 s intervals. Considering the sequence of impulses to be passed through an ideal lowpass filter of bandwidth $\sigma\pi$ rad/s $(0 < \sigma \leqslant 1)$, the filter output is

$$w_\sigma'(k, \tau) = \sum_{n=0}^{N-1} w_{nk}\, \mathrm{sinc}\, \sigma\pi(\tau - n) \qquad k = 0, \ldots K-1 \quad \ldots \quad (2)$$

where $\mathrm{sinc}\,\theta = (\sin\theta)/\theta$. $w_\sigma'(k, \tau)$ will be referred to as the σ factor Nyquist envelope of the kth sample set; in the case of the unit-factor Nyquist envelope, the weights are sample points of the envelope. We define the coefficient

$$F_\sigma' = \frac{\sum_{k=0}^{K-1}\sum_{n=0}^{N-1} [w_\sigma'(k, n) - w_{nk}]^2}{\sum_{k=0}^{K-1}\sum_{n=0}^{N-1} w_{nk}^2} \quad \ldots \quad (3)$$

as a normalised measure, averaged over the K sample sets, of the relative power content of the weighting-function spectral density in the frequency band $\sigma\pi \leqslant \omega \leqslant \pi$ (π rad/s is the Nyquist frequency). The frequency band $(1-\sigma)\pi$ may be thought of as a guardband, and F_σ' may be regarded as an indicator of the rate of roll-off of the spectral density adjacent to the Nyquist frequency. For a preset value of σ ($\sigma = \frac{1}{2}$ gives a reasonable guardband), we note that the smaller the value of F_σ', the smoother is the sample set. Likewise, the σ factor Nyquist envelope of the time variation of the nth weight $(n = 0, \ldots N-1)$ is

$$w_\sigma''(t, n) = \sum_{k=-\infty}^{\infty} w_{nk}\, \mathrm{sinc}\, \sigma\pi \left(\frac{K-1}{M-1}\right)(t-k) \qquad n = 0, \ldots N-1 \quad \ldots \quad (4)$$

where, mathematically, the contribution from all sample sets, past and future, must be included. Analogous to the coefficient F_σ', we define a coefficient

$$F_\sigma'' = \frac{\sum_{n=0}^{N-1}\sum_{k=0}^{K-1} [w_\sigma''(k, n) - w_{nk}]^2}{\sum_{n=0}^{N-1}\sum_{k=0}^{K-1} w_{nk}^2} \quad \ldots \quad (5)$$

Note that $w_\sigma'(k, n) \neq w_\sigma''(k, n)$, because ideal-filter smoothing is applied independently in the two time dimensions t and τ. Since eqn. 4 is not realisable, let us arbitrarily set future values of sample sets $(k = -1, -2 \ldots)$ equal to the present sample set $(k = 0)$. Also, let us disregard the effect of sample sets further in the past than, say, $k = 2K-1$; i.e. let

* BROWN, R. F.: 'Optimum measurement interval in real-time synthesis of linear time-varying systems'. Submitted for publication in *Proc. IEE*

Shenzhen Huiding Tech. Co., Ltd. - Exhibit 1006

Issues of Gestural Navigation in Abstract Information Spaces

David Allport[1], *Earl Rennison and Lisa Strausfeld*

MIT Media Lab
20 Ames St.
Cambridge, MA 02139
E-mail: *{dea,rennison,straus}@media.mit.edu*

ABSTRACT

Navigating large multidimensional information spaces presents a set of unique problems for user interface design. The key challenge is not to provide fast and accurate object manipulation, but to prevent the user from getting "lost", and to provide an intuitive way to move through the space. We have developed an interface that uses electrostatic field sensing to interpret natural hand gestures as motion controllers. We are investigating the conceptual models that provide intuitive mappings from hand gestures to movements in multidimensional information space.

Keywords: Gestural navigation, conceptual navigation models, input devices, abstract information spaces

THE "FLYING FISH"

We are using a "fish" electrostatic field sensor in human transmitter mode [4]. A cushion on the user's chair capacitively couples energy into the body, and four receivers mounted in "wings" around the bezel of a workstation monitor sense the fields emitted from the user's hands. An input on the fish's user port also allows two foot-switches to be connected, enabling us to select four different navigational modes.

By a comparison of the values received at the four corners of the monitor we can derive position sensing for up/down, left/right and forward/back, and thus implement a "virtual 3D joystick" where displacement from a central position is mapped to the velocity of navigational movement. This virtual joystick has the interesting property of being manipulable with one or two hands without any changes being made to hardware or software.

With this same "flying fish" sensing hardware we can implement a variety of other virtual 3D input devices in software. These could provide absolute position-to-position





Figure 1
a) *Steering a camera to the left, objects move right on screen.*

b) *Indicating the direction to move, objects move left on screen.*

The same hardware and software can support multiple different navigational models simultaneously, with the crucial variable being the conceptual mapping the user makes, as in the classic "which direction should the arrow point on a button?" problem. With our interface, the user can make different gestures supported by the different models, yet given the physics of our input sensors, the distinction for the input device between the gestures shown in (a) and shown in (b) is negligible.

1. Visiting scientist from HP Laboratories, Bristol, England.

Permission to copy without fee all or part of this material is granted provided that the copies are not made or distributed for direct commercial advantage, the ACM copyright notice and the title of the publication and its date appear, and notice is given that copying is by permission of ACM. To copy otherwise, or to republish, requires a fee and/or specific permission.
CHI' Companion 95, Denver, Colorado, USA
© 1995 ACM 0-89791-755-3/95/0005...$3.50

Shenzhen Huiding Tech. Co., Ltd. - Exhibit 1006

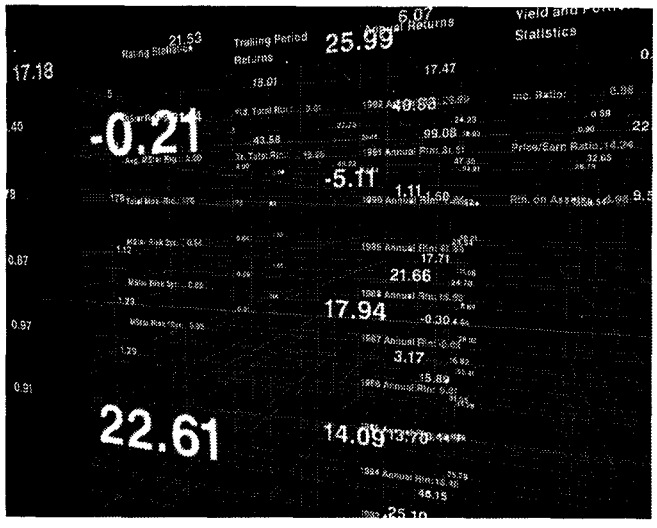


Figure 2 *Financial Viewpoints: A Euclidean information space.*

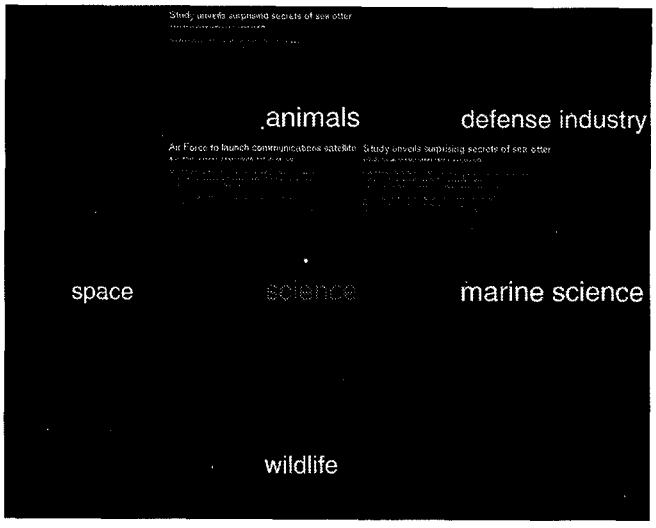


Figure 3 *Galaxy of News: An abstract, non-Euclidean information space.*

mapping (like a 3D tablet), or relative displacement-to displacement mapping (like a 3D relative mouse). But for navigation through very large spaces an absolute position-to-position mapping is impracticable, and a relative displacement-to-displacement mapping would be inconvenient because of the constant "nulling problem"[1] when moving to parts of the space not previously displayed.

CONCEPTUAL MODELS OF NAVIGATION

The "flying fish" provides a natural way to move through a 3D "virtual world", using gestures to point in the direction that we wish our virtual bodies to fly. We have implemented a financial information space whose form is analogous to a city with buildings, streets etc.[3]. From a distance, it can be thought of as an object like a planet floating in space. From close up, we can think of it as if we are "inside" the virtual buildings. However, it is unlike traditional virtual worlds in that the contents designated by the forms are entirely conceptual (see Figure 2).

Our experiences of navigating in this space have raised a host of issues concerning the underlying conceptual models. There are many different ways to think of what is flying through the space; is it the user's body, a steerable vehicle containing the user, a camera through which the user is looking, or is the user (directly or indirectly) acting upon the information "objects" themselves? (see Figure 1).

We are experimenting with providing a number of different "virtual intermediary devices", where the models which map gestures to navigational actions can change as the user moves into different spatial contexts. User expectations based upon familiar real-world motor skills and concepts can be used to reinforce the sense of immediacy of interaction.

A further set of issues arises when we are navigating through non-Euclidean spaces. We have developed an abstract news and information space whose form is 2-1/2D, in that it uses an orthogonal projection of multiple overlapping layers of news information [2], (seeFigure 3). However, as the viewer moves closer towards an object representing a particular topic, more details relating to that object appear, effectively reconstructing the space. As a result, navigation and movement become the only language of communication necessary for the dialogue between user and computer. The user not only browses "system output" by navigation, but also expresses "input commands" in the same manner.

Our bodies do not experience non-Euclidean spaces, but we can still use a natural gestural vocabulary that can be dynamically mapped onto different navigational modes by system software and/or by the user, to reflect whatever conceptual model is most appropriate for a given spatial context.

SUMMARY

We do not think that there is a single "right answer" to the question of how to move through multidimensional spaces. Rather we think that there are a range of natural gestures that users can employ to indicate 3D navigation, a large number of different types of virtual space that can be constructed, and a variety of different conceptual models that can be used to understand how gestures map to movements within (different parts of) these spaces. We have developed hardware and software that allows us to explore a large number of combinations of these different conceptual mappings.

REFERENCES

[1] Buxton, W. *There's more to Interaction than meets the eye: Some Issues in Manual Input.* In Norman, D.A and Draper,S.W (eds) User-centered System Design: New Perspectives on Human-Computer Interaction. Hillsdale, N.J. Lawrence Erlbaum Associates. 1986

[2] Rennison, E. Galaxy of News: An Approach to Visualizing and Understanding Expansive News Landscapes. *Proceedings of UIST 94.* November 1994.

[3] Strausfeld, L. Financial Viewpoints: Using Point-of-View to Enable Understanding of Information. Submitted to CHI 95. May 1995.

[4] Zimmerman, T.G.,. J.R. Smith, J.A. Paradiso, D. Allport, N. Gershenfeld. Applying Electric Field Sensing to Human-Computer Interfaces. *Proceedings of CHI 95.* May, 1995.

Shenzhen Huiding Tech. Co., Ltd. - Exhibit 1006

Toward Electric Field Tomography

by
Joshua Reynolds Smith

B.A., Computer Science, Philosophy
Williams College, Williamstown, MA
June 1991
B.A. Hons. Natural Sciences (Physics)
University of Cambridge, Cambridge, England
June 1993

Submitted to the Program in Media Arts and Sciences,
School of Architecture and Planning,
in partial fulfillment of the requirements for the degree of
MASTER OF SCIENCE IN MEDIA ARTS AND SCIENCES
at the
Massachusetts Institute of Technology
August 1995

© Massachusetts Institute of Technology, 1995
All Rights Reserved

Signature of Author _____
Program in Media Arts and Sciences
22 August 1995

Certified by _____
Neil Gershenfeld
Assistant Professor of Media Arts and Sciences
Program in Media Arts and Sciences
Thesis Supervisor

Accepted by _____
Stephen A. Benton
Chair
Departmental Committee on Graduate Students
Program in Media Arts and Sciences

Shenzhen Huiding Tech. Co., Ltd. - Exhibit 1006

Toward Electric Field Tomography

by
Joshua Reynolds Smith

Submitted to the Program in Media Arts and Sciences,
School of Architecture and Planning
on 22 August 1995
in partial fulfillment of the requirements for the degree of

Master of Science in Media Arts and Sciences

Abstract

This thesis addresses the problem of recovering three-dimensional location and shape information from measurements made with Electric Field Sensors. A single sensor functions as a proximity detector; two can be used as a mouse; three allow tracking of the hand in three dimensions, and each additional sensor allows us to extract additional shape information.

The ultimate goal of this work is to understand the entire hierarchy, from a single sensor up to an array of sensors. In this thesis, we take the first steps toward imaging, moving from simple proximity detection to imaging a single point in three dimensions. At every step along the hierarchy, we are interested in two questions: i) given a fixed number of sensors, how should they be arranged in space to enable us to extract the most information, and ii) given an arrangement of sensors, how should we infer "what's out there" from the data they return? We describe a probabilistic framework that can be used to answer these questions for any sensor configuration, from a single sensor to an array.

The thesis describes the physics of Electric Field Sensing, uses this discussion to find an approximate analytical solution to the forward problem of determining the sensor values from a conductivity distribution, shows how to use this analytical model in conjunction with probability theory to design optimal electrode layouts, and presents several methods of inverting the signals to recover information about a conductivity distribution from sensor values. As an example application, we present a non-contact three-dimensional mouse.

Thesis Supervisor: Neil Gershenfeld
Title: Assistant Professor of Media Arts and Sciences

Shenzhen Huiding Tech. Co., Ltd. - Exhibit 1006

Toward Electric Field Tomography

by

Joshua Reynolds Smith

The following people served as readers for this thesis:

Reader: _____

Stephen A. Benton
Professor of Media Arts and Sciences
Program in Media Arts and Sciences

Reader: _____

Seth Lloyd
Assistant Professor
Department of Mechanical Engineering

Shenzhen Huiding Tech. Co., Ltd. - Exhibit 1006

Acknowledgement

I thank my advisor, Neil Gershenfeld, for creating the Physics and Media Group and giving me a place in it; Joe Paradiso and Tom Zimmerman, for their work on the Fish and sensor array hardware, and for sharing some of their vast knowledge of electronics; Barrett, for writing the graphics code used in the 3-d mouse demo; the other members of the group, for generosity with their expertise; my readers, Steve Benton and Seth Lloyd, for their constructive comments; Linda Peterson and Santina Tonelli, for running the Media Arts and Sciences program so smoothly; David Waxman and Eric Metois for their friendship; my family, including my Grandmother, Ruth P. Smith, for their support; and Maggie Orth, for her patience.

This work was supported in part by Hewlett-Packard, Festo, and the News in the Future Consortium.

Shenzhen Huiding Tech. Co., Ltd. - Exhibit 1006

Contents

1 Introduction **7**
1.1 Electric Field Sensing . . . 7
1.1.1 Background: The Theremin and Capacitive Sensing . . . 7
1.1.2 Motivation for Electric Field Sensing . . . 7
1.1.3 Recent Work on Electric Field Sensing . . . 8
1.1.4 Alternatives to Electric Field Sensing . . . 8
1.2 Toward Electric Field Tomography . . . 9
1.2.1 Motivation for Electric Field Tomography . . . 9
1.2.2 Alternatives to Electric Field Tomography . . . 9
1.2.3 Background: Electrical Impedance Tomography . . . 10
1.2.4 Field Sensing Hierarchy . . . 12
1.2.5 Forward, Inverse, and Experimental Design Problems . . . 12
1.2.6 Bayesian Framework . . . 13

2 Physics of Electric Field Sensing **14**
2.1 Hardware . . . 14
2.1.1 Noise . . . 15
2.1.2 Contrast to Noise and Lengthscale . . . 16
2.2 Derivation of Circuit Model from Maxwell Equations . . . 18
2.2.1 Maxwell's equations . . . 18
2.2.2 Quasistatic limit . . . 20
2.2.3 Circuit Theory . . . 20
2.2.4 Laplace's equation in an inhomogeneous medium . . . 21
2.2.5 Electrostatics . . . 22
2.2.6 Capacitance . . . 22
2.3 Lumped Circuit Model and Sensing Modes . . . 23
2.3.1 Transmit Mode . . . 25
2.3.2 Transmitter Loading Mode . . . 25
2.3.3 Receiver Loading Mode . . . 25
2.3.4 Shunt Mode . . . 25

3 Forward Problem **28**
3.1 General Case . . . 28
3.2 Approximate effect of a small grounded object . . . 28
3.3 Modeling the field: the dipole approximation . . . 30
3.4 Modeling the sensor response . . . 30
3.5 Iso-Signal Shells . . . 32

Shenzhen Huiding Tech. Co., Ltd. - Exhibit 1006

3.6 Ground plane 32
3.6.1 Generalizations of hand model 33

4 Constructing the ambiguity class **34**
4.1 Uncertainty and optimal sensor geometry 36
4.2 Entropy 36
4.3 Example: Two dimensional mouse 37
4.3.1 Recovering orientation 42

5 Example Inverse Problem: 3D Mouse **43**

6 Conclusion **47**

A Backprojection Algorithm **49**

Shenzhen Huiding Tech. Co., Ltd. - Exhibit 1006

Chapter 1

Introduction

1.1 Electric Field Sensing

1.1.1 Background: The Theremin and Capacitive Sensing

Electric Field sensing has existed in some form since the Theremin was invented circa 1917.[Gal91, Oth92, Nic93] Before that time, only aquatic animals had used electric fields to sense their environments.[Bas94] The Theremin combined analog sound synthesis and an early form of Electric Field sensing in a single clever circuit. It may be surprising how little research attention has been focused since then on the use of electric fields for measuring the shape and motion of the human body. With the exception of the work of Mathews[Mat90] and Vranish[V$^+$92, V$^+$93], little effort has been made to improve upon the early, "capacitive" form of Electric Field sensing until recently.

However, it is worth remembering that before the advent of digital electronics, there existed very few devices that could be controlled by tiny currents. The Theremin represented not only the first application of Electric Field sensing, but also one of the first examples of electronically synthesized music of any kind. Furthermore, the computation needed to perform even the simplest interpretation of the signals produced by Electric Field Sensors was not available in an inexpensive and physically small form until quite recently. In Theremin's day, the word "computer" referred to women who tabulated ballistics tables. Thus there was little demand for methods of transducing the position of the human body into tiny currents.

In its time, the Theremin was clearly the "killer app," or rather the "only app," for capacitive sensing, since its analog synthesizer was one of the few existing devices that could be controlled by tiny currents, and since the signals required no inversion or gesture interpretation.

1.1.2 Motivation for Electric Field Sensing

Today, the supply of devices that can be controlled with tiny currents, in particular digital devices, is growing explosively. In one sense, controlling these devices is trivial: they can be programmed to map arbitrary messages into arbitrary actions. But the problem of translating human intention into those digital control messages is nontrivial; some would argue that it has become the main factor limiting their usefulness.

For example, the utility of 3-d graphics programs is limited by the fact that the most

Shenzhen Huiding Tech. Co., Ltd. - Exhibit 1006

sophisticated input device most people have access to is the 2-d computer mouse, which implements a straightforward mapping between motions of the mouse in a plane and motions of an on-screen pointer. In principle, arbitrary 3-d manipulations can be performed using the right combination of 2-d mouse moves (for example, clicking on-screen buttons to change rotation modes), but this is by no means a natural way to interact with a 3d environment.

The demand for more subtle and sophisticated means of physically interacting with digital devices and environments, plus the abundance of signal processing power, make this an auspicious time to develop Electric Field Sensing further. We will now survey recent efforts by members of the MIT Media Lab's Physics and Media Group to develop Electric Field Sensing further; this thesis is a continuation of this line of research.

1.1.3 Recent Work on Electric Field Sensing

In 1991, Gershenfeld[Ger91, Ger93] used a version of Electric Field sensing to measure the position of a cello bow with respect to the cello body. A transmitter on the cello body induces a signal in a resistive strip affixed to the bow. The received signal depends on the position of the bow relative to the body. Paradiso later applied these ideas in an accelerator alignment problem.[Par94, PM94]

The Physics and Media Group of the MIT Media Lab has developed this EF sensing technology further into non-contact sensors that detect the bulk conductivity of the human body[ZSP+95]. When part of a human body, which is typically coupled to ground, enters the field set up by a transmitter and receiver, some of the displacement current is diverted from the receiver and shunted to ground. This form of Electric Field sensing differs from previous, "capacitive" forms, because it is a three-terminal measurement, the sensed body part being the third terminal. The class of sensors usually called "capacitive," including Theremin's, Vranish's, Matthews', the cello and alignment sensors, and present industrial "capacitive sensors" are two terminal devices, in which the object being sensed functions as the second terminal.

This new form of Electric Field sensing, and variants, have been used in a variety of ways: with simple gesture recognition software to flip through the pages of an electronic newspaper[SPZG95], in a musical sculpture known as the Gesture Cube[Wax95, SPZG95], in a "musical chair" made for the magicians Penn and Teller[PGng], to fly through information spaces[ARS95, AZP+95], and in numerous musical installations by David Waxman[Wax95].

1.1.4 Alternatives to Electric Field Sensing

So far we have argued that the growing supply of digital devices presents a need for sophisticated sensing technologies, and that EF sensing is such a technology. In other words, EF sensing is sufficient to solve a problem of great practical interest. But to what extent is it necessary? Are there other sensing technologies that could solve the problem just as well?

There are, of course, other sensing mechanisms. Here we will briefly contrast some of the alternatives with EF sensing. Many sensors, including infra-red and pyroelectric, require a line of sight to the object being sensed. Electric Field Sensors can "see" through low conductivity materials, such as wood, paper, and cloth—they do not require a line of sight. Since EF sensors measure a bulk property of the body, impedance, surface properties of the object have no effect. By contrast, a change of clothing or lighting can change the response of video cameras and infra-red, pyroelectric, or sonar sensors. This is obviously

Shenzhen Huiding Tech. Co., Ltd. - Exhibit 1006

an advantage if one is interested in measuring surface or lighting properties. But often one is not. The fact the EF sensing functions independently of lighting conditions may be one of the reasons it is so prevalent in fish.

Magnetic sensors, such as the commercially available Polhemus, have none of the problems listed above. However, they tend to be much noisier than electric field sensors, and also are prone to hysteresis problems. One recent sensing technique, Micropower Impulse Radar,[Lab95] makes bulk measurements and does not require a line of sight to the object. But it is much more expensive than EF sensing, and while it can be used either as a simple proximity detector or an imager, it is unclear whether it could be used in regimes of intermediate complexity, such as for a non-contact 3-d mouse.

1.2 Toward Electric Field Tomography

The goal of the research begun in this thesis is to develop Electric Field sensing beyond the relatively simple applications surveyed in section 1.1.3, in which small numbers of sensors were used as proximity detectors, into a genuine imaging technology, Electric Field Tomography. At this point we have only taken the first steps, from proximity sensor to 3-d mouse, but the framework we introduce is very general should be applicable to much more complicated problems. We hope to gain a general understanding of how to extract information from a set of electric field sensors, and of the relationship between sensor geometry and the information they can provide. We are ultimately interested in the following questions: (1) Given a sensor geometry, how much information can be extracted from it? (2) To estimate a given quantity characterizing a matter distribution, what is the optimal sensor configuration (both number and geometry)? (3) How do we infer the information of interest about the distribution from the sensor values?

In this thesis, we introduce a framework for addressing these questions, and demonstrate its utility for a couple of relatively simple problems. But before continuing, let us consider some motivating applications and problems.

1.2.1 Motivation for Electric Field Tomography

Fast, inexpensive, and unobtrusive imaging of the human body will permit non-contact shape, motion, and gesture capture for hands, faces, and entire bodies, which will enable people to interact in new (and hopefully better) ways with digital devices, computer models, and other people. For example, as realtime three-dimensional computer graphics becomes more common, the need for techniques to measure 3-d gesture becomes more acute. Creating 3-d models, placing lights, and animating the models are all cumbersome procedures with present techniques. Creating and lighting models is often accomplished with a mouse, keyboard, or stylus. More sophisticated methods for capturing shape, and motion capture techniques, which we will review below, are typically more intrusive.

1.2.2 Alternatives to Electric Field Tomography

The CyberWare scanner, a laser-based shape capture device, requires a line of site between the apparatus and the object being scanned. Medical imaging techniques such as CT-scans, MRI, or PET are too costly, too large, and provide more data than is needed for human

Shenzhen Huiding Tech. Co., Ltd. - Exhibit 1006

interface and simple geometry-capture applications, since they provide images of the interior of the body.

All present motion capture or "performance animation" systems, which map human movement into that of three-dimensional graphic "puppets," are intrusive as well.[Rob94, Cha94] Magnetic motion capture devices such as the Polhemus require the user to wear tethered magnetic sensors whose response to a static field can be measured through the cable. The other popular motion-capture technology is video.

For human interface purposes, video provides both too much and too little data. The frame rate is too slow for musical and other demanding realtime control applications, so in that sense it doesn't provide enough data. One the other hand, when a video camera does deliver a frame, it provides as many as several million numbers. For control applications, these million numbers must be laboriously boiled down into the final control message, often just a few bytes. In this sense, a video camera provides far too much data.

To combat the second problem, video-based motion-capture systems require the user to wear black clothing and bright targets that the vision software can easily track. Video-based gesture recognition systems require large amounts of computing horsepower and often place restrictions on the background. Geometry capture systems require multiple cameras and consume large amounts of computing. Having surveyed the competition, we will now revisit the ancestors of Electric Field Tomography.

1.2.3 Background: Electrical Impedance Tomography

Electrical Impedance Tomography (EIT),[BB84, Web89] sometimes known as Applied Potential Tomography, is an imaging technique that has been used in medical and geophysical applications. It is closely related to Electric Field Tomography. In a typical medical EIT experiment, current is applied to electrodes attached to the skin, the resulting voltages are measured, and then, using a variety of inversion techniques, the conductivity distribution is recovered.

More formally, a current pattern is applied to the surface $\partial\Omega$ of body Ω, and the resulting electrical potential on $\partial\Omega$ is measured. The conductivity $\sigma \in \Omega$ is then inferred. The potential u in Ω satisfies $\nabla\cdot(\sigma\nabla u) = 0$, which is Laplace's equation with a finite conductivity field, and may also be viewed as the microscopic form of Ohm's and Kirchoff's laws. The current density j on $\partial\Omega$ given by $j = -\sigma\nabla_n u$ where n is the outward normal on $\partial\Omega$.

Comparison with Electric Field Tomography

EIT is similar enough to EFT that the mathematics used to show the feasibility of inversion appears to carry over directly, as we discuss in section 1.2.3. Though Electric Field Tomography and Electrical Impedance Tomography may be identical in the most general mathematical sense, there are substantial differences in practice. In EFT, we usually apply alternating voltages at the boundary and measure currents to find capacitances, rather than applying currents and measuring voltages to find conductances.

More significantly, the practical inversion problems are somewhat different. In EIT, the electrodes are in contact with the body. The goal is to image the small variations in conductivity in the interior. EIT imaging occurs in a very low-contrast regime. In Electric Field Tomography, on the other hand, the electrodes are not in contact with the person. There are essentially two, vastly different impedances: that of air, and that of the person's

Shenzhen Huiding Tech. Co., Ltd. - Exhibit 1006

hand. This is the high-contrast regime. Though EFT is an intrinsically easier problem (producing a 1-bit image should be easier than producing an 8-bit image), there are some advantages to the low-contrast regime: the image can be treated as a perturbation on a background conductivity, and linear approximations can be used.

Finally, note that EFT could be posed in a completely different way, in which all boundary potentials are known, but the boundary geometry is not known. This may turn out to be the most straightforward way of posing the problem.

Questions of Principle Answered in EIT

Extensive work has been done in the Electrical Impedance Tomography literature on the feasibility of the inverse problem. Basically, it has been shown that the problem is soluble in principle. Kohn and Vogelius proved the uniqueness of solutions of the inverse problem for a piecewise analytic conductivity.[KV84, KV85, KV83] Sylvester and Uhlman proved invertibility for $\sigma \in C^{\infty}(\Omega)$.[SU87] Though most of the EIT literature is posed in the context of DC conductivity, we will see in section 2.2.4 that there is an exact analogy between the Laplace equation for inhomogeneous media that describes the resistive forward problem, and the equation describing the capacitive forward problems, so that in the most general sense, arguments from one domain automatically apply in the other.

However, because of the different contrast regimes, algorithms for constructing the inverse are not automatically applicable in both domains. Furthermore, EFT has the additional practical complication that the object being imaged (a hand, say) is typically connected to a conductive body that is not in the sensing field, but is coupled capacitively to ground. Nevertheless, we will briefly survey the three classes of inversion algorithms used in EIT.

Backprojection

The backprojection algorithm for EIT, introduced by Barber and Brown,[BB84] was adapted from the algorithm of the same name that originally was used to reconstruct CT-scans. The classic backprojection algorithm is explained in Appendix 6. In the generalized version used in EIT, measurements are backprojected along the iso-signal surfaces, in Barber and Brown's case curved equipotential lines, since they measure voltage.

Barber and Brown's forward model makes perturbative linear approximations. It is at present unclear whether it could be adapted to our high-contrast regime.

Backprojection is reported to provide fast, high-quality, approximate reconstructions. If slower, more refined algorithms are to be employed, it may make sense to give them a head start by backprojecting first.

Spectral

Spectral methods typically provide a set of basis images and a matrix that transforms a vector of sensor readings into a vector of basis image coefficients. In EIT, these techniques rely on perturbative linear approximations. Since spectral techniques are analytical, they are more likely to give insight into algorithm stability, the ill-posedness of the inverse problem, and so forth.[AS91, Z^{+}91]

Shenzhen Huiding Tech. Co., Ltd. - Exhibit 1006

Iterative

Iterative numerical techniques are the only way of solving the inversion problem exactly. Based on the applied boundary conditions and a trial conductivity distribution, the free boundary conditions (sensor values) are predicted. An optimization technique such as Newton-Raphson is used to relax the conductivity distribution so as to reduce the error between the actual sensor values and those predicted by the trial conductivity distribution.[KM90, DL81]

A very interesting variational formulation of the inversion problem, which provides explicit estimate of the quality of the reconstruction, is developed by Berryman in [Ber89] and by Berryman and Kohn in [BK90]. They show that there is a close analogy between the electrical impedance tomography problem and the seismic travel-time inversion problem, which they solve using Fermat's principle.

1.2.4 Field Sensing Hierarchy

For many human interface applications, a full image may not be desirable. Therefore, rather than simply adopting one of the brute force imaging techniques from EIT, it would be nice to understand how to extract just the required information using only the necessary number of sensors. For example: roughly speaking, from one sensor it is possible to infer at most one number characterizing a matter distribution. The number might be an estimate of position or size, for example. With two sensors, one can estimate two position coordinates, or one size and one position. This field sensing hierarchy extends upwards, until we reach a continuum of sensors. When a large number of sensors is available, it becomes possible to extract a three-dimensional image of a conductivity distribution, as the arguments cited in section 1.2.3 show. In Chapter 4, we will show how to construct and analyze "ambiguity classes," which will make the notion of the field sensing hierarchy more precise.

This thesis is entitled "Toward Electric Field Tomography" because, although we have not yet arrived there, imaging is the endpoint toward which we are heading, and because our goal is to understand the entire hierarchy, from a single sensor up to a continuum. At this point, we have explored the hierarchy in a practical way as far as three sensors: we have made non-contact two- and three-dimensional mice. The user's body is the only moving part of these input devices.

1.2.5 Forward, Inverse, and Experimental Design Problems

Now that we have explained the ultimate destination of this research, we will describe the sub-problems that must be solved in order to arrive there. There are two obvious parts to the full imaging problem, and to any of the problems along the EF sensing hierarchy. The goal, of course, is to infer as much as possible about the conductivity distribution from the measurements returned by the sensors. We will refer to this as the inverse problem; before we can solve it, we must first understand the direct or forward problem of calculating the sensor values given a conductivity distribution and sensor geometry.

There is also a less obvious problem, which might be called the "experimental design" problem. When a large number of sensors is available, the problem is to decide which of the large number of measurements that could be made actually should be made. When a smaller number of sensors is available, the question is, how many are needed, and where should they be placed?

Shenzhen Huiding Tech. Co., Ltd. - Exhibit 1006

1.2.6 Bayesian Framework

We will introduce a general framework that allows us not only to solve inversion problems anywhere along the EF sensing hierarchy, but also to design optimal sensor geometries. Given a sensor geometry and data values, we will construct the ambiguity class of models that could explain the data. This ambiguity class takes the form of a probability distribution over model parameters. Once this distribution has been constructed, the problem of inverting the sensors (to find, say, the location of the hand from some sensor values) reduces to the optimization problem of maximizing the probability of the model, given the data.

This ambiguity function is also useful in chosing sensor geometries. The expected change in entropy of the ambiguity class will provide a measure of the quality of sensor geometries. By maximizing this quantity, optimal sensor geometries can be found.

Before we discuss methods of solving the inverse and experimental design problems in Chapters 4 and 5, however, we will explain the physics of electric field sensing in Chapter 2, and then, in Chapter 3, we will introduce approximations that allow us to predict efficiently the sensor values resulting from a simple matter distribution.

Shenzhen Huiding Tech. Co., Ltd. - Exhibit 1006

Chapter 2

Physics of Electric Field Sensing

In this chapter we will describe the hardware we use for Electric Field Sensing, and then discuss the physics underlying the hardware.

2.1 Hardware

The Electric Field Sensors[Ger93, ZSP+95] developed in the Physics Group of the MIT Media Laboratory provide high-precision, low-noise measurements of the bulk conductivity of a matter distribution. The "Fish" field sensing board[1] consists of a transmitter that can be tuned from 20kHz to 100kHz, and four receive channels that use synchronous detection. The transmitter consists of an oscillator connected to an op-amp. The op-amp defines the voltage on the transmit electrode, as specified by the oscillator, by putting out as much current as required to maintain the correct voltage. The amount of power that the user is exposed to is on the same order of magnitude as that received from a pair of stereo headphones, and is several orders of magnitude below FCC regulation.

Each receive channel consists of an op-amp gain stage, a multiplier, and another op-amp used as an integrator. The received signal is multiplied by the original transmitted signal, and the resulting function is integrated over an interval of 60 ms. The effect of these two operations is to project out, in a sense defined below, all the Fourier components of the received signal except for the component that was transmitted. The multiplier and integrator are computing (in analog electronics) the inner product of the transmitted signal function s_t and the received signal function s_r, with a window function set by the integration time. The sense in which the multiplier and integrator project out all undesirable Fourier components is the following: because all distinct pairs of Fourier components are orthogonal, the contribution to the inner product $< s_t, s_r >$ from all the undesirable (i.e. different from s_t and therefore orthogonal) components is zero. The input stage is therefore a very sharp filter that rejects all signals not of the proper frequency and phase.

It is also possible to describe the sensing circuitry in terms of amplitude modulation. The transmitter may be thought of as a carrier whose amplitude is modulated by the motions of a person's body. The receive multiplier mixes the carrier down to DC, and then the final

[1] It is called "Fish" because electric fish use similar mechanisms to sense their environments, and because we hope that the Fish, which navigates in three dimensions, might be the successor input device to the mouse, which only navigates in two.

Shenzhen Huiding Tech. Co., Ltd. - Exhibit 1006

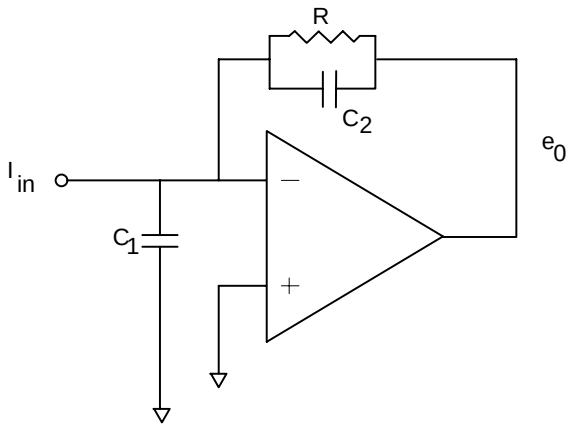


Figure 2-1: Diagram of front end gain stage for noise calculations.

lowpass filter rejects all signals other than those superimposed on the carrier.

2.1.1 Noise

There are two classes of op-amp noise to consider, *interference noise*, which is caused by external sources, such as coupling from the digital circuitry on the board, and *intrinsic noise,* which is due to the physics of the op-amp and feedback network components. We will calculate the intrinsic noise for the Fish front end, compare it to the observed noise, and conclude that interference noise dominates the intrinsic noise.

Intrinsic Noise Calculation

Intrinsic noise may be divided into voltage noise, current noise, and Johnson noise in the feedback and input resistors.[SS69] The most important component of the intrinsic noise turns out in our case to be voltage noise. For our front end gain stage, shown schematically in Figure 2-1, the output voltage noise e_o is given by $e_0 = Ne_n$ where e_n is this intrinsic voltage noise and the amplifier's noise gain N is given by

$$N = \frac{1}{\beta}\frac{1}{1+\frac{1}{A\beta}}$$

Here A is the amplifier's open-loop gain, and the feedback ratio

$$\frac{1}{\beta} = 1 + \frac{R}{1+RC_{2p}}(C_{1p})$$

with $R = 1M\Omega$ and $C1 = C2 = 1$pF. The impedance of C_1 is denoted $C_{1p} = \frac{1}{i\omega C}$. For the TL082CP op-amp used in the Fish front end, e_n is $\frac{18nV}{\sqrt{Hz}}$[Dev95]. This yields a voltage noise of $0.12mV$ rms. The current noise is $8.31 \times 10^{-18}V$ and the Johnson noise is $9.95 \times 10^{-7}V$. The quadrature sum of all the three intrinsic noise figures is essentially the same as that of the voltage figure, $0.119mV$.

The Fish board uses the 8-bit analog to digital converter on the Motorola MC68HC11,

Shenzhen Huiding Tech. Co., Ltd. - Exhibit 1006

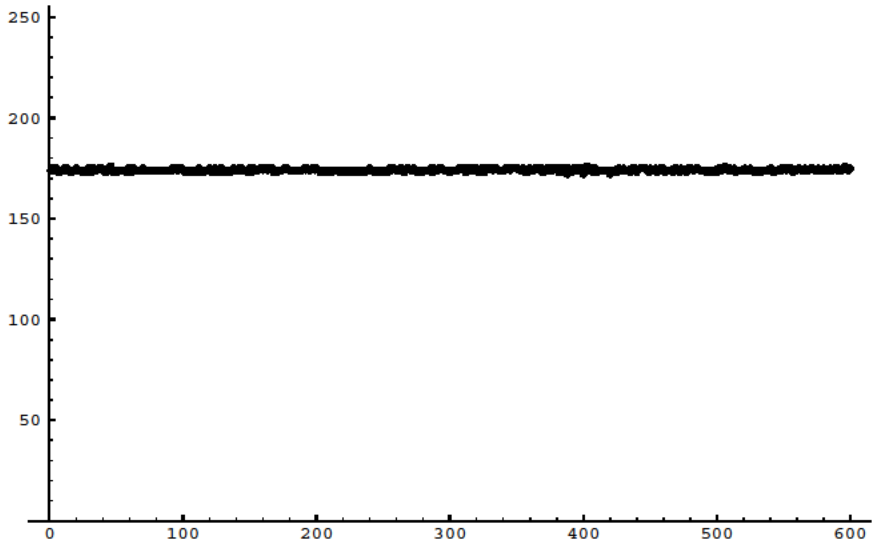


Figure 2-2: Timeseries of 600 sensor values showing quantization noise.

which has $\pm 1/2$ least significant bit accuracy[Mot91], so the quantization resolution is $5V/256 = .195V$. Since the quantization noise is 3 orders of magnitude greater than the intrinsic noise of the op-amp, we expect the readings to show the Gaussian profile typical of quantization noise.

Measured Noise

To study the noise characteristics of the final digitized signal, we chose the offset voltage so that the sensor gave a value comfortably far from clipping high or low (about 175 out of 255) when the field was unperturbed. We collected 600 samples at a sampling rate of 60 per second. The maximum likelihood estimate of the standard deviation of this data set is 0.66. Figure 2-2 shows this timeseries, Figure 2-3 shows its normalized histogram, and Figure 2-4 shows the normal distribution with the mean and standard deviation of the noise timeseries.

2.1.2 Contrast to Noise and Lengthscale

The signal received depends on the sensor geometry. Consider a parallel plate transmit-receive geometry. Since the capacitance goes as $1/d$, where d is the spacing between the plates, the unperturbed signal also falls off as $1/d$. Thus at a certain point the op-amp noise places a limit on how far we can see with the sensors, that is, on the lengthscale on which they are operable. In fact, however, the relevant quantity in determining the usefulness of the sensors is not signal to noise (the ratio of the unperturbed signal to the voltage or other noise), but *contrast* to noise, that is, the ratio of the difference between the maximum and minimum signal to the noise.

In order to maximize contrast to noise microscopically, one needs to set $\frac{d(\frac{S}{N})}{dp} = 0$, where S is signal, N is noise, and p is an adjustable parameter that affects both signal and noise.[Ros95]

Shenzhen Huiding Tech. Co., Ltd. - Exhibit 1006

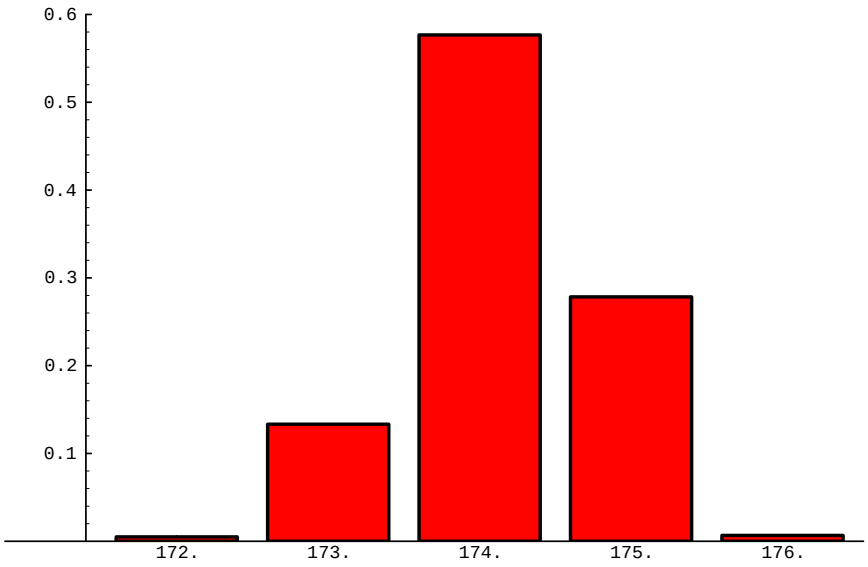


Figure 2-3: Normalized histogram of noise dataset.

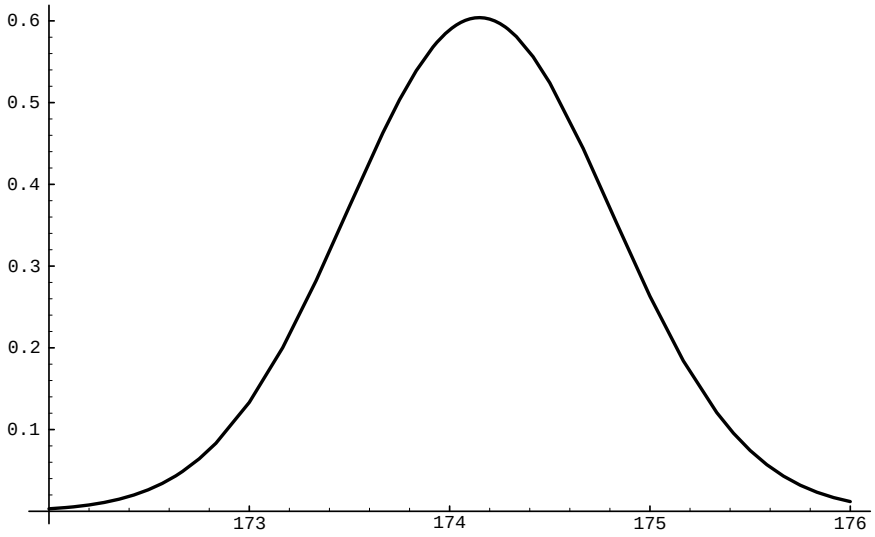


Figure 2-4: Normal distribution with mean and standard deviation of noise dataset.

Shenzhen Huiding Tech. Co., Ltd. - Exhibit 1006

2.2 Derivation of Circuit Model from Maxwell Equations

The goal of EFT imaging is to estimate a microscopic "impedance field" from macroscopic measurements provided by circuits such as the Fish. It will therefore be useful to be clear about the relationship between the circuit description and the field description of the sensing process. In the remainder of this chapter we will outline the derivation of the circuit description from the quasi-static approximation to the Maxwell equations, following the treatment in Chapter 6 of Fano, Chu, and Adler[FCA60]. In the next chapter, we will come full circle by using circuit concepts to describe fields, and introduce a hybrid circuit-field description that will allow us to predict the response of the sensors to simple conductivity distributions.

2.2.1 Maxwell's equations

Maxwell's equations can be written in the form

$$\nabla \times \mathbf{E} = -\frac{\partial \mathbf{B}}{\partial t} \tag{2.1}$$

$$\nabla \times \mathbf{H} = \mathbf{J}_f + \frac{\partial \mathbf{D}}{\partial t} \tag{2.2}$$

$$\nabla \cdot \mathbf{D} = \rho_f \tag{2.3}$$

$$\nabla \cdot \mathbf{B} = 0 \tag{2.4}$$

$$\nabla \cdot \mathbf{J}_f = -\frac{\partial \rho_f}{\partial t} \tag{2.5}$$

where, for linear and isotropic media,

$$\mathbf{D} = \epsilon \mathbf{E}$$

$$\mathbf{B} = \mu \mathbf{H}$$

$$\mathbf{J}_f = \sigma \mathbf{E}$$

As explained in section 2.1, Electric Field Sensing uses low frequencies. To study the properties of low-frequency solutions of the Maxwell equations, we can introduce a time-rate parameter α and a new, scaled time $\tau = \alpha t$. Small values of α map long periods of real time t into a unit of scaled time. Thus slow or low-frequency behavior corresponds to small values of α. The low-frequency behavior is therefore described by the low order terms in an expansion of the fields in a power series in α.

We can put a rough physical interpretation on α: its value is the ratio between the time τ for an electromagnetic wave to propagate across the longest lengthscale in the problem (the characteristic time for wave behavior), and the smallest time t of interest, in our case the period of the highest frequency that our oscillator can produce. We will say this quantitatively later, but for now note that the period of our oscillator is slow compared to the wave propagation time, so α is small. The expansion of $\mathbf{E}$ in powers of α has the form

$$\mathbf{E}(x,y,z,t) = \mathbf{E}(x,y,z,\tau,\alpha) = \mathbf{E}_0(x,y,z,\tau) + \alpha \mathbf{E}_1(x,y,z,\tau) + \alpha^2 \mathbf{E}_2(x,y,z,\tau) + \ldots$$

Shenzhen Huiding Tech. Co., Ltd. - Exhibit 1006

where

$$\mathbf{E}_0(x,y,z,\tau) = [\mathbf{E}(x,y,z,\tau,\alpha)]_{\alpha=0}$$

$$\mathbf{E}_1(x,y,z,\tau) = \left[\frac{\partial \mathbf{E}(x,y,z,\tau,\alpha)}{\partial \alpha}\right]_{\alpha=0}$$

$$\mathbf{E}_k(x,y,z,\tau) = \frac{1}{k!}\left[\frac{\partial^k \mathbf{E}(x,y,z,\tau,\alpha)}{\partial \alpha^k}\right]_{\alpha=0}$$

When the frequency is low enough that all but the zeroth and first order terms can be neglected, the solution is called quasi-static.[FCA60]

Using the new, scaled time τ, time derivatives will be multiplied by α, for example:

$$\frac{\partial \mathbf{B}}{\partial t} = \frac{\partial \mathbf{B}}{\partial \tau}\frac{\partial \tau}{\partial t} = \alpha \frac{\partial \mathbf{B}}{\partial \tau}$$

The three Maxwell equations involving time derivatives become

$$\nabla \times \mathbf{E} = -\alpha \frac{\partial \mathbf{B}}{\partial \tau} \tag{2.6}$$

$$\nabla \times \mathbf{H} = \mathbf{J}_f + \alpha \frac{\partial \mathbf{D}}{\partial \tau} \tag{2.7}$$

$$\nabla \cdot \mathbf{J}_f = -\alpha \frac{\partial \rho_f}{\partial \tau} \tag{2.8}$$

Substituting the expanded $\mathbf{E}$ and $\mathbf{B}$ fields back into the scaled Maxwell equation 2.6 and grouping terms, 2.6 becomes

$$\nabla \times \mathbf{E}_0 + \alpha(\nabla \times \mathbf{E}_1 + \frac{\partial \mathbf{B}_0}{\partial \tau}) + \alpha^2(\nabla \times \mathbf{E}_2 + \frac{\partial \mathbf{B}_1}{\partial \tau}) + \ldots = 0$$

Each term in the sum must equal zero individually for the equation to hold for all values of α. This defines a series of equations whose solution is the series of fields that make up our expansion. Because the $\mathbf{B}$ term in 2.6 is multiplied by α, and the $\mathbf{E}$ term is not, kth order $\mathbf{E}$ terms are related in the infinite series of equations to $k-1$th order $\mathbf{B}$ terms. The expansion of equation 2.7 will yield a series of equations coupling kth order $\mathbf{B}$ fields to $k-1$th order $\mathbf{E}$ fields. Since all fields are coupled only to lower order fields, any number of terms can be evaluated, by starting from the zeroth order solution, using that to find the first order, and so on. The zeroth order $\mathbf{E}$ field equations are

$$\nabla \times \mathbf{E}_0 = 0 \tag{2.9}$$

$$\nabla \times \mathbf{H}_0 = \mathbf{J}_{f0} \tag{2.10}$$

$$\nabla \cdot \mathbf{J}_{f0} = 0 \tag{2.11}$$

The Maxwell equations that do not involve time derivatives become:

$$\nabla \cdot \epsilon \mathbf{E}_0 = \rho_{f0} \tag{2.12}$$

$$\nabla \cdot \mu \mathbf{H}_0 = 0 \tag{2.13}$$

Shenzhen Huiding Tech. Co., Ltd. - Exhibit 1006

Next we will write out the first order fields. Since all values of α correspond to physically realizable fields, any field can be viewed as the original, "unscaled" field. Therefore no loss of generality results from setting $\alpha = 1$, and writing t instead of τ:

$$\nabla \times \mathbf{E}_1 = \mu \frac{\partial \mathbf{H}_0}{\partial t} \tag{2.14}$$

$$\nabla \times \mathbf{H}_1 = \epsilon \frac{\partial \mathbf{E}_0}{\partial t} + \mathbf{J}_{f1} \tag{2.15}$$

$$\nabla \cdot \epsilon \mathbf{E}_1 = \rho_{f1} \tag{2.16}$$

$$\nabla \cdot \mu \mathbf{H}_1 = 0 \tag{2.17}$$

$$\nabla \cdot \mathbf{J}_{f1} = -\frac{\partial \rho_{f0}}{\partial t} \tag{2.18}$$

Because the curl of any vector field V equals zero if and only if V can be written as the gradient of a scalar potential, equation 2.9 implies that $\mathbf{E}_0 = \nabla \phi_0$. In a region with no sources or sinks, any vector field satisfies $\nabla \cdot \mathbf{V} = 0$, so if there are no free charges, $\nabla \cdot \nabla \phi_0 = \nabla^2 \phi_0 = 0$; that is, ϕ_0 satisfies Laplace's equation. If free charges are present, then ϕ_0 satisfies Poisson's equation, by a similar argument.

2.2.2 Quasistatic limit

In terms of our expansion above, the quasi-static condition holds when $\alpha = \frac{\tau}{t} = \frac{L}{ct} \ll 1$, because higher powers of α are negligible when $\alpha \ll 1$. Again, τ is the time for an electromagnetic wave to propagate across the longest lengthscale in the problem, and t is the period of the transmit oscillator. If L is 10 meters and the transmit frequency is 100kHz, so that $t = 1.0 \times 10^{-5}$, then $\alpha = 3.3 \times 10^{-3} \ll 1$, so we are comfortably in the quasistatic regime.

When α is vanishingly small, so that only the zeroth order terms are required, we are in the regime of DC circuits. For small but finite rates of change, the first order terms must also be taken into account. This is the regime of AC circuitry. In the next section we will see in more detail how the concepts and laws of circuit theory emerge naturally as the quasistatic limit of the Maxwell equations.

2.2.3 Circuit Theory

There are three basic types of solutions to the zeroth and first order Maxwell equations, which correspond to the three basic types of circuit components: capacitive, inductive, and resistive. For Electric Field Sensing and Tomography, only the capacitive solutions are relevant;[2] for Electrical Impedance Tomography only the resistive solutions matter (for this reason the name Electrical Resistivity Tomography would be more accurate). We will see, however, that the equations specifying the "capacitive" and "resistive" fields are identical in form, which might be guessed from the fact that resistance and capacitance can be viewed as special cases of the generalized circuit concept of impedance.

The three types of quasi-static fields can be classified according to their zeroth-order terms. The first two types arise when there is no conduction current. In these first two

[2] We will see later that the situation is slightly more complicated than this.

Shenzhen Huiding Tech. Co., Ltd. - Exhibit 1006

cases the right side of equation 2.10 is zero, and there is no coupling between the electric and magnetic fields, so the two can be treated separately. The first type of quasistatic solution, electrical, has no magnetic component, and will be associated with capacitance, as we will explain below. A magnetic solution with no electrical component will be associated with inductance. The solution associated with resistance arises when conduction currents are present. If $\mathbf{J}_{f0} = \sigma \mathbf{E}_0$, then equation 2.10 becomes $\nabla \times \mathbf{H_0} = \sigma \mathbf{E}_0$. Thus in resistive solutions the zeroth order electric field is coupled to the zeroth order magnetic field through a finite conductivity.

To see why the electrical solution is associated with capacitance, first recall the circuit definition of capacitance:

$$I = C \frac{dV}{dt} \tag{2.19}$$

A capacitance couples a current to the time derivative of a voltage. Now consider the "capacitive" field. Because of equation 2.15, a zeroth order electric field induces a first order magnetic field proportional to the time derivative of the electric field. Associated with the zeroth-order electric field is a zeroth-order charge; by equation 2.18, the time derivative of this charge induces a first order current. Since the zeroth order electric field may be represented by a scalar potential, this first order current is coupled to the time derivative of the zeroth order potential. As we saw in equation 2.19, this type of coupling is referred to as capacitive in circuit theory. Similar arguments demonstrate the correspondance between the other types of fields and circuit components.

2.2.4 Laplace's equation in an inhomogeneous medium

For an inhomogeneous medium with embedded conductors at defined potentials, for example, the medium shown in Figure 2-5, the zeroth order electric field satisfies equation 2.12, which becomes

$$-\nabla \cdot \epsilon \mathbf{E_0} = \nabla \cdot (\epsilon \nabla \phi_o) = \epsilon \nabla^2 \phi_0 + \nabla \epsilon \cdot \nabla \phi_0 = 0 \tag{2.20}$$

in the region between the conductors. For a homogeneous medium, this reduces to the standard Laplace equation, $\nabla^2 \phi_0 = 0$. The third, resistive field solution leads to an equation analogous to 2.20, but with permittivity replaced by conductivity:

$$-\nabla \cdot \sigma \mathbf{E_0} = \nabla \cdot (\sigma \nabla \phi_o) = \sigma \nabla^2 \phi_0 + \nabla \sigma \cdot \nabla \phi_0 = 0 \tag{2.21}$$

Because these two equations have the same form, solutions pertaining to one physical situation are solutions to the other, as long as the boundary conditions are analogous. In fact, to determine the capacitance due to a body with a complex shape, Haus[HM89] (p. 274) recommends immersing the body in a tank filled with electrolytes and making conduction measurements, which he feels are easier experimentally.

Equation 2.21 describes the general forward problem in Electrical Impedance Tomography. Technically, equation 2.20 describes the forward problem in Electric Field Tomography. However, the bodies we image in EFT tend not to be isolated permittivities, as would be the case if we only wanted to use EFT to, for example, image the surface of a wooden desk and the books on top. For this sort of problem, all the machinery of Electrical Impedance Tomography applies in the most straightforward manner. In a typical EFT problem, however, the body being imaged is a perfect conductor coupled capacitively (through the shoes) to a defined potential, ground, which changes the problem somewhat. Practical approaches

Shenzhen Huiding Tech. Co., Ltd. - Exhibit 1006

will probably model the part of the body that is outside the sensing field as a lumped circuit component. For example, the parts of the body outside the field can probably be modeled as a capacitor to ground.

2.2.5 Electrostatics

Our expansion showed that static (zeroth order) electric fields satisfy Laplace's equation. The behavior of the static fields is crucial to Electric Field Sensing, because, as we shall see in section 2.2.6, though EF sensing requires first order fields to operate, no new information is contained in the first order fields; it is all present in the zeroth order. Therefore, we will now briefly discuss methods for solving electrostatic field problems.

There are two basic ways of viewing such problems: the boundary value perspective, and the superposition integral perspective. In the boundary value perspective, we find the potential and hence the field by solving Laplace's equation subject to specified boundary conditions. There are a variety of analytical methods useful for solving Laplace's equation in particular cases, but in general, one must resort to numerical methods. In describing the boundary value perspective, I have essentially just said "solve the zeroth order Maxwell equations for the electric field."

There is another way to view electrostatics problems, however. In the superposition integral approach, we assume that a charge distribution is known. We find the total field by superposing the fields induced by each charge separately. This approach works well for finding the field around a (non-conductive) molecule, since the charge density is essentially fixed. It is less convenient for dealing with conductors, since the charges are not in fixed locations. It may not be obvious how to relate the superposition integral perspective to our quasistatic solution of Maxwell's equations, and thus to the boundary value perspective. The relationship is that the $\mathbf{E}$ field due to a static point charge is the Green's function of Laplace's equation. The reason we can superpose the fields is that Maxwell's equations are linear.

2.2.6 Capacitance

In the previous two sections, we discussed the principles of how to find the static electric field due to a set of isolated conductors at known potentials, such as those shown in Figure 2-5, embedded in a medium (isotropic, but not necessarily homogeneous) of permittivity ϵ. We now will show how to use quasistatic field solutions to calculate macroscopic circuit quantities such as capacitance and received current.

The static charge on a conductor i is due to the $\mathbf{E}_0$ field:

$$Q_i = -\int_{S_i} \epsilon \mathbf{n} \cdot \nabla \phi_0 da$$

where S_i is the surface of i, $\mathbf{n}$ is the outward normal to S_i, and ϵ may be a function of position, since the medium need not be homogeneous.

Using the standard definition, the capacitance of conductor i due to a conductor j is the ratio between the charge on Q_i and the voltage between j and a reference. Of course if we know the capacitance and voltages for a pair of electrodes, we can find the charge induced on one by the other. Because of the linearity of all the equations involved, the total charge on i induced by all the other conductors is the sum of the separately induced

Shenzhen Huiding Tech. Co., Ltd. - Exhibit 1006

charges[FCA60] (note that the capacitances are not linear functions of position):

$$Q_i = \sum_j C_{ij} V_j \tag{2.22}$$

The off-diagonal terms of this capacitance matrix C_{ij} represent the ratio between Q_i and V_j when all the other Vs are zero. The diagonal "self-capacitance" terms C_{ii} represent the charge on i when it is held at V_i and all the other electrodes are at zero. In terms of our sensing hardware, the diagonal terms represent the intrinsic capacitance of the cable and the electrode. The matrix is symmetrical.

We will now see that from the capacitances, we can calculate the currents received at the electrodes. This is because equation 2.18 relates the first order current to the zeroth order charge. By charge continuity (expressed microscopically in equation 2.18), the current I_i entering receiver i is given by the time derivative of the charge on i: $I_i = \frac{dQ_i}{dt}$.

$$I_i = \frac{d}{dt} \sum_j C_{ij} V_j = \sum_j C_{ij} \frac{dV_j}{dt} \tag{2.23}$$

The currents that we measure in Electric Field Sensing are first order phenomena. However, we only use the currents to measure capacitance, the zeroth order property that is geometry dependent and therefore encodes the geometrical information that we ultimately want to extract. This tells us something about the physical limits on the time resolution of EF sensing: the "frame rate" must be much shorter than the characteristic time for first order phenomena, that is, the oscillator period.

2.3 Lumped Circuit Model and Sensing Modes

Now we will apply the framework developed in the previous section to Electric Field Sensing. We will present a lumped circuit model of a single transmit-receive pair with a single target object, whose proximity we are interested in. The various "modes" in which the Fish circuitry can be used have clear interpretations as current paths through the circuit diagram, shown in Figure 2-5. For each sensing mode, we will give a brief overview from a user's point of view, and then explain the physics of the mode in terms of this diagram.

Figure 2-5 shows the model. There are four "terminals": the transmitter, the receiver, the target object (shown as a hand), and ground. The $\frac{4\times3}{2} = 6$ distinct inter-conductor capacitances are shown. The small resistor and capacitor and C_i represent the body's internal capacitance and resistance. Capacitor C_5 is the target object's coupling to ground. If a person is being sensed, C_5 is usually dominated by the capacitance through the shoes. The ground terminal may either be a ground plane in close proximity to the transmitter and receiver, or the ambient room ground.

The sensors can be used in a variety of ways, explained below, each of which modifies these capacitances differently. We measure capacitance by measuring the current arriving at the receiver, as explained in section 2.1 and 2.2.6.

Shenzhen Huiding Tech. Co., Ltd. - Exhibit 1006

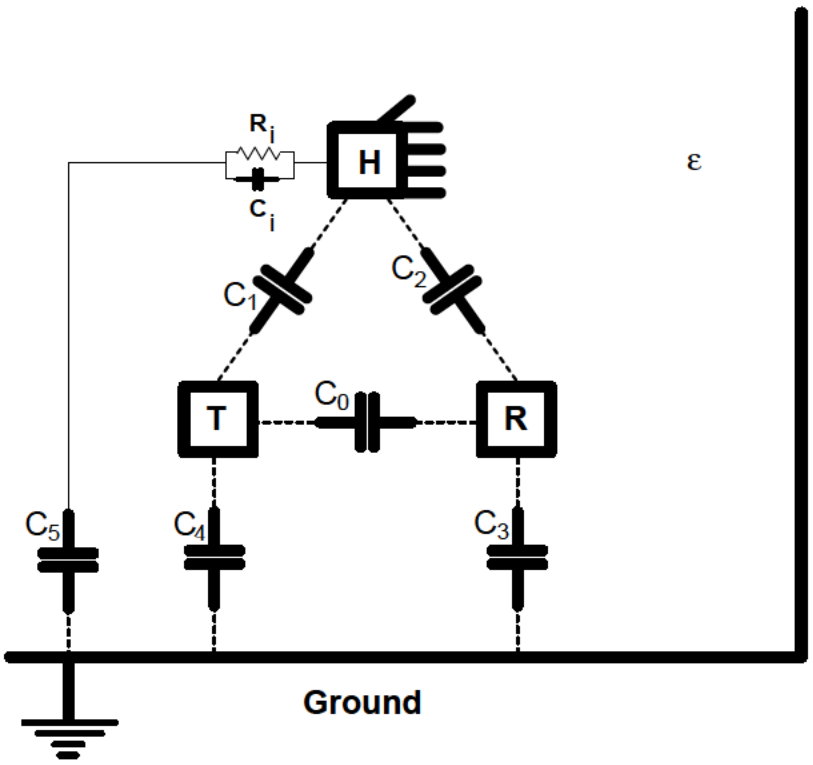


Figure 2-5: Lumped circuit model of Electric Field Sensing.

Shenzhen Huiding Tech. Co., Ltd. - Exhibit 1006

2.3.1 Transmit Mode

In transmit mode[GZA95], the transmit electrode is put in contact with the user's body, which then becomes a transmitter, either because of direct electrical connection, or AC coupling through the clothes, which is shown as current path C_1 in the circuit diagram.

When the hand moves, the spacing to the receiver changes, which changes the value of C_2. When the spacing from the hand to the receiver is large, the received signal goes roughly as $1/r^2$, because the hand acts like a point object and the field falls off as $1/r^2$. By Gauss's law then, the induced charge on the receiver also goes as $1/r^2$. Since the potentials on the electrodes are defined by the Fish circuit, we know the capacitance to be $C = Q/V$, and the received current $I_R = 2\pi f C V$, as explained in section 2.2.6. When the hand is very close to the receiver, C_2 (typically) has the geometry of a parallel plate capacitor, and the signal goes as $1/r$.

2.3.2 Transmitter Loading Mode

The Smart Fish[PG95] has circuitry to measure the current being lost at the transmit electrode. This is known as loading mode. It has also been investigated by Vranish et al.[V$^+$92, V$^+$93].

If the only object in our sensing apparatus that can move is the body that we wish to sense, then any change in the amount of current leaving the transmitter indicates a change in the value of C_1.

2.3.3 Receiver Loading Mode

Receiver loading mode is a pseudo mode, in that it relies on non-ideal characteristics of the op-amp. When a grounded object approaches the receiver, current may be shunted from the receiver, even if the receiver completely shields the transmitter from the ground.

I discovered this mode while trying to make a two-dimensional electric field mouse with touch click. The mode is useful for making very large pressure sensors that are *not* sensitive to matter until it touches the sensing surface. Additional proximity sensitive electrodes, for example those used to track the hand in the clickable two-d mouse, can be mounted on top of the touch surface; the touch sensor and the proximity sensors do not interfere with one another.

It is important for Fish users to know about this mode because it can often be an annoyance. If a receiver is placed against a wall, there is a current path from the receiver to the wall; this path appears as capacitor C_3 in the diagram. Because wall electrodes are usually placed flush against the wall, they behave like parallel plate capacitors, with a very small separation r between the plates. The reason this mode can be such a problem is that the capacitance k/r (where k is a constant) is very large. In particular, tiny changes in r, which may arise from air currents, lead to large changes in k/r, and therefore large offsets in signal. The mode can therefore introduce mysterious drifts in the sensor values, or be used to make very sensitive measurements.

2.3.4 Shunt Mode

In this thesis, we will be concerned primarily with shunt mode. Shunt mode is better suited to imaging, because it provides more informative measurements than other modes, as we

Shenzhen Huiding Tech. Co., Ltd. - Exhibit 1006

will explain below.

In shunt mode, neither the transmitter nor the receiver are in contact with the user's body. When the user's body is out of the field, current flows from transmitter to receiver through the effective capacitance C_0.

When part of the user's body, such as a hand, enters the field, it functions as a third terminal, and the capacitance matrix changes, often drastically. In particular, the value of C_0 shifts. Since the voltage between the transmitter and receiver is held constant, the change in C leads to a change in the current arriving at the receiver. From the amount of current that fails to arrive at the receiver, one can infer something—what, exactly, is the subject of the thesis—about the "amount of arm" in the vicinity of the sensor. [The rest of the body functions as a ground for the part that is in the field. It does so because, at these frequencies, the body is nearly a perfect conductor, and is a relatively large charge reservoir. The rest of the body is also capacitively coupled to an even larger charge reservoir, the earth or room ground; this current path is labeled C_5. Both effects (the body as a ground, and the body as a wire to ground) contribute to C_5.[Zim95]]

The sense in which shunt mode is more informative is the following: an n electrode array can make as many as $\frac{n(n-1)}{2}$ distinct measurements, since it uses pairs of electrodes. This number, rather than n^2, arises because electrodes cannot function simultaneously as receiver and transmitter (hence the $n(n-1)$). The factor of $\frac{1}{2}$ arises because the capacitance matrix is symmetrical: we learn nothing new when we interchange a transmitter and receiver. By contrast, an n-electrode array of sensors operating in transmit or loading mode can only make n distinct measurements. To see the difference more clearly, note that each shunt mode measurement has an associated length and orientation, that of the vector between the transmitter and receiver. A pair of electrodes far apart "sees" much further than a pair of electrodes close together (because the lengthscale of the $\frac{1}{r^3}$ field dependence is set by the spacing between the electrodes), and a pair oriented horizontally responds differently than a vertically oriented pair. So while both shunt and loading mode measurements have associated positions, a shunt mode measurement has an extra geometrical parameter, this sensor orientation vector.

Relationship to other modes The modes cannot actually be separated as cleanly as I have suggested. When the hand is close to both the transmitter and receiver, both C_1 and C_2 can become large. Their sum,[3] in fact, can become larger then C_0, and the current arriving at R can be greater than the current that arrived before the field was perturbed.

We usually refer to this as "coupling mode" or "crossover mode," meaning the pseudo mode in which the electrodes are configured for shunting, but the dominant effect is the transmit effect. As the hand approaches a transmit-receive pair in shunting configuration, the signal decreases as more displacement current is shunted from C_0 to C_1. But as the hand approaches the transmitter and receiver more closely, the signal starts increasing as the "transmit mode" current path through C_2 grows.

Variations in C_5 can affect the sensors dramatically. The C_5 of a person wearing 10 cm thick platform shoes would be one tenth that of a person wearing shoes with 1 cm thick soles. In fact, the value of C_5 can vary even more, for example when the person is on an actual platform such as a stage.[Par] This can be a serious problem.

[3] Since the arm is a conductor, C_1 and C_2 are connected in parallel, and therefore add.

Shenzhen Huiding Tech. Co., Ltd. - Exhibit 1006

For mice or imaging systems to work well, they must infer the global offset C_5, in addition to the $C1$ for each receiver. We usually try to suppress C_2, though for some applications it might be desirable to try to infer its value also.

Component Values

At the frequencies we are concerned with, the real impedance of free space is essentially infinite (capacitors block direct current), and the real impedance of the body is almost zero. Barber [BB84] gives resistivity figures on the order of $10\Omega m$ (Ohm-meters), plus or minus an order of magnitude: cerebrospinal fluid has a resistivity of $.65\Omega m$, wet bovine bone has $166\Omega m$, blood has $1.5\Omega m$, and a human arm has $2.4\Omega m$ longitudinally and $6.75\Omega m$ transverse.

Tom Zimmerman measured the capacitance between the right hand and the left foot, and found a value of 9.1 pF [Zim95]. A simple parallel plate model of feet in shoes with 1cm thick soles gives a capacitance of 35 nF, using $C = \epsilon_0 A/d$, and taking $A = 2$ feet $\times 20cm \times 10cm$ and $d = 1$cm. For 10 cm thick platform shoes, the value of $C = 3.5$nF. (We have neglected the dielectric constant of the soles, and all inductive effects.)

Shenzhen Huiding Tech. Co., Ltd. - Exhibit 1006

Chapter 3

Forward Problem

3.1 General Case

As we saw in section 2.2.4, the sensor values can be determined in the most general case by solving the Laplace equation with an inhomogeneous permittivity ϵ, equation 2.20:

$$-\nabla \cdot \epsilon \mathbf{E_0} = \nabla \cdot (\epsilon \nabla \phi_o) = \epsilon \nabla^2 \phi_0 + \nabla \epsilon \cdot \nabla \phi_0 = 0$$

However, for very simple imaging problems (such as imaging a single point, that is, making a two- or three-dimensional mouse), this model is too general. We cannot afford to solve Laplace's equation each time we move the mouse. In this chapter we will use some of the physics presented in Chapter 2 to motivate a an approximate forward model of the response of the sensor to a single point-like grounded object.

3.2 Approximate effect of a small grounded object

We want to model the effect of a small, perfect conductor h at a point $\mathbf{x}$ in space, connected to ground through a capacitance C_5 and a wire whose effect on the field is negligible. What we want is a simple model of how the presence of the conductor affects the capacitance between the transmitter and the receiver. As a "zeroth order" approximation, we will assume that the object's effect on the geometry of the field is negligible.[1] We will be more explicit below about what is meant by the geometry of the field.

Figure 3-1 shows both the unperturbed electric field impinging on the receiver, and the perturbed field. It will be helpful to define a "two-terminal" component model of a field line. Such a component is shown in the Figure, stretching from the perturbation to the receiver. The component is defined by a small tubular surface with the property that the tangent vector of its axis is everywhere parallel to the field. Since the tube is small, its sides are also parallel to the field, and its endcaps are perpendicular to the field. Because the sides are parallel to the field, there is no flux through the sides. The only flux into or out of the tube is through the endcaps. Since the endcaps are small and perpendicular to the field, the flux through an endcap is equal to the field strength at a point on the endcap

[1] It should be possible to do an expansion in the size of the perturbation, analogous to the expansion in the time rate parameter from Chapter 2, to make the "zeroth order" character of the approximation explicit.

Shenzhen Huiding Tech. Co., Ltd. - Exhibit 1006

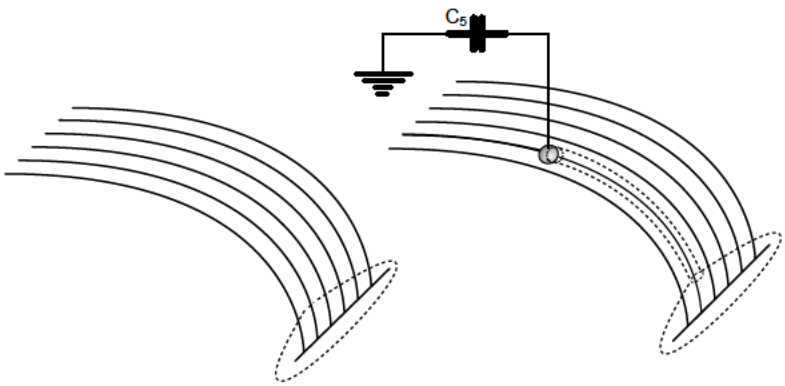


Figure 3-1: The unperturbed electric field impinging on the receiver, left, and the perturbed field, right. A two-terminal component model of a field line is shown between the perturbation and the receiver.

disk multiplied by the disk's area.

The divergence theorem says that the total flux through the tube's surface is equal to the integral of the enclosed source and sink terms ρ_f. The flux through a tube containing no sources or sinks (charge) is zero. Thus the flux leaving the bottom endcap of a sourceless tube equals the flux entering the top.

Now we can consider three contiguous tubes, the first starting at the transmit electrode (but not overlapping it) and ending just above the perturbation, the second enclosing the perturbation, and the third beginning just below and extending to the receiver. The net flux through the first tube is zero, since it contains no sources. The flux entering the small section of tube enclosing the perturbation is simply the field strength at the endcap disk multiplied by the disk's area, as explained earlier.

If the perturbation is a grounded, perfect conductor, it absorbs all the incident field lines: charge is induced on its surface in proportion to the incident flux. No flux leaves the bottom endcap, so that the net flux, rather than being zero as it would be in a charge-free region, is proportional to the induced charge.

Since none of the flux that left the first tube and entered the second arrives at the third, we can calculate an approximate change in the flux into the receiver, if we have made the "zeroth order" assumption that the object does not affect the field geometry (meaning the shapes of the tubes). The decrease in flux at the receiver is the amount that left the top tube, that is, the field strength at the perturbation, multiplied by the tube area.

If the object is connected to ground through an impedance, instead of directly, a voltage divider is a natural model to consider. The first tube would be modeled as one impedance, the third tube would be an impedance in series with it, and the connection to ground would be the load on the divider. This model is consistent with the case considered above, in which the impedance to ground is zero, and all the "current" is shunted to ground. When the impedance to ground is non-zero, some fraction of the flux entering the second tube

Shenzhen Huiding Tech. Co., Ltd. - Exhibit 1006

would also leave, and arrive at the receiver. We will be investigating the utility of this model further.

Now we have introduced a model for how an object changes the received signal that depends on the field strength at the object's location. Next we will need a model of the field itself.

3.3 Modeling the field: the dipole approximation

We will approximate the field due to a pair of small, identical, rectangular electrodes of dimension $b \times c$ and displaced from one another by a along the x-axis as a dipole with the same spacing. The dipole moment of a charge distribution is

$$\mathbf{p} = \int \mathbf{x}' \rho(\mathbf{x}') d^3x' \tag{3.1}$$

If the distribution on the electrode surfaces had a uniform value of ν,[2] then 3.1 yields

$$p_x = \nu abc$$

and

$$p_y = 0$$

The expression for p_x makes sense: νbc yields the total charge on one electrode, so we could write $p_x = Qa$. Thus the pair of rectangular electrodes displaced from one another by a and charged to $+Q$ and $-Q$ has the same dipole moment as a pair of point charges $+Q$ and $-Q$ displaced by the same amount.

To justify the dipole approximation more rigorously, we would have to solve for the charge distribution on the electrode surfaces, and then perform a multipole expansion of the charge distribution. The dimensions at which the higher order terms became significant would be the limits of the approximation's validity.

3.4 Modeling the sensor response

Using the point absorber model together with the dipole approximation of the field geometry, we can model the sensor response data measured using a small grounded object as a hand phantom. Figure 3-2 shows a plot of the function $C - |E(\mathbf{x})|$, where C is a constant and $E(\mathbf{x})$ is a dipole field, given by the gradient of the dipole potential $\frac{\mathbf{p}\cdot\hat{\mathbf{r}}}{r^2}$. The dipole moment $\mathbf{p}$ is a constant representing charge multiplied by the vector from the center of the transmitter to the center of the receiver.

Figure 3-3 shows sensor measurements along the z-axis, perpendicular to the transmit-receive axis, and the dipole response model. Since x and y are zero, the dipole model simplifies to $\mathbf{E}(0,0,z) = \frac{1}{z^3}$. Scale and offset parameters for the distance (abcissa) and sensor value (ordinate) have been fit to the data. The function plotted is shown at the top of the graph.

[2] The surface charge distribution is not in fact uniform, though the surface is an equipotential. These two statements are by no means equivalent.

Shenzhen Huiding Tech. Co., Ltd. - Exhibit 1006

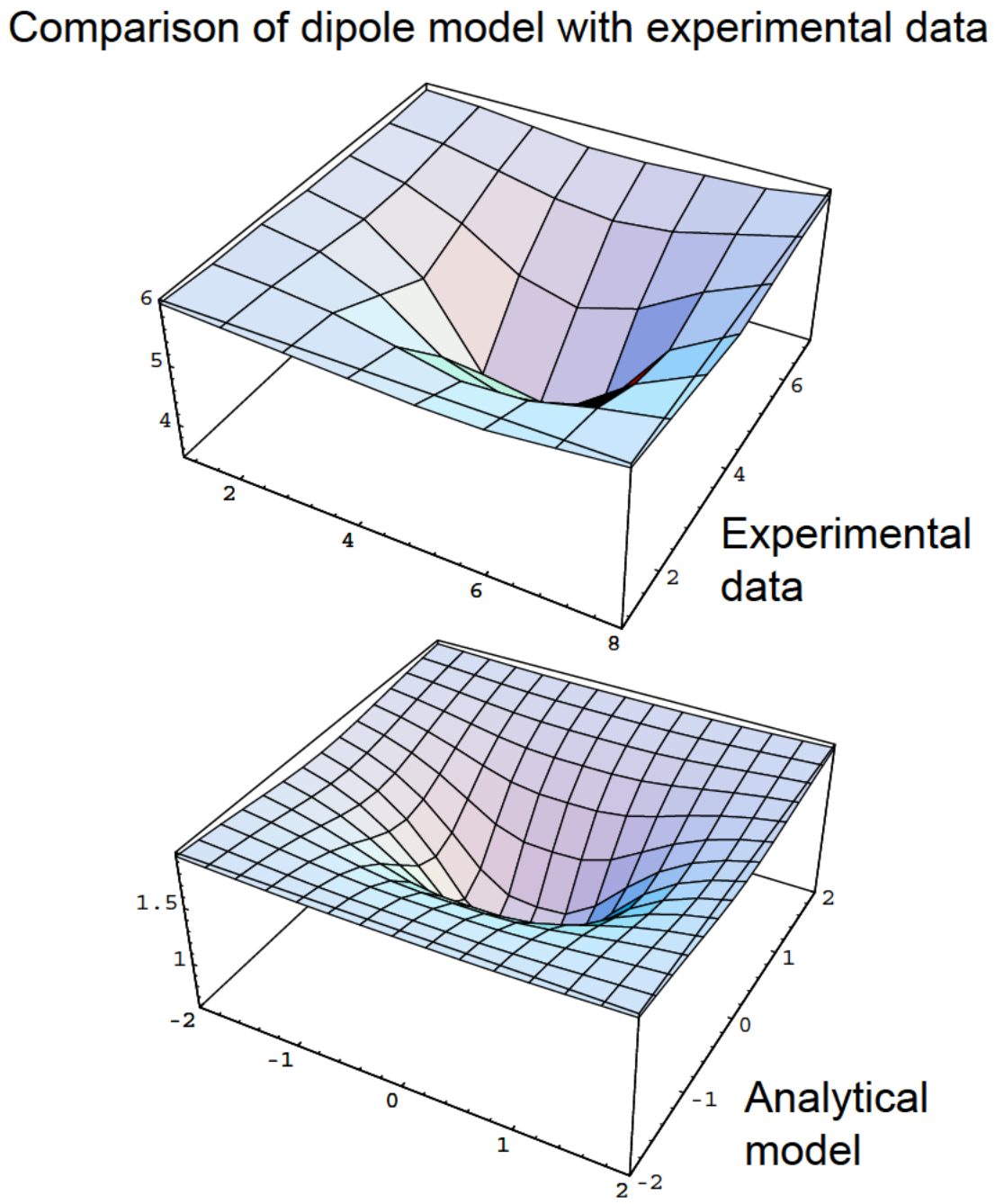


Figure 3-2: Comparison of functional form of dipole model with experimental data. Measurements were made in a plane parallel to the dipole axis, using a grounded metal cube as a hand phantom. The theoretical plot is for a plane parallel to dipole axis, at a distance of $.9a$ above the dipole axis, where a is the dipole spacing.

Shenzhen Huiding Tech. Co., Ltd. - Exhibit 1006

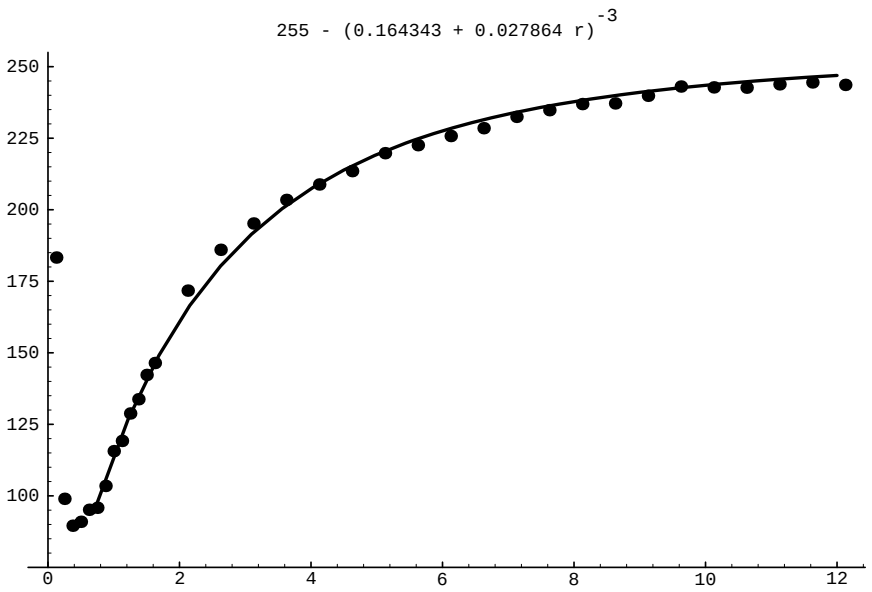


Figure 3-3: Comparison of functional form of dipole model with experimental data. Measurements were made along a line originating at the dipole origin, and extending outward, perpendicular to the dipole axis. At very short distances, transmit mode starts to dominate, and the signal rises again.

3.5 Iso-Signal Shells

Given this field model, we can plot surfaces of constant sensor readings. These plots are very helpful in shaping one's intuition about the behavior of the sensors. The surfaces are ellipsoidal shells. The central axis of the ellipsoid is the dipole axis. Figure 3-4 shows two nested iso-signal shells, for two different sensor readings. The outer shell has been cut away to reveal the inner one. As we will see in Chapter 4, these shells, with a Gaussian thickness to represent uncertainty due to sensor noise, are the ambiguity classes for single sensor measurements.

3.6 Ground plane

The dipole approximation is also a good model of the response of a sensor in the presence of a groundplane. Note that in the presence of a groundplane, the functional form of the response of a sensor is no longer simply the field strength, since many field lines starting at the transmitter end on the groundplane, instead of on a receiver, and are therefore irrelevant to the signal measured. In the non-groundplane case, almost all the field lines leaving the transmitter arrive at the receiver, so the sensor response is proportional to the absolute field strength.

The electric field between a transmit-receive pair in the presence of a groundplane is not dipolar. The field due to a single transmitter might be modeled as a dipole, but it would be one whose axis was perpendicular to the groundplane (by the method of images). Nevertheless, the response of the sensor can be modeled almost as well by the field strength of a dipole whose axis runs between the transmitter and receiver, parallel to the groundplane.

Shenzhen Huiding Tech. Co., Ltd. - Exhibit 1006

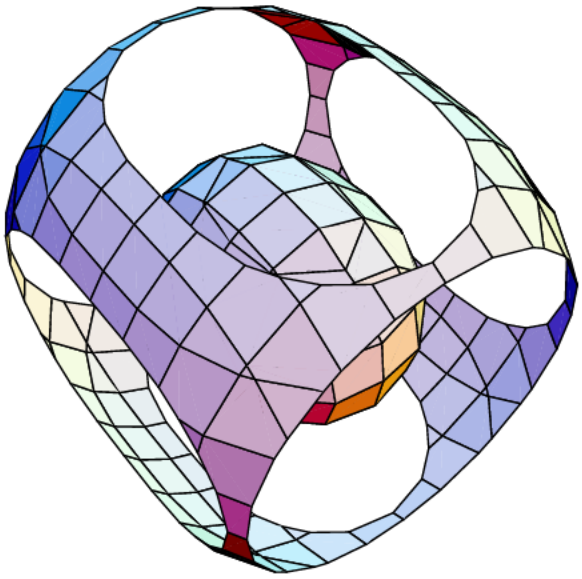


Figure 3-4: Two nested iso-signal shells, for two sensor values. The outer shell has been cut away to reveal the inner one. The dipole generating the field lies along the central axis of the ellipsoid.

Evidently the density of field lines that leave the transmitter and arrive on the receiver, rather than on groundplane, has this dipolar form, which is not surprising since this set of field lines has at least the very least the same bilateral symmetry as those produced by a pair of isolated electrodes.

We now have an analytical model for the behavior of a single transmit-receive pair in the presence of a groundplane, and this has useful consequences. Since receivers are virtual grounds, the field configuration due to, say, one transmitter, should not be changed by replacing a patch of groundplane with a receiver. In other words, the field due to a transmitter surrounded by groundplane is identical to that produced by a transmitter surrounded by a patchwork of receivers and ground. This in turn means that, in the presence of a groundplane, receivers do not affect one another—they are entirely independent dipoles. For small objects at least, we have an analytical solution to the forward problem of predicting the sensor values given a hand location, and this will be very helpful in solving the inverse problem.

3.6.1 Generalizations of hand model

It is an open research question whether the sort of approximations we have been using can generalized and applied to more complex conductivity geometries, for example, to the case of two hands, and for the general imaging problem. If there is a way to do so, we will be able to make faster algorithms. In the worst case, we will have to solve Laplace's equation each time we need to evaluate the forward model. This is a computationally slow but well-understood procedure.

Shenzhen Huiding Tech. Co., Ltd. - Exhibit 1006

Chapter 4

Constructing the ambiguity class

In this chapter we will introduce a general probabilistic framework that will allow us solve inversion problems anywhere along the EF sensing hierarchy, and also provide a means of designing optimal sensor geometries. This approach, applied to full imaging problems, is described by Jaynes in [Jay83], Hurwitz in [HHL79], Gull and Daniell in [GD78], and Skilling and Gull in [SG83].

The essence of the approach is to view imaging (or proximity detecting, or hand finding) as an inference problem. We define a model whose parameters we wish to know, and a probability distribution over those parameters. As more data becomes available (for example, as we consider additional sensors), the volume of the feasible set of model parameters, which we will call the ambiguity class, decreases and the probability distribution becomes increasingly peaked around the "true" values of the parameters.

The inverse curvature of a peak in a particular direction gives the uncertainty of the estimate of the parameter value (or linear combination of parameter values) corresponding to that direction. The amount of information provided by a measurement can by quantified by the change in entropy of the distribution that resulted from the measurement. Ill-posed (underdetermined) problems can be made well-posed by specifying additional constraints on the feasible set. (This is the Bayesian view of regularization.) These constraints can be encoded in the prior probability distribution that defines the initial feasible set. The problem of designing sensor arrays may be posed in terms of maximizing the expected information provided by a measurement.

Since, as we saw in section 2.1.1, the sensors are subject to additive Gaussian noise, the probability of the data given some setting of model parameters is given by

$$p(D|m) = \sqrt{\pi}\sigma e^{\frac{(D-f(m))^2}{\sigma^2}}$$

where σ is the standard deviation,[1] d is a data value, $f(m)$ is the data value predicted by our analytical forward model given a model configuration (hand position) m. This distribution is normalized: if we integrate over all values of d, we get 1. By Bayes' theorem,

$$p(m|D) = \sqrt{\pi}\sigma \frac{e^{\frac{(D-f(m))^2}{\sigma^2}} p(m)}{p(D)}$$

[1] It will not represent conductivity in this chapter.

Shenzhen Huiding Tech. Co., Ltd. - Exhibit 1006

For the case of a two- or three-dimensional mouse, we can chose a prior $p(m)$ that renders the inversion well-posed, by, for example, restricting the possible hand positions to positive coordinate values. A useful prior for for one of the model parameters is $p(m) = \frac{c}{1+e^{-\beta x}}$, defined in some finite range of x, where c is a normalizing constant and β is a sharpness parameter. This function is a way to approximate a step function with a closed form expression. A possible advantage of using this function over a hard step function is that numerical optimization techniques are able to follow it back into the high probability region, since it is smoothly varying. The prior for our entire model is the product of the priors for x, y, and z.

$$p(m|D) \propto e^{\frac{(D-f(m))^2}{\sigma^2}} \frac{c}{1+e^{-\beta x}}$$

Apart from the prior, which we might have chosen to be a constant over some region, the functional form of $p(m|D)$ is identical to that of $p(D|m)$. The remarkable fact that the $p(m|D)$ distribution and the $p(D|m)$ distribution, which have completely different meanings, happen always to have the same functional form is the content of Bayes' rule. However, the similarity in functional form is in some sense superficial. Consider the normalization of $p(m|D)$. Rather than performing the trivial Gaussian integral over d (trivial and Gaussian because when we integrated $p(D|m)$, m and therefore $f(m)$ was fixed), we must integrate over all values of m, which means integrating our forward model composed with a Gaussian. The difficulty of performing this integration depends on the form of f. This normalization constant, which Bayesians grandly call the evidence, is not important for finding the best setting m of the model paramters, since a scaling of the dependent variable (probability) has no effect on the location of maxima. However, it does become important when making any sort of comparison between different functions f, or calculating entropies. The difficulty of performing this integration would be the Achilles' heel of Bayesian methods, were it not for the fact that for small σ, $p(m|D)$ can be well approximated by a Guassian, which is trivial to integrate.

Information collected by multiple sensors can easily be fused: simply multiply the $p(m|D)$ terms due to each sensor to get the joint probability of a model given all the data. Thus if we use D to denote the set of N measurements d_i, where i indexes the sensor,

$$p(m|D) \propto \prod_i^N e^{\frac{(D_i-f_i(m))^2}{\sigma^2}} \prod_j \frac{c}{1+e^{-\beta x_j}}$$

Notice that, since log is a monotonically increasing function, if we maximize $\log p(m|D)$, we will get the same m as if we had maximized $p(m|D)$. It will be desirable in practice to work with log probabilities rather than probabilities, for several reasons: we can save computation time since exponentials disappear and multiplication and division become addition and subtraction. Furthermore, when we multiply many probabilities together, the numbers become very small, so that numerical precision can become a problem. Using log probabilities alleviates this problem, and reduces computation time, since exponentials appear so often, in each of our Gaussian probability distributions.

$$\log p(m|D) = \sum_i^N \frac{(D_i - f_i(m))^2}{\sigma^2} - \sum_j \log(1+e^{-\beta x_j}) + c$$

Shenzhen Huiding Tech. Co., Ltd. - Exhibit 1006

This has the familiar interpretation of the sum of squared errors between the data and the data predicted by the model, with an additional error term derived from the prior.

4.1 Uncertainty and optimal sensor geometry

Once the basic degeneracies have been broken, either by collecting sufficient data or imposing constraints via a prior, so that there is a single maximum in the log probability, the uncertainty about the best setting of model parameters may be represented by the inverse Hessian matrix A^{-1} evaluated at the maximum. To see why, we will consider the Hessian and its properties. The Hessian A gives the curvature, which is a measure of confidence or certainty. In A's eigenvector basis, in which it is diagonal, the diagonal elements (the eigenvalues) A_{ii} represent the curvature along each of the eigenvector directions (known as the principal directions). The curvatures along the principal directions are called the principal curvatures. The product of the curvatures, the Gauss curvature, which serves as a summary of the certainty at a point, is given by the determinant of A. The average curvature is given by $\frac{1}{2}$ trace $A = \frac{A_{11}+A_{22}}{2}$. Finally, the curvature in a particular direction $v = (cos\theta, sin\theta)$ is given by Euler's formula:[Mor93]

$$\kappa = v^T A v = \kappa_1 cos^2\theta + \kappa_2 sin^2\theta$$

The inverse of A in this basis is the matrix with diagonal elements $1/A_{ii}$. Thus the inverse Hessian specifies "radii of curvature" of the probability distribution, which can be used a measure of uncertainty. The determinant and trace of the Hessian are independent of coordinates, so we may use these as local measures of the "Gauss uncertainty" and mean uncertainty.

4.2 Entropy

The most general global measure of uncertainty is the entropy. The change in entropy of the $p(m|d)$ distribution resulting from the collection of new data measures the change in uncertainty about the values of the model parameters, including uncertainty due to multiple maxima, given a set of measurements. The change in total entropy ΔH of the ambiguity class m resulting from a measurement d_{n+1} is

$$\Delta H(m|D_{n+1}) = H(m|D_{n+1}) - H(m|D_n)$$

where

$$H(m|D_n) = \int p(m|D_n) \log p(m|D_n) dm$$

The expected change in entropy when we collect a new piece of data, that is, the change in entropy averaged over possible data values, gives a basis for comparing sensor geometries. The expected value of $H(m|D)$ is

$$I = \int p(D) H(m|D) dD$$

I is thus measure of the quality of a sensor geometry. By analogy with coding theory, the best measurement procedure (for single measurements) reduces the entropy as much as

Shenzhen Huiding Tech. Co., Ltd. - Exhibit 1006

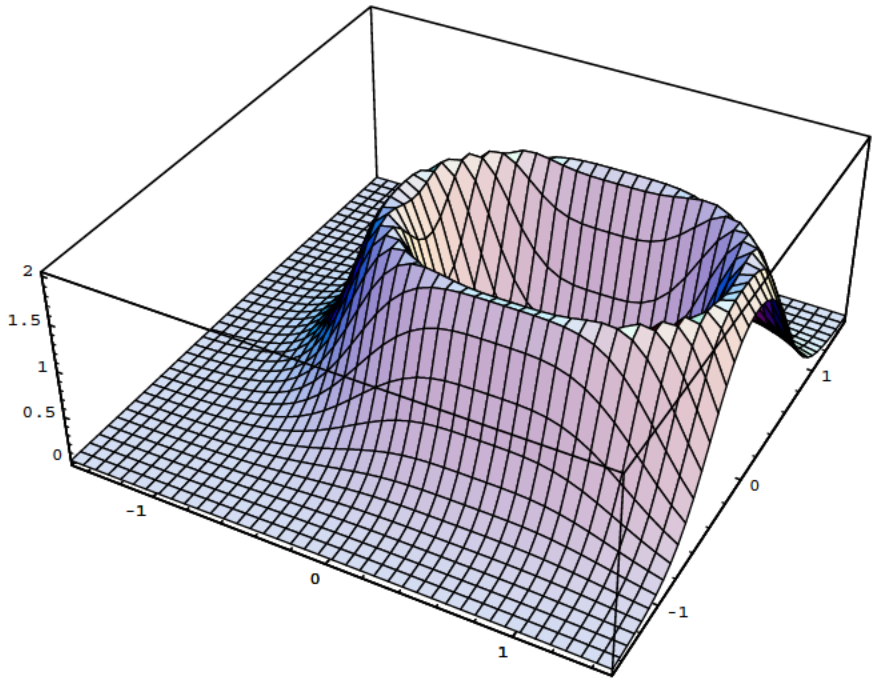


Figure 4-1: Forward probabilities for sensor 1.

possible. One could therefore search for optimal sensor geometries by maximizing I.[Mac91, Lut85, Lin56]

4.3 Example: Two dimensional mouse

Here we use this technique to construct the ambiguity class and find the most likely model parameters given two sensor readings. We want to infer the position of the hand in two dimensions from two sensor readings. So the model consists simply of two numbers, representing the position of the object purported to explain the sensor readings. The sensor axes are oriented perpendicular to one another, and the transmit electrode is shared.

Figures 4-1 and 4-2 below show the forward probability distributions $p(D|m)$ for the two sensors, oriented perpendicular to one another. To make the figure easier to view, the the noise has been exagerated dramatically. If we were to use the actual noise levels for the sensors, as measured in section 2.1.1, the features of the surfaces would be so minute that the plot routine would miss them.

Figure 4-3 shows these two distributions in the same space. Their product, the joint forward probability, $p(D1, D2|m) = p(D1|m)p(D2|m)$, is shown in Figure 4-4. The inverse probability distribution, $p(m|D1, D2)$ is the same picture, multiplied by a prior and divided by a normalizing constant.

The surfaces in Figures 4-1 through 4-3 are not normalized with respect to m (i.e. they show $p(D|m)$ not $p(m|D)$), because the heights of the two marginal distributions are not in fact the same. Their actual heights would make Figure 4-3 less clear. The important feature of that picture is the point where the straight sections of the ovals intersect perpendicularly. In Figure 4-4, which shows the normalized joint distribution (the product of the first two

Shenzhen Huiding Tech. Co., Ltd. - Exhibit 1006

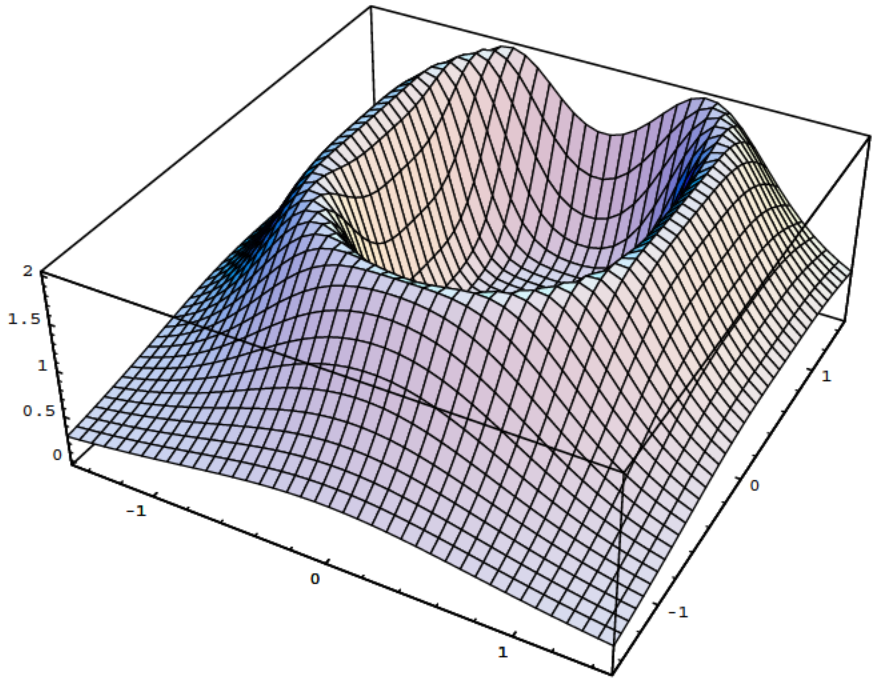


Figure 4-2: Forward probabilities for sensor 2.

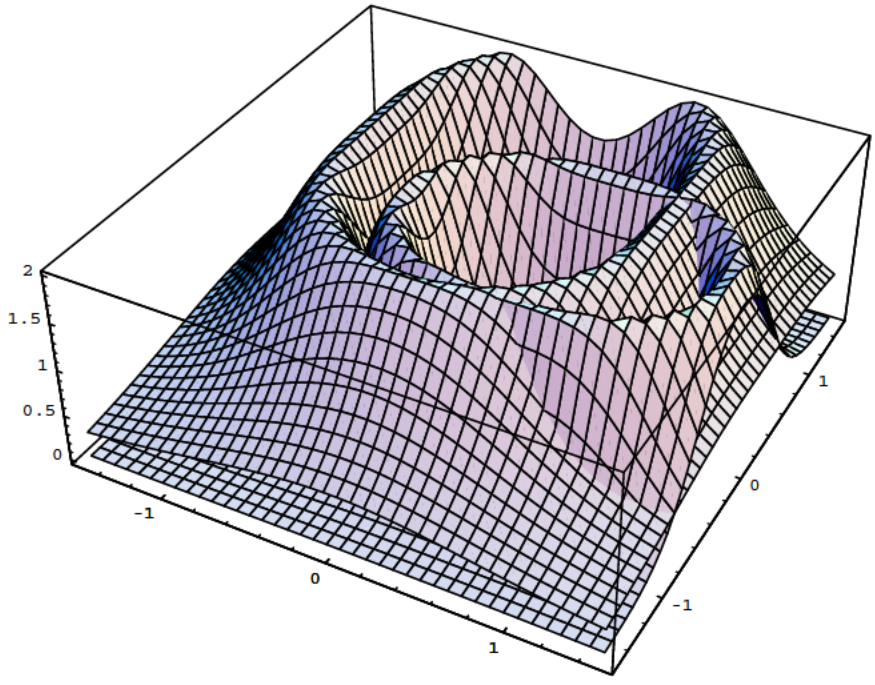


Figure 4-3: Forward probabilities for sensor 1 and sensor 2.

Shenzhen Huiding Tech. Co., Ltd. - Exhibit 1006

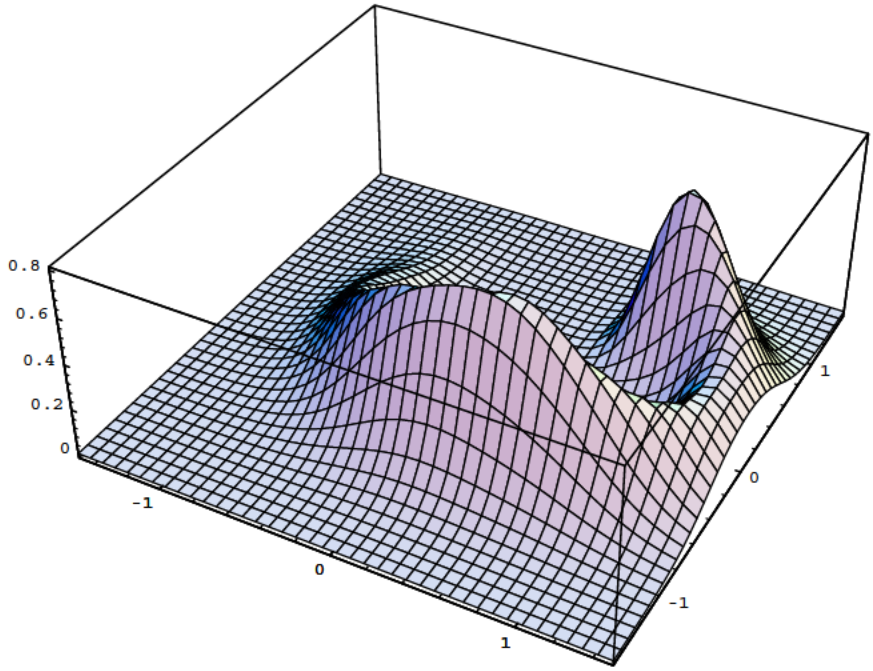


Figure 4-4: The ambiguity class: joint forward probabilities.

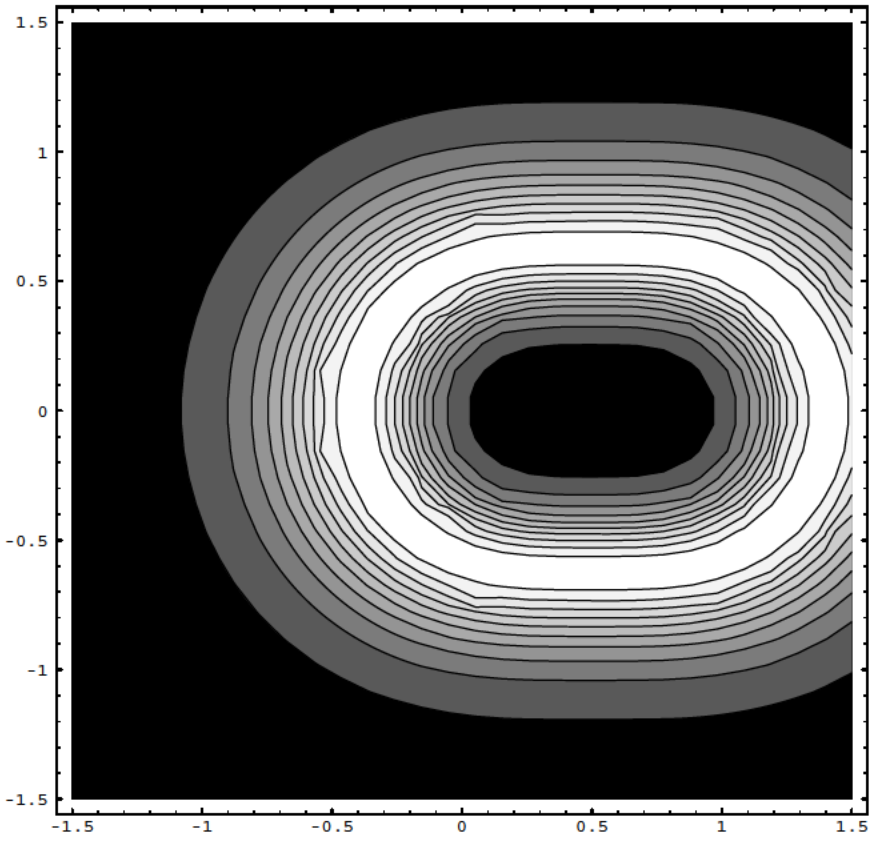


Figure 4-5: Forward probabilities for sensor 1.

Shenzhen Huiding Tech. Co., Ltd. - Exhibit 1006

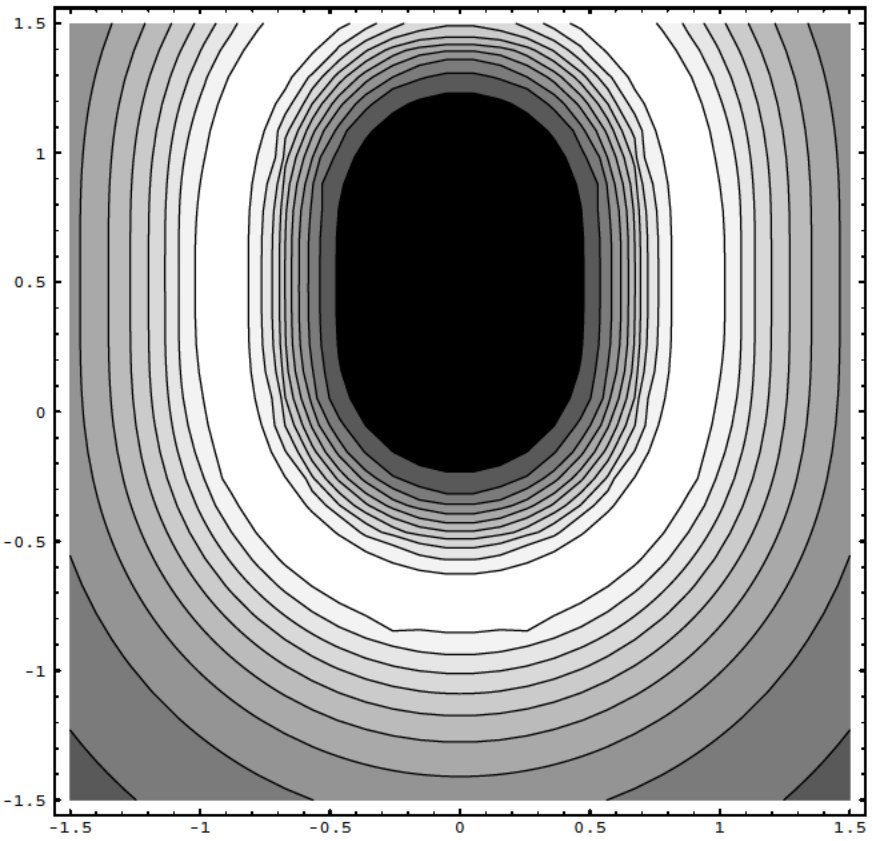


Figure 4-6: Forward probabilities for sensor 2.

Shenzhen Huiding Tech. Co., Ltd. - Exhibit 1006

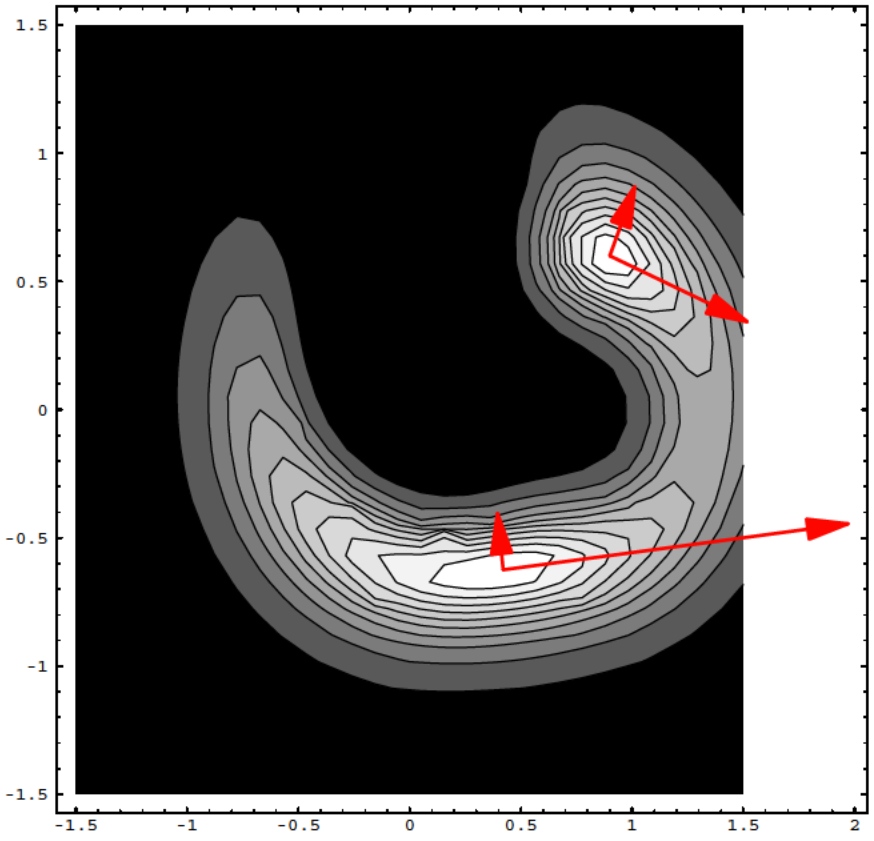


Figure 4-7: The ambiguity class: joint forward probabilities, with error bars, the principal components of the inverse Hessian evaluated at each peak. The larger error bar on the less sharply defined peak has been scaled down by 1/3 to fit it on the page.

Shenzhen Huiding Tech. Co., Ltd. - Exhibit 1006

distributions, normalized), this intersection point appears as the sharper peak. Figure 4-7 shows a contour plot of the joint distribution, with the "principal uncertainties," or error bars, evaluated at the two maxima, superimposed on the maxima. The three smallest arrows have been scaled up by a factor of 10 to make them more visible. The larger arrow on the less sharply defined peak has only been scaled up by $3\frac{1}{3}$, so that it fits on the page.

4.3.1 Recovering orientation

Since in our calculations we have been assuming that the hand is point-like, the uncertainties seen here are due to the field, not the hand. But if the hand were not point-like, this would presumably introduce additional uncertainties, flattening the distribution further, at least in some directions. If we "calibrated out" the intrinsic ambiguities due to the sensor layout, for example by multiplying the uncertainties at each point by the principal curvatures for the single-point ambiguity class, or by subtracting the same, then any ambiguities we did detect would presumably represent a spread in the distribution being measured. This may provide a way to estimate the size and orientation of the object: simply use the "uncertainty ellipsoid" defined by the principal curvatures.

Shenzhen Huiding Tech. Co., Ltd. - Exhibit 1006

Chapter 5

Example Inverse Problem: 3D Mouse

In this section we will present another application of the discussion in Chapter 4: a three-dimensional mouse. We will chose a sensor geometry and construct its ambiguity class for an example hand position. It is possible to check the suitability and quality of a sensor layout and prior by examining the ambiguity class: if there are multiple maxima, the inversion is ill-posed, and if the peak is not sharp (if the maximum has high radii of curvature, that is, a high value of the determinant of the inverse Hessian matrix) the value is very uncertain.

Figure 5-1 shows the layout we selected. In section 4.1 we discussed criteria for optimal sensor design. Evaluating the entropy integrals, and averaging over all possible data values, represents a substantial practical challenge. Efficient means of doing so may require sophisticated Monte-Carlo techniques, except in special cases.

Therefore, we will simply satisfy ourselves that this layout does not lead to ill-posed inversion problems by examining its ambiguity class. Figure 5-2 shows the (log) ambiguity class for our sensor layout with the hand at $.5, .5, .5$, measured in units of the sensor dipole spacing. Each image shows a slice through the three-dimensional joint probability distribution, parallel to the $X - Y$ plane.

Unlike in Chapter 4, where we plotted the probability directly because it led to a clearer figure, here we have plotted the log probability, which is the more useful quantity. In this case, the same figure made with probability instead of log probability, is not very interesting: every frame is black except one, which has a small white area in the region of the maximum. The log figure is easier to read.

Actually to invert the signals (as opposed to showing that they can be inverted), we can maximize the log probability, which corresponds to minimizing the prior term plus the sum of squared error between the measured value and that predicted by the current estimate of the hand position. We have done so for this example case, and found that the maximum was the at the expected location of $.5, .5, .5$.

For the practical mouse we have made, we have taken a cruder approach. The inversion process is computationally intensive, so we have generated a set of input-output data using the forward model, and fit to this dataset surfaces mapping sensor values to hand positions. Once the surfaces are fit, evaluating them is more computationally efficient than maximizing a function each time. However, function fitting can be very difficult. In fact, we never found a full, satisfactory map from all 3 sensor values to all 3 axes. We ended up fitting a map

Shenzhen Huiding Tech. Co., Ltd. - Exhibit 1006

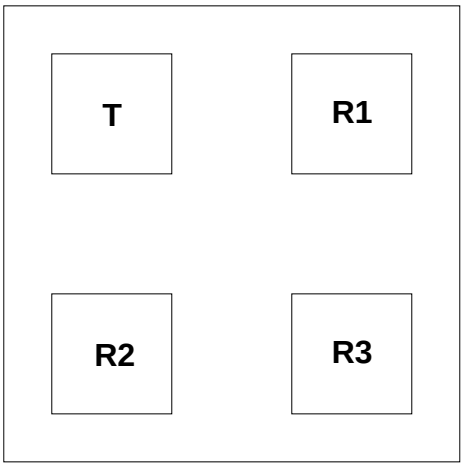


Figure 5-1: Sensor geometry for three-d mouse.

from 2 of the sensor values to x and y, and then estimating the z separately. This allows horizontal motions to be tracked well, but the approach is fundamentally flawed, and it leads to other problems: as the hand moves left and right, there is a large change in z, because the left-right change also changes the value of the third (diagonal) sensor.

The Bayesian approach, if it can be realized in real time, is free of these flaws, and gives the actual position and error, to the extent that the forward model is correct. We plan to try an alternate implementation of the mouse in which we solve the optimization problem in real time. In addition to the fitting difficulties we encountered, the fitting approach will not be applicable to harder inverse problems, in which we are trying to infer more parameters. Furthermore, possibility raised in section4.3.1 that curvatures in the ambiguity class may reveal size and orientation information is tantalizing. Finally, even if some other inversion technique is employed, the Bayesian formalism we have introduced can be used offline to design optimal sensor configurations, by minimizing the expected change in the entropy of the ambiguity class resulting from a typical measurement.

Figure 5-3 shows a screen-shot of the mouse.[1] The user's hand motion is mapped onto the motion of the hand icon. The hand can pick up the small cube shown, move it around the space, and set it back on the floor. Because we cannot yet extract hand size, we have used a "sticky hand, sticky floor" protocol for grasping and releasing the cube. The small cube starts on the floor. When the hand first touches the cube, the hand closes and the cube "sticks" to the hand and moves with it until the hand returns to the floor, at which point the hand opens and the cube sticks to the floor, where it remains until the hand returns.

[1] The 3d graphics for the mouse was created by Barrett Comisky.

Shenzhen Huiding Tech. Co., Ltd. - Exhibit 1006

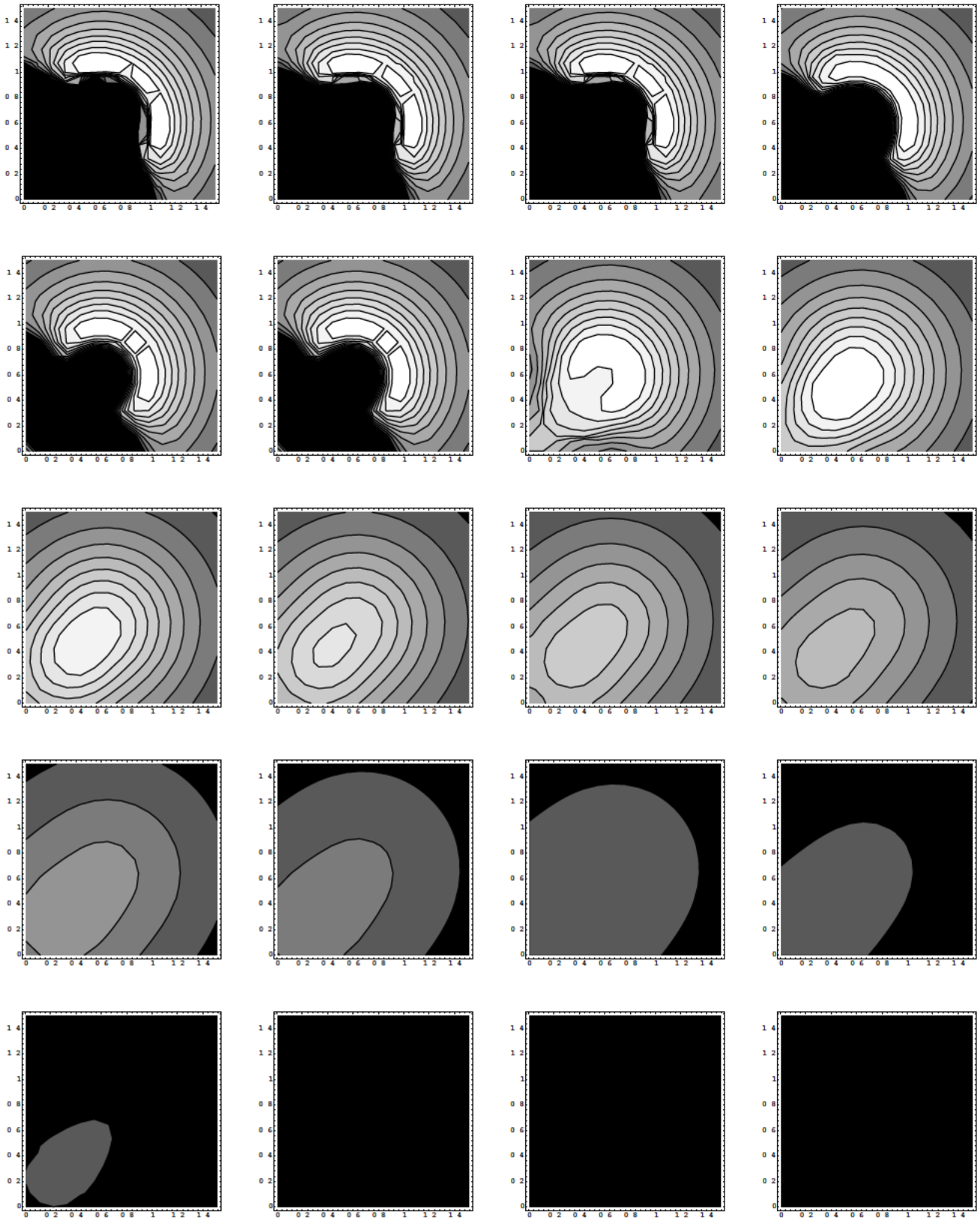


Figure 5-2: Ambiguity class for sensor geometry pictured in the previous figure, with hand at location .5, .5, .5.

Shenzhen Huiding Tech. Co., Ltd. - Exhibit 1006

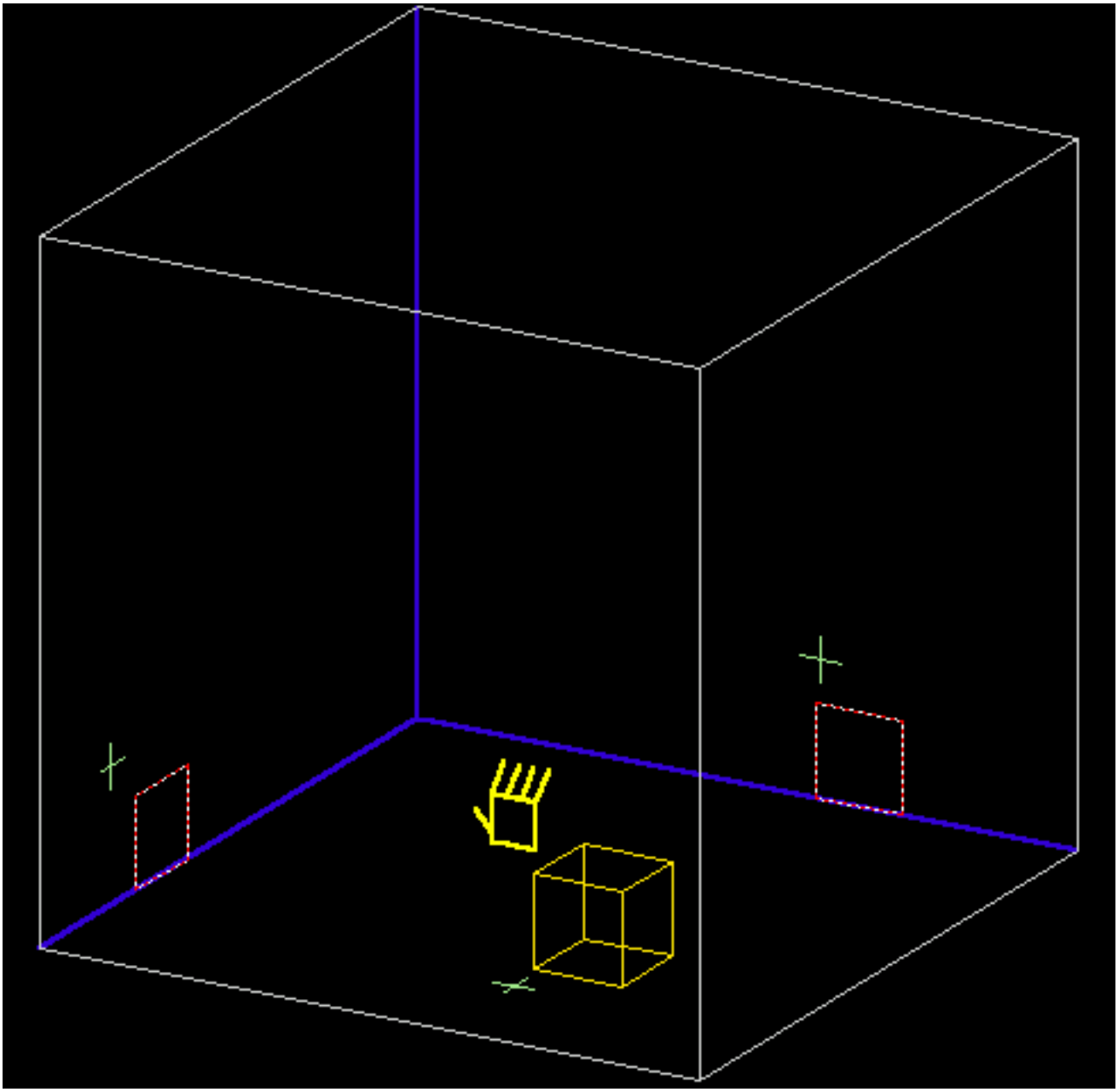


Figure 5-3: Three-d mouse.

Shenzhen Huiding Tech. Co., Ltd. - Exhibit 1006

Chapter 6

Conclusion

We have taken the first steps toward Electric Field Tomography, moving from simple proximity detector to 3-d mouse. We have introduced a general mathematical framework with which it should be possible to solve the inversion and optimal sensor design problems for any number of sensors.

In Chapter 2, we explained the physics of Electric Field Sensing. Starting from Maxwell's equations, we found that Laplace's equation with an inhomogeneous permittivity is the general solution to the forward problem of predicting the sensor values given a permittivity distribution and boundary conditions. But with an eye toward the simplified problem of imaging a single point, in Chapter 3 we introduced an approximate analytical forward model. This model has two parts: one describes how the object interacts with the field, and the other describes the field itself.

Next, in Chapter 4 we introduced a framework that allows us to discuss both inversion and optimal sensor placement. Given a forward model, in this framework we define a probability distribution over the model parameters. Additional data sharpens the distribution around the "true" parameter values. The most likely set of model parameters is found by maximizing the probability, or log probability. The uncertainty of the final estimate of model parameters (the error bars) is given by the curvature of the log probability. An optimal sensor layout can be chosen by minimizing the expected change in the entropy of the ambiguity class. Finally, we showed how to use the Bayesian framework to image a single point in two and three dimensions.

One open question is whether the forward model introduced in Chapter 3 will continue to be useful with more complicated distributions, for example with multiple small objects. As long as the approximation on which it is based remains valid, it should work with multiple objects. The only question is whether multiple objects start to distort the field so much that the zeroth order approximation is no longer good enough. Answering this question will require additional experimental and theoretical work. Another issue that must be addressed is that of incorporating a variable impedance to ground into our model. A suggestion for how to do this was presented at the end of section 3.2, but it must be tried experimentally.

If the forward model can be generalized successfully, then there is truly a path from the 3-d mouse to imaging. If it cannot be, then we will have to take a brute force approach, and solve Laplace's equation numerically in order to image more complex geometries. Even if our present forward model cannot be generalized, however, all the inference and inversion techniques introduced here are applicable, since they treat the forward model as a black

Shenzhen Huiding Tech. Co., Ltd. - Exhibit 1006

box. And even if the 3-d mouse is not a path to imaging, developing it for its own sake, perhaps by using the principle curvatures of the log probability to extract orientation and size information, will interesting and useful. If the long-term project is successful, we will be able unobtrusively to extract 3-d shape information using electric field measurements, which could profoundly affect the way people interact with machines.

Shenzhen Huiding Tech. Co., Ltd. - Exhibit 1006

Appendix A

Backprojection Algorithm

The standard backprojection algorithm is a computationally efficient means of recovering an image of the cross section of an object from a set of projections. A projection is a line integral of some parameter of the object, for example X-Ray opacity (as in CT-scans). We will restrict the discussion in this Appendix to the case of parallel projections, that is, integrals along straight lines that are parallel to one another. Figure A-1 shows an object $f(x, y)$, and (schematically) a single parallel projection $P_\theta(t)$.

The mathematical basis of the backprojection algorithm is the Fourier Slice Theorem, which equates the Fourier transform of $P_\theta(t)$ with a sample (or slice) along the projection angle θ, of $F(u, v)$, the two-dimensional Fourier Transform of $f(x, y)$. The proof of the Fourier Slice Theorem, following Kak and Slaney [KS88], is straightforward:

Consider the coordinate system (t, s), a rotated version of (x, y):

$$\begin{bmatrix} t \\ s \end{bmatrix} = \begin{bmatrix} \cos\theta & \sin\theta \\ -\sin\theta & \cos\theta \end{bmatrix} \begin{bmatrix} x \\ y \end{bmatrix} \tag{A.1}$$

In this coordinate system, a projection along lines of constant t is written

$$P_\theta = \int_{-\infty}^{\infty} f(t, s)ds$$

Its Fourier Transform is given by

$$S_\theta(\omega) = \int_{-\infty}^{\infty} P_\theta(t)e^{-2\pi i\omega t}dt = \int_{-\infty}^{\infty} \left[\int_{-\infty}^{\infty} f(t, s)ds\right] e^{-2\pi i\omega t}dt = \int_{-\infty}^{\infty}\int_{-\infty}^{\infty} f(t, s)e^{-2\pi i\omega t}dsdt$$

We can transform the expression for $S_\theta(\omega)$ back into the (x, y) frame using A.1:

$$S_\theta(\omega) = \int_{-\infty}^{\infty}\int_{-\infty}^{\infty} f(x, y)e^{-2\pi i\omega(x\cos\theta + y\sin\theta)}dxdy$$

This expression represents the two-dimensional Fourier Transform at a spatial frequency of $(u = \omega\cos\theta, v = \omega\sin\theta)$, that is, along a line through the origin at angle θ:

$$S_\theta = F(\omega, \theta) = F(\omega\cos\theta, \omega\sin\theta)$$

.

Shenzhen Huiding Tech. Co., Ltd. - Exhibit 1006

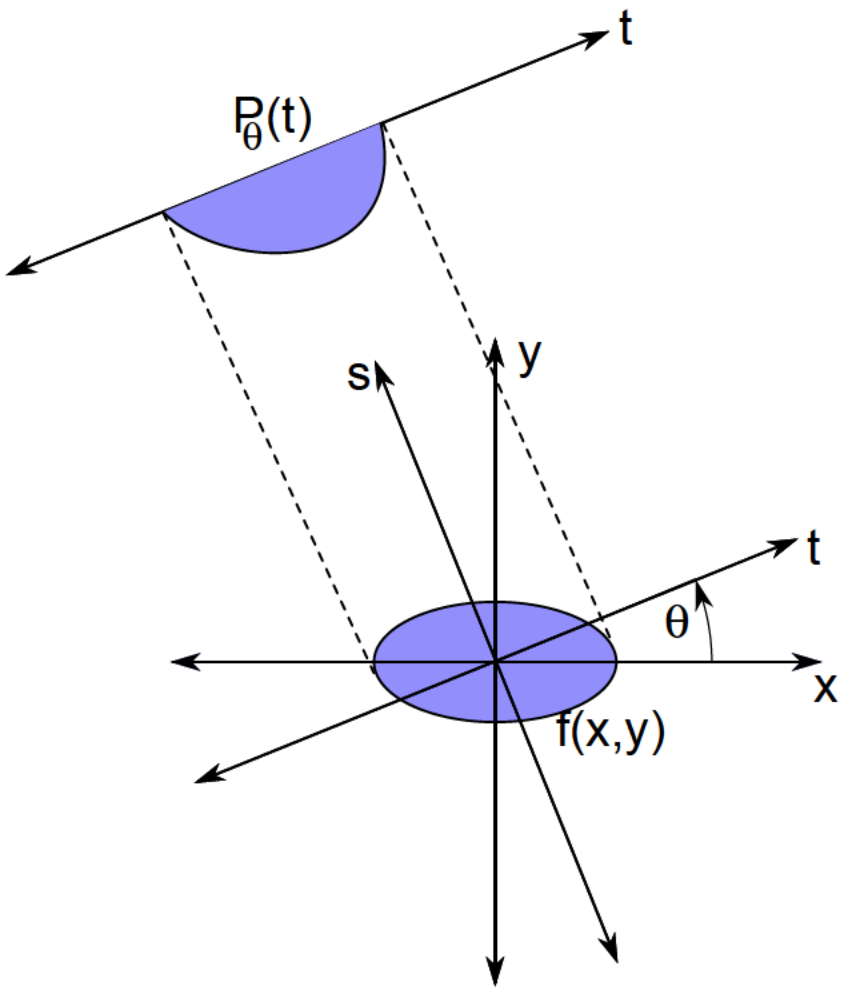


Figure A-1: The projection $P_\theta(t)$ of an object $f(x, y)$.

Shenzhen Huiding Tech. Co., Ltd. - Exhibit 1006

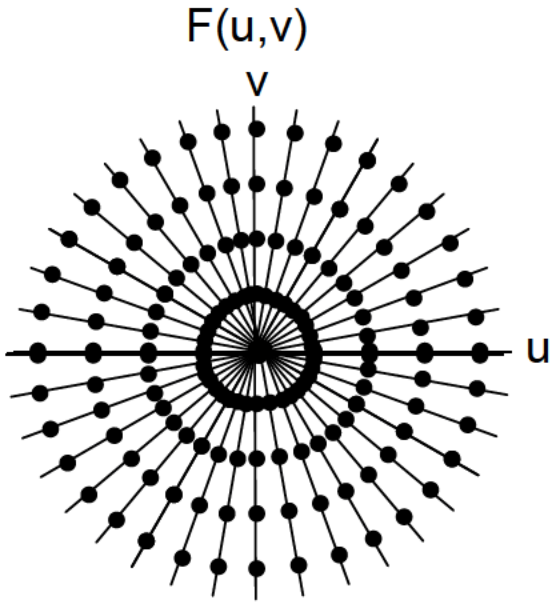


Figure A-2: The non-uniform sampling of k-space corresponding to a set of projections 10 degrees apart.

Now that we have explained the Fourier Slice Theorem, we can use it to analyse the process of collecting projections. This will lead us to the backprojection algorithm. The following explanation of backprojection is a combination of Kak[KS88], Rosen[Ros95], and my own explanation.

The Fourier Slice Theorem tells us that a series of projections in increments of 10 degrees, for example, provides a set of samples of the Fourier transform plane along a set of lines 10 degrees apart, as shown in Figure A-2. To reconstruct the image $f(x, y)$, we might naively sum all the samples of the Fourier Transform plane and then take the inverse transform. But this would introduce a systematic error. The low spatial frequencies in the center of the Fourier Transform plane have been sampled more densely than the higher spatial frequencies at the outskirts of the plane, because we sampled along lines through the origin. In particular, the origin (the spatial DC component) received a contribution from each sample line. To correct this, in the we could scale each frequency domain sample by $|k_r|$, where $|k_r|$ is the distance of the sample from the origin in k space (the Fourier Transform plane). This is a high-pass filtering operation. Notice that this removes the overemphasized DC component entirely, which is no loss, since it contained no spatial information (just a global "brightness" that would typically be adjusted to make the picture look best anyway).

The final reconstruction could be found by adding together the two-dimensional inverse Fourier Transform of each weighted slice. But to carry out the reconstruction, we do not actually have to perform the forward and inverse Fourier transforms. We can implement the filtering (weighting), by convolving each projection with the Fourier transform h of our one-dimensional "ramp" weighting/filtering function $|k_r|$. The (t, s) space counterpart of adding together the weighted k-space samples is adding the functions $h(t) * P_\theta(t)$. Since this function has no explicit or implicit s dependence, $h(t) * P_\theta(t)$ has the same value for

Shenzhen Huiding Tech. Co., Ltd. - Exhibit 1006

all s. This means that the value of pixel $p(s,t)$ is given by

$$p(s,t) = \sum_{\theta} h(t) * P_{\theta}(t)$$

This means that we are "smearing" the values $h(t)*P_{\theta}(t)$ along all values of s, or backprojecting, and summing the backprojections for each θ value. This is the filtered backprojection algorithm.

Note that if we forget the k-space picture completely, backprojection still makes some intuitive sense: we smear the measured values back along the set of pixels that could have contributed to the measurement; additional projections sharpen the image, because the pixels where the object actually is receive contributions from many projections. Nevertheless, we are always left with an unwanted spatial "DC" term, in all the pixels that received contributions from, say, just one projection, so we perform a highpass filtering operation to eliminate this DC component.

The backprojection algorithm can be generalized to handle non-parallel, non-straightline projections. The backprojection algorithm used in Electrical Impedance Tomography backrojects along curved equipotentials. This is discussed further in Chapter 1.

The set of pixels $p(s,t)$ along which we "smear" the measured value $h(t) * P_{\theta}(t)$ bears some resemblance to the ambiguity class for the projection measurement, to use the terminology of Chapter 4. However, the ambiguity class in fact is more general. It is the probability distribution over all possible states of the model. So in this case, it is the probability distribution over each possible brightness setting of the pixel values in the set $p(s,t)$. Backprojection may be viewed as an approximation of this approach in which the probability distribution over the possible brightness values of each pixel is summarized by the mean value. Using the Bayesian approach with the Gaussian approximation amounts to keeping the first two moments of the ambiguity class, instead of just the mean. This allows us to put error bars on each pixel brightness.

Shenzhen Huiding Tech. Co., Ltd. - Exhibit 1006

Bibliography

[ARS95] D. Allport, E. Rennison, and L. Strausfeld. Issues of gestural navigation in abstract information spaces. In *CHI 95 Human Factors in Computing Systems*, pages 206–207, Denver, Co, 1995. ACM Press.

[AS91] A. Allers and F. Santosa. Stability and resolution analysis of a linearized problem in electrical impedance tomography. *Inverse Problems*, 7:515–533, 1991.

[AZP+95] D. Allport, T.G. Zimmerman, J.A. Paradiso, J.R. Smith, and N. Gershenfeld. Electric field sensing and the flying fish. Article submitted to ACM special issue on Multimedia and Multisensory Virtual Worlds, December 1995.

[Bas94] J. Bastian. Electrosensory organisms. *Physics Today*, pages pp.30–37, February 1994.

[BB84] D.C. Barber and B.H. Brown. Applied potential tomography. *Journal of Physics E*, 17:723–733, 1984.

[Ber89] J.G. Berryman. Fermat's principle and nonlinear traveltime tomography. *Physical Review Letters*, 62:2953–2956, 1989.

[BK90] J.G. Berryman and R. V. Kohn. Variational constraints for electrical-impedance tomography. *Physical Review Letters*, 65:325–328, 1990.

[Cha94] D. Chase. The human factor: Figuring it out with performance animation. *Millimeter*, February:pp.34–44, 1994.

[Dev95] Analog Devices. Analog circuit data book, 1995.

[DL81] K.A. Dynes and R.J. Lytle. Analysis of electrical conductivity imaging. *Geophysics*, 46:1025–36, 1981.

[FCA60] R.M. Fano, L.J. Chu, and R.B. Adler. *Electromagnetic Fields, Energy, and Forces*. John Wiley & Sons, New York, 1960.

[Gal91] B.M. Galeyev. L.S. Termen: Faustus of the twentieth century. *Leonardo*, 24(5):pp.573–579, 1991.

[GD78] S.F. Gull and G.J. Daniell. Image reconstruction from incomplete and noisy data. *Nature*, 272:686–690, 1978.

[Ger91] N. Gershenfeld. Sensors for real-time cello analysis and interpretation. In *Proceedings of the ICMC*, Montral, Canada, 1991.

Shenzhen Huiding Tech. Co., Ltd. - Exhibit 1006

[Ger93] N. Gershenfeld. Method and apparatus for electromagnetic non-contact position measurement with respect to one or more axes. *U.S. Patent No. 5,247,261*, Sept 21, 1993.

[GZA95] N. Gershenfeld, T. Zimmerman, and D. Allport. Non-contact system for sensing and signalling by externally induced intra-body currents. *U.S. Patent Application*, May 8, 1995.

[HHL79] G.T. Herman, H. Hurwitz, and A. Lent. A Bayesian analysis of image reconstruction. In G.T. Herman, editor, *Image Reconstrucion From Projections: Implementations and Applications*, pages pp.85–103. Springer-Verlag, 1979.

[HM89] H.A. Haus and J.R. Melcher. *Electromagnetic Fields and Energy*. Prentice Hall, Englewood Cliffs, NJ, 1989.

[Jay83] E.T. Jaynes. Prior information and ambiguity in inverse problems. *SIAM AMS Proceedings*, 14:151–166, 1983.

[KM90] R.V. Kohn and A. McKenney. Numerical implementation of a variational method for electrical impedance tomography. *Inverse Problems*, 6:389–414, 1990.

[KS88] A.C. Kak and M. Slaney. *Principles of Computerized Tomographic Imaging*. IEEE Press, New York, 1988.

[KV83] R.V. Kohn and M. Vogelius. Identification of an unknown conductivity by means of measurements at the boundary. *SIAM AMS Proceedings*, 14:113–123, 1983. A less formal and more accessible introduction to the approach developed in the other papers by the authors.

[KV84] R.V. Kohn and M. Vogelius. Determining the conductivity by boundary measurements. *Communications on Pure and Applied Mathematics*, 38:289–298, 1984.

[KV85] R.V. Kohn and M. Vogelius. Determining the conductivity by boundary measurements II, interior results. *Communications on Pure and Applied Mathematics*, 38:643–667, 1985.

[Lab95] Lawrence Livermore National Lab. Micropower impulse radar specifications, 1995.

[Lin56] D.V. Lindley. On a measure of the information provided by an experiment. *Annals of Mathematical Statistics*, 27:pp.986–1005, 1956.

[Lut85] S.P. Luttrell. The use of transinformation in the design of data sampling schemes for inverse problems. *Inverse Problems*, 1:pp.199–218, 1985.

[Mac91] D.J.C. MacKay. *Bayesian Methods for Adaptive Models*. PhD thesis, CalTech, 1991.

[Mat90] M. Matthews. Three dimensional baton and gesture sensor. *U.S. Patent No. 4,980,519*, December 25, 1990.

Shenzhen Huiding Tech. Co., Ltd. - Exhibit 1006

[Mor93] F. Morgan. *Riemannian Geometry: A Beginner's Guide*. Jones and Bartlett, Boston, 1993.

[Mot91] Motorola. MC68HC11 reference manual, 1991.

[Nic93] M. Nicholl. Good vibrations. *Invention and Technology*, Spring:pp.26–31, 1993.

[Oth92] A.N. Other. Leon Theremin. *Keyboard*, February:pp.47–54, 1992.

[Par] J.A. Paradiso. Personal Communication.

[Par94] J.A. Paradiso. A simple technique for measuring axial displacement in stretched-wire alignment systems. Technical Report GEM-TN-94-60, Draper Labs GEM Collaboration, May 1994.

[PG95] Physics and Media Group. *Smart Fish Technical Manual*, 1995.

[PGng] J.A. Paradiso and N. Gershenfeld. Electric Field Sensing. *Computer Music Journal*, Forthcoming.

[PM94] J.A. Paradiso and D.R. Marlow. Electronics for precision alignment of the gem muon system. In *Proceedings of the International Conference on Electronics for Future Colliders*, number GEM-TN-94-636. LeCroy Corporation, May 11-12 1994.

[Rob94] B. Robertson. Caught in the act: Motion captured from live beings helps animators create animations faster and makes live performances of 3d characters possible. *Computer Graphics World*, September:pp.23–28, 1994.

[Ros95] B. Rosen. Course notes for Magnetic Resonance: Analytic, biochemical, and imaging techniques. MIT course 22.561J, 1995.

[SG83] J. Skilling and S.F. Gull. The entropy of an image. *SIAM AMS Proceedings*, 14:167–188, 1983.

[SPZG95] J.R. Smith, J.A. Paradiso, T.G. Zimmerman, and N. Gershenfeld. Activating space with electric field sensing. *SIGGRAPH Technical Sketch*, 1995.

[SS69] L. Smith and D.H. Sheingold. Noise and operational amplifier circuits. *Analog Dialogue*, 3(1):pp.19–31, 1969.

[SU87] J. Sylvester and G. Uhlman. A global uniqueness theorem for an inverse boundary value problem. *Annals of Mathematics*, 125:153–169, 1987.

[V+92] Vranish et al. Driven shielding capacitive proximity sensor. *U.S. Patent No. 5,166,679*, November 24, 1992.

[V+93] Vranish et al. Phase discriminating capacitive array sensor system. *U.S. Patent No.5,214,388*, May 25, 1993.

[Wax95] D. Waxman. Digital theremins: Interactive musical experiences for amateurs using electric field sensing. Master's thesis, MIT Media Lab, 1995.

Shenzhen Huiding Tech. Co., Ltd. - Exhibit 1006

[Web89] J.G. Webster, editor. *Electrical Impedance Tomography*. Adam Hilger, New York, 1989.

[Z+91] M. Zadehkoochak et al. Spectral expansion analysis in electrical impedance tomography. *Journal of Physics D: Applied Physics*, 24:1911–1916, 1991.

[Zim95] T.G. Zimmerman. Personal Area Networks (PAN): Near-field intra-body communication. Master's thesis, MIT Media Lab, 1995.

[ZSP+95] T.G. Zimmerman, J.R. Smith, J.A. Paradiso, D. Allport, and N. Gershenfeld. Applying electric field sensing to human-computer interfaces. In *CHI 95 Human Factors in Computing Systems*, pages 280–287, Denver, Co, 1995. ACM Press.

Shenzhen Huiding Tech. Co., Ltd. - Exhibit 1006

US005914701A

United States Patent [19]

Gershenfeld et al.

[11] **Patent Number: 5,914,701**

[45] **Date of Patent: Jun. 22, 1999**

[54] **NON-CONTACT SYSTEM FOR SENSING AND SIGNALLING BY EXTERNALLY INDUCED INTRA-BODY CURRENTS**

[75] Inventors: **Neil Gershenfeld**, Somerville, Mass.; **Thomas Zimmerman**, Flushing, N.Y.; **David Allport**, Boston, Mass.

[73] Assignee: **Massachusetts Institute of Technology**, Cambridge, Mass.

[21] Appl. No.: **08/907,062**

[22] Filed: **Aug. 6, 1997**

Related U.S. Application Data

[63] Continuation of application No. 08/436,982, May 8, 1995, abandoned.

[51] **Int. Cl.**[6] **H04B 5/00**; G09G 5/00

[52] **U.S. Cl.** **345/156**; 340/870.37; 340/825.71; 455/41; 455/100; 345/157; 345/158

[58] **Field of Search** 345/156, 158, 345/157, 174; 340/562, 561, 407.1, 870.37, 563, 564, 825.71; 341/21, 31, 32, 33; 434/12; 455/41, 100; H04B 5/00

[56] **References Cited**

U.S. PATENT DOCUMENTS

4,688,037	8/1987	Krieg	340/825.72
4,903,012	2/1990	Ohuchi	340/709
4,918,737	4/1990	Luethi	381/68.4
4,988,981	1/1991	Zimmerman et al.	340/709
5,204,672	4/1993	Brooks	340/825.71
5,367,315	11/1994	Pan	345/156
5,380,983	1/1995	Cavada et al.	219/250
5,488,204	1/1996	Mead et al.	178/18

FOREIGN PATENT DOCUMENTS

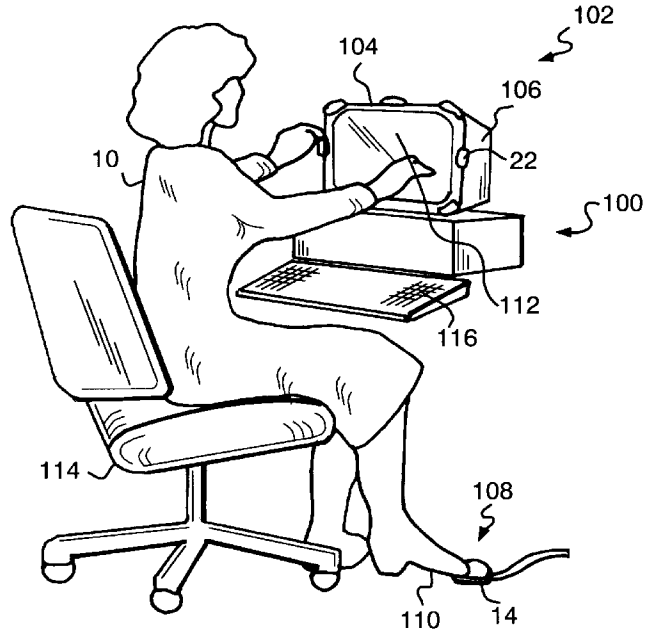
60-250731	5/1986	Japan .
61-046639	7/1986	Japan .
2 129 176	5/1984	United Kingdom .

Primary Examiner—John K. Peng
Assistant Examiner—Linus M. Lo
Attorney, Agent, or Firm—Cesari and McKenna, LLP

[57] **ABSTRACT**

A wireless system includes one or more transmitters and one or more remote receivers that are respectively coupled through one or more users and room ground. The transmitters each produce low-frequency, low power signals that, through capacitive coupling, pass as displacement currents into and from the body of the user, which acts as a conductive node. A receiver that couples capacitively to the user responds to the displacement currents and reproduces the signals. The transmitter includes a signal generator and a pair of electrodes. The signal generator produces modulated signals that vary the voltage between the electrodes, a first one of which is closely coupled capacitively to the user's body such that the "quasi-electrostatic" field resulting from the electrode potential causes a displacement current to pass to the user's body. The second electrode is oriented so that its coupling to the room ground is stronger than that of the first electrode, such that room ground acts as a return path for the current from the receiver. The signal generator may modulate the information to be transmitted using, for example, a pseudorandom code, to produce spread spectrum signals. This increases noise immunity and allows multiple transmitters, each using a different modulation code, to operate at the same time. The receivers each include a detector/demodulator that acquires and tracks the signals from the one or more transmitters.

25 Claims, 9 Drawing Sheets



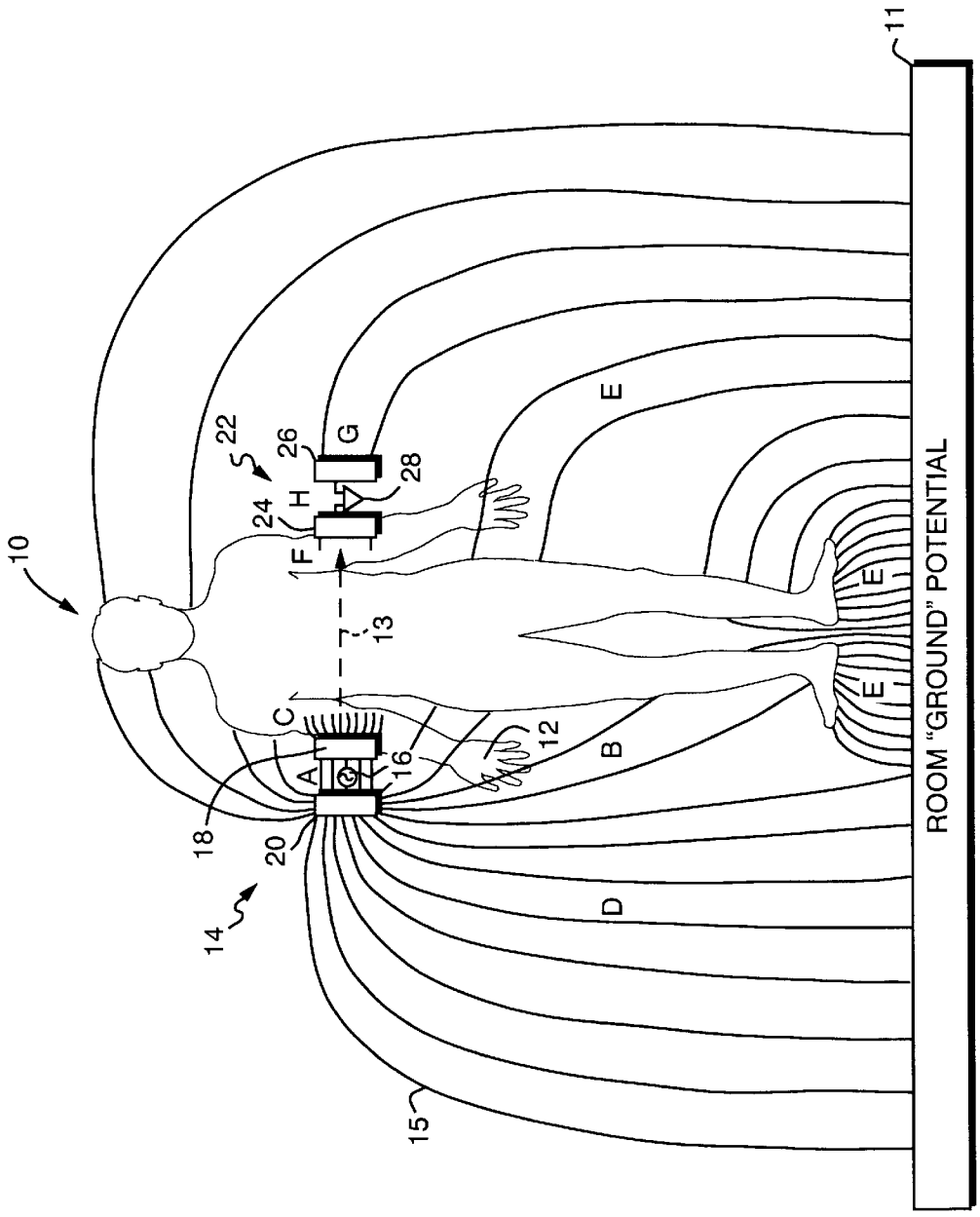

10
11
ROOM "GROUND" POTENTIAL
22
24
26
28
G
H
F
E
E
E
E
13
7
C
A
B
D
12
16
18
20
14
15

FIG. 1

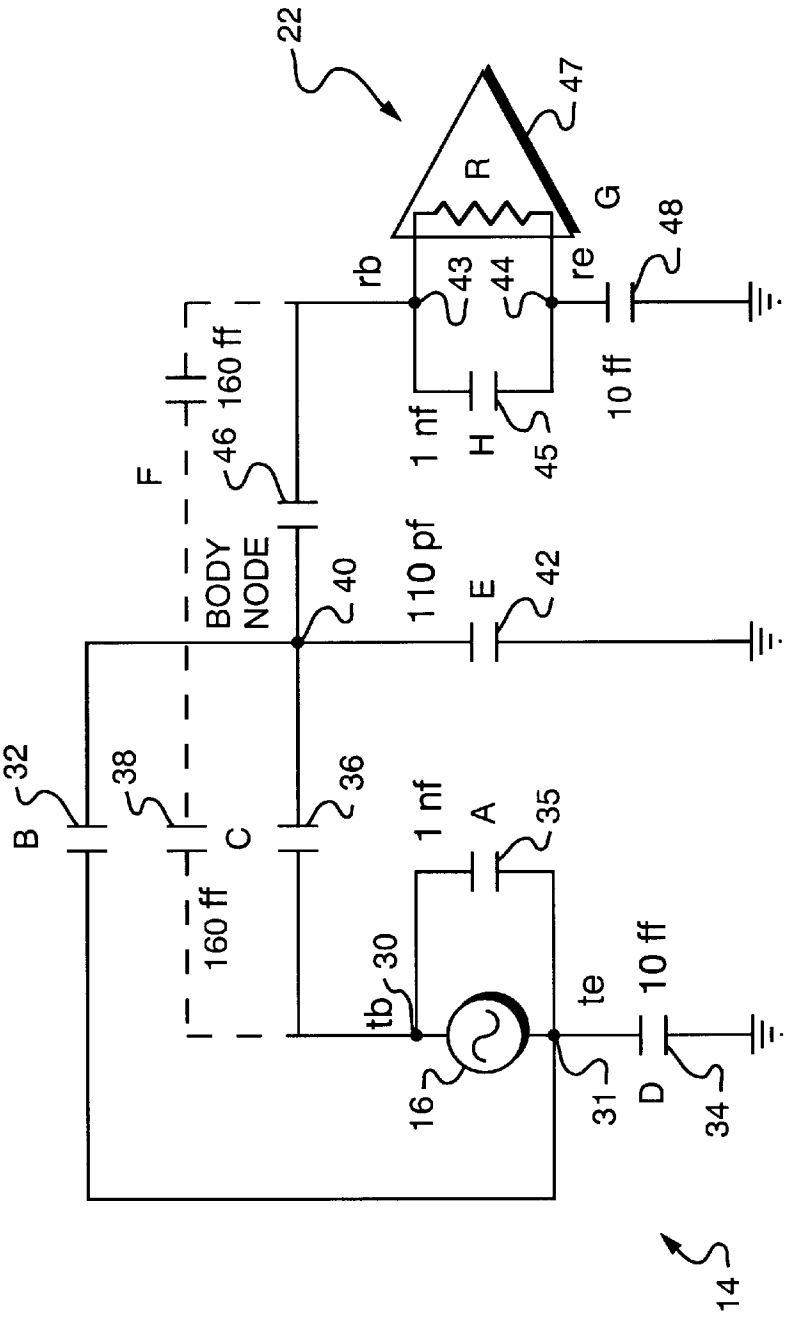

22
47
R
G
48
rb
43
44
re
10 ff
1 nf
H
45
F
160 ff
46
BODY NODE
40
110 pf
E
42
B
32
38
C
160 ff
36
1 nf
A
35
tb
30
te
10 ff
D
16
31
34
14

FIG. 2

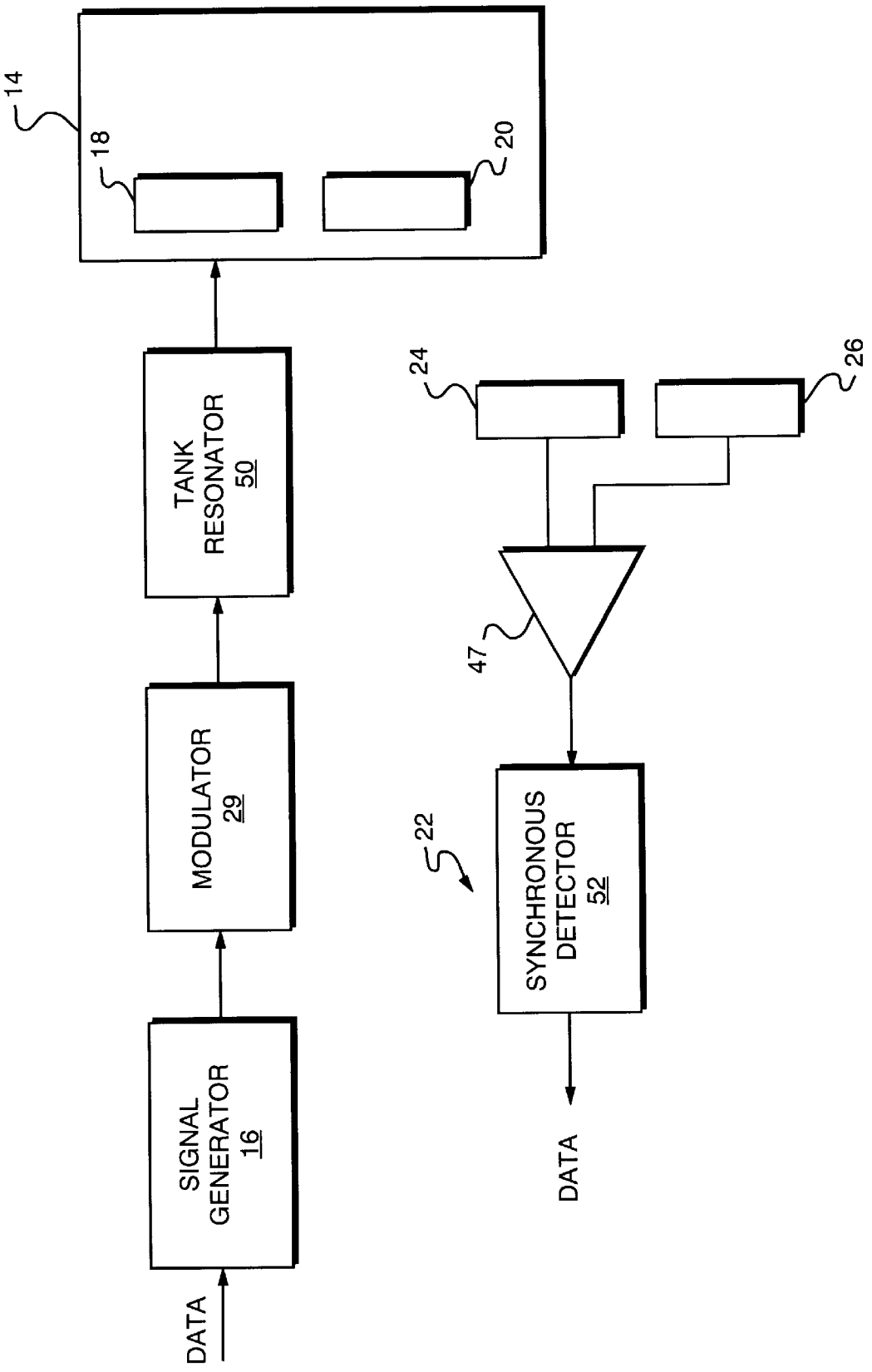

14
18
20
TANK RESONATOR 50
MODULATOR 29
SIGNAL GENERATOR 16
DATA
24
26
47
22
SYNCHRONOUS DETECTOR 52
DATA

FIG. 3

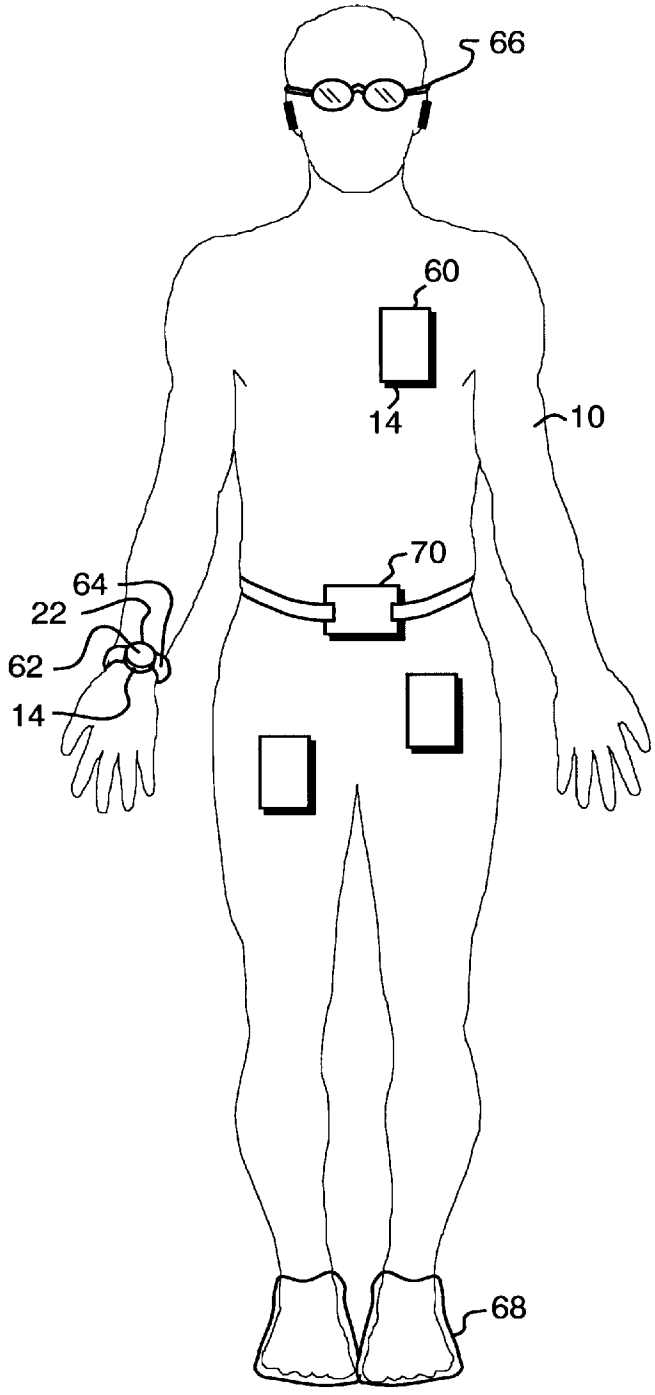


FIG. 4

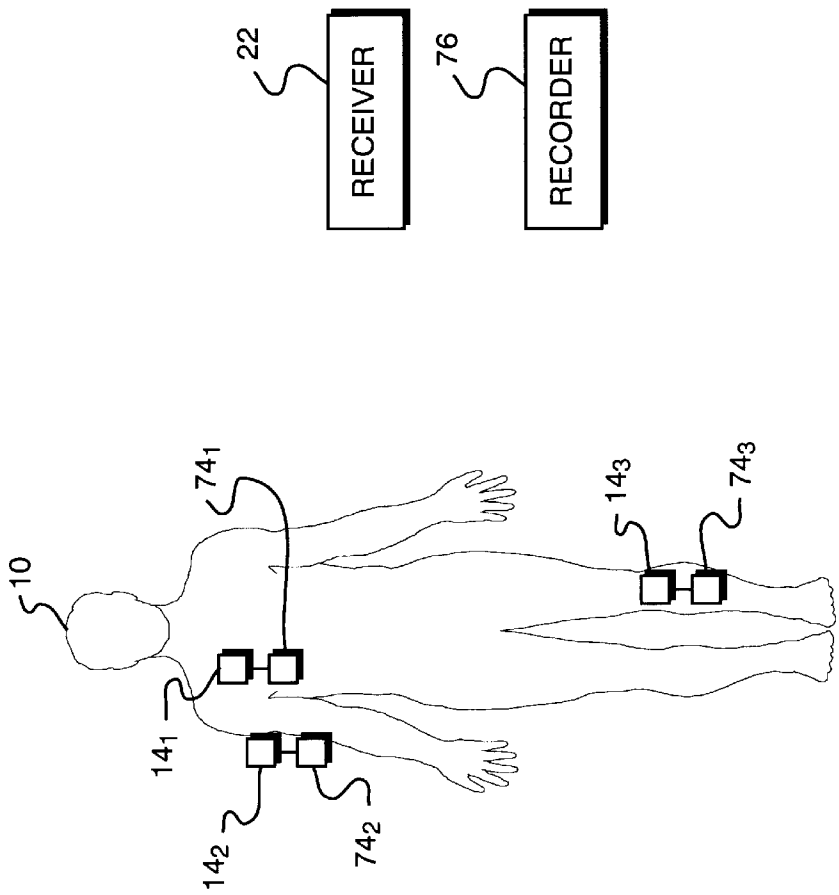


FIG. 5

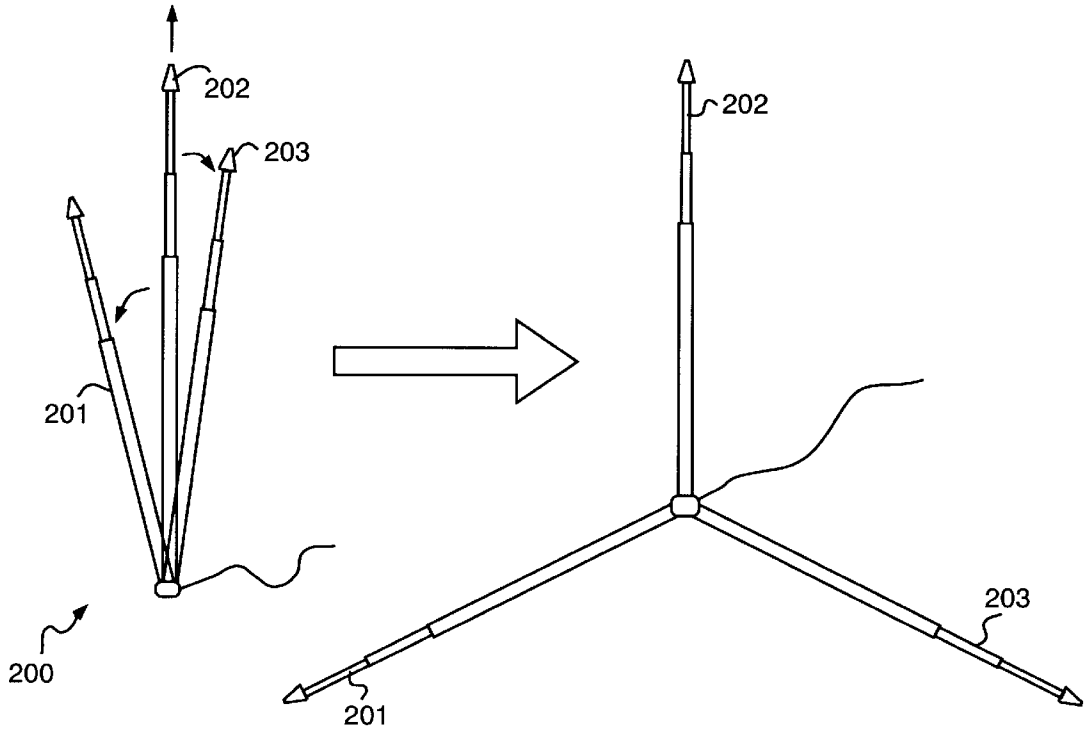


FIG. 9

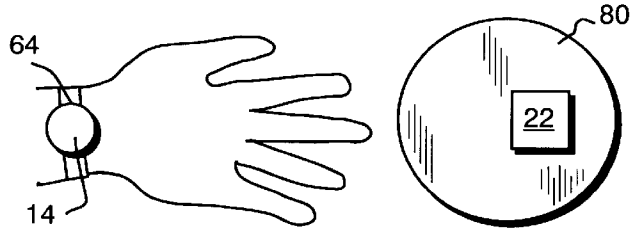


FIG. 6

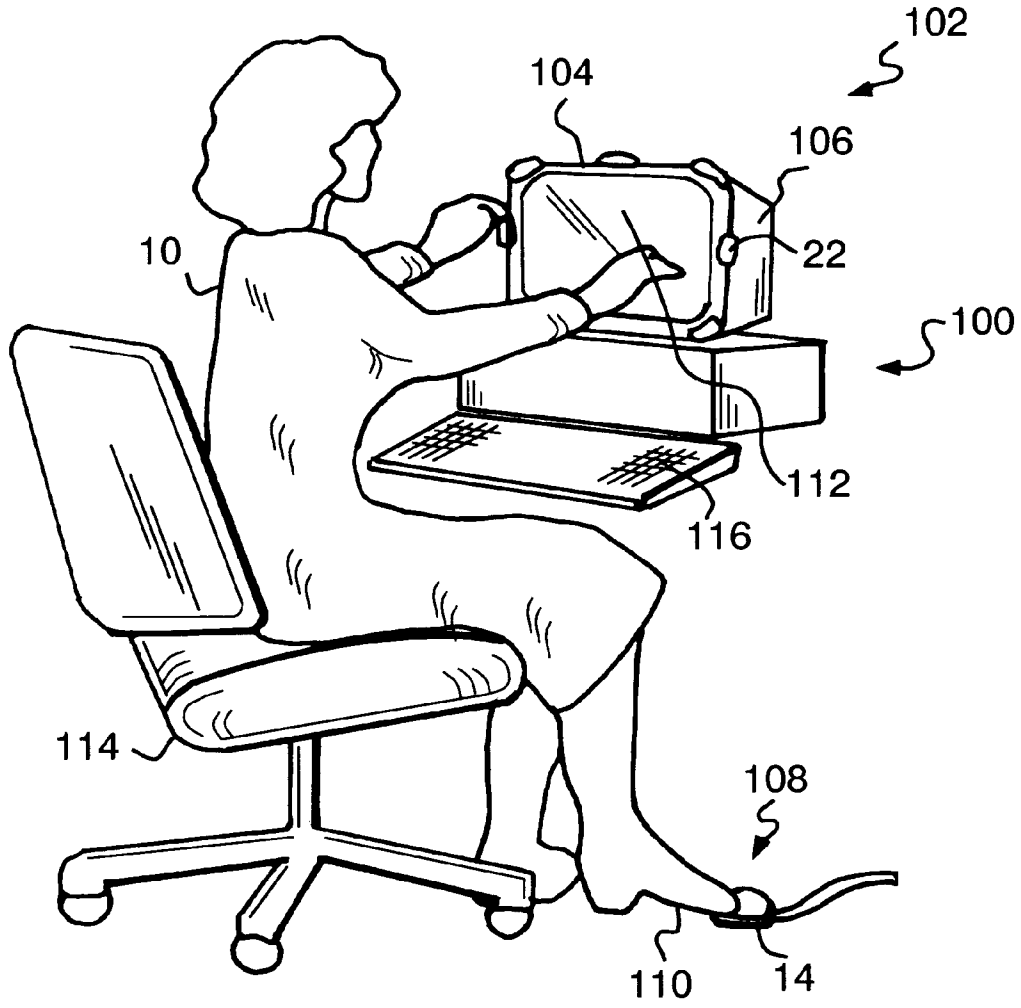


FIG. 7

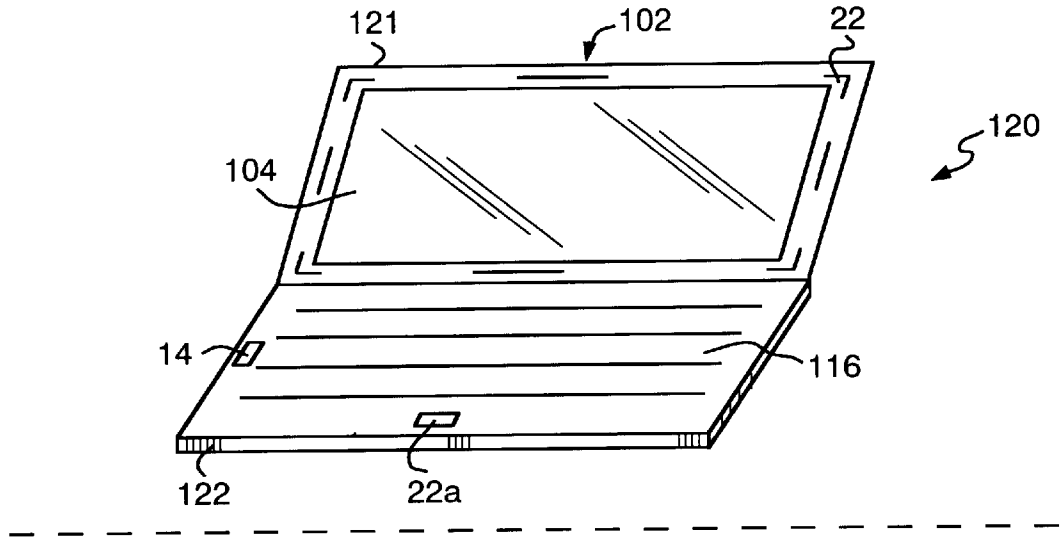


FIG. 8

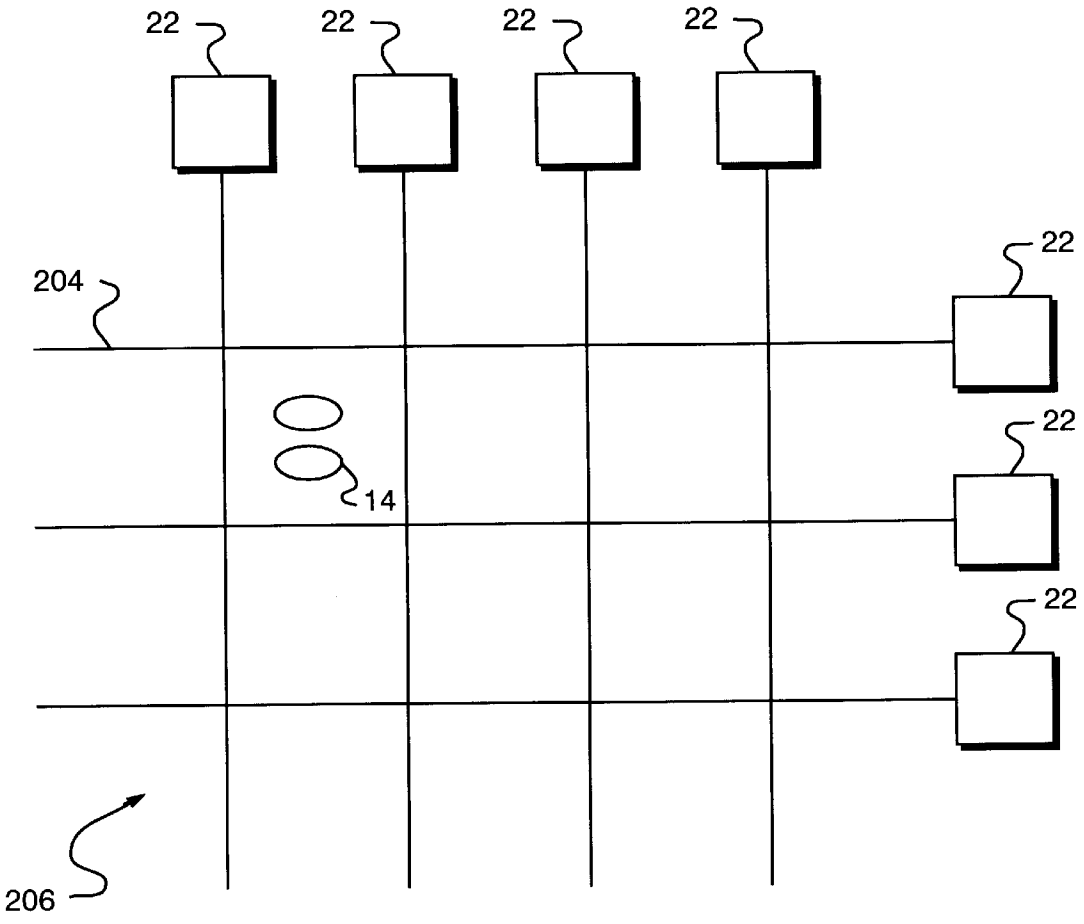


FIG. 10

NON-CONTACT SYSTEM FOR SENSING AND SIGNALLING BY EXTERNALLY INDUCED INTRA-BODY CURRENTS

This application is a continuation of Ser. No. 08/436,982 filed on May 08, 1995 now is abandoned.

FIELD OF THE INVENTION

This invention relates generally to the use of small currents externally induced in people by electrostatic field coupling, and more particularly, to systems that can be used for wireless communication among proximate devices, and for sensing a person's position for use in control tasks.

BACKGROUND OF THE INVENTION

There is a need for personal communication systems that allow portable devices, such as pagers, telephones, computer terminals, and so forth, carried on the person to communicate with each other and with fixed location devices. For example, a user may want to store in a personal computer a message received over the air by a paging terminal. Known prior personal communication systems typically require that these two devices be interconnected by wire, which makes it cumbersome to affix them to users and/or interconnect them to each other, and thus, inconvenient to use.

In medical environments, systems for gathering information such as blood pressure, EKG readings, and so forth typically require that instruments taking the readings from a patient be connected, by wire, to a patient-carried system component that monitors or stores the information. These system are also cumbersome to affix to a user.

In other applications, wireless systems are currently used to transmit information between system components by, for example, radio waves, microwaves, infra-red signals and so forth. These systems may not be suitable for sending information between the user-mounted system components discussed above because of problems with interference in the immediate environment or between the signals transmitted from the various devices.

For example, devices in systems that use infra-red signals should optimally communicate with line-of-sight transmissions, which are not always possible between devices carried by a user. Further, the infra-red systems suffer from interference with ambient light, which can not always be controlled by the user. And, for systems transmitting signals at high frequencies, the users' bodies absorb the radiating energy, and thus, degrade the signals.

Further, such systems are subject to government regulation, since their signals radiate significantly. Also, these systems allow others to eavesdrop on the transmissions.

Wireless transmission systems have also been used to determine relative position. Such systems determine the position of a transmitter based on the timing or strength of signals received by various receivers. These systems are not well suited for and can be unreliable for determining position and orientation at close distances.

SUMMARY OF THE INVENTION

The invention is a wireless system in which a transmitter and a receiver are coupled through a user and room ground, rather than by wire or by optical or high frequency transmitted signals. The transmitter produces low-frequency, low power signals that, through capacitive coupling, pass as displacement currents into and from the body of the user.

The user's body acts as a conductive node and a receiver that is capacitively coupled to the user's body responds to the displacement currents passed to it from the body, to detect the low frequency signals. The user's body thus becomes part of the system rather than an impediment to signal propagation. Also, since the transmitter and receiver do not couple with one another directly, the shared room ground provides the return path for the current.

The transmitter includes a signal generator and a pair of electrodes, referred to hereinafter as inner and outer electrodes. The signal generator produces modulated signals that vary the voltage between the electrodes. The inner electrode is closely coupled capacitively to the user's body such that the "quasi-electrostatic" field resulting from the electrode potential causes a displacement current to pass to the user's body. The outer electrode is oriented so that its coupling to the room ground is stronger than that of the inner electrode, such that room ground acts as a return path for the current from the receiver.

The signal generator may modulate the information to be transmitted using, for example, a pseudorandom code, to produce spread spectrum signals. This increases noise immunity and allows multiple transmitters, each using a different modulation code, to operate at the same time.

The receiver includes a pair of electrodes and a detector/demodulator that acquires and tracks the spread spectrum signal. One of the electrodes is closely coupled capacitively to the user's body such that displacement current that passes from the body passes to that electrode. The current then flows through detector circuitry to the other electrode, which is asymmetrically coupled capacitively to room ground, to complete the path for the current. The current varies in accordance with the current passed to the body from the transmitter, and thus, in accordance with the signals produced by the signal generator.

The detector circuitry detects the current and operates in a conventional manner to recover the transmitted information therefrom.

There are a number of uses for the system—to communicate information both "intra-body" and "inter-body," to receivers that are capacitively coupled to the user. The system may also be used as a position-sensor, with an array of multiple receivers determining the position of the person based on the relative strengths of the received signals coupled out of the person. Since the signals are not transmitted as radiated energy, small (compared to a wavelength) and essentially flat electrodes may be used in the transmitters and receivers. These electrodes efficiently couple to the user by virtue of their surface area and can, for example, be readily incorporated into a watch, a credit card sized component, a shoe, and so forth. These electrodes are in contrast to the antennas required to efficiently transmit and receive radiated energy. Moreover, since there is negligible radiation of the electromagnetic energy from the electrodes, the system does not fall under government regulations directed to transmitting systems. Further, the system does not have the problem that planar capacitive sensing system have with transmitting over an intervening ground plane.

In one configuration the system passes information between carried or worn components of, for example, a paging system. In this configuration a users carries in his pocket a paging terminal that includes a transmitter. The user also wears a watch that includes a display and a receiver. Both the transmitter and the receiver are capacitively coupled to the user and to room ground, such that signals from the transmitter pass to the receiver as displacement

currents to and from the user, respectively. When the paging terminal receives a paging message over the air, the transmitter passes the message to the receiver for display. The transmitter passes the message to the user as a displacement current, and the receiver receives the message from the user as a displacement current.

In an alternative configuration the system passes to a receiver that is worn or carried by a user, information from medical instruments that are monitoring the physiological condition of the user. In this configuration, each of the medical instruments is connected directly to an associated transmitter that is worn by the user. Each of these transmitters is capacitively coupled to the user and to room ground, such that the signals are passed as displacement currents to the user and from the user to the receiver.

In an alternative embodiment, a transmitter carried by the user passes signals to one or more nearby receivers carried by other users or located in fixed positions. In the quasi-electrostatic field produced by the transmitter the user is capacitively coupled to the receivers through the atmosphere. Accordingly, the user need not physically contact the receivers to pass information to them. For example, two users shaking hands may transfer information between transmitters and receivers they each carry. The proximity of the hands provides a conductive path for the signal current. The return path can be a combination of air and earth ground. Any materials in the vicinity of the transmitter and receiver, such as metal cabinets, reinforcement studs, and so forth, also contribute to the return path.

An alternative system may be incorporated into a general-purpose computer and provide the user with a multi-dimensional input device. Such a system includes an array of receivers and one or more transmitters. The array of receivers are mounted around the periphery of the computer screen and the transmitter may be carried by the user or mounted on, for example, the side of a keyboard.

The user repositions an on-screen object in two-dimensional space or three-dimensional virtual space displayed on the screen by making contact with the transmitter with one hand, for example, his left hand, and moving his right in front of the screen. A processor connected to the receivers in the array determines, based on the relative strengths of the received signals, the relative position of the user's right hand and moves the object to the corresponding on-screen position.

To allow a user to select, or "click on," a particular on-screen object, one or more auxiliary receivers may be mounted on the key board, for example, below the space bar. The user directs the object to a desired location by moving his right hand in front of the screen and clicks on that location by moving the thumb of this left hand closer to the auxiliary receiver in the keyboard. Since the user need not make contact with the auxiliary receiver, the receiver can be combined with, or incorporated directly into, the spacebar or one or more keys of the keyboard.

When the system is be used to move three-dimensional objects or the user, that is, move the user's viewpoint, in three-dimensional virtual space, the array of receivers senses the relative position of the user's hand in front of the screen and based on that position determines if the user desires to move through the virtual space forward, backward, up, down, left or right, and also how fast the user desires to move, as discussed in more detail below. In addition, a foot pedal may be used as an accelerator to further control the "granularity" of the movement of the user through the virtual space, as discussed below.

The system may include a portable, scalable receiving device that consists of an array of three orthogonal electrodes that are, respectively, connected to three receivers. A processor connected to the three receivers determines, based on the signals received by the individual receivers, the relative position of the user. The electrodes are extended or collapsed, as necessary, to accommodate the relative scale of the user's physical movements to the movements of the user within, for example, the three-dimensional virtual space displayed on an associated screen.

BRIEF DESCRIPTION OF THE DRAWINGS

The above and further advantages of the invention may be better understood by referring to the following description in conjunction with the accompanying drawings, in which:

FIG. **1** is a functional block diagram of a system constructed in accordance with the invention;

FIG. **2** is a simplified schematic of the system of FIG. **1** showing typical numbers for capacitances;

FIG. **3** is a functional block diagram of a transmitter and receiver of FIG. **1**;

FIG. **4** illustrates an exemplary use of the system with a plurality of transmitters;

FIG. **5** illustrates an alternative use of the system;

FIG. **6** illustrates an alternative configuration of the system;

FIG. **7** illustrates a use of the system as part of a personal computer;

FIG. **8** illustrates a use of the system as part of laptop computer;

FIG. **9** depicts a scalable receiver; and

FIG. **10** depicts an alternative system.

DETAILED DESCRIPTION OF ILLUSTRATIVE EMBODIMENTS

FIG. **1** depicts a user **10** who has attached to one arm **12** a transmitter **14** that consists of a signal generator **16** connected between a pair of electrodes **18** and **20**, referred to individually as an inner electrode **18** and an outer electrode **20**. As discussed in more detail below, the inner and the outer electrodes **18** and **20** are capacitively and assymetrically coupled, respectively, to the user **10** and to room ground denoted in the drawing by the numeral **11**. The signal generator **16** produces between these electrodes **18** and **20** a voltage that gives rise to a quasi-electrostatic field depicted in the drawing by solid lines **15**. A resulting displacement current passes between the inner electrode **18** and the user **10**. A portion of this current flows through the user in a path **13**, depicted in the drawing by a dotted line, and passes as a displacement current to a receiver **22** that is attached to the user's other arm **12**.

The receiver **22** includes a detector **28** and a pair of electrodes **24** and **26**, referred to individually as an inner electrode and an outer electrode. The inner electrode **24** is closely coupled capacitively to the user **10** and the outer electrode **26** is coupled capacitively to room ground, such that a displacement current passes from the user **10** to the inner electrode **24**. The current then flows through the detector **28** to ground, and thus, back to the transmitter **14**. The detector **28** detects the current and extracts therefrom the transmitted information.

Current flows also along other paths (not shown) through the user. Most notably, the current flows from the user to room ground. This results in an attenuation of the current

that passes to the receiver **22**. Accordingly, the receiver must be capable of detecting, or measuring, relatively small currents.

The transmitter **14** may modulate the signals by using, for example, direct-sequence spread spectrum modulation. This increases the system's immunity to noise. Also, it allows multiple transmitters, each using a different modulation code, to transmit information at the same time, as discussed in more detail below. Alternatively, the modulation may instead be simply binary on/off modulation, and if multiple transmitters are used each transmits at a different frequency.

A simplified electrical model of the wireless system is shown in FIG. **2**. The signal generator **16** produces low frequency signals, preferably between 100 and 1000 kilohertz. At these frequencies and with the relative impedances involved in the circuit, the user can be considered as a conductive node **40**.

The signal generator **16** is connected between two nodes **30** and **31** that represent, respectively, the inner and outer electrodes **18** and **20**. The signals produced by the signal generator **16** result in a current passing from node **30** to a node **40**, to which it is coupled by a capacitance **36**. The current passes from the user-node **40** to a node **43** that represents the inner electrode **24** of the receiver **22**. A capacitance **46** represents the coupling between these two nodes. The current then flows through the receiver **22**, that is, through a detector **47** and node **44**, to ground through a coupling represented by a capacitance **48**. The node **31** of the transmitter provides the return path for the current, as represented by a capacitance **34**.

There is direct capacitive coupling between the electrodes **18** and **20** of the transmitter **14**, as represented by a capacitance **35** between the nodes **30** and **31**. The node **30** is also capacitively coupled to the receiver **22**, through the air, by a capacitance **38**. This coupling is relatively weak, however, because of the distance between the transmitter and the receiver.

The node **31** is coupled to the user-node **40**, through the air, as represented by a capacitance **32**. This coupling provides additional current paths for the transmitted signal traveling through the user-node **40**.

The user-node **40** is coupled to ground, as represented by a capacitance **42**. This coupling shorts a relatively large portion of the current to ground, and thus, significantly attenuates the current passed from the user to the receiver.

The coupling from the inner electrode **24** to the outer electrode **26** of the receiver is represented by a capacitance **45**. If the detector **47** is detecting current, this coupling has little affect since the current measuring resistance, denoted by R in the drawing, of the amplifier **47** is typically smaller than the impedance of the capacitance **45**. If the detector **47** is detecting a potential, the coupling between the nodes creates a current leakage path through the receiver **22** to ground.

Referring now to FIG. **3**, the transmitter preferably includes the signal generator **16** and a direct-sequence spread spectrum modulator **29**. The modulator modulates the signals produced by the signal generator in accordance with a pseudorandom code, and supplies the modulated signal through a tank resonator **50** to the electrodes **18** and **20**. The tank resonator **50** converts square waves to sine waves at the frequency of interest, without radiating energy at the higher-frequency components of the square wave.

The receiver **22** includes the amplifier **47**, which amplifies a signal that corresponds to the displacement current that passes from the user to the inner electrode **24**, though a synchronous detector **52** to the outer electrode **26**. A synchronous detector **52**, operating in a conventional manner, demodulates the signal and reproduces the transmitted information.

As discussed, multiple transmitters **14** may be included in the system. Each transmitter uses a different pseudorandom code in its modulator **29**. This allows the receiver to distinguish the signals transmitted simultaneously by various transmitters, based on the codes. Alternatively, the transmitters may transmit at different carrier frequencies or at different times, in which case the receiver distinguishes between the various signals based on these frequencies or times of transmission.

FIG. **4** depicts one application for the system. In this configuration the system is incorporated into various components of a paging system that the user wears or carries. The user carries, for example, in his pocket, a paging terminal **60** that receives paging messages over the air in a conventional manner. The paging terminal includes the transmitter **14**, which is capacitively coupled to the user and to ground. The transmitter produces signals that include information from the received messages and passes the signals to the user as displacement currents.

A display device **62** that is incorporated in, for example, the user's watch **64**, includes a receiver **22** that is capacitively coupled to the user. The receiver **22** reproduces the signals from the displacement current passed to it, and the display then presents the information included therein to the user. The watch **64** may also include one or more buttons (not shown) that a user may use to select, for example, storage options for the paging messages. The various system components may instead be incorporated into the user's glasses **66**, shoes **68**, belt buckle **70**, and so forth.

There is no wire connection between the receiver and the transmitter, since they are each capacitively coupled to the user and to room ground, and thus, communicate through the user's body. Accordingly, the system does not interfere with the user's clothing or restrict his movements.

Another application for the wireless system is to pass information that represents the user's physiological condition between a plurality of transmitters and a receiver that are each capacitively coupled to the user. Referring now to FIG. **5**, a plurality of transmitters 14_1,14_2,14_3 . . . are connected, respectively, to instruments 74_1,74_2,74_3 . . . that measure blood pressure, take EKG readings, and so forth. Each transmitter receives data from the associated instrument and produces modulated signals that include the data. These signals result in displacement currents passing between the transmitters and the user **10** and from the user **10** to the receiver **22**, which is connected to a recorder **76** that records the data.

Referring now to FIG. **6**, the system may also be used to pass signals inter-body to a receiver that is proximate to but not mounted or carried on the user's body. As discussed above, the return path for the current is through room ground, and no connecting wires are required. A user wears the transmitter **14**, for example, as part of his watch **64**, and the receiver **22** is mounted on a door (not shown) or within a doorknob **80** that controls the opening of the door. The transmitter **14** produces a modulated signal that includes a personal identification number. This signal is capacitively coupled to the receiver **22** when the user grasps or comes sufficiently close to the doorknob. The receiver **22** determines if it recognizes the number, and if so locks or unlocks the door, as appropriate.

Similarly, two users shaking hands can each exchange information between receivers and transmitters that they are carrying, to exchange, for example, electronic business cards.

Other applications of the system are discussed below, with reference to FIGS. **7** and **8**. In these applications an array **102** of receivers **22** is at a fixed location. The receivers **22** determine the relative position of a user-carried transmitter from the relative strengths of the received signals.

FIG. **7** depicts the wireless system incorporated into a personal computer **100**. The system provides to the user a multi-dimensional input device that allows a user, with hand gestures, to move in two dimensions an on-screen object such as a cursor, or in three dimensions a three-dimensional on-screen object or herself, that is, her viewpoint, through a virtual space that is displayed on the screen.

The system includes the array **102** of receivers **22**, which are mounted in close proximity to a screen **104** of a monitor **106**. The transmitter **14** is incorporated into a foot pedal **108** that the user contacts when she desires to move an on-screen object or, her virtual space viewpoint.

The user places her foot **110** on the foot pedal **108** and moves one of her hands **112** in front of the screen **104**. As discussed above, the transmitter **14** is capacitively coupled to the user **10** and to ground. The signals produced by the transmitter **14** are passed as currents through the user and from the user's hand **112** to the array **102** of receivers **22**. A processor **111***a,* which is housed in the computer drive **111**, connected to receive signals from the array **102** determines the relative position of one or both of the user's hands, based on the relative strengths of the signals received by the various receivers. The processor then moves, for example, the on-screen object to a corresponding location on the screen.

When the system is used to move the user or an object in a three-dimensional virtual space that is displayed on the screen, the system determines where the user's hand is relative to a predetermined "neutral" position that corresponds to a mid-point in the range of movement to which the receiver responds. If, for example, the receiver responds to movements of the user's hand when the hand is at most one meter from the screen and ten centimeters to the left, right, above or below the screen, the neutral position is the center of the screen at the distance between the screen and one meter that corresponds to the middle of the operational range of the receivers.

If the user moves one of her hands between the neutral position and the screen the system moves the user forward through the virtual space. If the user also moves one of her hands to the left of the neutral position, the system moves the user at a corresponding angle to the left in the space, and so forth. As the user moves one or both of her hands farther and farther from the neutral position, the system moves the user faster and faster through the virtual space in the direction that corresponds to the relative position of the user's hand.

In an alternative arrangement of this system, the transmitter **14** is included on the keyboard **116** or in a chair cushion **114**, instead of in the foot pedal **108**. In this arrangement, the foot pedal may optionally be used to control the "granularity" of the user's movement in the virtual space, that is, to control the scale of the movements through the space. The user depresses the foot pedal to speed the user's overall movement in the virtual space and released to slow that movement. If, for example, the user is moving between buildings in the virtual space she depresses the foot pedal to accelerate her progress through the space and repositions her hand to regulate and direct the accelerated movements. When the user enters a room in the building, she releases the foot pedal to slow her movements, and again uses her hand to regulate and direct the decelerated movements.

The wireless system readily translates the three-dimensional movements of a user's hand to movements of the user through three-dimensional virtual space. This is in contrast to input devices that operate in two-dimensions and cannot readily convey simultaneously backward or forward, up or down, and left or right movements to the on-screen objects. Further, the user may direct the movement using one or both of her hands, as appropriate.

Referring now to FIG. **8**, a laptop computer **120** incorporates the wireless system to replace the mouse and/or control the movement of the user through three-dimensional virtual space. The array **102** of receivers **22** is mounted adjacent to the screen **104** in the lid **121** of the laptop. The transmitter **14** is incorporated into the base **122** of the laptop, on one side of or next to the keyboard **116**. A user touches the transmitter **14** with one hand, for example, her left hand, and controls the movements of objects displayed on the screen by positioning her right hand in front of the screen, as discussed above with reference to FIG. **7**

One or more auxiliary receivers **22***a* may be mounted on the keyboard **116**, to allow a user to select, or "click on," a particular on-screen object. The user makes her selection by moving the thumb of her left hand proximate to the appropriate auxiliary receiver **22***a*.

FIG. **9** depicts a portable, scalable input device **200** that consists of an array **201** of receivers **22**. The array includes three orthogonal, electrically isolated electrodes **201–203** that are part of three receivers **22**. Each electrode is capacitively coupled, through the air and through room ground, to a user (not shown) who is nearby. A processor **205** connected to process the signals received by the electrodes determines the relative position of the user based on the strengths of the signals received by each of the electrodes. This array may be used instead of the array **102** depicted in FIGS. **7** and **8**.

The electrodes **201–203** can be extended or collapsed over a range of several inches to two feet, as necessary, to scale the expected range of movement of the user or users to the range of movements of on-screen objects in, for example, three-dimensional virtual space. The electrodes can be selectively extended and collapsed to accommodate fully the expected range of movement. The device **200**, when collapsed fits into a pocket for easy transport.

FIG. **10** illustrates an alternative wireless system that includes multiple receivers **22** that are connected to lines **204**. The lines are arranged in a grid **206** and may be included in a rug or floor. A user carries a transmitter **14**, preferably in his or her shoes. The wireless system determines the position of the user by determining which receivers receive the strongest signals from the transmitter. The receivers distinguish individual users based on the modulation codes associated with their respective transmitters. Again, the return path for current is through room ground, and thus, the transmitter and receiver electrodes pass the signals capacitively instead of as radiated energy.

The foregoing description has been limited to a specific embodiment of this invention. It will be apparent, however, that variations and modifications may be made to the invention, with the attainment of some or all of its advantages. Therefore, it is the object of the appended claims to cover all such variations and modifications as come within the true spirit and scope of the invention.

What is claimed is:

1. A wireless communication system including:

A. a transmitter for producing low frequency signals that include data, the transmitter being capacitively coupled to a user and to ground, the transmitter passing to the user a current that is associated with the low frequency signals; and

B. a receiver that is displaced from the user and is coupled to ground for receiving when capacitively coupled to the user a current that is associated with the signals produced by the transmitter, the receiver reproducing the transmitted signals and recovering the data.

2. The wireless communication system of claim **1**, wherein the transmitter includes:

i. a pair of electrodes; and

ii. a signal generator connected between the electrodes, the signal generator generating the low frequency signals that result in an associated displacement current between the electrodes and the user.

3. The wireless communication system of claim **2**, wherein the receiver includes:

i. a pair of electrodes; and

ii. a signal detector connected between the electrodes, the signal detector reproducing the low frequency signals from a displacement current developed between the electrodes and the user.

4. The wireless communication system of claim **1** wherein the system further includes

a. a plurality of receivers; and

b. a processor for determining from the signals reproduced by the receivers the position of the user relative to one or more of the receivers.

5. The wireless communication system of claim **4** wherein:

the receivers are mounted on the periphery of a computer screen; and

the processor moves a cursor to a position on the screen that is associated with the position of the user relative to one or more of the receivers.

6. The wireless communication system of claim **2** wherein the transmitter further includes a signal modulator for spread spectrum modulating the signals with a predetermined pseudorandom code.

7. The wireless communication system of claim **6** wherein the system further includes a plurality of transmitters, each of the transmitters being associated with a predetermined code that differs from the codes associated with the other transmitters in the system, the receiver using the codes to distinguish between the signals passed from each of the transmitters in the plurality of transmitters.

8. The wireless communication system of claim **7** wherein each of the transmitters in the plurality of transmitters is capacitively coupled to a different user, and the receiver receives signals respectively from the individual transmitters when the receiver is capacitively coupled to the individual transmitters.

9. The wireless communication system of claim **8** wherein the system further includes:

a. a plurality of receivers; and

b. a processor for determining from the signals reproduced by the receivers the relative positions of the users.

10. The wireless communication system of claim **9** wherein:

the receivers are mounted on the periphery of a computer screen; and

the processor moves one or more objects to positions on the screen that are associated with the positions of one or more of the users relative to one or more of the receivers.

11. A computer system including:

A. a screen for displaying on-screen objects;

B. a keyboard for data entry to the system;

C. a transmitter for producing low frequency signals, the transmitter being capacitively coupled to a user to pass to the user a current that is associated with the low frequency signals;

D. a plurality of receivers mounted on the periphery of the screen, each of the receivers in the plurality receiving from the user, through capacitive coupling to the user, a current that is associated with the signals produced by the transmitter, the receivers determining the position of the closest extremity of the user's body relative to one or more of the receivers; and

E. a processor for controlling the screen display, the processor directing the screen to display the objects in positions that correspond to the position of the user's extremity as determined by the receivers.

12. The computer system of claim **11** wherein the transmitter is incorporated into the keyboard.

13. The computer system of claim **11** further including a receiver that is mounted on the keyboard, the receiver determining, based on the strength of the received signals if the user is selecting the information that is displayed below the cursor, the system determining that the user is selecting the information if the strength of the signals received by the receiver mounted on the keyboard is above a predetermined threshold.

14. A wireless communication system including:

A. a plurality of transmitters for producing low frequency signals, the transmitters being capacitively coupled to one or more users and to ground and, respectively, including a pair of electrodes and connected between the electrodes a signal generator that generates low frequency signals, each transmitter passing to the associated user a current that is associated with the low frequency signals; and

B. a plurality of receivers coupled to ground for receiving, respectively, from the one or more users to which they capacitively couple one or more currents associated with the signals produced by the transmitters, the receivers reproducing the transmitted signals; and

C. a processor for determining from the signals reproduced by the receivers the respective positions of the users relative to one or more of the receivers.

15. The wireless communication system of claim **14** wherein:

i. the transmitters each, respectively, transmit signals associated with a different predetermined code; and

ii. the receivers distinguish between the signals produced by the individual transmitters based on the codes.

16. The wireless communication system of claim **14** wherein the receivers distinguish between the signals produced by the individual transmitters based on the times the signals are transmitted.

17. The wireless communication system of claim **14** wherein:

i. the transmitters each, respectively, transmit signals at different predetermined frequencies; and

ii. the receivers distinguish between the signals produced by the individual transmitters based on the frequencies.

18. A system including:

A. a screen for displaying one or more on-screen objects including a cursor;

B. a keyboard for data entry to the system;

C. a transmitter for producing low frequency signals, the transmitter being capacitively coupled to a user to pass

to the user a current that is associated with the low frequency signals;

D. a plurality of receivers mounted on the periphery of the screen, each of the receivers in the plurality receiving from the user, through capacitive coupling to the user, a current that is associated with the signals produced by the transmitter, the receivers determining the position of the closest extremity of the user's body relative to one or more of the receivers;

E. a selection receiver mounted on the system for determining, based on the strength of the received signals, if the user is selecting the information that is displayed below the cursor, the system determining that the user is selecting the information if the strength of the signals received by the selection receiver is above a predetermined threshold; and

F. a processor for controlling the screen display, the processor directing the screen to display one or more of the objects in positions that correspond to the position of the user's extremity as determined by one or more of the plurality of the receivers.

19. The system of claim **18** wherein the selection receiver is mounted on the keyboard.

20. The system of claim **19** wherein the system further includes a plurality of selection receivers.

21. The wireless communication system of claim **1** wherein the receiver is mounted on an object.

22. The wireless communication system of claim **1** wherein the receiver is coupled to another user.

23. The wireless communication system of claim **1** wherein the system further includes:

a. a plurality of transmitters that are capacitively coupled to one or more users;

b. a plurality of receivers that are displaced from the users; and

c. a processor for determining from the signals reproduced by the receivers the positions of the one or more users relative to one or more of the receivers.

24. The wireless communication system of claim **23** wherein:

i. the transmitters also receive signals; and

ii. the receivers also transmit signals.

25. The wireless communication system of claim **1** wherein:

i. the transmitter also receives signals; and

ii. the receiver also transmits signals.

* * * * *

Towards the Distributed Visualization of Usage History

Paul Michael Yarin

BSE Mechanical Engineering, University of Pennsylvania, 1995
MS Mechanical Engineering, Stanford University, 1997

ARCHIVES

MASSACHUSETTS INSTITUTE OF TECHNOLOGY

JUL 20 2001

LIBRARIES

Submitted to the Program in Media Arts and Sciences,
School of Architecture and Planning,
in partial fulfillment of the requirements for the degree of
Master of Science in Media Arts and Sciences
at the Massachusetts Institute of Technology

© Massachusetts Institute of Technology, 1999

September 1999

Author Signature redacted
Program in Media Arts and Sciences
August 6, 1999

Certified by Signature redacted
Hiroshi Ishii
Professor of Media Arts and Sciences
Program in Media Arts and Sciences

Accepted by Signature redacted
Stephen A. Benton
Chair, Departmental Committee for Graduate Students
Program in Media Arts and Sciences

Shenzhen Huiding Tech. Co., Ltd. - Exhibit 1006

Towards the Distributed Visualization of Usage History

Paul Michael Yarin

**Submitted to the Program in Media Arts and Sciences,
School of Architecture and Planning, on August 6th, 1999,
in partial fulfillment of the requirements for the degree of
Master of Science in Media Arts and Sciences
at the Massachusetts Institute of Technology**

Abstract

Because they require focused visual attention and explicit user control, current computer interfaces have either limited computer augmentation to highly specialized environments or have necessitated major changes to work practice. "Situated usage history displays," devices that indicate the former use of physical objects and surfaces enable convenient access to information without disruption of existing environments or behavior. Prototype systems for monitoring the usage of handheld objects, storage containers, medication bottles and other devices are presented; underlying technologies for sensing and display are also described. The design space of situated usage history displays is characterized through discussion of key opportunities and constraints.

**Thesis Advisor:
Hiroshi Ishii
Professor of Media Arts and Sciences
Massachusetts Institute of Technology**

Shenzhen Huiding Tech. Co., Ltd. - Exhibit 1006

APPENDIX EE

Towards the Distributed Visualization of Usage History

Thesis Committee

Thesis Reader	Signature redacted	**Hiroshi Ishii** **Associate Professor of Media Arts and Sciences**
Thesis Reader	Signature redacted	**Mitchel Resnick** **Associate Professor of Media Arts and Sciences**
Thesis Reader	Signature redacted	**Scott Snibbe** **Member, Research Staff, Interval Research Corporation**

Shenzhen Huiding Tech. Co., Ltd. - Exhibit 1006

Your notes here

Acknowledgments

Hiroshi Ishii
For providing an engine, premium fuel, and a heavy foot on the pedal

Scott Brave, Andy Dahley, Matt Gorbet, Craig Wisneski, Victor Su, Phil Frei, Jay Lee, Seungho Choo, and James Patten
For being exciting, creative, and fearless colleagues

Josh Smith, Tom White, Rich Fletcher, Golan Levin, and Jon Ferguson
For sharing time and talent as collaborators

Hiroshi Ishii, Mitch Resnick, and Scott Snibbe
For their efforts to review and improve this document

Clay Harmony and James Hsiao
For their diligent project execution

David, Naoko, and Peter Yarin
For the gift of a happy and loving family

Joanna Berzowska
For her insight and charm

Brygg Ullmer and John Underkoffler
For being omnivorous in intellect, if not in diet

John Maeda, Neil Gershenfeld, Marvin Minsky, Henry Jenkins, Larry Leifer, Ed Carryer, Dennis Boyle, Hale Rowland, Tommy Cowan, and Bob Goody
For teaching me well

Scamper
For teaching me to be a dog, well

Shenzhen Huiding Tech. Co., Ltd. - Exhibit 1006

Table of Contents

1	INTRODUCTION	8
	1.1 Motivation	8
	1.2 Research Topic	9
	1.3 Thesis Overview	10
2	BACKGROUND AND RELATED WORK	11
	2.1 Computer-augmented environments	11
	2.2 Situated information spaces	12
	2.3 History-enriched digital objects	13
	2.4 Tangible interfaces	14
	2.5 Artificial intelligence, perception, and emotion	15
3	DESIGN APPROACH	17
	3.1 Objectives	17
	3.2 Design Parameters	17
4	GESTURAL INTERACTION DEVICES	20
	4.1 Introduction	20
	4.2 FishFace	20
	4.3 ShakePad	25
	4.4 Discussion	26
5	AUGMENTED CONTAINER STORAGE SYSTEM	29
	5.1 Background	29
	5.2 Implementation	30
	5.3 Interaction techniques	31
	5.4 Discussion	34

Shenzhen Huiding Tech. Co., Ltd. - Exhibit 1006

6	OBJECT IDENTIFICATION AND TRACKING SURFACES	37
	6.1 Introduction	37
	6.2 SensePad	39
	6.3 IDPad	45
	6.4 Discussion	49
7	EVALUATION AND FUTURE WORK	51
	7.1 FishFace and ShakePad	51
	7.2 TouchCounters	52
	7.3 SensePad and IDPad	52
8	CONCLUSION	54
	8.1 Summary	54
	8.2 Personal vision	54
A	APPENDIX: ADDITIONAL INTERACTIVE DEVICES	56
	A.1 Tactile Pad	56
	A.2 Network Meter	59
B	APPENDIX: PROJECT INFLUENCE MAP	61
C	APPENDIX: DESIGN PARAMETERS	62
	REFERENCES	63

Shenzhen Huiding Tech. Co., Ltd. - Exhibit 1006

1 Introduction

1.1 Motivation

The basic operations of work are exchanges between people, information, and physical objects (Cooper98). Although computers have greatly facilitated the ease and efficacy of interpersonal communication, similar benefits have yet to be widely conferred upon interactions with physical objects.

One reason is that most computer interfaces are poorly suited for mediating interactions with physical objects. The dominant paradigm for computer interaction is the "graphical user interface" or GUI, in which users monitor a detailed display of text and graphics while typing on keyboards and manipulating pointing devices. While well suited to applications in which the computer is the focus of attention, this type of interaction is difficult to carry out in conjunction with inherently physical tasks—the sorting of items on a table, the location of physical objects or containers, or the use of physical tools.

Under these circumstances, users stand to benefit most from "lightweight" interfaces, those with which data can be usefully recorded or retrieved with minimal cognitive and physical effort. To enable lightweight interactions with information, interfaces should be

- physically present and visible at the location of use
- easy to comprehend through use of visual patterns
- responsive to simple physical actions
- capable of conveying relevant information

The successful design of these systems demands more than simply extrapolating the design of the GUI to larger and smaller form factors. Lightweight interfaces depend upon the careful integration of sensing technology, display, and interaction techniques in a physical form suitable to the environment of use. Simplicity and efficiency, rather than raw computational power determine real-world utility.

Shenzhen Huiding Tech. Co., Ltd. - Exhibit 1006

1.2 Research Topic

To address the above goals, I have chosen to develop various computational devices that demonstrate a possible approach. These devices aim to enhance collaboration by displaying visual representations of locally recorded physical data. Unlike the cumbersome, generic computers of today, these devices are envisioned as integral and unobtrusive features of living and working environments, acquiring and displaying information silently and automatically. Because these devices portray the past histories of objects and environments, their means of interaction may be termed "the distributed visualization of usage history."

This phrasing requires some clarification. *Distributed* refers not to a method of data analysis but rather to the simultaneous exchange of data at multiple physical locations. *Visualization* refers to the visual representation of information in a manner that facilitates understanding. *Usage* refers broadly to any physical activity performed repeatedly to achieve a useful function. *History* signifies data that has been accumulated over time, whether or not the temporal dimension is explicitly represented to the user.

The concept of usage frequency as an aid to collaboration has roots in both online media, in its use of relevance queries and popularity rankings, as well as in physical indications of wear: walking trails worn by repeated passage, fingerprints on the popular pages of repair manuals, and date stamps in the backs of popular library books (Hill92). This work concerns electronically synthesizing such phenomena in response to physical actions.

The arguments in favor of measuring usage history include its flexibility, simplicity, and robustness. The measurement of usage frequency applies equally to characterizing the histories of either people or objects. The many available sensing technologies make detection of a wide variety of physical events feasible at a low cost, and with a high level of reliability. (Note that this technique may, but need not, take advantage of remotely stored, computed, or acquired data; networking is not a prerequisite for measurements of usage history.) As measurement of history can be readily automated, these systems can acquire data without the intervention of a human operator.

Distributed visualization describes both the presentation of information from multiple, individual displays, and the techniques that allow data to be compared through concurrent viewing of multiple displays in parallel. Techniques for information visu-

Shenzhen Huiding Tech. Co., Ltd. - Exhibit 1006

alization are well established in the computer graphics community (Card99), but are rarely applied to augmenting of physical objects or spaces with multiple displays.

Displays designed to integrate with physical structures can be positioned within the visual field of the user. This greatly reduces the cost of attending to the interface, as setup and tear-down times become essentially nonexistent. In addition, the use of multiple displays in parallel allows identification of trends in relative use across objects and spaces; this is especially well suited to objects contained in furniture with regular geometries like shelves, drawers, or pegboards.

1.3 Thesis Overview

This document presents prototypes and conceptual models of situated usage history displays. Related work in computer-augmented environments, information visualization, and digital histories are described. In the next section, the design space for situated usage history displays is outlined through several key parameters. The development of the several prototype systems are then presented. The next chapter evaluates these systems and describes recommendations for future work. Finally, a brief summary is presented with a description of a personal vision for this work.

The first Appendix described two additional prototypes that fall somewhat outside the scope of this work. The second charts the conceptual connections between projects; the third lists the design dimensions in greater detail.

APPENDIX EE

Shenzhen Huiding Tech. Co., Ltd. - Exhibit 1006

2 Background and Related Work

This work draws upon a variety of influences and research findings in computer-augmented environments, context-aware computing devices, interaction histories for software objects, information visualization, and tangible interfaces. Related projects not discussed here include augmented reality (Feiner93), distributed sensing devices (Poor99), and computational learning tools (Resnick98).

2.1 Computer-augmented environments

A wide variety of projects claim to address the integration of computing technologies with physical spaces. Most, however, assume that people exchange the same *types* of information in shared physical spaces as they do when using desktop computers—messages, meeting notes, indications of attendance, etc. As a result, most systems tend to incorporate scaled versions of desktop-style graphical user interfaces—pointing devices, icons, multimodal, and high-resolution displays.

Ubiquitous computing

The Ubiquitous Computing concept (Weiser91) anticipated the widespread proliferation of networked computing devices throughout interior environments. Wall-sized projected whiteboards and tablet-sized computers were demonstrated, in addition to a handheld device called the ParcTab. The later companion concept of "calm technology" (Weiser97) emphasized the importance of subtle and peripheral indicators of human activity.

While the "UbiComp" vision has been influential and prominent for many years, few usable design principles or prototypes have been developed since the original concept was articulated. This work is consistent with the broad vision of Ubiquitous Computing, but is more explicit about the types of hardware and interactions it hopes to support.

Cooperative buildings

More recently, the concept of UbiComp has influenced the field of computer-supported collaborative work (CSCW). The first conference on Cooperative Buildings (Darmstadt, Germany, February, 1998) centered upon integrating technologies



Figure 2.1: ParcTab device (Weiser93)

Shenzhen Huiding Tech. Co., Ltd. - Exhibit 1006

APPENDIX EE

with workplace environments. The motivation for this trend was described in the conference proceedings:

> The introduction of information and communication technology has already changed processes and contents of work significantly. However, the design of work environments, especially physical work spaces such as offices and buildings, remained almost unchanged. It is time to reflect these developments in the design of equally dynamic, flexible, and mobile work environments. (Streitz98a)

A representative example of this approach is the "i-LAND" system described in (Streitz98b). This specially constructed room contains a wall-sized, rear-projected display, chairs with tablet computers installed within swiveling armrests, and a bottom-projected tabletop display. Users interact with the devices, and transfer data between them, by using pens and by pointing. The equipment is intended to support group meetings and discussions.

The design of i-LAND, like that of many other computer-augmented environments, implies several common assumptions about computer-augmented interaction:

- that collaboration support systems require specialized, dedicated facilities
- that users in this environment are concerned only with the manipulation of virtual information
- that physical objects are not intrinsic features of collaborative physical environments (no environmental objects appear in the images, aside from a single plant)
- that graphical interaction techniques, with some modifications, are well-suited for multi-user interaction
- that displays must be engaged at distances of 0-10 feet

Collaborative documentation and meeting support may be well served by such facilities, but actions involving physical objects are unknown and irrelevant to them. As a result, it is difficult to imagine how these systems could be employed in environments where physical tasks and objects are central.

2.2 Situated information spaces

The concept of "situated information spaces" proposed by George Fitzmaurice has a somewhat stronger relationship to this work. This work emphasized the importance of physical objects and space in providing a meaningful context for interaction.

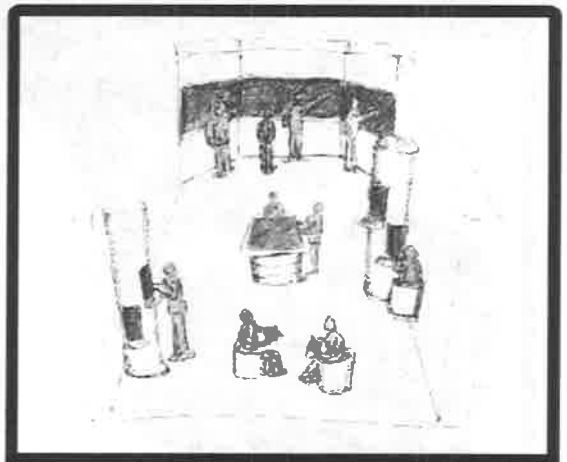


Figure 2.2: "i-LAND" concept sketch (Streitz98b)



Figure 2.3: "i-LAND" "roomware" (Streitz98b)

Shenzhen Huiding Tech. Co., Ltd. - Exhibit 1006

APPENDIX EE

> Wherever possible, we should look for ways of associating information with physical objects in our environment.... Our goal is to go a step further by grounding and situating the information in a physical context to provide additional understanding of the meaning of the space and to improve user orientation. (Fitzmaurice93)

Situated information spaces were to be enabled by the technology of "spatially aware palmtop computers," handheld displays carried by users as they navigated personal spaces. These devices, typified by the "Chameleon" prototype, were equipped with sensors to detect their positions and orientation. Movement of the device caused the displayed image to scroll over a virtual workspace. The device acted as a "lens" that could reveal a virtual world hidden within the physical.

In addition, proprioceptive displays might be used in conjunction with a distributed system of displays embedded in physical storage structures. Though such a system was never implemented, Fitzmaurice imagined a computer-augmented library with touch-sensitive LCD indicators along the front edges of the shelves: "as we walk through the music section, books on the topic of interest as well as related material will be highlighted by indicator lights..." (Fitzmaurice93)

Again, while the broad observations regarding physical context do relate to this work, significant constraints are imposed by the choice of implementation. Use of a small, handheld display requires attention to be focused upon a small screen, and offers no benefit to other users of the same space. Wielding the device continuously also seems incompatible with other concurrent activities. The means to determine the books' positions (for registration with the LCD's) was not addressed, nor were issues of power, networking, data storage, or latency.

2.3 History-enriched digital objects

The concept of automatically embedding representations of history was first proposed in a seminal paper by James Hollan and Will Hill (Hill92). Interestingly, the notion was conceived as a means to facilitate collaboration over digital objects, rather than physical ones:

> The basic idea is to maintain and exploit object-centered interaction histories: Record on computational objects (e.g. documents, menus, spreadsheets, images, email) the events that comprise their use, and then, on future occasions, when the objects are used again, display useful graphical abstractions of the accrued histories as parts of the objects themselves.

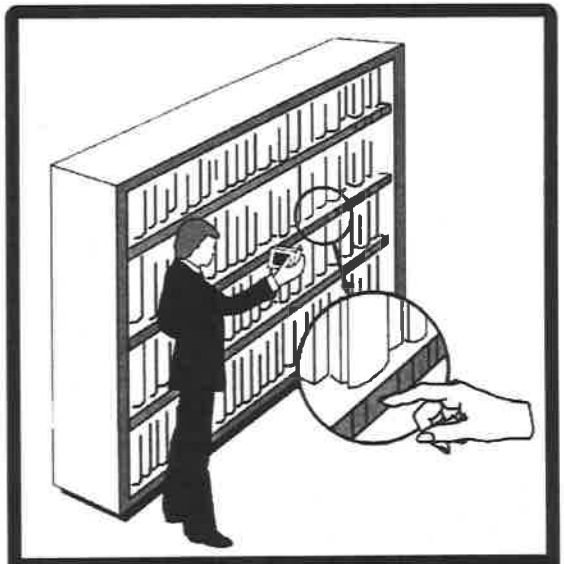


Figure 2.4: Computer-augmented library concept (Fitzmaurice93)

APPENDIX EE

Shenzhen Huiding Tech. Co., Ltd. - Exhibit 1006

Hill and Hollan implemented tools for recording the cumulative time spent editing or reading each line of a document. This data was then represented visually as a simple graphic in the "attribute-mapped scroll bars" alongside the document. This was an elegant solution in that it overlaid the visualization with the area of the screen used for navigation.

In addition to describing their implementation, Hill and Hollan pointed out the possibility of inventing new "physics" when generating wear through computation:

> Computation enables the creation of virtual worlds that resemble the real world and allow us to exploit our extensive knowledge of the world in interacting with them... these same techniques also allow us to create virtual worlds that give concrete existence to abstract entities operating according to a physics of our choice. The entities and their physics can be designed to highlight aspects of phenomena not normally available to us but that are important for supporting understanding and task performance.

This point applies equally to "wear" represented in physical environments; use data can indicate information about users, object attributes, modification dates, etc. as well as accumulated use.

2.4 Tangible interfaces

The work of the Tangible Media Group, founded and led by Professor Hiroshi Ishii, was the immediate context from which this research emerged. "Tangible media," a phrase that signifies both physical embodiment and ease of comprehension, was defined broadly as "the seamless interfacing of physical and digital worlds." (Ishii97) Since its inception, the group has engaged in a series of design projects that have served to demonstrate new concepts, forms, and applications of information technologies. Presented here are some themes that have recurred throughout several different projects.

One theme is the use of physical objects as representations of electronically stored information. Various projects have employed physical objects as "containers, conduits, and controls" for digital information. (Ullmer98) Such systems have the benefits of allowing agile manipulation of data elements, concurrent manipulation by multiple users (Fitzmaurice95), expression of correlations and hierarchies between multiple

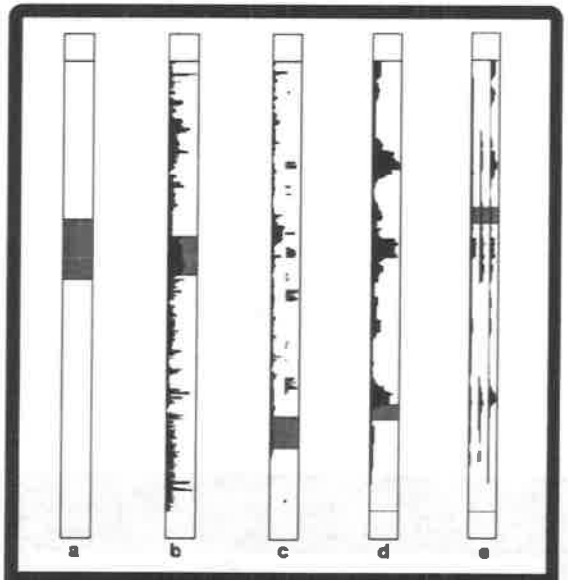
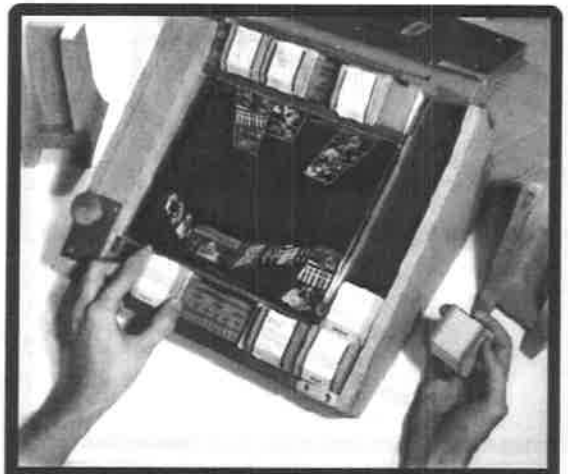


Figure 2.5: Attribute-mapped scroll bars (Hill92)


Figure 2.6: MediaBlocks sequencer (Ullmer98)

Shenzhen Huiding Tech. Co., Ltd. - Exhibit 1006

APPENDIX EE

data elements (Gorbet98), and the learning of motor tasks through object manipulation (Underkoffler98).

Another theme has been the representation of remotely acquired information streams. "inTouch" (Brave97) allows direct and conscious communication between remote parties through the concurrent manipulation of electronically coupled physical objects. Other systems display remote activity or information though a variety of abstract representations: patches of light projected onto walls, rows of spinning pinwheels, ripple patterns on the ceiling of a room. These projects raised many issues about representing remote data displaced from its original context (Wisneski98, Dahley98).

A third area of research has been the degree to which information systems require conscious attention to the display of data. In the ambientRoom and Ambient Fixtures projects (Dahley98), attempts were made to provide "background information," typically live data streams represented through physical phenomena or abstract visualizations. In theory, users could remain unaware of these information sources until sudden changes brought them into the "foreground."

Unfortunately, while a number of novel display devices have been constructed, none were in practice linked to live data streams. Examples of online data sources were suggested—changing stock values, quantity of incoming email messages, activity of a family member in a remote location, etc., but none seemed compelling enough to warrant the effort of implementing a working connection. One problem, it seems, is that most data available online are already well supported by the design and usage context of the personal computer. Conversely, the types of information about which we care most—the activity of people in a different space or time—are simply unavailable online. One goal of my work is to provide information sources to address this problem.

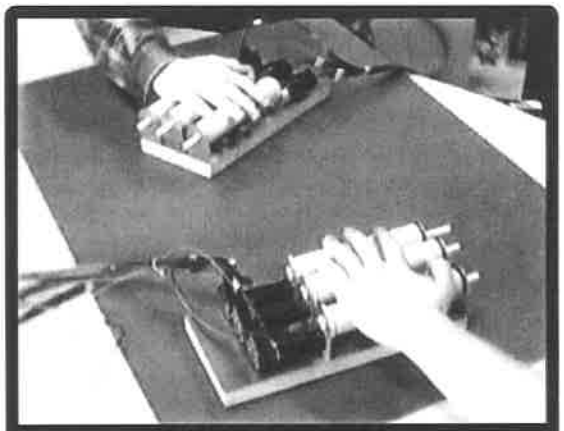


Figure 2.7: inTouch prototype (Brave97)

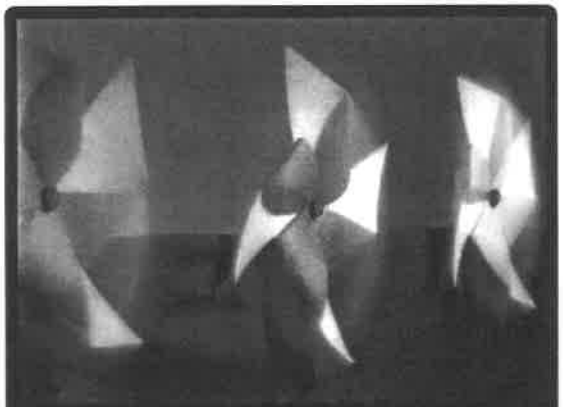


Figure 2.8: "Pinwheels" (Dahley98)

2.5 Artificial intelligence, perception, and emotion

Limitations in the interfaces to computer systems are also being addressed by efforts to grant computers human-like cognitive, perceptual, and emotional abilities. These are mentioned here because many people imagine computers of the future as agents, robots, or anthropomorphic computers that engage users in humanoid dialogue and social behavior. Perhaps the difficulty of achieving these goals should underscore the

APPENDIX EE

Shenzhen Huiding Tech. Co., Ltd. - Exhibit 1006

importance of applying good design practice to existing technologies. In any case, humanoid computers can only benefit from knowledge of human physical actions.

Artificial intelligence

Artificial Intelligence seeks to imbue computers with human-like cognitive abilities through the structured representation of memory and thought processes. While great strides have been made in certain areas—natural language processing, expert systems, and image processing, for example—the general-purpose thinking machine seems at least several decades away, and is perhaps is for our lifetimes a utopian fantasy (Minsky85; Dennett98).

Perceptual user interfaces

The field of Perceptual User Interfaces is a recent outgrowth of computer vision research. It amassed sufficient interest to open its first conference recently (Turk97). "Perceptual" interfaces involve the use of vision, speech recognition, and/or speech synthesis to enable sound- or gesture-based communication with computers. While some systems emphasize passive monitoring of user actions, most are intended as controllers for the familiar GUI workstation.

Affective computing

The focus of Affective Computing (Picard97) is the emotional state of humans and of machines. Various sensing technologies are used to infer information about a user's emotional state. Gesture, posture, speech, and physiological analysis are used to determine the user's level of arousal or confusion when using a computer system. Affective computing has begun to investigate wearable, passive devices for recording emotions as well. For example, the StartleCam project (Healey98) records digital video whenever the user's orientation response exceeds a particular threshold.

Shenzhen Huiding Tech. Co., Ltd. - Exhibit 1006

3 Design Approach

3.1 Objectives

The approach taken in this work is "research through design." While many useful sensing and display technologies exist, the majority of them require significant effort to adapt to human-computer interaction. Realizing working prototypes that employ these technologies, preferably in forms that can be conveniently reused, is a major goal of this work. A concurrent goal is to propose interaction techniques for this new class of devices. The basic approach has been articulated, but these concepts must be instantiated through specific applications, environments, and types of data. A final goal is to establish conceptual models and maps that help to define the design space for these devices.

3.2 Design Parameters

The possible universe of situated usage history displays is quite large. As an aid to navigation, we propose a set of design parameters that characterize the dimensions by which these devices can differ. This list is intended to motivate the prototypes described in the bulk of this document. After these artifacts have been presented in detail, they will be examined in light of these properties. Of course, the properties listed here are somewhat subjective, and this list is not exhaustive.

Quantity of measurement

The choice of the quantity of measurement to determine "usage" is critical. Generally, the quantities of interest are affected by human activity, but tracking the use of individual objects may be more directly useful than tracking people directly. Thus both human- and object-sensing technologies are of interest. Additionally, measuring devices might count discrete events, such as the number of sheets produced by a printer, or continuous values, such as the overall noise level in a room.

In determining the appropriate quantity of measure, designers should consider

- The utility of the measured data in the task's "action present" (Hill92)
- The cost, complexity, and difficulty of obtaining the measurement
- The extent to which measurement requires changes to existing practice

Shenzhen Huiding Tech. Co., Ltd. - Exhibit 1006

Physical form

Situated displays may take a variety of physical sizes and forms. Devices can be integrated into large, permanent fixtures like walls or shelves or can be portable devices that are body-worn or carried. Compact, portable usage monitors can also be attached (parasitically) to larger pieces of equipment. Perhaps most interestingly, devices be can small individually, but can act as a large display collectively.

The technology underlying usage history displays need not be complex. For example, imagine a "book monitor" the size of a pack of gum, containing only a battery, capacitor, mercury switch, and a blinking LED. This device could attach to the spine of a book, such that its capacitor would charge whenever the book was tilted into a reading position. The LED would then blink for several hours thereafter, until the capacitor was fully discharged. Thus, one could easily identify which books in a library had been read recently.

The type of data connectivity between devices has both technical and conceptual implications. Remote storage of data may result in unpredictable time lags, while batteries may result in power failure. Only if data, display, and power are local to a device can it be treated as a self-contained, "active" object.

The physical appearance of a device should ideally communicate aspects of its functionality: whether it can be attached or detached, the location of its physical controls, in which direction it should be oriented. If a display represents an attribute of a "referent" object, permitting detachment may lead to ambiguity about the correlation of attribute to object.

Interaction techniques

Interaction, the dialogue between user and machine, must also be designed for the context of use. Users may be active controllers of the interface, casual observers, or may completely ignore or avoid the output of the displays.

In general, all situated usage history displays should have some automated display functionality; they should make the cost of seeking information as low as possible. In this sense, situated displays are like signs posted in public spaces. However, it may be advantageous to instrument existing actions in an attempt to provide more specifically contextualized information.

Quantity of measurement
type of phenomenon measured
method of counting
degree of user adaptation
criticality of information
Physical form
physical mobility of displays
physical aggregation with other displays
integration with other physical structures
physical location of stored data
Interaction techniques
degrees of user involvement
number of modes
Visualization
degree of abstraction
temporal representation
responsiveness/dynamism
relativity of comparison

Table 3.1: Design parameters for situated usage history displays

Shenzhen Huiding Tech. Co., Ltd. - Exhibit 1006

For example, imagine an electronic music synthesizer that recorded the frequency of use of each key, and that represented this frequency by making the keys glow with different levels of brightness. One might program the system to respond to the user by detecting the most recently played note, and illuminating only other notes played in conjunction with that note in the past (as accompaniment or as parts of a chord).

Under some circumstances, it may be useful to add features that allow deeper queries (perhaps into the histories or attributes of objects). In supporting these operations, one must weigh the functionality against the added complexity of moded behavior. Multiple interaction modes should be represented explicitly, and should be triggered only by explicit user actions.

Visualization

The choice of a visual representation of history data is as important as the choice of the data itself. Depending on whether absolute or relative usage is more important, one might choose a numerical or graphical display of quantity. Many techniques from the field of scientific data visualization (Card99) can be appropriated for this purpose.

Time may or may not be represented explicitly. Displays can show either a single value that represents accumulated usage over time (like the time-in-use counters used in forklifts and industrial equipment), accumulated use over a given time period, or the level of use over time (like the scrolling humidity recorders in museums).

The use of dynamism in graphics is a delicate issue. Large moving graphics draw attention and trigger orienting responses (Reeves96), and thus should probably be used sparingly—only, perhaps, on a single display at the focus of attention. Small movements on multiple displays may be tolerable, however; small, synchronized lateral movements may be perceptually similar to the motion of trees in the wind. Dynamic graphics can be very effective at indicating the coupling of a user's physical actions to their graphical representation, a circumstance in which demanding attention is appropriate.

A final note is that color appears to be a very effective filtering criteria in attentional studies (Pashler98), and thus may be a useful technique for visualization of a phenomenon across multiple displays.

Shenzhen Huiding Tech. Co., Ltd. - Exhibit 1006

4 Gestural Interaction Devices

FishFace and ShakePad

4.1 Introduction

The first interaction devices developed in this research were portable, self-contained, motion sensing devices. "FishFace" detects hand motion through an electric field sensing device called the Lazy Fish; "ShakePad" senses its own tilting and shaking through an accelerometer. Both use an array of color LED's as an output, and similar graphics were implemented on both devices.

While both record "history" in a technical sense (i.e., they save sampled data points over time), they do so on the order of seconds rather than days or years. Rather, the property that makes them interesting for lightweight interaction is the ease by which they can be located, physically acquired, and controlled. Their design is also interesting in that they can be completely self-contained, including their power supplies; thus they both demonstrate technologies that could easily be integrated into the design of other objects.

4.2 FishFace

The FishFace project was enabled by the availability of a particular sensing technology. Joshua Smith, of the Physics and Media Group, had been developing electric field sensing devices for several years. FishFace was the product of his collaboration with the author during the November 1997 course on Tangible Interfaces. In addition to being familiar to Josh, electric field sensing seemed well suited to interfaces involving handheld physical objects.

Electric Field Sensing

Electric field sensing detects the motion of objects by measuring the changes in electric fields between multiple electrodes in the proximity of the moving object. The oscillating fields are generated by "transmitter" electrodes and are detected by "receiver" electrodes.

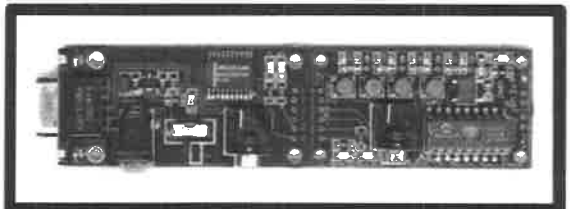


Figure 4.1: Lazy Fish circuit board

APPENDIX EE

Shenzhen Huiding Tech. Co., Ltd. - Exhibit 1006

These electrodes can be constructed in various sizes and configurations to detect different scales and types of motion. Unlike joysticks, magnetic position tracking devices, and sensing gloves, electric field sensors can detect hand or finger motion without requiring direct contact with the user's skin. This can potentially allow freer motion, greater comfort, improved durability, and lower cost. This freedom from equipment and from wear could be particularly advantageous, for example, in public information kiosks.

Prior to the FishFace project, several people at the Media Lab had employed Josh's electric field sensing modules. In general, the modules were used as non-contact pointing devices for computer displays; users could scroll screens or vary parameters by waving their hands in front of the display. All of these systems were relatively large and stationary. However, Josh had almost completed the "Lazy Fish" module, a self-contained electric field sensing circuit with updated hardware and software. The new module, about 2 x 1 x ½ inches, was much more compact than an earlier version. Josh's goal was to implant the sensors into handheld objects.

FishFace Concept

The field sensing technology was a good match for a different technology that had intrigued the author: the LED (light-emitting diode) matrix. This component is a square plastic tile about 2½ inches square. 64 LED's are embedded in the tile as a grid in 8 rows of 8. Though several students around the Lab had these parts, none seemed to be using them. While their resolution was coarse by computer display standards, they seemed appropriate for a small, simple device driven by a microprocessor. (Ultimately, these devices played a major role in all future projects.)

Several factors made this concept appealing. One was the compactness of the technology. As detection range was approximately equivalent to the electrode dimensions, a device the size of a deck of cards could detect finger motion within a 2" control volume. Thus a user could hold the device in the non-dominant hand while gesturing with the other. Another interesting aspect was the ability to detect motion *prior* to contact—a device might "awaken" as a hand approached it, reacting instantly upon contact. The concept of a single compact device also suggested that unexpected interactions might arise from a multiplicity of such devices.

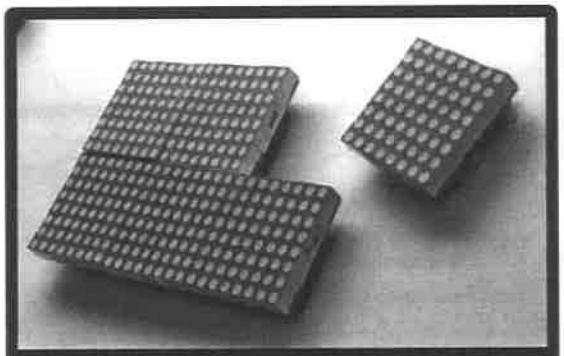


Figure 4.2: LED matrix tiles

Shenzhen Huiding Tech. Co., Ltd. - Exhibit 1006

APPENDIX EE

The combination of the LED matrix with the "Fish" sensor was sufficiently specific to allow consideration of possible uses and interaction techniques. However, there were several open design questions:

- Would the device be self-contained? Would the LED's simply provide visual feedback about the detected signal, or would the entire unit act as a controller and display for an external system?

- What types of graphics could be shown on the display? Could treating the display as a window onto a larger, "virtual" space mitigate the resolution limitations? In such a case, the user might move a finger relative to the display to scroll it vertically or horizontally.

- Could the workspace be divided into virtual, invisible "cells," triggered only when a finger moved into that region? For example, the square could be divided into a 3x3 grid of squares, as are the digits 1 to 9 on a telephone keypad; the entire display could display the numeral corresponding to the selected region.

- Could a pair of these devices be used as a communications medium, like a pair of walkie-talkies? If so, how would local data be mapped to the remote device? Would local data be represented visually?

- What degree of abstraction was appropriate for the graphics on the display? The display was barely capable of representing a single alphabetic character legibly; was there any sense in trying to scroll text messages? Could a simple graphic, e.g. an electronic schematic symbol, be depicted realistically?

As we were able to implement only a few of the many possible configurations, many of these questions remain open.

Original Prototype

The prototype was constructed from two modules: the Lazy Fish sensing board and a new LED matrix control board. Each board had a PIC microprocessor; the two were interconnected by a pair of serial cables. As this was the author's first exposure to programming the PIC microcontroller, much of the development effort was expended on simply achieving bi-directional communication between the two circuit boards.

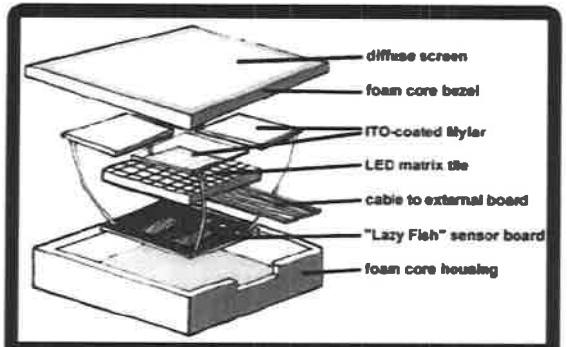


Figure 4.3: Original FishFace assembly diagram

Shenzhen Huiding Tech. Co., Ltd. - Exhibit 1006

The electrodes were cut from a sheet of Mylar coated with indium tin oxide (ITO), a transparent, conductive material. The transparency allowed the electrodes to be mounted directly atop the LED matrix without obscuring the display. In later versions, the transparent film was replaced by L-shaped cutouts of copper tape mounted around the corners of the display.

Housings were built from a variety of materials—foam core, acrylic, and fused deposition polymer— but were similar in their plain, white appearance. The housings ranged from about three to four inches square in size.

Interaction modes

Several modes of interaction were implemented in the microprocessor code for FishFace. The code for each interaction mode was quite straightforward and differed only subtly from the others. However, the experience of manipulating each one was strikingly different.



Figure 4.4: Original FishFace displaying "Snake" patterns

In the simplest mode, the sensor's x-y position data was mapped to the position of a single pixel illuminated on the display. The illusion was that the user's fingers were projecting a glowing dot onto the surface of the display, or that an invisible extension of the user's fingers was made visible by the surface. In a slightly different mode, a snakelike chain of pixels follows the user's finger, elongating when moved quickly and collapsing when slowed.

Finally, in a third mode, finger proximity is detected as well as x-y position; a moving square of light appears around the user's finger, expanding as the finger ap-

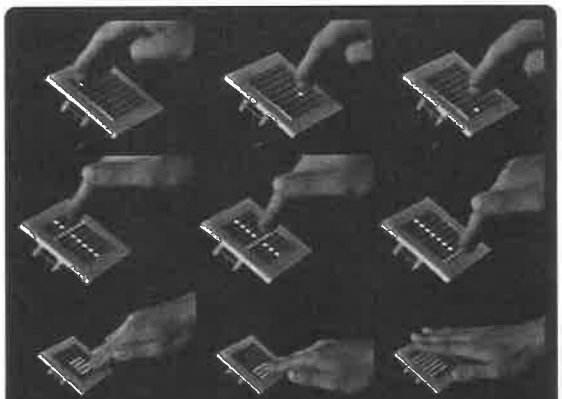


Figure 4.5: FishFace interaction modes "Dot," "Cross," and "Zoom"

Shenzhen Huiding Tech. Co., Ltd. - Exhibit 1006

proaches the surface. In this mode, the finger seems to dip into a virtual liquid, the cross-sectional area of the contact plane expanding with increased depth.

Wireless Communications

For an in-class demonstration of the FishFace system, two FishFace devices were linked by a pair of short-range radio-frequency transceivers. The system was implemented hurriedly and with a number of flaws, but for a short time a bi-directional link was operational. The originally self-contained FishFace devices were thus converted to synchronous, portable communication devices, like a pair of walkie-talkies.

To explore this further, one would have to select a model of the mapping of information between the two devices. In a simple case, the paths traced by each user's gestures might be displayed simultaneously on both displays. Another straightforward approach would be to display each user's gesture as a separate color; this would require a bicolor display. Or, rather than displaying each user's motions directly, each user's current position could be used as an endpoint of a line interconnecting the two; thus the line's length would indicate the difference between the user's positions. The inTouch system is a model of another approach; the two displays could indicate a common graphic computed by interpolating between each user's position values.

Performance

The original FishFace display had many technical limitations. The display was monochromatic (red), and thus information could not be communicated through color. Because the display was driven directly from the microprocessor, the available current was barely sufficient to illuminate the display. Room lights had to be dimmed for the display to be easily visible.

Also, reactions to the diffuse overlay were mixed. Some liked the organic appearance of the glowing lines; others found it unnecessarily blurry. The screen was successful in disguising the coarse resolution of the display, however; many assumed that the underlying resolution was much higher than 8x8.

4.3 ShakePad

Several months after the development of FishFace, a similar system called ShakePad was constructed. Like FishFace, ShakePad was a handheld, white, square object with

Shenzhen Huiding Tech. Co., Ltd. - Exhibit 1006

no visible controls. Instead of detecting hand motion through electric field sensing, ShakePad detects its own motion through an accelerometer contained within its enclosure. Tilting or shaking the device triggers changes in the patterns displayed.

Acceleration Sensing

The accelerometer, manufactured by Analog Devices, Inc., is a convenient and versatile sensor. An electronic package about 10mm square, it can be easily integrated into the design of a printed circuit board. Only a few external components are necessary for its operation, and it consumes fairly little power. The two axes of acceleration measurement are in the plane of the device.

Acceleration measurement techniques respond to two different types of motion. Slow, tilting motions are sensed through measurement of the direction of the gravitational acceleration vector *g*. This has a fixed magnitude (9.81 m/s^2) and is directed towards the ground. Thus, if the device is stationary, components of this vector present in the x- or y- axes can be used to compute the angle of inclination. Alternately, if the device is held horizontal but is shaken laterally, acceleration will be detected in the x- and y- axes. As a result, either tilting or shaking the device can produce identical acceleration values.

Graphics

The graphics implemented for ShakePad were based upon those used in FishFace. One difference was the use of bicolor LED matrices; now the colors green and orange were available in addition to red. The use of external LED driver components also made the display much brighter than that of FishFace (which was driven directly from the PIC processor).

In designing graphics for such a system, some filtering must be performed in software to permit accurate control of the dynamic graphics. If shaking is expected to be the dominant mode of device operation, a "high-pass" filter can be used to reduce the effects of gravitational acceleration. Alternately, if accurate tilt measurement is paramount, a "low-pass" filter can be used to attenuate the high-frequency shaking signals. In practice, this technique made the graphics slower to respond, as several values were recorded in order to average the results.

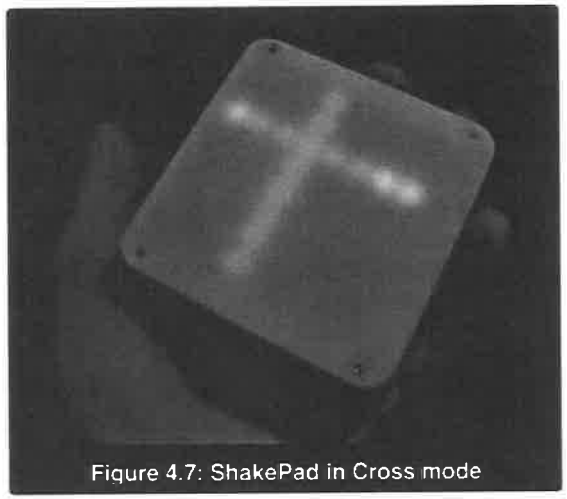


Figure 4.7: ShakePad in Cross mode

APPENDIX EE

Shenzhen Huiding Tech. Co., Ltd. - Exhibit 1006

The "snake" mode, which featured a collapsing trail of pixels, was implemented for ShakePad. The "head" of the snake, i.e. the most recently recorded pixel, was red, while the snake's "body" was green. Minimal filtering was performed, such that the snake was very responsive to both tilting and shaking. The inherent noise of the accelerometer was not damped, so the snake always appeared to jump between nearby pixels. The dynamism and color of this interaction made it very satisfying; the snake indeed seemed like an excited creature trapped within the white box.

For the "cross" mode, data was averaged over several readings to reduce the jittering of the previous mode. The display showed a horizontal red line and a vertical green

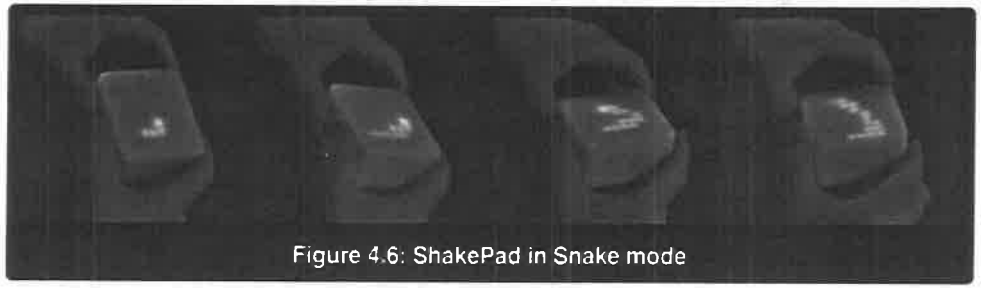


Figure 4.6: ShakePad in Snake mode

line; the position of each depended on the angle of tilt of the display.

4.4 Discussion

LED displays

LED matrices have far lower resolution than common computer displays like liquid-crystal displays (LCD's), and cathode-ray tubes (CRT's). Those displays can address over 5000 independent pixels in a square inch, while an LED matrix can manage only 16! Although RGB models are now becoming available, the majority of LED's can display only red, green, or a combination. LCD's, of course, can show a full spectrum of colors. In addition, LED matrices consume far more power than LCD's; this is the main reason they are rarely used in battery-operated equipment.

Nevertheless, LED's have characteristics that enable fundamentally different types of interaction than the ubiquitous computer displays. Unlike LCD's, which are reflective or transmissive, LED matrices are emissive. Their high contrast ratio permits viewing at a distance, through diffuse screens, and even through translucent objects.

APPENDIX EE

Shenzhen Huiding Tech. Co., Ltd. - Exhibit 1006

In addition, the viewing angle of LED matrices is essentially a full hemisphere, while LCD's decrease in brightness when viewed off-axis. The low resolution of LED's, while limiting graphical detail, permits a concurrent reduction in the data that must be sent to the display. An array of LED matrices can easily be driven by a small, inexpensive microprocessor, and a "graphics driver" can be written in a matter of hours. Finally, the displays can be tiled to cover a large physical area without a significant increase in cost; LCD displays cannot be scaled in this way.

The combination of low data rates, high brightness, wide viewing angle, and simplicity give LED's a decided advantage under many circumstances. Most significantly, LED matrices seem well suited for the display of simple information at a distance.

Coupling and responsiveness

User of FishFace and ShakePad experienced the sensation of directly manipulating the glowing pixels. One might expect this to be no more interesting than moving a computer mouse while watching the response of the cursor on-screen. Yet this simple visual feedback was striking—why?

One reason seems to be that the visual feedback was highly responsive—the delay between motion and response was approximately 100 milliseconds. Unless hand motion was very fast, this degree of latency was imperceptible. This made the interactions seem like a physical phenomenon, like a shadow beneath a moving object.

When the positions of graphical objects are continuously controlled by physical gestures, the latency in the control loop seems to affect the perceived nature of the interaction dramatically. (Of course, this is why personal computers have dedicated hardware for handling mouse input.) In both ShakePad and FishFace, the collocation of the display with the interaction space reinforced this illusion. Because the output was closely coupled to the physical input, the moving pixel seemed like a direct extension of the user's body.

Social uses of usage history

The FishFace and ShakePad prototypes are computational devices that can be operated as easily as physical objects can be manipulated. They can be engaged with instantly, and their responses are easily seen and comprehended. Of course, neither of these devices performs any of the functions of traditional computing devices. How might people use them? What roles might they serve in people's lives?

APPENDIX EE

Shenzhen Huiding Tech. Co., Ltd. - Exhibit 1006

The usage frequency of physical objects can have social and psychological implications. Heavy use may make objects seem more desirable, as popularity may suggest quality, or less so, as repeated use may imply degradation or contamination. Thus, heavily used books, video rentals, tools, or pool cues may be sought out, but heavily used public phones or toilet seats might be avoided. Visible indicators of usage frequency might charge common objects with a new dimension of valence or desirability. Today, the frequent use of communications gadgets confers status; cellular phones with prominent usage displays might become the fetish objects of the week. If every toy in the chest contained a ShakePad that displayed its popularity, what six year-old wouldn't try to grab the brightest one first?

Architecture could also be transformed by the integration of devices that make past contact visible. Imagine an office hallway lined with FishFace devices spaced every twenty feet. The "temperature" of each display could increase with the "body heat" of each passerby, creating a subtle indication of the level of activity in each part of the building. Over time, people would begin to react to this new artifact in their environment. Perhaps they would pause before the displays, swaying back and forth to actively increase their brightness. Or perhaps the ubiquity of these indicators would make less-traveled areas seem especially lifeless and desolate.

Invading people's personal spaces with these devices might have even stronger effects. Consider an airport, bus terminal, or subway car with FishFace devices installed in the benches. The patterns of light could take on the contours of people sitting upon them, only to "evaporate" over time after their users had risen. Would people feel uncomfortable about sitting upon the residual "heat" left by strangers, or would they do so willingly? Would they derive a sense of contact or community from sharing the seat with the shadow of another person, or would they avoid the glowing benches entirely?

Shenzhen Huiding Tech. Co., Ltd. - Exhibit 1006

5 Augmented Container Storage System

TouchCounters Prototype

5.1 Background

TouchCounters is an integrated system of electronic modules, physical storage containers, and shelving surfaces for the support of collaborative physical work.

TouchCounters evolved from the work environment in which FishFace and ShakePad were developed: the shared physical workspace of the Tangible Media Group. This 20x20 foot area is crammed with workbenches, storage boxes, computers, and raw materials. A revolving set of about a dozen people shares the space. Supplies and materials are stored in 80 to 100 identical plastic containers, labeled inconsistently by attributes such as type of contents, user's name, or project.

The pace of this environment is often rushed and chaotic. Under time pressure and without supervision, people often remove boxes from the shelves and replace them in different positions, thus making it difficult for people to locate specific boxes in a hurry. Reordering of supplies is often done on an emergency basis, and without any tracking of overall usage or efficiency.

Initial prototype

Portraying usage frequency seemed an appropriately robust solution for the inherent disorder of this environment. The bright displays of FishFace and ShakePad seemed well suited for use as indicators of box usage, status, and categorization. The original concept was simply to fit each box with a contact sensor, thus enabling its popularity to be seen. This led to the concept of a "touch counter," a "hit counter for physical objects."

In May 1998, a prototype "augmented container" was developed. A permanent magnet was installed in the lid of the box; a magnetic reed switch on the box could then count the number of opening and closing events. The box was powered by an onboard battery and stored its usage records internally. However, this direction was rejected in favor of a system in which the shelving structure became the substrate for interaction with the system. The shelves would be fitted with multiple "docks" that



Figure 5.1: Storage containers in shared workspace of Tangible Media Group



Figure 5.2: Attaching electronic label to storage container

Shenzhen Huiding Tech. Co., Ltd. - Exhibit 1006

APPENDIX EE

would provide both power and network connections to the boxes. This would eliminate the need for power supplies on the boxes themselves. During the summer of 1998, this system was implemented.

5.2 Implementation

Labels and containers

The TouchCounters modules were designed to contain the LED matrix, about 2.5x2.5 inches. Each was equipped with a magnet sensor, an accelerometers, and a identification chip etched with a unique 48-bit ID. The electrically erasable microprocessor, the PIC16F84, allowed rapid uploading of new code through a programming connector. Infrared transmitter and receiver modules allowed wireless communication through standard TV remote protocols.

Data was exchanged with the server through a series of connectors on the modules, storage containers, and shelves. Conductive, magnetic snaps were used to link the label modules to the containers. These connectors, sold in the garment industry as snaps for leather purses, carried both power and data signals. The labels could be easily attached and detached with one hand, and tactile and audible "clicks" indicated engagement of the magnets. It was imagined that these labels might serve as generic, reusable usage indicators, perhaps connecting to telephones or to furniture, but those uses have not yet been attempted.

The receptacles on the shelves were wired to a common bus connected to a central server. Standard telephone connectors were used to permit easy expansion. As identical snaps were installed on the containers and the shelves, the act of placing a container upon the shelf activated communication with its label.

Web Server

Originally, the web server was a standard desktop computer running Java™ code. Serial I/O classes enabled the server to read data from the machine's serial port. To allow remote users to dynamically alter the code executed on this machine, Java's remote method invocation (RMI) routines were employed. All data was exchanged as ASCII text to facilitate debugging.

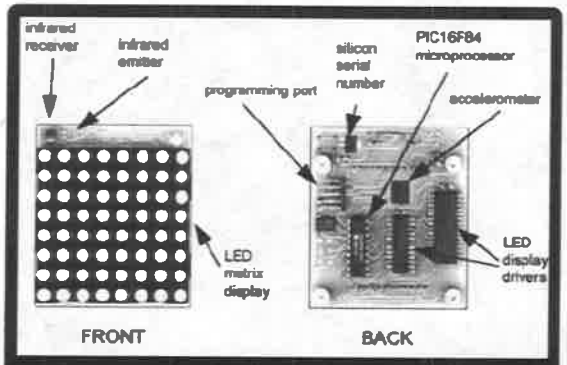
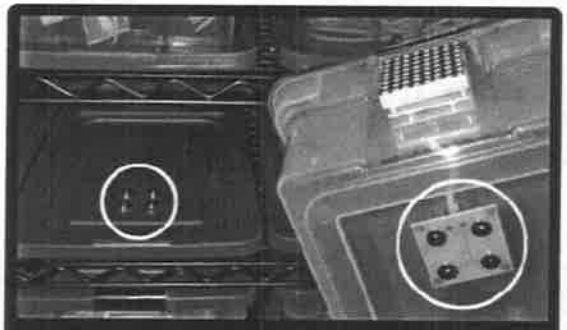


Figure 5.3: Components of label modules


Figure 5.4: Magnetic snap connectors, circled, on containers and shelves

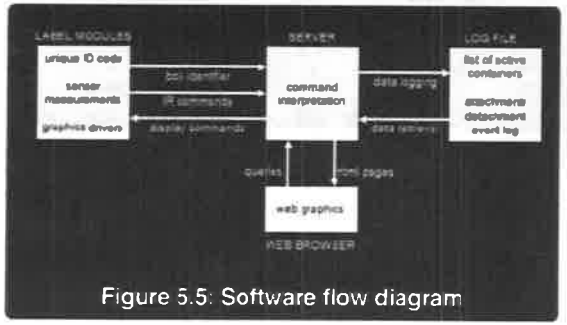


Figure 5.5: Software flow diagram

Shenzhen Huiding Tech. Co., Ltd. - Exhibit 1006

Later, however, a tiny embedded web server replaced the desktop machine. Its physical compactness suggested the potential for an entirely new type of furniture, designed from the start with integrated sensing and connectivity. This influenced the design of SensePad, discussed in the following section.

In this system, the labels served only as tags and displays, retaining no memory locally; all processing was performed by the server. Descriptions of the containers' contents were manually encoded. Usage correlation was measured both through count information relayed from the labels, and by measuring the time that a box unit was offline and therefore removed from the shelf. Each access event was stored in a continually updated matrix of variables. Likewise, frequency-of-use information was logged in a file available online. A Java applet displayed box status to remote users, and also allowed data to be sent to the labels.

5.3 Interaction techniques

The labels, containers, shelving, and server together supported varying degrees of user involvement in use of the system. These are presented in order of increasing degree of active engagement.

Visualization of usage frequency

The default state of the system is the display of box usage frequency. The label on each box shows a dot pattern that indicates its recent frequency of use; each pixel represents a single use of the container within "short-tem memory," usually a few days. When the entire set of containers is viewed from across a room, the aggregated displays comprise a spatial map of usage frequency.

This provides several types of functionality. As a small fraction of the containers are subject to much heavier use than the average; these "hot spots" can be used as starting points when searching for a commonly used item. In addition, the relative counts can be used to facilitate the manual task of optimizing box placement. For example, the most active ones can be placed at hand- or eye-level. The use indicators also provide an indirect indication of the presence of specific users, as many boxes are associated with individuals. In theory, records of use could be used to prompt replacement of the contents as well.

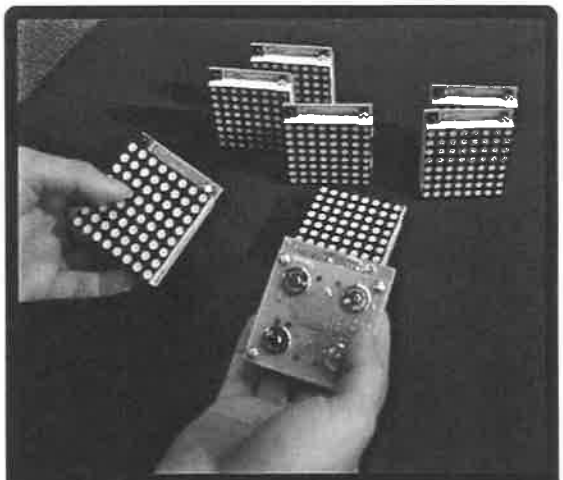


Figure 5.6: TouchCounters label modules



Figure 5.7: Usage frequency distribution of multiple containers

Shenzhen Huiding Tech. Co., Ltd. - Exhibit 1006

APPENDIX EE

Visualization of usage correlation

A second mode of operation is the display of usage correlation. Through analysis of the record of box accesses, the system generates a matrix of values that represent the correlation of use between boxes—how many times they have been removed within one minute of each other.

While usage frequency is displayed persistently, this correlation display appears only for the few seconds following the removal of a box from the shelf. (After this time the labels return to the frequency display mode.) To distinguish this mode from the usage frequency display mode, both color and graphical patterns were changed. The normally green graphics changed to red, and the pattern changed from a "solid fill" to a pseudo-random pattern of pixels.

As two or more containers were often used in combination, the correlation display facilitates the rapid location of several related items on the shelf. In this way, the search for a related item can be accelerated by looking at the brightest displays in the area. This data can also be used to improve container placement, as strongly related boxes can be positioned near each other.



Figure 5.8: Correlation of usage to container just removed

Direct annotation

In addition to displaying automatically recorded data, the system allowed users to explicitly annotate the boxes. By pointing an infrared remote control at the boxes, users could attach symbols or "glyphs" that indicated common associations between several containers. Holding a button on the remote transmitted repeated bursts of data, so multiple boxes could be rapidly labeled by "dragging" the controller across physical space.

The categorization labels were imagined to be arbitrary attributes ascribed by the user, as are the colored "labels" in the Macintosh™ OS. For example, users could indicate associations of boxes with specific users or specific steps in a project. Alternately, a group of users could agree upon certain symbols as indications of the state of completion of various prototypes.

Potentially, users might use other infrared-enabled devices to interact with the labels. Users with personal digital assistants could attach electronic "notes" indicating that an item had been borrowed. Alternatively, users could wear infrared-emitting name tags (Resnick98) to recall personal settings for the system



Figure 5.9: Labeling individual containers with infrared remote control

Shenzhen Huiding Tech. Co., Ltd. - Exhibit 1006

APPENDIX EE

Online status display

Finally, users could view the state of the entire system remotely by opening a web page with an embedded Java applet. As a demonstration of the bi-directional interaction, users could also click on these web-based images; this triggered changes to the physical displays.

This was a trivial example of how a conventional graphical interface might be used in conjunction with the distributed displays of the TouchCounters system. The GUI can more easily support complex, textual queries, while the physical visualizations would support the frequent and rapid "lightweight" interactions. The GUI's separation from the physical objects is tolerable or even advantageous in some circumstances; a remote supplier of parts or an inventory manager might access the system to analyze patterns of consumption.

However, the most interesting opportunities seem to arise when fundamentally digital operations can be performed on physical objects. If objects were labeled with metadata describing their contents, users, times of use, and so on, they might be digitally indexed, searched, and located *in situ*. This is a new type of functionality that centralized graphical interfaces simply cannot provide.

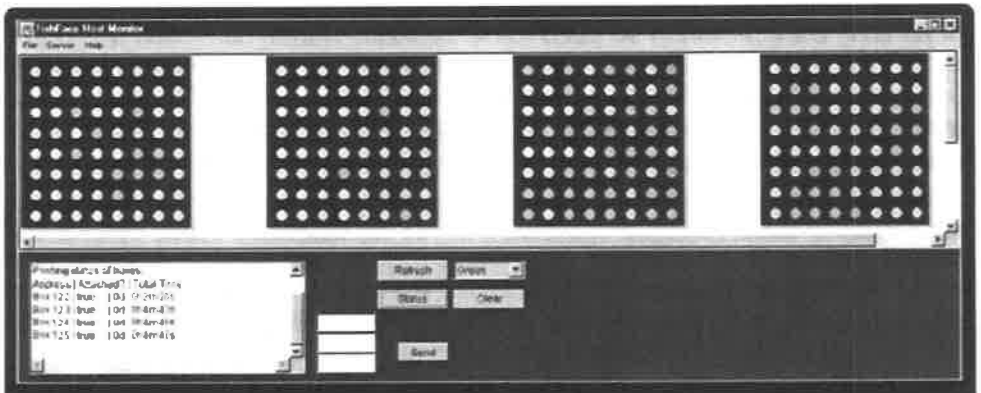


Figure 5.11: Applet indicating status of physical containers on web page



Figure 5.10: "Dragging" remote control across containers to label multiple objects

APPENDIX EE

Shenzhen Huiding Tech. Co., Ltd. - Exhibit 1006

5.4 Discussion

User feedback

Some qualitative feedback about the system was obtained from members of the group. While no substitute for formal testing, this did provide some guidance for design. Sixteen containers were fitted with the labels and networking hardware; the remainder were left unchanged.

Generally, users responded positively to the display graphics, and expressed interest in the complete implementation of the system. In particular, users liked the visual feedback that accompanied labeling with the remote control. Some users asked how messages could be left on the containers themselves; for example, a note that an item had been borrowed from a box. Others asked whether the users of each box could be identified, such that personalized settings or histories could be retrieved.

Interaction at range

The TouchCounters displays were bright enough to be seen from across a room. Three types of viewing could be distinguished, which correlate approximately to three scales of distance between user and display. From 10-20 feet away, the glowing of the displays simply indicated that the system was present and operational. At a range of 5-10 feet, patterns on the multiple displays could be compared. Within three feet of the boxes, the printed container labels could be examined, each pixel on the display could be seen, and the box could be accessed physically.

These levels of scale had implications for the design of the display graphics. The visibility of the displays made it important to prevent them from becoming distracting. In particular, animated graphics were not used as they attracted attention from all points in the room. This made the switch from usage frequency mode to usage correlation mode very noticeable.



Figure 5.12: Viewing TouchCounters at long-, medium- and close-range

wire	solder	scissors	velcro
serial cables	ethernet	serial adapters	foam
fabric	magnets	abrasives	adhesives
paint	markers	tape	monitor cables

Table 5.1: Materials tracked while testing TouchCounters

Shenzhen Huiding Tech. Co., Ltd. - Exhibit 1006

Different representations of quantity were used in the usage frequency and correlation modes. Both represented only a single value that represented accumulated use, but they suggested different meanings. The "scatter pattern" was intended to appear random, but many interpreted the pattern as a two-dimensional encoding of information. Others complained that the "fill" pattern should fill from the bottom, as a liquid fills a glass. More sophisticated indications of usage history could be represented on the matrix displays, such as a histogram that indicated the temporal distribution of usage events. (See the Network Meter in Appendix A.)

Because all of the individual displays showed the same type of data, they acted in concert as a single, room-filling "meta-display." As persistent fixtures of the environment, the usage indicators might fade into the "background" of one's awareness, noticed only if sudden changes occurred (Ishii97).

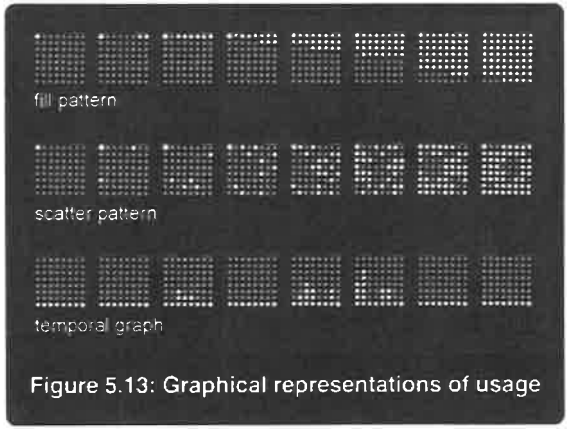


Figure 5.13: Graphical representations of usage

Conceptual models and new technologies

The expectations of any new technology are strongly influenced by prior experience with other technologies. When faced with new developments, analogies to familiar precedents are employed to exploit existing conceptual models. New devices are understood in terms of parallels to older or simpler devices. Thus, designers of radically new interfaces must reflect upon which assumptions engendered by conceptual association must be preserved, and which can be discarded.

Imagine the task of explaining the modern personal computer to a person who missed the last 50 years. One might make reference to a variety of somewhat older technologies:

- television, as a source of dynamic representational images viewed on a screen
- telephones, as a means for synchronous interpersonal communication that transcends distance
- light bulbs, as a consumer of energy and a source of light and heat
- automobiles, as complex machines requiring skill to operate, as means of personal empowerment
- books, as repositories of information
- record players, an automated mechanism for streaming media playback
- human beings, as information input and output systems that make use of language, memory and cognition

Shenzhen Huiding Tech. Co., Ltd. - Exhibit 1006

To extend the use of TouchCounters to uses beyond storage management, one might attempt to characterize them through analogy to other physical devices. In one sense, TouchCounters can be considered tags or labels, as they are unique identifiers that attach directly to their physical referents (although this operation was not used as part of the interface). They are augmentations to existing objects rather than tools in themselves. However, while a single module indicates the use of an individual object, collectively they portray the activity level of an environment. Also, they are a mechanism for sharing group knowledge in a public space. In these senses, they seem like signs. But unlike traditional signs, TouchCounters show dynamic information. This suggests that that they are indicators, embedded displays of dynamic variables often viewed in parallel.

The point is that when physical devices are augmented by computational mechanisms—memory, communications, procedural behavior—the scope of potentially available uses and functions suddenly explodes. Thus, designs for lightweight interactions must weigh each additional level of functionality against its additional disruption of existing conceptual models. Often the challenge concerns not sophistication but simplicity; the difficulty lies in identifying the few features that can be both useful and easily understood.

	SIMILARITIES	DIFFERENCES
Labels	Describe specific physical objects	Mainly static; edited manually
Signs	Describe physical environments; can be viewed at a distance	Static; not associated with physical objects
Indicators	Show dynamic information, can view several concurrently	Not associated with physical objects, fixed mapping

Table 5.2: Comparison of TouchCounters to other types of physical indicators

APPENDIX EE

Shenzhen Huiding Tech. Co., Ltd. - Exhibit 1006

6 Object Identification and Tracking Surfaces

SensePad and IDPad Prototypes

6.1 Introduction

While the TouchCounters system was based on an existing system of physical storage, its physical design was a hodge-podge of appendages and modifications to existing equipment. Labels, connectors, and docks clung like barnacles to the shelves and plastic containers, while computers huddled nearby, tethered by many umbilical cables. This was appropriate for the demonstrating the various interaction concepts, but for the deployment of usage history displays on a broader scale.

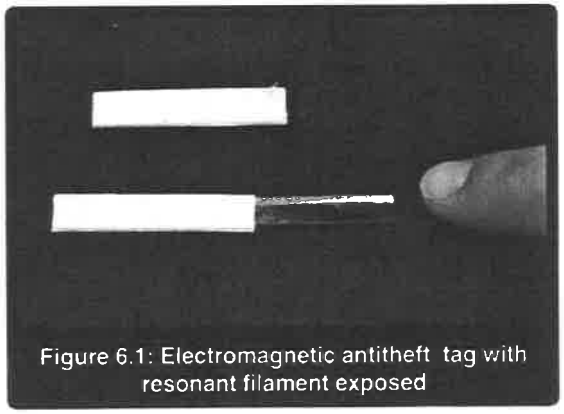


Figure 6.1: Electromagnetic antitheft tag with resonant filament exposed

The SensePad and IDPad projects were attempts to integrate sensing and display technologies into the design of new types of furniture, such that they could be incorporated into various environments with minimal disruption. This goal had several components: (1) to make the sensing technologies more reliable and robust, (2) to reduce the size and the cost of the labels used to identify the objects, and (3) to develop modular physical platforms that could be integrated into tables, desks, shelves, and other furniture upon which objects often reside.

Tagging Technologies

Broadly defined, a tag is a device designed to facilitate the automated identification of a physical object. The majority of tags are inexpensive "labels" that are affixed to various objects, and which are then identified by "readers." A wide variety of tagging devices exist, but in this section we concern ourselves only with wireless identification tags—those that can be identified without direct contact through interrogation with electromagnetic signals.

Two of the most popular tag technologies are printed optical tags, such as bar codes, and radio-frequency identification (RFID) tags. Optical tags require a direct line of sight between an optical sensor or imaging device and the surface of the tag. While optical tags can be made very inexpensively, they pose difficulties stemming from occlusion, surface contamination, and registration. The most common RFID tags are batteryless electronic chips that contain a simple identification number. These tags can be "read" by exposing them to an oscillating electromagnetic field. While draw-

Shenzhen Huiding Tech. Co., Ltd. - Exhibit 1006

APPENDIX EE

ing power from this field, these tags then transmit an identification number by modulating the field. While these tags are compact, convenient, and offer both read and write capabilities, their high cost has prevented them from replacing optical tags. (Typically, RFID tags cost from $0.50 to $10.)

Another common type of identification tag is the electromagnetic anti-theft tag, of the type manufactured by Sensormatic and Checkpoint. These tags allow stolen goods to be detected upon their removal from a store's premises. While these tags are very inexpensive ($0.01), they have essentially no memory capacity and thus cannot be used to distinguish amongst multiple items.

"Materials Tags"

Rich Fletcher, a doctoral candidate in the Physics and Media Group, was developing ultra-low-cost wireless tagging technologies. Rather than storing information on semiconductor memories, these tags would store unique patterns in soft magnetic materials; thus they were called "materials tags" (Fletcher96). The spectral response of these tags would be modulated by the magnetic materials. If realized, materials tags could dramatically expand the application of tagging technologies; for example, every item in a supermarket could bear a unique tag. Clearly, a variety of new interface needs would be created.

As a short-term substitute for the eventually forthcoming materials tags, EAS (electronic article surveillance) tags manufactured by Sensormatic could be detected by tuning the device to 58kHz. The frequency of these tags could be increased up to 70kHz by opening their plastic packages, removing the metal strips inside, approximately trimming their lengths with clippers, reinserting them into their plastic shells, and then graphing their frequency response using a PC-based application. A limitation of this approach was that the tags did not exhibit a single resonant frequency but instead "double peaks" a few kHz apart. This limited the number of tags differentiable in the 58-70kHz range to perhaps 20.

Tag Reader

The primary product of Rich's efforts was a swept-frequency tag reader optimized for materials characterization. Through measurement of the frequency and strength of the reflected signal, the reader could determine the tags' proximity to the antenna, as well as their identities. Unlike commercial tag readers, this device could be tuned to detect tags at frequencies from 0 to 300 kHz. In addition it was capable of reading

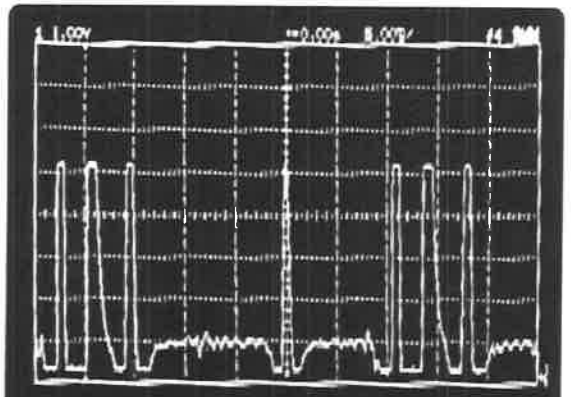


Figure 6.2: Frequency response of several LC tags; distinct "peaks" are visible

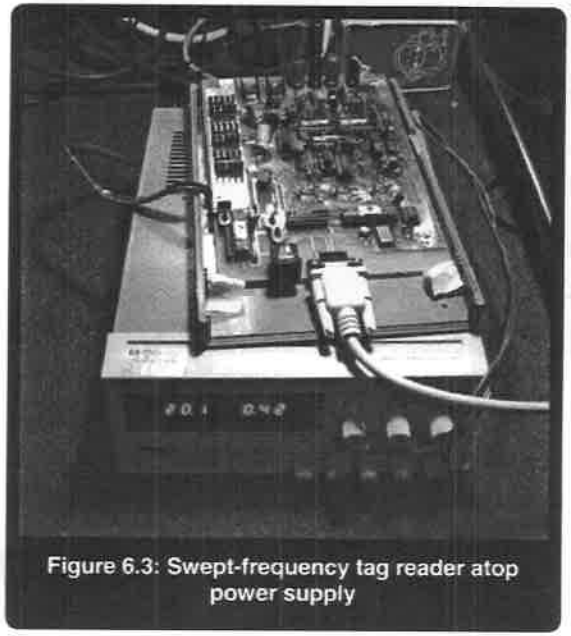


Figure 6.3: Swept-frequency tag reader atop power supply

Shenzhen Huiding Tech. Co., Ltd. - Exhibit 1006

both magnitude and phase of the detected signals, a requirement for reading materials tags. The tag reader's physical form was a 6x8" circuit board in a blue plastic enclosure. It was usually connected to a 20" diameter loop of coiled wire in a plane perpendicular to the tags. The same coil would be used to alternately "excite" any tags in its proximity and to detect the oscillations of any tags present.

6.2 SensePad

SensePad was intended to be a device that displayed graphical patterns directly beneath objects placed onto its surface. The system was designed to both recognize and track the positions of objects bearing wireless identification tags. Unfortunately, despite a prolonged development period of over 18 months, its intended features were never completely realized. The IDPad project, which arose somewhat serendipitously, later achieved some of the goals of SensePad.

SensePad Concept

From the spring of 1998, the author collaborated with Rich Fletcher to develop a visual interface to Rich's tag reader. The interface was envisioned as an "interactive surface" that would react to small, tagged objects placed upon it. After some discussion, it was agreed that the device would be an oblong platform with LED's upon its top face; it would reside on a tabletop and would exchange information with a desktop computer. The graphical display would indicate (1) the position of each object along the length of the strip, (2) the proximity of each object to the surface of the strip, and (3) a symbol that distinguished each object from the others.

A real-world application had emerged in parallel with the development of the SensePad concept. "Medication non-compliance," estimated to cost $1 billion per year, has been addressed by a wide variety of technologies—electronic bottle caps, voicemail messages, pill box alarms, pill removal sensors, etc. (Cramer91) These systems provided either the function of reminding patients to take their medication, or a means to record whether medication had actually been taken. Becton-Dickinson, a Media Laboratory sponsor, expressed interest in a device that could record the usage of medications in the home.

As a visual interface to information about tagged objects, an interactive surface like SensePad seemed well suited to serving this function. As a reminding device, SensePad could illuminate icons beneath medicine bottles upon its surface to indicate

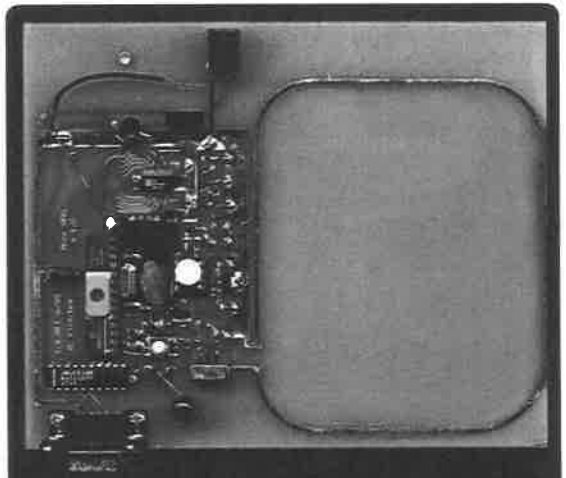


Figure 6.4: "Mini" tag reader, developed later; antenna coil requires only one loop

APPENDIX EE

Shenzhen Huiding Tech. Co., Ltd. - Exhibit 1006

which ones were due for consumption. As a recorder, SensePad could detect when each bottle was removed (and its contents, presumably, consumed). Furthermore, SensePad could be sized to fit into a user's home medicine cabinet.

Additional functionality specific to medication monitoring could be added as well. Information about a patient's medication regimen could be downloaded from a remote database or perhaps stored in the medicine bottles themselves. Potentially, the system could also indicate warnings if a contra-indicated medications were taken together.

First Prototype

The development of SensePad was a protracted and somewhat inconclusive effort. This process is documented here for readers interested in the underlying technology; others can skip to the next section.

In keeping with the above concept, the initial prototype was a 2.5"x12" pad with a monochrome red 8x32 pixel display (comprised of 4 LED matrices). As with FishFace, the graphics would be coarse but bright and responsive. The detection of tag position would be achieved by measuring signal values at each of 4 coils along the length of the strip.

The device would connect to Rich's tag reader through an external cable. Because Rich's device was designed to use only a single RF coil, a switching circuit on the new device would be necessary to allow communication with multiple coils. In this prototype, switching between coils would be performed by a series of electromechanical relays controlled by a microprocessor on the device. In addition, a separate microprocessor (the Microchip PIC16C73A used in FishFace) would be used to generate graphics on each of the LED matrices. An additional processor of the same type would be configured as a "master" that would control the four "slaves." Finally, a small beeper would provide auditory feedback.

The circuit board for the first prototype was designed in mid-April 1998; components were installed and test software written over the next few weeks. Unfortunately, a number of problems made the board virtually unusable. To illustrate the technical difficulties that characterize this type of work, these will be described in some detail.

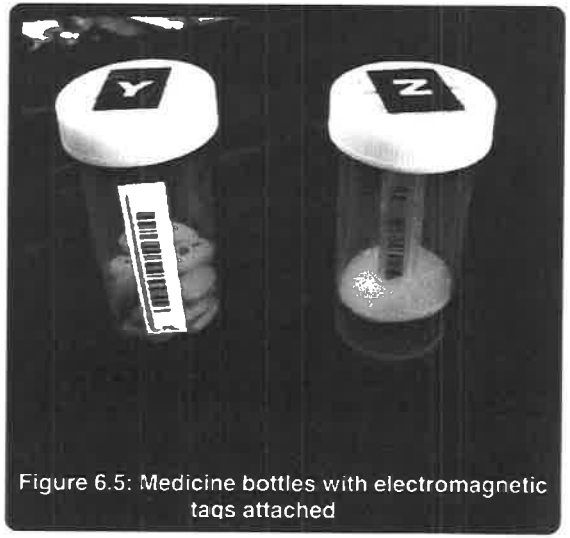


Figure 6.5: Medicine bottles with electromagnetic tags attached

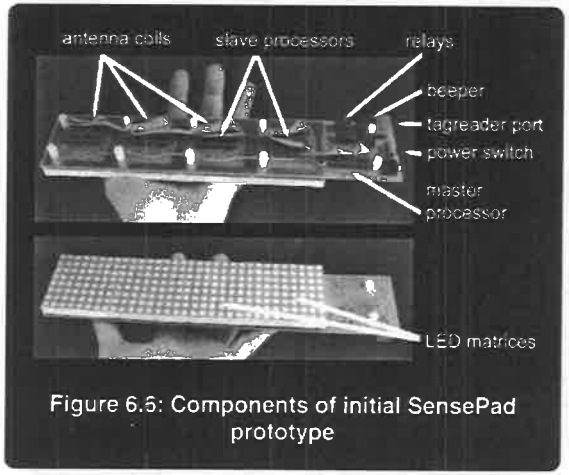


Figure 6.5: Components of initial SensePad prototype

APPENDIX EE

Shenzhen Huiding Tech. Co., Ltd. - Exhibit 1006

The first problem was that the tag reader could not successfully interrogate the tags. The coils, both smaller and with fewer turns than the original coil, could not excite tags placed near their edges. Thus, unless tags were placed in the center of each square, they could not be detected at all. In addition, the proximity of the analog antenna traces to the digital data and graphics traces caused noise on the tag signals.

Electromagnetic interference was another problem. Rapid switching of the relays caused inductive interference that frequently reset the microprocessors. No mechanism was available for resetting an individual processor; the entire board had to be shut down if the code on one failed. The switching also created a loud, unsettling clicking noise.

Another set of problems concerned the multi-processor architecture. Revising the graphics required the tedious removal, erasure, programming, and replacement of five microprocessors. As the slaves handled communications in software (rather than by hardware UART), command reception could not occur in parallel with the display of graphics; this made the display flicker visibly.

Difficulties also plagued the exchange of data between the master, the slaves, and the processors on the external tag reader board. These commands were series of ASCII characters sent via the RS-232 serial protocol. As the tag reader's software had been successfully written and debugged earlier, it was taken to be immutable. However, that software was optimized for materials characterization, rather than instantaneous response. Several command variables had to be sent to the reader between coil-switching operations; this slowed its operation.

Other problems included the brightness of the display, as dim as that of the original FishFace, and various difficulties in assembly of the board. Clearly, a major redesign was in order.

Second Prototype

A number of improvements were made for the next version. The first addressed the problem of read range. Fortunately, the tag reader had separate terminal connections for coil excitation and detection—these functions could be performed by separate coils if they were close to each other. On the revised board, a single, large transmit coil was created that would surround the four original coils. Its field would thus ex-

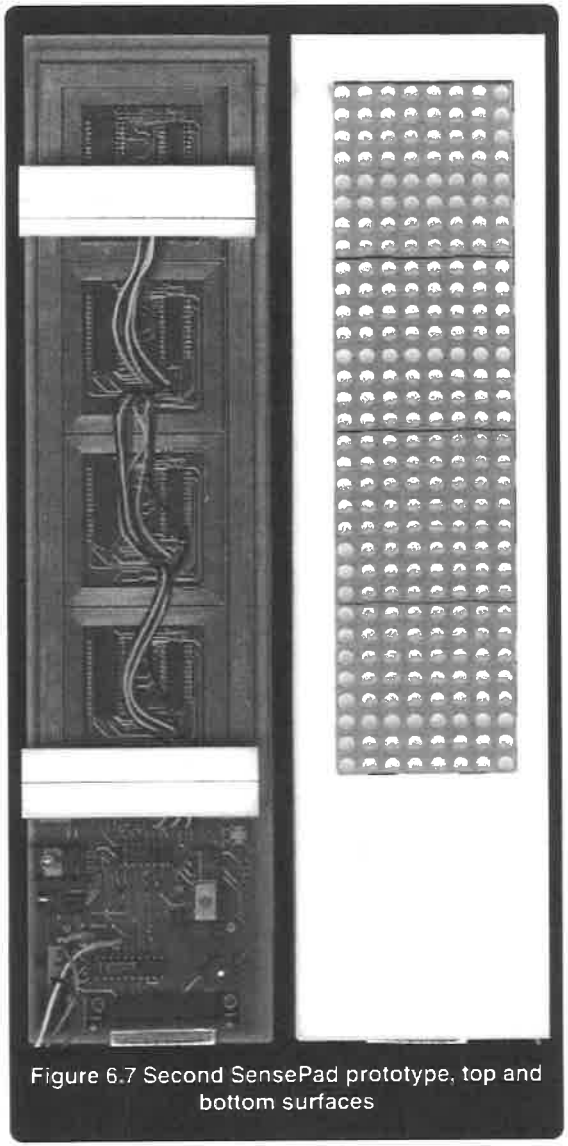


Figure 6.7 Second SensePad prototype, top and bottom surfaces

APPENDIX EE

Shenzhen Huiding Tech. Co., Ltd. - Exhibit 1006

cite all tags on the SensePad surface, while the original coils could then be used for detection.

Separation of the transmit and receive coils offered another advantage. While current through the transmit coil had to be high, the current induced in the receive coils was low. As the transmit signals no longer were switched, the relays could be replaced by an analog multiplexer chip with a relatively high impedance. This device would switch the received signals electronically, thus eliminating the electrical and acoustic noise caused by the relay inductors.

To reduce the complexity, cost, and instability of the five-processor configuration, each slave was replaced by a pair of LED driver chips. These devices could be chained sequentially, thus allowing a single processor to control the entire array. The drivers were capable of sourcing a high, constant level of current; this would allow the displays to be uniformly bright. They also supported more output lines than did the PIC microprocessors. This allowed 24-pin, bicolor LED matrices to replace the original monochrome displays. Each pixel could appear green, red, or a yellow-orange combination of the two.

In addition, the "brains" of the device were now split across two circuit boards. Communication with the tag reader board would be handled by a microprocessor mounted directly on that board; the chip on SensePad itself would handle only graphics and coil switching. This change required manufacturing a new tag reader board as well as a new SensePad. The new circuit board designs were dispatched for manufacture in mid-July, but returned with some errors; a corrected version was first assembled in August.

The device could now measure the response of electromagnetic tags placed upon each of the four coils. The reflected signal was strongest when tags were placed at the center of each coil, and diminished as they moved towards the edges. Thus, the position of a tag could be approximately computed by weighting the signal strength of a tag at each coil by a number representing that coil's position. The proximity of the tag could be computed by simply summing the strength values at each coil. This technique had the limitation that position could not be accurately determined if the tag was placed at the extreme ends of the pad, past the centers of the first and last coils. This meant that only three-fourths of the display area could not be used for sensing. Nevertheless, the simple weighting scheme allowed reasonably accurate position tracking.

Shenzhen Huiding Tech. Co., Ltd. - Exhibit 1006

At last, the board's sensing hardware was sufficiently operational to allow experimentation with the graphical output. The control processor could now compute the identity, position, and proximity of each tag. For demonstration purposes, it was decided that a graphical patterns for to three to five tagged objects would be sufficient to indicate the device's functionality. It seemed natural to employ a graphical symbol or "sprite" that would follow the position of the tagged object, as a shadow follows a physical object. The sprite for each tag could then have a different shape. To indicate proximity, the shape would "grow" as the tag approached the SensePad surface.

The shapes had to be visually distinct, and had to be larger than the footprint of a medicine bottle but no larger than the width of the display. Since orientation information was not measured, only radially symmetric patterns would be used. (This also allowed a reduction in memory space consumed by each graphic.) A rounded, "disc" shape, a square, and an expanding spiral shape were the first shapes chosen. For each type, eight variations were generated in sizes ranging from 4x4 to 8x8 pixels. In summary, the following mappings were used to indicate the object's parameters:

- object's identity: shape and color of symbol
- object's location: position of symbol
- object's proximity: size of symbol

At the inception of this project, the graphics were imagined as shadows that would closely follow the motion of the tagged objects. Of course, such an effect would depend upon the rapid tracking of object motion. Unfortunately, as the tag reader took 2-3 seconds to measure the position of each tag; the graphics lagged the objects' motion very noticeably. For demonstration purposes, it was necessary to move the objects very slowly to create the illusion of coupling. It was clear that improving the speed of the tag reader was essential.

This system was demonstrated to various sponsors at the Things That Think Consortium meeting in September 1998. During the following week, a meeting was held with several executives from Becton-Dickinson Corporation. They felt that the device was too small to accommodate the medication collections of some patients, and suggested that, to be effective as a medication monitor, the device be redesigned to hold at least 20 bottles simultaneously.

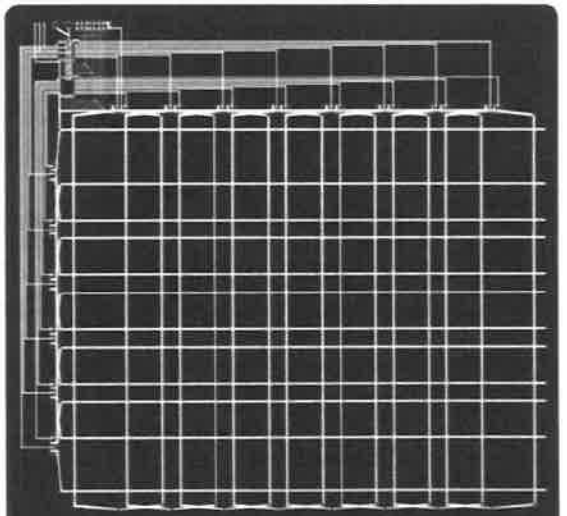


Figure 6.8: Antenna coil for third prototype



Figure 6.9: Second SensePad prototype tracking two medicine bottles

APPENDIX EE

Shenzhen Huiding Tech. Co., Ltd. - Exhibit 1006

Third Prototype

Many changes were made in the next version. First, the display surface was expanded from four to twelve tiles, arranged in a 3x4 pattern. This size could accommodate 20 medicine bottles comfortably. The display area was now approximately equal to the printable area of a 8½x11" sheet of paper; future applications were envisioned involving printed templates backlit by the display. Because many more pixels would have to be updated per second, a faster processor was needed to drive the display. The Hitachi SH-2, a 32-bit processor, was chosen for its high speed, low cost, and convenient development tools.

Meanwhile, in parallel with the development of this prototype, Rich had constructed a smaller, faster, and less expensive tag reader. This so-called "mini" tag reader was a much simpler, faster, and lower-power circuit for use with high-frequency "LC" tags in the 5-15 MHz frequency range. Because of the higher frequency, this reader required only a single loop of wire for excitation and detection; this allowed the entire device, including antenna, to be constructed on a single 4x6" PCB.

The simple antenna format enabled the layout of a two-dimensional tracking array. A new PCB was designed with 6 horizontal and 8 vertical loops. By testing each of these overlapping coils in sequence, the 2D position of a tagged object could be determined. Two multiplexers were used to switch the high and low sides of the signal.

This tracking array was designed to fit on top of, rather than beneath, the display surface. Although it could not transparent, it was designed such that a large rectangular window could be cut from the center of the PCB to allow the display to show through. The missing traces would be replaced by thin wires stretched taut across the window in both horizontal and vertical orientations. The display would then be covered with a diffuse screen to conceal the wires beneath.

The LC tags, which consist of an inductor and a capacitor in series, could be designed in various form factors to specific frequency values. The inductor for this type of tag could be made from a spiral trace on a printed circuit board or from wire finely wound into a loop, while the capacitor was a standard electronic component. The LC tags had sharper and more stable frequency "peaks" than the electromagnetic tags. This meant that more unique tags could occupy a given frequency range.

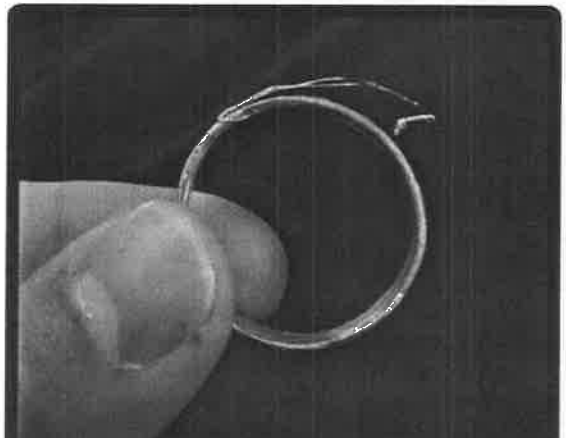


Figure 6.10: "LC" tag made from coiled wire and capacitor

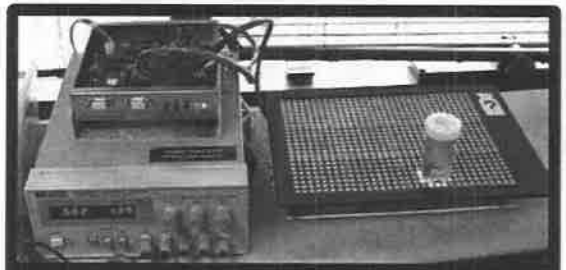


Figure 6.11: Expanded display for third prototype; power supply and control board also

Shenzhen Huiding Tech. Co., Ltd. - Exhibit 1006

The new display circuit was bright and flicker-free. The SH-2 also provided a much more professional development environment. The sensing circuit, however, had some problems. The multiplexers' ON-state resistance seemed to interfere with the reading of the signal. In addition, the mini tag reader lacked sufficient transmit power to drive these coils; it would have to be redesigned with a high-power output stage.

Conclusion

While these problems were not intractable, due to timing complications, they were never completely resolved. The author hopes that another party may be able to complete the design in the near future. Nevertheless, a functional wireless tag tracking system was eventually constructed—the "IDPad" system described in the following section.

6.3 IDPad

The IDPad is an alternative tag-tracking interface device that was originally built as an test platform for a revised version of TouchCounters. After its construction, however, it seemed useful as a platform for direct manipulation of objects rather than usage history tracking. Nevertheless, the technologies and design issues are discussed for their relevance to the broader work.

IDPad Concept

IDPad was an outgrowth of the TouchCounters project, rather than of SensePad. The design of the TouchCounters system had required different components on the label modules, containers, and docks. Many of the connection points were unreliable, which made continued operation of the system very difficult. A second-generation system was conceived in which the displays and sensors would be embedded in the shelves, while the boxes would simply bear RFID tags. No electrical connections would be engaged or disengaged during operation, thus improving reliability.

Each shelf in the storage rack would be augmented with the following components:

- A commercial RFID tag reader board
- Four large antenna coils mounted along each shelf's surface
- An RFID reader controller board to link the tag reader with each of the four antennae
- Four 4x8 LED matrix displays mounted along the front edges of the shelf
- A driver board for controlling the LED matrices

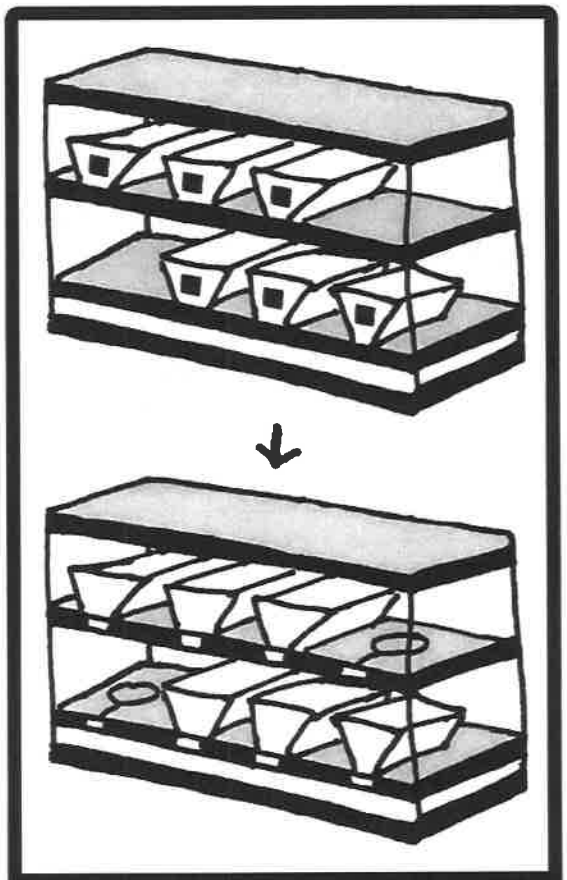


Figure 6.12: Concept for revised TouchCounters system: displays integrated into shelving

Shenzhen Huiding Tech. Co., Ltd. - Exhibit 1006

As soon as a box was placed upon the shelf, the RFID controller would identify the tag attached to its underside, and would then send this information to a central server over a serial bus. The server would then generate a graphic pertaining to that particular object and send it to the display controller on that shelf. The display beneath the newly inserted box would then illuminate with the graphic. These operations were intended to occur "instantly" (within 200-300 milliseconds).

RFID Technology

While the LC and electromagnetic tags used in SensePad prototypes are simple, single-frequency resonators, RFID tags are complete semiconductor devices with onboard memory and logic. RFID tags draw power from radio waves oscillating at a given frequency. Communication between tag reader and tag is based on modulation of this field; any arbitrary sequence of bits can be sent in this fashion. Thus, RFID tags can have far more sophisticated functionality than the simple antenna-like materials tags. Far more objects can be uniquely identified, as they have rewriteable memory of 256 bits or more.

RFID is an inherently digital, while resonant tag sensing is analog. The signals of resonant tags fall off slowly as they move farther from a sensing coil, while RFID signals simply stop at a certain threshold. An important implication is that the position of RFID tags cannot be tracked continuously, but only at the discrete locations of multiple coils. This constraint was fully acceptable for the TouchCounters application, as placing the four containers at discrete positions was not inconvenient.

Implementation

Around March 1999, the RFID reader was obtained, and the RFID controller and display boards were designed. In order to test these components prior to their installation, an enclosure was fabricated using a laser cutter. This enclosure was a long, narrow pad sized to contain the four antenna coils and four displays.

The author was determined to avoid the technical failures of the SensePad project, especially those involving tag reading technology. Thus the tag and reader devices were chosen from proven, commercially available components.

Tag reader. Despite the relative ubiquity of RFID technology, it was difficult to locate a tag reader vendor that sold unit quantities at reasonable prices. Eventually, a small design company was located in the UK; it had developed a PIC-based tag

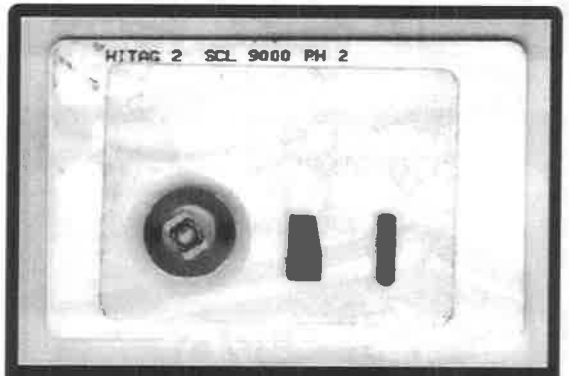


Figure 6.13: Card-, coin-, wedge-, and pill-sized RFID tags

Shenzhen Huiding Tech. Co., Ltd. - Exhibit 1006

reader that could read and write Philips tags in the 125kHz range. The device was conveniently postage-stamp sized, and could be controlled by TTL-level RS-232 signals. The company, IB Technology, provided invaluable technical support over the telephone.

Tags. Tags were also surprisingly difficult to obtain. Strangely, it was impossible to obtain tags from Philips, the manufacturer. Dozens of calls, faxes, and emails eventually unearthed a few vendors with short lead times and small quantities. Several tags were obtained in several form factors. One was an opaque, white, and the size of a credit card; another was thin, flat, and nickel-sized; yet another was a tiny, pill-shaped glass capsule intended for animal injection. The type primarily used, however, was a black plastic wedge 12x6x3mm in size.

A significant limitation of the tag protocol was the inability to communicate with multiple tags concurrently—a feature known as "anti-collision technology." If any two tags were within range of a single coil, all reading or writing was disabled. Thus, the four-coil surface could identify at most one tag per coil.

Antenna coils. After brief experiments with hand-wound coils of enameled wire, the antenna coils were designed on a PCB layout program. The first iteration proved unusable due to an accidental 200% scaling error made during use of the software. The corrected coils fit on 6" square segments of circuit board. An outside vendor manufactured the coils on printed circuit boards; no further treatment was necessary.

RFID controller board. This board was designed with a socket to hold the matchbook-sized tag reader as if it were a single component. Matt Reynolds, a student with years of RF experience, recommended the use of triac-output optoisolators to switch the antenna signals. These permitted a low-voltage PIC processor to control the 140VAC signals without risk of damage or interference. An important constraint was to ensure that the antenna coil was not switched during the tag reader's communication with the coil; this would disrupt communications between the board and the tag, resulting in a faulty read or write operation. The PIC monitored a Clear-to-Send line on the tag reader, switching the coils as soon as this signal was detected. Upon detection of a valid tag, the PIC sent the ID to the adjacent LED driver board.

LED driver board. By this point, designing LED drivers had become second nature. This board used a PIC to control four 4x8 LED matrices. Every tag in the system was

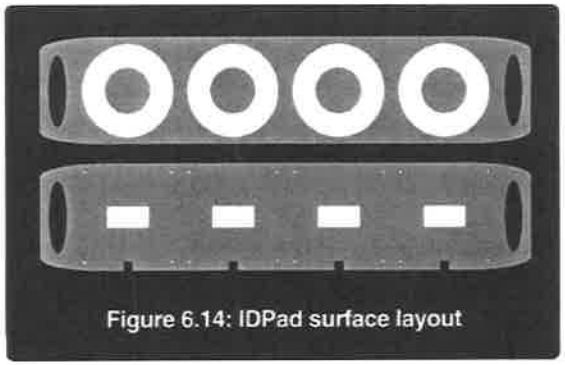


Figure 6.14: IDPad surface layout

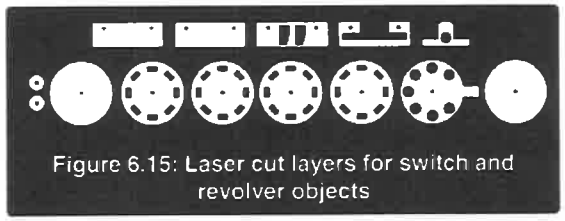


Figure 6.15: Laser cut layers for switch and revolver objects

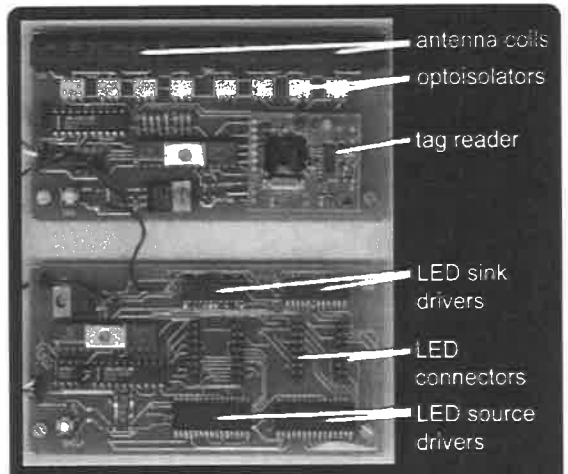


Figure 6.16: RFID controller board (top) and LED driver board (bottom)

Shenzhen Huiding Tech. Co., Ltd. - Exhibit 1006

associated with a unique graphical pattern. When a tag ID was received from the RFID controller, this tag was displayed; if no tag was present the display went blank.

Pad surface. As mentioned previously, the enclosure for this system was intended only to permit testing of the electronics prior to installation in a shelving system. Thus it was shaped to fit a row of four antenna PCB's, with the addition of handles at the ends for carrying. It was designed and cut one afternoon on the laser cutter, and was then assembled using standard machine screws.

Simple token objects. The objects used upon the surface of the IDPad were at first intended simply as handles for manipulation of the RFID tags. Because the wedge tags contained very directional antennae, they had to be held perpendicular to the field lines in order to be detected. A simple enclosure of clear acrylic was laser-cut; the name "bishop" reflects its similarity to a game piece. Another design which used several layers of clear acrylic was shaped like a loaf of bread.

Parameter control objects. During experimentation with the token objects, it was discovered that a strong magnetic field in the proximity of the wedge tags prevented communication with them. This was because the wedge tags, unlike the card and disc tags, used antennae with ferrite cores to concentrate field lines through their antennae. Magnetizing the ferrite material displaced the resonant frequency of the tag from 125kHz, thus preventing the tag's power circuit from operating.

This property inspired the design of objects with multiple physical states that could be distinguished wirelessly. These "parameter control objects" contained multiple tags and a number of small permanent magnets. The mechanisms inside the objects moved the magnets in relation to the tags, selectively disabling all but one of them. The "switch" object operates exactly like a toggle switch, enabling one of two tags embedded within. The "revolver" operates similarly, permitting selection of one of eight tags. One fortunate outcome of the magnet-suppression technique was that because the magnets were attracted to the individual tags, the switch and revolver objects tended to "snap" to discrete positions that represented different states.

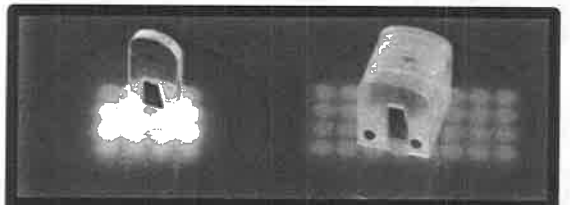


Figure 6.17: Bishop and bread objects on IDPad surface

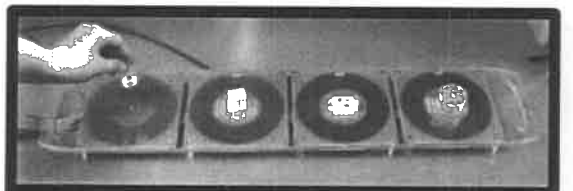


Figure 6.18: Objects on surface of IDPad

APPENDIX EE

Shenzhen Huiding Tech. Co., Ltd. - Exhibit 1006

6.4 Discussion

Application concepts

Time did not permit development of an application that took advantage of IDPad's properties. However, for example's sake, consider an example inspired by MediaBlocks, Music Bottles, and other tools for media navigation and playback.

In a performance of electronic music, prerecorded audio samples are layered and modulated into dense compositions; they are accelerated, slowed, distorted in pitch and volume, echoed, appended, truncated, and concatenated. IDPad could allow all of these operations to be carried out through manipulation of the physical objects. Parameter control objects could serve to represent either objects or operations, while adjusting the controls could trigger switching between samples or could modulate effects performed on the samples. Because tag position is identified as well as identity, operations could also be distinguished by *location* rather than by object; thus common operations like recording and playback might be separated spatially on a control platform.

Also, the revolver object could be used to control relative rather than absolute identity. Thus, an digital album of 100 photographs could be browsed with an eight-position wheel by simply maintaining a position index in software. Another interesting aspect is that because the objects retain physical state, the modification of object attributes can occur without requiring the presence of the interactive surface.

Tangible interfaces vs. augmented physical interactions

Both SensePad and IDPad allow arbitrary information sources to be associated with physical objects; both have similar size, displays, and identification technology. Differences in the physical objects employed, however, illustrate a key distinction between this work and other "tangible interfaces."

The manipulation of collocated, untethered physical objects has been the focus of perhaps half of the tangible interface systems developed to date. The metaDesk, Triangles, Illuminating Light, Urp, Music Bottles, and the Media Blocks "sequencer rack" all respond to the presence and relative positioning of a set of token objects. These objects are designed to serve as easily manipulable and identifiable tokens for control of the interface, and are thus integral and inseparable components of the sys-

APPENDIX EE

Shenzhen Huiding Tech. Co., Ltd. - Exhibit 1006

tem. Any prior or concurrent physical uses (such as containment of liquids in Music Bottles) are incidental to their main function as interface control objects. The IDPad is another example of this type of system. The IDPad objects bear no resemblance to existing physical objects, and are useless without the system that recognizes them. By contrast, SensePad and TouchCounters are fundamentally based upon the existing uses of objects as physical containers to transport, organize, identify, and protect their contents. IDPad represents a new form of interaction, while SensePad represents an augmentation of existing interaction.

Category	Projects	Interactions	Object properties
Object manipulation systems	• Triangles • Bottles • I/O Bulb • metaDesk • MediaBlocks (sequencer) • IDPad	• Manipulation of collocated, fixed set of objects • Operations include selection, binding, sequencing, relative positioning	• Objects designed as part of system, lack functionality apart from use in the system • Sensing technology, extent of physical representation, and ergonomics
Distributed awareness systems	• InTouch • MediaBlocks (slots) • ambientRoom • Ambient Displays • musicBox • Network Meter	• Remote monitoring/transmission of data • Closely attended or passively monitored • Uni- or bidirectional communication	• Object represents either specific or generic data source • Object's properties must changes perceptibly to indicate changes in data
Augmentation systems	• PPP • TouchCounters • SensePad	• Existing uses of object are maintained; digital information "augments" uses	• Tags and readers or recognition systems are fitted to existing objects

Table 6.1: Categorization of past Tangible Media Group projects

The success of these two types of systems depend on somewhat different factors. Compelling applications of IDPad, should they ever be developed, will hinge upon the digital functionality of the interactive system to which they are connected. The success of usage history displays like SensePad will depend upon the ability to provide and record useful data without negating the existing objects' functionality.

Shenzhen Huiding Tech. Co., Ltd. - Exhibit 1006

7 Evaluation and Future Work

This section describes the main contributions of the systems presented in the previous three chapters, and describes opportunities for future work.

7.1 FishFace and ShakePad

The FishFace and ShakePad projects demonstrated the feasibility of simple, self-contained interfaces with physically coincident input and output. They revealed the intrinsic attractiveness of bright, responsive graphics coupled closely to physical gesture. They also highlighted the sensitivity of the perceptual experience to slight variations in software implementation. The appeal of FishFace and ShakePad suggests that usage history displays can be interesting or even enjoyable to operate.

Because neither was applied to recording and displaying long-term histories of use, the immediate practical utility of FishFace and ShakePad remains unknown. Essentially, they are proofs-of-concept for both environmental and portable display devices.

To make FishFace and ShakePad better indicators of usage history, several technical improvements would be necessary. Increasing their "memory span" from seconds to hours or days would allow them to mediate interactions between temporally separated collaborators. To augment environments, longer-range sensing could be employed to detect body-scale motion. To augment portable objects, low-power displays such as "electronic ink" could be used to extend battery life.

Both FishFace and ShakePad are independent modules that can represent usage history without network connectivity. Reducing their physical size would increase the range of objects they could augment. In the long term, these modules could conceivably be miniaturized into independent, microscopic clusters that react to pressure, light, or temperature fluctuations. Such devices could be brushed onto surfaces like paint, instantly augmenting surfaces with history information.

Shenzhen Huiding Tech. Co., Ltd. - Exhibit 1006

7.2 TouchCounters

The TouchCounters system showed that tracking of containers rather than loose items confers several benefits. First, this approach simplified technical implementation, as numerous, heterogeneous, consumable items did not have to be tracked individually. Second, an existing physical categorization scheme was preserved and exploited. (Grouping items in a container is, in a sense, the ascription a common attribute to each item.) Finally, the array of evenly spaced containers was used to structure the visual presentation of multiple displays in parallel.

TouchCounters raised several questions regarding the complexity appropriate for a display of usage history. If usage history displays are simply visual representations of physical wear, are annotation or remote visualization operations necessary? Does passive tracking of objects constitute an invasion of privacy? Finally, what should be the balance of automatically triggered data presentation and the direct manipulation or control of data?

Controlled user testing of TouchCounters would be a strong step towards determining the appropriate complexity and feature set for a given environment. While the existing interaction modes were general enough for early testing, some customization to specific users, rooms, or industries would ultimately become necessary. Evaluation by real users might well result in reducing the number of features.

To conduct such long-term tests, the system would have to be made much more robust. Use of IDPad's contactless tracking system, rather than mechanical connectors, would greatly improve reliability. This technology would also allow the easy extension of the tracking system to a variety of object storage systems, including bookshelves, file folders, media storage racks, etc.

7.3 SensePad and IDPad

The SensePad project attempted to show that surfaces designed for storage and manipulation of objects could be redesigned as interfaces for information query and retrieval. In addition, it intended to demonstrate the low cost of augmenting objects through materials tagging technology. Although the tagging technology was not sufficiently developed for these goals to be fully realized, two elements of SensePad were significant steps towards lightweight interaction interfaces.

Shenzhen Huiding Tech. Co., Ltd. - Exhibit 1006

First, the contactless tags allowed identification and tracking of objects without swiping, scanning, or orientation towards a camera or other reader device. Second, the "digital shadows" were an effective mechanism for rapidly and unambiguously correlating attribute data with their physical referents. While the technique of collocating graphics with objects was used in the metaDesk, MediaBlocks and Luminous Room projects, only specific, custom-constructed objects were employed; SensePad showed this technique could be extended to augment objects with pre-existing functions and associations.

The IDPad prototype realized several of SensePad's objectives with the notable exception of continuous position tracking. IDPad showed responsive, object-specific graphical underlays in action, and pioneered the use of rewriteable identification tags. While IDPad was intended only as a test platform for an augmented shelving system, it led to such a different direction that its original application was never implemented. The token objects with their parametric controls are better examples of tangible interfaces than displays of usage history.

In addition to debugging SensePad's tagging and tracking technologies, greater effort could be spent to incorporate these technologies into the design of new types of furniture. New types of desks, tables, and shelves could be designed with integrated displays and tracking coils. This "computational furniture" would have immediate applications in retail environments, offices, libraries, and process automation, as well as in homes.

An opportunity not yet explored involves inverting the token/reference frame relationship of SensePad and IDPad. By making the tag reader into a compact, handheld object, the device could be used as a means to embed messages and annotations in objects throughout interior environments. Museums, kitchens, and bookstores could be annotated collaboratively by their users.

Shenzhen Huiding Tech. Co., Ltd. - Exhibit 1006

8 Conclusion

8.1 Summary

In this document, I have presented the concept of "situated displays of usage history," computational mechanisms for portraying the past history of physical objects and spaces. I have described the relationship of this concept to past and current research in human-computer interaction, and have outlined the space of devices that could potentially exist. From this space I have developed several specific prototypes that illustrate issues in design and application of these devices. I have also discussed social, economic, and psychological constraints upon the deployment of these systems.

From this work a few main points should be clear.

- Situated usage history displays are feasible and useful augmentations of existing environments.
- The tracking of human beings and of physical objects are parallel and complementary approaches, and many technologies are available for these purposes.
- To permit "lightweight interactions," situated usage history displays must be designed with particular sensitivity to preservation of existing patterns of use and understanding.
- In general, situated usage history displays should be used first to visualize data at the point of collection, rather than in a remote space. While more sophisticated functionality may be justifiable under some circumstances, the increased learning, orientation, and development time should be weighed carefully.

8.2 Personal vision

As one whose experience straddles research and product development, my tone throughout this document has been either analytical or pragmatic. The perspective of the artist—one compelled to express or elevate through creation—has been absent from my discussion. In closing, however, I will mention an aesthetic vision that has influenced my personal interest in this work.

APPENDIX EE

Shenzhen Huiding Tech. Co., Ltd. - Exhibit 1006

I have a mental image of an entirely new sort of architecture or environmental space. This world is reactive, dynamic, and even organic, despite being man-made. In this world, all objects are alive and are responsive to human presence and action. Devices are omnipresent but unobtrusive, with individual visual indicators that can be seen only if examined at close range. As one steps away to survey a larger space, these tiny blips of light combine to form larger, flickering constellations.

One navigates this space as easily as one strolls through breezy, moonlit woods, gathering cues from brightness, color, spatial arrangement, and movement. Objects react instantly to human contact, just as frogs jump and croak when people approach. The environment continually evolves and breathes as a reflection of the people who inhabit it. "Sensors" and "displays" are symbiotic extensions of the structures that support them, and are found wrapped around pillars and walls like ivy vines. "Pixels" exist not upon planar, Cartesian surfaces, but speckled throughout space and buried deep within materials.

The behavior of each element of this world is extremely simple, but through the unpredictable interaction of its thousands of components, a world emerges that is magical, surprising, and alive. These crude prototypes are a far cry from approaching this vision, but perhaps they represent a small step.

Shenzhen Huiding Tech. Co., Ltd. - Exhibit 1006

A Appendix: Additional Interactive Devices

Tactile Pad and Network Meter Prototypes

This section presents two additional modular device prototypes that employed a variety of new sensing and display technologies. Conducted in an atmosphere of exploration and self-education, this work illustrates some elements of interaction relevant beyond the limited domain of the artifacts themselves. In addition, these projects served to develop technical proficiency that facilitated the implementation of later projects.

COMPUTATION	PIC microprocessors
DISPLAY	electromagnet arrays LED matrix displays
SENSING	electric field sensing acceleration sensing network data sensing
COMMUNICATIONS	serial interfaces radio communications

Table A.1: Interactive technologies explored in early prototypes

A.1 Tactile Pad

This project, the first I implemented at the Media Lab, was the construction of a haptic output mechanism for a colleague. While it has little direct relation to the other research, it is included for completeness and to highlight the evolution of the prototyping techniques throughout this work.

Background

Tom White, a student in the Aesthetics and Computation Group, had developed an input device using a silicone bladder filled with an opaque liquid (soy sauce). When a user pressed this bladder against the glass supporting it, a camera mounted underneath the glass could detect the shape of its "contact patch." This shape could then be used for the control of interactive graphics. Having developed an input device based on "liquid haptics," Tom's attention turned to the output side.



Figure A.1: "Lilliput" tactile array by Andrew Dahley

The idea of a high-resolution, responsive, tactile output array is often raised in discussions of haptics, but most employ mechanical pistons or vibrators. One example is the "Lilliput," an array of vibrating speakers controlled by a similar array of buttons.

Tom hoped to use magnetorheological fluid, which hardens during exposure to a magnetic field, as a kind of "haptic display." A square, flat bladder containing this material would rest atop an array of electromagnets. A computer could then control these electromagnets in order to generate patterns of stiff material throughout the bladder. The physical patterns would be the tactile equivalent of graphics. As a warm-up project, the author agreed to construct a prototype of this device.

Shenzhen Huiding Tech. Co., Ltd. - Exhibit 1006

Implementation

The system hardware was constructed in several days. Magnetorheological fluid was obtained from Lord Corporation, then a Media Lab sponsor; electromagnets were ordered by mail. The electromagnets were mounted in the grid holes of a sheet of pegboard bought at a hardware store. A total of 64 electromagnets were placed in an 8x8 grid. In order to maximize the field couplings through the material in the bladders, the electromagnets were wired in a "checkerboard" pattern, such that half of the alternate cells had reverse-polarity.

The electromagnets were driven by a set of transistors on a breadboard. These provided the electromagnets with high-current power, but could be controlled by low-power signals from the electronic circuitry. As each electromagnet had to be addressed independently, a separate driver transistor was used for each of the solenoids. The transistors were controlled by a set of eight octal latches that could "sample and hold" data from the PIC microcontroller. (The technique of "row/column addressing" was used in later projects to control LED arrays.)

Powering the array of electromagnets was not a trivial problem. Since each electromagnet drew 350mA current, the complete array could draw over 20 amps. A car battery was considered as a power source, but eventually a behemoth 24V, 20A power supply was obtained. This monstrosity, which lacked an enclosure and weighed over 30 pounds, posed the various hazards of fire, electrical outage, and crushing injuries.

An enclosure for the system was made by cutting and gluing pieces of black foam core around the circuitry; the bladder rested on the top surface. An LED display was installed for debugging, but was never fully implemented.

Performance

In designing this project, the author underestimated the difficulty of implementing a high-current drive system. Inductive loads on the solenoids caused a variety of electrical noise problems. Eventually, these problems were eliminated, but the system's performance remained unsatisfactory. The solenoids used were simply not strong enough to generate ridges of noticeable depth in the bladder fluid. However, dynamic changes were easier to detect; Tom White took advantage of this by creating "graphics" modes in which invisible forces swept across the pad array.



Figure A.2: Electromagnet array for Tactile Pad

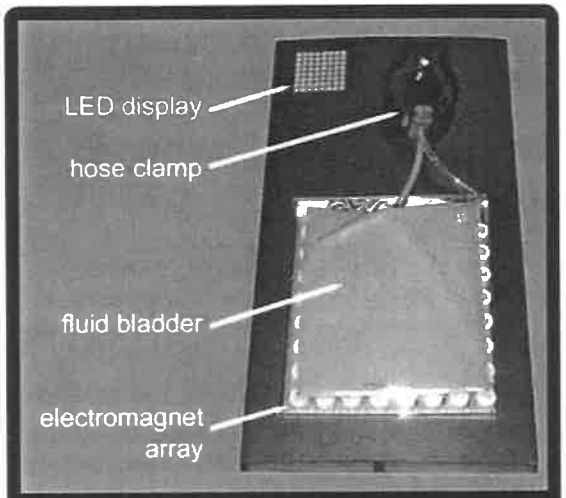


Figure A.3: Components of Tactile Pad

Shenzhen Huiding Tech. Co., Ltd. - Exhibit 1006

Discussion

Visual, auditory, or tactile displays can be used to communicate dynamic information. Visual displays, the most common, include monitors, LED displays, and projectors. Speakers, beepers, etc., are auditory displays, and tactile displays are usually motorized objects or vibrating actuators. (see table) The Tactile Pad was the only project to employ a non-visual output modality. Are haptic or vibrotactile actuators more appropriate for the task of distributed visualization?

The auditory transfer of information is usually serial. Since, in general, users must initiate contact with tactile displays to obtain information, touch is often serial as well. This is confirmed by Roger Whitehouse, designer of tactile maps for the blind:

> Sighted individuals can scan their surroundings and simultaneously become aware of the multiple possible structures and destinations within their purview; theirs is a complex and three-dimensional spatial understanding of the relationships of all of these things. The blind individual, on the other hand, experiences the environment sequentially, discovering first the door handle, then the door, then the frame, then the wall, then the wastebasket, then the chair, and so on. (Whitehouse99)

Certainly, tactile displays may be appropriate for surfaces that are not directly visible, such as furniture surfaces such as bench tops and seat backs. However, visual displays seem best for the representation of multiple, spatially distinct, moderate-bandwidth information streams. This is because engagement with such displays can be very rapid, information transfer can occur in parallel streams, and interference with physical manipulation tasks is low.

	Visual	Auditory	Tactile
spatialization of multiple sources	HIGH	MED	HIGH
physical contact required	NO	NO	YES
data bandwidth	HIGH	MED	LOW
interference with human-human communication	MED	HIGH	LOW
interference with concurrent manipulation tasks	MED	LOW	HIGH

Table A.2: Suitability of common output mechanisms for distributed visualization

Shenzhen Huiding Tech. Co., Ltd. - Exhibit 1006

A.2 Network Meter

Of the projects presented here, the Network Meter was both the most rapidly implemented and the longest in continuous operation. The device is a simple display that shows the level of network traffic between the Media Lab and the external Internet. It is a logarithmic graph that scrolls to the left as time passes.

Background

The Network Meter, which never had an official name, was installed at the suggestion of Jon Ferguson. Jon held a systems administration position at NeCSys, the Media Lab's Network Computing Systems office. To monitor the utilization of the lab wide Internet connection, Jon had written a Unix program that computed the current network bandwidth. Its output was an ASCII graph that advanced vertically up the screen of a workstation in the NeCSys office. Inspired to make this information available to the passersby, Jon inquired about the use of the LED displays he had seen in the TouchCounters project.

Implementation

Adapting an existing label for this purpose was quite straightforward, and was done within a few days. The existing Unix script continued to perform the computation; Jon simply added a routine to send the display graphics commands via serial cable. PIC code was written to represent temporal data using a histogram. The vertical axis indicated the logarithmic bandwidth, which was normalized to a maximum value; the horizontal axis represented time. The rightmost column of the display showed the current bandwidth, and was updated every few seconds. Every 10 seconds, the average value during that time scrolled to the left by one column.

Performance

The Network Meter has been extremely robust in practice, and has been displaying data almost continuously since its installation. Systems whose electrical connections never change seem, in general, far easier to construct than reconfigurable systems.

Discussion

The electronic labels designed for the TouchCounters project had a modular design that made them easy to re-purpose for use in both ShakePad and Network Meter. This

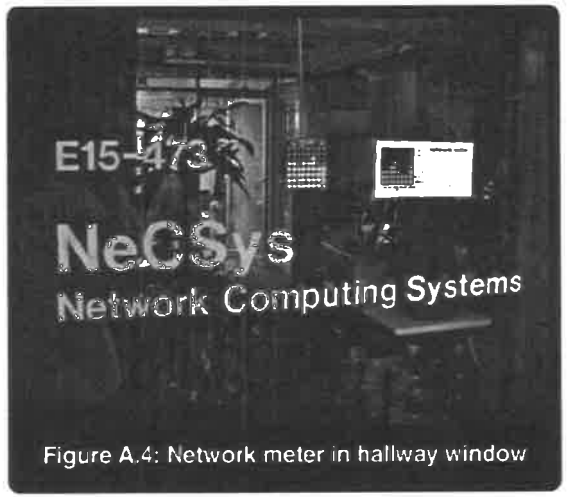
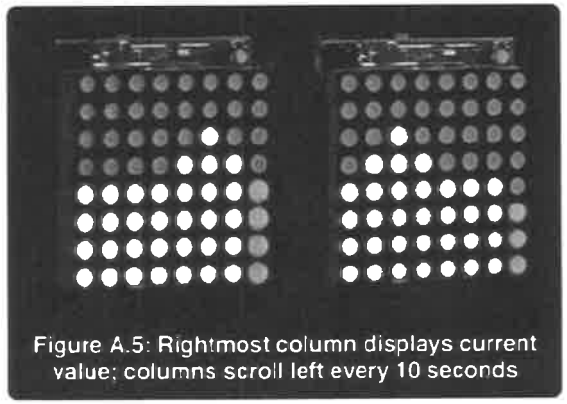


Figure A.4: Network meter in hallway window


Figure A.5: Rightmost column displays current value; columns scroll left every 10 seconds

Shenzhen Huiding Tech. Co., Ltd. - Exhibit 1006

highlights the value of modularity, not only for products but for prototypes as well. Modularity in design implies both flexibility and scalability; FishFace could easily have been replicated to cover entire walls.

The Network Meter was hardly the first device to display network traffic in a public space. The Live Wire, created by artist Natalie Jeremijenko, was a ceiling-mounted device from which dangled a gyrating tube of rubber. For every Ethernet packet that passed over the local network, the tube twitched, thus providing an evocative physical indicator of network activity. Likewise, the Tangible Media Group's Pinwheels and Water Lamps are well-suited towards the physical manifestation of dynamic information streams.

The Network Meter, a simple visual readout, featured a far less radical representation than any of these projects. However, it did raise an important issue regarding the visualization of temporal data at multiple scales simultaneously. The network traffic value was refreshed every second or so, but were the display to advance every second, only a few seconds could be represented on the display. Thus it was necessary to divide the display area of the device into "current" and historical data.

If the display had been physically larger—a row of 100 LED matrices instead of one—this would not have been necessary. Such a structure would also have permitted the integration with auxiliary information, such as an event calendar.

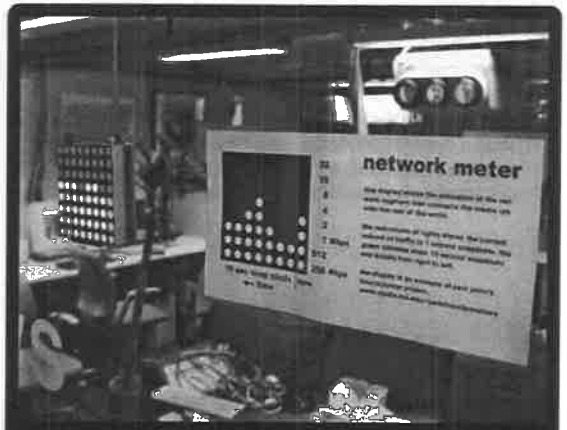
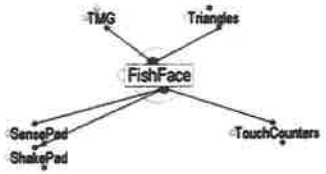


Figure A.6: Network meter legend

Shenzhen Huiding Tech. Co., Ltd. - Exhibit 1006

B Appendix: Project Influence Map

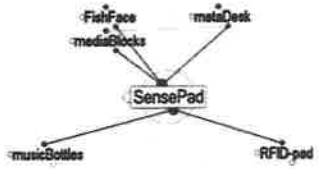
FishFace
FishFace was fairly original in its use of a bright, responsive, portable display. It borrowed the use of embedded PIC processors from Triangles.





ShakePad
ShakePad was directly based upon FishFace, and can be seen as leading to Curlybot, a self-contained, proprioceptive device.

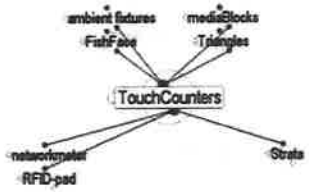
SensePad
SensePad utilized graphical underlays, employed in both metaDesk and MediaBlocks, as well as tagged passive objects as in MediaBlocks. Music Bottles also employs tagged bottles, and the IDPad tracks tagged objects with low-resolution graphical shadows as well.





IDPad
IDPad employed tagged objects, as do SensePad and TouchCounters; it also shared the responsive visualization. New, however, are the parameter controls on the individual objects.

TouchCounters
TouchCounters drew heavily on past work: ambient fixtures for persistent, peripheral visualization, MediaBlocks for tagged objects, Triangles for physical/digital connectors and embedded PIC's, and FishFace for responsive visualization. The Network Meter and IDPad are outgrowths, as is Strata's architectural visualization.





Network Meter
The Network Meter borrowed hardware directly from TouchCounters, but is based on an older concept from ambient fixtures: a single-purpose, statically-mapped display for continuous, remote data.

Shenzhen Huiding Tech. Co., Ltd. - Exhibit 1006

C Appendix: Design Parameters

Quantity of measure	
preservation of existing work practice	*existing actions vs. learned behavior*
usage type measured	*time-in-use vs. discrete events vs. value levels (temperature, movement, network traffic)*
criticality of information	*optional, augmentation information (boxes) vs. critical-path information (e.g. medication)*
Physical form	
physical distribution of displays	*scattered, object-centered vs. central cluster vs. environmental*
integration with other physical structures	*occasional attachment vs. removable label vs. integrated into design of object*
physical location of stored data	*locally stored (FishFace/ShakePad) vs. buffered (SensePad) vs. network storage (Touch-Counters)*
User interaction techniques	
degree of user involvement	*explicitly controlled (passive) vs. context-triggered (reactive) vs. automatic visualization*
modedness in interface	*persistent mapping (simple counting) vs. multi-modal (annotation+correlation functionality)*
Visualization	
temporal representation	*immediate (closely coupled) vs. historical (stored memory)*
responsiveness/dynamism	*dynamic, real-time interaction vs. slowly changing static display*
relativity of comparison	*single object in isolation vs. spanning multiple objects*
generality	*abstract or symbolic vs. literal or specific*

Shenzhen Huiding Tech. Co., Ltd. - Exhibit 1006

References

1. Brave, S. and Dahley, A. (1997) inTouch: A Medium for Haptic Interpersonal Communication. In *Extended Abstracts of CHI '97*. Atlanta: ACM Press, 1997.
2. Card, S., MacKinlay J.D., Shneiderman, B., eds. (1999) Information Visualization. In *Readings in Information Visualization: Using Vision to Think*. San Francisco: Morgan Kaufmann, 1999, pp.1-38.
3. Cooper, Ken. (1998) Personal conversation, September 1, 1998.
4. Cramer, J. and Spilker, B., eds. (1991) *Patient Compliance in Medical Practice and Clinical Trials*. New York: Raven Press, 1991.
5. Dahley, A., Wisneski, C., and Ishii, H. (1998) Water Lamp and Pinwheels: Ambient Projection of Digital Information into Architectural Space. In *Extended Abstracts of CHI'98*. Los Angeles: ACM Press, 1998.
6. Dennett, D. (1998) *Brainchildren: Essays on Designing Minds*. Cambridge, MA: MIT Press, 1998.
7. Edwards, Paul N. (1994) From 'Impact' to Social Process: Computers in Society and Culture. In Sheila Jasanoff et al., eds., *Handbook of Science and Technology Studies*. Beverly Hills, CA: Sage Publications, 1994, pp. 257-285.
8. Feiner, S., MacIntyre, B., and Seligmann, D. (1993) Knowledge-based augmented reality. In *CACM* 36(7), July 1993, pp. 52-62.
9. Fishkin, K., Moran, T., and Harrison, B. (1998) Embodied User Interfaces: Towards Invisible User Interfaces. In *Proceedings of EHCI'98*. Heraklion, Crete, September 1998. In Press.
10. Fitzmaurice, G. (1993) Situated Information Spaces and Spatially Aware Palmtop Computers. In *CACM* 36(7), July 1993, pp.38-49.
11. Fitzmaurice, G., Ishii, H., and Buxton, W. (1995) Bricks: Laying the Foundations for Graspable User Interfaces. In *Proceedings of CHI'95*. ACM Press, 1995, pp. 442-449.
12. Fletcher, R. (1996) *Low-Cost Electromagnetic Tagging Technology for Identification, Sensing, and Tracking of Objects*. MS Thesis, MIT Media Lab, 1996.
13. Gorbet, M., Orth, M. and Ishii, H. (1998) Triangles: Tangible Interface for Manipulation and Exploration of Digital Information Topography. In *Proceedings of CHI '98*. Los Angeles: ACM Press, 1998, pp. 49-56.

Shenzhen Huiding Tech. Co., Ltd. - Exhibit 1006

14. Healey, J. and Picard, R. (1998) StartleCam: A Cybernetic Wearable Camera. In *Proceedings of the International Symposium on Wearable Computing*. Pittsburgh, Pennsylvania: ISWC, 1998, pp. 42-49.

15. Hearst, Marti A. (1995) TileBars: Visualization of Term Distribution Information in Full Text Information Access. In *Proceedings of CHI'95*. ACM Press, 1995, pp. 59-66.

16. Hill, W. C., Hollan, J. D., Wroblewski, D., and McCandless, T. (1992) Edit Wear and Read Wear. In *Proceedings of CHI'92*. New York City, New York: ACM Press, 1992, pp. 3-9.

17. Ishii, H. and Ullmer, B. (1997) Tangible Bits: Towards Seamless Interfaces between People, Bits and Atoms. In *Proceedings of CHI '97*, Atlanta: ACM Press, 1997, pp. 234-241.

18. Ishii, H., Wisneski, C., Brave, S., Dahley, A., Gorbet, M., Ullmer, B. and Yarin, P. (1998) ambientROOM: Integrating Ambient Media with Architectural Space (video). In *Summary of CHI '98*. Los Angeles: ACM Press, 1998, pp. 173-174.

19. Kirsh, D. (1995a). The Intelligent Use of Space. In *The Journal of Artificial Intelligence*, 73(1-2), 1995, pp. 31-68.

20. Kirsh, D. (1995b) Complementary Strategies: Why We Use Our Hands When We Think. In *Proceedings of 7th Annual Conference of the Cognitive Science Society*. Hillsdale, NJ: Lawrence Erlbaum, 1995.

21. Minsky, M. (1985) *The Society of Mind*. New York: Simon and Schuster, 1985.

22. Norretranders, T. (1998) *The User Illusion: Cutting Consciousness Down to Size*. Viking Press, 1998.

23. Pashler, H. (1998) *The Psychology of Attention*. Cambridge: MIT Press, 1998, pp. 1-99.

24. Philips Hitag Information Page. (1999) Available at: http://www.semiconductors.com/identification/products/contactless/hitag

25. Picard, R.W. (1997) *Affective Computing*. Cambridge, MA: MIT Press, 1997.

26. Poor, R. (1999) The iRX 2.1 ...where atoms meet bits. Available at: http://www.media.mit.edu/~r/projects/picsem/irx2_1/

27. Raskin, J. (1999) Presenting Information. In *Information Design*, Robert Jacobson, ed. Cambridge, MA: MIT Press, 1999, pp.341-348.

Shenzhen Huiding Tech. Co., Ltd. - Exhibit 1006

28. Rekimoto, J, and Nagao, K. (1995) The world through the computer: computer augmented interaction with real world environments. In *Proceedings of UIST'95.* ACM Press, 1995, p. 29.

29. Resnick, M., et al. (1998) Digital Manipulatives: New Toys to Think With. In *Proceedings of CHI'98*, 1998, pp. 281-287.

30. Reeves, B. and Nass, C. (1996) *The Media Equation.* New York: CSLI Publications, 1996, pp. 219-226.

31. Smith, J. (1996) Field Mice: Extracting Hand Geometry from Electric Field Measurements. In *The IBM Systems Journal*, Volume 35, No. 3&4, 1996.

32. Streitz, N., Geißler, J.,and Holmer, T. (1998a) Roomware for Cooperative Buildings: Integrated Design of Architectural Spaces and Information Spaces. In *Proceedings of CoBuild'98: First International Workshop on Cooperative Buildings.* GMD, Darmstadt, Germany, 1998.

33. Streitz, N., Konomi, S,H.-J. Burkhardt (Eds.): (1998b) *Cooperative Buildings: Integrating Information, Organization, and Architecture.* First International Workshop, CoBuild'98, Darmstadt, Germany, February 1998. Available at: http://link.springer.de/link/service/series/0558/papers/1370/1370000v.pdf

34. Turk, M. (1997) *Workshop on Perceptual User Interfaces* (website). Available at: http://research.microsoft.com/PUIWorkshop97/

35. Ullmer, B., Ishii, H. and Glas, D. (1998) mediaBlocks: Physical Containers, Transports, and Controls for Online Media. In *Proceedings of SIGGRAPH '98.* Orlando, Florida: ACM Press, 1998, pp. 379-386.

36. Underkoffler, J., and Ishii, H. (1998) Illuminating Light: An Optical Design Tool with a Luminous-Tangible Interface. In *Proceedings of CHI'98.* ACM Press, 1998, pp. 542-549.

37. Want, R., Fishkin, K., Gujar, A. and Harrison, B. (1999) Bridging physical and virtual worlds with electronic tags. In *Proceedings of CHI'99.* ACM Press, 1999, pp. 370-377.

38. Weiser, M. (1991) The Computer for the 21st Century. In *Scientific American*, 265(3), pp. 94-104.

39. Weiser, M. (1993) Some Computer Science Issues in Ubiquitous Computing. In *Communications of the ACM*, Vol. 36, No. 7 (July 1993), Pages 75-84.

40. Weiser, M. and Brown, J. S. (1997) Designing Calm Technology. In *CHI'97 Workshop on Research Issues in Ubiquitous Computing*. Atlanta, GA: ACM Press, 1997.

Shenzhen Huiding Tech. Co., Ltd. - Exhibit 1006

41. White, T. (1998) *Introducing Liquid Haptics in High Bandwidth Human Computer Interfaces. MS Thesis*, MIT Media Lab, May 1998.

42. Whitehouse, R. (1999) The Uniqueness of Individual Perception. In Robert Jacobson, ed. *Information Design.* Cambridge, MA: MIT Press, 1999, pp. 103-129.

43. Wisneski, C., Ishii, H., Dahley, A., Gorbet, M., Brave, S., Ullmer, B., Yarin, P. (1998) Ambient Displays: Turning Architectural Space into an Interface Between People and Digital Information. In *Proceedings of CoBuild'98: First International Workshop on Cooperative Buildings*. GMD, Darmstadt, Germany, 1998.

44. Yarin, P. and Ishii, H., (1999) TouchCounters: Designing interactive electronic labels for physical containers. In *Proceedings of CHI '99*. Pittsburgh: ACM Press, 1999, pp. 362-369.

45. Zimmerman, M. (1989) The Nervous System in the Context of Information Theory. In R.F. Schmidt and G. Thews. eds. *Human Physiology*, 2d ed. Berlin: Springer-Verlag, 1989, p. 172. As quoted in (Norretranders98).

Shenzhen Huiding Tech. Co., Ltd. - Exhibit 1006

Orlando, Florida
November 11-14, 2001

UIST 01

Proceedings of the
14th Annual
ACM Symposium on
User Interface Software
and Technology

CHI Letters Vol 3, Issue 2

sponsored by
ACM SIGGRAPH
ACM SIGCHI
in cooperation with
ACM SIGSOFT

Shenzhen Huiding Tech. Co., Ltd. - Exhibit 1006

Orlando, Florida
November 11-14, 2001

01 UIST

Proceedings of the 14th Annual ACM Symposium on User Interface Software and Technology

CHI Letters Vol 3, Issue 2

sponsored by
ACM SIGGRAPH
ACM SIGCHI
in cooperation with
ACM SIGSOFT





Shenzhen Huiding Tech. Co., Ltd. - Exhibit 1006

The Association for Computing Machinery
1515 Broadway
New York New York 10036

Copyright 2001 by the Association for Computing Machinery, Inc.(ACM). Permission to make digital or hard copies of portions of this work for personal or classroom use is granted without fee provided that copies are not made or distributed for profit or commercial advantage and that copies bear this notice and the full citation on the first page. Copyright for components of this work owned by others than ACM must be honored. Abstracting with credit is permitted. To copy otherwise, to republish, to post on servers or to redistribute to lists, requires prior specific permission and/or a fee.Request permission to republish from: Publications Dept. ACM, Inc. Fax +1 (212) 869- 0481 or <permissions@acm.org>.

For other copying of articles that carry a code at the bottom of the first or last page, copying is permitted provided that the per-copy fee indicated in the code is paid through the Copyright Clearance Center, 222 Rosewood Drive, Danvers, MA 01923, +1-978-750-8400,+1-978-750-4470 (fax).

Notice to Past Authors of ACM-Published Articles
ACM intends to create a complete electronic archive of all articles and/or other material previously published by ACM. If you have written a work that was previously published by ACM in any journal or conference proceedings prior to 1978, or any SIG Newsletter at any time, and you do NOT want this work to appear in the ACM Digital Library, please inform permissions@acm.org, stating the title of the work, the author(s), and where and when published.

ACM ISBN: 1-58113-438-x

Additional copies may be ordered prepaid from:

ACM Order Department
PO Box 11405
New York, NY 10286-1405

Phone: 1-800-342-6626
(US and Canada)
+1-212-626-0500
(all other countries)
Fax: +1-212-944-1318
E-mail: acmhelp@acm.org

ACM Order Number: 429012
Printed in the USA

DiamondTouch: A Multi-User Touch Technology

Paul Dietz and Darren Leigh
Mitsubishi Electric Research Laboratories
201 Broadway
Cambridge, MA 02139 USA
+1-617-621-7500
{dietz,leigh}@merl.com

ABSTRACT

A technique for creating a touch-sensitive input device is proposed which allows multiple, simultaneous users to interact in an intuitive fashion. Touch location information is determined independently for each user, allowing each touch on a common surface to be associated with a particular user. The surface generates location dependent, modulated electric fields which are capacitively coupled through the users to receivers installed in the work environment. We describe the design of these systems and their applications. Finally, we present results we have obtained with a small prototype device.

KEYWORDS: DiamondTouch, multi-user, touch, collaborative input, single display groupware

INTRODUCTION

DiamondTouch is a multi-user touch technology for tabletop front-projected displays. It enables several different people to use the same touch-surface simultaneously without interfering with each other, or being affected by foreign objects. It also allows the computer to identify which person is touching where.

During the course of research on Human-Guided Simple Search [1] some of our colleagues have constructed a collaborative workspace in which multiple users work on the same data set. The environment consists of a ceiling-mounted video projector displaying onto a white table around which the users sit. A single wireless mouse is passed around as different users take the initiative. Our colleagues proposed that the collaboration would be improved if the users could independently and simultaneously interact with the table, and considered using multiple mice.

The use of multiple mice in a collaborative environment is particularly problematic. It can be challenging for users to keep track of one pointer on a large surface with lots of activity. Keeping track of many mice is nearly impossible. This leaves users physically pointing at their virtual pointers to tell other users where they are. Also, relying on a separate physical device keeps us from utilizing the natural human tendencies of reaching, touching and grasping. [1]



Figure 1: The collaborative work environment for Human-Guided Simple Search.

Using a large touch-screen as the table surface would seem to be an answer, but existing touch technologies were inadequate. Most allow only a single touch and do not identify users. While schemes have been developed where users take turns [3], we wanted the interaction to be simultaneous and spontaneous.

Unlike electronic whiteboards or other vertical touch systems, the tabletop nature of our display creates a problem: people tend to put things on tables. With a pressure-sensitive surface, foreign objects create spurious touch-points causing single touch systems to malfunction.

Optimally, we would like a multi-user touch surface to have the following characteristics:

Permission to make digital or hard copies of all or part of this work for personal or classroom use is granted without fee provided that copies are not made or distributed for profit or commercial advantage and that copies bear this notice and the full citation on the first page. To copy otherwise, to republish, to post on servers or to redistribute to lists, requires prior specific permission and/or a fee.
UIST 01 Orlando FLA
Copyright ACM 2001 1-58113-438 -x/01/11...$5.00

[1] Plus see the discussion in [2] for advantages of touch tablets over mice.

Shenzhen Huiding Tech. Co., Ltd. - Exhibit 1006

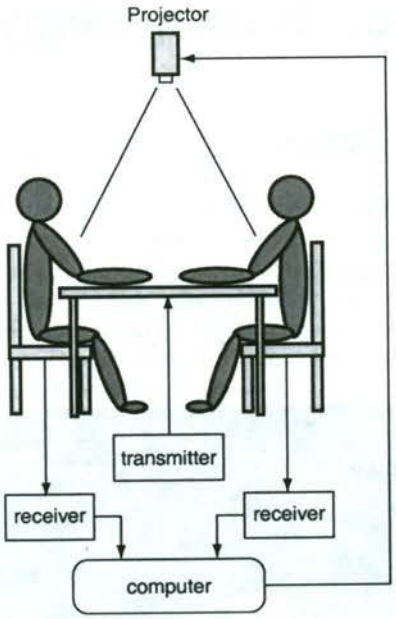


Figure 2: DiamondTouch works by transmitting signals through antennas in the table. These signals are capacitively coupled through the users and chairs to receivers, which identify the parts of the table each user is touching. This information can then be used by a computer in the same way as mouse or tablet data.

1. Multipoint: Detects multiple, simultaneous touches.
2. Identifying: Detects which user is touching each point.
3. Debris Tolerant: Objects left on the surface do not interfere with normal operation.
4. Durable: Able to withstand normal use without frequent repair or re-calibration.
5. Unencumbering: No additional devices should be required for use – e.g. no special stylus, body transmitters, etc.
6. Inexpensive to manufacture.

The DiamondTouch technology meets all of these requirements. In the following sections, we describe its operating principles, the sorts of interactions that are possible, and the results of our experience with a small prototype device. We also present some ideas for future work and applications.

DiamondTouch

DiamondTouch works by transmitting a different electrical signal to each part of the table surface that we wish to uniquely identify. When a user touches the table, signals are capacitively coupled from directly beneath the touch point, through the user, and into a receiver unit associated with that user. The receiver can then determine which parts of the table surface the user is touching.

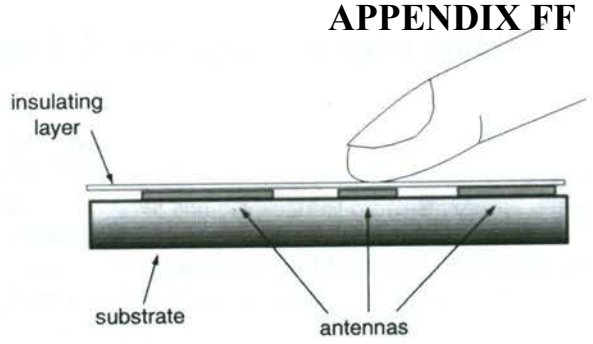


Figure 3: A set of antennas is embedded in the tabletop. The antennas are insulated from each other and from the users.

The table surface is a constructed with a set of embedded antennas which can be of arbitrary shape and size. The antennas are thin pieces of an electrically conductive material which are insulated from each other. Since the coupling of signals to the users is done capacitively, the antennas are also insulated from the users, and the entire table surface can be covered by a layer of insulating, protective material as shown in Figure 3. Each antenna extends over a single area of the table to be unambiguously identified: the system cannot tell where on the antenna a user touches, just that the user touches that antenna. A transmitter unit drives each antenna with its own signal that can be distinguished from the signals of the other antennas. Users are capacitively coupled to their receivers through their chairs, and the receivers are connected back to the transmitter through a shared electrical ground reference.

When a user touches the table, a capacitively coupled circuit is completed. The circuit runs from the transmitter, through the touch point on the table surface, through the user to the user's receiver and back to the transmitter.

With proper design, capacitive coupling [4] through the human body [5] can be quite reliable. The first consideration is that we wish to operate via "near field" (i.e. capacitive) coupling. By limiting the transmitting frequencies so that the dimensions of the entire system are very short compared to a wavelength, very little energy is radiated. This reduces problems with radio frequency interference and with unwanted coupling between the antennas. For reasonably sized tables, frequencies should be in the sub-MHz range.[2]

The system can be understood with the aid of a simplified equivalent circuit as shown in Figure 4. C_{table} represents the capacitance between the user's finger and a transmitting antenna in the table. C_{chair} represents the capacitance between the user and a conducting chair. The coupling capacitance is

[2] At a frequency of 1 MHz, the wavelength is about 300 meters.

Shenzhen Huiding Tech. Co., Ltd. - Exhibit 1006

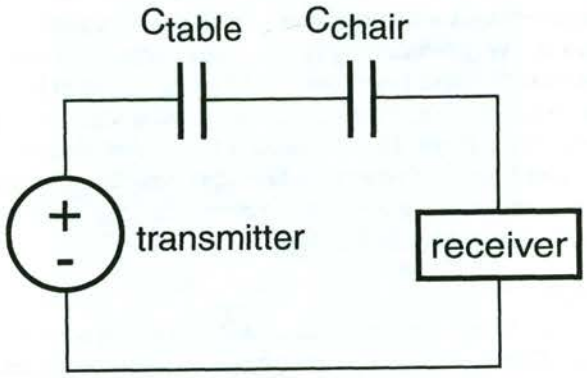


Figure 4: The equivalent circuit for the DiamondTouch system.

the series combination of these two capacitances:

$$C_{coupling} = \frac{C_{table} \times C_{chair}}{C_{table} + C_{chair}}$$

Since the coupling area of a finger is very small compared to the entire body in a conducting chair, C_{table} tends to be very small compared to C_{chair}. Thus, the equation reduces to $C_{coupling} \approx C_{table}$. This means that the precise capacitive coupling via the chair is inconsequential, as long as it is large enough. If it were desirable to have the users stand on conductive floor plates instead of sitting in conductive chairs, the coupling area would be substantially smaller, but still very large compared to a finger. Experience has shown that even thick-soled shoes do not present a problem in this scenario.

When a user's finger is far from the table, C_{table} is very small and little or no signal is coupled from the transmitter to the receiver. As the user's finger approaches the table, C_{table} increases, the coupling to the receiver increases and so the received signal strength increases. The signal strength is also proportional to the area of the touch: using a thumb or the heel of a hand will produce a higher received signal strength than using a little finger.

DiamondTouch requires reasonable electrical isolation between the users. This constraint is violated if two or more users (or their chairs) are touching, or are in very close physical proximity. In this regard, social norms of "personal space" have been sufficient to keep the inter-user coupling acceptably small. However, this behavior can be explicitly exploited. By touching another user (or their chair), the touches of either user are interpreted as touches for both users. Typically, the coupling "through" a second user is somewhat weaker, and so it is usually possible to determine the "primary" user versus "shared" users. This provides a simple and intuitive mechanism for users to jointly indicate a selection.

UNIQUE SIGNALS

Because a user may touch several antennas at once, it is important that the receiver be able to distinguish between and identify any mix of incoming signals. We can do this if the signals are "separable", or in signal processing terms "mutually orthogonal".

There are many ways of generating such signals.[3] For example, each antenna could be driven with a sinusoid of a different frequency. A receiver that is coupled to several antennas could determine which ones they are by examining the frequency spectrum of the received signal. Unfortunately, generating the numerous frequencies required for a large array is complicated and relatively expensive, so we rejected simple "frequency-division multiplexing" in our prototype.

Time-division multiplexing is another option. In this case, each antenna is separately driven in turn by a given signal while the other antennas are not. The timing of the received signals is used to determine which antennas are coupled to the receiver. While this system is very simple to implement, it may not be appropriate for larger arrays. The problem is caused by the interplay of various constraints. To provide good response time, the entire array must be scanned 10 to 100 times per second. However, as noted previously, practical modulating frequencies are limited to the sub-MHz range. This leaves very few modulation cycles per antenna, making receiver design difficult, especially in the face of other interfering noise sources. There are some clever ways of reducing the scan time [6] that help to extend the practicality of time-division multiplexing schemes, but these are beyond the scope of this paper.

Another way to construct a set of orthogonal signals is by code-division multiplexing, which is a spread spectrum technique. In fact, this turns out to be a particularly elegant approach for large arrays because very simple hardware operations (shifts, XORs, etc.) can be used to generate the large number of spreading codes. The simple hardware can even be cascaded, so that smaller touch devices can be tiled to make much larger ones. The spread spectrum approach will actually provide a significant gain in signal-to-noise ratio for large arrays.

ANTENNA PATTERNS

As we stated before, the antennas embedded in the tabletop can be of arbitrary shape and size. A designer may choose to implement just a few large "buttons" or a much more complicated array. Of course, a general, configurable solution is more desirable than a particular one that is designed into the hardware.

The most general solution is a "full matrix" pattern, in which a very large number of antennas are arranged in a rectan-

[3] A concise explanation of these various types of multiplexing can be found in [7]. For more general information on orthogonal signals, and spread spectrum information, see [8].

Shenzhen Huiding Tech. Co., Ltd. - Exhibit 1006

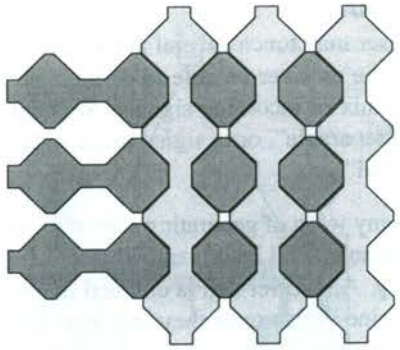


Figure 5: The row-column antenna pattern that our prototype uses. Each row or column is composed of diamond shapes connected in one direction and isolated in the other. This allows the maximum surface area for both layers without the upper one shielding too much of the lower one.

gular grid. Such a matrix of individually driven antenna "pixels" allows an unambiguous determination of multiple touch locations, even for a single user. Unfortunately, this is also the most difficult pattern to manufacture due to the very large number of connections required and the correspondingly large amount of supporting circuitry. In reality, the full matrix pattern may be unnecessary for many applications. Although the simultaneous, multi-user feature is essential, it is usually sufficient for each user to indicate at most a single touch point or bounding box. This functionality can be obtained with a simple row/column pattern that drastically reduces the number of antennas.

The rows and columns will usually be on two different layers. Due to shielding effects, there is some subtlety to creating a good row/column antenna pattern. A simple rectangular pattern of columns on the upper layer will overlap and cover too much of the equivalent set of rows on the lower layer. This will decrease the amount of area through which the rows can capacitively couple signals, weakening their sensitivity. A good antenna pattern will minimize the area in which the rows and columns overlap, while maximizing their total areas. We have found the connected diamond pattern shown in Figure 5 to be a good choice. This pattern has the interesting property that the row conductors are identical to the column conductors, rotated ninety degrees. In our prototypes, this allowed us to create a single conductor pattern and use it for both rows and columns, saving manufacturing costs.

In use, a touch will most likely span multiple rows and columns with different degrees of coupling. The received signal strengths can be used to estimate a centroid for the touch, obtaining positioning finer than the row and column spacing. However, an alternative way of using this information is to present a bounding box for the touch event, defined by the outermost rows and columns that have significant coupling. This leads to an interesting use of the device – a single user might touch two points to define a bounding box. This is a very natural way of selecting a rectangular area. In practice, we have found two modes of operation to be useful: when the coupled area is small, assume that the user is indicating a point. When it spans a larger area, assume that the user is trying to specify a bounding box. The end result is that even this simplified row/column design allows some multi-touch capability for single users.[4]

PROTOTYPE

In order to test these concepts, we have created a small DiamondTouch prototype, part of which is shown in Figure 6. The prototype has an active area of approximately 20 centimeters by 20 centimeters containing 80 antennas arranged as 40 rows and 40 columns. The half-centimeter pitch was chosen so that a typical finger touch would span at least two rows and two columns. A 0.5 millimeter thick double-sided printed circuit board was designed to be either the row or the column array, depending upon the rotation. Since we would like the coupling to either rows or columns to be about the same, the boards were arranged with the antenna arrays sandwiched in the middle of the stacked row and column boards with a very thin insulator in-between. Thus the gap to the top surface was very similar, varying only by the thickness of the insulator.

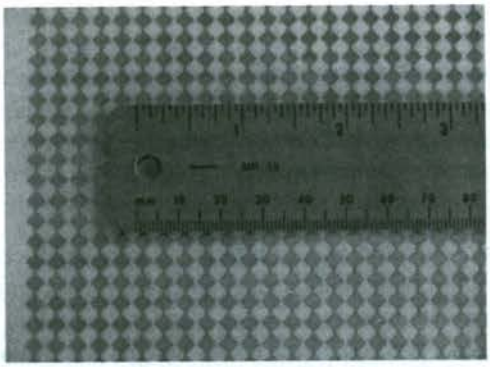


Figure 6: Part of the prototype's antenna array. Compare with Figure 5.

The antenna arrays are driven by a transmitter board that appears in Figure 7. For the moment, we have implemented time-division multiplexing where each antenna, in turn, is driven with 10 cycles of a 100 kHz square wave. While this board is capable of driving the antennas with a 60 volt swing,

[4]Of course, it would be better if a row/column pattern could distinguish multiple touches from a single user. The problem is that, given two X and two Y coordinates, the system cannot tell if the intended touches are $(X1, Y1)$ and $(X2, Y2)$ or $(X1, Y2)$ and $(X2, Y1)$. In most cases, timing information might be used to disambiguate the two cases. If you had $(X1, Y1)$ and then $(X2, Y2)$ appeared later, you could safely guess the pairings. A case where this method fails is if the two touch points come together and then separate.

Shenzhen Huiding Tech. Co., Ltd. - Exhibit 1006

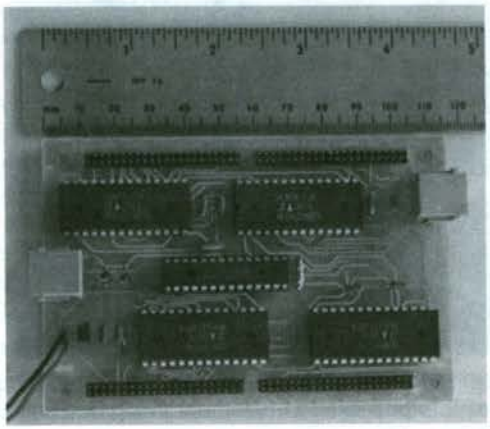


Figure 7: The prototype's transmitter board based around a PIC microcontroller. It is small and uncomplicated.

we have found 5 volts to be quite sufficient. Using a higher voltage produces a better signal-to-noise ratio which can be useful in electrically noisy environments.

The receivers are attached (via shielded cables) to padded, folding metal chairs that serve as the user coupling devices. Just about any conductive chair can be used for this application as long as there is sufficient capacitive coupling between the occupant and the receiver cable. Non-conductive chairs will work if a conductive "cushion" (a layer of metal foil, perhaps padded for comfort) is used to couple the user to the receiver.

Figure 8 shows one of the prototype receivers. For maximum noise immunity, the receivers use synchronous demodulation, and thus require appropriate synchronization signals from the transmitter board. The receivers digitize the results and send them in raw form to a PC via fast RS-232 serial connections. There is a separate receiver board for each user. The entire table is scanned 75 times per second and the PC receives a coupling value for each user for each row and each column. The 75 Hz update rate and negligible latency to the computer allow the prototype to be very responsive.

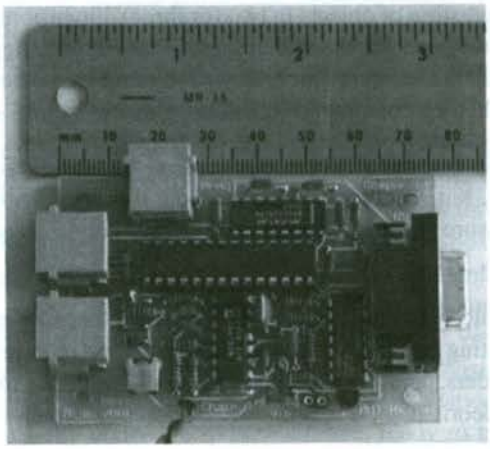


Figure 8: One of the prototype's receiver boards, based around a PIC microcontroller. One is needed for each user.

The table is considered to be "touched" when the received signal at an antenna is high enough. In theory, we could use a simple threshold to determine this. However, given component drift, user variations, and varying noise levels, we have found it more practical to adapt a threshold based on current estimates of minimum coupling and noise levels. This works satisfactorily, but more sophisticated methods may yield better results. A problem case arises when the rubber-footed chairs are dragged across the carpet. "Static electricity" causes large noise spikes that require better filtering.

The transmitter and receiver boards are based on PIC microcontrollers and other inexpensive, off-the-shelf electronic components. The most expensive parts we used were the printed circuit boards for the table itself, and these would be much cheaper in a massed produced product.

We have written test software that generates a bar graph display of the coupling level, for each row and column and each user, along the appropriate axes. Different colors are used for each user. The calculated touch points are graphically displayed: a cross-hair cursor is shown for small touch areas, and a bounding box is show for larger ones.

RESULTS

The prototype DiamondTouch system works quite well. Figures 9 and 10 show the results for two people touching the table at once. The functionality of each user is quite independent.

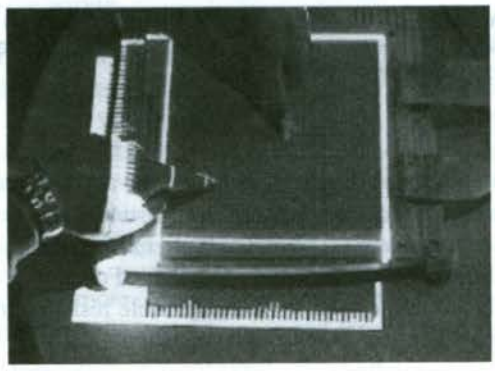


Figure 9: Two users are interacting with the table independently.

We have stated that DiamondTouch operation is largely unaffected by objects carelessly left on the surface. Figure 11

Shenzhen Huiding Tech. Co., Ltd. - Exhibit 1006

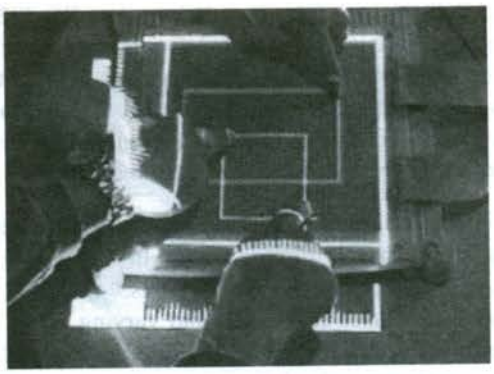


Figure 10: Here two users are creating bounding boxes. Note that the operations are independent and they do not interfere with each other.

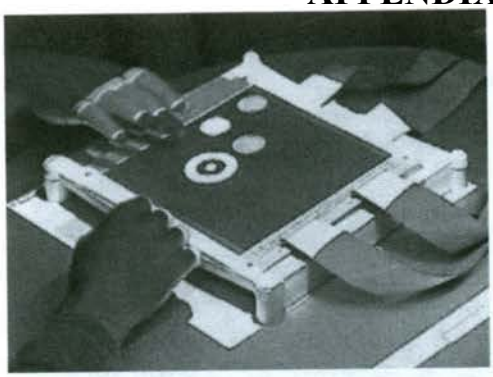


Figure 12: Two users are playing the Pop-A-Bubble game. It is possible to implement this game only because the table can identify who is touching where.

shows that a conducting object left on the surface does not cause a problem. While normal objects do not affect the table, it is possible to design special ones that do. This could be very useful in applications that use tangible and graspable objects as part of their user interface.

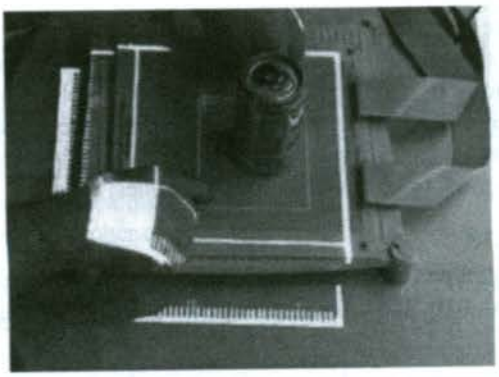


Figure 11: An aluminum can has been placed on the table, but it does not affect operation, despite being electrically conductive.

Because the insulating layer between the antenna array and users does not require any special properties, it can be manufactured from a variety of materials to make the table robust under different environmental conditions. For example, glass or plastic could be used to make the table resistant to liquid and chemical spills. Our prototype was made from a fiberglass laminate called GML1000 [9], whose thermal properties allowed us to operate the table temporarily (and without damage) while it was covered with burning alcohol.

A Game

We have implemented a simple game to demonstrate some of the capabilities of DiamondTouch. Multi-player "Pop-a-Bubble" pits up to four players against each other in a real-time game of reflexes. Colored "bubbles" appear and disappear on the table. The four players are each assigned a color (red, green, blue or yellow) and they get points for "popping" bubbles of their color. They lose points for trying to pop other players' bubbles. Cyan bubbles are "wild" and any player will receive points for popping one. Magenta bubbles are "poison" and players who pop them lose points.

The game shows off DiamondTouch's main features. The interaction is both spontaneous and simultaneous: the players reach out and act naturally, without having to worry about turn-taking or dealing with extra "gadgets". Scoring is easily handled because the game can identify which player touched the table at what location and at what time. And it's fun to play!

RELATED WORK

Many different technologies have been developed for sensing the position of objects in two (or three) dimensions. Here we discuss some of the technologies that we investigated in our work on DiamondTouch, as well as some that others suggested that we compare to it.

Resistive and capacitive touch screens have been sold for decades, but are confused by multiple touches. Those that are pressure sensitive cannot tolerate any debris objects left on them.

Ultrasonic systems [10] [11] have recently become popular for creating electronic whiteboards, but they require active pen holders, and do not generally allow multiple touches. Larger debris objects may cause "shadowing" which will degrade performance.

One system that can support more than one touch while identifying the tool used is the Wacom Intuos graphics tablet [12]. This has a feature called "Dual Track" that allows two tools (styluses or mice) to be used simultaneously. Unfortunately, the Intuos is smaller and more expensive than we wanted and is limited to two touches only.

Shenzhen Huiding Tech. Co., Ltd. - Exhibit 1006

Other multi-touch systems that cannot identify users include the FingerWorks FingerBoard [13] and Tactex [14] smart fabric technology. Although the FingerBoard is not shipping as of this date, it appears to use a two-dimensional array of capacitance sensors to obtain a 2-D "image" of the object placed on it. The Tactex technology senses pressure by changes in the optical properties of the material.

Some optical-based input systems have been designed which track hands or other objects around a 2-D area. HoloWall [15] uses a camera and infrared illumination to find objects near a glass wall. Strickon and Paradiso [16] have done something similar in free space using a scanning laser rangefinder. Both system can sense multiple "touches" but cannot easily distinguish between different users.

Near-field electric field (capacitive) sensing has been used for decades in applications as simple as touch switches. More elaborate forms of capacitive sensing were introduced to the user interface community in recent years. Zimmerman, et al described this technology in depth in [17] and introduced the Fish, a device used to measure the position of a hand in three space using electric fields. Related work can be found in [18] and [19]. These systems attempt to detect a hand or other object that is several centimeters from one of the electrodes, and use field strength to determine the position. DiamondTouch differs by requiring that the sensed object be very close (millimeters or less) to an electrode, but uses a large array of these to sense the position.

CONCLUSIONS AND FUTURE WORK

DiamondTouch multi-user touch technology achieves all of our stated goals. It detects simultaneous, multiple touches, identifying which user is touching each point. It is largely unaffected by objects left on the surface, and is extremely durable. There is no stylus to lose, and the entire system can be manufactured inexpensively.

Larger and Different Systems

We are interested in building units much larger than our prototype and see no barriers to doing so. Scaling the electronics should not present a problem. The prototype was small because it was made from printed circuit boards, and these are expensive to make in larger sizes and small quantities. Large antenna arrays could be manufactured very cheaply by etching sheets of metalized plastic. We believe that these could be so inexpensive that we can envision a day when most white-boards sold will include a DiamondTouch antenna array under the writing surface, ready to plug into a separately-sold electronics package if the owner wishes to have touch-input capability.

We have designed and are having manufactured a small run of larger prototype DiamondTouch units. These will be made by silk-screening conductive ink onto flexible plastic, and will measure 80 cm by 48 cm with the same 0.5 cm row and column pitch as the original prototype. They will connect to the host computer via a USB interface instead of several serial ports.

While we have described DiamondTouch's use in a front-projected format, the technology is certainly not limited to this. Because the signals are capacitively coupled, very little electric current flows through the antennas so these can be made of a relatively high-resistivity material. This means that transparent conductors such as indium tin oxide can be used, and that the technology will be useful for rear-projection applications as well. Our experiments with such materials are just beginning but show promise.

New Applications

The ability for simultaneous, identifying interaction opens some interesting possibilities. One of the more intriguing ideas is the ability to create virtual personal work areas. We originally envisioned DiamondTouch as a method to allow group collaboration on a common surface, but in practice, individuals will sometimes want to "break away" to briefly address some subset of the problem, and then wish to integrate their result into the whole. When these situations arise, DiamondTouch can create a virtual personal work area in front of the appropriate user that only responds to that user. The user can be manipulating objects in this space, without impacting the larger work effort of other users but for the loss of some table space. Since these virtual personal work areas are software defined, they can be created and destroyed on the fly, in any shape as desired.

The concept of virtual personal work areas can be extended to special "privileged objects". A privileged object is an icon that allows only certain classes of users to perform certain operations with that object. For example, a plumber and an electrician may be viewing the same house plan, but only the plumber can modify the pipes and only the electrician can modify the wiring.

DiamondTouch's capability of providing public and private spaces is the input dual of "Single Display Privacyware" [20], which does the same thing with displayed output. Meshing these two technologies could provide some interesting user interface abilities. We are doing research into public/private display systems here at MERL and plan to experiment with a combination of these and DiamondTouch.

Undoubtedly, more new and interesting applications will arise as we gain experience with more and larger DiamondTouch devices.

ACKNOWLEDGMENTS

The authors would like to thank Joe Marks and Kathy Ryall of MERL for both motivating this work, and encouraging us to publish in this forum.

REFERENCES

1. Anderson, Anderson, Lesh, Marks, Mirtich, Ratajczak and Ryall, *Human-Guided Simple Search* in Proceed-

Shenzhen Huiding Tech. Co., Ltd. - Exhibit 1006

ings of AAAI 2000, July 30–August 3, 2000. Austin, TX, USA.

2. Buxton, W., Hill, R. and Rowley, P., *Issues and Techniques in Touch-Sensitive Tablet Input* in Proceedings of Siggraph '85 (July 22-26, San Francisco), ACM/Siggraph, 1985, pp. 215–224.

3. Inkpen, K., McGrenere, J., Booth, K. S., and Klawe, M., *Turn-Taking Protocols for Mouse-Driven Collaborative Environments* in Proceedings of Graphics Interface '97, Kelowna, BC, May 1997, pp. 138–145.

4. Baxter, L. *Capacitive Sensors Design and Applications*, IEEE Press, Piscataway, NJ, USA, 1997.

5. Zimmerman, T. G., *Personal Area Networks: Near-field intrabody communication* in IBM Systems Journal, vol. 35, nos. 3&4, 1996, pp. 609–617.

6. Lee, S. K., Buxton, W. and Smith, K. C., *A Multi-Touch Three Dimensional Touch-Sensitive Tablet* in Proceedings of CHI '85 (April 1985), ACM/SIGCHI, NY, 1985, pp. 21–25.

7. Glisic, S. and Vucetic, B. *Spread Spectrum CDMA Systems for Wireless Communications*, Artech House, Norwood, MA, USA, 1997, pp. 340–341.

8. Dixon, R. *Spread Spectrum Systems*, 2^{nd} edition, Wiley-Interscience, NY, USA, 1984.

9. GML1000 is a copper clad laminate designed for use in antennas and high frequency circuits requiring low loss. It is available from GIL Technologies of Collierville, TN USA. `http://www.gilam.com`

10. The Mimio electronic white board. `http://www.mimio.com`

11. The eBeam Presenter. `http://www.e-beam.com`

12. The Wacom Intuos graphics tablet. `http://www.wacom.com`

13. The FingerWorks FingerBoard. `http://www.fingerworks.com`

14. Tactex Smart Fabric Technology. `http://www.tactex.com`

15. Matsushita, N. and Rekimoto, J., *HoloWall: Designing a Finger, Hand, Body and Object Sensitive Wall* in Proceeding of the ACM UIST '97 Symposium on User Interface Software and Technology, 209-210.

16. Strickon, J. and Paradiso, J., *Tracking Hands Above Large Interactive Surfaces with a Low-cost Scanning Laser Rangefinder* in Proceedings of CHI '98 Extended Abstracts, ACM Press, NY, April 1998, pp. 231–232.

17. Zimmerman, T., Smith, J., Paradiso, J., Allport, D. and Gershenfeld, N. *Applying Electric Field Sensing to Human-Computer Interfaces* in Proceedings of CHI '95; ACM Conference on Human Factors in Computing Systems, pp. 280–287.

18. Smith, J. R. *Field Mice: Extracting hand Geometry from electric field measurements* in IBM Systems Journal, vol. 35, nos. 3&4, 1996, pp. 587–608.

19. Smith, J., White, T., Dodge, C., Paradiso, J., and Gershenfeld, N. *Electric Field Sensing for Graphical Interfaces* in IEEE Computer Graphics and Applications, vol. 18, no. 3, May-June 1998, pp. 54–60.

20. Shoemaker, G. and Inkpen, K., *Single Display Privacyware* in Proceedings of CHI 2001, pages 522-529, ACM Press, 2001.

Shenzhen Huiding Tech. Co., Ltd. - Exhibit 1006

Code-Division Multiplexing of a Sensor Channel: A Software Implementation

Joshua R. Smith, Christopher Salthouse, and Neil Gershenfeld, *Member, IEEE*

***Abstract*—This paper demonstrates the use of software radio techniques in the context of sensing, rather than communications. It describes code-division multiplexing (CDMA) and time-division multiplexing (TDMA) of a receiver channel in an electric field sensing system. The only hardware used is a front-end gain stage consisting of two opamps and a microcontroller. The modulation and demodulation operations are implemented entirely in the microcontroller software. Multiple coded waveforms are transmitted simultaneously, and induce a combined signal on a single receive electrode. The combined signal, after passing through a single analog front end terminating in an analog-to-digital converter, is separated into the four original component signals by a software demodulation operation.**

The signal-to-noise ratio (SNR) achieved by the code-division multiplexed system given a fixed measurement time is compared to the SNR achieved by a time-division multiplexed implementation given the same total measurement time. The paper also compares the scaling of TDMA and CDMA performance with the number of transmitted channels and the number of demodulated channels.

***Index Terms*—CDMA, electric field sensing, sensing, software radio, spread spectrum.**

I. Introduction

THIS paper demonstrates the use of software radio techniques in the context of sensing, rather than communications. It describes code-division multiplexing (CDMA) and time-division multiplexing (TDMA) of a receiver channel in an electric field sensing system. The demodulation operation is performed entirely in software. Several sensor signals can simultaneously share the same analog front-end hardware, including ADC, because software performs different processing operations on one set of samples to extract several distinct signals. This means that the number of channels that may simultaneously be received is not rigidly fixed by hardware. Additional receiver channels are extra processing steps on the data already being collected. Additional coded waveforms do appear as noise to the other channels (in the CDMA case), or require additional sensing time (for TDMA), so additional channels are not "free," but the number of channels is not fixed by the hardware. As long as one is able to pay the price in either signal-to-noise ratio (SNR) or measurement time, and also in processing time, additional channels may be added. Furthermore, the software receiver readily changes which particular channels it is demodulating.

The work is set in the context of electric field sensing, which is introduced below, but the same principles could be applied in virtually any sensing or measurement system in which the quantity being sensed is modulated by a carrier. For example, these techniques could be applied to systems of ultrasound or infrared emitters and detectors.

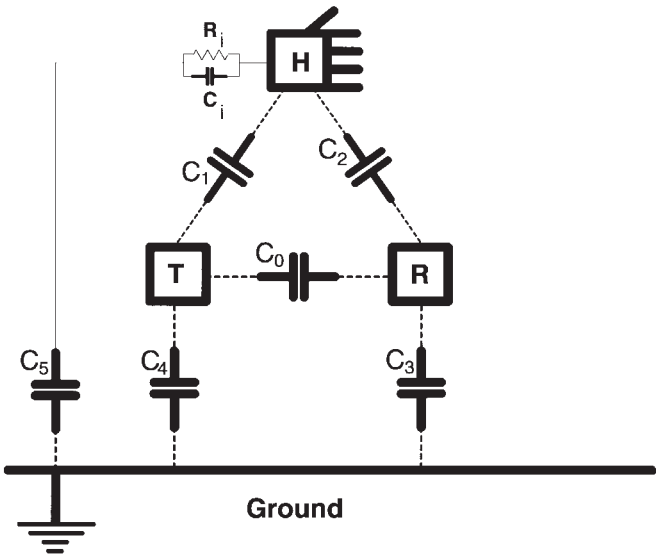


Fig. 1. Lumped circuit model of electric field sensing.

II. Motivation: Electric Field Sensing

The term electric field sensing refers to a family of noncontact methods for measuring the position and orientation of the human body, or parts of the human body such as a hand. Electric field sensing has been used for human–computer interface [1], to make a three-dimensional noncontact mouse [2], for creating new musical instruments (3-D) [3], and in the automotive industry as a solution to the rear-facing infant seat problem.[1]

In a typical implementation of electric field sensing, a low-frequency (from 10–100 kHz) voltage is applied to a transmit electrode (labeled T in Fig. 1), and the displacement current induced at a receiver R is synchronously detected. Fig. 1 shows a lumped circuit model of the electrodes and the body.

Manuscript received September 1997; revised June 19, 1998 and July 31, 1998.

J. R. Smith is with the Escher Laboratories, Cambridge, MA 02142 USA.
C. Salthouse and N. Gershenfeld are with the Physics and Media Group, M.I.T. Media Laboratory, Cambridge, MA 02139 USA.

Publisher Item Identifier S 0733-8716(99)02976-5.

[1] Because the violent inflation of an airbag can injure infants in rear-facing infant seats, it is desirable to sense the orientation of the child and disable the airbag as appropriate [4].

0733–8716/99$10.00 © 1999 IEEE

Shenzhen Huiding Tech. Co., Ltd. - Exhibit 1006

The term capacitive sensing ordinarily refers to measuring the change in the loading of the transmitter as the hand approaches, increasing the value of C_1. There is no distinct receiver in this measurement, so C_1 is the only significant capacitance in the problem. This type of measurement is called a *loading mode* measurement.

But the other current pathways in the diagram suggest other measurement techniques. In transmit mode, the transmitter is coupled strongly to the body—C_1 is very large—and the body is essentially at the potential of the transmitter. As the body approaches the receiver, the value of C_2 (and C_0—the two are not distinct in this mode) increase, and the received signal increases.

Shunt mode measurements are most relevant to this paper. In the shunt mode regime, C_0, C_1, and C_2 are of the same order of magnitude. As the hand approaches the transmitter and receiver, C_1 increases and C_0 decreases, leading to a drop in received current: the displacement current that had been flowing to the receiver is shunted by the hand to ground (hence, the term shunt mode). The sensed signal is defined to be the magnitude of the decrease in received current as the hand moves in from infinity. In other words, one measures a baseline received current when the hand is at infinity, and then subtracts later readings from this baseline. Thus, when the hand is at infinity, the signal is zero, and as the hand approaches the sensor, the signal increases.

With n ordinary capacitive sensors (loading mode), one can collect n numbers. These n numbers turn out to be the diagonal of the capacitance matrix for the system of electrodes. In shunt mode, one measures the $n(n-1)$ off-diagonal elements.[2]

As the size of the electrode array grows, it becomes possible to infer more about the geometry of the hand or other body parts—as n gets large (say, above 10), a kind of fast, cheap, low resolution 3-D imaging becomes possible [5]. However, the large amounts of data are not without a cost. If one were to measure sequentially each value of the capacitance matrix, the time required would be $O(n^2)$. Fortunately, it is possible to make all of the receive measurements for a single transmitter simultaneously. This brings the measurement time down to $O(n)$. One might expect the measurement time to be constant rather than linear since all of the measurements are being made simultaneously. However, as will be explained in the section on resource scaling, the simultaneous measurements interfere with one another, leading to linear rather than constant scaling. But before the scaling is considered in more detail, the basics of code-division multiplexing will be reviewed.

III. Direct-Sequence Spread-Spectrum and Code-Division Multiplexing

In direct-sequence spread spectrum [6], [7], the signal is modulated with a pseudorandom carrier, usually generated by a maximum length linear feedback shift register (LFSR). With code-division multiple access (CDMA), multiple users share the same physical channel by choosing different coded waveforms. Another common channel-sharing technique is time-division multiple access, in which transmitters avoid transmitting simultaneously.

The simple implementation of direct sequence spread spectrum for electric field sensing can be understood in terms of linear algebra. Each measurement is made using a single short pseudorandom measurement burst, during which the hand is assumed to be stationary.

If the pseudorandom carrier signal for transmitter i at time t is $\phi_i(t)$, then the signal received on electrode j, as modified by the capacitance matrix to be measured, is

$$R_{ij}(t) = C_{ij}\phi_i(t) + N_{ij}(t)$$

where C_{ij} is a constant because the hand geometry, and therefore the capacitance matrix, are assumed to be static on the time scale of a sensing burst, and $N_{ij}(t)$ is noise. The noise is indexed by the transmitter and receiver because, for each demodulation operation, the signal from the other transmitters appears as noise. Thus, the noise depends not only on the receiver, but also on which transmitter is being demodulated.

In the ideal case, the transmitted waveforms would be orthogonal to one another, so that channels do not interfere

$$\langle \phi_i, \phi_j \rangle = \frac{1}{s}\sum_{t=1}^{s} \phi_i(t)\phi_j(t) = G^2\delta_{ij}$$

where s is the number of chips in a burst and G^2 is the average power per chip. One can view time division multiplexing as a case in which the carriers do not overlap, and thus satisfy this orthogonality condition exactly.

In CDMA systems, there are nonzero cross correlations between different code sequences. This can be a serious problem in a communications scenario in which receivers may spuriously lock onto the wrong code sequence. However, in the sensing application, there is no synchronization problem because the transmitter and receiver are on the same circuit board, so the only problem is a decrease in SNR due to interference between the channels.

It would be best if the basis functions were also orthogonal to the ambient noise N. In reality, they are not completely orthogonal to N; if they were, one could sense using arbitrarily little energy or time. Since the noise is uncorrelated with the carrier, then by the law of large numbers, the fluctuations around zero of the inner product of the carrier and the noise are on the scale of $1/\sqrt{s}$, where s is the number of samples

$$\langle \phi_i, N \rangle = \frac{1}{s}\sum_{t=1}^{s} \phi_i(t)N(t) \approx 0 \pm \frac{1}{\sqrt{s}}.$$

To measure an entry in the capacitance matrix, form the inner product of the received signal R_{ij} with the transmitted signal ϕ_i

$$D_{ij} = \langle R_{ij}, \phi_i \rangle = \frac{1}{s}\sum_{t=1}^{s} R_{ij}(t)\phi_i(t) = G^2C_{ij} \pm \frac{1}{\sqrt{s}}. \quad (1)$$

[2] Because the capacitance matrix is symmetrical, there are ideally only $(1/2)n(n-1)$ distinct values. In practice, apparent deviations from symmetry can be used to calibrate the measurement system.

Shenzhen Huiding Tech. Co., Ltd. - Exhibit 1006

IV. Resource Scaling

With the code-division sensor multiplexing techniques explored in this paper, one might argue that it should be possible in constant time to collect data that completely characterize the n^2 entries in the capacitance matrix. Each transceiver unit would simultaneously transmit its coded carrier, measure the combined signal induced by the other transmitters, and store its measurement samples in memory. The vector of samples in unit $\hat{\imath}$ contains a complete, but encoded, representation of all of the $C_{\hat{\imath}j}$ values.

Of course, the "constant time" figure ignores deviations from orthogonality of the coded waveforms. A simple algebraic argument suggests that the number of samples necessary to maintain orthogonality grows linearly with n. If sinusoids are used instead of pseudorandom sequences, then the length of the measurement vector must be equal to (or greater than) the number of sensor channel amplitudes to be extracted since the DFT matrix is square. Thus, more realistically, one can form a complete but computationally encoded representation of the capacitance matrix using measurement time proportional to n, and storage of n values in each of the n units.

So far, this discussion has ignored the computational operations necessary for unit $\hat{\imath}$ to do signal separation, transforming the raw measurement vector into an explicit representation of the n capacitance values. The naive separation algorithm (for a single rseceiver unit—multiple receivers can process in parallel) requires time mT, where T is the number of samples in the measurement vector and m is the number of channels being demodulated. By the argument from the previous paragraph, T cannot be less than n, and in practice, should be some constant multiple of n. In the case in which one wishes to demodulate all n channels (so that $m = n$), then the naive demodulation algorithm requires n^2 time. (It is natural to wonder whether an n log n fast spread-spectrum demodulation algorithm exists, analogous to the fast Fourier transform, that could be used with coded rather than sinusoidal carriers. A pseudorandom generator with hidden symmetry properties would probably be needed.) The naive algorithm to extract just a small number m of the possible n sensor values would require time mn.

In the time-division multiplexed (TDMA) case, the transmitted carriers are exactly orthogonal to one another since they do not overlap at all. As in the CDMA case, the total measurement time for one unit is proportional to n. Because the carriers are exactly orthogonal, the time required for a single measurement is constant, rather than proportional to n as in the CDMA case. The amount of computation required to demodulate TDMA is also proportional to n. Thus, in the limit in which all possible measured values are actually demodulated, TDMA appears to have an advantage, requiring n rather than n^2 or n log n time. In the limit in which just a few of the possible sensor values are extracted, the algorithms scale similarly since TDMA still requires linear measurement time, and CDMA's processing time becomes linear instead of quadratic.

In the practical examples discussed in this paper, there were four transmitters and one receiver (rather than measuring the full 5×5 capacitance matrix of this five-electrode system), so m was four. The theoretical discussion above considers the measurement and processing time required to achieve the same SNR using software TDMA and CDMA. In the examples, the same total measurement and processing time is allotted to the two schemes, so that a meaningful comparison of the resulting SNR may be made.

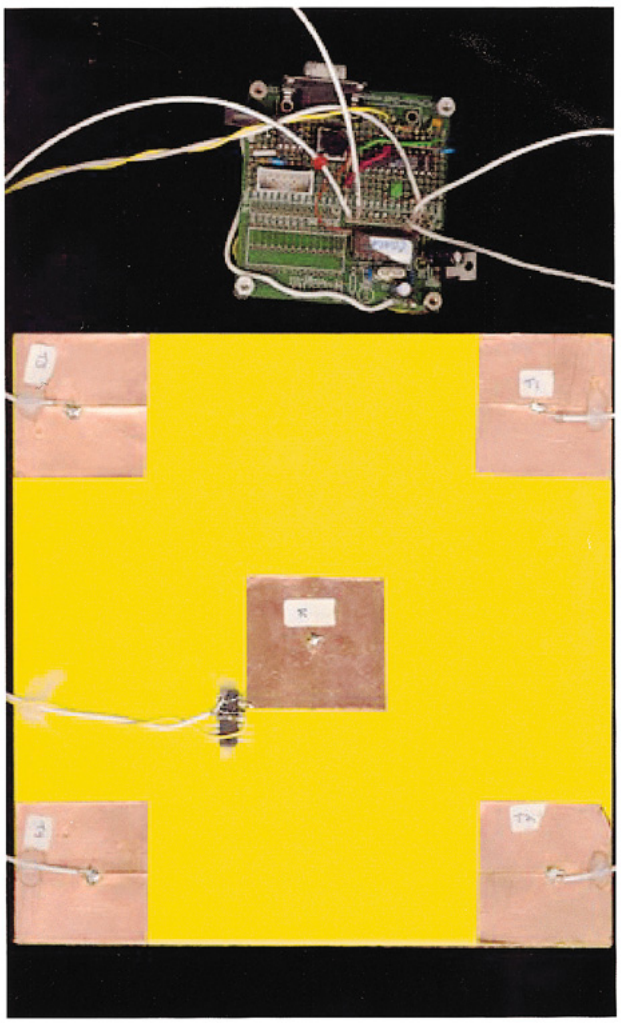


Fig. 2. Hand-wired prototype circuit board used to make measurements, together with electrode array. In the center is a receive electrode, with front-end op-amp attached. In the corners are the transmit electrodes.

The next sections describe the hardware and software used to implement the sensing schemes introduced above.

V. Hardware

The analog front end consists only of a MAX 474 dual opamp. It is configured as a transimpedance amplifier with a 1M resistor and 22 pF capacitor in its feedback network, followed by an inverting voltage gain stage with a 10K input resistor and 100K feedback resistor, for a gain of 10. Because the opamp uses a single supply (5 V), but the received signals are bipolar (positive and negative), 2.5 V was used as analog ground. The amplified signals are read by the analog-to-digital converter on the PIC16C71 microcontroller. The PIC transmits data through a Maxim MAX233 RS-232 transceiver to a host computer for display and analysis. Fig. 2 shows the

Shenzhen Huiding Tech. Co., Ltd. - Exhibit 1006

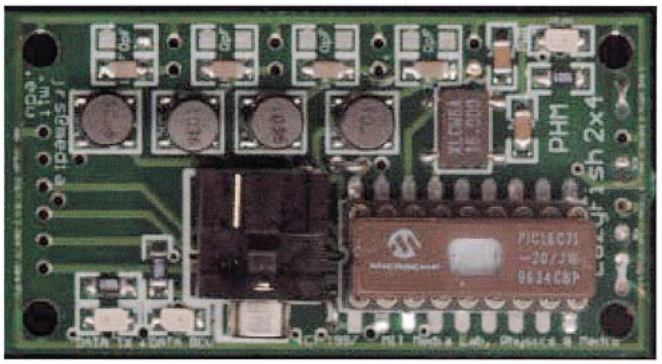


Fig. 3. Later printed circuit board implementation that supports four transmit and two receive channels.

hand-wired prototype board used to make the measurements described in this paper, along with the electrodes. Fig. 3 shows a later printed circuit board implementation that supports four transmit and two receive channels.

VI. Software Demodulation

If the gain variable G from Section III is unity, then the multiplications in the inner product operation described in Section III become additions and subtractions. Performing the demodulation in software requires an accumulation variable in which to store the value of each inner product as it is being calculated. When the first transmitter is high, the processor adds the current ADC value to the first accumulator; if the second transmitter is low, the processor subtracts that same ADC value from the second accumulator. The same ADC value is operated upon differently for each of the demodulation calculations. The addition operation can be thought of as a multiplication by +1 followed by addition to the accumulator; the subtraction is a multiplication by -1 followed by addition to the accumulator. Thus, the operation just described effectively takes the inner product of a vector of samples with a vector representing a transmitted waveform.

An 8-bit LFSR was used, with taps at bits 3, 4, 5, and 7 (counting from zero). This set of taps is known to be maximal [8]. The C code fragment below calculates the four LFSR's, and then sets the states of the transmit pins accordingly.

```
for(k = 0; k < 3;  k++) { // k indexes the 4 LFSRs
  low = 0;
  if(lfsr[k]&8) // tap at bit 3
    low++;  // each addition performs
            // XOR on low bit of low
  if(lfsr[k]&16) // tap at bit 4 low++;
  if(lfsr[k]&32) // tap at bit 5 low++;
  if(lfsr[k]&128) // tap at bit 7 low++;
  low&= 1;  // keep only the low bit
  lfsr[k] <<= 1;  // shift register up to make
                  // room for new bit
  lfsr[k]|= low;  // or new bit in
}
```

```
OUTPUT_BIT(TX0, lfsr[0]&1);  // Transmit according
                             // to LFSR states
OUTPUT_BIT(TX1, lfsr[1]&1);
OUTPUT_BIT(TX2, lfsr[2]&1);
OUTPUT_BIT(TX3, lfsr[3]&1);
```

The variable `lfsr` is an array of four bytes. Each byte in the array represents the state of one LFSR. The variable `low` also holds a byte. It is used as temporary storage to calculate the new value of the LFSR's low bit, which must be set to the sum modulo 2 of the current "tap" bits. The value of the least significant bit of `low` contains the appropriate modulo 2 sum after the compare and increment operations above. Its LSB is then masked off and ORed into the low bit of `lfsr`.

The next code fragment performs the demodulation operation. Each value returned by the ADC is operated upon differently for each channel, as specified by the appropriate LFSR.

```
meas = READ_ADC();  // get sample
for(k = 0; k < 3;k++) {
  if(lfsr[k]&1){ // check LFSR state
    next = accuml[k];  // keep backup of low
                       // byte of accum
    accuml[k]+= meas;  // add measured val to accum
    if(accuml[k] < next)accumh[k]++;
    // if overflow, then carry
  }
  else {
    next = accuml[k];
    accuml[k]-= meas;
    // subtract measured valfrom accum
    if(accuml[k] > next)accumh[k]--;
    // carry if necessary
  }
}
```

On the host computer, the final sensor value is found by dividing the accumulated value (`accumh*256 + accuml`) by s, the number of samples taken, as in (1). Because of the division by s, the fluctuations diminish as $1/\sqrt{s}$, but the typical magnitude of the sensed value (that is, the mean of the random variable describing the final sensed value) is independent of s.

VII. Results: Comparison with Time Division

The performance of the CDMA and TDMA techniques was compared by measuring four channels in 105 ms. The ADC on the current PIC16C71 can sample at about 40 kHz. Calculating the four LFSR's, performing the ADC, and doing the four demodulation computations, the PIC's chip time was 136 μs or 7.4 kchip/s. To examine the limit in which the processing time is negligible compared to the ADC time, one compares the performance of the CDMA algorithm with a TDMA algorithm generating a 3.7 kHz square wave (7.4 kchip/s). The total

Shenzhen Huiding Tech. Co., Ltd. - Exhibit 1006

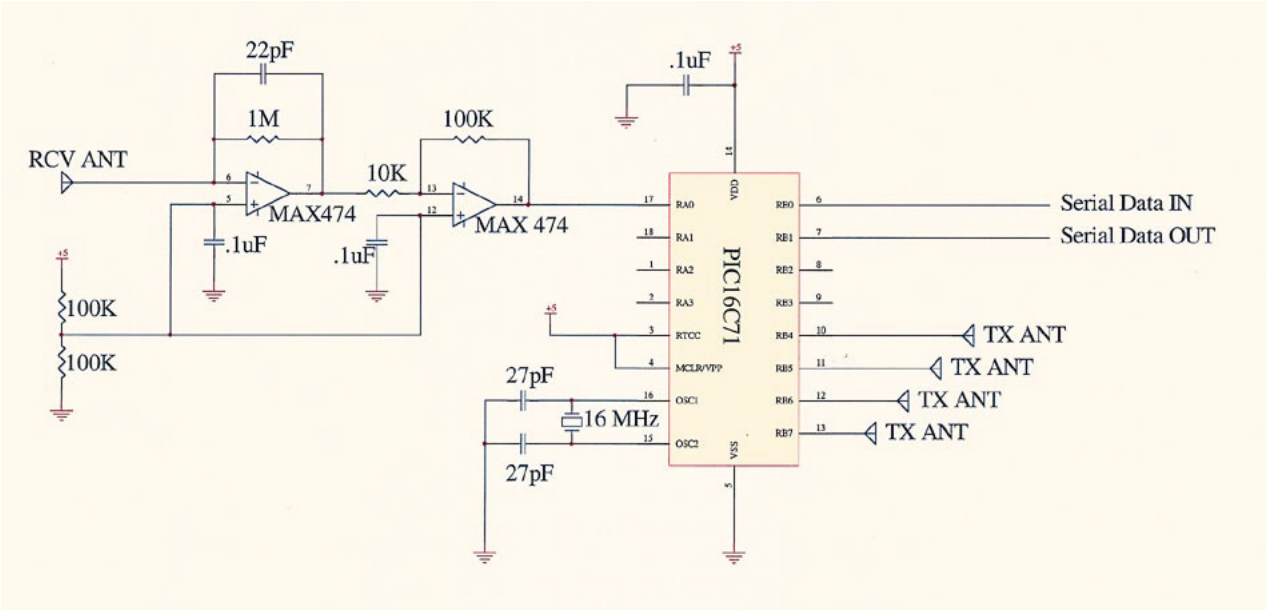


Fig. 4. Analog front end consists of two opamp gain stages. These feed into the ADC built into the PIC. Demodulated values are sent serially to a host computer for display analysis.

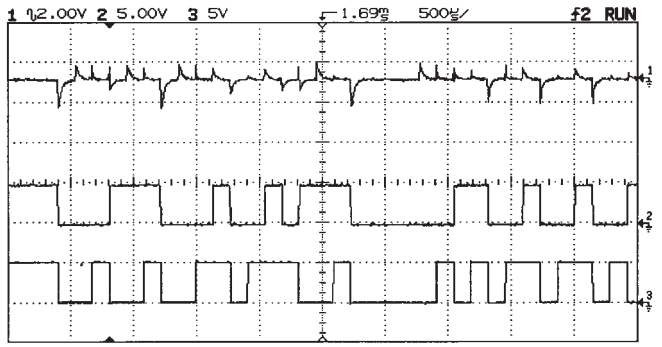


Fig. 5. Top trace: received signal induced by four coded waveforms. Middle and bottom traces: two of the four transmit channels.

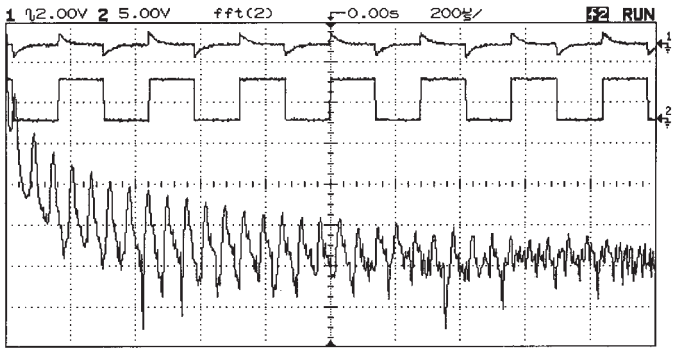


Fig. 6. Top trace: received signal from one transmitted square wave. Middle trace: transmitted square wave. Bottom trace: Fourier transform of transmitted square wave (frequency span: 244.1 kHz; 10 dB/division).

measurement time for the four time multiplexed channels was fixed at 105 ms. An additional comparison was made in which the PIC generated a square wave at top speed (given the time required for analog-to-digital conversion and demodulation calculations), which was 13.5 kHz.

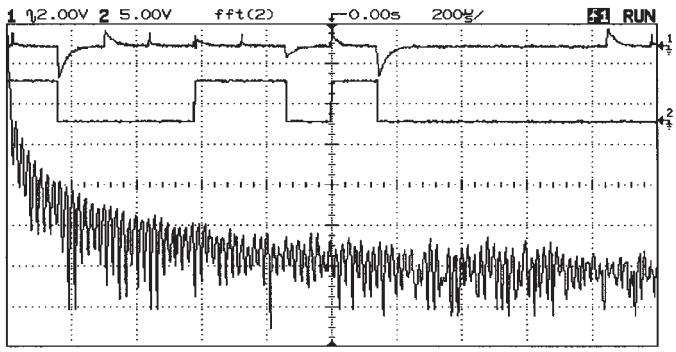


Fig. 7. Top trace: signal received from four coded waveforms. Middle trace: one of the transmit channels. Bottom trace: Fourier transform of one transmit channel (frequency span: 244.1 kHz; 10 dB/division). Notice how much more uniformly the LFSR-generated carrier fills the bandwidth than the square wave of Fig. 6.

To measure the SNR on a particular channel requires calibration of the maximum and minimum observed values as a hand moved from outside the sensor's active region (defined to be zero signal) to the sensor's most sensitive point (maximum signal). With the hand outside the sensitive region, 100 samples were used to calculate the standard deviation. The SNR estimate is an average of five ratios of maximum signal to standard deviation.

When limited to the same chip rate, the SNR for the CDMA and TDMA approaches were as follows: for CDMA, the SNR was 340, or 51 dB, or 8.4 bits; for TDMA, the SNR was 320, or 50 dB, or 8.3 bits. When the TDMA system was operated at the maximum data rate, the SNR increased to 55 dB. This is not surprising. The total output signal power is higher in the higher chip-rate case, and so the SNR should be higher. Thus, in the practical systems of today, the higher computational cost of generating the pseudorandom sequence (which limits the chip rate) diminishes the performance. When the computation

Shenzhen Huiding Tech. Co., Ltd. - Exhibit 1006

time becomes negligible compared to the ADC time, there is little difference between the performance of time-division and code-division multiplexing.

VIII. Conclusion

There are clear advantages for sensing applications of a software-multiplexed analog front end over hardware multiplexing or multiple analog channels. There are minimal requirements for special-purpose hardware and increased flexibility. Channels may be added without hardware modifications.

Comparing the two software channel-sharing schemes, there are no significant performance differences between CDMA and TDMA. There is a slight practical advantage at present to TDMA. The advantage is that TDMA does not require the computation time to calculate the LFSR's. But even with present technology, this difference could be eliminated by a more efficient algorithm.

Although the mean SNR values were the same for CDMA and TDMA, the variance of the SNR's for TDMA was higher. In the TDMA scheme, each single-channel measurement is based on a smaller number of samples. Thus, even though the average channel properties are the same, there are larger fluctuations in the noise levels in the TDMA channel. In CDMA, the several transmit channels appear as noise to one another, but in this sensing application, with its fixed electrode geometry, the level of that self-induced noise is consistent. Since each TDMA sensor value is formed from a smaller number of samples, the TDMA channels are more "bursty." Although the mean SNR is the same for the two modulation techniques, the distribution of SNR measurements is scattered more broadly about the mean for the TDMA technique than for the CDMA technique. For bulk communications purposes, the increased SNR variance does not matter, but for streamed data or sensor values, this is a distinct disadvantage. The performance of a sensor system is only as good as the worst case SNR, measured in short windows of time. During a bulk communications operation like an FTP download, the short time performance of the channel is irrelevant; the relevant figure of merit is the global performance, calculated over the entire time required to complete the operation.

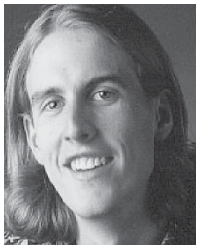
Apart from the subtle SNR variance advantage over TDMA, it is difficult to determine whether the properties of CDMA sensing channels make them significantly more attractive than TDMA channels. The additional flexibility—such as the possibility of determining which sensor channels, or how many, to extract after the raw measurements have been made—might be useful in certain applications. For making multiple measurements with an array of sensors, the more consistent noise levels may make CDMA more attractive than TDMA. In either case, it is useful to process multiple channels of sensor data using a single analog front end, ADC, and DSP software. And while it is common practice to send multiple streams of communications data simultaneously through a single physical channel, it is historically less common (although fundamentally no different) to use a single analog front end and ADC to simultaneously process multiple-sensor channels.

Despite the appeal of CDMA sensing, the most practical implementation of electric field sensing to date, the "LazyFish" board shown in Fig. 3, uses LC resonant circuits to transform the four 5-V square-wave microcontroller outputs into 80-V sinusoidal carriers. These four transmit channels are time-division multiplexed into two analog front ends. The resonators, which provide a significant increase in SNR, are useless with a spread-spectrum excitation. For the practical system, the SNR advantage of resonant transmission tipped the balance decisively in favor of TDMA.

The practical system benefits from one additional application of software radio techniques. The LazyFish performs quadrature demodulation in software, which enables it to be invariant to phase shifts, such as those caused by cable capacitance. In a hardware implementation, quadrature demodulation would require almost doubling the amount of analog hardware—only the front-end amplification could be shared by the in-phase and quadrature channel associated with a particular receiver. Each receiver would require an additional analog multiplier and low-pass filter for the additional quadrature channel. The LazyFish board fits 16 sensing channels (counting quadrature channels) into a 1 in $\times$ 2 in footprint. Its small size would not have been possible without shifting the division of labor from hardware to software.

References

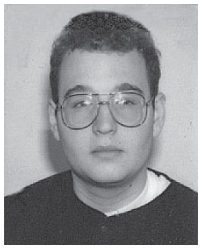
[1] T. G. Zimmerman, J. R. Smith, J. A. Paradiso, D. Allport, and N. Gershenfeld, "Applying electric field sensing to human-computer interfaces," in *CHI'95 Human Factors in Comput. Syst.*., Denver, CO, 1995, pp. 280–287, ACM Press.
[2] J. R. Smith, "Field mice: Extracting hand geometry from electric field measurements," *IBM Syst. J.,* vol. 35, no. 3 and 4, 1996.
[3] J. A. Paradiso and N. Gershenfeld, "Musical applications of electric field sensing," *Comput. Music J.,* 1997.
[4] NEC Automotive Electronics, *Smart Airbags and the Future of Automotive Sensing Technologies from NEC,* World Wide Web page, http://www.nectech.com/auto 1997.
[5] J. R. Smith, "Electric field imaging," Ph.D. dissertation, Massachusetts Inst. Technol., Cambridge, Feb. 1999.
[6] R. C. Dixon, *Spread Spectrum Systems with Commercial Applications.* New York: Wiley, 1994.
[7] M. K. Simon, J. K. Omura, R. A. Scholtz, and B. K. Levitt, *The Spread Spectrum Communications Handbook.* New York: McGraw-Hill, 1994.
[8] P. Horowitz and W. Hill, *The Art of Electronics.* Cambridge, England: Cambridge Univ. Press, 1990.



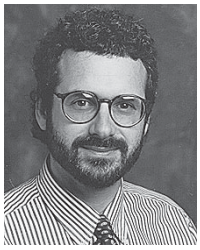
Joshua R. Smith received double B.A. degrees in computer science and philosophy from Williams College, the M.S. degree from the M.I.T. Media Lab, the M.A. degree in physics from Cambridge University and the Ph.D. degree from the M.I.T. Media Lab.

He is Director of Escher Laboratories, Cambridge, MA. He holds, along with N. Gershenfeld, several patents on electric field sensing. While at M.I.T., he co-invented the Pixel Tag family of digital watermarking alrogithms. He has had visiting positions at the Santa Fe Institute, Los Alamos National Lab, Yale University Department of Computer Science, and NASA's Goddard Institute for Space Studies.

Shenzhen Huiding Tech. Co., Ltd. - Exhibit 1006



Christopher Salthouse is an undergraduate majoring in electrical engineering and computer science at M.I.T. He worked in the Physics and Media Group as an Undergraduate Research Opportunity Student.



Neil Gershenfeld (S'80–M'81) received the B.A. degree in physics (with high honors) from Swarthmore College and the Ph.D. degree from Cornell University, studying order–disorder transitions in condensed matter systems.

He is an Associate Professor of Media Arts and Sciences. He leads the Physics and Media Group at the M.I.T. Media Lab, and codirects the Things That Think industrial research consortium with sponsors including HP, Motorola, Microsoft, Fedex, Nike, and Disney. His laboratory investigates the interface between the content of information and its physical representation, from building molecular quantum computers to building musical instruments for collaborations ranging from Yo-Yo Ma to Penn and Teller. Research in his lab has found application in products in markets such as computers, automobiles, and toys. He was a Technician at Bell Labs using lasers for atomic and nuclear physics experiments, and he was a junior fellow of the Harvard Society of Fellows, where he organized an international study hosted by the Santa Fe Institute on forecasting the behavior of complex systems.


Dixon
SPREAD SPECTRUM SYSTEMS
Second Edition
WILEY-
INTERSCIENCE

SPREAD SPECTRUM SYSTEMS

Second Edition

Robert C. Dixon

Shenzhen Huiding Tech. Co., Ltd. - Exhibit 1006

Schnur



SPREAD SPECTRUM SYSTEMS

Shenzhen Huiding Tech. Co., Ltd. - Exhibit 1006

SPREAD SPECTRUM SYSTEMS

Second Edition

Robert C. Dixon

A Wiley-Interscience Publication
JOHN WILEY & SONS
New York • Chichester • Brisbane • Toronto • Singapore

Shenzhen Huiding Tech. Co., Ltd. - Exhibit 1006

Copyright © 1984 by John Wiley & Sons, Inc.

All rights reserved. Published simultaneously in Canada.

Reproduction or translation of any part of this work beyond that permitted by Section 107 or 108 of the 1976 United States Copyright Act without the permission of the copyright owner is unlawful. Requests for permission or further information should be addressed to the Permissions Department, John Wiley & Sons, Inc.

Library of Congress Cataloging in Publication Data:

Dixon, Robert C. (Robert Clyde), 1932–
Spread spectrum systems.

"A Wiley-Interscience publication."
Bibliography: p.
Includes index.

1. Spread spectrum communications. I. Title.
TK5102.5.D55 1984 621.38'043 83-26080
ISBN 0-471-88309-3

Printed in the United States of America

10 9 8 7 6

Shenzhen Huiding Tech. Co., Ltd. - Exhibit 1006

PREFACE TO THE FIRST EDITION

Spread spectrum systems encompass communications, data transmission, message privacy, signal hiding, and position location within their repertoire. These systems are a unique blend of analog (usually RF) and digital disciplines. The coding methods used are the key to providing a spread spectrum system's capabilities.

This book represents an effort to unify at least the terminology used by those working in the spread spectrum field. It is intended to introduce working engineers and students to the philosophy and some of the details of spread spectrum technology. As far as is practical, this book is self-contained. Those who wish to dig deeper, pursue historical development, or investigate rigorous proofs will find in Appendix 3 a comprehensive listing of references in spread spectrum and related areas.

Most of the concepts of spread spectrum systems have been understood for many years, but the components and techniques for building systems capable of reliable operation have been available for a much shorter time. J. P. Costas concluded in 1959 that "for congested-band operation, broadband systems appear to offer a more orderly approach to the problem and a potentially higher average traffic volume than narrow-band systems." At that time, however, transistors and other components were not available to build a reliable, reasonably sized spread spectrum system.

Today components have advanced to the point at which large parts of a spread spectrum system can be contained in a single integrated circuit. A code generator, for instance, which even in 1967 would have required at least 100 discrete transistors, can easily be incorporated in a single small package only slightly larger than one of the transistors. In the future a complete subsystem may well be reduced to one similarly small package. The point is that the use of spread spectrum techniques is no longer constrained by *constituent electronic* components, within limits.

Spread spectrum applications started with the first communicator who set up a scheduled time to send and receive messages. This scheduling may

Shenzhen Huiding Tech. Co., Ltd. - Exhibit 1006

have come about through a desire to avoid heavy traffic (consider, for instance, 10 Indian smoke signalers talking at once) or a desire to avoid interception by surprising the would-be interceptor. The same technique of timing was adapted by radio operators, but they added a new dimension—frequency. The radio operator not only could schedule his transmissions for a time unknown to an interceptor but could transmit at one of many frequencies, which forced the interceptor to "find" his transmission in addition to guessing his schedule. Encoding of messages for error correction and improved time and frequency selection naturally followed.

Modern spread spectrum communications circuits and systems have evolved from just these simple concepts. Both of the most important communications and data systems (frequency hopping and direct sequence) use code-controlled frequency-time keying to avoid interception and minimize interference. These systems have grown in capability and in application since the late 1940s and have been applied today in many areas. Though almost all of the applications to date have been military, commercial equipment is available, and the major test equipment manufacturers have introduced instruments specific to the spread spectrum area.

The material in this book has been gathered from many sources—technical articles, internal memos, military contract reports, private conversations, and my personal experience. References are listed whenever they were available.

The first chapter is an introduction to spread spectrum systems and the reasons for their being. Chapter 2 describes the different types of systems in some detail. Subsystems are described in Chapters 3 through 8, with the emphasis placed on describing advantages and disadvantages of various implementations. Also, successful designs typical of real systems are included. Application of spread spectrum techniques is the subject of Chapter 9. I hope that some ideas for new applications will be generated by this chapter.

The gestation period for this book has spanned a number of years. The idea for it came about in 1963. Since then many people have contributed to its growth. A list of those who have influenced it would fill another book. Edward Guyer of the Northrop Corporation, P. M. Hooten and C. F. White of the Naval Research Laboratories, R. D. Matson and H. J. Schmidt of the Air Force Avionics Laboratories, D. R. Bitzer of D. O. D., and Dr. I. J. Gabelman of Rome Air Development Center all are due special thanks for their help in bringing the book to reality.

To those who insist on strict rigor and abundance of mathematical precedence no apology is given. There is enough of this material already existing to define completely all that is said here many times over. That is precisely the problem I have tried to overcome—hoping to separate enough of the trees from the forest that the usefulness and practical

Shenzhen Huiding Tech. Co., Ltd. - Exhibit 1006

aspects of spread spectrum systems can be seen—simply and in their own context—without the myriad qualifying statements and assumptions that would otherwise be required. There are, listed within the bibliography of this book, enough of the works of those whose world is rigor and precedence to satisfy the needs of their fellows.

Those who, like me, are afflicted with the need for practical applications to secure their understanding have, I hope, found a book useful to them.

ROBERT C. DIXON

Cypress, California
June 1975

Shenzhen Huiding Tech. Co., Ltd. - Exhibit 1006

PREFACE

Since the first edition of this book in 1976, spread spectrum communication techniques have been recognized as a viable method to gain an advantage in interference environments. Many new military-oriented systems have been initiated and some civil systems have been attempted, but few are in regular operation. Some of the new systems are mentioned in Chapter 9.

Some of the recent technical literature regarding spread spectrum systems and techniques are listed in Appendix 2. There has been so much interesting literature generated since 1976 that it is difficult to provide a comprehensive listing. However, it is hoped that enough of the titles in the areas of interest have been included to help the reader narrow the field of search in particular subjects.

I am indebted to many people for their kindness and encouragement, and hope that this somewhat expanded version of *Spread Spectrum Systems* is not a disappointment to them. I am also indebted to my daughter, Theresa Vanderpool, to Linda Nellany, and to Carol Minikus for their diligent and painstaking typing. Any mistakes, misstatements, and misunderstandings included here are strictly my own.

The organization of this edition is the same as the earlier book, with expansion for further interpretation and inclusion of updated material, and a few deletions in the case of superseded information.

The purpose here, as always, is to aid system designers and others to avoid the mistakes I have made in spread spectrum system design and development; and to speed their efforts. If this much is accomplished, then this book can be counted as a success.

ROBERT C. DIXON

Cypress, California
March 1984

Shenzhen Huiding Tech. Co., Ltd. - Exhibit 1006

To

Nancy
David and Suzi
Theresa and Jeff
Robbie
Matthew and Sean

CONTENTS

1 THE WHATS AND WHYS OF SPREAD SPECTRUM SYSTEMS 1

1.1 What is a Spread Spectrum System? 1
1.2 Why Bother? 7
1.3 Process Gain and Jamming Margin, 9

2 SPREAD SPECTRUM TECHNIQUES 13

2.1 Direct Sequence Systems, 15

Characteristics of Direct Sequence Signals, 16
Radio Frequency Bandwidth in Direct Sequence Signals, 21
Direct Sequence Process Gain, 25
Direct Sequence Code and Spectrum Relationships, 27
The Minimum Shift Key Technique, 28

2.2 Frequency Hopping, 28

Characteristics of Frequency Hopping Signals, 29
Determining Frequency Hopping Rate and Number of Frequencies, 34
Avoiding the Repeat Jammer, 40

2.3 Time Hopping, 42

2.4 Pulsed FM (Chirp) Systems, 44

Characteristics of Chirp Signals, 44

2.5 Hybrid Forms

Frequency Hopped/Direct Sequence Modulation, 48
Time-Frequency Hopping, 52
Time Hopping Direct Sequence, 53

Shenzhen Huiding Tech. Co., Ltd. - Exhibit 1006

3 CODING FOR COMMUNICATIONS AND RANGING 56

3.1 Maximal Sequences, 58

Run-Length Distribution, 60
Autocorrelation, 61
Linear Addition Properties, 62
State Exhaustion, 64

3.2 Linear Code Generator Configuration, 64

3.3 Autocorrelation and Cross-correlation of Codes, 71

3.4 Composite Codes, 79

Gold Code Sequence Generators, 79
Syncopated-Register Generators, 82
JPL Ranging Codes, 83

3.5 Bit Rate and Code Length, 84

3.6 Choosing a Linear Code, 86

3.7 Generating High Rate Codes, 91

3.8 Software-Implemented Codes, 97

3.9 Code Selection and Signal Spectra, 98

3.10 Code Baseband Spectra, 103

3.11 Error Detection and Correlation Codes, 104

4 MODULATION AND MODULATORS: GENERATING THE WIDEBAND SIGNAL 108

4.1 Balanced Modulation, 109

Effects of Carrier and Code Rate Spurious (Lack of Suppression), 117
Quadriphase Modulation, 117
Carrier Modulation Trade Offs, 120
Effect of Synch Acquisition, 120
Sidelobe Energy Output, 121

Shenzhen Huiding Tech. Co., Ltd. - Exhibit 1006

4.2 Frequency Synthesis for Spread Spectrum Modulation, 126

Indirect Synthesis, 131
Direct Synthesis, 132
Synthesis from Digital Words, 136

4.3 Sending the Information, 136

Carrier Modulation, 138
Clock Rate Modulation, 139
Code Modification, 141
Digitizing Methods, 142
Frequency Hopping Code Modifiers, 149

5 CORRELATION AND DEMODULATION 153

5.1 Remapping the Spread Spectrum, 153

In-Line Correlation, 154
Heterodyne Correlation, 156
Code Timing Offset Effects on Correlation, 158

5.2 Effect of Nonsynchronous Input Signals, 162

Correlator Output with Interference, 167
Direct Sequence Reaction to Interference, 171
Frequency Hopping Reaction to Interference, 181

5.3 Baseband Recovery, 186

Phase-Lock Loops, 187
Squaring Loops, 191
Costas Loop Demodulators, 193
Frequency Modulation Feedback Demodulators, 196
PDM Demodulation, 198
Frequency Hopping Demodulation, 198
Integrate-and-Dump Filters, 203
The Dehopped Signal, 204
m-ary Detection, 210

6 SYNCHRONIZATION 214

SOURCES OF SYNCHRONIZATION UNCERTAINTY, 214

6.1 Initial Synchronization, 217

The "Sliding" Correlator, 218
Synchronization Preambles, 221

Shenzhen Huiding Tech. Co., Ltd. - Exhibit 1006

Frequency Hop Synchronization, 223
Transmitted-Reference Methods, 224
Universal Timing, 226
Burst Synchronization, 226
Sequential Estimation, 227
Special Coding for Synch Acquisition, 228
Matched-Filter Synchronizers, 229
Synch Recognition, 234

6.2 Tracking, 248

Tau-Dither Tracking, 248
Delay-Lock Tracking, 252
Split-Bit Tracking, 257
Coherent Loss Due to Bandpass Filtering, 258

7 THE RF LINK, 261

7.1 Noise Figure and Cochannel Users, 261

7.2 Dynamic Range and AGC, 265

7.3 The Propagation Medium, 272

Line-of-Sight Loss, 272
Absorptive Losses, 273
Differential Phase Delay, 274
Multipath, 275

7.4 Overall Transmitter and Receiver Design, 278

The Transmitter, 279
Power Amplification, 280
VSWR, 283
Receiver RF Considerations, 283
Receiver Signal Handling Capacity, 284
Wideband Front Ends, 284
The Ideal RF Section, 285
Bandwidth and Phase-Shift Effects, 288

8 NAVIGATING WITH SPREAD SPECTRUM SYSTEMS 291

8.1 Ranging Techniques, 291

Tone Ranging, 295
Sources of Range Error, 296

Shenzhen Huiding Tech. Co., Ltd. - Exhibit 1006

Frequency Hopping Range Measurement, 298
More on the Selection of a Clock Rate, 298
Selecting the Ranging Code, 300
Hybrid-Ranging System, 301

8.2 Direction Finding, 306

Special Antennas, 306

9 APPLICATIONS OF SPREAD SPECTRUM METHODS 313

Space Systems, 313
Avionics Systems, 325
Test Systems and Equipment, 330
Message Protection, 334
Position Location, 334
Real Systems, 335
A Final Word, 335

APPENDIX 1 GLOSSARY OF TERMS 336

APPENDIX 2 BIBLIOGRAPHY ON SPREAD SPECTRUM SYSTEMS AND RELATED TECHNOLOGY 342

APPENDIX 3 EQUIVALENCE OF SIMPLE AND MODULAR SEQUENCES 388

APPENDIX 4 MULTIPLICATION OF DIRECT SEQUENCE SIGNALS 390

APPENDIX 5 LINEAR CODE SEQUENCE VULNERABILITY 392

APPENDIX 6 THE RELATION BETWEEN ω_n AND $\omega_{3\,dB}$ 398

APPENDIX 7 GOLD CODE SELECTION 403

ANSWERS TO PROBLEMS 406

INDEX 419

Shenzhen Huiding Tech. Co., Ltd. - Exhibit 1006

SPREAD SPECTRUM SYSTEMS

Shenzhen Huiding Tech. Co., Ltd. - Exhibit 1006

1

THE WHAT AND WHYS OF SPREAD SPECTRUM SYSTEMS

Spread spectrum techniques, applied in recent years, have produced results in communications, navigation, and test systems that are not possible with standard signal formats. In many applications the advent of high-speed transistors and/or integrated circuits was the key to practical-sized-and-powered equipment based on spread spectrum modulation. But what is a spread spectrum system? What are the advantages of spread spectrum modulation? To be sure, there are also disadvantages, but what are they?

These questions and others are posed in this chapter and in those that follow. It is hoped that the reader will find the answers he or she needs in a useful form.

1.1 WHAT IS A SPREAD SPECTRUM SYSTEM?

Before we attempt to define a spread spectrum system, let us be sure that we understand what is meant by a spectrum. Every transmitting or modulating system has a characteristic signature that includes not only the frequency at which the signal is centered, but also the bandwidth of the signal when modulated by the intended signaling waveform. A spectrum, as we speak of it here, is the frequency-domain[1703] representation of the signal and, for our purposes, especially the modulated signal. We most often see signals presented in the time domain (that is, as functions of time). Any signal, however, can also be presented in the frequency domain, and transforms (mathematical operators) are available for converting frequency- or time-domain functions from one domain to the other and back again. The most basic of these operators is the Fourier transform, for which the relationship between the time and

Shenzhen Huiding Tech. Co., Ltd. - Exhibit 1006

frequency domains is defined by the pair of integrals

$$F(f) = \int_{-\infty}^{\infty} f(t) \exp -j\omega t \, dt$$

which transforms a known function of time to a function of frequency, and

$$f(t) = \int_{-\infty}^{\infty} F(f) \exp j\omega t \, df$$

which performs the inverse operation.

Fourier transforms do not exist for some functions because they require the existence of the integral

$$\int_{-\infty}^{\infty} f(t) \, dt$$

Therefore discontinuous signals must often be transformed by use of the Laplace integral

$$L(s) = \int_{0}^{\infty} f(t) \exp -st \, dt$$

Tables of Fourier and Laplace transform pairs for many functions have been generated and well documented (e.g., see 1714 and 1716).

Figure 1-1 illustrates some of the Fourier transforms that are most important in our considerations of spread spectrum systems. For example, we will be interested in the spectra of carriers modulated by pseudorandom binary data streams. Also of some interest will be the spectra of frequency hopped carriers—especially where those carriers are to be used in multiple-access applications, and it is necessary to restrict any interference between mutual users of the same band of frequencies. Note that the frequency spectrum produced by modulation with a square pulse is a $(\sin x)/x$ function, while modulation having a $(\sin x)/x$ envelope produces a square spectrum. Other spectra that will be of special interest to us are those that are produced by triangular or trapezoidal envelopes and the Gaussian-shaped pulse. Still others will be introduced in the following chapters.

Even as an oscilloscope is a window in the time domain for observing signal waveforms, so is a spectrum analyzer a window in the frequency domain. The many spectrum presentations in this book are almost all spectrum analyzer representations, generated by sweeping a filter across

Shenzhen Huiding Tech. Co., Ltd. - Exhibit 1006

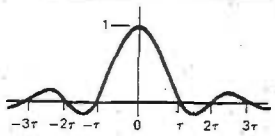
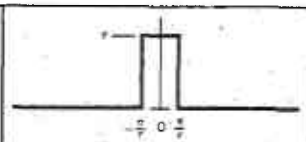
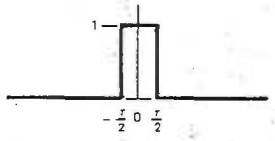
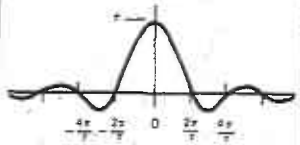
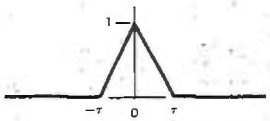
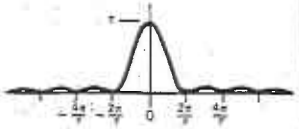
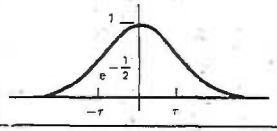
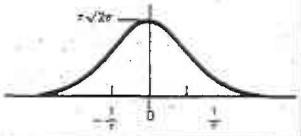
	Time function		Frequency function		
$\sin x$ x Envelope		$f(t) = \dfrac{\sin(\pi t/\tau)}{\pi t/\tau}$	$F(\omega) = \begin{cases} \tau, \lvert\omega\rvert < \pi/\tau \\ o, \lvert\omega\rvert > \pi/\tau \end{cases}$		Rectangular frequency spectrum
Rectangular envelope		$f(t) = \begin{cases} 1, \lvert t\rvert < \tau/2 \\ o, \lvert t\rvert > \tau/2 \end{cases}$	$F(\omega) = \tau \dfrac{\sin(\omega\tau/2)}{\omega\tau/2}$		$\dfrac{\sin x}{x}$ Frequency spectrum
Triangular envelope		$f(t) = \begin{cases} 1 - \lvert t\rvert/\tau, \lvert t\rvert < \tau \\ o, \lvert t\rvert > \tau \end{cases}$	$F(\omega) = \tau \dfrac{\sin^2(\omega\tau/2)}{\omega\tau/2^2}$		$\left(\dfrac{\sin x}{x}\right)^2$ Frequency spectrum
Gaussian envelope		$f(t) = e^{-(t/\tau)^2/2}$	$F(\omega) = \tau\sqrt{2\pi}\, e^{-(\tau\omega)^2/2}$		Gaussian frequency spectrum

Figure 1.1 Four important Fourier transforms and their corresponding time and frequency functions.

Shenzhen Huiding Tech. Co., Ltd. - Exhibit 1006

the band of interest and detecting the power falling within the filter as it is swept. This power level is then plotted on an oscilloscope. All spectra referred to are power spectra.

Literally, a spread spectrum system is one in which the transmitted signal is spread over a wide frequency band, much wider, in fact, than the minimum bandwidth required to transmit the information being sent. A voice signal, for example, can be sent with amplitude modulation in a bandwidth only twice that of the information itself. Other forms of modulation, such as low deviation FM or single sideband AM, also permit information to be transmitted in a bandwidth comparable to the bandwidth of the information itself. A spread spectrum system, on the other hand, often takes a baseband signal (say a voice channel) with a bandwidth of only a few kilohertz, and distributes it over a band that may be many megahertz wide. This is accomplished by modulating with the information to be sent and with a wideband encoding signal.

The most familiar example of spectrum spreading is seen in conventional frequency modulation in which deviation ratios greater than one are used. Bandwidth required by an FM signal is a function not only of the information bandwidth but of the amount of modulation. As in all other spectrum spreading systems, a signal-to-noise advantage is gained by the modulation and demodulation process. For FM signals this gain advantage (referred to as "process gain") is

$$3\beta^2 \left(\frac{S}{N}\right)_{\text{info}}$$

where β = deviation ratio, or $\Delta f_{\text{carrier}}/f_{\text{modulations}}$
$(S/N)_{\text{info}}$ = signal-to-noise ratio in the baseband or information bandwidth.

Wideband FM could be classified as a spread spectrum technique from the standpoint that the RF spectrum produced is much wider than the transmitted information. In the context of this book, however, only those techniques are of interest in which some signal or operation other than the information being sent is used for broadbanding (or spreading) the transmitted signal.

Three general types of techniques will be accepted here as examples of spread spectrum signaling methods:

1. Modulation of a carrier by a digital code sequence whose bit rate is much higher than the information signal bandwidth. Such systems are called "direct sequence" modulated systems.
2. Carrier frequency shifting in discrete increments in a pattern dictated by a code sequence. These are called "frequency hoppers." The

Shenzhen Huiding Tech. Co., Ltd. - Exhibit 1006

transmitter jumps from frequency to frequency within some predetermined set; the order of frequency usage is determined by a code sequence.

3. Pulsed-FM or "chirp" modulation in which a carrier is swept over a wide band during a given pulse interval.

Closely akin to the frequency hoppers are "time hopping" and "time-frequency hopping" systems whose chief distinguishing feature is that their time of transmission (usually of low duty cycle and short duration) is governed by a code sequence. In time-frequency hoppers it follows that the code sequence determines both the transmitted frequency and the time of transmission.

Figure 1.2 shows frequency spectra typical of direct sequence and frequency-hopping systems. These spectra are often tens to hundreds of megahertz wide, where conventional signals are usually confined to bandwidths in the range of 10–100 kiloHertz.

The basis of spread spectrum technology is expressed by C. E. Shannon in the form of channel capacity:

$$C = W \log_2 \left(1 + \frac{S}{N}\right)$$

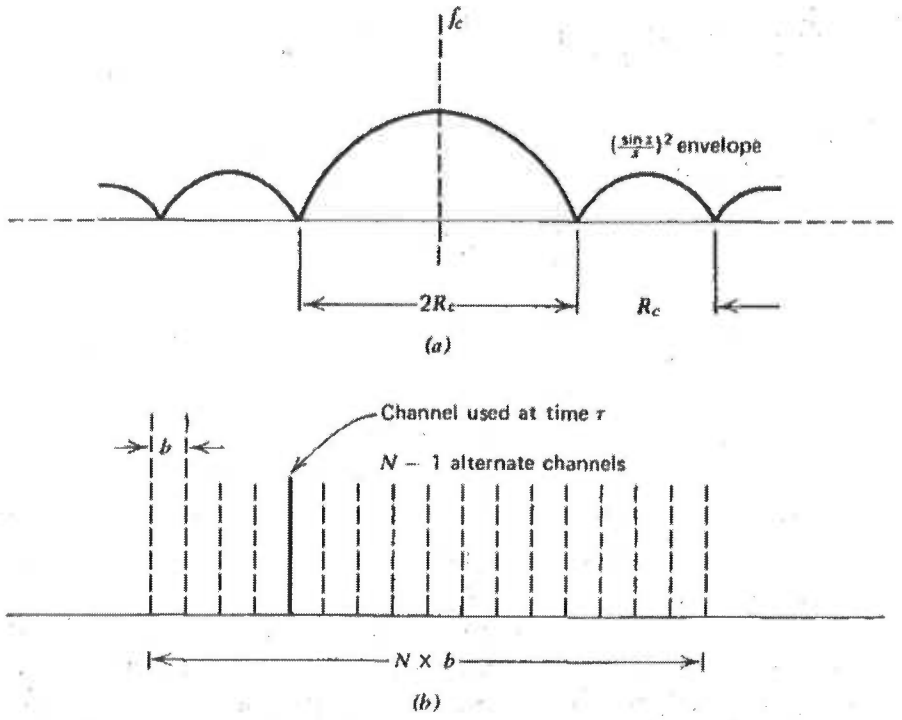


Figure 1.2 Ideal spectra of typical spread spectrum signals: (*a*) direct sequence signal spectrum; (*b*) frequency-hopping signal spectrum.

Shenzhen Huiding Tech. Co., Ltd. - Exhibit 1006

where C = capacity in bits per second,
W = bandwidth in hertz,
N = noise power,
S = signal power.

This equation shows the relationship between the ability of a channel to transfer error-free information, compared with the signal-to-noise ratio existing in the channel, and the bandwidth used to transmit the information.

Letting C be the desired system information rate and changing bases, we find

$$\frac{C}{W} = 1.44 \log_e \left(1 + \frac{S}{N}\right)$$

and for S/N small, say $\leqslant 0.1$ (as one would wish it to be in an antijam system),

$$\frac{C}{W} = 1.44 \frac{S}{N}$$

since

$$\log_e \left(1 + \frac{S}{N}\right) = \frac{S}{N} - \frac{1}{2}\left(\frac{S}{N}\right)^2 + \frac{1}{3}\left(\frac{S}{N}\right)^3 - \frac{1}{4}\left(\frac{S}{N}\right)^4 \cdots \left(-1 < \frac{S}{N} < 1\right)$$

by the logarithmic expansion.

From this equation we find

$$\frac{N}{S} = \frac{1.44W}{C} \approx \frac{W}{C}$$

and

$$W = \frac{NC}{S}$$

thus we see that for any given noise-to-signal ratio we can have a low information-error rate by increasing the bandwidth used to transfer the information; for example, if we want a system to operate in a link in which the interfering noise is 100 times greater than the signal and our information rate 3 kilobits per second (kbps) then our 3-kbps information must be transmitted with a bandwidth of

$$W = \frac{1 \times 3 \times 10^5}{1.44} = 2.08 \times 10^5 \text{ Hz}$$

Incidentally, the information itself may be embedded in the spread spectrum signal by several methods. The most common is that of adding the information to the spectrum-spreading code before its use for spreading modulation. This technique is applicable to any spread spectrum system that uses a code sequence to determine its RF bandwidth (either direct sequence or frequency hopping systems are good candidates). Of course, the information to be sent must be in some digital form because addition to a code sequence involves modulo-2 addition to a binary code. Alternately, information may be used to modulate a carrier before spreading it. This is usually done by some form of angle modulation, for the need in spread spectrum systems is often to output a constant-power RF envelope.

A spread spectrum system, then, must meet two criteria: (1) the transmitted bandwidth is much greater than the bandwidth or rate of the information being sent and, (2) some function other than the information being sent is employed to determine the resulting modulated RF bandwidth.

This is the essence of spread spectrum communications—the art of expanding the bandwidth of a signal, transmitting that expanded signal, and recovering the desired signal by remapping the received spread spectrum into the original information bandwidth. Furthermore, in the process of carrying out this series of bandwidth trades the purpose is to allow the system to deliver error-free information in a noisy signal environment.

1.2 WHY BOTHER?

The first reaction common among those encountering spread spectrum techniques is "why bother?" The answers are varied and seldom the same. In a world beset by too little RF spectrum to satisfy the ever-growing demands of military, commercial, and private users the question "why spread spectrum" must certainly be considered valid, for spread spectrum systems have almost as many reasons for being as they have users.

Some of the properties that may be cited are the following:

1. Selective addressing capability.
2. Code division multiplexing is possible for multiple access.
3. Low-density power spectra for signal hiding.
4. Message screening from eavesdroppers.

Shenzhen Huiding Tech. Co., Ltd. - Exhibit 1006

5. High-resolution ranging.
6. Interference rejection.

These properties come about as a result of the coded signal format and the wide signal bandwidth that results. A single receiver or group of receivers may be addressed by assigning a given reference code to them, whereas others are given a different code. Selective addressing can then be as simple as transmitting the proper code sequence as modulation.

Not all of these characteristics, however, are necessarily available from the same system at the same time. It is somewhat anomalous, for instance,

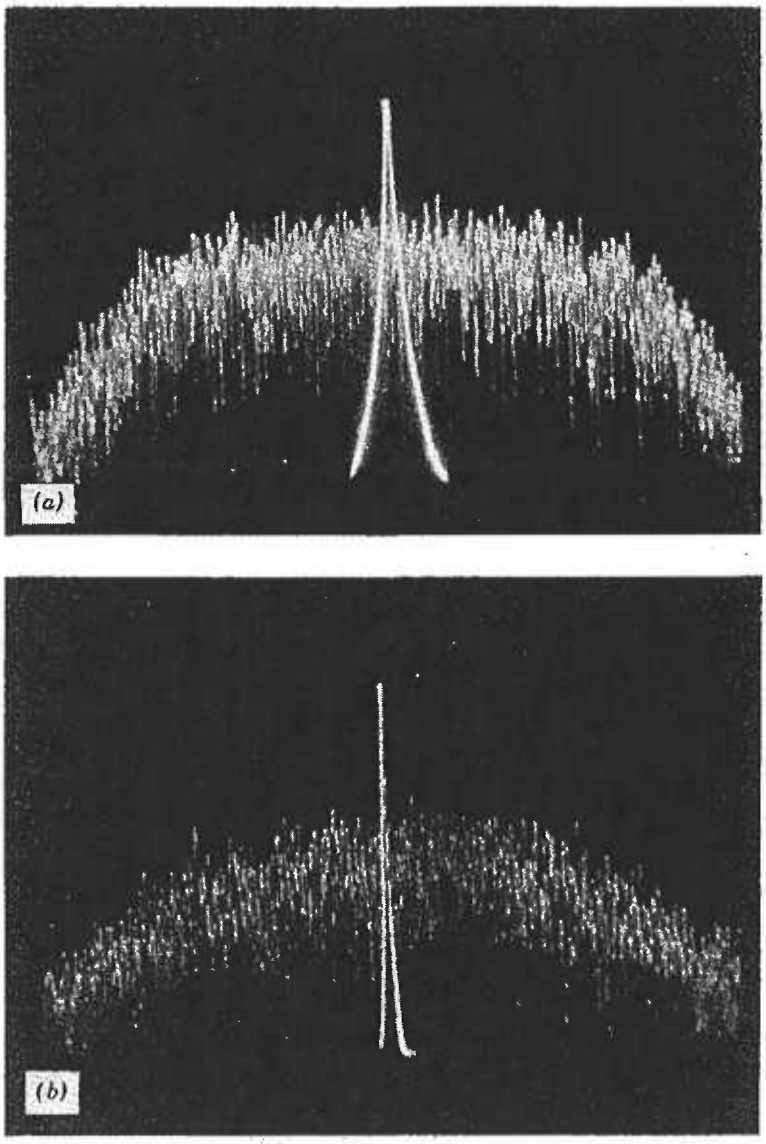


Figure 1.3 Illustration of power density showing equal power spread spectrum and CW signals, for spread spectrum bandwidth of (*a*) 2 MHz (0.88 MHz, 3 dB) and (*b*) 10 MHz (4.4 MHz, 3 dB).

to expect, at the same time, a signal that is easily hidden but can also be received in the face of a large amount of interference. Signal-hiding requirements and inferference rejection are often at odds, but the same system might be used for both by using low-power transmissions when low detectability is desired and high-power transmissions when maximum interference rejection is needed.

When codes are properly chosen for low cross correlation, minimum interference occurs between users, and receivers set to use different codes are reached only by transmitters sending that code. Thus more than one signal can be unambiguously transmitted at the same frequency and at the same time; selective addressing and code-division multiplexing are implemented by the coded modulation format.

Because of the wideband signal spectra generated by code modulation, the power transmitted is low in any narrow region. At any rate, the density of a spread spectrum signal is far less than that of more conventional signals in which all the transmitted power is sent in a band of frequencies commensurate with the baseband information bandwidth. Again, because of the coded signals employed, an eavesdropper cannot casually listen to messages being sent. Though the systems may not be "secure," some conscious effort must be made to decode the messages.

Figure 1.3 illustrates the difference in the power density of continuous-wave and typical spread spectrum signals.

Resolution in ranging is afforded in accordance with the code rates used, and the sequence length determines maximum unambiguous range. Ranging has been the most prominent and certainly the best known use of spread spectrum systems.

1.3 PROCESS GAIN AND JAMMING MARGIN

The most commonly used quantity in spread spectrum systems is that of "process gain," although it must be pointed out that what is usually intended is not process gain but "jamming margin." Process gain is a readily available quantity, if the bandwidth employed in a system is known and the information rate is available. In Section 1.1, we considered Shannon's information-rate theorem, which shows that one can send information without error, if some method can be devised that employs a wide enough bandwidth to transmit the information. The process gain that we consider here is just an embodiment of that theorem, in which the signal is spread, and the process gain produced by the spreading and despreading process is equal to the bandwidth ratio between the information and the RF bandwidth used to send it.

A spread spectrum system develops its process gain in a sequential signal bandwidth spreading and despreading operation. The *transmit* part of the process may be accomplished with any one of the band-

Shenzhen Huiding Tech. Co., Ltd. - Exhibit 1006

spreading modulation methods. Despreading is accomplished by correlating the received spread spectrum signal with a similar local reference signal. When the two signals are matched, the desired signal collapses to its original bandwidth before spreading, whereas any unmatched input is spread by the local reference to its bandwidth or more. A filter then rejects all but the desired narrowband signal; that is, given a desired signal and its interference (atmospheric noise, receiver noise, or jamming), a spread spectrum receiver enhances the signal while suppressing the effects of all other inputs. This process is described in detail in Chapter 2.

The difference in output and input signal-to-noise ratios in any processor is its "process gain." A given processor, for instance, with an input signal-to-noise ratio of 10 dB and an output signal-to-noise ratio of 16 dB would have a process gain of 6 dB.

In spread spectrum processors the process gain available may be estimated by the rule of thumb:

$$\text{process gain} = G_p = \frac{\text{BW}_{\text{RF}}}{R_{\text{info}}}$$

where the RF bandwidth (BW_{RF}) is the bandwidth of the transmitted spread spectrum signal and the information rate (R_{info}) is the data rate in the information baseband channel. This does not mean, however, that a processor can perform when faced with an interfering signal having a power level larger than the desired signal by the amount of the available process gain. Another term, "jamming margin," which expresses the capability of a system to perform in such hostile environments, must be introduced.

Jamming margin is that quantity that is usually intended in the specification of spread spectrum systems, but it is less readily predicted from bandwidth and information-rate information. One can be sure, however, that jamming margin in any given system is always less than the process gain available from that system.

Jamming margin takes into account the requirement for a useful system output signal-to-noise ratio and allows for internal losses; that is,

$$\text{jamming margin} = G_p - \left[L_{\text{sys}} + \left(\frac{S}{N} \right)_{\text{out}} \right] = M_j$$

where L_{sys} = system implementation losses,
$(S/N)_{\text{out}}$ = signal-to-noise ratio at the information output;

for example, a system with 30-dB process gain, minimum $(S/N)_{\text{out}}$ of 10 dB, and L_{sys} of 2 dB would have an 18-dB jamming margin (M_j). It could not be expected to operate with interference more than 18 dB above the desired signal.

Shenzhen Huiding Tech. Co., Ltd. - Exhibit 1006

The "jamming threshold" of a particular system is of interest in determining how well that system will operate in the presence of interference. Consider the following processor model with signal and noise inputs (the noise input includes interference):

$$\left.\begin{matrix}\text{signal in}\\ \text{noise in}\end{matrix}\right\} \left(\frac{S}{N}\right)_{\text{in}} \bullet\!\!\rightarrow \boxed{G_p} \rightarrow \left(\frac{S}{N}\right)_{\text{out}} = \left(\frac{S}{N}\right)_{\text{in}} \times G_p$$

For the region of interest $S \ll N$. Converting to decibels, we have

$$\left(\frac{S}{N}\right)_{\text{out}} (\text{dB}) = \left(\frac{S}{N}\right)_{\text{in}} (\text{dB}) + G_p\,(\text{dB})$$

but

$$\left(\frac{S}{N}\right)_{\text{in}} (\text{dB}) = -\frac{J}{S}(\text{dB})$$

Therefore

$$\left(\frac{S}{N}\right)_{\text{out}} (\text{dB}) = G_p(\text{dB}) - \frac{J}{S}(\text{dB})$$

for the region above the jamming threshold, where the threshold for a particular system is that level for which (see Figure 1.4)

$$\left[\, G_p(\text{dB}) - \frac{J}{S}(\text{dB}) \,\right]_{\text{Ideal}} - \left[\, G_p(\text{dB}) - \frac{J}{S}(\text{dB}) \,\right]_{\text{meas'd}} = 1 \text{ dB}$$

The cause of thresholding lies in such things as tracking loss, nonlinearities, and thresholding of the postcorrelation detector. No system can be designed without a jamming threshold, but with care the threshold point can be placed beyond the normal operating region. All possible thresholding sources would tend to degrade at the same point, for when one part of the system operates at interference levels beyond the others the overall system performance does not improve.

Table 1.1 compares the process gain from spread spectrum processing techniques with that provided by other methods, such as antenna pointing or electronic interference cancellation.

Antenna-cancellation techniques employ the directivity of an antenna to reject a would-be jammer. Such techniques have been used but are not always practical because of positioning restrictions. When geometry is fixed, antenna rejection of interference is limited only by the particular antenna's directivity.

Shenzhen Huiding Tech. Co., Ltd. - Exhibit 1006

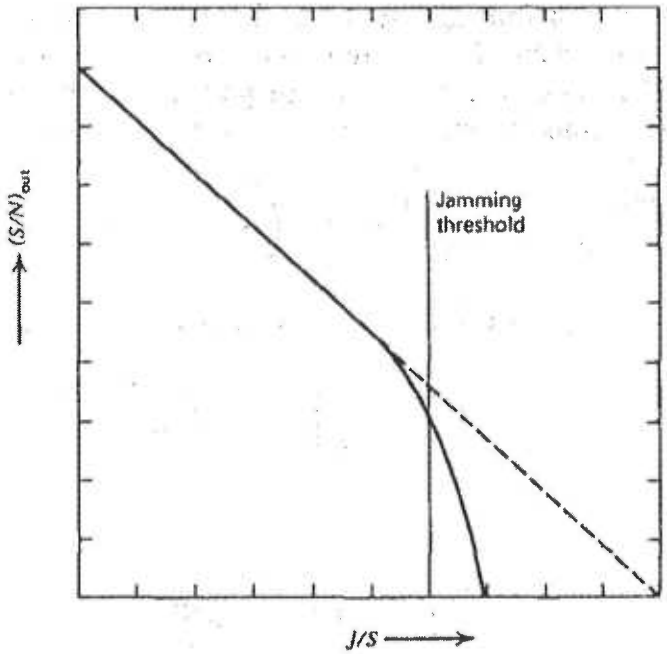


Figure 1.4 Typical process gain curve.

For effective electronic interference cancellation a duplicate of the signal to be rejected must be generated. This replica is then subtracted from the combined interfering and desired signals. The result is a residue consisting of the desired signal only. This technique has proved to be useful but is limited to those situations in which few interfering signals occur (a separate signal simulator and subtractor is required for each signal) and in which relatively noncomplex interfering signals are encountered.

Table 1.1 Comparison of Process Gains Available for Various Techniques, Including Signal Rejection and Cancellation

System	Process Gain
Direct sequence	$\frac{BW_{RF}}{R_{info}} = TW$
Frequency hopping	$\frac{BW_{RF}}{R_{info}} = TW$ = number of frequency choices
Time hopping	$\frac{1}{\text{transmit duty cycle}}$
Chirp	Compression ratio = $\tau\, dF = TW$
Antenna rejection	Antenna gain
Electronic cancellation	Depends on accuracy of replica; sometimes 40 dB
Selective rejection	High but useful only against narrowband interference.

Shenzhen Huiding Tech. Co., Ltd. - Exhibit 1006

Selective rejectors such as notch filters are useful for removing interference signals but are limited to narrowband signals such as CW. Rejection of a wideband signal with a filter could also reject much of the desired signal, which would degrade system operation and net no gain in performance, even though the interference were rejected.

In general, spread spectrum processing offers the most flexible means of providing unwanted signal rejection because it is not necessary to design for rejection of any particular kind of interference and geometric considerations are not normally important. Spread spectrum processing does not, however, offer the highest process gain (or undesired signal rejection) for every situation. The alternatives mentioned here may be combined with spread spectrum techniques to produce a compatible system with the advantages of spread spectrum and other signal-to-noise improving methods.

Conventions in This Book

The following conventions will be employed:

Direct Sequence Bandwidth. All direct sequence signal bandwidths are assumed to be equal to the 3-dB bandwidth of the spectrum. Thus, the bandwidth will vary, depending on the particular type of carrier modulation employed such as biphase, quadriphase, or minimum shift key.

Frequency Hopper Bandwidth. Frequency hoppers are assumed to have BW_{RF} equal to m times the channel bandwidth, where m is the number of frequency channels available.

Information Rate. Information rate is a function of the type of information transferred over the links discussed and is the minimum bit rate necessary for satisfactory reproduction of the information at the receiver. For voice transmission 3 kHz is the analog bandwidth. Data are consistent with the minimum rate sufficient to convey analog signals,* or digital data.

Chip Rate. Chip rate is equivalent to the code generator clock rate, or in frequency-hopping systems, the hop rate.

Postcorrelation Bandwidth. The signal bandwidth following the receiver correlation process is the two-sided information bandwidth produced by the baseband modulating signal or by a frequency hopped carrier.

All other bandwidths are 3-dB bandwidths.

*Data rate representing an analog signal is at least the Nyquist rate, or 2 bits per Hertz. The actual rate depends on the A/D technique used.

Shenzhen Huiding Tech. Co., Ltd. - Exhibit 1006

PROBLEMS

1. Given a requirement for operating in an environment in which an interfering signal is 250 times the desired, how much jamming margin is required?
2. If in the system described above a 10-dB output signal-to-noise ratio is required, what is the minimum process gain allowable?
3. Information rate is 6 kbps. What is the minimum RF bandwidth needed?
4. Assume that a direct sequence approach has been employed. What code rate should be used?
5. How many channels would be required by a frequency hopper for a similar performance?
6. Given that chirp modulation is required and the information rate is 10 kbps, what RF sweep bandwidth is the minimum that would produce a 20-dB process gain?
7. A direct sequence system has a code rate of 1 Mcps (cps = chips per second) and an information rate of 100 kbps. Is it worth it?
8. A frequency hopper has a 5-MHz RF bandwidth available and an information rate of 100 kbps. Comment.
9. How does a chirp system meet the criterion that the RF transmission bandwidth employed is not a function of the information sent?
10. How does a direct sequence system meet the same criterion?
11. Same question for frequency hopping.
12. What is the prime limiting factor in the processing gain of a time-hopping system?

Shenzhen Huiding Tech. Co., Ltd. - Exhibit 1006

2

SPREAD SPECTRUM TECHNIQUES

Several basic spread spectrum techniques available to the communications system designer, are listed in Chapter 1 and described in a general way. This chapter gives detailed descriptions of the various techniques and the signals generated. In addition to the two most important (or at least most prevalent) forms of spread spectrum modulation, other useful techniques such as chirping, time hopping, and various hybrid combinations of modulation forms are described. Each is important in that it has useful application. Curiously enough, there has been little competition between the different techniques. The historical tendency has been to confine each form to a particular field. Chirp modulation, for instance, has been used almost exclusively in radar. Here all are presented together to give the reader a reasonably complete picture of contemporary spread spectrum technology.

2.1 DIRECT SEQUENCE SYSTEMS

Direct sequence (or, to be more exact, directly carrier-modulated, code sequence modulation) systems are the best known and most widely used spread spectrum systems. This is because of their relative simplicity from the standpoint that they do not require a high-speed, fast-settling frequency synthesizer. The JPL ranging technique described in Golomb et al. *Digital Communications with Space Applications*[219] and used in various space applications is a direct sequence approach. Today, direct sequence modulation is being used for communication systems and test systems, and even laboratory test equipment capable of producing a choice of a number of code sequences or operating modes is available. It is reasonable to expect that direct sequence modulation will become a familiar form of modulation in many areas in the foreseeable future. Even now, commercial applications of such systems are being contemplated.

Shenzhen Huiding Tech. Co., Ltd. - Exhibit 1006

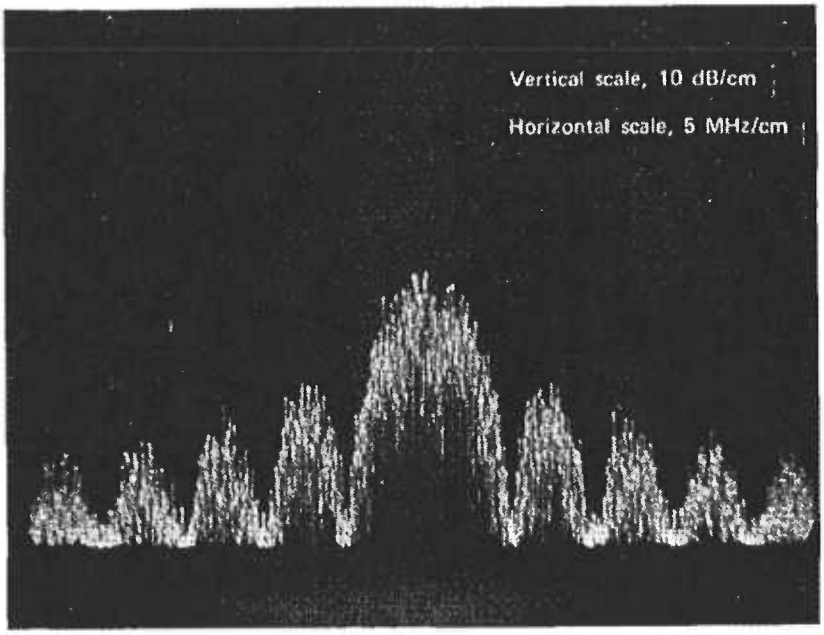


Figure 2.1 Direct sequence spread spectrum signal 180° biphase-modulated by a 5 Mcps code.

Characteristics of Direct Sequence Signals

Direct sequence modulation, as mentioned in Chapter 1, is just exactly that—modulation of a carrier by a code sequence. In the general case, the format may be AM (pulse), FM, or any other amplitude- or angle-modulation form. Very common, however, is 180° biphase phase-shift keying, though the reasons for it may not be immediately obvious. The basic form of direct sequence signal is that produced by a simple, biphase-modulated (PSK) carrier. A spectrum typical of this signal format is shown in Figure 2.1. The main lobe bandwidth (null-to-null) of the signal shown is twice the clock rate of the code sequence used as a modulating signal. Each of the sidelobes has a bandwidth from null-to-null that is equal to the clock rate; that is, if the code sequence being used as a modulating waveform has a 5-Mcps (cps = chips per second) operating rate, the main lobe bandwidth will be 10 MHz and each sidelobe will be 5 MHz wide. This is exactly the case in Figure 2.1.

Typically, the direct sequence biphase modulator has the form shown in Figure 2.2. A balanced mixer whose inputs are a code sequence and an RF carrier operates as the biphase modulator. In the time domain the biphase-modulated carrier looks like the signal shown in Figure 2.3. There the carrier is transmitted with one phase when the code sequence is a "one" and a 180° phase shift when the code sequence is a "zero." In the usual biphase-modulated system, which phase is of little consequence. It is worthy of note that, although other modulation forms such as PAM

Shenzhen Huiding Tech. Co., Ltd. - Exhibit 1006

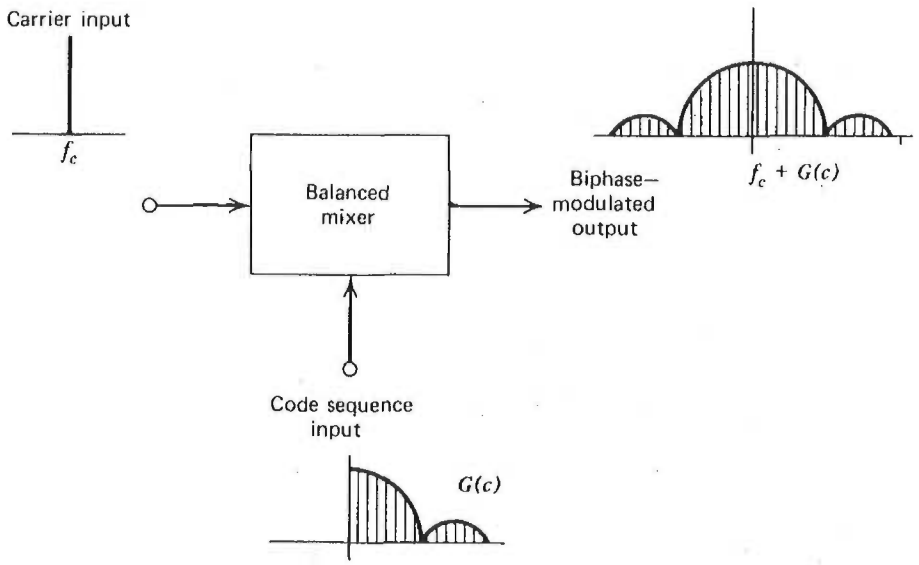


Figure 2.2 Direct sequence modulator (biphase).

(pulse-amplitude modulation) could be used, balanced* modulation is the most common in direct sequence systems. This is true for several reasons:

1. The suppressed carrier produced is difficult to detect without resorting to somewhat sophisticated methods. Figure 2.4 shows a typical direct sequence signal (as does Figure 2.1 in less detail) with carrier suppression. It is obvious that a conventional receiver would not be useful for detecting the carrier here because it is well below the level of the "noise" produced by the code modulation. For comparison, Figure 2.5 shows the same modulator but without carrier balance; therefore, the carrier is no longer suppressed.
2. More power is available for sending useful information because the transmitter power is used to send only the code-produced signal.
3. The signal has a constant envelope level so that transmitted power efficiency is maximized for the bandwidth used. PAM modulation in which a carrier would be pulse modulated by a code as in Figure 2.6 is acceptable; it produces a similar $[(\sin x)/x]^2$ power spectrum but lacks the same effective power at the receiver. Thus for the same range of operation higher peak power would be necessary.

*Biphase-balanced modulation, for example, is well adapted to code modulation in that one carrier phase may be transmitted for a one in the code and the opposite phase for a zero. This produces a signal $A \cos \omega_c t \cos \omega_m t = A \cos (\omega_c \pm \omega_m) t$ after filtering in which the carrier term is absent. Balanced modulation is discussed in detail in Chapter 4.

Shenzhen Huiding Tech. Co., Ltd. - Exhibit 1006

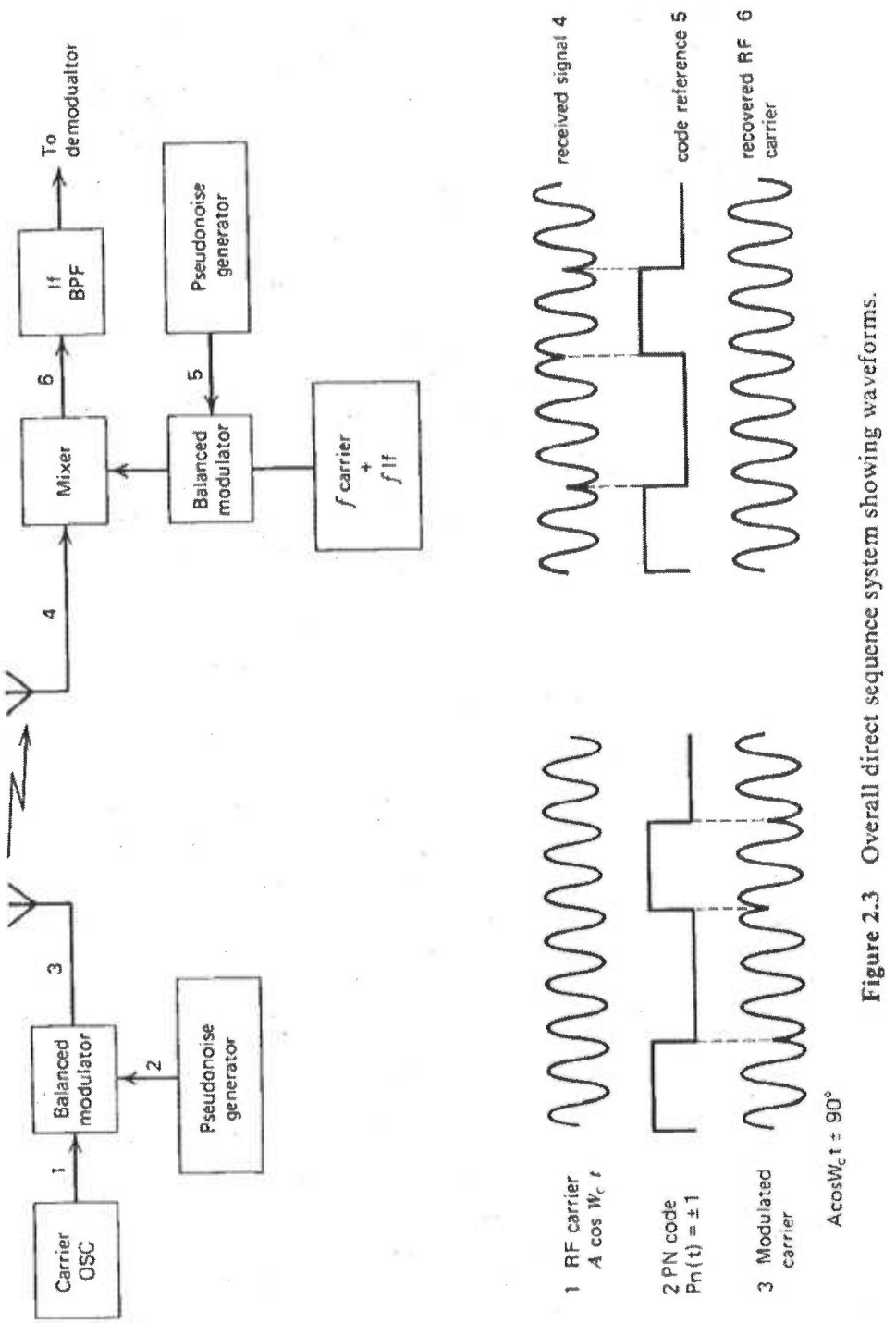


Figure 2.3 Overall direct sequence system showing waveforms.

Shenzhen Huiding Tech. Co., Ltd. - Exhibit 1006

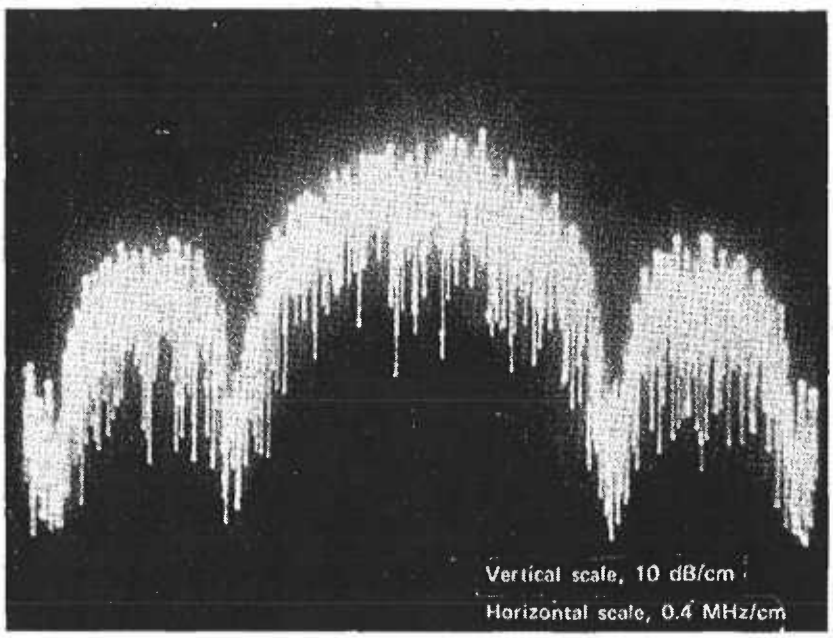


Figure 2.4 Direct sequence, suppressed carrier spectrum-biphase, code-modulated.

The simplified block diagram in Figure 2.3 illustrates a typical direct-sequence communications link. It shows that the direct sequence system is similar to (and, in fact, can be) a conventional AM or FM communications link with code modulation overlaid on the carrier. In actual practice the carrier is not usually modulated by baseband information. The baseband information is digitized and added to the code sequence. For

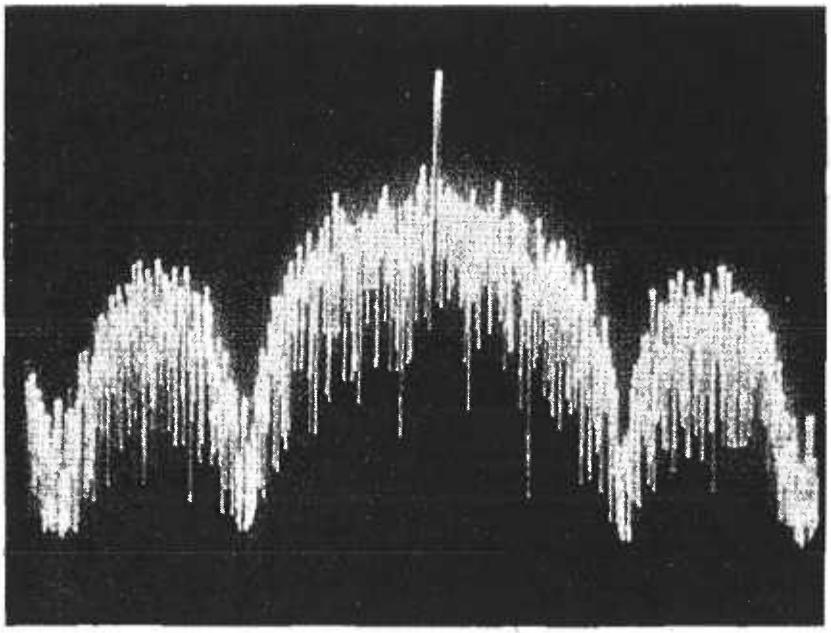


Figure 2.5 Direct sequence unsuppressed carrier, spectrum biphase and code modulated.

Shenzhen Huiding Tech. Co., Ltd. - Exhibit 1006

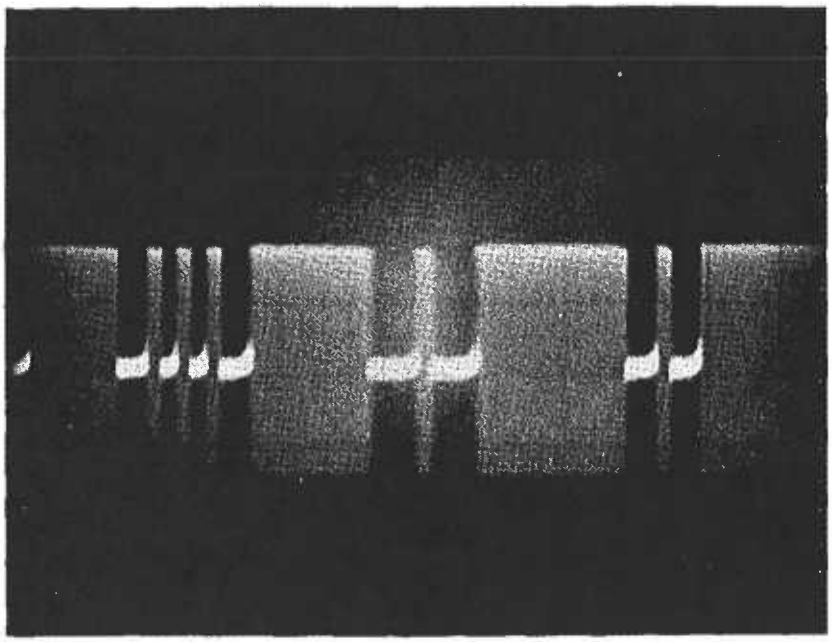


Figure 2.6 Pulse amplitude-modulated carrier, code modulated.

this discussion, however, we will assume that the RF carrier has been modulated before code modulation because this somewhat simplifies discussion of the modulation–demodulation process.

After being amplified, a received signal is multiplied by a reference with the same code and, assuming that the transmitter's code and receiver's code are synchronous, the carrier inversions transmitted are removed and the original carrier restored. This narrowband restored carrier can then flow through a bandpass filter designed to pass only the baseband-modulated carrier.

Undesired signals are also treated in the same process of multiplication by the receiver's reference that maps the received direct sequence signal into the original carrier bandwidth. Any incoming signal not synchronous with the receiver's coded reference (a wideband signal) is spread to a bandwidth equal to its own bandwidth plus the bandwidth of the reference; that is, the receiver's multiplier output signal variance is the covariance of its input signals.

Because an unsynchronized input signal is mapped into a bandwidth at least as wide as the receiver's reference, the bandpass filter can reject almost all the power of an undesired signal. This is the mechanism by which process gain is realized in a direct sequence system; that is, the receiver transforms synchronous input signals from the code-modulated bandwidth to the baseband-modulated bandwidth. At the same time non-synchronous input signals are spread at least over the code-modulated bandwidth.

System information bandwidth sets the postcorrelation filter bandwidth, and this filter in turn determines the amount of power from an

Shenzhen Huiding Tech. Co., Ltd. - Exhibit 1006

unsynchronized signal which reaches the information demodulator. Therefore we see that, as already stated, the multiplication-and-filtering sequence provides the desired signal with an advantage or "process gain."

Radio-Frequency Bandwidth in Direct-Sequence Systems

Radio-frequency (RF) bandwidth in direct sequence systems, as discussed in the preceding sections, directly affects system capabilities. If a 20-MHz bandwidth is available, the process gain possible is limited by that 20 MHz.

Several approaches are useful in choosing the proper bandwidth in a signal-hiding application; the interest is in reducing the power transmitted per Hertz of bandwidth, and wide bandwidths are used. When maximum process gain for interference rejection is desired, bandwidth again should be large. When either frequency allocation or the propagation medium does not permit wide RF bandwidth, some restraint must be applied.

A prime consideration in spread spectrum systems (and especially direct sequence systems) is the bandwidth of the system with respect to the interference furnished to other systems (that may not necessarily be spread spectrum systems) operating in the same or adjacent channels. Referring to Figures 2.4 and 2.5 will show that high sidelobe energy is present in some direct sequence formats, even though the content of the signal is not enhanced by transmitting the sidelobes. In systems such as JTIDS (Joint Tactical Information Distribution System), for example, the band employed is shared with both IFF and TACAN systems. Therefore, a special form of direct-sequence modulation called MSK (minimum shift key) is used.

There are, in fact, a number of waveforms, all closely related, that can be employed in direct sequence systems to control the level of energy contained in the unneeded sidelobes. We shall discuss these in detail in Chapter 4, but for now we simply summarize the characteristics of the available waveforms in Table 2.1. That the simple biphase or quadriphase

Table 2.1 Comparison of Direct Sequence Waveforms

Waveform	Null-to-null Main Lobe BW	3-dB BW	First Sidelobe	Rolloff Rate
BPSK	2 × code clock	0.88 × code clock	−13 dB	6 dB/octave
PAM	2 × code clock	0.88 × code clock	−13 dB	6 dB/octave
QPSK	2 × code clock[a]	0.88 × code clock	−13 dB	6 dB/octave
QQPSK	2 × code clock[a]	0.88 × code clock	−13 dB	6 dB/octave
MSK (classic)	1.5 × code clock	0.66 × code clock	−23 dB	12 dB/octave

[a]Requires two codes at same rate as single BPSK code.

Shenzhen Huiding Tech. Co., Ltd. - Exhibit 1006

direct sequence signal has a $[(\sin x)/x]^2$ spectrum can be simply shown: Given a rectangular pulse whose duration is T and whose amplitude is A over $T \pm T/2$ and zero elsewhere:

$$C_n = \int_{-T/2}^{T/2} A \exp(-j\omega t)\,dt = \frac{A}{j\omega} \exp(-j\omega t) \int_{-T/2}^{T/2}$$

$$= \frac{A \exp(j\omega\ T/2) - A \exp(-j\omega\ T/2)}{j\omega}$$

$$= \frac{2A}{\omega} \sin \frac{\omega T}{2} = TA \frac{\sin \omega T/2}{\omega T/2}$$

This expression is obviously of the form $(\sin x)/x$: It is the voltage distribution for the signal whose power distribution is then $[(\sin x)/x]^2$. This shows what is readily apparent when using a spectrum analyzer—the spectrum of biphase and quadriphase signals has a $[(\sin x)/x]^2$ distribution. Pulse shaping, as we shall see, can provide significantly improved power distribution, and that is the approach used in the other forms of direct sequence modulation that we will discuss.

In any case, the direct sequence system has a main lobe bandwidth that is a function of the waveshape and the code rate used. For example, in Figure 2.1 the code rate is 5 Mcps, Figure 2.4 is generated with a code rate of 25 Mcps, and the chip rate in Figure 2.7 is a very high 100 Mcps. All of these signals are from biphase modulators, but the spectra are identical to

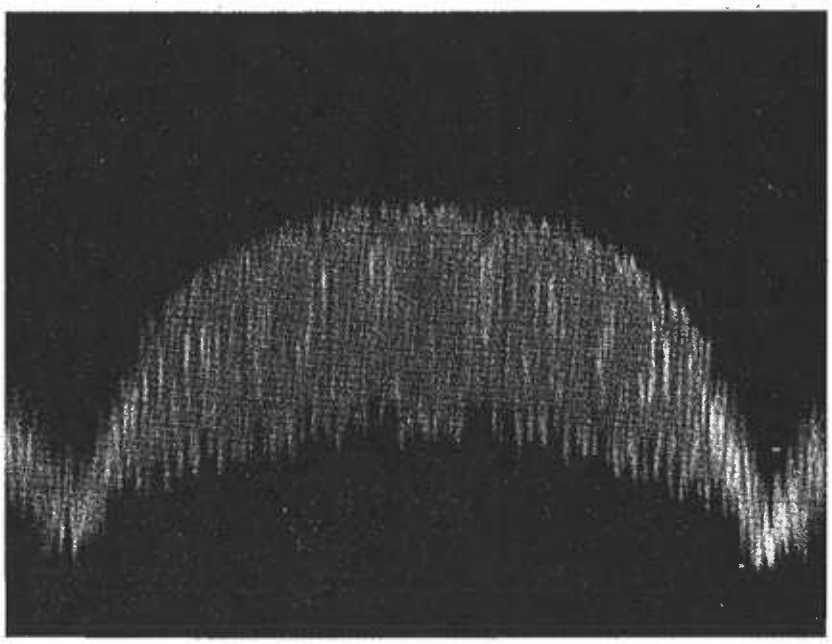


Figure 2.7 High-speed code-modulated direct sequence (BPSK) spectrum.

Shenzhen Huiding Tech. Co., Ltd. - Exhibit 1006

those that would be produced by the equivalent quadriphase or offset quadriphase modulator. Comparison of these spectra will show that the spectral shape is $[(\sin x)/x]^2$ and the null-to-null bandwidth is $2R_c$.

The signal lost as a result of accepting only the main lobe is small. Only 10% of the power in a BPSK or QPSK signal is contained in the sidelobes (see Figure 2.8). Signal-power loss is not the only effect of bandwidth restriction, however. The sidelobes contain much of the harmonic power of the modulation. Thus restriction to a narrow RF bandwidth is the equivalent of restricting the rise and fall times of the modulating code. Also, the sharply peaked triangular correlation of a coded signal is rounded by a bandwidth restriction. Figures 2.9 and 2.10 show the effect of band restriction on the RF envelope and correlation function of a direct sequence signal.

Quadriphase (QPSK) transmission (discussed in Chapter 4) is one method of restricting RF bandwidth when a given code rate is to be used. QPSK does halve the RF bandwidth required, but processing gain is then a function of the halved bandwidth. More than four phases can also be used to restrict bandwidth further, but the same rationale holds; for example, a system with a 22.75 Mcps code rate and 10 kbps data to be sent would require a 20 MHz (null-to-null) bandwidth using the standard form of BPSK modulation. Its process gain would be 20 MHz/10 kbps $= 2 \times 10^3$. On the other hand, QPSK could reduce the bandwidth

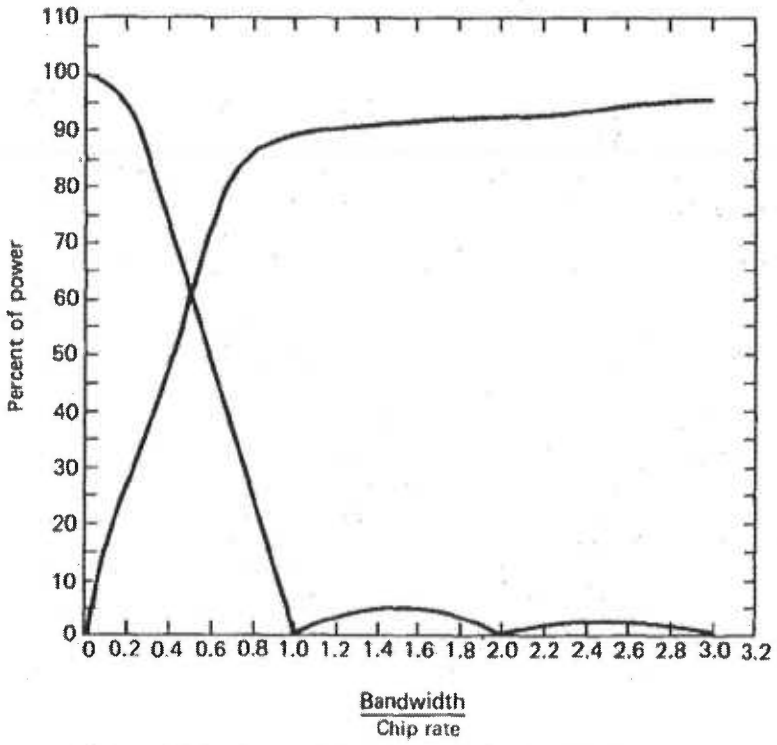


Figure 2.8 Power distribution in $[(\sin x)/x]^2$ spectrum.

Shenzhen Huiding Tech. Co., Ltd. - Exhibit 1006

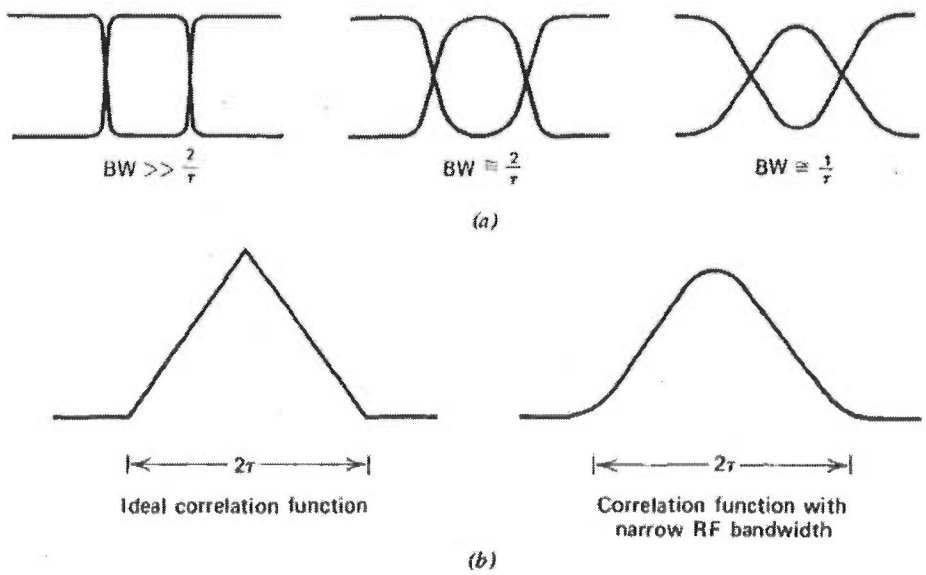


Figure 2.9 RF bandwidth restriction and its effect on typical direct sequence signals: (a) RF envelope of direct sequence signal for various RF bandwidths; (b) effect of bandwidth restriction on correlation function.

required to only 10 MHz but would also reduce process gain to 10 MHz ÷ 10 kbps = 1×10^3, or 3 dB less.

The choice of modulation and code rate is highly dependent on the system in which they are to be used. One must consider bandwidth availability, process gain required, and the basic data rates. RF bandwidth restriction is of more than usual importance in direct-sequence

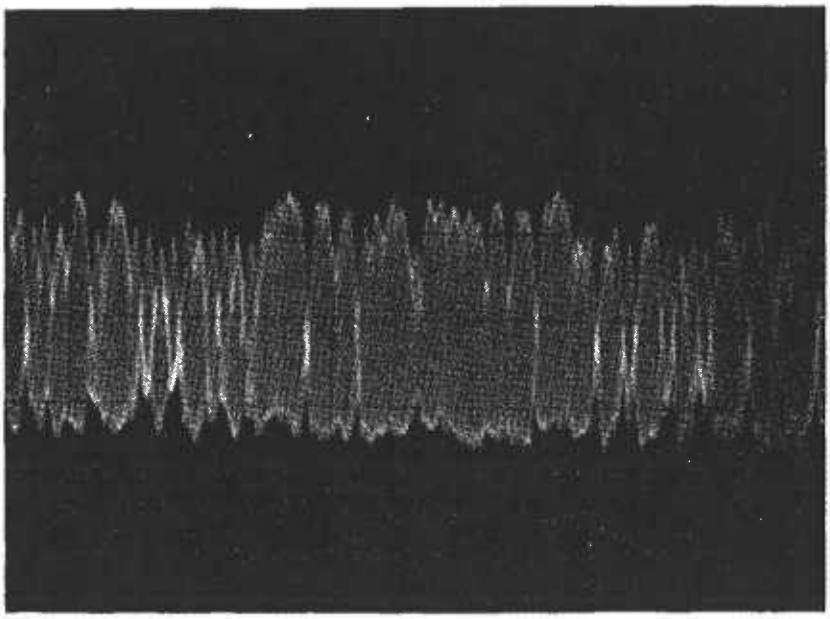


Figure 2.10 This photograph shows amplitude distortion of a bandlimited direct sequence signal.

ranging systems, for degradation of the correlation function, as shown in Figure 2.9, could result in a loss of ability to measure timing precisely. Bandwidth restriction, therefore, can reduce range resolution (i.e., increase the minimum measurement).

Distribution of the power in a direct sequence signal (whether biphase or quadriphase) is plotted in Figure 2.8 along with a plot that shows the relative amplitudes of the first two sidelobes over a region equal to three times the code rate. Figure 2.8 shows that 90% of the total power is contained in a bandwidth equal to twice the bit rate, 93% of the total power in four times the bit rate, and 95% of the total power is in six times the bit rate.

Further consideration of RF bandwidth in both direct sequence and frequency-hopping systems is discussed in Chapter 7 with respect to the RF transmission and reception link. Here it is sufficient to say that direct sequence-signal bandwidth is a direct function of code rate, modulation envelope, and the number of phase positions employed.

Direct Sequence Process Gain

Process gain in a direct sequence system is a function of the RF bandwidth of the signal transmitted compared with the bit rate of the information. The gain in question is exhibited as a signal-to-noise improvement resulting from the RF-to-information bandwidth tradeoff.

The usual assumption taken is that the RF bandwidth is that of the main lobe of the $[(\sin x)/x]^2$ direct sequence spectrum, which is 0.88 times the bandwidth-spreading code clock rate. Therefore, for a system having a 10 Mcps code clock rate and a 1 kbps information rate the process gain would be $(0.88 \times 10^7)/(1 \times 10^3) = 8.8 \times 10^3$ or 39 dB. (Such parameters are typical for practical systems.)

Let us consider the limitations that exist with respect to expanding the bandwidth ratio arbitrarily so that process gain may be increased indefinitely. (Unfortunately, physical limitations prevent this increase.) Only two parameters are available to adjust process gain. The first, RF bandwidth, depends on the code rate used. If we wish to have an RF (null-to-null) bandwidth 100-MHz wide, the code rate would be at least 50 Mcps. On this basis, how wide is it practical to make the system RF bandwidth? At present, integrated circuits are available that allow limited code generation at rates up to 200 or even 300 Mcps. Is there a profit in going higher or, for that matter, in using these bit rates? Consider higher bit rates: doubling the present state-of-the-art code rates would increase process gain by only 3 dB, which is at best a modest gain when compared to the effort required to double the operating speed of present circuits.

Another consideration is that as code rates go higher, operating errors must go lower in inverse proportion. To be operationally useful a code generator should be able to operate for hours or even days without error.

Shenzhen Huiding Tech. Co., Ltd. - Exhibit 1006

If we consider what this means in error rate, we see that a 100-Mcps code sequence generator must operate error free for 3.6×10^{11} bits, just to allow a system to operate for 1 hr. On the other hand, high-speed logic circuits tend toward noise sensitivity and are more susceptible to error.

Finally, but not of least concern, is that high-speed digital circuits consume large amounts of current and power dissipation is high. High-speed code generators often consume as much as 1.0 W/stage.

The foregoing reasons, coupled with the problems of spectrum occupancy, equipment implementation (both RF and digital), and propagation constraints, tend to limit the code rates used for band spreading. For the near future, it appears that code rates of 50–100 Mcps are the highest that are practical for general use.

Reiterating an important point, we state that to improve process gain significantly beyond that obtainable with a 100-Mcps code, we would be forced to generate codes in the 1×10^9 bps region. This, at present, is not practical for the long, multifeedback sequence generators required for useful communications systems. Though codes generated at rates near 500 Mcps have been shown as laboratory curiosities, they have been extremely short and exhibited errors at rates in the 1×10^{-3} range. A 100-Mcps code generator with even a 1×10^{-8} error rate could be expected to make one mistake every second. This would prevent data transmission even if it permitted system synchronization. (It is unlikely that the system could be synchronized.)

Data rate reduction to improve process gain is limited in its extent by the willingness of a user to slow information transfer and by the overall stability of the transmission link. Once data rate is slowed to the tens of bits-per-second area or lower such things as local oscillator phase noise or instability in the propagation medium become significant and can cause errors. It is conceded that systems with 1 bps and lower data rates have been built. Here, however, 10 bps is recommended as a lower limit.

Now, if we consider systems with code rate limited at 100 Mcps and data rate limited at 10 bps, we see that for practical systems process gain is limited at about

$$\frac{0.88 \times 10^8}{10} = 0.88 \times 10^7, \quad \text{or } 69 \text{ dB}$$

It is realized that future systems will transmit data at gigabit rates and that even as this paragraph is being written techniques for building such systems are being worked out. Thus, in setting a seat-of-the pants practical limit of 100 Mcps on spread spectrum code generators for direct sequence communications, it is realized that this limit appears paradoxical. However, there is a difference in high-speed codes used for RF spectrum spreading and in high-speed data (the high-speed data would also result in a wide RF spectrum, of course), even though both are

Shenzhen Huiding Tech. Co., Ltd. - Exhibit 1006

bit streams. The difference in the two lies in the action of errors on the system; that is, an error (or, for that matter, many errors up to some correctible limit) might be tolerated in a data-modulated system, whereas an error in a code generator would completely disable the code-modulated system until resynchronization occurs.

Direct Sequence Code and Spectrum Relationships

It has been repeatedly stated here, and emphasized in illustrations, that the spectral power envelope of a direct sequence signal is of a $[(\sin x)/x]^2$ form. This is an expected result since any good set of Fourier transform pairs[1714] will show that the frequency function corresponding to a square pulse is $(\sin x)/x$ (which is a voltage distribution function) and code modulation produces a series of pulses. Because the power envelope is a function of the voltage squared, the $[(\sin x)/x]^2$ power spectrum results. {As an aside, we point out that a spectrum-analyzer presentation of a direct sequence signal always appears to have a $[(\sin x)/x]^2$ distribution because spectrum analyzers do not display phase information, only amplitude.}

Any code sequence used to modulate a direct sequence system produces a similar power envelope, but what about the details of distribution within that envelope?

Observation of a pseudonoise code sequence will show that it is made up of a series of variable-period pulses, which could be viewed as half-period square waves. Figure 2.11 illustrates this concept. These square wave half-periods vary in duration from one code clock chip to n chips for a linear maximal sequence $2^n - 1$ bits in length. Each of these half-periods has a $(\sin x)/x$ spectrum associated with it. As a code sequence modulates a direct sequence transmitter, the output spectrum is actually

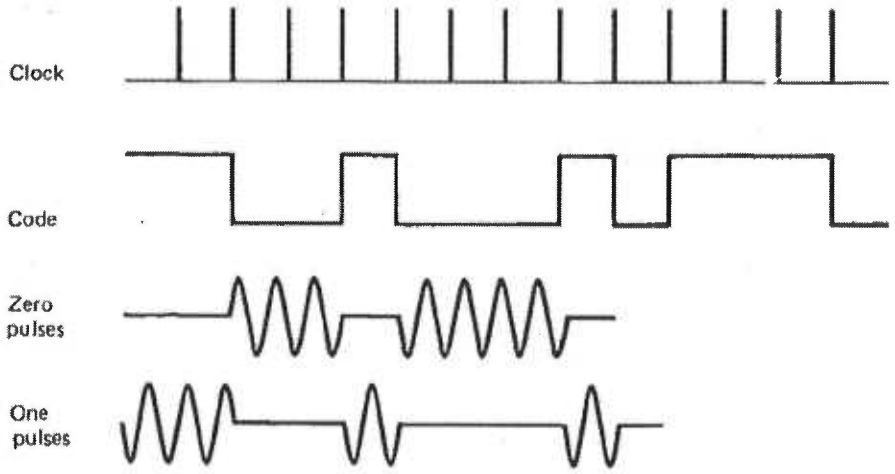


Figure 2.11 Direct sequence transmission as a pulse series.

Shenzhen Huiding Tech. Co., Ltd. - Exhibit 1006

a composite made up of a series or group of spectra produced by the various half-wave components of the code.

Because the pulse of shortest duration in any code sequence is equal in length to the code sequence clock period, it follows that the frequency spectrum for the composite modulation containing that code sequence must have a main-lobe bandwidth such that its first nulls fall at the code clock rate. Reinforcing this expectation is the fact that the distribution of single ones and zeros in a code sequence is such that they outnumber all other pulse lengths. Chapter 3 includes a detailed discussion of the distribution of the half-periods (or runs) in a pseudonoise code sequence. For now, it is enough that one-fourth of the runs in a maximal code are one chip long and that the number of runs or lengths longer than one decreases by half for each chip of increase in run length.

The number of frequency sets available is a function of the length of the code (and code generator being used). For an n-chip sequence generator, there are $n + 1$ frequency sets, and the spacing of individual frequency components is as narrow as $R_c/(2^n - 1)$, where the code length is $2^n - 1$ (maximal), n is the sequence generator length, and R_c is the code chip or clock rate.

The Minimum Shift Key Technique

Minimum shift keying (MSK) is a direct sequence modulation technique that offers exceptionally good suppression of signal sidelobes and fast side lobe rolloff. MSK has a main lobe whose power distribution is approximately the same as BPSK and QPSK, but the null-to-null bandwidth is $1.5R_c$.* Although somewhat more difficult to implement than BPSK or QPSK, MSK does offer some advantages that other forms of direct sequence modulation cannot match. We hasten to state that there are many forms of MSK modulation, each with different spectrum and characteristics. Offset QPSK is, in fact, one form of MSK modulation. We will further discuss these forms and compare their characteristics in detail in Chapter 4.

2.2 FREQUENCY HOPPING†

"Frequency hopping" modulation is more accurately termed "multiple-frequency, code-selected, frequency shift keying." It is nothing more than FSK (frequency shift keying) except that the set of frequency choices is greatly expanded. Simple FSK most often uses only two frequencies; for example f_1 is sent to signify a "mark," f_2 to signify a "space." Frequency

*Classic MSK.

†See the Bibliography, Sections 1, 7, and 8.

Shenzhen Huiding Tech. Co., Ltd. - Exhibit 1006

"hoppers," on the other hand, often have thousands of frequencies available. One real system[111] has 2^{20} discrete frequency choices, randomly chosen, each selected on the basis of a code in combination with the information transmitted. The number of frequency choices and the rate of hopping from frequency to frequency in any frequency hopper is governed by the requirements placed on it for a particular use.

Characteristics of Frequency Hopping Signals

A frequency hopping system or "frequency hopper" consists basically of a code generator and a frequency synthesizer capable of responding to the coded output from the code generator. A great deal of effort has been expended in developing rapid-response frequency synthesizers for spread spectrum systems.

Ideally, the instantaneous frequency hopper output is a single frequency. Practically, however, the system user must be satisfied with an output spectrum which is a composite of the desired frequencies, sidebands generated by hopping, and spurious frequencies generated as by-products.

Figure 2.12 is a simplified block diagram of a frequency hopping transmission system. The frequency spectrum of this frequency hopper is shown in Figure 2.13.

Over a period of time, the ideal frequency hopping spectrum would be perfectly rectangular, with transmissions distributed evenly in every available frequency channel. The transmitter should also be designed to transmit, to a degree as close as practical, the same amount of power in every channel.

The received frequency hopping signal is mixed with a locally generated replica, which is offset a fixed amount such that $\{f_1, f_2, \cdots, f_n\} \times \{f_1 + f_{IF}, f_2 + f_{IF}, \cdots, f_n + f_{IF}\}$ produces a constant difference frequency f_{IF} when transmitter and receiver code sequences are in synchronism.

As in a direct sequence system, any signal that is not a replica of the local reference is spread by multiplication with the local reference. Bandwidth of an undesired signal after multiplication with the local reference is again equal to the covariance of the two signals; for example, a CW signal appearing at the frequency hopping receiver's input would be identical to the local reference when translated to the IF frequency. A signal with the same bandwidth as the local reference (but nonsynchronous) would have twice the reference bandwidth at the IF. The IF following the correlator, then, can reject all of the undesired signal power that lies outside its bandwidth. Because this IF bandwidth is only a fraction of the bandwidth of the local reference, we can see that almost all the undesired signal's power is rejected, whereas a desired signal is enhanced by being correlated with the local reference.

Shenzhen Huiding Tech. Co., Ltd. - Exhibit 1006

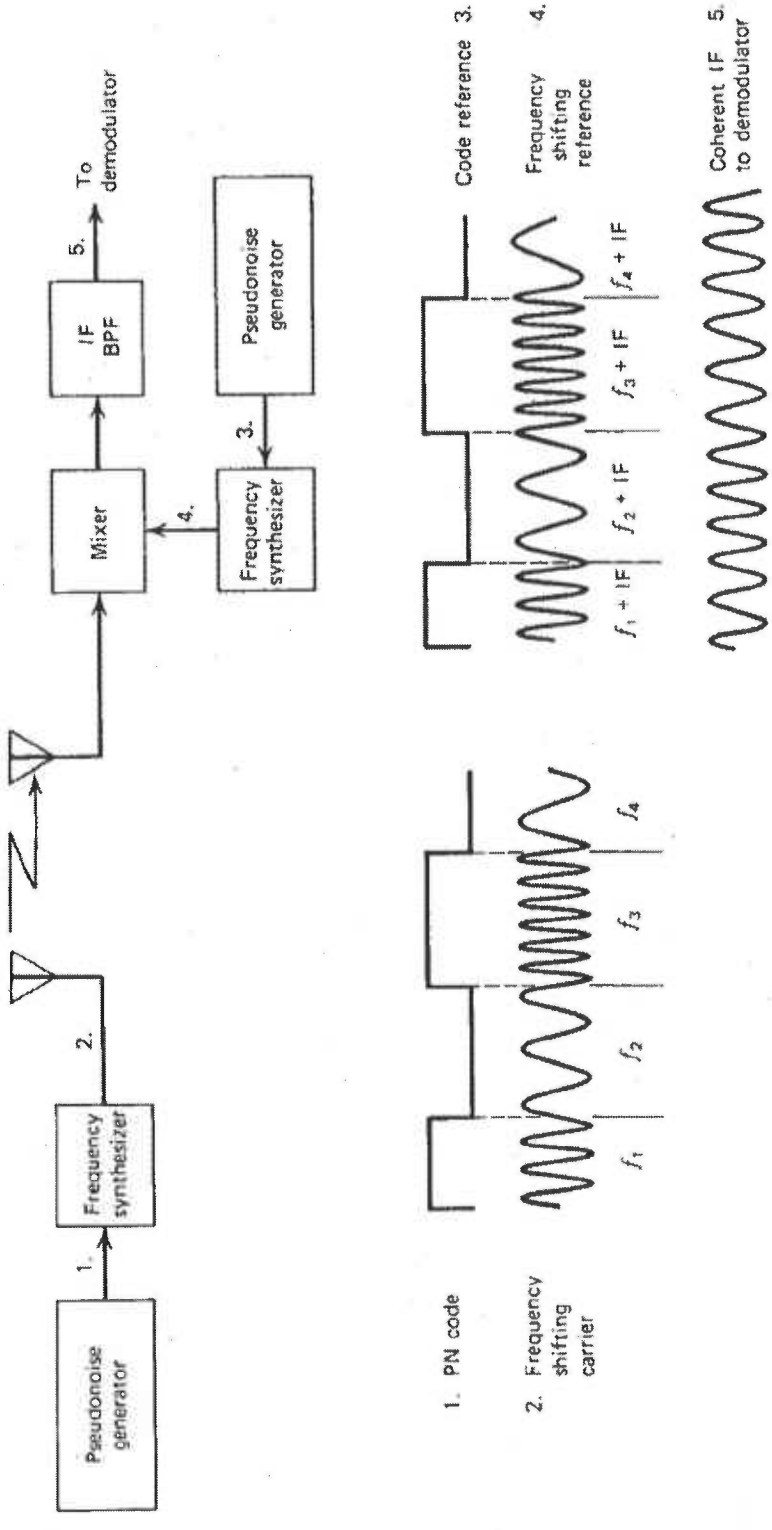


Figure 2.12 Basic frequency hopping system with waveforms.

Shenzhen Huiding Tech. Co., Ltd. - Exhibit 1006

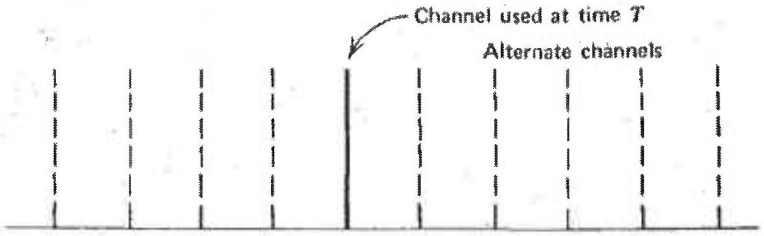


Figure 2.13 Ideal Frequency Hopping signal spectrum.

In the preceding section on direct sequence systems, we saw that a direct sequence system's operation is identical from the standpoint of undesired signal rejection and remapping of the desired signal. From this general viewpoint direct sequence and frequency hopping systems are identical; they are different, however, in the details of their operation.

Process gain for the frequency hopping system (in which channels are contiguous) is the same as that for the direct sequence system; that is,

$$G_p = \frac{\mathrm{BW}_{\mathrm{RF}}}{R_{\mathrm{info}}}$$

If the channels are not contiguous, a better measure of process gain is

$$G_p = \text{the number of available frequency choices} = N$$

which also holds for contiguous channels; for example, a frequency hopping system containing 1000 frequency choices could have 30 dB available process gain.

The only restriction in use of these simple calculations for process gain is that interchannel interference (crosstalk) is neglected. When IF

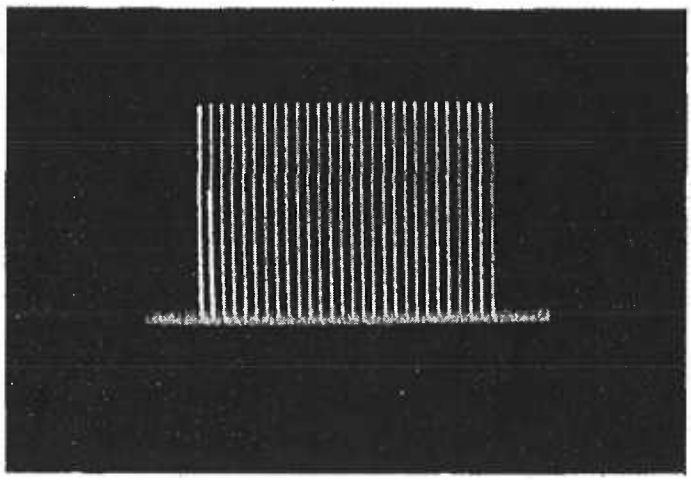


Figure 2.14 Ideal frequency hopper output spectrum.

Shenzhen Huiding Tech. Co., Ltd. - Exhibit 1006

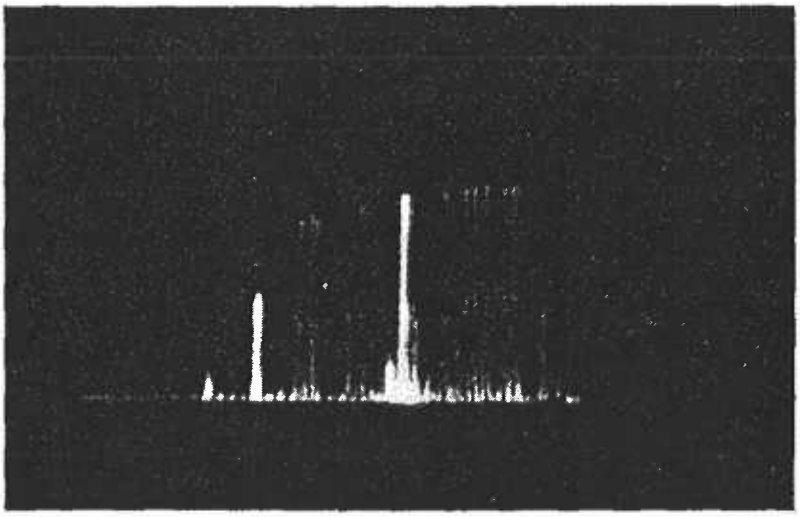


Figure 2.15 Multifrequency hopper spectrum with CW interference.

bandwidth or channel overlap does not provide for unambiguous channel recognition, an allowance must be made for this source of error, which reduces process gain.

Figures 2.14 through 2.17 illustrate actual frequency hopping signals typical of those that might be seen with a spectrum analyzer.

Figure 2.14 shows an ideal frequency hopping spectrum, actually far better than those normally seen from wideband, multifrequency synthesizers. This particular spectrum would be seen from a narrowband frequency hopper (only 28 frequencies are shown), so that the output level is flat over the output band. Compare this spectrum with those of Figures 2.15 and 16.

Figure 2.15 is a time exposure of a several-thousand-frequency hopper output. The bright center trace is a CW carrier equal in power to the

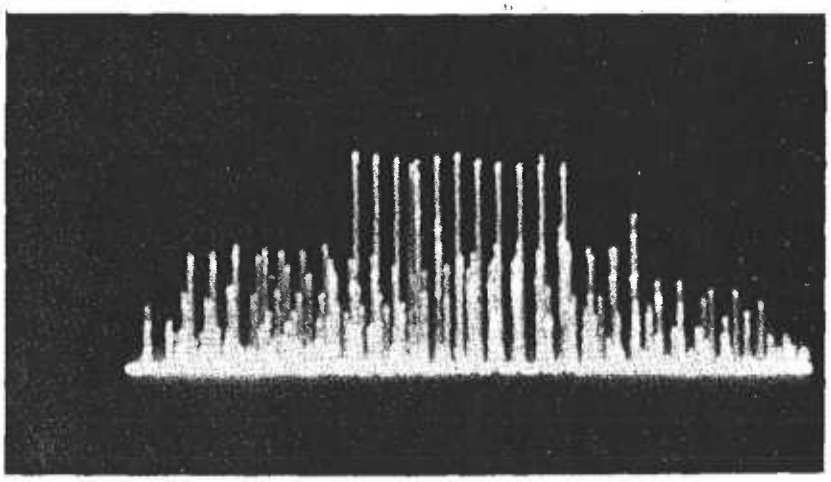


Figure 2.16 Multifrequency hopper spectrum with partial band multitone interference.

Shenzhen Huiding Tech. Co., Ltd. - Exhibit 1006

frequency hopping signal. Note that the output spectrum of this wider-band synthesizer is not so flat in amplitude as the preceding narrowband hopper.

A wideband frequency hopper, combined with partial band interference, is shown in Figure 2.16. The interference is the larger set of signals at its center. The actual frequency hopping signal is the set of smaller, much-wider-band signals. Here again it is obvious that amplitude linearity across the band is less than perfect, as is spurious suppression.

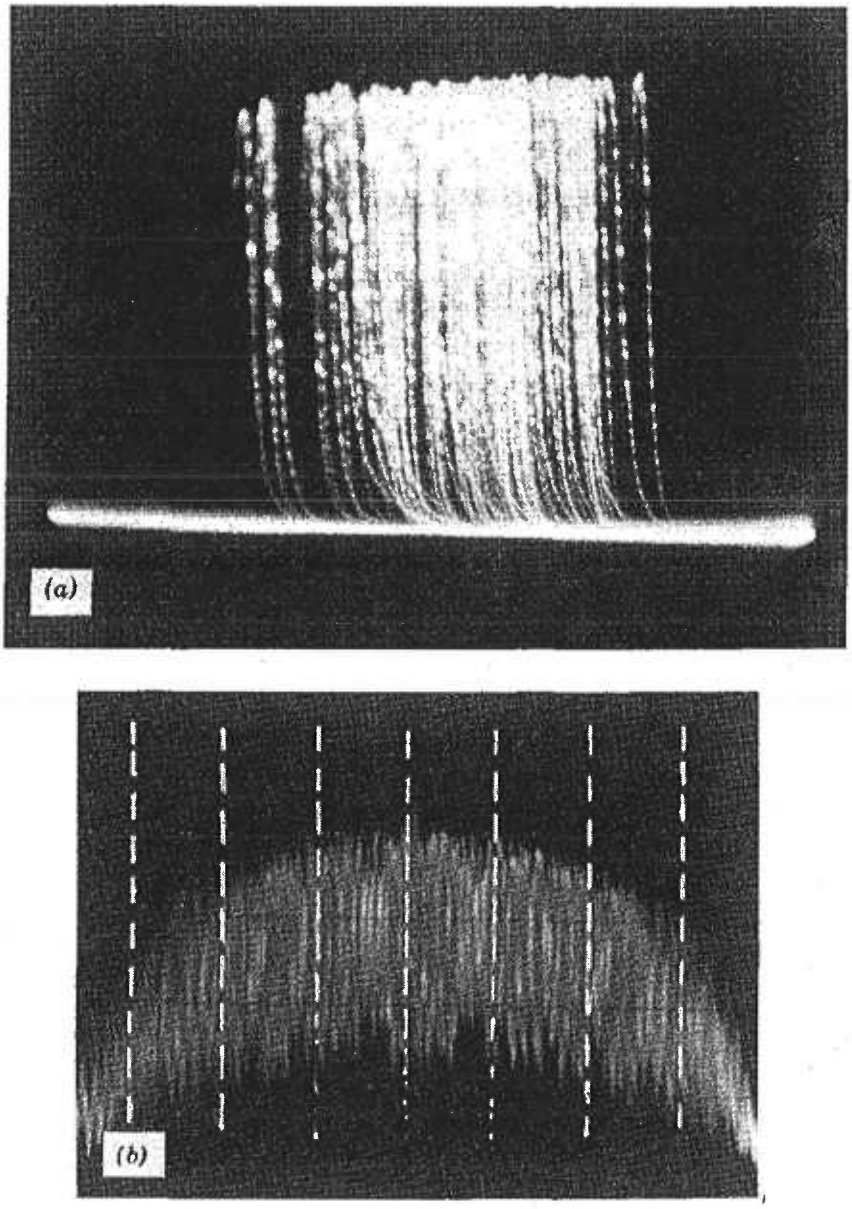


Figure 2.17 Frequency hopping and direct sequence signal comparison. (*a*) Integrated circuit synthesizer at 500 hops/sec, frequency separation 10 kHz. (*b*) Direct sequence signal compared to equivalent-power frequency hopped signal.

Shenzhen Huiding Tech. Co., Ltd. - Exhibit 1006

Where spurious signal suppression is desired, it is necessary to use pulse shaping of the frequency hopped carrier. Transmission of a rectangular pulse results in (as might be expected) a $(\sin x)/x$ spectrum centered at each frequency cell. This is the origin of most of the spurious signals seen in Figure 2.16.

It is not necessarily obvious that the output spectrum for a frequency hopping system needs to be flat. If bit decisions are made on the basis of signal-power comparison in alternate channels, it becomes important that transmitted signal variation be small. When the mark/space detector has a narrow threshold band, interference must be within that band to be effective. Use of a narrow decision band depends, however, on having a transmitter that has closely controlled amplitude from channel to channel.

Determining Frequency Hopping Rate and Number of Frequencies

The minimum frequency switching rate usable in a frequency hopping system is determined by a number of parameters:

1. The type of information being sent and its rate.
2. The amount of redundancy used, if any.
3. Distance to the nearest potential interferer.

Information in a frequency hopping system may be transmitted in any way available to other systems. Usually, however, some form of digital signal is used, whether the information is a digitized analog signal or data. Assume for the present that some digital rate is prescribed and that frequency hopping has been chosen as the transmission medium. How, then, is the frequency hopping or "chip" rate chosen?

A frequency hopping system must have a large number of frequencies usable on demand. The number required is dependent on the system error rate; for instance, a library of 1000 frequencies could provide good operation when interference or other noise is evenly distributed at every available frequency. For equal distribution of noise in every channel the noise power required to block communications would approach 1000 times desired signal power (in other words, jamming margin would be 30 dB). Unless some form of redundancy that allows for bit decisions based on more than one frequency is used, however, a single narrowband interferer would cause an error rate of 1×10^{-3}, which is generally acceptable for digital data. For a simple frequency-hopping system without any form of transmitted data redundancy, the expected error rate is just J/N, where J equals the number of interferers with power greater than or equal to signal power and N equals the number of frequencies available to the system. We see then that some form of data transmission

Shenzhen Huiding Tech. Co., Ltd. - Exhibit 1006

other than simple binary frequency hopping is required because of the inherent high error rates caused by a small amount of interference.

Error rate for a frequency-hopping system, in which we assume that binary redundant FSK is used (f_a = mark, f_b = space) may be approximated* by the expression for the cumulative binomial expansion:

$$P_e = \sum_{x=r}^{c} \binom{c}{r} p^x q^{c-x}$$

where p = error probability for a single trial = J/N,
J = the number of jammed channels,
N = the number of channels available to the frequency hopper,
q = probability of no error for a single trial = $1 - p$
c = the number of chips (frequencies sent per bit of information),
r = the number of wrong chip decisions necessary to cause a bit error.

A chip decision is defined as occurring any time the interference power in a "space" channel exceeds the power in an intended "mark" channel (or vice versa) by some amount e that is sufficient to cause a decision in favor of what was not intended.

If three or more† frequencies (chips) are sent for each bit of information, we find that performance with interference is greatly enhanced. When the receiver's bit decision is made on the basis of two out of three being correct, a single-channel interferer would cause no more than

$$\binom{3}{2} p^2 q^{3-2} = 3p^2 q^{3-2} = 3p^2 q$$

but $q = 1 - p$, therefore, $3p^2 q = 3(p^2 - p^3)$ errors

*This error-rate approximation is good to the extent that the effects of interference falling into the occupied signal channel are ignored; that is, in addition to the probability J/N of falling into the channel that signifies the opposite of what is intended, there is a probability (also J/N) that an interfering signal will fall into the intended or occupied channel. When this happens, the phase relationship of the two signals occupying the channel determines what occurs. To complicate matters further, there is the probability that an interfering signal will fall in both the intended and opposite channels, in which case, the mark/space decision is based on whether the signal in the opposite channel is greater than the composite of the signals in the intended channel.

†Three or more chips per bit of information allows a majority decision (or some other decision) to be made. Usually an odd number of bits is used. In majority decision systems (in which a decision is based on two of three, three of five, · · ·, trials) an odd number of trials (r) is always better than $r + 1$ or $r - 1$ trials because another trial gives no more information but does increase the chance of error. A three-of-five decision, for instance, allows two errors in five, yet gives a correct decision. Increasing the number of trials to six requires four of the six to be correct and still allows only two errors.

Shenzhen Huiding Tech. Co., Ltd. - Exhibit 1006

Returning to our 1000-channel system, we see that p is $1/1000$ and $q = 1 - 1/1000 = 0.999$ and the error rate is now

$$3\left(\frac{1}{10^6} - \frac{1}{10^9}\right) \approx 3 \times 10^{-6}$$

which is far better than the 1×10^{-3} error rate given by the simple one-chip-per-bit system.

We have paid for the reduction in errors with a threefold increase in transmission (hop) rate; our frequency synthesizer must now hop three times as fast. Given that the synthesizer can do so, however, it is almost always advantageous to make the three-for-one trade in speed to reduce errors 3000 to 1.

The probability of increasing redundancy (and, with it, the hop rate) to improve bit error rate depends on the system parameters. It is obvious that the more chips sent for a bit, the lower the bit error rate is. The hopping rate required and the RF bandwidth increase in direct proportion. If either the bandwidth allocated or the frequency capability of the frequency synthesizer is limited, then some tradeoff must be made between sending a larger number of chips per bit and reducing the number of frequencies available. As an example, assume that a data source at 1 kbps is to be transmitted and that a 10 MHz RF bandwidth is allowable. The 1 kb data rate suggests that frequency hopping be at least 1 khps, so that the main lobe of the dehopped $[(\sin x)/x]^2$ carrier spectrum is 2 kHz wide. Therefore, if no overlap is allowed (ignoring sidelobes), 10 MHz/2 kHz = 5000 frequency hopping channels are available. Maximum desired error rate is assumed to be 1×10^{-3}, when the interference-to-signal ratio is 100:1.

Now if only one chip is sent per bit of data, $P_s + e$ interference power in 100 of our 5000 available channels (which would equal our desired 100:1 interference power ratio) would have a probability of causing errors once chips are sent for each bit of information, the transmission rate goes to 3000 hps and the received signal bandwidth to 6 kHz. Thus the number of nonoverlapping signal channels available is 10 MHz/6 kHz = 1666 and the 100:1 interference ratio gives us $J/N = 100/1666 = 0.06 = P_e$ for 100 channels containing interference among the 1666 available. The error-rate could then be expected to be

$$\sum_{x=2}^{3} \binom{3}{x} 0.06^x 0.94^{3-x} = 1.2 \times 10^{-2}$$

which still does not reach our error-rate goal.

Observing Figure 2.18, we see that to reach the desired error rate (1×10^{-3}) it is necessary to decrease the ratio J/N or change the decision

Shenzhen Huiding Tech. Co., Ltd. - Exhibit 1006

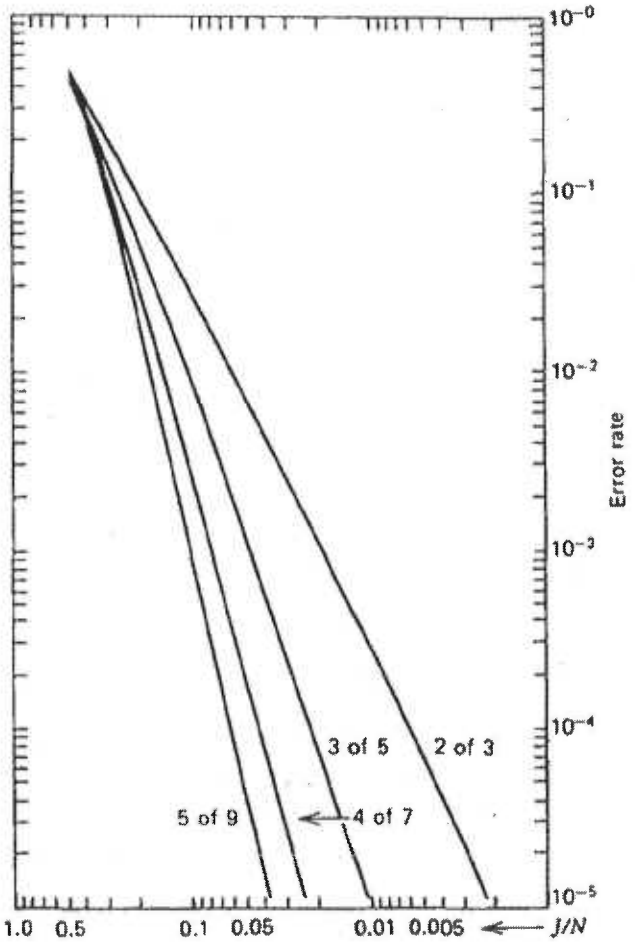


Figure 2.18 Error rate versus fraction of channels jammed (J/N) for various chip decision criteria in multichip transmissions.

criteria. For a two-out-of-three (one error allowable in three) decision at a 10^{-3} error rate we see that J/N can be no greater than 0.019 and that $100/0.019 = 5260$ transmit frequencies are the minimum allowable for 100:1 interference rejection. At three chips per bit of information the receiver dehopped-signal bandwidth is 6 kHz. Therefore, the RF bandwidth would be $6 \times 5260 \times 10^3 = 31.5$ MHz.

Alternatively, if the number of chips is increased to five per information bit, we see that J/N is increased to 0.047 at a 10^{-3} error rate. For the same interference ratio (100:1) we are required to use $100/0.047 = 2130$ channels. Because the contiguous (nonoverlapping) dehopped-signal bandwidth is now 10 kHz, the RF bandwidth must be 21.3 MHz, or approximately one-third less than that required for decisions made on the basis of two of three chips.

Figure 2.19 plots bandwidths required for various data rates, desired jamming margin, and J/N. Note that any kind of bit decision that can be made on the basis of one error allowed in three, or two in five, etc., would

Shenzhen Huiding Tech. Co., Ltd. - Exhibit 1006

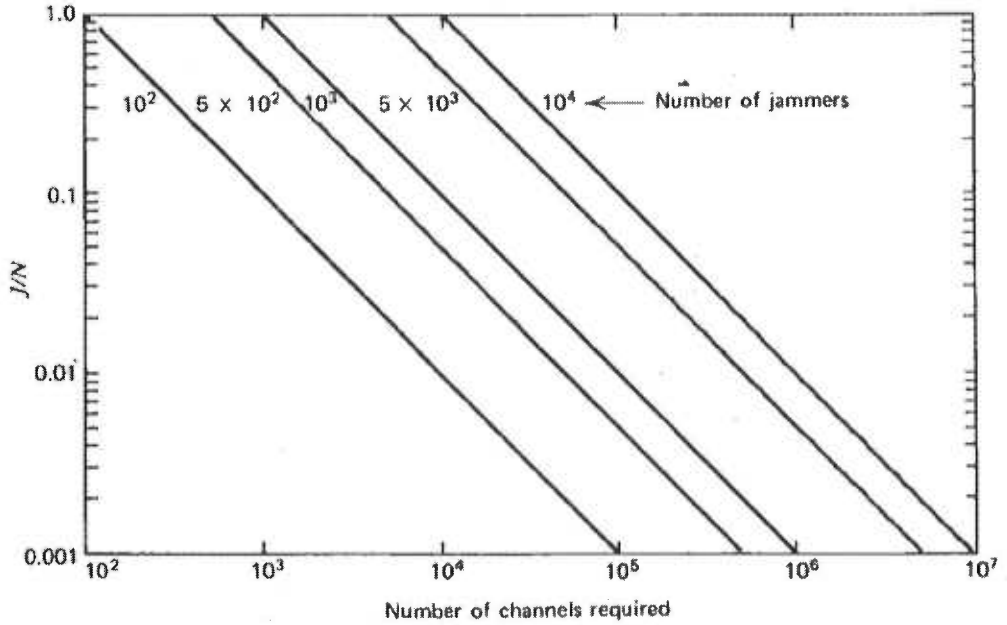


Figure 2.19 Number of channels required versus fraction of channels jammed (J/N) and number of jammers.

give the same result. Here the use of simple majority bit decisions has been implied. Any other form of error allowance would do just as well. It is worthy of mention that there are techniques for forcing three out of three chip errors before causing a bit error.

It is been assumed for the frequency hopping systems discussed so far that contiguous frequency spacing is used; that is, the dehopped signal appearing at the receiver is not allowed to overlap from one channel into another. This is not strictly a true picture. In many systems, depending on the receiver used, transmit spacing can be such that significant overlap occurs. This overlap greatly reduces the RF bandwidth required for the transmitted spread spectrum signal. Figure 2.20 illustrates overlapping channels and the bandwidth savings. Between Figures 2.20*a* and 2.20*b*, there is a doubling of channels in the same bandwidth. Overlapping is such that the center of one channel falls at a null for the adjacent channels (we are assuming noncoherent carrier reception). Here, then, is a technique for allowing the frequency hopping system in our example to meet the RF bandwidth restrictions imposed while keeping chip rate low. The three-chip-per-bit system of the example would have only 15.5 MHz bandwidth, whereas the five-chip-per-bit system would come close to the 10 MHz bandwidth goal with a 10.6 MHz requirement.

One other significant consideration regarding chip rate is the effect of signals which are received at the same frequency as the desired signal but are different in phase. These signals are due to multipath or, even worse, deliberate interference. In most cases, the multipath signal arriving at a receiver is much smaller than the desired signal and is therefore not of

Shenzhen Huiding Tech. Co., Ltd. - Exhibit 1006

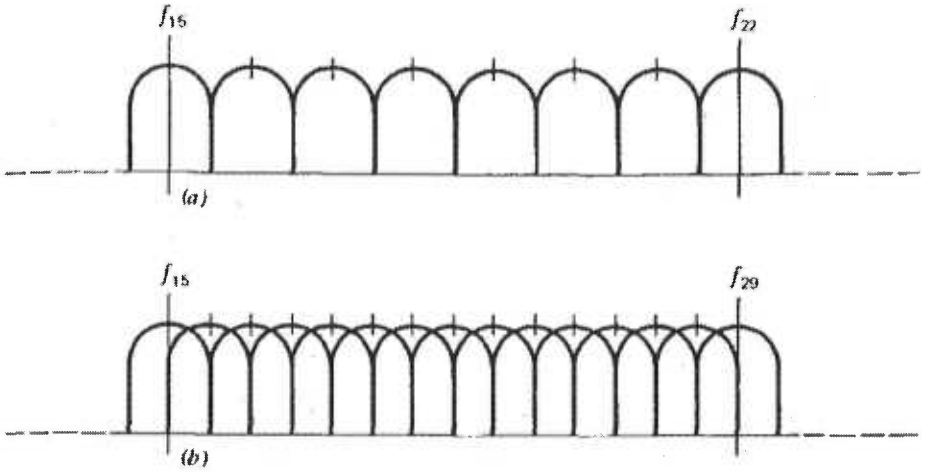


Figure 2.20 Illustration of contiguous versus overlapping channels showing gain in channels per unit bandwidth; (a) contiguous channel spacing; (b) overlapping channel spacing

great consequence. The deliberate interferer who receives a signal from the frequency hopping transmitter, amplifies it, modulates with noise (or, if he or she knows the key, transmits the complement) can be extremely effective with transmitter power similar to the friendly one. Against this kind of threat, the frequency hopper might have no advantage. To combat the threat the frequency hopper must hop at a rate that allows it to skip to another frequency before the interferer can respond to the last one. The desired hopping rate is then greater than $(T_r - T_d)^{-1}$, where T_r is the total propagation time from the frequency hopping transmitter to the interferer and from there to the intended receiver. T_d is direct path delay, illustrated in Figure 2.21.

As we observe Figure 2.21, we see that the minimum required hopping rate is a function of distance to the interfering station and the angle of offset from the direct path. For fixed stations, we can derive a minimum

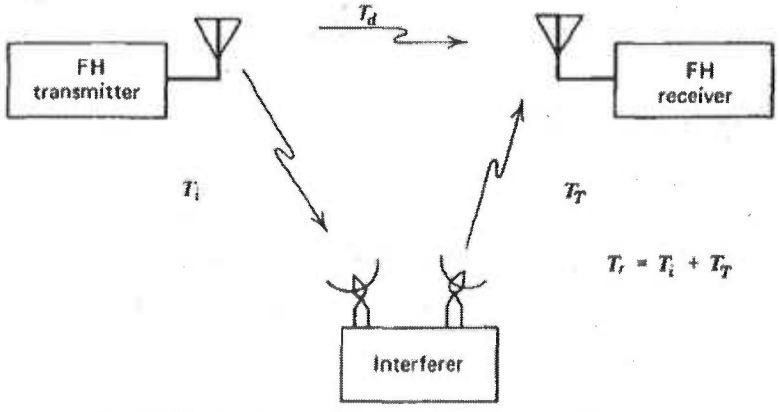


Figure 2.21 Repeater-type interference diagram

Shenzhen Huiding Tech. Co., Ltd. - Exhibit 1006

hop rate, but for mobile applications the conclusion must be to "make the system hopping rate as fast as possible."

To give an idea of the magnitude of a possible problem assume that the transmitter and desired receiver are 10 miles apart and that the interferer is 8 miles from each of them; $T_r - T_d = 109 - 68 = 41\,\mu s$ and the hopping rate should be at least 24.2 khps. This is a readily achievable hopping rate.

Because of its importance in frequency hopping, let us recap what has been said:

Frequency hopping rate is a function of information rate.

Information error rate cannot be reduced below J/N unless some form of redundant* transmission is used.

The number of frequency channels required is determined by the desired interference rejection capability (jamming margin) and chip error tolerance.

The correlated (dehopped) signal seen in a noncoherent frequency hop receiver is $[(\sin x)/x]^2$ in shape and has main-lobe bandwidth equal to twice the chip rate.

Chip rate is bounded on the low side by multipath and repeater interference considerations. The best rule for variable geometry situations is to hop as fast as possible.

Avoiding the Repeat Jammer

We have mentioned that frequency hopping systems can be faced with the prospect of a jamming signal which follows the signal from frequency to frequency, and can thus have an effect on the desired signal similar to that which a single-frequency jammer would have on a nonhopping signal. It is possible to negate or at least greatly reduce the effects of the repeat jammer by relatively simple techniques, using a noncoherent detector.

One simple approach is to use frequency hopped on–off keying. That is, if a One is intended, let the transmitter send a signal selected from the library by the code. If a zero is intended, however, the transmitter sends nothing. The repeat jammer then has no advantage since:

Transmission of a One provides a signal for the jammer to detect and repeat, but doing so will in most instances only help the receiver to detect the signal and make the correct decision that a One has been sent. The only hope that the jammer has to cause an incorrect decision is to attempt to arrive at the receiver with a signal that is identical to the

*"Redundant" includes error detection and correction coding.

Shenzhen Huiding Tech. Co., Ltd. - Exhibit 1006

desired signal but opposite in phase, and this is a highly improbable (if not impossible) state to maintain.

When a zero is intended, the desired signal transmitter sends nothing, so the jammer can only make a guess at random as to the correct signal frequency if a One were being sent. In this case, the jammer's probability of causing an error is just J/N.

The repeat jammer is similarly ineffective against other frequency hopping techniques as long as the frequency hopped carrier is unmodulated, and the receiver uses noncoherent detection. Thus in many applications the repeat jammer can generally be ignored as a viable threat to the frequency-hopping system.

Let us turn for a moment to m-ary frequency hopping systems in which a block of $\log_2 m$ coded data bits is sent by transmitting one of a set of m frequencies. (This corresponds in an analog system to one of m levels.) When such transmissions are used, an interfering signal needs only to hit in any one of the $m - 1$ channels not intended for transmission to cause a block error. In an 8-ary system this means that one-seventh the number of jamming signals is required to cause the same probability of a chip error that would be required in a simple binary system. This is a clear loss of 8.5 dB in processing gain. Of course, the reason for using an m-ary transmission format is to reduce chip rate, not to reduce errors or increase jamming margin. Chip-rate reduction, however, is not necessarily a good thing when we are faced with the "look-through" or repeating jammer.

At any rate, for m-ary frequency hopping, only N/m* m-ary channels or sets are available, which not only reduces the processing gain available (to $10 \log N/m$ dB) but increases the probability of chip error per jammed (single) channel. Chip error rates for m-ary transmitters may then be calculated on the basis of J/N_c = number of jammed channels per number of m-ary sets. Character or block error rate for m-ary transmission would be

$$p(\epsilon) = \sum_{a=r}^{m} \binom{m}{a} p^a q^{m-a}$$

which gives the probability distribution for independent trials with probability p of a correct bit and $q = 1 - p$ incorrect bit probability for any given chip. In the case of m-ary signaling $p - J/N_c$ and $q = 1 - J/N_c = (N_c - J)/N_c$. Given a probability of error that is acceptable, we can determine the number of jamming signals that will produce this error.

*N is the number of channels available. For contiguous channels $N = \mathrm{BW}/R$, where BW = bandwidth available, R = chip rate.

Shenzhen Huiding Tech. Co., Ltd. - Exhibit 1006

Table 2.2 Block Error Rate for *m*-ary Transmission of Three-, Five-, and Seven-Bit Blocks with Various Numbers of Errors Corrected

	Percent of Channels Jammed									
Corrected	5	10	15	20	25	30	35	40	45	50
	Error Rate									
1 in 7	0.04	0.15	0.28	0.42	0.56	0.67	0.76	0.84	0.89	0.93
2 in 7	0.004	0.026	0.073	0.15	0.24	0.35	0.47	0.58	0.68	0.77
3 in 7	0.0002	0.003	0.012	0.033	0.07	0.13	0.2	0.29	0.39	0.5
1 in 5	0.022	0.081	0.16	0.26	0.37	0.47	0.57	0.66	0.74	0.81
2 in 5	0.0012	0.0086	0.027	0.058	0.10	0.16	0.24	0.32	0.41	0.5
1 in 3	0.007	0.03	0.06	0.1	0.16	0.22	0.28	0.35	0.43	0.5

Table 2.2 lists the percentage of jammed channels allowable for various levels of error, correctable in blocks of three, five, and seven bits.

The prime advantage of *m*-ary transmissions in frequency hopping is that they are well adapted to the use of some powerful error-correction techniques without a great increase in the hopping rate being required. A good example is the TATS technique, which will be discussed in Chapter 4 in more detail. That system employs an octal Reed–Solomon error-correcting code in such a way that six-bit input data blocks are converted to seven-octit output symbols. Each octit (a three-bit word) is then transmitted as one of eight contiguous frequency hopping signals. Two advantages accrue from this format: One is that up to three errors in seven symbols can be corrected, and up to four errors in seven symbols can be detected. The second advantage is that the technique (which converts from binary to octal and back again) permits the use of an extremely powerful error-correcting code while increasing the symbol and hopping rates (the symbol rate is the rate at which the system sends encoded information) by a factor of only $\frac{7}{6}$.

2.3 TIME HOPPING

Time hopping, in other words, is the familiar pulse modulation; that is, the code sequence is used to key the transmitter on and off, as in Figure 2.22. Transmitter on and off times are therefore pseudorandom, like the code, which can give an average transmit duty cycle of as much as 50%. This form of signal, as spread spectrum modulation, has found its major application in combination with frequency hopping as in the RACEP systems developed by the Martin Marietta Corp. The fine point of difference separating time frequency and plain frequency hopping is that in frequency hopping systems the transmitted frequency is changed at

Shenzhen Huiding Tech. Co., Ltd. - Exhibit 1006

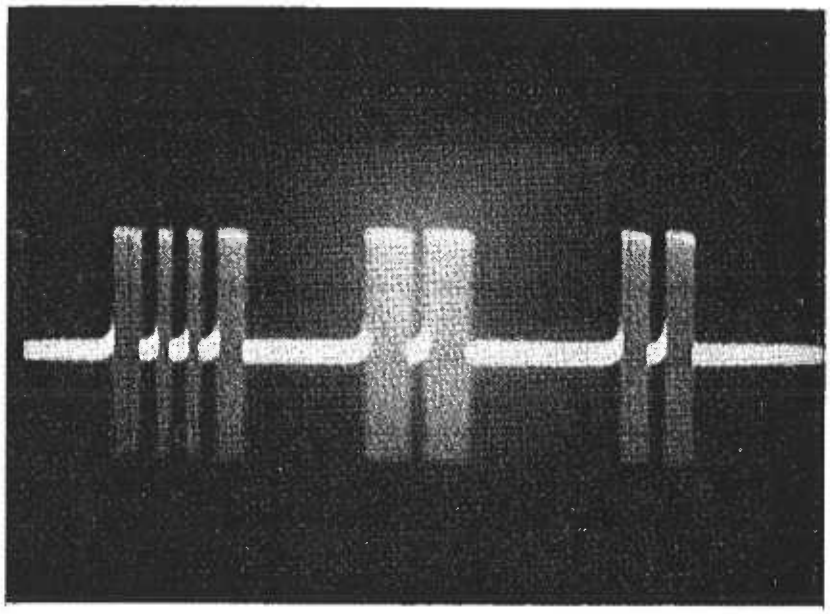


Figure 2.22 Pseudorandom code-keyed (time-hopping) signal waveform.

each code chip time, whereas a time-frequency hopping system may change frequency only at one/zero transitions in the code sequence. Figure 2.23 shows a time-hopping system in block form. The simplicity of the modulator is obvious. Any pulse-modulatable signal source capable of following code waveforms is eligible as a time-hopping modulator.

Time hopping may be used to aid in reducing interference between systems in time-division multiplexing. Stringent timing requirements must be placed on the overall system to ensure minimum overlap between

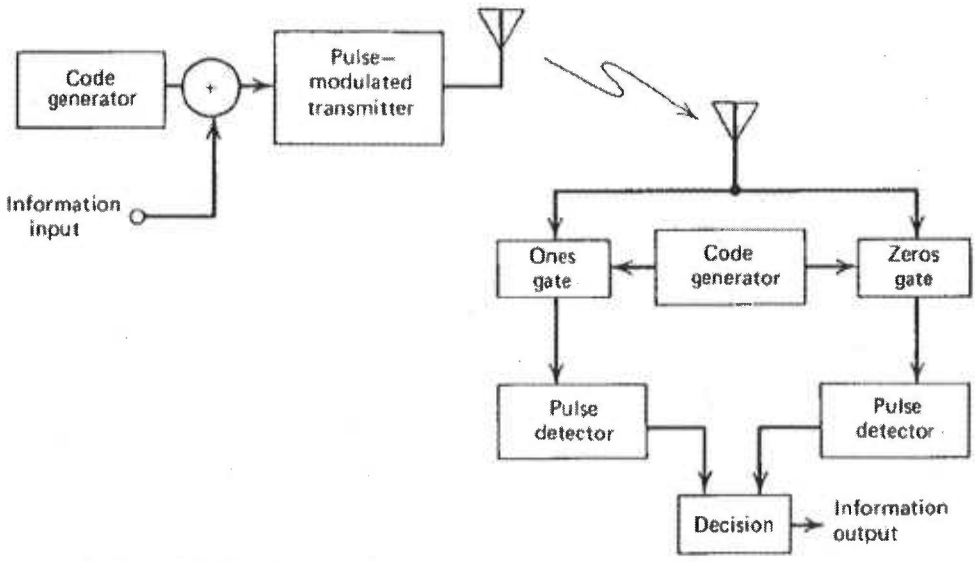


Figure 2.23 Simple time-hopping (pseudorandom pulse) system.

Shenzhen Huiding Tech. Co., Ltd. - Exhibit 1006

transmitters, however. Also, as in any other coded communications system, the codes must be considered carefully from the standpoint of their cross-correlation properties.

Simple time-hopping modulation offers little in the way of interference rejection because a continuous carrier at the signal center frequency can block communications effectively. The primary advantage offered is in the reduced duty cycle; that is, an interfering transmitter to be really effective would be forced to transmit continuously (assuming the coding used by the time hopper is unknown to the interferer). The power required of the reduced-duty-cycle time hopper would be less than that of the interfering transmitter by a factor equal to the signal duty cycle.

Because of this relative vulnerability to interference, simple time-hopping transmissions should not be used for antijamming unless combined with frequency hopping to prevent single frequency interferers from causing significant losses. For ranging, multiple access, or other special uses time hopping may be especially useful, if only because of the simplicity of generating the transmitted signal.

2.4 PULSED FM (CHIRP) SYSTEMS

Characteristics of Chirp Signals

One type of spread spectrum modulation that does not necessarily employ coding but does use a wider bandwidth than the minimum required so that it can realize processing gain is "chirp" modulation. This form has found its main application in radar but is also applicable to communications. Chirp transmissions are characterized by pulsed RF signals whose frequency varies in some known way during each pulse period. The advantage of these transmissions for radar is that significant power reduction is possible. The receiver used for chirp signals is a matched filter, matched to the angular rate of change of the transmitted frequency-swept signal. Coding is not normally used with this type of matched filter.

The transmitted frequency-swept-signal chirp signal is just that produced by a common laboratory sweep generator because most chirp systems use a linear sweep pattern. Any pattern, suitable to the requirement that a matching receiver filter must be built, is suitable. Here, however, we consider only linearly swept signals. Figure 2.24 illustrates typical waveforms that exist in a chirp system.

Letting $\mu = d\omega/dt$ for the frequency sweep rate, we see that the linearly swept transmitted signal (and the input to the chirp filter) is

$$F(t) = A \cos(\omega_c t + \tfrac{1}{2}\mu t^2)$$

Shenzhen Huiding Tech. Co., Ltd. - Exhibit 1006

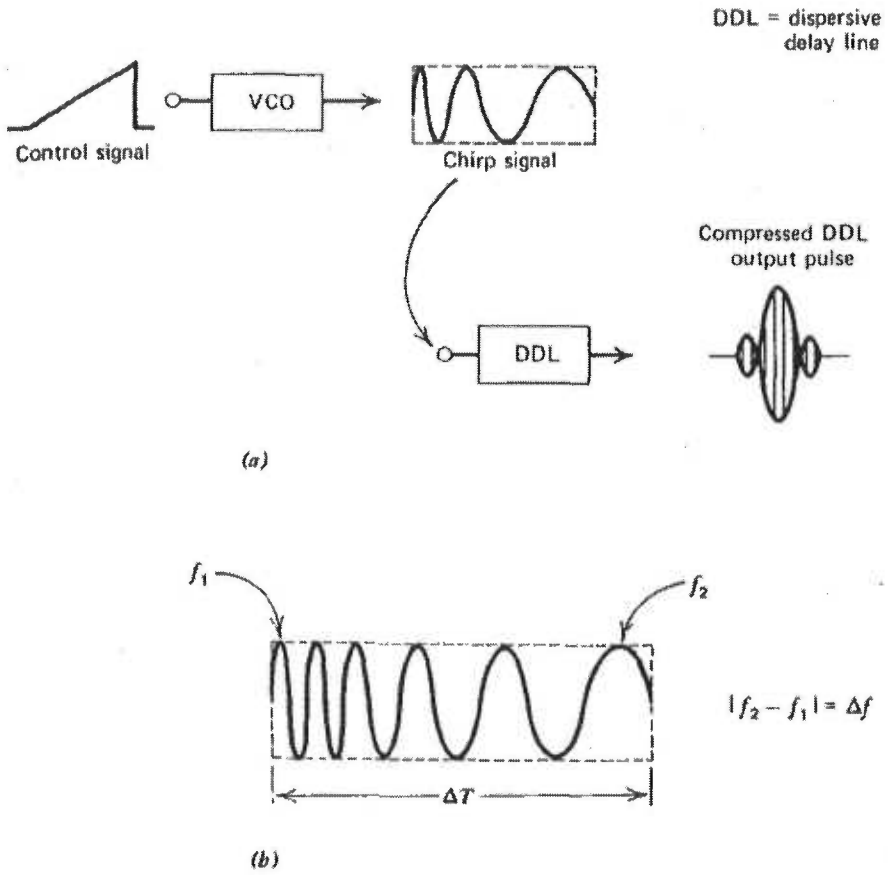


Figure 2.24 Chirp system waveform: (a) typical chirp waveforms; (b) transmitted chirp signal (one sweep).

over the linear range of frequency sweep. For the larger compression ratios of interest here amplitude distribution in our linear FM pulse is quite flat. Cook[210] and Klauder et al.[223] have shown that the chirp signal is distributed according to the Fresnel integral

$$Z(u) = \int_0^u e^{i\pi\alpha^{1/2}} d\alpha$$

and have plotted spectral amplitude for compression ratios as high as 130:1. Their plots confirm that ripple decreases as compression ratio increases.

The dispersive filter at the heart of a chirp receiver is a storage and summing device that accumulates the energy received over an interval, assembles it, and releases it in one coherent burst. We may visualize the filter's operation by imagining a transmitter that sends a series of signals over a time period, each of which is tagged in some way. The receiver then

Shenzhen Huiding Tech. Co., Ltd. - Exhibit 1006

sorts the signals according to their tags and assembles them so that they add together within a much shorter time period, reinforcing one another to produce a much stronger signal.

In actual practice, the "tagging" process used by the transmitter is its frequency sweep (which may be in either direction—low to high or high to low), with each increment in frequency denoting a new signal to be sorted and stored by the receiver. A received signal is stored until the entire ensemble of frequencies in one sweep arrives and the summed power at all frequencies is output at one time.

The transmitted signal may be developed in several ways, the simplest of which is application of a linear voltage sweep to a voltage-controlled oscillator. An alternative to the voltage-controlled oscillator is the chirp-generating filter. This is a filter whose impulse response is such that its output is a time series of output frequency components; that is, an impulse with a "continuous" frequency spectrum causes a series of output signals whose time delay is dependent on the frequency component being delayed. If the delay slope dt/df is linear (constant over the range of interest), the output is a linear frequency sweep and the chirp-generating filter can be made to be the exact complement of the receiver's dechirping filter. In fact, if chirp filters were designed as bilateral devices, a chirp-generating filter could also be used to dechirp.

The transmitted chirp signal has two parameters of primary interest. Once these parameters are defined, system performance is also defined, and the rest of the problem is making use of the capability inherent in the chirp signal. These parameters are (1) the frequency sweep $|f_2 - f_1| = \Delta f$ and (2) the amount of time ΔT used to sweep the Δf band. We assume that any amplitude change during ΔT is negligible.

The dispersive delay line or chirp-matched filter compresses a frequency sweep, usually linear, which provides an improvement in output

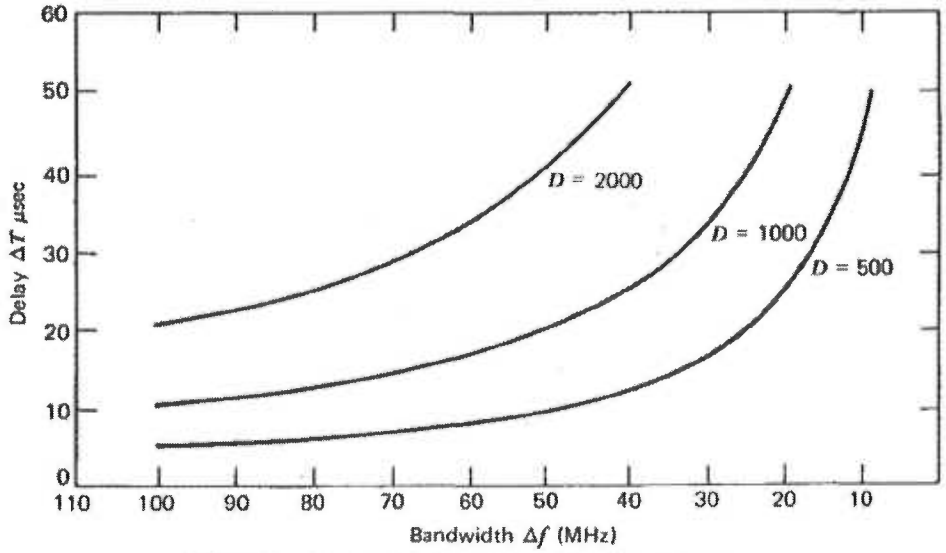


Figure 2.25 Chirp filter TW product curve.

Shenzhen Huiding Tech. Co., Ltd. - Exhibit 1006

signal (voltage) to noise ratio equal to $\sqrt{D}$, where the compression ratio is

$$D = \Delta T \, \Delta f$$

Δf is defined as the frequency sweep $|f_2 - f_1|$ and ΔT is defined as the time occupied by the sweep in frequency.

All signal parameters are transformed by the factor D between the filter's input and output as given below:

	Input	Output
Frequency sweep	Δf	$\Delta f / D$
Sweep time (signal duration)	ΔT	$\frac{\Delta T}{D} = \tau$
Signal (peak) power	$\hat{P}_i$	$DP_i = \hat{P}_0$
Time resolution	ΔT	$\pm\frac{\Delta T}{D} = \pm\frac{1}{\Delta f}$
Frequency resolution	Δf	$\pm\frac{\Delta f}{D} = \pm\frac{1}{\Delta T}$

Chirp systems are not the only ones that employ matched filters for reception. Matched filters made up of delay elements matched to a coded signal are also used. These are discussed in Chapter 6.

Figure 2.25 illustrates typical delay and bandwidth parameters available in contemporary delay lines of the dispersive type.

2.5 HYBRID FORMS

In addition to the more usual forms of spread spectrum modulation, there are the hybrid combinations of modulation that offer certain advantages over, or at least extend the usefulness of, the direct sequence and frequency hopping techniques. The most often used combination (or hybrid) spread spectrum signals are made up of (1) simultaneous frequency hopping and direct sequence modulations, (2) simultaneous time and frequency hopping, and (3) simultaneous time-hopping and direct sequence modulations.

The advantage in combining two spread spectrum modulation methods is usually that characteristics can be provided which are not available from a single modulation method. Implementation is not necessarily increased in difficulty by the same factor, however; that is, a combined frequency hopping and direct sequence transmitter might be built up of readily constructed code sequence generators and frequency synthesizers whereas a straightforward direct sequence modulator or frequency hopper could not be constructed to do the same job.

The specific construction of the various subsystems is not discussed

Shenzhen Huiding Tech. Co., Ltd. - Exhibit 1006

here because it is covered elsewhere. The emphasis here is on describing the hybrid techniques in use and reasons for that use.

Frequency Hopped/Direct Sequence Modulation

As suggested by its title, frequency hopped/direct sequence (FH/DS) modulation consists of a direct sequence modulated signal whose center frequency hops periodically. Figure 2.26 illustrates the frequency spectrum from such a modulator. The spread spectrum signal shown is made up of a number of spread spectrum signals. A direct sequence signal covering a part of the band appears instantaneously, and the entire signal appears in other parts of the band as dictated by a frequency hopping pattern.

Hybrid FH/DS signals are used for various reasons:

To extend spectrum spreading capability.

For multiple access and discrete address.

For multiplexing.

When the maximum in reliable sequence generator clock speed has already been obtained or a limit in the number of frequency hop channels has been reached, a hybrid modulator can be especially valuable. Say, for example, that a RF spectrum 1 GHz wide is wanted. The system designer could specify a 1136 Mcps code sequence generator to support a direct sequence transmitter, a frequency synthesizer with 200,000 5-kHz-spaced outputs for frequency hopping, or a hybrid combination. By combining the direct sequence and frequency hopping approaches we could construct a signal that has a 1 GHz spread spectrum bandwidth by using a 114 Mcps code sequence generator and a frequency synthesizer with only twenty 50-MHz-spaced frequencies available. It is obvious that the difficulty of building the hybrid modulator is significantly lower than that of either of the other approaches. Both the 114 Mcps code sequence generator and the 20-frequency synthesizer could be readily constructed today, which is much more than can be said for a 1136 Mcps code sequence generator or a 200,000 frequency, 1 GHz bandwidth frequency synthesizer.

Hybrid FH/DS transmitters are straightforward superimpositions of direct sequence modulation on a frequency hopping carrier, as shown in

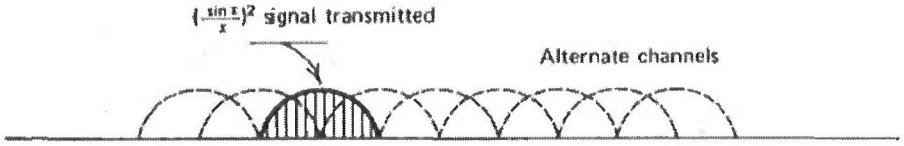


Figure 2.26 Frequency spectrum of hybrid FH/DS system.

Shenzhen Huiding Tech. Co., Ltd. - Exhibit 1006

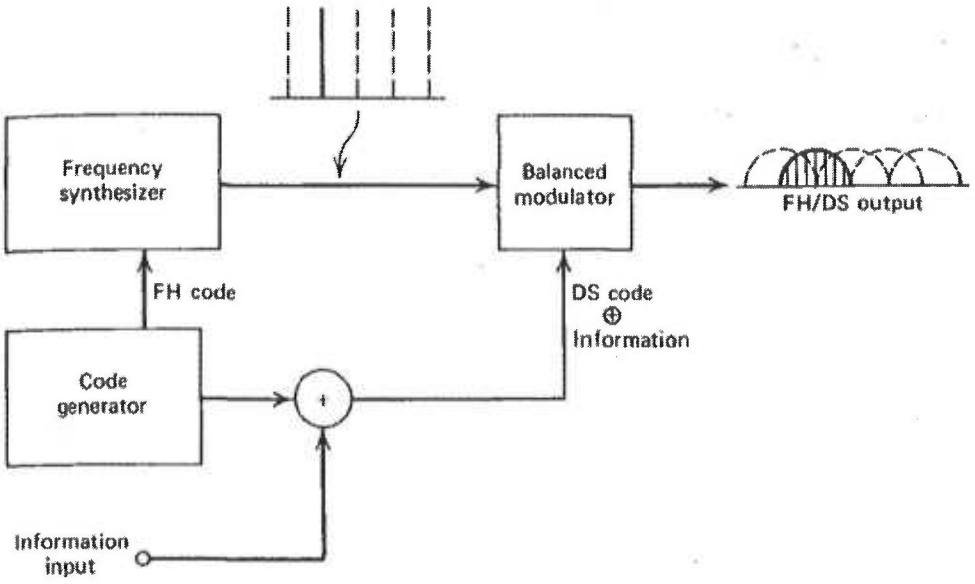


Figure 2.27 Hybrid FH/DS modulator.

Figure 2.27. This modulator differs from a simple direct sequence modulator mainly in that the carrier frequency is varying (hopped) rather than being at a constant frequency, as for simple DS modulation. Note also that the same code sequence generator can supply code data both to the frequency synthesizer to program its hopping pattern and to the balanced modulator for direct modulation.

Synchronism between the FH and DS code patterns means that whenever a given sector of the DS code pattern is transmitted the frequency channel will be the same. It should be noted that the DS code rate is normally much faster than the rate of frequency hopping. Therefore, many chips of DS modulation occur in a single frequency channel. Also, the number of frequency channels available is usually much smaller than the number of code chips so that in the course of a complete code length all the frequency channels are used many times. The pattern of their use, however, is as random (or pseudorandom) as the code itself.

The correlator used to strip off the spread spectrum modulation in a receiver, before baseband demodulation, is, for FH/DS hybrids, again a superimposition of a direct sequence correlator on a frequency hopping correlator; that is, the local reference signal becomes a hybrid FH/DS signal, which is then multiplied with all received input signals. Figure 2.28 shows a typical FH/DS receiver configuration in which the local reference generator is essentially a replica of the transmitting modulator, with two exceptions: (1) the local reference center frequency is offset an amount equal to the IF and (2) the DS code is unmodified by baseband input.

The process gain for FH/DS hybrids is a composite of that furnished

Shenzhen Huiding Tech. Co., Ltd. - Exhibit 1006

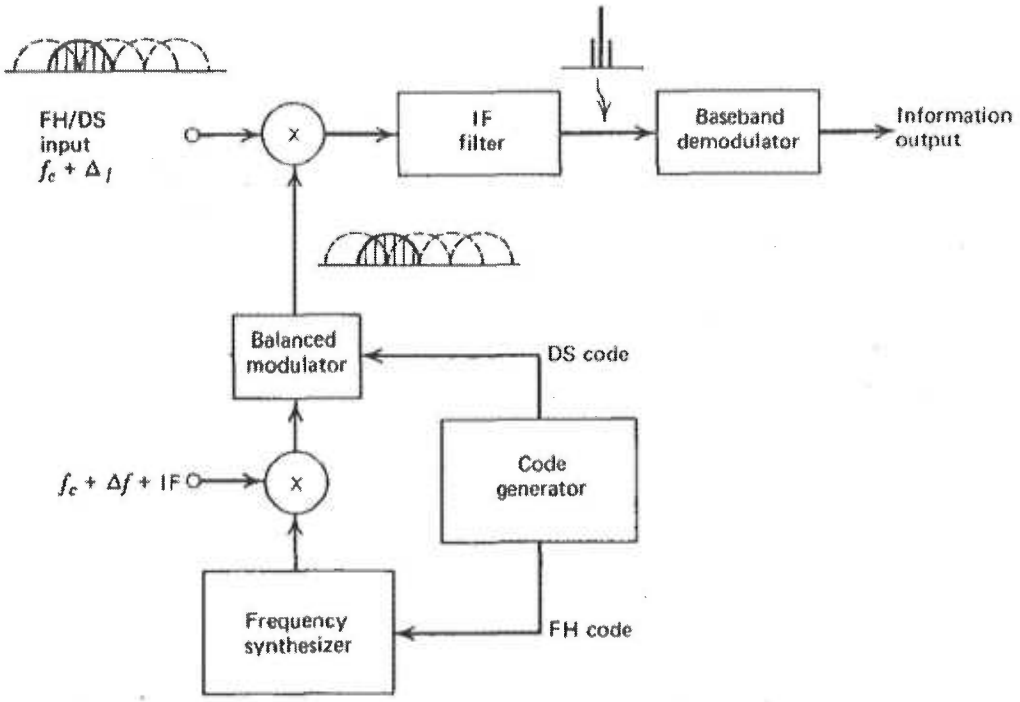


Figure 2.28 Hybrid FH/DS receiver.

separately by the frequency hopping and direct sequence modulations, with certain restrictions; that is, from an overall view the process gain is a function of

$$\frac{\text{BW}_{\text{RF}}}{R_{\text{info}}} = \text{FH/DS process gain}$$

When viewed with respect to particular signals, however, we see that this does not hold true when predicting jamming margin; for a hybrid FH/DS system, jamming margin is not necessarily related to process gain by the relation (see Chapter 1)

$$\text{jamming margin} = G_p - \left[L_{\text{sys}} + \left(\frac{S}{N} \right)_{\text{out}} \right]$$

although from an overall standpoint the relation holds. The reason is that in any particular segment of the overall input spectrum the FH/DS receiver can reject only that amount of interference commensurate with the spread spectrum bandwidth of the partial-band direct sequence signal; that is, if we refer to out 1 GHz bandwidth example, in which the DS signal bandwidth was 100 MHz, the process gain in that segment is limited by the 100 MHz DS bandwidth. This is true because an interfering signal (say a CW carrier) whose power falls wholly within one sector of the 1 GHz band is spready by only the bandwidth of the DS signal

Shenzhen Huiding Tech. Co., Ltd. - Exhibit 1006

whenever the signal hops into that sector. This means than when the signal lies in that one sector, a narrowband interferer can cause a loss of performance, with significantly less power than is required to interfere with the entire FH/DS signal structure.

The reason for pointing out this possible loss in partial-band jamming margin is that when the separated direct sequence channels are used as access channels for multiplexing more than one DS signal on a frequency hopping carrier it is possible for a single frequency interfering signal to interfere with only one channel, with no significant effect on the others. To prevent one user (or channel) from being completely lost, while spreading the effect of interference across all channels, we need to change the order of channel use periodically so that each user employs all available frequencies equally. In this way, even though an interfering signal causes complete loss of one frequency channel, each of the multiplexed signals would be affected only a part of the time equal to

$$\frac{\text{number of jammers}}{\text{number of channels}}$$

Thus, if our 20-channel system had an interfering signal in one channel, it would be affected 1/20th of the time, and if all users shared that channel, a particular user would be affected 1/400th of the time. It is reasonable to say, then, that process gain in decibels for a properly designed FH/DS hybrid system is the sum of the process gains produced by two overlaid spread spectrum modulations; that is

$$\begin{aligned} G_{p(\text{FH/DS})} &= G_{p(\text{FH})} + G_{p(\text{DS})} \\ &= 10 \log (\text{number of channels}) + 10 \log \frac{\text{BW}_{\text{DS}}}{R_{\text{info}}} \end{aligned}$$

Comparing the results of our 1-GHz spread spectrum example, we have process gain for a straightforward direct sequence system (assuming a 5-kbps information rate):

$$G_p = 10 \log \frac{1 \times 10^9}{5 \times 10^3} = 53 \text{ dB}$$

for a straightforward frequency hopper with 200,000 frequencies,

$$G_p = 53 \text{ dB}$$

for the FH/DS system,

$$G_{p(\text{FH/DS})} = 10 \log 20 + 10 \log \frac{1 \times 10^8}{5 \times 10^3} = 56 \text{ dB}$$

Shenzhen Huiding Tech. Co., Ltd. - Exhibit 1006

Process gain is actually 3 dB higher for the FH/DS system because of overlap allowed in the twenty 100-MHz-wide channels. (The same degree of overlap in a straightforward frequency hopper would produce 400,000 channels for a 56-dB process gain.) We emphasize that jamming margin may be significantly less than the simple FH or DS system, however.

Time-Frequency Hopping

Time-frequency hopping modulation has found its greatest application in those systems in which a large number of users with widely variable distances or transmitted power are to operate simultaneously in a single link. Such systems tend to employ simple coding, primarily as an addressing medium, rather than to spread the spectrum specifically. The general tendency is to design for the equivalent of a wireless telephone switching system in which random access and discrete address are the prime operational goals. For such uses time-frequency hopping is well adapted; it offers one of the few (and perhaps only) viable solutions to the near–far problem.

Consider for a moment two receiving and transmitting links whose receivers and transmitters are spaced as in Figure 2.29 and in which the receiver for each link is positioned so that the other link transmitter causes interference. The problem in this system lies in the difference in distance from a receiver to its desired transmitter and to the nearby transmitter.

The antijamming capacity of spread spectrum systems aids in such a situation but unfortunately is not enough under most conditions to overcome the disparity seen in nearby and remote signals. A close transmitter, for instance (say within a mile), would normally produce signals attenuated by 40-plus dB (the plus is a function of transmitting frequency), whereas another transmitter 20 miles away would produce

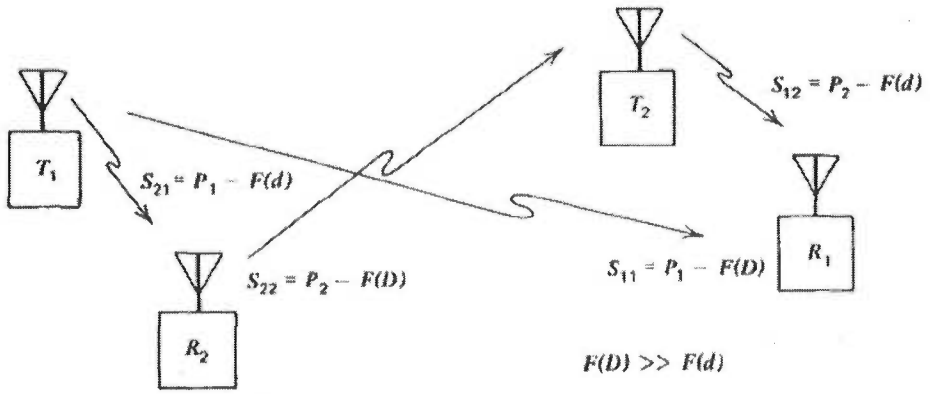


Figure 2.29 Two-link communication system illustrating the near-far problem.

Shenzhen Huiding Tech. Co., Ltd. - Exhibit 1006

signals attenuated by 63-plus dB. To operate in such an environment a receiver would need process gain in the order of 35 dB with no allowance for fading. Processing alone is not really the answer to near–far reception difficulties. A much better solution is to time all transmissions so that the desired and undesired transmitters are never transmitting at the same time. Even better, with time-frequency hopping the two transmitters can be programmed to transmit on different frequencies as well as at different times. Many links can then be operated at once if their time slots and frequency hopping channels are properly synchronized.

Time-Hopping Direct Sequence

When direct sequence transmission is used and code division multiplexing does not permit sufficient access to the link, time-hopping has proved to be a useful way of adding time-division multiplexing (TDM) to aid in traffic control. The high degree of time synchronization between direct sequence transmit–receive terminals because of their code correlation requirements leads ideally to time-hopping; that is, because a direct sequence receiver must align its local reference code within a fraction of a *pn* code chip time, it already has timing good enough to support TDM operation.

All that is required to add time-hopping TDM to a direct sequence system is on–off switching and control. For time-hopping the on and off decision can be easily derived from the same code sequence generator used to derive the spectrum spreading code. An easily implemented keying control would be an n-input gate which senses some previously chosen shift register state and turns the transmitter on or off at the appearance of that state. Figure 2.30 illustrates a time-hopping direct sequence (TH/DS) transmitter. The receiver for this system would operate similarly, except that the control signal would be used to block or enable the receiver front end synchronously with the expected transmit signal.

When selecting the code state for time control, we choose a shift register state that occurs repeatedly and detect the occurrence of that state. For an n-stage maximal-connected shift register generator there are $2^n - 1$ unique states, each occurring once per repetition of the m-sequence. By choosing a number of register stages $(n - r)$ and sensing an all-ones condition in those stages, we could expect to see that condition 2^r times a code sequence and the distribution of that occurrence would be (pseudo-) random.

On the average, the state sensed would occur at a rate

$$\frac{R_c 2^r}{2^n - 1} = \text{average state occurrence for } (n - r) \text{ stage vector}$$

Shenzhen Huiding Tech. Co., Ltd. - Exhibit 1006

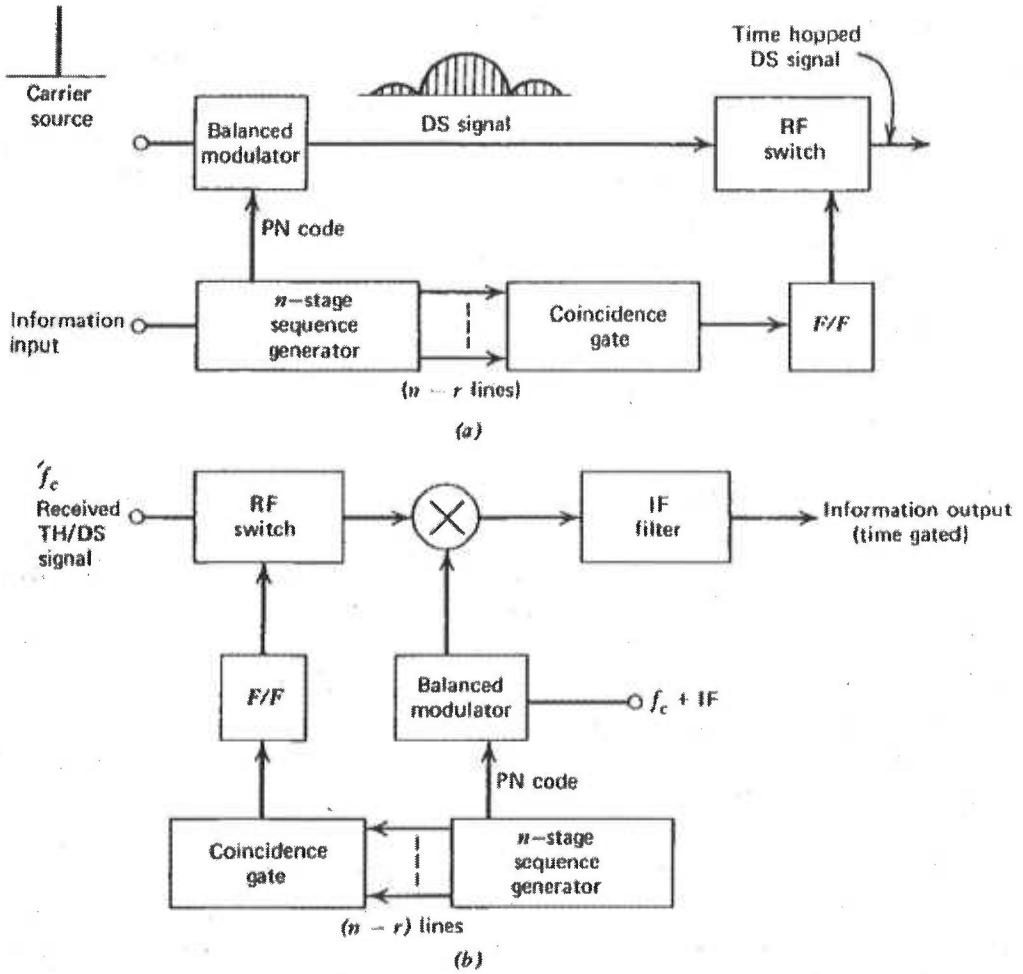


Figure 2.30 TH/DS system block diagrams: (a) time-hopping/direct sequence transmitter; (b) TH/DS receiver.

and the direct sequence "on" periods would occur at an average rate

$$\frac{R_c 2^r}{2^{n+1} - 2} = \text{average pulse occurrence for TH/DS transmission}$$

where R_c = code clock rate,
n = shift register length,
r = register stages not sensed.

We could then select the average frequency of occurrence of direct sequence output, with the actual output occurring at pseudorandom intervals for a pseudorandom duration, as dictated by the code. This pseudorandom time division can permit more channel users, improve operation over simple code division multiplex, and allow more accesses. Again, as in all other applications of codes for signal discrimination, code cross-correlation should be well defined before a TH/DS operation is attempted.

Shenzhen Huiding Tech. Co., Ltd. - Exhibit 1006

PROBLEMS

1. Why employ a balanced mixer to generate a direct sequence spread spectrum signal?
2. Remembering that a direct sequence signal has a $[(\sin x)/x]^2$ power spectrum, what is the signal's 3-dB bandwidth? What is the peak power level of the first sidelobe compared with that of the main lobe?
3. What percentage of total signal power is contained in the main lobe of a direct sequence signal?
4. Compare the power densities that would exist at a point 5 MHz removed from the center frequency of a 20 MHz wide (a) frequency hopped signal, and (b) direct sequence signal, BPSK, QPSK, classic MSK.
5. What number of channels is required by a frequency hopper whose maximum bit error rate is 0.01 and which must have a 30-dB jamming margin?
6. What RF bandwidth would this frequency hopper employ if its frequency cells were contiguous, its data rate were 1 kpbs, and three chips were transmitted per bit?
7. For the same 30-dB jamming margin, 0.01 bit error rate, and 1 kbps data, what RF bandwidth would be required by a direct-sequence system?
8. The process gain expected from a hybrid FH/DS system with a 20 Mcps code rate, 100 frequency cells, and 3 kbps data rate would be how many decibels?
9. Compare the demodulator bandwidth required on coherent and non-coherent frequency hopping systems.
10. Compare demodulator bandwidth for one- and three-chip-per-bit frequency hopping systems.
11. What would be the effect of a Doppler frequency shift on an upchirp–downchirp system?
12. Compare multipath sensitivity for direct sequence and frequency hopping systems.
13. How might time/frequency hopping be employed to overcome near–far and transmitter imbalance problems?
14. Determine the minimum hop rate that should be used for a fixed receiver when an interferer is 10 miles away and the desired signal transmitter is 100 miles away at a 45° angle from the desired signal. The interferer is a repeater.
15. Compare power density for a chirp signal with that of direct sequence and frequency hopping signals.

Shenzhen Huiding Tech. Co., Ltd. - Exhibit 1006

4

MODULATION AND MODULATORS: GENERATING THE WIDEBAND SIGNAL

The wideband signals characteristic of spread spectrum systems are generated in different ways in the basic techniques of interest here. In a direct sequence system the encoding signal is used to modulate a carrier, usually by phase-shift keying at the code rate; that is, for a "one" in the code pattern, one carrier phase is transmitted and for a "zero" a different carrier phase is sent. More complex phase-shift mappings are also used (such as quadriphase), but in each there is a one-to-one correspondence between the carrier phase transmitted and the code reference or references. It is of some interest to note that balanced modulation* is often used, because this suppresses carrier components and helps to hide the signal. In addition, no power is wasted in transmitting a carrier that would contribute nothing to interference rejection or information transfer.

Frequency hopping systems generate their wideband signal spectra in a different manner from direct sequence systems, although the modulation is still dictated by a code sequence. The relation of the code sequence to the RF output is such that it commands the frequency of a carrier signal rather than directly modulating the carrier; that is, for a given code state the system transmits at one frequency and for any other code state transmits at a different frequency. In each state the code commands the system output frequency. Therefore, the carrier "hops" from one frequency to another in synchronism with code state changes.

*Balanced modulation multiplies a carrier $A \cos w_c t$ with a modulation term $B \cos w_m t$. The resulting signal is $AB \cos w_c \cos w_m t = AB \cos w_r + w_m t$, for which there is theoretically no carrier term. In practice carrier suppression for such modulators is between 20 and 60 dB.

Shenzhen Huiding Tech. Co., Ltd. - Exhibit 1006

Typically, a frequency hopping system may have a few thousand available frequencies to choose from and a code sequence generator with at least that number of states; for example, a system with a frequency synthesizer capable of outputing any one of 10,000 frequencies separated by 1 kHz would have an RF bandwidth of 10 MHz. Its code generator should then be able to generate a code sequence at least 10,000 chips long so that each of the frequencies available can be used. A 14-stage shift register sequence generator could be used for this purpose because it can generate sequences up to $2^{14} - 1 = 16{,}383$ chips. The wideband signal spectrum from a frequency hopper is not generated by carrier modulation like the direct sequence signal. Instantaneously, the system has only one output rather than a set of symmetrically distributed outputs.

Information is normally embedded in the code sequence that determines frequency for a frequency hopper or spectrum spreading for a direct sequence system. Therefore, it does not matter which type of spread spectrum system one is dealing with, from the standpoint of information transmission, if the information to be sent is a part of the code sequence. The same code might be used for a direct sequence biphase or quadriphase modulator or at a lower rate to determine the frequencies over which a frequency hopper spreads its output.

The point is that both direct-sequence and frequency-hopping systems generate wideband signals under the control of a code sequence generator. In one case, the code is used as direct carrier modulation (direct sequence) and in the other (frequency hopping) the code commands the carrier frequency. This chapter shows spectrum spreading subsystems and circuits typical of those used in practical systems and discusses the problems most often encountered.

4.1 BALANCED MODULATION

An important tool in any suppressed carrier system is the balanced modulator used to generate the transmitted signal. Balanced modulation is employed in many applications in which either one or both of the signals applied to a modulator must be suppressed at its output. Balanced modulation for carrier suppression is at least 60 years old; a patent for this purpose was filed by J. R. Carson in 1915.

Here we intend to show the specific application of balanced modulation in direct sequence spread spectrum systems. We also illustrate the effects of various circuit problems on the output signal.

Almost as many kinds of balanced-modulator (or balanced mixer, depending mainly on who is using it) circuits exists as there are applications. Recent advances in semiconductor diodes (in particular, hot carrier diodes and wideband transformers) and their application to ring-configured diode modulators[1019,1022,1023] (see Figure 4.1) have generally

Shenzhen Huiding Tech. Co., Ltd. - Exhibit 1006

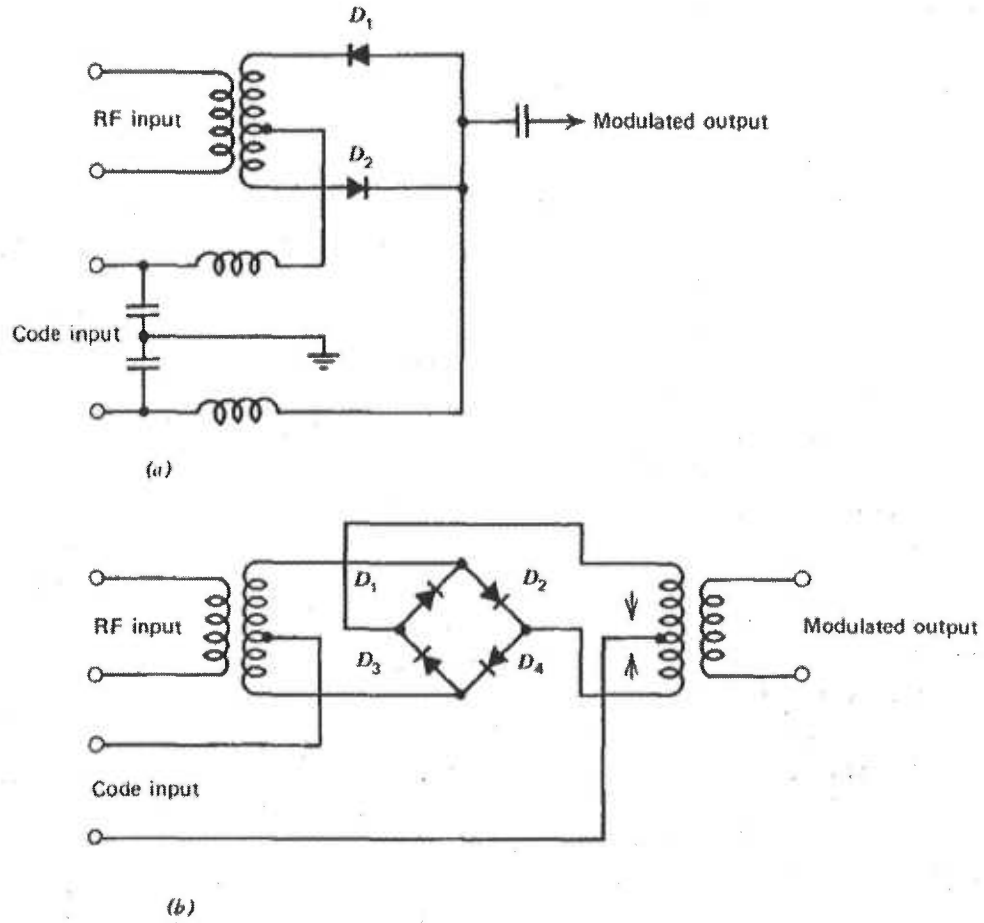


Figure 4.1 Diode-balanced modulator configurations: (*a*) typical single-balanced mixer/modulator; (*b*) typical double-balanced mixer/modulator schematic diagram.

made obsolete all others for most applications. Therefore, our emphasis is on the diode modulator. Commercially available single- and double-balanced diode modulators cover most frequency ranges and offer excellent performance from the standpoint of input signal suppression, low loss, and stable operation.

A simple form of balanced mixer/modulator is a double throw switch, connected so that it switches between two 180°-separated input signals at a modulating signal rate. This configuration would work quite well for digital data modulation and in fact is the same in function as a modulo-2 adder. Figure 4.2 shows a balanced mixer output signal as modulated by a binary switching signal. (The binary switching signal is for out purposes a code sequence, with embedded information. This is true for biphase or quadriphase signals. Note that since the code includes the transmitted information, the single spectrum spreading, balanced-modulation operation satisfied both information transmission and RF signal spreading requirements.)

For code-modulated RF signals the balanced-modulator output is a

Shenzhen Huiding Tech. Co., Ltd. - Exhibit 1006

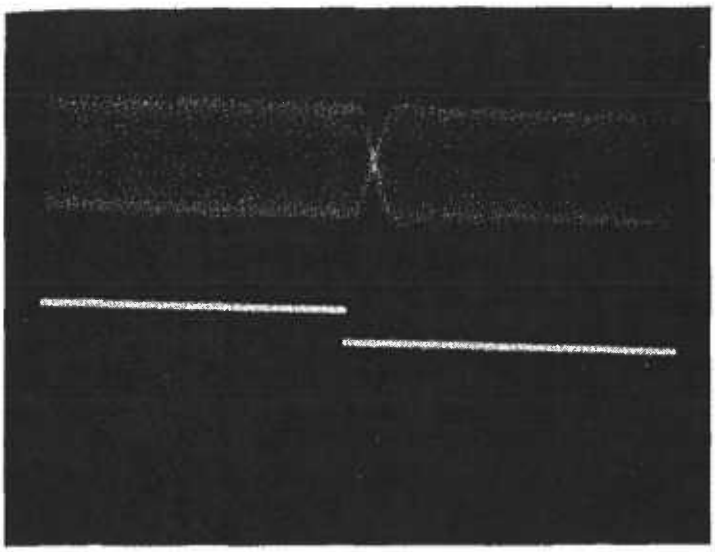


Figure 4.2 An actual balanced mixer output signal.

square wave modulated carrier rather than the familiar sine-wave-modulated balanced signal. For sine wave modulation, the signal may be expressed as

$$A \cos \omega_c t \; B \cos \omega_m t$$

Similarly for data modulation the signal is

$$A \cos \omega_c t \; B \cos \omega_s t$$

where ω_s is a time-varying set of frequencies harmonically related to the data bit rate and run lengths.

Output waveforms from sine-wave- and data-modulated balanced modulators are shown in Figure 4.3.

Spectral outputs of the two modulating signals are $AB\cos(\omega_c + \omega_m)t$ for sine wave modulation in which only two sidebands are represented and $AB\cos(\omega_c + \omega_s)t$ for data. Those familiar with single-sideband systems will recognize the signal in Figure 4.3*a*.

The code-modulated spectrum is not a single pair of sidebands but a set of symmetrical $[(\sin x)/x]^2$-distributed sidebands due to the many code frequency components. In any case, the carrier signal is suppressed an amount that depends on the design of the balanced modulator and on the carrier waveform.

When a code is used to generate a spread spectrum output from a balanced mixer/modulator, a great deal of care must be exercised to provide both carrier and code clock suppression. Figures 4.4 through 4.10 are actual photographs of spread spectrum output signals. The single-balanced mixer of Figure 4.1*a* suppresses only the RF input by inverting

Shenzhen Huiding Tech. Co., Ltd. - Exhibit 1006

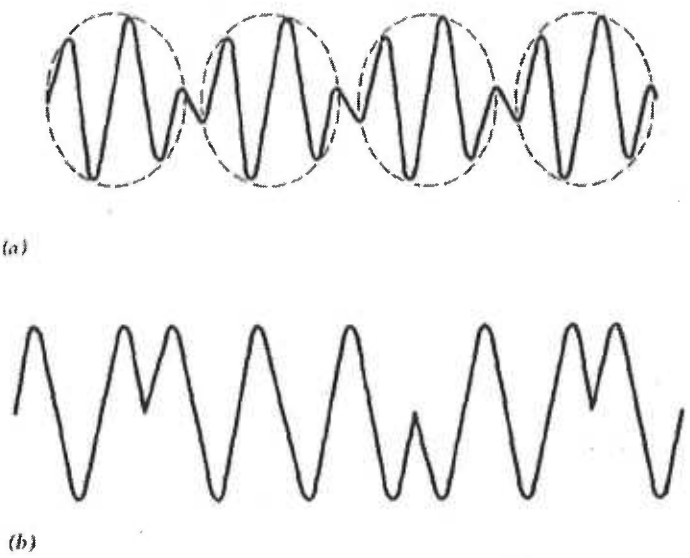


Figure 4.3 Balanced modulator output waveforms: (*a*) sine-wave-modulated balanced mixer output signal; (*b*) data (code)-modulated balanced mixer output signal.

the phase of the RF carrier at a code-determined rate. A code input turns on either diode one (D_1) or diode two (D_2) and turns off the other diode, depending on the relative polarity of the input. Because the code input is complementary, one input is always at a higher DC level than the other, and if the difference between the two exceeds a diode's forward voltage drop, one of the two will conduct. (In practice, the code input voltage should be higher than the carrier input level.) Diode conduction then allows one phase of the RF carrier to pass to the output.

For improved overall input suppression, the double-balanced configuration of Figure 4.1*b* is recommended. Here a diode bridge is used and an output transformer is added. Operation is similar to the single-balanced mixer/modulator in that the polarity of the code input lines determines whether D_1 and D_4 or D_2 and D_3 are conducting and thereby determines which RF carrier phase appears at the output. In addition, the balanced windings on the transformers allow suppression of the code input signal at the output. This suppression occurs because code-related current is in opposition in both input and output transformers and thus tends to cancel.

The spectrum of a properly operating biphase modulated signal is shown in Figure 4.4. The power distribution of this signal is $[(\sin x)/x]^2$, with line separation within this distribution equal to the repetition rate of the code modulating signal; for example, if a 1023 chip code with a 1 Mcps rate were used, the code would repeat $(1 \times 10^6)/1023 = 977$ times per second and the line separation in the modulated signal would be 977 Hz. Because of the pseudorandum character of the code, however, the appearance of any particular spectral component in time is also pseudorandom. Therefore, the direct sequence modulated signal appears to be noise with a $[(\sin x)/x]^2$ distribution.

Shenzhen Huiding Tech. Co., Ltd. - Exhibit 1006

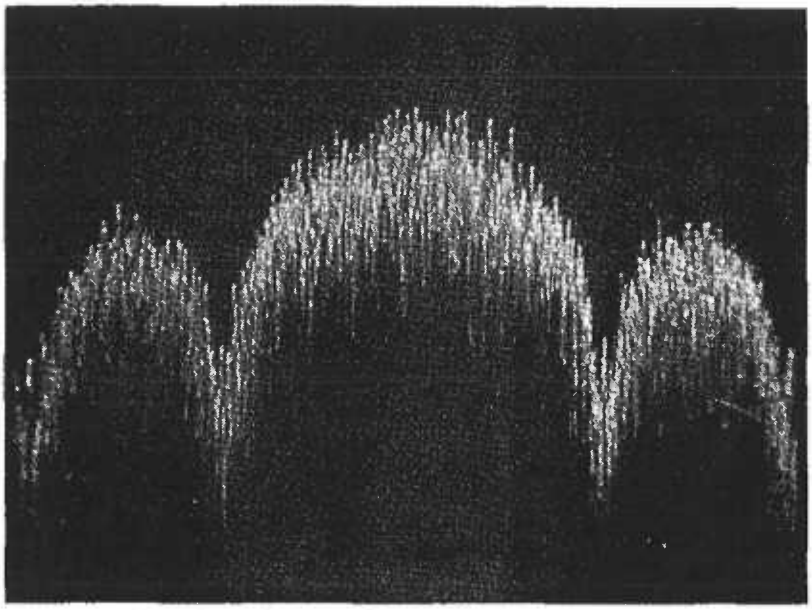


Figure 4.4 Satisfactory balanced mixer/modulator output.

Figure 4.5 illustrates the effect of poor carrier balance, which could be caused by imbalance in the transformers of Figure 4.1, an open diode, or any other cause that might give the effect of unequal 180° carrier inputs. The two phases of the carrier must also be well matched to provide satisfactory balance. (In the diode mixer/modulator of Figure 4.1 the two carrier phases are provided by the input transformer.) Either amplitude inequality or less than 180° phase shift can cause the carrier to be present in the modulated output.

Figure 4.6 is a phasor diagram of the modulated output, which is

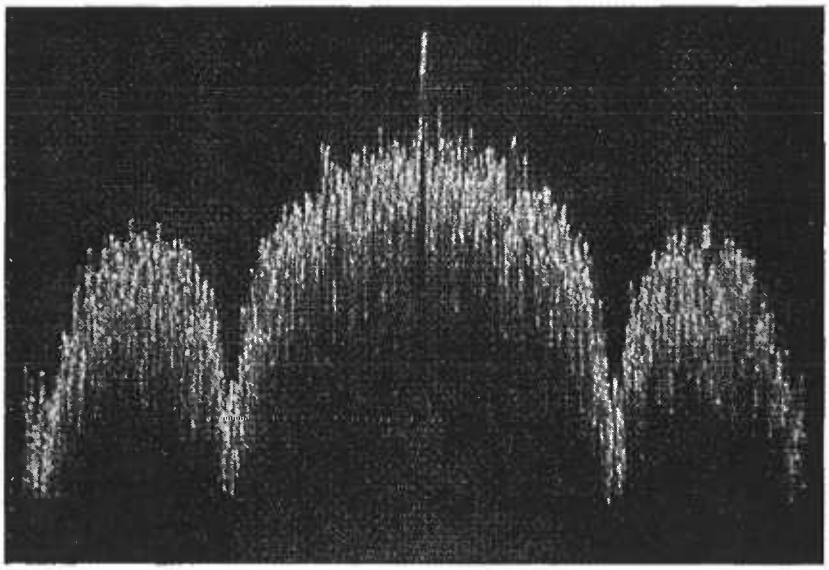


Figure 4.5 Balanced mixer/modulator output showing lack of carrier balance.

Shenzhen Huiding Tech. Co., Ltd. - Exhibit 1006

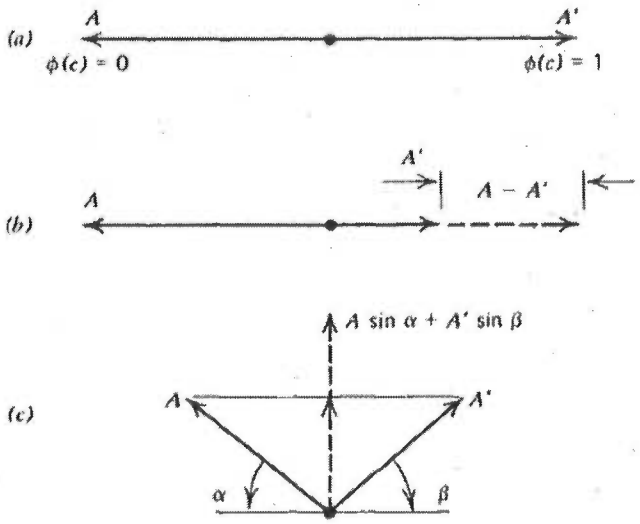


Figure 4.6 Vector diagram of biphase-balanced modulation.

recognized as antipodal. The carrier output that results is zero when the $\phi(c)$ corresponding to the one and zero code inputs are balanced and in phase opposition.

A difference in amplitude of the two output phases results in imbalance $A - A'$ as illustrated in Figure 4.6*b*, and a less than 180° phase relationship is shown by Figure 4.6*c*.

Carrier suppression may be expressed in decibels below the output desired by the expression

$$V = 10 \log \frac{B}{A \sin \alpha + A' \sin \beta} \text{ dB}$$

where B = amplitude of the correct output signal (i.e., $A = A'$ and $\alpha = \beta = 0$),
A = zero degree signal amplitude,
A' = 180° signal amplitude,
α = A phase offset,
β = A' phase offset.

In some cases a controlled amount of carrier signal is deliberately sent for use in carrier tracking without code demodulation as in the Air Force's SGLS space ground link subsystem system. For such an application the system is usually designed so that $\alpha = \beta$, $A = A'$, and $V = (10 \log B)/(2 \sin \alpha)$.

Phase modulation by less than 180° is also used when the modulated signal is multiplied by an even number. Unfortunately, this is not practical for 180° biphase modulation because even-order multiplication of any signal that is symmetrical in the frequency domain removes the symmerical sidebands and produces an unmodulated output at the

Shenzhen Huiding Tech. Co., Ltd. - Exhibit 1006

frequency multiple desired. This problem is overcome by phase modulating by $\pm 90/k$ degrees before multiplication by the factor k. When carrier suppression is critical, however, the technique is not recommended, for modulation at odd phase angles can be quite difficult to maintain and any departure from the desired $90/k$ modulation angle would significantly reduce carrier suppression after multiplication.

Alternatives to less than $\pm 90°$ modulation in which multiplication is involved are the following:

1. Separately multiply the carrier, then modulate. In general, this is a practical solution because balanced mixers and modulators are commercially available to several gigahertz.
2. Multiply by the odd order, because odd-order multiplication preserves symmetrical modulation.

A typical direct sequence output signal in which the carrier signal is poorly suppressed is shown in Figure 4.5. In most instances poor balance might not be so clearly evidenced. Often, however, a constant signal component is detectable in the output spectrum when carrier balance is not as it should be. The best method for checking carrier suppression is to remove the code modulation and substitute a square wave. This permits observation of the carrier component in comparison to the square-wave-modulation sidebands without noiselike code components (see Figure 4.7). Varying the square wave frequency over the range of code frequency components (code rep rate^{-1} to clock rate/2) also allows a check of modulator balance with code modulation.

Figures 4.8 and 4.9 show the effects of (1) nonsymmetry in the code modulating sequence and (2) simultaneous code nonsymmetry and lack of carrier balance. Code symmetry is more difficult to provide in a practical system than carrier balance because of the characteristics of the circuits used to drive the balanced modulator with a code sequence. Many integrated-circuit flip-flips are capable of driving a diode-balanced mixer/modulator directly and offer the best general symmetry; that is, both discrete circuits and separate drivers tend to exhibit more differ-

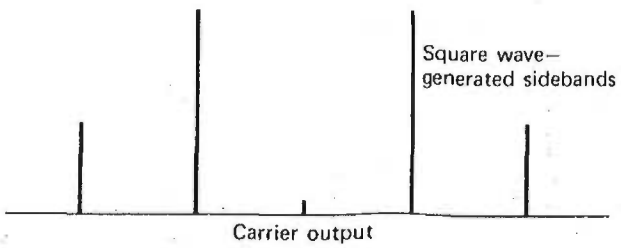


Figure 4.7 Typical square-wave-balance modulation test spectrum for checking carrier suppression.

Shenzhen Huiding Tech. Co., Ltd. - Exhibit 1006

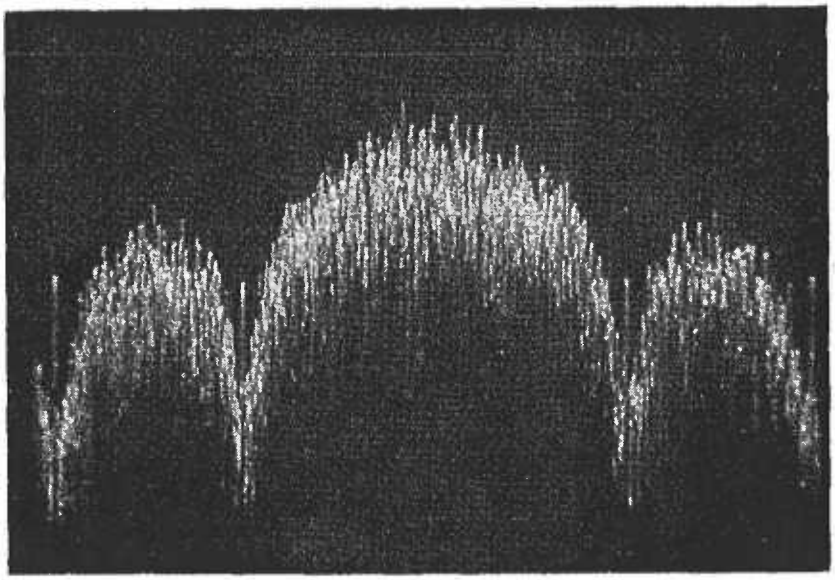


Figure 4.8 Balanced mixer/modulator output showing poor code balance.

ential change in output signal than complementary outputs from a single integrated-circuit flip-flop.

The problem is this: to exhibit good code-rate suppression a balance-modulated output signal must weight the signal corresponding to a one at the same value as a signal corresponding to a zero; that is,

$$A \int_0^{\tau} G_1(c)\, dt$$

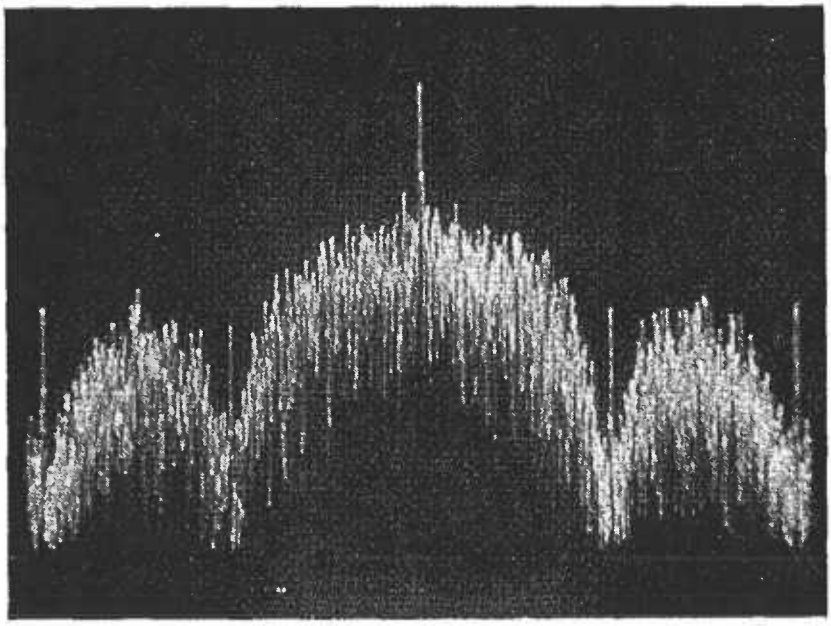


Figure 4.9 Balanced mixer/modulator output showing both carrier and code imbalance.

Shenzhen Huiding Tech. Co., Ltd. - Exhibit 1006

must equal

$$A' \int_{\tau_1}^{\tau_2} G_0(c)\, dt$$

where $G_1(c)$ is the signal envelop corresponding to a one and $G_0(c)$ is the signal envelope corresponding to a zero. Also, the periods $\{\tau_1 - 0, \tau_2 - \tau_1\}$ and amplitudes $\{A, A'\}$ must equal one another.

Now, in flip-flop output stages the rise and fall times of the output signals are not the same. Furthermore, temperature change causes characteristic changes and the two may not maintain the same relationship. Therefore, we caution the designer that no matter how good the balanced modulator may be some attention must be paid to code symmetry or his or her work will be of little value for code-rate suppression.

Effects of Carrier and Code-Rate Spurious (Lack of Suppression)

What is the effect of having a modulated output like that in Figure 4.9? In the transmitter the most significant effect is that after having gone to the trouble of code modulation our output spread spectrum signal has stationary, easily detected signals in its midst, which defeat one purpose of spread spectrum modulation by causing narrowband interference, transmission of wasted power, and relatively easy detection.

In spread spectrum receivers a narrowband signal due to carrier or code imbalance is even less desirable. These signals can render the receiver unusable because undesired narrowband input signals may be translated directly into the IF (see Section 5.2). Figure 4.10 shows the effect of excessive code clock leakage through or around the balanced mixer/modulator so that the output is not only balanced-modulated by the code but amplitude-modulated by the code clock. This is usually simple to prevent, but the undesired output signals can cause the same kinds of spurious signals already discussed.

Quadriphase Modulation

Quadriphase modulation is an extension of biphase-balanced modulation and is often used in direct sequence systems. The main reasons for quadriphase, despite its extra complexity, are that (1) a quadriphase signal is not so seriously degraded as a biphase signal when passed through a nonlinearity simultaneously with interference and (2) the RF bandwidth for a quadriphase signal is half that required by a biphase signal, given the same data rate. Alternatively, twice as much data might be transmitted in the same bandwidth with a quadriphase signal as with a

Shenzhen Huiding Tech. Co., Ltd. - Exhibit 1006

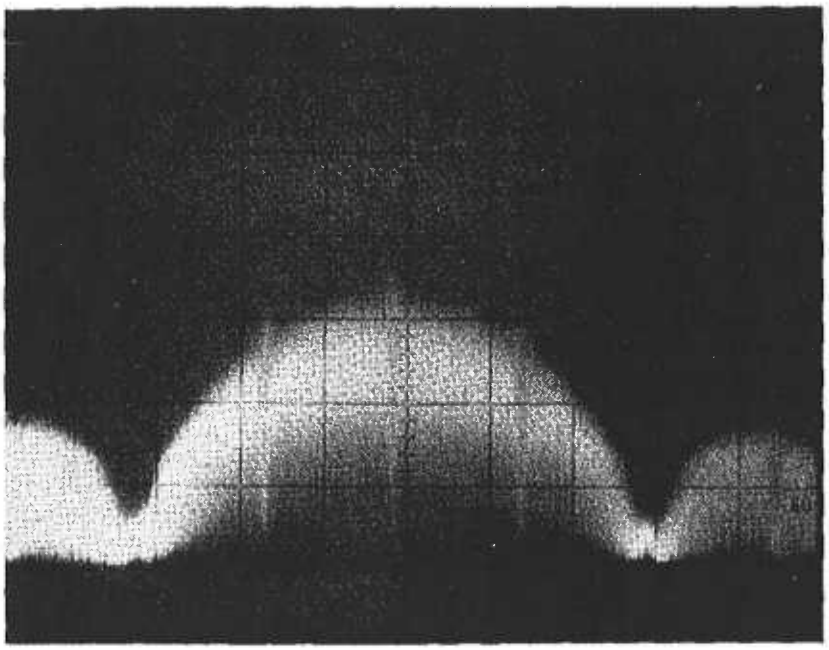


Figure 4.10 Balanced mixer/modulator output showing code clock leakage.

biphase signal. A quadriphase modulator shifts between one of four carrier phases spaced at 90° intervals. Thus 2 bits of binary data are required to select the phase to be transmitted. A typical scheme for such selection might be

Data Bits		
A	*B*	Transmitted Phase
0	0	0°
0	1	90°
1	0	270°
1	1	180°

Of course, any other one-to-one correspondence between the data and the transmitted phase is just as good. The only requirement is that a transmitter and receiver both employ the same data-to-carrier phase relationship.

The block diagram in Figure 4.11 shows a common quadriphase modulator configuration that consists of a combined pair of biphase modulators. An input RF carrier is phase shifted by 90° and applied in the original and quadrature form to a pair of biphase modulators. Separate binary inputs drive the two modulators and their outputs are summed (Figure 4.12). Any combination of carrier phases from the two biphase modulators (a, a' and b, b' are not allowed) results in a summed output that is one of the four desired carrier phases.

Shenzhen Huiding Tech. Co., Ltd. - Exhibit 1006

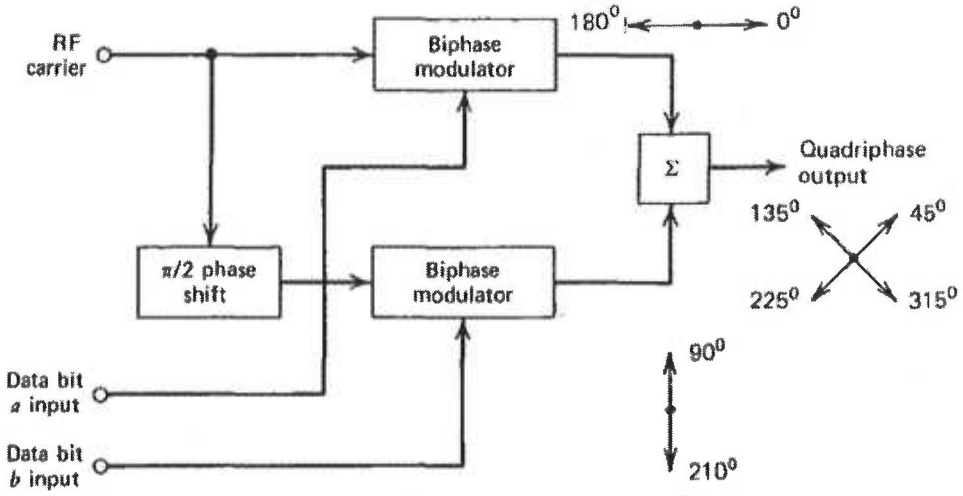


Figure 4.11 Quadriphase modulator block diagram.

The capability of quadriphase signals to pass through limiting with minimal processing loss has a great deal of importance but is left for discussion in Chapter 7.

The power envelope of a quadriphase signal has the same shape as a biphase modulated signal; that is, $(\sin_2 x)/x^2$. The main-lobe bandwidth, however, is only half that of the biphase signal for the same code rate; that is, the first null of the $(\sin^2 x)/x^2$ spectrum occurs at chip rate/2, and successive nulls occur at the same interval. We recall that the biphase-modulated signal has a main lobe whose first null occurs at the chip rate, with succeeding nulls also separated by the chip rate. Figure 4.13 illustrates this relationship.

In typical QPSK-modulated spread spectrum systems the spectrum employed has the same bandwidth as a BPSK-modulated system using

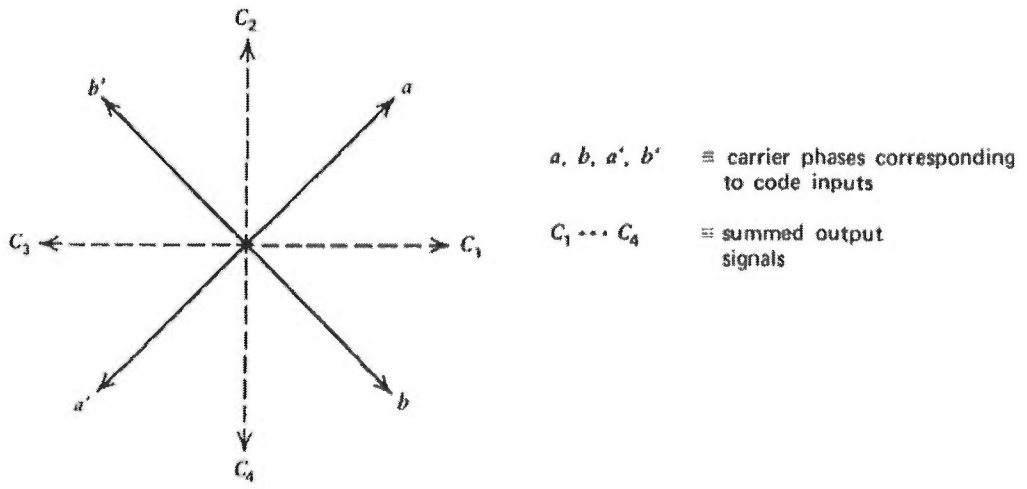


Figure 4.12 Output carrier phase derivation corresponding to data input.

Shenzhen Huiding Tech. Co., Ltd. - Exhibit 1006

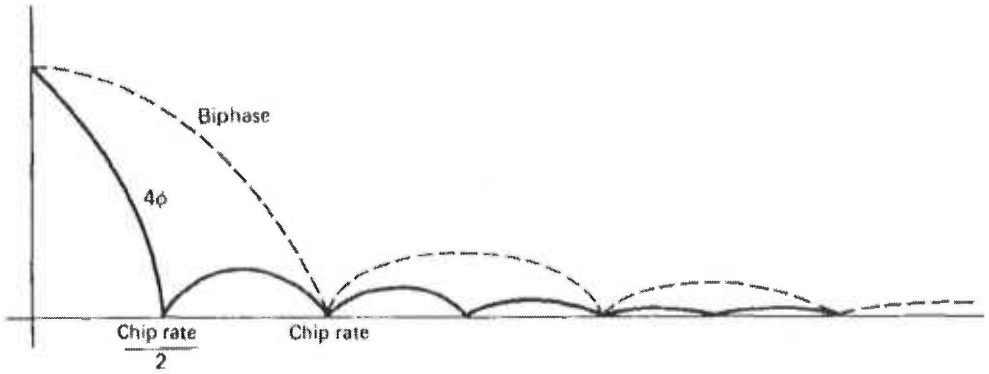


Figure 4.13 Comparison of biphase and quadriphase signal spectra for the same code rate (one code only).

the same code rate. This is accomplished by using two codes in the QPSK systems that have the same rate as the single code used in a BPSK system. This is done to avoid the loss in processing gain that would occur if the RF bandwidth were reduced.

Carrier Modulation Trade Offs

The major concerns in choosing a modulation waveform that must be taken into account in a spread spectrum are:

Effect on synch acquisition technology.

Sidelobe energy output (splatter) and bandwidth.

Complexity of modulators and demodulators.

Effects of jamming on the system.

Impact of the technique on size, weight, power requirements, and reliability.

Effect of Synch Acquisition

The waveform employed is a primary force in determining the synch acquisition capability of a spread spectrum system. Direct sequence modulation, for example, employed high-chip-rate code sequences that force a receiver to synchronize to within a very narrow time window (often as narrow as a few nanoseconds), while frequency hopping with its lower code rates, permits timing uncertainties as great as a few milliseconds. This means that the techniques employed for synchronizing in the various systems are quite varied, depending on the waveform employed. Representative acquisition and tracking techniques are (see also Chapter 6):

Shenzhen Huiding Tech. Co., Ltd. - Exhibit 1006

1. Direct Sequence:
   (a) Initial acquisition:
   Serial and/or sequential search—slowest
   Sequential estimation—fast but poor AJ performance
   Universal timing—depends on small time uncertainty
   Matched filters/convolvers—fastest, but still has problems
   (b) Tracking:
   Delay lock loops—classic or dithered

2. Frequency Hopping:
   (a) Initial acquisition:
   Serial and/or sequential search—works well because of reduced uncertainty
   Universal timing—works well due to low drift rates
   (b) Tracking:
   Split-bit tracking—similar to delay lock

(Some frequency hopping systems operate without tracking loops, due to their relative stability and long chip time.)

Sidelobe Energy Output

Production of unwanted sidelobe energy is much higher in some common direct sequence modulating approaches than in others, and is typically high in frequency hopping, although frequency hopping sidelobe energy is well contained inside the signal band. (With frequency hopped signals, one must remember that the signal is a pulsed carrier, and that the spectrum of the signal produced by pulsing the carrier is strictly dependent on the pulse envelope.) Typical rectangular-pulse frequency hopped carriers have $[(\sin x)/x]^2$ power spectra, with sidelobes at −13 dB, and that roll off at a 6 dB/ octave rate. Techniques for pulse shaping exist, however, that can reduce the sidelobe energy, and these may be employed in a system design, where they are applicable.

Also of interest are the techniques needed for use in reducing sidelobe energy output in direct sequence modulated systems. Of the modulation techniques available—biphase phase shift keyed (BPSK), quadriphase shift keyed (QPSK), offset quadriphase shift keyed (OQPSK), and minimum shift keyed (MSK)—the MSK-like signals appear to be most promising.

MSK, or minimum shift keying, is actually a family of signal structures that must satisfy two conditions:

1. The modulating pulse $g(t)$ is symmetrical about $t + T/2$ and 0 otherwise.

Shenzhen Huiding Tech. Co., Ltd. - Exhibit 1006

2. The modulated carrier has a constant envelope. That is,

$$g^2(t) + g^2(t + T/2) = 1$$

Some examples of such waveforms are:

$$\text{(a)} \quad g(t) = \cos\left(\frac{\pi t}{2T} - U\sin\frac{2\pi t}{T}\right) \qquad -T \leqslant t \leqslant T$$
$$= 0 \text{ otherwise}$$

(For classical MSK, $U = 0$ and for SFSK, $U = 0.25$.)

$$\text{(b)} \quad g^{(n)}(t) = \left(\frac{\sin(\pi t/2T)}{\pi t/2T}\right)^n \qquad -2T \leqslant t \leqslant 2T$$

Figure 4.14 shows the (half-pulse) envelope of some signals satisfying equation (a), and Figure 4.15 and 4.16 show the spectral density and out-of-band power, respectively, for three forms of MSK. (OQPSK, though often listed separately, is actually a form of MSK, where the pulse used is square, instead of shaped as in the more usual forms.) Figure 4.17 compares the autocorrelation functions of OQPSK, and two other forms of MSK modulation (classic MSK with $U = 0$, and SFSK with $U = 0.25$).

The OQPSK form does have a more sharply peaked autocorrelation function (this is true only for unfiltered OQPSK), and rolls off linearly. This makes it optimum for ranging systems. MSK and SFSK, on the other hand, have rounded correlation functions, which make them less synchronization-critical.

Complexity of the basic modulators is compared in Figure 4.18. The BPSK and MSK modulators are least complex, and appear identical on a block-diagram basis. The filters employed are very different, however, although the balanced modulators are the same.

BPSK modulation, though simple, is too readily vulnerable, and should not be processed in a limiting channel. Figure 4.19 illustrates the problem seen when passing a BPSK-modulated signal $B \cos \omega_0 t \pm 90°$ through a limiter, together with a strong CW jamming signal $J \cos \omega_0 t$. The result of the process, when the frequency of the jammer is exactly at center frequency, is that the small desired signal amplitude modulates the jamming signal. This results in amplitude modulation that is completely removed by the limiter, so that nothing remains but an unmodulated carrier.

Even in the best case, desired signals are suppressed by larger jamming signals by up to 6 dB and all this must be considered when designing a spread spectrum system. Table 4.1 summarizes the significant characteristics of the various carrier modulation techniques useful for direct-sequence modulation.

Shenzhen Huiding Tech. Co., Ltd. - Exhibit 1006

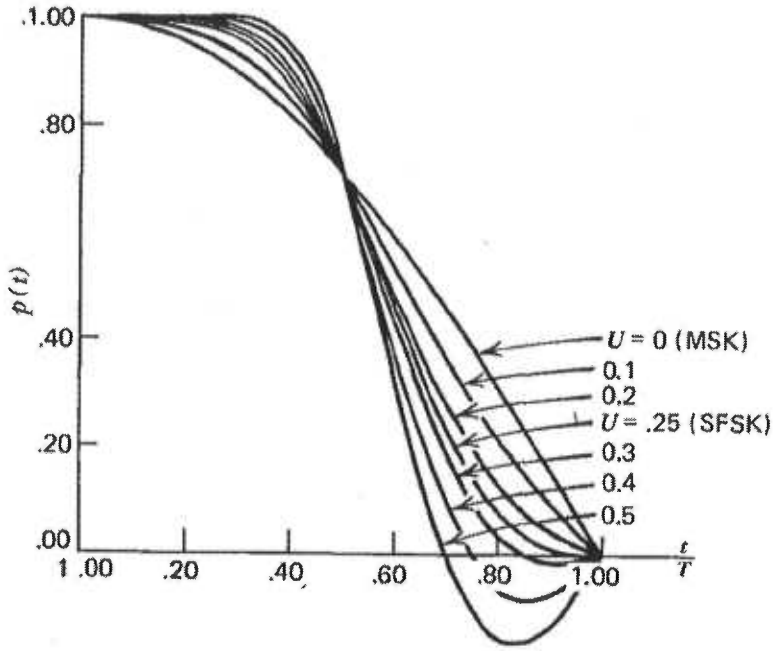


Figure 4.14 Pulses suitable for MSK format.

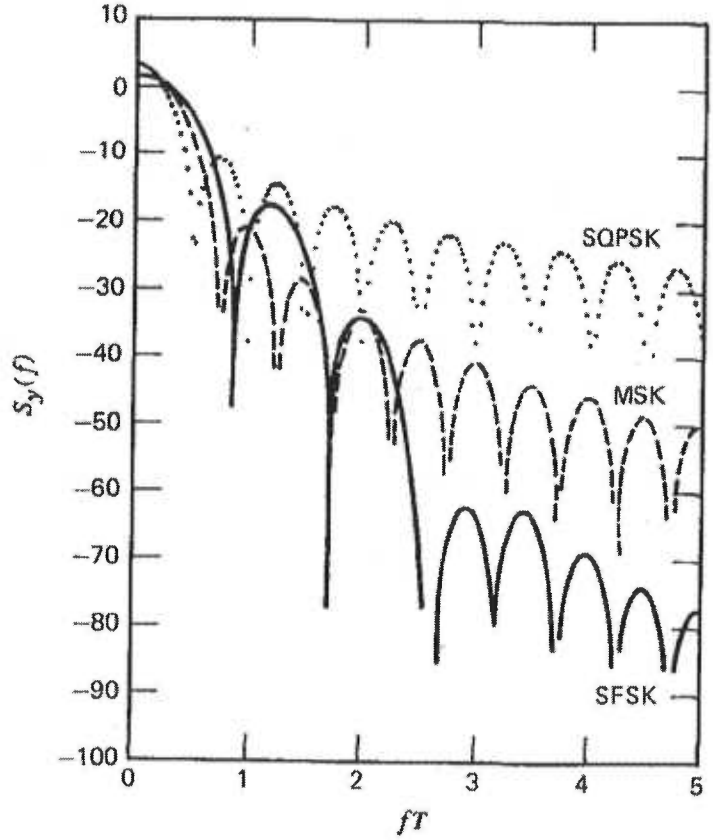


Figure 4.15 Comparison of the equivalent low-pass power spectral densities for OQPSK, MSK, and SFSK.

Shenzhen Huiding Tech. Co., Ltd. - Exhibit 1006

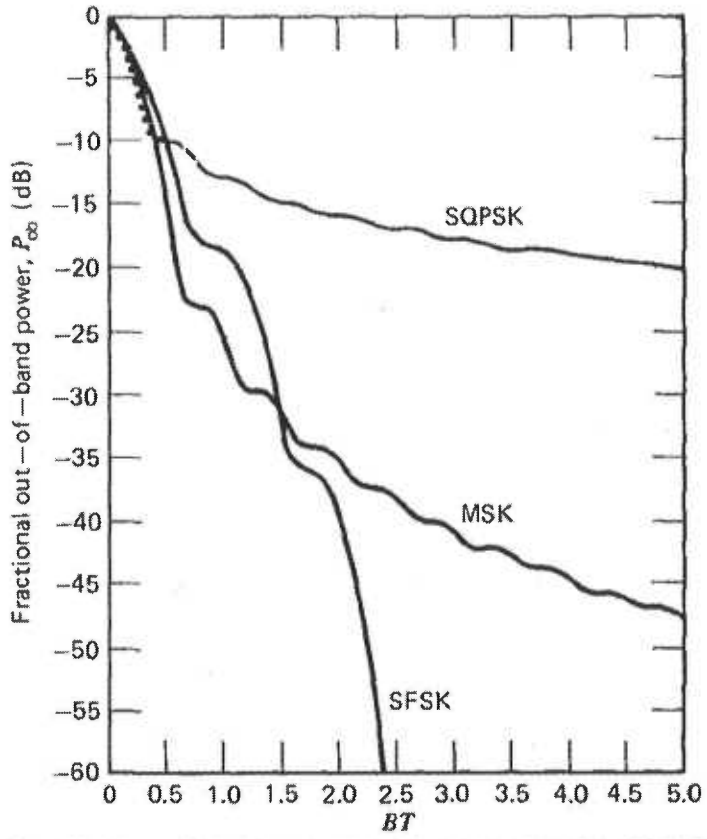


Figure 4.16 Comparison of fractional out-of-band powers for OQPSK, MSK, and SFSK.

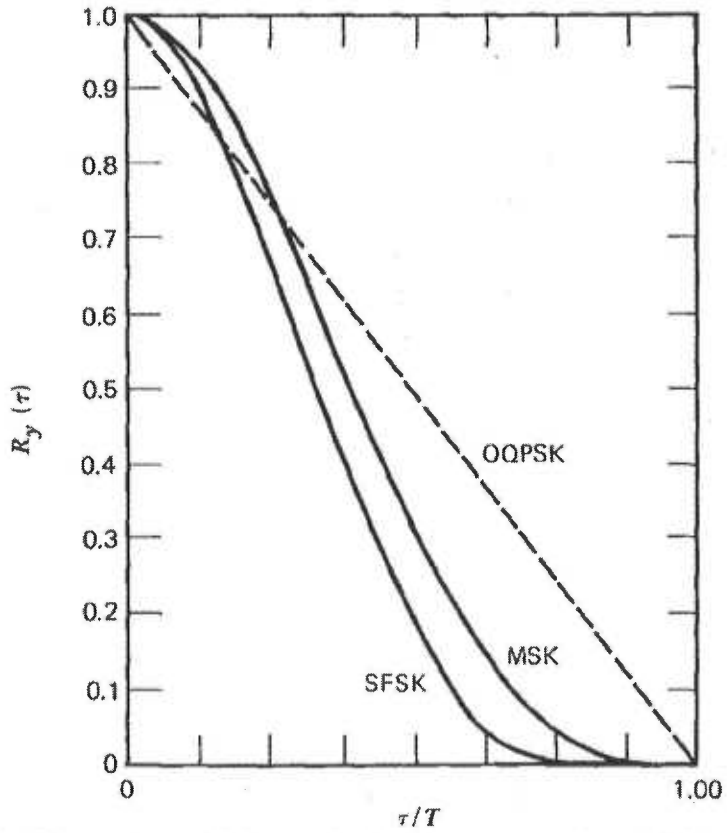


Figure 4.17 Comparison of the equivalent low-pass autocorrelation functions for OQPSK, MSK, and SFSK.

Shenzhen Huiding Tech. Co., Ltd. - Exhibit 1006